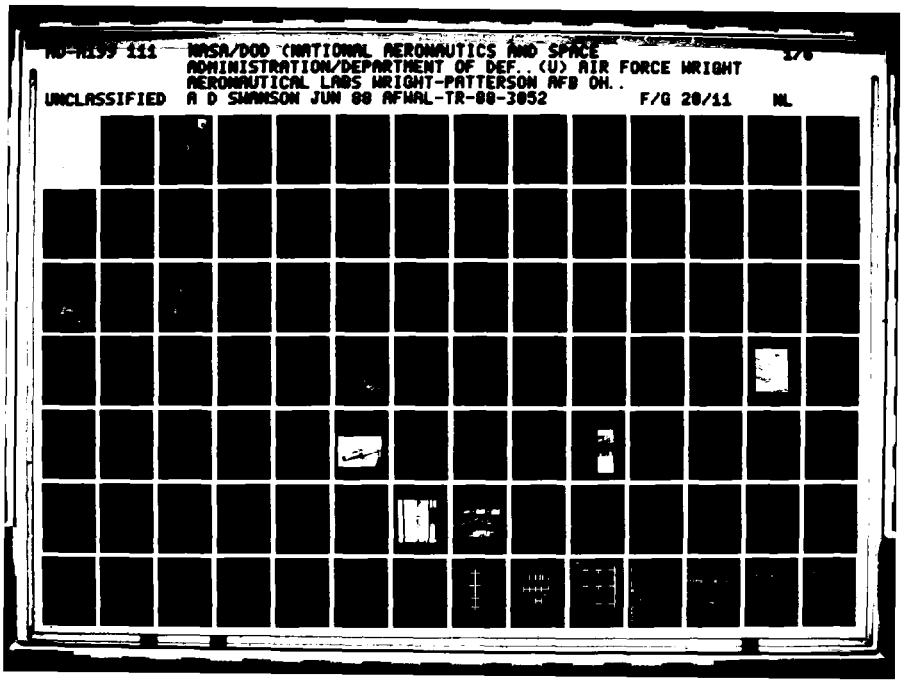
AD-A199 111 NASA/DOD (NATIONAL AERONAUTICS AND SPACE ADMINISTRATION/DEPARTMENT OF DEF.. (U) AIR FORCE WRIGHT AERONAUTICAL LABS WRIGHT-PATTERSON AFB OH..
UNCLASSIFIED A D SWANSON JUN 88 AFWAL-TR-88-3052 F/G 20/11 NL

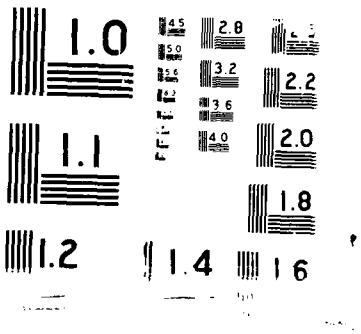
1.0
1.1
1.2
1.4
1.6
1.8
2.0
2.2
2.8
3.2
3.6
4.0
4.5
5.0

DTIC FILE COPY

AFWAL-TR-88-3052

AD-A199 111

NASA/DOD CONTROL/STRUCTURES INTERACTION TECHNOLOGY 1987

Andrew D. Swanson, Lt
Structural Vibration Branch
Structures/Dynamics Division

June 1988

Final Report for Period 17 November - 19 November 1987

DTIC
ELECTE
SEP 2 0 1988
S D
CWD

Approved for Public Release; Distribution is Unlimited

FLIGHT DYNAMICS LABORATORY
AIR FORCE WRIGHT AERONAUTICAL LABORATORIES
AIR FORCE SYSTEMS COMMAND
WRIGHT-PATTERSON AIR FORCE BASE, OHIO 45433-6553

88 9 2

UNCLASSIFIED

SECURITY CLASSIFICATION OF THIS PAGE

ADA199111

REPORT DOCUMENTATION PAGE

Form Approved OMB No 0704-0188

1a. REPORT SECURITY CLASSIFICATION: Unclassified	1b. RESTRICTIVE MARKINGS
2a. SECURITY CLASSIFICATION AUTHORITY: N/A	3. DISTRIBUTION/AVAILABILITY OF REPORT: Approved for public release; distribution is unlimited.
2b. DECLASSIFICATION/DOWNGRADING SCHEDULE: N/A	
4. PERFORMING ORGANIZATION REPORT NUMBER(S): AFWAL-TR-88-3052	5. MONITORING ORGANIZATION REPORT NUMBER(S)
6a. NAME OF PERFORMING ORGANIZATION: Flight Dynamics Laboratory; 6b. OFFICE SYMBOL (If applicable): AFWAL/FIBG	7a. NAME OF MONITORING ORGANIZATION
6c. ADDRESS (City, State, and ZIP Code): Wright-Patterson AFB OH 45433-6553	7b. ADDRESS (City, State, and ZIP Code)
8a. NAME OF FUNDING/SPONSORING ORGANIZATION; 8b. OFFICE SYMBOL (If applicable)	9. PROCUREMENT INSTRUMENT IDENTIFICATION NUMBER
8c. ADDRESS (City, State, and ZIP Code)	10. SOURCE OF FUNDING NUMBERS

PROGRAM ELEMENT NO	PROJECT NO	TASK NO	WORK UNIT ACCESSION NO
62201F	2401	04	32

11. TITLE (Include Security Classification)

NASA/DOD CONTROL/STRUCTURES INTERACTION TECHNOLOGY - 1987

12. PERSONAL AUTHOR(S)

Compiled by Lt Andrew D. Swanson

13a. TYPE OF REPORT	13b. TIME COVERED	14. DATE OF REPORT (Year, Month, Day)	15. PAGE COUNT
Final	FROM 17NOV87 TO 19NOV87	1988 June	523

16. SUPPLEMENTARY NOTATION

Spacecraft

17. COSATI CODES		
FIELD	GROUP	SUB-GROUP
20	11	

18. SUBJECT TERMS (Continue on reverse if necessary and identify by block number)

active control, large space structures, passive damping, control/structures interaction, vibration control.

19. ABSTRACT (Continue on reverse if necessary and identify by block number)

This report is a compilation of 32 technical papers presented at the Second NASA/DOD Control/Structures Interaction Technology Conference, Colorado Springs, Colorado, 17-19 November 1987. The conference was sponsored by the Air Force Wright Aeronautical Laboratories, Wright-Patterson Air Force Base, Ohio and hosted by the Air Force Academy. The emphasis of the second CSI conference was the marriage of control system design and structural implementation, especially in the areas of system analysis, hardware, and testing and validation techniques. The conference consisted of five sessions on integrated controls and structures: (1) Design, Hardware, and Testing for CSI Technology; (2) Control of Flexible Structures (COFS); (3) Design and Analysis; (4) Hardware; and (5) Testing and Validation.

20. DISTRIBUTION/AVAILABILITY OF ABSTRACT	21. ABSTRACT SECURITY CLASSIFICATION
[X] UNCLASSIFIED/UNLIMITED [ ] SAME AS RPT [ ] DTIC USERS	Unclassified

22a. NAME OF RESPONSIBLE INDIVIDUAL	22b. TELEPHONE (Include Area Code)	22c. OFFICE SYMBOL
Lt Andrew D. Swanson	(513)255-5236	AFWAL/FIBG

DD Form 1473, JUN 86 Previous editions are obsolete

SECURITY CLASSIFICATION OF THIS PAGE

UNCLASSIFIED

PREFACE

The Department of Defense and the National Aeronautics and Space Administration are cooperating in the development of a validated technology base in the areas of control/structure interaction, deployment dynamics, and system performance for large, flexible spacecraft. The development of these technologies is essential for the successful operation of new classes of spacecraft whose missions require unprecedented performance, reliability, and low cost. To fulfill these goals, the Air Force Wright Aeronautical Laboratories and the NASA Langley Research Center have agreed to sponsor alternately a series of annual control/structures interaction technology conferences.

This publication is a compilation of the unclassified papers presented at the Second NASA/DOD Control/Structures Interaction Technology Conference, held in Colorado Springs, Colorado, on 17-19 November 1987, sponsored by the Air Force Wright Aeronautical Laboratories and hosted by the Air Force Academy. The proceedings were produced from the original manuscripts provided by the individual authors as camera-ready copy. Special thanks are due to the authors for their care in preparing the manuscripts, and to Nancy Gass of the Air Force Academy for her efforts in arranging for transportation and a secure conference room for the classified portion of the conference.

DTIC COPY INSPECTED 1

Accession For
NTIS GRA&I
DTIC TAB
Unannounced
Justification
By
Distribution/
Availability Codes
Dist Special
A-1

TABLE OF CONTENTS

INTEGRATED CONTROLS & STRUCTURES SESSION I:
DESIGN, HARDWARE, AND TESTING FOR CSI TECHNOLOGY

ASPECTS OF THE INTEGRATED DESIGN OF CONTROLLED FLEXIBLE SPACECRAFT....1
Brantley R. Hanks

OPPORTUNITIES FOR GROUND TEST OF LARGE SPACE STRUCTURES.....19
Keto Soosaar and Laura Larkin

REPORT ON SDIO/NASA MULTIBODY SIMULATION WORKSHOP.....37
R. A. Laskin and G. K. Man

CONTROL OF FLEXIBLE STRUCTURES (COFS)

MAST FLIGHT SYSTEM ENGINEERING DEVELOPMENT AND SYSTEM INTEGRATION....46
Ronald C. Talcott, John W. Shipley, Thedro Kimball,
and Scott W. Greeley

MAST RELATED TEST AND ANALYSIS RESEARCH.....66
Garnett C. Horner and Nancy A. Nimmo

ASTRO 1750A COMPUTER SYSTEM.....75
James McKelvy and Harold Tinsley

CONCEPTUAL DESIGN OF A SPACE STATION DYNAMIC SCALE MODEL.....87
Robert Letchworth, Paul E. McGowan, Marc J. Gronet,
and Edward F. Crawley

INTEGRATED CONTROLS & STRUCTURES II:
DESIGN AND ANALYSIS

OPTIMIZATION OF LARGE SPACE STRUCTURES WITH ACTIVE CONTROLS.....121
A. L. Hale, F. D. Hauser, and N. S. Khot

EFFICIENT CONTROLLER REDUCTION.....136
H. OZ

A CONCEPTUAL SYSTEM DESIGN FOR ANTENNA THERMAL AND DYNAMIC
DISTORTION COMPENSATION USING A PHASED ARRAY FEED..... 145
G. R. Sharp, R. J. Acosta, E. A. Bobinsky, and F. J. Shaker

ADAPTIVE STRUCTURES.....163
B. Wada, J. Garba, J. Fanson, J. Chen, and G-S Chen

METHODS RESEARCH USING EIGENSYSTEM ANALYSIS.....176
Jer-Nan Juang, Richard W. Longman, and John L. Junkins

COMMENTS ON LDCM ACTUATORS.....195
Douglas K. Lindner, Jeff L. Sulla, and Eric Ide

METHODOLOGY FOR OPTIMAL SENSOR LOCATIONS IN DYNAMIC SYSTEMS.....208
Firdaus E. Udwadia

ROBUSTNESS AND POSITIVITY FOR STRUCTURAL CONTROL SYSTEMS.....218
G. L. Slater

RETARGETING CONTROL OF FIGHTING MIRRORS.....234
Steven Ginter and Gunter Stein

INTEGRATED CONTROLS & STRUCTURES III:
HARDWARE

COST EFFECTIVE DEVELOPMENT OF A NATIONAL TEST BED.....250
Henry B. Waites and Victoria L. Jones

RECENT LABORATORY RESULTS ON THE CONTROL OF FLEXIBLE STRUCTURES.....268
P. C. Hughes and T. Hong

RECENT DEVELOPMENTS ON MBCT.....282
B. Wada and C. P. Kuo

QUIET STRUCTURES FOR PRECISION POINTING.....295
P. A. Studer and H. W. Davis

A FACILITY FOR CONTROL STRUCTURE INTERACTION TECHNOLOGY VALIDATION..317
D. Eldred and H. Vivian

EMULATING A FLEXIBLE SPACE STRUCTURE: MODELING.....330
S. C. Rice, V. L. Jones, and H. B. Waites

SLEWING AND VIBRATION SUPPRESSION FOR FLEXIBLE STRUCTURES.....353
P Madden

ASTREX - A FACILITY FOR INTEGRATED STRUCTURES AND CONTROL RESEARCH..364
Richard Quartararo and James Harris

INTEGRATED CONTROLS & STRUCTURES IV:
TESTING AND VALIDATION

ACTUATOR STRUCTURE INTERACTIONS.....376
D. C. Zimmerman and D. J. Inman

EXPERIMENT IN MODELING AND PARAMETER ESTIMATION OF FLEXIBLE
STRUCTURES.....389
Alok Das

OAST IN-SPACE TECHNOLOGY EXPERIMENTS.....401
Jon S. Pyle

STRUCTURAL DYNAMICS RESEARCH ON SCALE MODEL SPACECRAFT TRUSSES.....419
Paul E. McGowan, Harold H. Edighoffer, and Joseph M. Ting

LARGE SPACE STRUCTURES TECHNOLOGY PROGRAM (LSSTP).....438
Robert Gordon

EXPERIMENTAL FAILURE DETECTION RESULTS USING THE SCOLE FACILITY.....457
Mathieu Mercadal and Wallace E. Vander Velde

SINGLE STEP OPTIMAL CONTROL IMPLEMENTED ON THE SCOLE.....484
D. Sparks, Jr. and J. P. Williams

PROBLEMS ASSOCIATED WITH REACTION MASS ACTUATORS USED IN
CONJUNCTION WITH LQG CONTROL ON THE MINI-MAST.....496
D. Ghosh and R. C. Montgomery

ASPECTS OF THE INTEGRATED DESIGN OF CONTROLLED FLEXIBLE SPACECRAFT

Brantley R. Hanks

NASA Langley Research Center
Hampton, Virginia

ASPECTS OF THE INTEGRATED DESIGN OF CONTROLLED FLEXIBLE SPACECRAFT

Brantley R. Hanks
NASA Langley Research Center
Hampton, Virginia

INTRODUCTION

As spacecraft become larger and performance requirements more stringent, an expected future trend, it becomes more difficult to assure structures sufficiently stiff that control-structure interactions are avoided. Furthermore, even if it were not difficult, doing so may be undesirable from standpoints of required control forces and energy as well as launch weight. Using the potential capability of the control system to damp flexible motions may prove the most efficient approach. The relative importance of these factors is not well understood, however, owing primarily to a separation of the structures and controls functions during design. A major hurtle in overcoming this separation is the development of a common mathematical formulation for design purposes and subsequent applications to candidate systems.

This paper discusses the concept that the design of controlled flexible spacecraft is amenable to an integral formulation in which the structure and control system are both modeled in the same way. Basically, structural elements are considered to be special cases of control devices and all controls, including rigid-body controls, are modeled in closed-loop form. Linear Quadratic Regulator theory is interpreted in physical terms as an aid to choosing weighting matrices and interpreting results. An alternate, quick, approach for obtaining an initial system design is offered which is amenable to trading off mass, stiffness and damping. Guidelines are presented for configuring initial designs to obtain good performance characteristics.

TYPES OF SPACECRAFT STRUCTURES

Different types of spacecraft present different challenges from a standpoint of flexible structure control design. Methods which are successful for one type may fail for another. Spacecraft with a few highly concentrated masses connected by low-mass structure are best controlled by devices located directly on the masses. This is the case for the Space Station and most current-day interplanetary and communications spacecraft. As the number of masses become larger, control actuators on each mass become impractical and all significant responses cannot be controlled directly. This situation is at worst in spacecraft with highly distributed mass, such as antenna dishes and solar arrays. In these cases, the control difficulty can be reduced by extremely stiff structure, provided such structure can be designed and put into orbital operation at a reasonable cost.

A third type of spacecraft control problem is that in which subsystems must be isolated, pointed and/or shaped with precision in the presence of disturbances or operations elsewhere on the spacecraft. This problem is made less difficult if the structure to which the subsystem is attached is massive and stiff relative to the subsystem.

Future spacecraft may include combinations of the above three types. A question of growing importance is how to trade off structural stiffness and mass against control complexity and operational cost in spacecraft design.

- CONCENTRATED MASSES WITH LOW-MASS CONNECTIONS
- AREA-TYPE WITH MASS DISTRIBUTED OVER ENTIRE STRUCTURE
- LOCAL COMPONENTS ATTACHED TO MASSIVE SUPERSTRUCTURE

REQUIREMENTS FOR PRECISION, RESPONSE TIME, AND DECAY TIME GENERALLY DIFFER FOR EACH TYPE. THE CONTROL-STRUCTURE DESIGN PROBLEM ALSO DIFFERS.

Figure 1.

BASIC CONTROL DEVICE FUNCTIONS

There are three basic control device functions in spacecraft. Each is a variation on the fundamental function of sensing an output and applying a force in proportion to it. They differ only in the physical location of these actions. In the simplest case, the device senses the state at one point, operates on that signal, and applies a force at another point in proportion to the operator output. Special cases of this function include sensing and operating at the same point, i.e. grounding, and dual cross-coupling of state and force between two points. These forms are equally valid as passive or active devices; and springs and dampers, as well as structural elements, may be considered as subsets of the latter two cases.

In the general case, where the operation is applied to combinations of state measurements at multiple locations, and the operator output controls several actuators, the distributed control problem reaches its greatest complexity. However, for purposes of design, structural members and passive dampers may be considered as simple control devices in even the most complex systems.

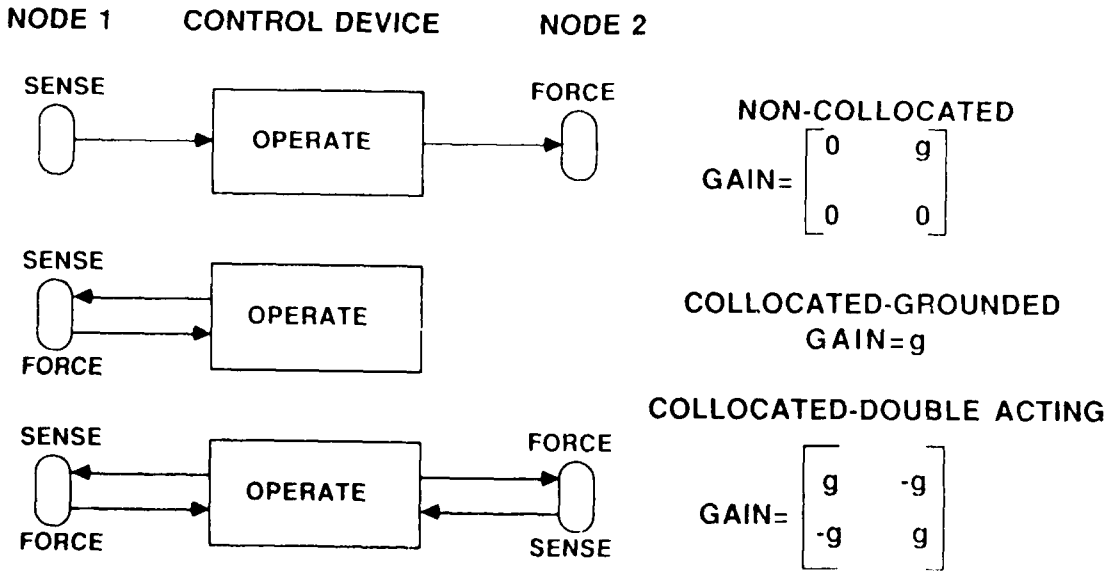

Figure 2.

VISUALIZATION OF RIGID-BODY CONTROL AS MECHANICAL LINKS

The control of a spacecraft or component in free translation or rotation, i. e. rigid-body motion, is generally perceived in design as a process of applying external forces to achieve some desired state or trajectory. For conceptual purposes, however, an alternate view is useful in which the measurement reference against which the control system compares its error, and the control forces proportional to it, in effect act as mechanical links. This is implied by requirements of observability and controllability of rigid body modes in the design analysis. These in effect say that such a linkage must be possible in the closed-loop system in order for a stable solution to exist. The foregoing concept does not change or improve the control design problem, it merely clarifies the similarity between the functions of structure and control. The mathematical effect of either is similar although the mechanization is quite different.

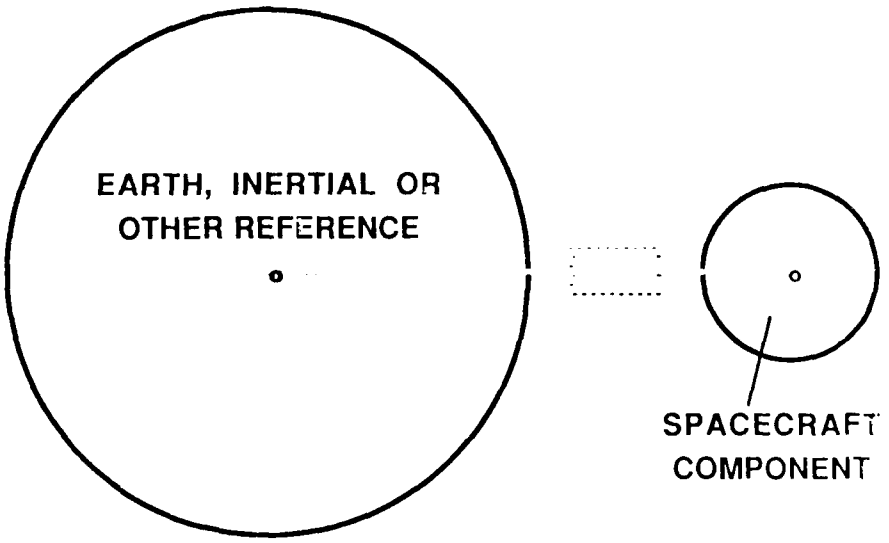

CLOSED-LOOP CONTROLLABILITY/OBSERVABILITY IMPLIES EXISTENCE OF K&C AND INVERSE OF K&C

Figure 3.

MOMENTUM EXCHANGE IN CONTROL

The crucial difference in spacecraft control and in most earthbound control/structures problems is in the control of rigid-body motion. The control system cannot actually complete the virtual force loop suggested in the previous figure. There is no earth, atmosphere, water or other sink against which to push in reacting forces. Therefore control forces must be reacted by changing the momentum of some mass, such as by expelling gases or accelerating/decelerating masses. For rigid motion control, the motion of the momentum sink, in opposition to the application of a control force/moment to the spacecraft, is usually of little concern. The sink mass is allowed to move at will, within the mechanical limits of the hardware (saturation).

For flexible motion control, except by gas jets, the momentum remains on board and the direction of momentum transfer reverses with each cycle. The vibratory inertia of the sink becomes integral to the system dynamics and must be retained in the design analysis.

In the special case of linear momentum exchange devices, sometimes used for vibration control, the vibratory component is key to the device's operation. The momentum exchange facilitates dissipation of energy as heat rather than storing energy as momentum in the device. These devices are not appropriate for controlling rigid-body modes and eliminating the rigid-body mode of linear momentum exchange devices by use of a centering mechanism is necessary. Including its dynamics in the design analysis is absolutely necessary.

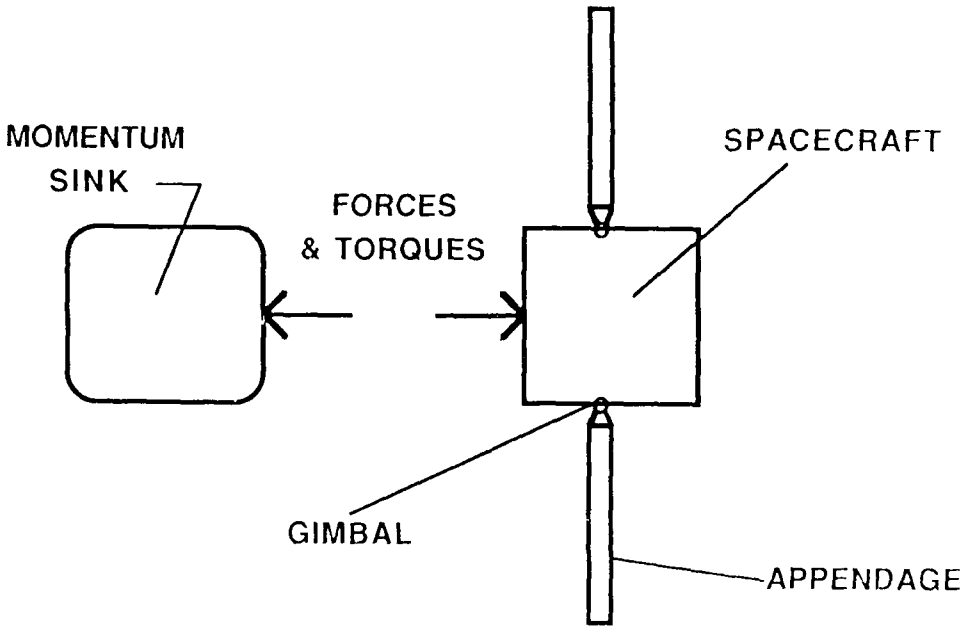

FLEXIBLE MOTION CONTROL REQUIRES MODELING THE MOMENTUM-SINK DYNAMICS

Figure 4.

ACTUATOR TYPES AND APPLICATIONS

The choice of actuators in flexible spacecraft control is not a simple one. Basically, any device capable of transferring and/or dissipating momentum in order to oppose motion is a candidate. This chart shows some popular choices and their applications. Passive structural members and dampers are included here in a departure from general practice. In keeping with the concepts of Figure 2, the design of integrated structures and control systems can best be accomplished by treating both in the same mathematical format. The important point of this figure is that the choice of actuator type is not simple but neither is it completely arbitrary. In cases where structure can substitute for active control, or vice versa, an integrated design approach is needed to make the most beneficial choices.

APPLIC. / TYPE	RIGID SLEW	RIGID TRANSL	DAMP (FLEX)	STIFFEN	ISOLATE	RECONFIGURE
WHEELS	X		X	?	X	ARTIC/POINT
LIN. MASS			X	?	X	
ACTIVE STR			X	X	X	X
JETS	X	X	X	?		ARTIC/POINT
PASSIVE*			X	X	X	

* INCLUDES STRUCTURAL MEMBERS, DAMPERS, SPRINGS, ETC

Figure 5.

DYNAMICS AND CONTROL FORMULATIONS

The three basic formulations the equations of motion of linear dynamic systems shown here represent the primary approaches to dynamic system redesign. They are shown in full-state, physical coordinates but are also frequently transformed to other spaces or projected on subspaces.

The ultimate purpose of a dynamic redesign is to determine system changes (controls) which improve some measure of performance (objective function). In the Newton-Lagrangian formulation, usually used in structures, changes are sought in the stiffness, mass and/or damping matrices, or their modal equivalents, to produce the desired performance.

In control theory, two types of formulations are usually seen. The first, the Linear Quadratic Regulator, assumes complete feedback of all the system states. Projection to subspaces. is usually carried out before the control gains, P, are computed and physical changes are then inferred from the resulting controls. In the Output Feedback formulation, physical connections where changes/controls will be placed are assumed and the gains, G, to produce the optimal dynamic system are then computed.

All three formulations result in a revised linear set of mass, stiffness, and damping matrices which may include active (powered) and/or passive changes to the system.

o NEWTON-LAGRANGIAN

$$\ddot{X}=(M+\Delta M)^{-1}(C+\Delta C)\dot{X}+(M+\Delta M)^{-1}(K+\Delta K)X$$

o LINEAR QUADRATIC REGULATOR

$$\begin{bmatrix}\dot{X}\\ \ddot{X}\end{bmatrix}=\begin{bmatrix}0 & I\\ -M^{-1}K & -M^{-1}C\end{bmatrix}\begin{bmatrix}X\\ \dot{X}\end{bmatrix}-BR^{-1}B^{T}P\begin{bmatrix}X\\ \dot{X}\end{bmatrix}$$

o OUTPUT FEEDBACK

$$\begin{bmatrix}\dot{X}\\ \ddot{X}\end{bmatrix}=\begin{bmatrix}0 & I\\ -M^{-1}K & -M^{-1}C\end{bmatrix}\begin{bmatrix}X\\ \dot{X}\end{bmatrix}-BGH\begin{bmatrix}X\\ \dot{X}\end{bmatrix}$$

Figure 6.

TIME-INVARIANT LINEAR QUADRATIC REGULATION

The solution of the design problem of the previous figure is usually accomplished differently in structures and controls designs. In structures, hundreds of degrees of freedom are required and permissible changes are highly constrained. Solution of the design problem is generally by constrained nonlinear search of the design space. Controls hardware, on the other hand, allows considerable implementation freedom and, until recently, required only a few (10-30) degrees of freedom in the equations. Connections among measurements and actuators are assumed to occur in a computer and any combination is theoretically possible.

The hypothetically perfect control is given by the Linear Quadratic Regulator solution shown here. The system equations on the first line of the figure are the equivalent of the regulator equations on the previous figure where the vector $z^T=(x\ \dot{x})^T$. The revised system equations are shown on the last line where the matrix BG contains the effective changes in the mass, stiffness, and damping matrices. The solution is exact, when it exists, and is given by the relatively complicated Riccati Equation shown on line four. Difficulties arise in applying this solution to physical systems for several reasons too complex for discussion here. However, the first is in choosing the arbitrary weighting matrices, Q and R, which quantitatively set the objective "potential" and the relative change which will be allowed in the system in achieving this objective, respectively. Both enter into the optimal solution and, hence, the initial assumption governs the result.

SYSTEM: $\dot{z} = Az + Bu$

CONTROLLED VARIABLES: $y = Hz$

OBJECTIVE: $\min_u \int_0 \left\{ \underbrace{[y^T Qy]}_{\text{RESPONSE}} + \underbrace{[u^T Ru]}_{\text{CONTROL}} \right\} dt$ Q AND R ARE WEIGHTING MATRICES

OPTIMAL CONTROL: $u_{opt} = -R^{-1} B^T Pz = -Gz$ WHERE P IS THE SOLUTION

$TO - PA - A^T P + PBR^{-1} B^T P - H^T QH = 0$ (ALGEBRAIC RICCATI EQUATION)

FINAL SYSTEM: $\dot{z} = [A - BG]\, z = [A + \Delta A]\, z$

Figure 7.

COMPATIBILITY CONSIDERATIONS

The terminology of the previous figure causes much confusion in applications where the problem solved must represent a physical system. Numerous or inexplicable choices of R, in particular, are frequently used and the resulting solution, though exact, may not be as good as that produced by a nonlinear search or other inexact techniques.

Investigation of the dimensions of the LQR equations of Figure 7 by imposing the dimensions of the equations of motion, Figure 6, on the solution provides some physical intuition in choosing Q and/or R. Figure 8 shows that five relationships occur containing six undefined terms. (The term $B^TR^{-1}B$ repeats in all five relationships and will carry the dimensions shown for R if B is not dimensionless.) Note that Q and P in Figure 7 are 2n by 2n matrices where the mass, stiffness, damping, Q_{ij}, P_{ij} and R matrices here are n by n.

CLOSED-LOOP SYSTEM:

$$J = E_0 + \int_0^T \begin{bmatrix} x' & \dot{x}' \end{bmatrix} \begin{bmatrix} (Q_{11} + P_{12}B'R^{-1}BP_{21}) & (Q_{12} + P_{22}B'R^{-1}BP_{21}) \\ (Q_{21} + P_{12}B'R^{-1}BP_{22}) & (Q_{22} + P_{22}B'R^{-1}BP_{22}) \end{bmatrix} \begin{Bmatrix} x \\ \dot{x}' \end{Bmatrix} dt$$

$$\begin{Bmatrix} \dot{x} \\ \ddot{x} \end{Bmatrix} = \begin{bmatrix} 0 & I \\ M^{-1}K - B'R\ BP_{21} & M^{-1}C - B'R^{-1}BP_{22} \end{bmatrix} \begin{Bmatrix} x \\ \dot{x} \end{Bmatrix}$$

FIVE DIMENSIONAL RELATIONSHIPS:

$$Q_{11};P_{12}B'R^{-1}BP_{21} \qquad Q_{12};P_{12}B'R^{-1}BP_{22} \qquad Q_{22};P_{22}B'R^{-1}BP_{22}$$
$$M^{-1}K;B'R^{-1}BP_{21} \qquad M^{-1}C;B'R^{-1}BP_{22}$$

SIX UNDEFINED TERMS:

R, Q_{11}, Q_{12}, Q_{22}, P_{12}, P_{22} (B ASSUMED DIMENSIONLESS)

ONLY ONE OF THESE TERMS CAN BE FIXED ARBITRARILY

Figure 8.

SOME DIMENSIONALLY-COMPATIBLE CHOICES IN WEIGHTING MATRICES

Choosing a form for any one of the undefined terms in Figure 8 fixes the form of all the others. Choosing a form for more than one implies adding constraints among the others. The table shown in Figure 9 gives some combinations which can result if B is assumed dimensionless. Various forms of quantity being minimized can be recognized among them including strain energy, kinetic energy, velocity, displacement, acceleration, etc. Interpretation of the meaning of these terms is assisted by remembering that K/M is related to natural frequency squared and KM is related to critical damping squared. By inspection of the first row, it is seen that if total energy is minimized (i.e., Q_{11}=K and Q_{22}=M), then C is constrained to the form KM and modal damping must occur as the optimal solution form. The sixth row shows this constrained set and the seventh row shows the constrained set which results when the often-assumed case of a unity Q matrix is considered.

Q_{11}	Q_{12}	Q_{22}	R	P_{12}	P_{22}	Comment
K	C	C^2/K	M^2/K	M	MC/K	
MK^2/C^2	MK/C	M	M^3/C^2	KM^2/C^2	M^2/C^2	
K^2/C^2	K/C	1	M^2/C^2	KM/C^2	M/C	
1	C/K	C^2/K^2	M^2/K^2	M/K	MC/K^2	
K^2/M^2	KC/M^2	C^2/M^2	1	K/M	C/M	Pij same as A matrix terms
K	C	M	M^2/K	M	M^2/C	Implies C^2 ~ KM Constraint
1	1	1	M^2/K^2	M /K	M/C	Implies K~ C Constraint

Figure 9.

BASIC EQUATIONS

As mentioned in the discussion of the previous figure, choosing Q to be the sum of kinetic and potential energies requires C^2 proportional to KM and constrains Q_{12} to be a damping term. It is well known that the integral of the sum of kinetic and potential energies is minimized by the standard equations of motion as shown in this figure provided the damping is of so-called proportional or Rayleigh form; that is, C is diagonalized by the eigenvalues of the undamped system. The same can be easily shown for the integral form shown where the energies are coupled by a dissipation term. The equations of motion can be directly derived from dV/dt=0. Thus proportional damping makes the coupled energy quadratic an extremum over the entire trajectory, no matter what its magnitude. An infinite number of solutions exist and this corresponds to the infinite number of arbitrary values of the weighting matrix R in the LQR solution. A more precise approach to guide design is needed.

MINIMIZE J SUBJECT TO $M\ddot{x} + C\dot{x} + Kx = 0$ WHERE

$$J = \int_0^T \begin{bmatrix} x' & \dot{x}' \end{bmatrix} \begin{bmatrix} K & C'/2 \\ C/2 & M \end{bmatrix} \begin{Bmatrix} x \\ \dot{x} \end{Bmatrix} dt = \int_0^T E\, dt$$

J IS MINIMIZED BY THE SOLUTION TO $M\ddot{x} + C\dot{x} + Kx = 0$ PROVIDED C IS PROPORTIONAL DAMPING, i.e. CAN BE DIAGONALIZED BY THE EIGENVECTORS OF THE UNDAMPED SYSTEM

Figure 10.

ALTERNATE FORMULATION

An alternate approach to making the integrand of the objective function an extremum is shown here for the energy formulation. It produces critical damping as the solution in this case but can be applied to other formulations. The solution shown is not unique. It satisfies the equations of motion independently of the other two equations. Other possibilities include satisfying each equation independently and all simultaneously.

J IS ALSO MINIMIZED IF $\dot{E} = 0$, i.e.

$$[\, x' \quad \dot{x}' \quad \ddot{x}' \,] \begin{bmatrix} 0 & K & C/2 \\ K & (C'+C)/2 & M \\ C'/2 & M & 0 \end{bmatrix} \begin{Bmatrix} x \\ \dot{x} \\ \ddot{x} \end{Bmatrix} = 0$$

THIS CONDITION IS SATISFIED BY THE EQUATIONS OF MOTION AND THE CONSTRAINT

$$C' M^{-1} C = 4K$$

FROM WHICH

$$C/2 = \sqrt{M}\sqrt{K} = (\Phi^{\mathrm{T}})^{-1} \Omega \Phi^{-1}$$

Figure 11.

BASIC FORM OF OPTIMAL SOLUTION

A quick approach to implementing the result of the previous figure to obtain the basic form of an optimal dynamic system design is shown in this figure. It consists of choosing the closed-loop system parameters such that the quadratic to be minimized has the property shown. The rank of the overall Q matrix is reduced, i. e. eigenvalues of the closed-loop objective function become non-oscillatory. Several variations are shown in the figure including an output-feedback form which has very promising properties, as will be shown later. The most recognizable form is that of minimizing the energy (also directly transformable to modal coordinates) which produces a ratio of critical damping as the optimum solution. The rank of the energy matrix is reduced from 2n by 2n to n by n. It is clear in the physical energy form that locating controls at the points of maximum product of mass and stiffness is likely to be the best initial assumption.

The key advantage of the proposed approach is that it gives a unique answer for any Q matrix. In output feedback form, it has the additional property that, given any two of the mass, stiffness or damping matrices, a unique physical solution is found directly. Reduction of gains to fit practical constraints is also direct as is computing the resulting effect on other parameters. The sub-optimal problem where desired gains cannot be achieved at desired locations will be discussed in a later paper.

$$Q_{21} Q_{22}^{-1} Q_{12} = Q_{11}$$

$$\begin{bmatrix} \sqrt{Q_{11}}^{T} \\ \sqrt{Q_{22}}^{T} \end{bmatrix} \begin{bmatrix} \sqrt{Q_{11}} & \sqrt{Q_{22}} \end{bmatrix} = \begin{bmatrix} Q_{11} & Q_{12} \\ Q_{21} & Q_{22} \end{bmatrix}$$

$$\begin{bmatrix} \sqrt{K}^{T} \\ \sqrt{M}^{T} \end{bmatrix} \begin{bmatrix} \sqrt{K} & \sqrt{M} \end{bmatrix}$$

$$\begin{bmatrix} B_1 \sqrt{G_1}^{T} \\ B_2 \sqrt{G_2}^{T} \end{bmatrix} \begin{bmatrix} \sqrt{G_1} H_1 & \sqrt{G_2} H_2 \end{bmatrix}$$

Figure 12.

OPTIMAL DAMPING - 2 DEGREE-OF-FREEDOM SYSTEM

The results of applying the approach shown in the previous figure is illustrated by the simple 2-mass system shown in this figure. Given masses M_1=1 and M_2=2 and springs K_1=1.586, K_2=1.414, and K_3=0.586, respectively, the optimal solution given by the root matrix form is the damping matrix shown. It results from 3 dampers with damping values totalling 5.97. The response, as indicated by the displacement and velocity curves, is highly damped, permanently falling below 10 percent of the initial in about 6 seconds.

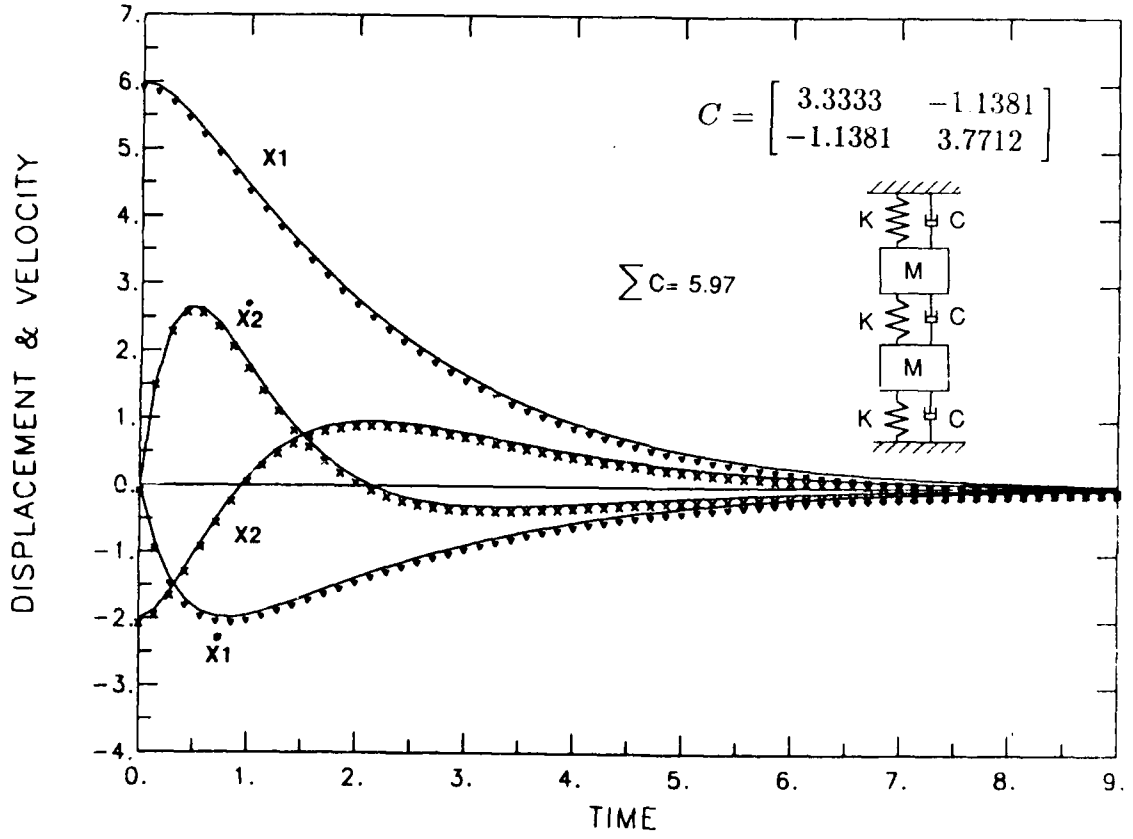

Figure 13.

OPTIMAL DAMPING - 2 DAMPER SIMPLE SYSTEM

The results of a slightly different approach to the same problem as shown in Figure 14 is illustrated in this figure. Using a variation on the output feedback approach in which the system is decomposed such that G is diagonal, the optimal solution given by the root matrix form is the damping matrix shown. It results in only 2 dampers (to ground) rather than 3 and the damping values total 5.00, about 16 percent less than in the previous case. The response, as indicated by the displacement and velocity curves, is again highly damped, permanently falling below 10 percent of the initial value in about 4 seconds, or 33 percent faster than in the previous case.

The two results to the same problem differ primarily in that the higher frequency response component is less damped in the second case but settles within the response time of the first mode. A more significant fact is that the second solution was quickly calculated by hand. A linear regulator analysis would require solving a 4th-order Matrix Riccati Equation, possibly for several values of the R weighting matrix. A nonlinear search would require several iterations, depending on the accuracy of the starting parameter assumptions. Not obvious here, but clear in the calculation process, is that rate feedback to ground will always be the most important control component even for flexible modes. Taking advantage of this approach and supplementing it with passive dampers to assure stability of high frequency flexible modes is recommended as the best initial design assumption.

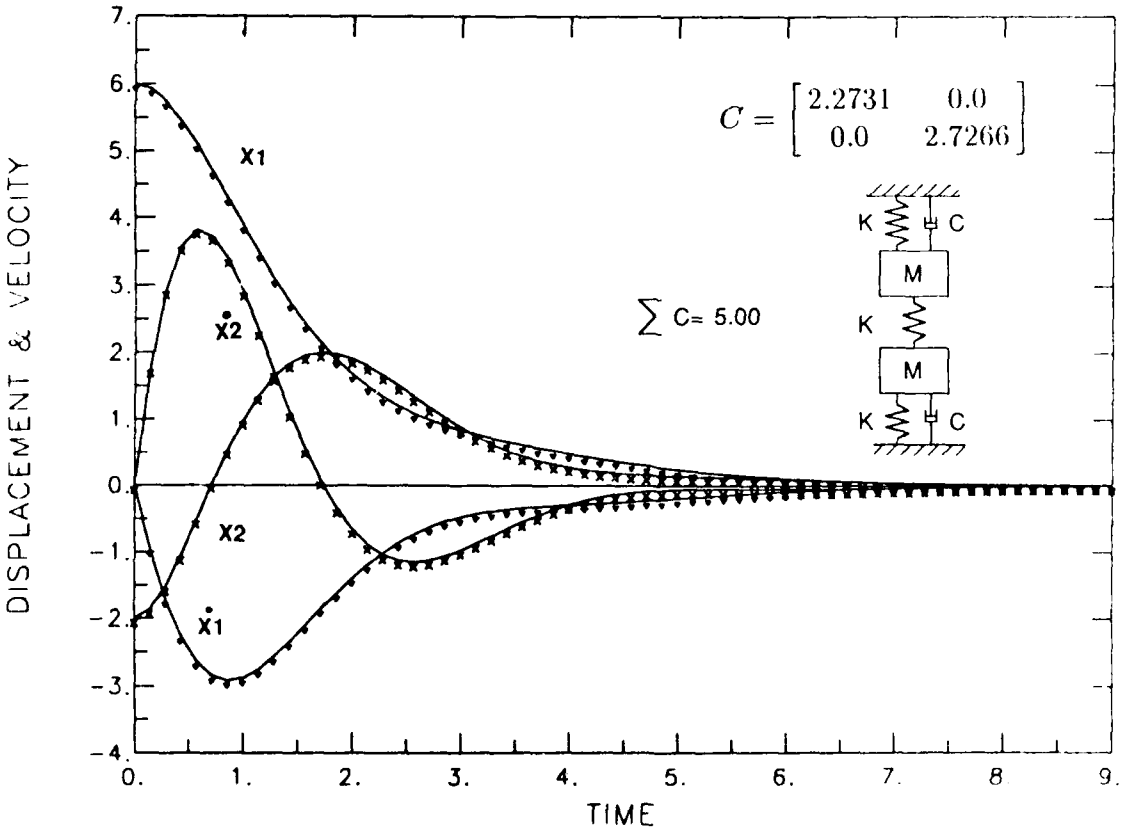

Figure 14.

DESIGN GUIDELINES FOR FLEXIBLE SPACECRAFT CONTROL

Key results of the design approach of the previous 3 figures are summarized in this figure with some elaboration which follows from the earlier discussion. With design guidelines such as these, initial designs which have a high potential for success can be formulated. In addition, a basis for trading controls and structure in the same design process rather than by passing data between two separate design processes is a direct result. Treatment of non-symmetry and instability was not discussed but is a straightforward extension of the same approach.

- o CONCENTRATE MASS IN AS FEW LOCATIONS AS POSSIBLE
- o APPLY HIGHEST STIFFNESS AT LOCATIONS OF HIGHEST MASS
- o APPLY DAMPERS (RATE FEEDBACK CONTROL) AT LOCATIONS OF HIGHEST PRODUCTS OF MASS AND STIFFNESS (PROPORTIONAL CONTROL)
- o CONTROL LOWEST FLEXIBLE MODES WITH RIGID-BODY CONTROLLER AND USE FILTERS AND PASSIVE DAMPING TO AVOID EXCITATION OF HIGHER MODES
- o KEEP MASS & INERTIA AS LOW AS POSSIBLE AND SET FIRST MODE FREQUENCY SUCH THAT CRITICALLY-DAMPED TIME CONSTANT EQUALS REQUIRED RESPONSE TIME

Figure 15.

SUMMARY

This paper has discussed the concept that the design of controlled flexible spacecraft is amenable to an integral formulation in which the structure and control system are both modeled in the same way. Basically, structural elements can be treated as special cases of control devices and all controls, including rigid-body controls, are modeled in closed-loop form. An approach for obtaining an "optimal" initial system design is offered which is amenable to trading off mass, stiffness and damping. Figure 16 lists some of the inferences which can drawn from the results of this approach.

- STRUCTURES AND CONTROLS ARE AMENABLE TO THE SAME ANALYSIS/DESIGN TECHNIQUES
- DESIGN OF BOTH IN THE SAME PROCESS IS NECESSARY
- THE SOLUTION DIFFERS FOR DIFFERENT TYPES OF MASS DISTRIBUTIONS
- USE OF RIGID-BODY ACTUATORS AND PASSIVE DAMPERS TO CONTROL FLEXIBLE MOTIONS IS RECOMMENDED

Figure 16.

OPPORTUNITIES FOR GROUND TEST OF LARGE SPACE STRUCTURES

Keto Soosaar and Laura Larkin
Cambridge Research
A Division of Photon Research Associates, Inc.
Cambridge, Massachusetts 02138

TASKS UNDERTAKEN

To evaluate ground test opportunities, test verification and validation of SDI and NASA systems were studied in detail. SDI systems specifications and requirements were identified. The information was combined with our existing extensive NASA database, and system comparisons were made. Numerous sources were utilized for this study, including the NASA Space Systems Technology Model (SSTM), the Air Force Military Space System Technology Plan (MSSTP), and a variety of SDIO basic material from unclassified sources.

With these data, mission classes were determined and testing issues explored. Ground test and other prelaunch verification limitations and benefits were identified. Effects of the earth environment were also studied to determine impact.

Some recent ground testing experience was studied to aid in devising and evaluating future test scenarios. Although ground testing with its inherent limitations may not provide 100% confidence, it will remain the most feasible method for prelaunch verification for future SDI missions. Therefore, it is important that the advantages and limitations of scaled, artificially suspended test articles be thoroughly understood.

1) SURVEY ALL SDIO SYSTEMS TO ESTABLISH PERFORMANCE REQUIREMENTS AND COMPARE WITH NASA GOALS.

2) ESTABLISH CATEGORIES OF VERIFICATION REQUIREMENTS.

3) DEVISE AND EVALUATE TEST SCENARIOS WHICH CAN BE USED TO MEET VERIFICATION REQUIREMENTS.

NASA MISSIONS

The planned future civilian space systems where structure/control interaction is important may be divided into three categories: optical systems, large platforms, and antennas. This figure shows a NASA mission from each of these classes. On the left is the Large Deployable Reflector (LDR), which will be a dedicated observatory to explore the far infrared/near millimeter wave spectral region which is meshed by the earth's atmosphere. The baseline concept consists of a Cassegrain telescope with a segmented, actively controlled 20-m primary reflector. Active control of the optics will be utilized to control the position and orientation of each optical segment. Alternate schemes are in development as well, utilizing reimaging approaches where all of the wavefront correction is done on a small reimaged system. The central picture shows the proposed Space Station, typical of a large multibody platform system. The International Space Station (ISS) will be 189 meters in length. The growth version is expected to be over 320 meters in length. Structural models of these systems predict fundamental modes below 1/4 Hz. Current analysis estimates indicate marginal freedom from structure/control interaction, but whether the future extensions to the larger platform have these properties remains to be seen. The third picture indicates a generic large NASA antenna. These are encountered in many communications, radiometric, or actively transmitting formats, and at the typical sizes of 30 m and up will be expected to exhibit needs for active surface control and flexible body pointing.

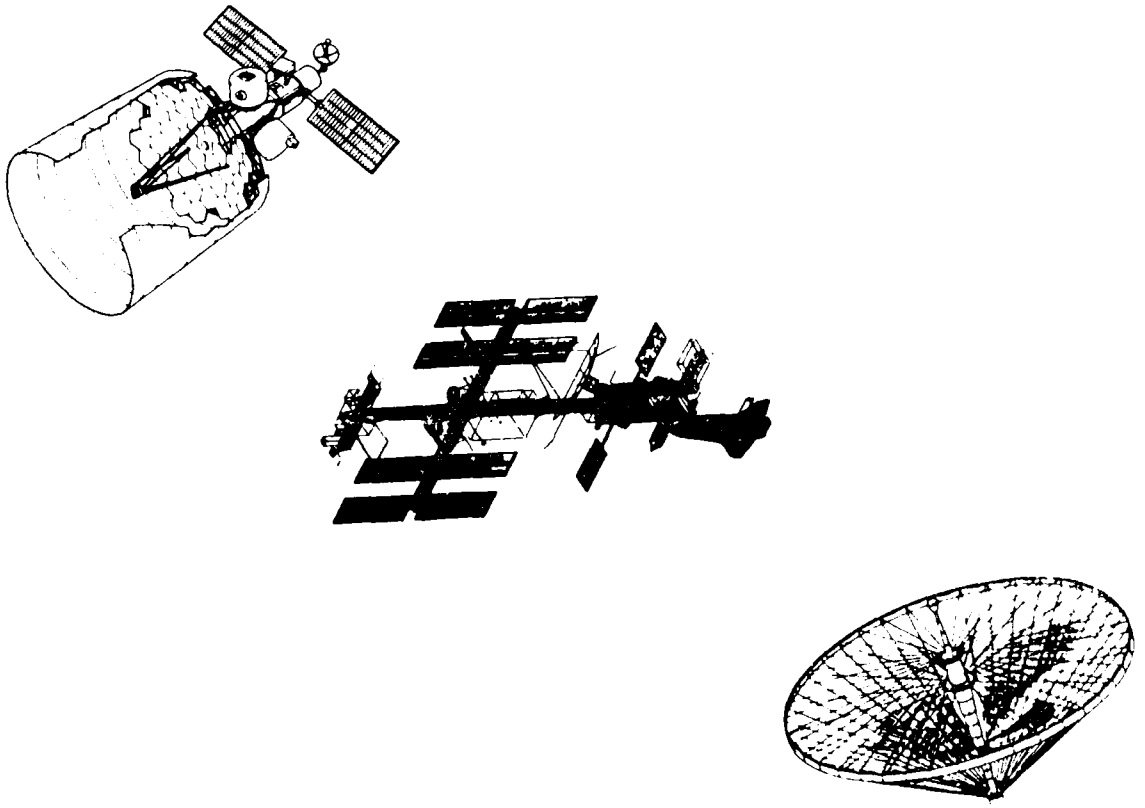

MAJOR CLASSES OF NASA SYSTEMS

These three categories of space missions show distinct structures, dynamics, and controls issues. Testing and verification requirements also differ among the classes. The optical systems are spacecraft which support a large precision short wavelength sensor. Several proposed NASA missions, such as the Infrared Interferometer and the Thinned Aperture Telescope, fit this category. The antennas are long wavelength systems used for communication and radar. The Gravity Wave Interferometer and the Very Long Baseline Interferometer are good examples of this class. The platform systems are large, mostly "planar" structures, including Space Station, Geostationary Platform, and Earth-Observing System.

The optics require extreme pointing stability and accuracy. Although the structural frequencies are higher than the other two categories, control/structure interaction and control of a flexible structure is still a major concern. The large size of these systems may require on-orbit deployment. The main test requirement is the demonstration of precision pointing, stability, and figure control in the 0-g space environment.

The antennas are characterized by very low structural frequencies. Although pointing and stability requirements are not very stringent, some systems may require control of the antenna mesh. On-orbit deployment of these lightweight membrane structures is a primary concern. Validating this deployment is a major test issue.

The platforms are also expected to have low structural frequencies. These systems are characterized by multibody dynamics, which is a primary [illegible] verification area.

SYSTEM TYPE	EXAMPLES	KEY FEATURES IN STRUCTURES, DYNAMICS AND CONTROL	MAJOR VERIFICATION AND TEST NEEDS
PRECISION SHORT WAVELENGTH SENSORS (OPTICAL TELESCOPES)	LOR, AXAF, INFRARED INTERFEROMETER COSMIC, TAT	POINTING STABILITY AND ACCURACY OF FLEXIBLE CONTROLLED STRUCTURE; FIGURE AND ALIGNMENT CONTROL; DEPLOYMENT OF PRECISION STRUCTURE; LOW TO MEDIUM STRUCTURAL FREQUENCIES	POINTING STABILITY AND FIGURE CONTROL IN ZERO-G
LARGE COMMUNICATION AND RADAR ANTENNAS (LONG WAVELENGTH)	VLBI, GRAVITY WAVE INTERFEROMETER, SETI	SURFACE QUALITY MAY REQUIRE CONTROLLED MESH. AUTOMATIC DEPLOYMENT A MAJOR CONCERN. VERY LOW TO LOW STRUCTURAL FREQUENCIES	SURFACE CONTROL IN ZERO-G; ZERO ATM[illegible] MODAL PROPERTIES; DEPLOYMENT IN ZERO-G
LARGE CONSTRUCTED MULTI-PURPOSE PLATFORMS (POSSIBLY MANNED)	SPACE STATION, EARTH-OBSERVING SYSTEM, GEO-STATIONARY PLATFORM	MULTIBODY DYNAMICS WITH FLEXIBLE COMPONENTS AND ATTACHED PRECISION POINTING EXPERIMENTS VERY LOW TO LOW STRUCTURAL FREQUENCIES	FLEXIBLE MULTI-B[illegible] BEHAVIOR; DYNAMIC STABILITY; [illegible] ENVIRONMENT FOR EXPERIMENTS; A[illegible] CONSUMABLES, [illegible] DURING [illegible]

SDI MISSIONS

This picture shows several SDI missions, which also may be divided into the three spacecraft classes. The top row shows three concepts of optical systems. These are drawings of the Space-Based Laser (SBL) and the space relay portion of the Ground-Based Laser (GBL). The middle row provides artist renderings of the two SDI platform systems: Neutral Particle Beam (NPB) and Kinetic Energy Weapon (KEW). The bottom row depicts antenna systems--one a reflector type, the other a phased-array configuration that might be used for space-based radar.

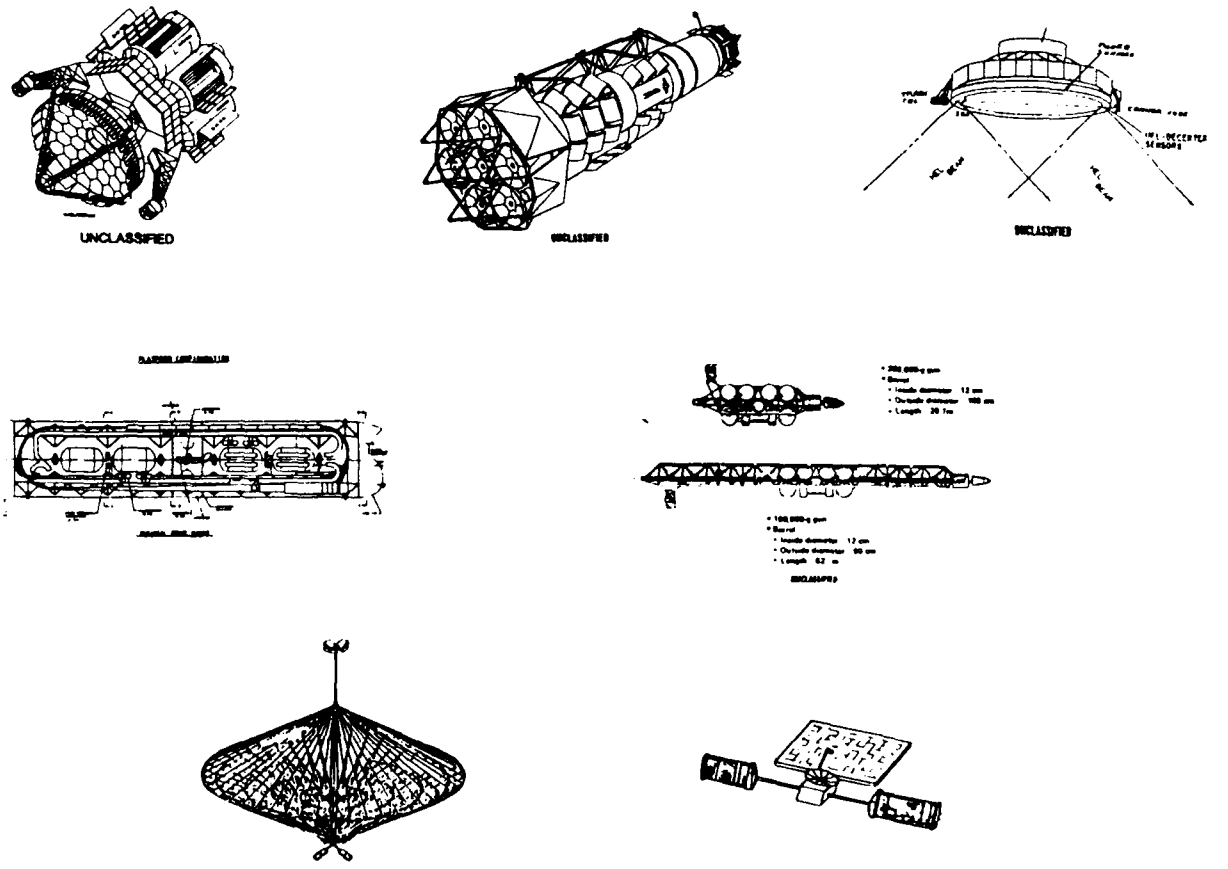

MAJOR CLASSES OF SDIO SYSTEMS

The SDI classes of systems are very similar to the NASA systems. Many of the same issues exist in the areas of structures, dynamics, controls, and test verification. One of the major differences is the extremely large internal disturbances which will act on the optical and platform systems.

In addition to precision pointing, figure control, and stability, the optical systems must provide isolation of the disturbances. Testing requirements include demonstration of precision slewing, system-level isolation, and structural control in the 0-g space environment.

The features and test needs of the large antenna system mirror those of NASA systems. Very low structural frequencies will dominate these very large, lightweight systems. Deployment validation will be a major challenge.

The SDI platforms also have many of the same features as the NASA platforms. Multibody behavior may be significant. In addition, large disturbances must be isolated.

SYSTEM TYPE	EXAMPLES	KEY FEATURES IN STRUCTURES, DYNAMICS AND CONTROLS	MAJOR VERIFICATION AND TEST NEEDS
PRECISION SHORT WAVELENGTH OPTICAL SYSTEMS	SBL, GBL SURVEILLANCE IR	POINTING STABILITY AND ACCURACY OF FLEXIBLE CONTROLLED STRUCTURE; FIGURE AND ALIGNMENT CONTROL; MAJOR ISOLATION OF DISTURBANCES; PRECISION ASSEMBLED STRUCTURE; MODERATELY HIGH FREQUENCIES; MULTIBODY CONFIGURATIONS.	SYSTEM-LEVEL ISOLATION AND STRUCTURAL CONTROL IN 0-G; FIGURE AND WAVEFRONT CONTROL IN 0-G; PRECISION SLEW IN 0-G; MULTI-BODY BEHAVIOR.
LARGE ANTENNAS	SURVEILLANCE RADAR	BEAM QUALITY MAY REQUIRE CONTROLLED SURFACE; ALIGNMENT AND BEAM POINTING (?) CONTROL AUTOMATIC DEPLOYMENT A MAJOR CONCERN; VERY LOW STRUCTURAL FREQUENCIES.	SURFACE QUALITY AND CONTROL IN 0-G; ON ORBIT MODAL PROPERTIES; 0-G DEPLOYMENT
LARGE 1-DIMENSIONAL PLATFORMS	NPB KEW	ALIGNMENT MAY REQUIRE CONTROL POINTING AND SLEW WITH FLEXIBLE STRUCTURE; SIGNIFICANT DISTURBANCES; ON-ORBIT DEPLOYMENT, ASSEMBLY OR CONSTRUCTION; MULTIBODY POSSIBLE	ON-ORBIT MODAL PROPERTIES; MULTIBODY BEHAVIOR; POINTING AND ALIGNMENT STABILITY.

ANALOGOUS MISSIONS

The features, issues, and concerns of these mission categories exist in both NASA and SDI systems. This chart shows the missions and categories previously described, grouped according to class and government agency.

SYSTEM	SDIO	NASA
OPTICS	GBL SBL SSTS	LDR AXAF I^2 COSMIC TAT
RADAR	SBR	VLBI GWI SETI
LARGE PLATFORMS	NPB KEW	SPACE STATION EOS GEO PLATFORM

STRUCTURES, DYNAMICS, AND CONTROL VALIDATION/DEMONSTRATION ENVIRONMENTS

There are several methods to validate a space structure prior to mission operation. These vary in complexity, expense, and level of confidence. Some combination of these six may be required for each system. Every spacecraft will undergo analytical modeling to test performance and specifications. This method allows relatively inexpensive investigation of a wide variety of parameters. The major drawback is in modeling phenomenologies which are not fully understood.

Ground testing, either full or reduced scale, allows human modifications during testing of hardware. Power and data processing capabilities are unconstrained by weight and volume in contrast to flight experiment limitations. The main disadvantage is the effect of the earth environment, which requires thermal and atmospheric test tanks and suspension systems. Reduced-scale models are usually less expensive, but have the difficulties of scaling phenomena such as damping, tolerances, and nonlinear joint effects. This scaling leads to a reduced confidence when transferring results to the actual system, especially if the scale factor is large.

Flight experiments yield the highest confidence of mission success, but are very expensive. Space tests are feasible only for flight-ready hardware, which occurs at the end of the development schedule. Experience has shown that the space verification test process often uncovers design and manufacturing problems. A discovered anomaly may require redesign, retrofit, repair, and subsequent retesting. In the case of a shuttle-attached experiment, scaling and man-rating may be required. The environment is quite good--zero gravity, vacuum, thermal cycling, but the dynamics are not truly free due to shuttle attachment. A free-flyer test sends a very close copy of the intended system into space. As expected, the cost is quite high and the experiment/test must provide its own power, computation, navigation, and communication. The obvious advantage is the truly free dynamics in an identical operational environment. Space Station based testing is similar to Shuttle testing in that the dynamics are slightly constrained, some human modifications may be possible, and human safety factors are of concern.

TYPE OF TEST	ADVANTAGES	DISADVANTAGES
FULL-SCALE GROUND	• UNCONSTRAINED POWER, DATA PROCESSING • QUICK MODIFICATIONS POSSIBLE	• ZERO-G SUSPENSIONS DIFFICULT • ZERO ATMOSPHERE LIMITED BY TANK
REDUCED-SCALE GROUND	• AS IN FULL SCALE, BUT EASIER REQUIREMENTS ON ZERO-G SUSPENSIONS AND VACUUM TANKS • MUCH CHEAPER THAN FULL SCALE	• SCALE EFFECT PHENOMENA: JOINTS, DAMPING • NEEDS REDUCED-SCALE ACTUATORS, SENSORS IF SCALE FACTOR TOO LARGE
ANALYTICAL/ COMPUTATIONAL	• STRONG COST ADVANTAGE • OPPORTUNITY TO EXPLORE PARAMETERS	• LIMITED TO PHENOMENOLOGIES FULLY OBSERVED, UNDERSTOOD AND MODELABLE
SHUTTLE-ATTACHED EXPERIMENT	• MANNED PRESENCE IN SPACE EXPERIMENT - LIMITED MODIFICATIONS • ZERO G, ZERO ATMOSPHERE BUT WITH SOME LIMITATIONS • SOME LIMITED CONSTRUCTION POSSIBLE	• SCALE MUST BE APPROPRIATE TO SHUTTLE PERFORMANCE • ALL COMPONENTS MUST BE MAN-RATED • EXPENSIVE • LIMITED POWER, PROCESSING • NOT TRULY FREE DYNAMICS • ENVIRONMENT MILDLY CONTAMINATED
FREE-FLYER TEST	• TRULY FREE DYNAMICS • COMPONENTS NEED NOT BE MAN-RATED • SCALE - SHOULD BE LAUNCHABLE	• REQUIRES OWN POWER, COMPUTATION, NAVIGATION AND COMMUNICATION
SPACE-STATION BASED TESTING	• TEST ARTICLE LESS OF LIMITATION • MANNED PRESENCE--MANY MODIFICATIONS • LARGE POWER, COMPUTATION • POSSIBLY CHEAPER THAN SHUTTLE OR FREE-FLYER • LONG-TERM TESTS POSSIBLE • MORE CONSTRUCTION POSSIBLE	• SAFETY MAY LIMIT SOME TESTS • DYNAMICS STILL CONSTRAINED

FULL-SCALE SYSTEMS TESTING - OPTICS

Full-scale ground testing for prelaunch verification of large optical systems may be limited by existing cryovac facilities. For a complete demonstration of pointing accuracy and stability, thermal and atmospheric control is required. This limits the testable size to 5 - 10 meters. Gravity off-loading is not a major concern for these relatively stiff structures. For some system validation, scaled and component testing may prove adequate. Wavefront and pointing control may be validated through scaled subsystem testing. Isolation control may be limited to a planar demonstration in the earth environment.

LARGE OPTICS

- 5 TO 10 M WITHIN CURRENT CRYOVAC CAPABILITIES
- NATURAL FREQUENCY > 10 HZ
  - STIFF STRUCTURE, LITTLE OR NO SUSPENSION NEEDED
- CLOSED-LOOP PERFORMANCE
  - GRAVITY LOADS ON ACTUATORS ARE SIGNIFICANT - SOME RELIEF MUST BE INSTALLED
- CONTROL REQUIREMENTS
  - WAVEFRONT CONTROL - SUBSYSTEM SCALED TEST
  - POINTING CONTROL - SUBSYSTEM SCALED TEST
  - ISOLATION CONTROL - 2-D ONLY
  - VIBRATION CONTROL - FULL SCALE ONLY

FULL-SCALE SYSTEMS TESTING - ANTENNAS

Full-scale, full-fidelity ground testing of the very large antenna systems proves to be difficult, if not impossible. The 50 - 200 meter diameter systems exceed existing and proposed facilities and will require suspension systems to off-load gravity effects. Careful analysis must be conducted to avoid interaction between the suspension and structural modes. Control verification most likely will have to be conducted on scaled models.

LARGE ANTENNAS

- 50 TO 200 M EXCEEDS EXISTING AND PROPOSED FACILITIES
- NATURAL FREQUENCIES << 1 HZ
  - FLEXIBLE STRUCTURE, SUPPORT IN 1-G NEEDED, SUSPENSION WILL INTERACT WITH MODES
  - FLEXIBLE NON-LINEAR JOINTS MUST BE TESTED
- CONTROL REQUIREMENTS
  - SURFACE CONTROL - STATIC POSSIBLE, DYNAMIC DIFFICULT
  - ATTITUDE CONTROL - NOT TESTABLE AT FULL SCALE

SCALING CONSIDERATIONS

Dynamics problems have three independent dimensional variables--length, mass, and time. If one chooses to reproduce the prototype at a reduced model scale but with the actual prototype materials, these three independent scale factors have already been determined. Obviously, if the same materials are utilized, the elastic modulus of the model, E_m, must equal the elastic modulus of the prototype, E_p. Therefore, the scaling factor F_E must be 1. Likewise, the specific mass of the model, G_M, is equal to that of the prototype, G_p, and scaling factor F_M must be 1.

Since these variables represent three independent relationships involving all dimensional variables, no other choices are possible and scaling is reduced to one scale factor, F_L. This form of scaling--replica scaling--preserves much of the behaviors that are unscaleable, such as strain, damping ratio, and angular motion.

- DYNAMICS PROBLEM HAS 3 INDEPENDENT DIMENSIONAL VARIABLES
  - LENGTH, MASS, TIME
- BY SCALING LAWS (BUCKINGHAM π ,ETC) CAN CHOOSE 3 DIMENSIONALLY INDEPENDENT RELATIONSHIPS BETWEEN THEM
- IN PRACTICE, ONE IS LIMITED BY REAL MATERIALS AND NEEDS TO REPRODUCE NONDIMENSIONAL VARIABLES SUCH AS
  - STRAIN, DAMPING RATIO, ANGULAR MOTION
- INVARIABLY ONE IS THUS LED TO REPRODUCE THE PROTOTYPE AT REDUCED MODEL SCALE BUT WITH PROTOTYPE MATERIALS
  - LENGTH $R_M = F_L \times R_P$ (DIMENSION L)
  - ELASTIC MODULUS $E_M = F_E E_P$ (DIMENSION $ML^{-1}T^{-2}$) $F_E = 1$
  - SPECIFIC MASS $G_M = F_M G_P$ (DIMENSION ML^{-3}) $F_M = 1$
- SINCE THESE REPRESENT 3 INDEPENDENT RELATIONSHIPS INVOLVING ALL DIMENSIONAL VARIABLES, NO FURTHER CHOICES ARE POSSIBLE

SCALING CONSIDERATIONS (CONT.)

Once the scale factor is chosen, other replica scale factors may be determined from nondimensional equations of motion. These additional scaling laws are listed in the figure below.

- THUS SIZE RATIO (F_L) IS THE ONLY VARIABLE LEFT. HENCE BY INSPECTION

$\text{LENGTH}_M = F_L \times \text{LENGTH}_P$ $\qquad$ $\text{ELASTIC MOD}_M = 1 \times \text{ELASTIC MOD}_P$

$\text{DISPLACEMENT}_M = F_L \times \text{DISP}_P$ $\qquad$ $\text{STRESSES}_M = 1 \times \text{STRESSES}_P$

$\text{SPEC MASS}_M = 1 \times \text{SPEC MASS}_P$

$\text{MASS}_M = F_L^3 \times \text{MASS}_P$

- CAN FURTHER DERIVE

$\text{TIME}_M = F_L \times \text{TIME}_P$ $\qquad$ $\text{FREQ}_M = F_L^{-1} \times \text{FREQ}_P$

$\text{VELOCITY}_M = 1 \times \text{VELOCITY}_P$ $\qquad$ $\text{ACCEL}_M = F_L^{-1} \times \text{ACCEL}_P$

$\text{FORCE}_M = F_L^2 \times \text{FORCE}_P$ $\qquad$ $\text{TORQUE}_M = F_L^3 \times \text{TORQUE}_P$

$\text{AREA}_M = F_L^2 \times \text{AREA}_P$ $\qquad$ $\text{INERTIA}_M = F_L^5 \times \text{INERTIA}_P$

$\text{VOLUME}_M = F_L^3 \times \text{VOLUME}_P$

SCALING CONSIDERATIONS (CONT.)

From the scaling laws on the previous page, it is shown that frequencies shift proportionally with the scale factor. Joint stiffness, damping, and tolerances require precise modeling, and the actual damping phenomenology may change at reduced scales. Decreasing fabrication tolerances with scale may result in unrealizable miniaturization.

Several controls issues arise with model scaling. The system bandwidth increases with scale, and other relationships such as force imply that the scale model may require different sensors and actuators from those of the prototype. This may also introduce new uncertainties in noise, quantization, and device dynamics.

Multibody dynamic interaction and scaling present unique problems. Since rigid-body and elastic phenomena will be present to interact nonlinearly, and control devices will need to be included, a truly scaled multibody test is somewhat difficult. The important contribution of multibody ground testing, when it can be arranged, is to verify the validity of analytical tools which then can be used to predict on-orbit behavior.

- STRUCTURAL BEHAVIOR
  - FREQUENCIES SHIFTED PROPORTIONALLY TO LENGTH SCALE
  - JOINT CHARACTERISTICS (STIFFNESS, DAMPING, NONLINEARITY) REQUIRE PRECISE MODELING
  - DAMPING PHENOMENOLOGIES MAY CHANGE
    E.G. FORCE SCALING FOR COULOMB, STRAIN RATE/FREQUENCY FOR VISCOELASTIC
  - USEFUL DATA POSSIBLE WITH CARE EXERCISED

- CONTROLS TESTING
  - SYSTEM BANDWIDTH INCREASED WITH SCALING
  - SENSOR, ACTUATOR : RANGE AND RESOLUTION TIGHTENED WITH SCALE
  - QUANTIZATION, NOISE, CONTROL DEVICE DYNAMICS REQUIRE SCALING AS WELL

- MULTIBODY TESTING
  - IF STRICTLY SCALED THEN OUT OF THE QUESTION
    - CONFLICTING SCALING LAWS ON FORCE, TORQUE, MASS, INERTIA, VELOCITY, ETC.
  - POSSIBILITY EXISTS IF WILLING TO DISTORT CERTAIN VARIABLES
    - VERIFICATION THEN ONLY OF ANALYTICAL TOOLS

ACTUAL SUSPENSION ISSUES

All of the large antenna systems and many of the platform systems will require some type of support system to off-load 1-g effects. An ideal suspension system would eliminate the gravity-induced stresses in a test article. In addition, it would support the model in a way that permits rigid body motion by 1) simulating free-free boundary conditions, 2) allowing unrestrained motion in all six degrees of freedom, 3) adding no weight to the model or changing the modal mass, and 4) creating no dynamic structural interaction with the test specimen.

Actual suspensions fall into two broad categories: 1) stiff, rigid cables and 2) flexible, soft cords. Stiff cables permit small rigid-body motion in the plane parallel to the floor only. Vertical motion is restrained by the cable stiffness. Pendulum and string modes may be present and can couple or interact to cause additional vibration. Flexible, soft cables permit large motion and therefore become quickly limited by the size of the test facility [Hanks, 1985; Hanks and Pinson, 1983; Venneri, Hanks, and Pinson].

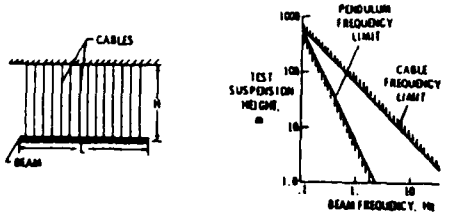

PENDULUM SUSPENSION IN A GRAVITY ENVIRONMENT

- STIFF CABLES PERMIT SMALL RIGID-BODY MOTIONS IN THE PLANE PARALLEL TO THE FLOOR ONLY.
- CABLE STIFFNESS RESTRAINS VERTICAL MOTION.
- PENDULUM MODES MAY BE PRESENT AND CAN COUPLE WITH SYSTEM MODES.
- STRING MODES MAY CAUSE CABLE VIBRATION.
- FLEXIBLE CABLES QUICKLY BECOME FACILITY LIMITED BY DEFLECTIONS.

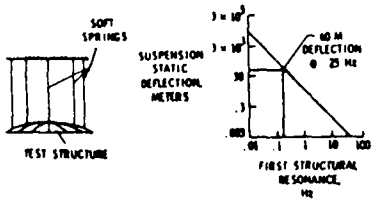

SOFT SUSPENSION IN A GRAVITY ENVIRONMENT

FREQUENCY VS. CABLE STRAINS - FULL AND QUARTER SCALES

A first-order, lumped-mass model analysis for a suspension system was conducted. The equation for the ratio of the lowest system structural frequency to the lowest structural frequency of the cable plunge mode was derived. In order to ensure no interaction between the structure and suspension, this ratio should be 5 or greater. By setting the ratio equal to 5 and assuming available cable length, the limiting system frequency as a function of cable strain was calculated and plotted.

The low frequency of the antenna systems falls below all curves, and this class will not be able to utilize soft suspensions. Model/suspension interaction will be a problem if fundamental structural frequencies drop below 1 - 5 Hz. Clearly some missions can be tested this way, and others not.

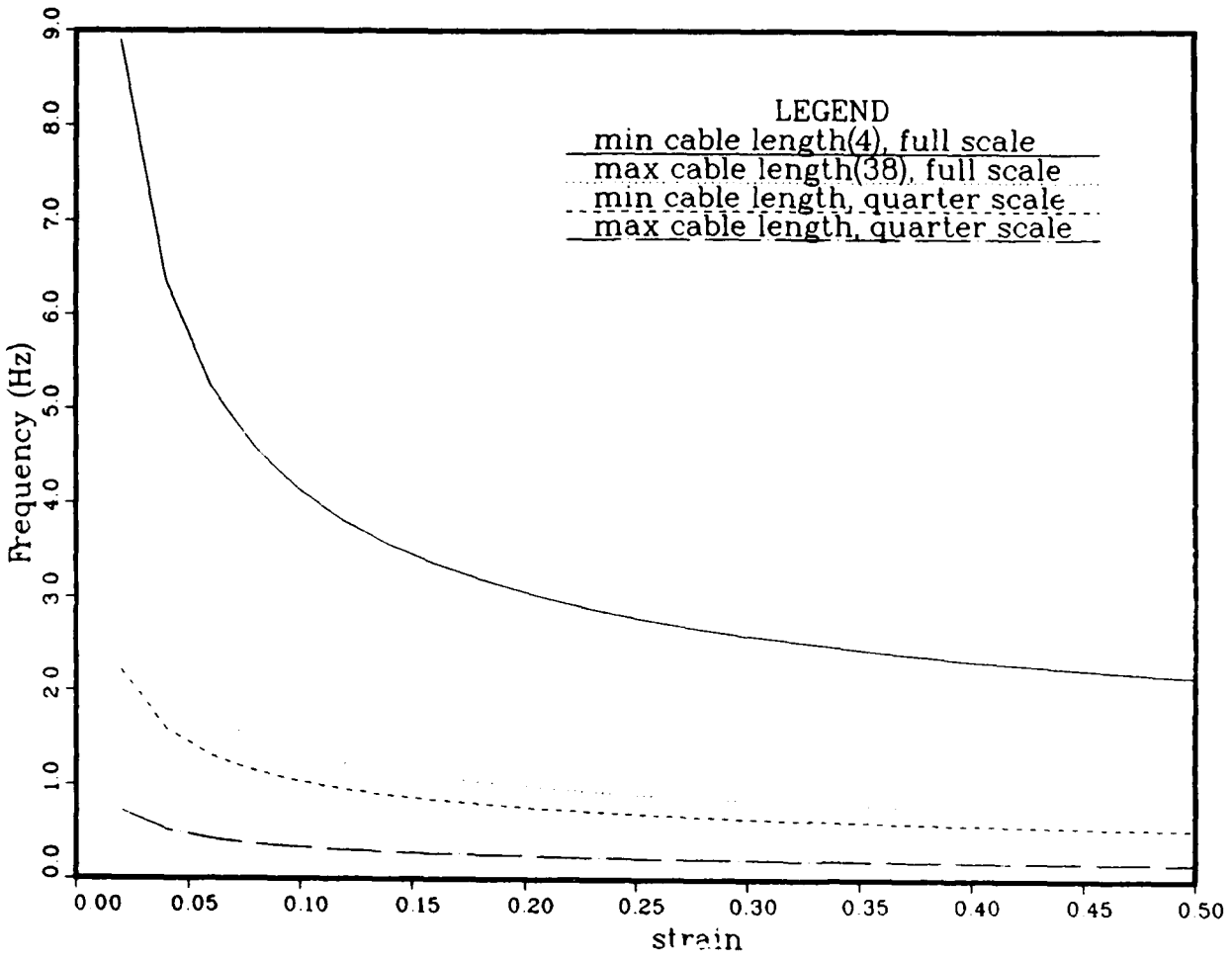

15-METER HOOP/COLUMN ANTENNA

Some recent experience has been gained from studies of the NASA/LaRC-Harris 15-meter hoop/column antenna. This structure is intended to eventually be flown. As a representative antenna structure, the hoop/column is relatively large, extremely flexible and lightweight, and the structural dynamics are dominated by the joints. Dynamic tests were performed both in air and vacuum to assess the effects of atmospheric damping.

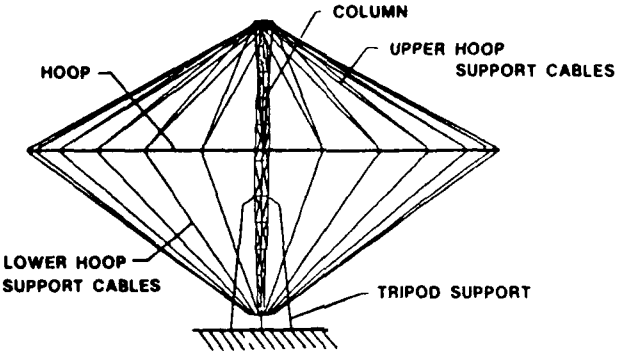

- DEPLOYMENT AND TESTING OF A REPRESENTATIVE JOINT-DOMINATED, LARGE, FLEXIBLE, LIGHTWEIGHT SPACE STRUCTURE
- STATIC AND DYNAMIC TESTING WAS PERFORMED TO VALIDATE THE STRUCTURAL MODELS, MEASURE DAMPING, AND EVALUATE THE IMPACT OF TESTING IN AIR

15-METER HOOP/COLUMN OBSERVATIONS

Some important discrepancies were found between the analytical model and the test results. Differences were attributed to unmodeled phenomena, especially joint characteristics. A further analysis was conducted incorporating test data to modify stiffness. With this test-in-the-loop analysis, correlation between analysis and test was quite good. However, this implies that without structural testing, good dynamics predictions are difficult to obtain.

- EXPERIMENTERS CONCLUDED THAT JOINT UNMODELLED CHARACTERISTICS CAUSED SIGNIFICANT DIFFERENCES BETWEEN ANALYSIS AND TEST
- "REFINED ANALYSIS" USED STATIC TEST DATA TO MODIFY STIFFNESS TO MATCH TEST RESULTS; GOOD CORRELATION RESULTED
- AIR DAMPING WAS NOT FOUND SIGNIFICANT

CONCERN

- STATIC GROUND TESTS BECOMING PART OF DYNAMIC MODELLING
- IS THIS A FORWARD OR BACKWARD STEP FOR ZERO-G DYNAMIC PREDICTION?

SUMMARY AND CONCLUSIONS

Several SDI and NASA missions have similar requirements and specifications. Both agencies anticipate missions in the three categories described--optics, antennas, and platforms. Since both groups share interests in technology development and verification goals, joint programs could reduce costs and shorten schedules.

Ground testing will continue to be the main process to ensure mission success. In most cases, flight tests are prohibitively expensive and pure simulation is not regarded as proof of success.

Several issues need to be addressed and resolved for each main class of future space systems. The earth environment, existing test facilities, and test setup interactions all affect ground testing confidence. Further detailed study is required to fully ensure successful transition from ground test to mission operation of future large, lightweight, flexible spacecraft.

- SDI AND NASA MISSIONS GREATLY RESEMBLE EACH OTHER
- GROUND TESTING WILL REMAIN PRIMARY METHOD OF ENSURING SUCCESS
  - SIMULATION NOT ACCEPTED IN PLACE OF TESTING
  - FLIGHT TESTING TOO EXPENSIVE FOR MOST SYSTEMS
- EARTH ENVIRONMENT AND FACILITIES LIMIT BEHAVIOR PREDICTION
  - ANTENNA CLASS MOST SENSITIVE TO GRAVITY, ATMOSPHERE, THERMAL CYCLING
- TEST MODELS SIZE LIMITED BY EXISTING FACILITIES
  - SCALING REQUIRED FOR ANTENNAS AND PLATFORMS
- SUSPENSION SYSTEMS MAY ADD SIGNIFICANT DYNAMICS TO MODEL
  - LOW-FREQUENCY ANTENNAS MOST AFFECTED

REPORT ON SDIO/NASA MULTIBODY SIMULATION WORKSHOP

R. A. Laskin and G. K. Man
Jet Propulsion Laboratory
California Institute of Technology
Pasadena, California

A group of 140+ international scientists and engineers representing five countries convened at the Embassy Suites Hotel in Arcadia, California, 1-3 September 1987, for a three-day intensive workshop on Multibody Simulation. Jet Propulsion Lab hosted the meeting under joint SDIO/NASA sponsorship.

The workshop devoted sessions to applications, formulation methods, existing codes, model reduction and validation, and computational methods and architecture. A substantial amount of time was also set aside for open discussion and these discussion periods were rich in ideas and information exchange. For many they constituted the highlight of the workshop.

Prior to the workshop a Steering Committee, chaired by Dr. Peter Likins, President of Lehigh University, was selected and charged with focussing workshop technical discussions, establishing community consensus where possible, and issuing a recommended course of action for on-going activity in the field. The salient recommendation was for the institution of a national code evaluation program to compare current and future NASA and DOD space mission requirements to existing simulation capability. The most promising technical paths for improving upon the current state-of-the-art were also identified and highlighted.

SUMMARY

- **WORKSHOP HELD SEPTEMBER 1-3 IN ARCADIA, CALIFORNIA**
  - 140+ ATTENDEES FROM FIVE COUNTRIES
  - HOSTED BY JPL
  - SPONSORED BY SDIO AND NASA
- **SESSIONS**
  - APPLICATIONS
  - FORMULATION METHODS
  - EXISTING CODES
  - MODEL REDUCTION AND VALIDATION
  - COMPUTATIONAL METHODS AND ARCHITECTURE
- **PRINCIPAL STEERING COMMITTEE RECOMMENDATION:**
  - INSTITUTE A NATIONAL CODE EVALUATION PROGRAM TO COMPARE CURRENT AND FUTURE NASA/DOD SPACE MISSION REQUIREMENTS TO EXISTING SIMULATION CAPABILITY

WORKSHOP OBJECTIVES

The workshop had three primary objectives: (1) provide a window into current SDIO and NASA multibody simulation research and development by allowing prominent researchers in the multibody simulation field to exchange ideas on the correctness, efficiency, and usability of current multibody codes; (2) identify important issues and unsolved problems of current interest which can be dealt with by possible future SDIO/NASA/Industry/University combined efforts; (3) recommend actions that should be undertaken (if any) to verify current capabilities and to extend the state-of-the-art.

WORKSHOP OBJECTIVES

- **EXCHANGE INFORMATION**
  - **STATUS OF SDIO/NASA APPLICATIONS**
  - **STATUS OF MULTIBODY RESEARCH AND DEVELOPMENT**
- **ESTABLISH COMMUNITY CONSENSUS ON IMPORTANT UNSOLVED PROBLEMS**
- **ISSUE RECOMMENDED COURSE OF ACTION**

MULTIBODY SIMULATION APPLICATIONS

Galileo is an example of a NASA spacecraft for which multibody simulation programs have been used. DISCOS was used extensively to verify the scan platform pointing control design. DISCOS was chosen because of its ability to simulate the dynamics of interconnected flexible bodies. This was a necessity for Galileo due to the flexibility of a number of spacecraft sub-bodies.

The Space Relay Experiment spacecraft represents a design concept for use in an SDIO laser beam relay proof-of-concept experiment. With two independently articulated two degree of freedom gimbals, each supporting a magnetically suspended mirror, there is an obvious need for multibody simulation capability for control design and verification.

Robotics, manipulators, and mechanisms represents another area of application for multibody programs. The figure depicts a teleoperated grappling application that would be extremely challenging to simulate since it not only involves multiple flexible bodies but also time varying dynamic constraints that change as the workpiece is grappled and released.

MULTIBODY SIMULATION APPLICATIONS

- **NASA SPACECRAFT**

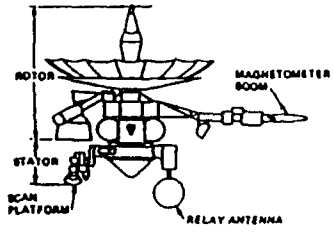

- **SDIO SPACECRAFT**

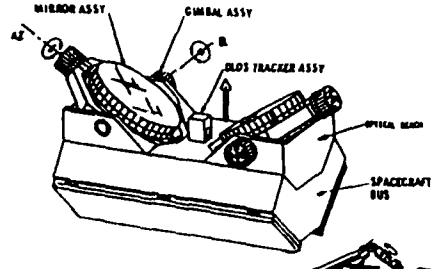

- **ROBOTICS, MANIPULATORS AND MECHANISMS**

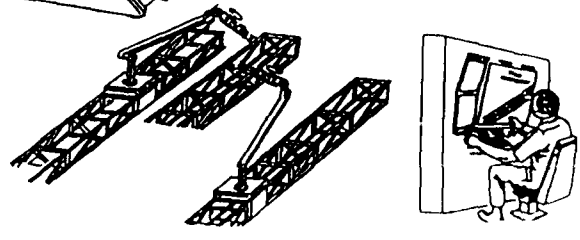

One of the sessions at the workshop was devoted to formulation methods. Topics covered included: methods for handling nonlinear geometric effects such as spin induced structural stiffening; continuum methods vs discrete methods; flexible body dynamics for control design (as opposed to control verification); deployment dynamics; and equation formulation for computation. The topic of geometric nonlinearities, in particular, generated varying points of view and would seem to represent a fertile area for future research. It was not clear, however, the degree of practical importance that ought to be attached to this subject.

Another session was devoted exclusively to multibody simulation codes that currently exist and are in use, either in the public domain or on a proprietary basis in industry. Presenters were asked to concentrate not on the theoretical foundations of the codes but on user issues such as runtime, portability, interfaceability, support, types of problems handled, user interface, and so forth. Presentations were given on the following programs: DISCOS, CONTOPS, ADAMS, DADS, SADACS, DYNACON, MEDYNA, SD/EXACT and SD/FAST, LATDYN, AUTOLEV, and DART.

WORKSHOP TOPICS

FORMULATION METHODS

- METHODS FOR HANDLING SPIN STIFFENING EFFECTS
- CONTINUUM METHODS
- FLEXIBLE BODY DYNAMICS FOR CONTROLS DESIGN
- DEPLOYMENT DYNAMICS
- EQUATION FORMULATION FOR COMPUTATION

EXISTING CODES

- DISCOS, CONTOPS, ADAMS, LATDYN, MEDYNA....

Model reduction and code validation were the subjects of another session. Much of the model reduction discussion centered around the distinction between system model reduction and component model reduction. The former addresses the situation where a system level structural model is available and only small displacements, both elastic and articulation, are anticipated. There are several approaches that exist for addressing this class of essentially linear problem, although further work is certainly warranted. By far the lesser explored problem is that of component model reduction which comes into play when a structural system consists of several flexible components, each of which can be articulated through large angles relative to the others. The question arises: how to reduce the model order of each component body for input into a multibody code such that the overall system will retain its proper modal characteristics in every possible system configuration. Experimental facilities capable of doing validation experiments of mutibody codes were also discussed. Two facilities, one at Marshall Space Flight Center and the other at the University of Toronto, were identified as having the capability of carrying out such work.

The workshop's final session was devoted to computational methods and architecture. Topics covered included: symbolic manipulation, parallel processing, high speed algorithms, user interface, data handling, and numerical considerations.

WORKSHOP TOPICS Cont.

MODEL REDUCTION AND VALIDATION

- SYSTEM AND COMPONENT MODEL ORDER REDUCTION
- VERIFICATION/VALIDATION- APPROACHES AND FACILITIES

COMPUTATIONAL METHODS AND ARCHITECTURE

- SYMBOLIC MANIPULATION
- PARALLEL PROCESSING
- ORDER N ALGORITHMS
- COMPUTATIONAL ASPECTS
- USER INTERFACE
- DATA HANDLING

PRELIMINARY STEERING COMMITTEE RECOMMENDATIONS

The recommendations are preliminary in that the workshop final report is still under review by the members of the steering committee. Nevertheless, the overriding concern identified at the workshop was that the realm of applicability of existing codes has never been properly established. To remedy this situation the steering committee will recommend that a national technology assessment program for multibody simulation codes be undertaken. Such an endeavor should start with a careful definition of the mission and simulation requirements that flow from the target SDIO/NASA mission set. A set of test problems, both mathematical and experimental, that spans the requirements space should then be developed and these tests should be executed and evaluated. The mathematical models developed for exercising the simulation codes should include both simple and complex cases. Experimental work should include both ground and flight tests. At the end of the effort a final report documenting multibody simulation technology readiness should be prepared and disseminated. Jet Propulsion Lab was chosen to lead the planning and coordination of this national effort.

PRELIMINARY

STEERING COMMITTEE RECOMMENDATION

CONCERN

- THE REALM OF APPLICABILITY HAS NOT BEEN ESTABLISHED FOR CURRENT TOOLS

OPPORTUNITIES

- INSTITUTE A NATIONAL TECHNOLOGY ASSESSMENT PROGRAM FOR MULTIBODY SIMULATION CODES
  - REQUIREMENT DEFINITIONS- MISSION AND SIMULATION
  - TEST DESIGN
    - SIMPLE AND COMPLEX MATHEMATICAL MODELS
    - GROUND EXPERIMENTS
    - FLIGHT EXPERIMENTS
  - TEST EXECUTIONS AND EVALUATION
- JPL WILL LEAD THE PLANNING AND COORDINATION OF THIS EFFORT

A workshop consensus also developed around another pervasive concern, namely that current tools represent a limiting factor in today's control design and verification process and are likely to be wholly inadequate for future needs. However, several very promising research areas are maturing rapidly, each one of which has the potential to offer order of magnitude improvement in simulation runtime. These areas are component model order reduction and synthesis, recursive algorithms, concurrent processing, and symbolic manipulation. In concert these techniques might well enable real time simulation of complex, flexible, multibody systems. The advent of this capability would greatly enhance engineering productivity. It would also enable man-in-the-loop simulations and thereby potentially revolutionize the development of telerobotic and related systems.

TECHNOLOGY DEVELOPMENT OPPORTUNITIES

CONCERN

- CURRENT TOOLS ARE A LIMITING FACTOR IN TODAY'S CONTROL DESIGN ANALYSIS, AND ARE INADEQUATE FOR FUTURE NEEDS

OPPORTUNITIES

- SEVERAL TECHNOLOGY DEVELOPMENT AREAS OFFER ORDER OF MAGNITUDE *RUNTIME IMPROVEMENT*
  - COMPONENT MODEL ORDER REDUCTION
  - RECURSIVE ALGORITHMS
  - CONCURRENT PROCESSING
  - SYMBOLIC MANIPULATION
- IN CONCERT THESE TECHNIQUES WOULD ENABLE REAL TIME SIMULATION OF COMPLEX, FLEXIBLE, MULTIBODY SYSTEMS

ACKNOWLEDGMENT

The research described in this paper was carried out by the Jet Propulsion Laboratory, California Institute of Technology, under a contract with the National Aeronautics and Space Administration.

MAST FLIGHT SYSTEM ENGINEERING DEVELOPMENT AND SYSTEM INTEGRATION

RONALD C.TALCOTT
DR. JOHN W. SHIPLEY
THEDRO KIMBALL
SCOTT W. GREELEY

MAST FLIGHT EXPERIMENT FLIGHT SYSTEM CONCEPT

The Mast Flight System provides a research tool for space experiments which is needed to build and utilize the next generation of space structures. In so doing, it will bridge the gap between current design practice and planned large space system applications.

The Deployable Mast Subsystem (DMS) is the primary subsystem in the Mast Flight System. The other subsystems interface the DMS to effect the experiment. The DMS consists of a 60 meter joint dominated graphite epoxy and titanium deployable truss beam assembly. Integral to the beam assembly are actuators, sensors and associated electronics which provide excitation damping and performance measurements for the system. The beam structural characteristics can be varied via the Parameter Modification Device which is installed at the tip of the beam. All data including sensor outputs and actuator commands are transmitted along the beam on a standard 1553 bus. Experiments are controlled by the Modular Distributed Information Subsystem (MDIS) which functions as the bus controller. The MDIS includes two 1750A computers to provide redundant safing. Excitation and control algorithms reside in the Excitation and Damping Subsystem (EDS) computer which is available to the experimenter. The Mast interfaces the orbiter through the STEP pallet and the Mast Support system. The physical relationship of the Subsystems is shown below.

MAST FLIGHT SYSTEM CONCEPT

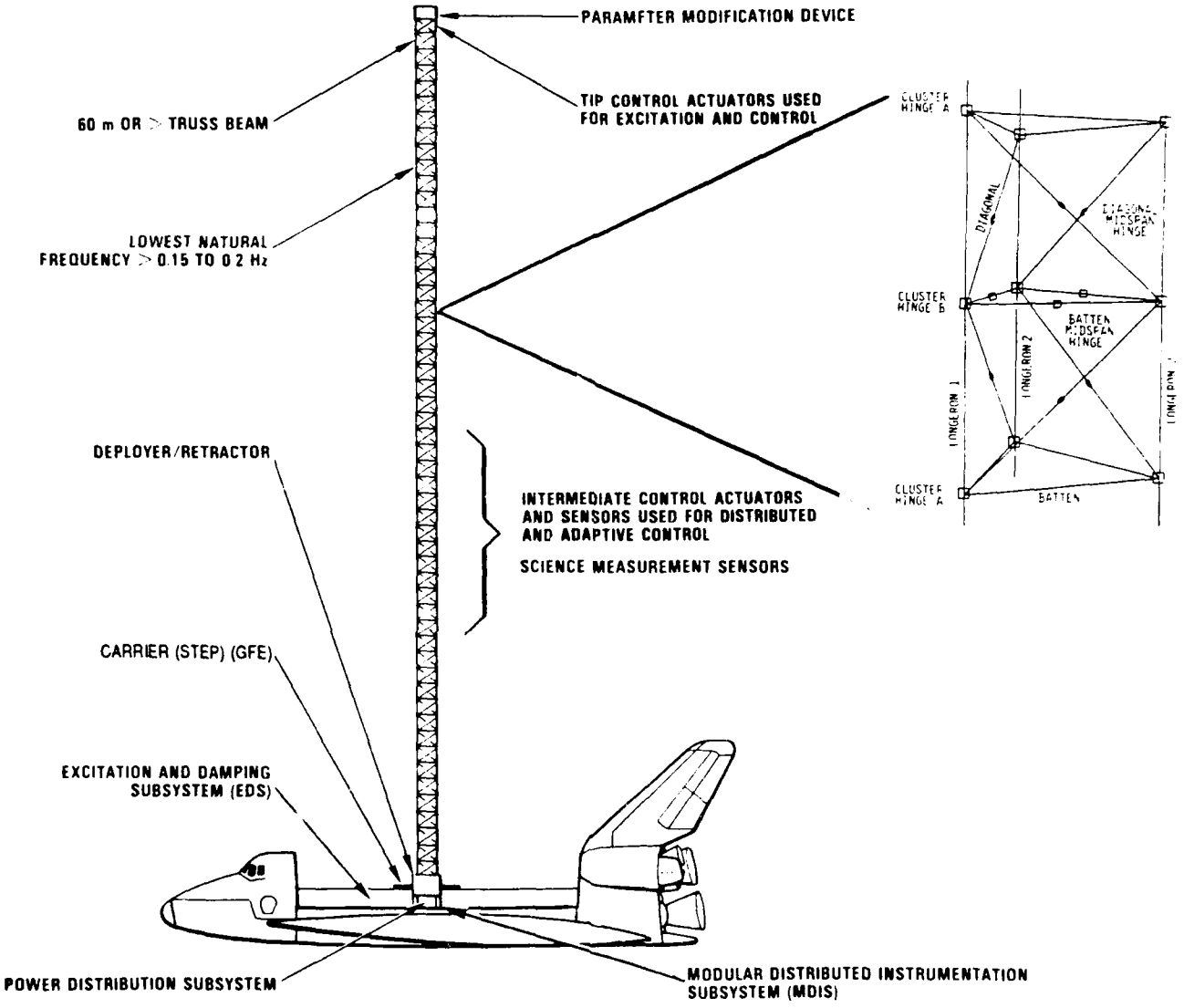

MAST FLIGHT SYSTEM BLOCK DIAGRAM

The block diagram shown below illustrates the primary elements of the system and provisions for commands and data gathering. The mission specialist interfaces the system from the orbiter aft flight deck through the DDCU. All experiment commands including beam deployment, retraction, excitation and control are executed through this interface. In addition to a baseline damping algorithm, which is to be used for checkout and for damping between experiment modes, basic commands such as sine excitation, random excitation, PMD position and experiment setup will be available for the experimenter's use.

All experimental data is passed through the HRM to the high rate link through TDRSS to the ground where it is stored for post flight analysis. A limited amount of selectable data can be reviewed on the ground in near real time.

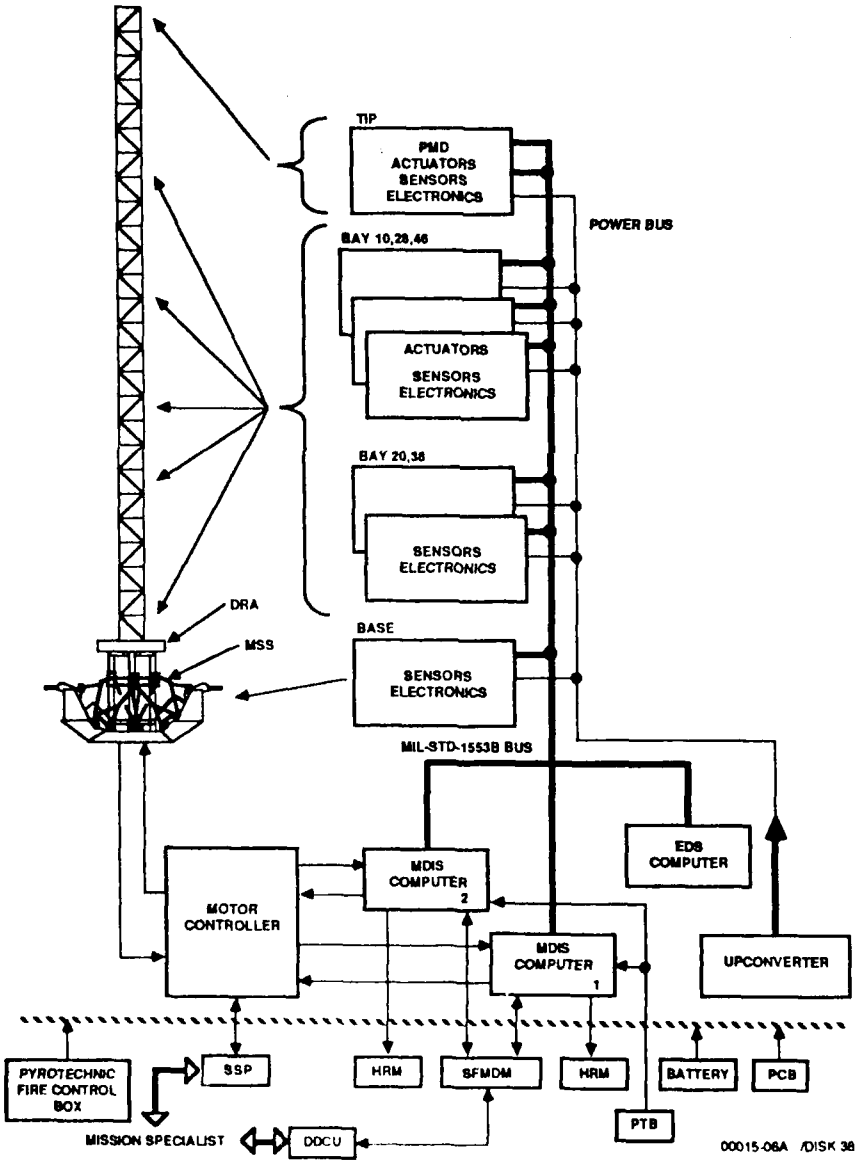

PROGRESS DURING PAST YEAR

During the past year effort has been concentrated on developing the detailed subsystem level requirements from the system level functional reqiurements and the concept of operation. Areas where significant progress has been realized included:

- Development of detailed requirements for all subsystems and components.
- Conducted a System Requirements review.
- Implementation of the Z-beam design including the Deployer/Repacker Assembly into the system baseline.
- Implementation of the mast support structure into the system baseline.
- LDCM motor compensator development including detailed analysis, characterization, simulation and test.
- Initiated development of the MDIS and EDS computers.
- Breadboard fabrication and test of the upconverter, power supply, remote interface unit and motor controller.
- Development of a detailed Craig-Bampton structural model which includes detailed models of the Orbiter, Step Pallet, Mast Support System and Deployable Mast System.
- Detailed characterization of the beam performance and simulation.

PARAMETER MODIFICATION DEVICE

Beam structural characteristics can be coarsely altered by varying the beam length. This provides the ability to approximately coalesce the first torsion and second bending mode frequencies. The parameter modification device shown below can be used to improve frequency matching by varying the moment of inertia of the tip station. Geometric coupling of torsion and bending modes can be achieved using the PMD by changing the center of gravity of the tip station.

The parameter modification device operation is shown below.

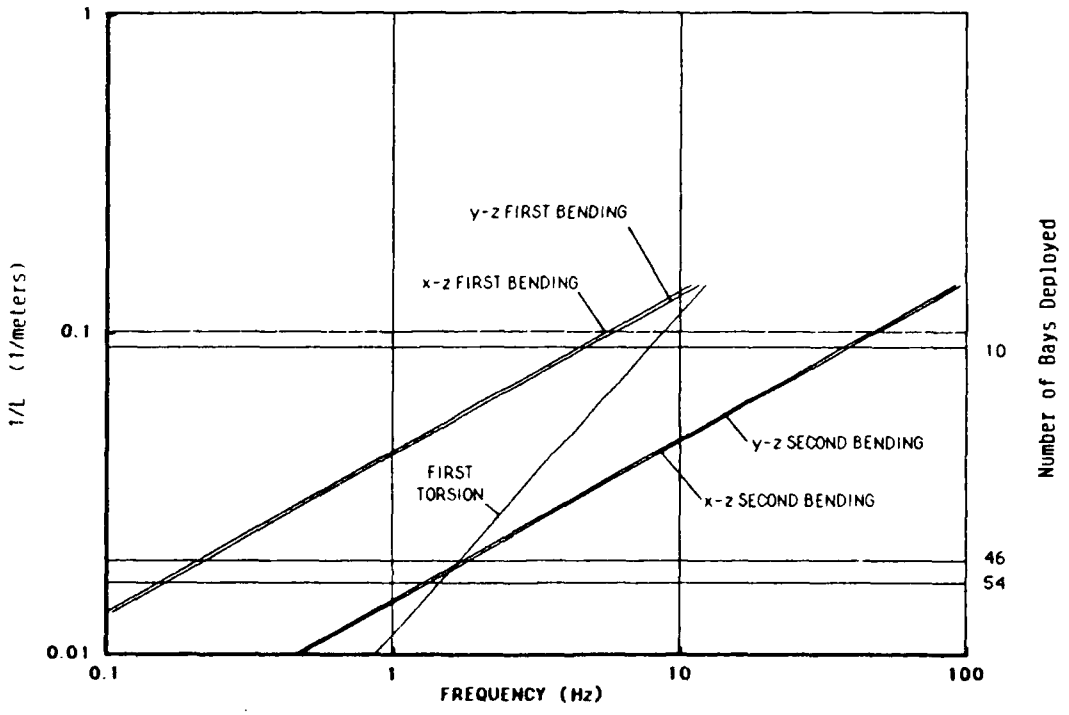

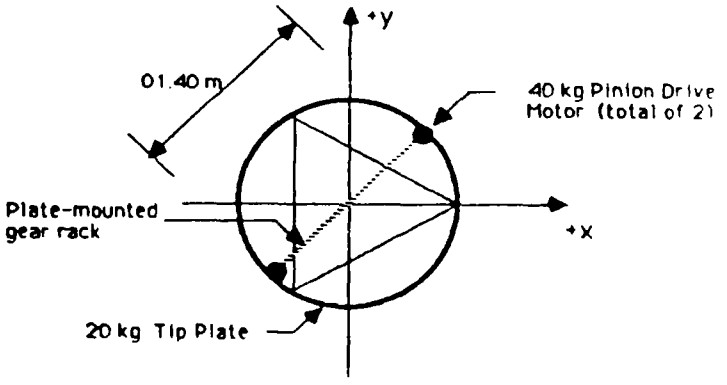

MAST-226

MAST FLIGHT SYSTEM MODAL CHARACTERISTICS

The first ten Mast Flight System modes include four y-z plane bending modes,four x-z plane bending modes and two torsion modes. Mode shapes for the y-z bending and torsion modes are shown below. The x-z bending mode shapes are the same as the y-z bending mode shapes. The data includes the effects of the orbiter and pallet; however, these elements are not shown for clarity.

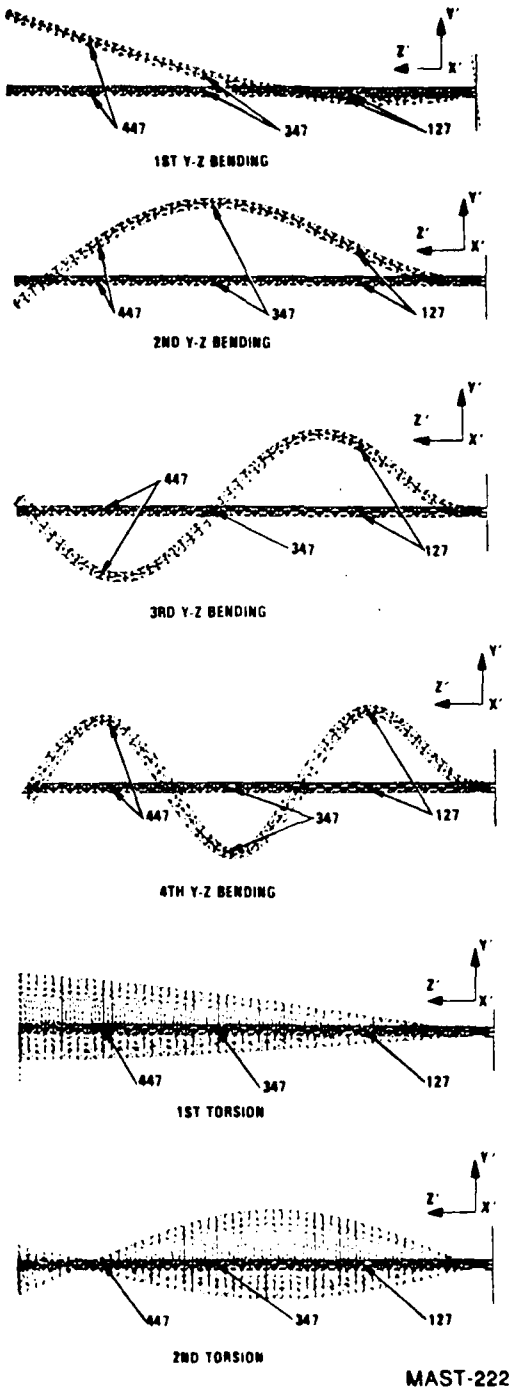

MAST-222

LINEAR DC MOTOR DESIGN

Linear DC Motors (LDCMs) are used for both primary and secondary actuators. Four type I LDCMs are used at the tip station to excite both bending and torsion (primary actuators) and a pair of LDCMs are used bay locations 10, 28 and 46 to excite bending (secondary actuators). The LDCM employs a magnetically driven reaction mass as shown below. A secondary mounted accelerometer provides feedback to improve force resolution.

LDCM TYPE I BREADBOARD MODEL

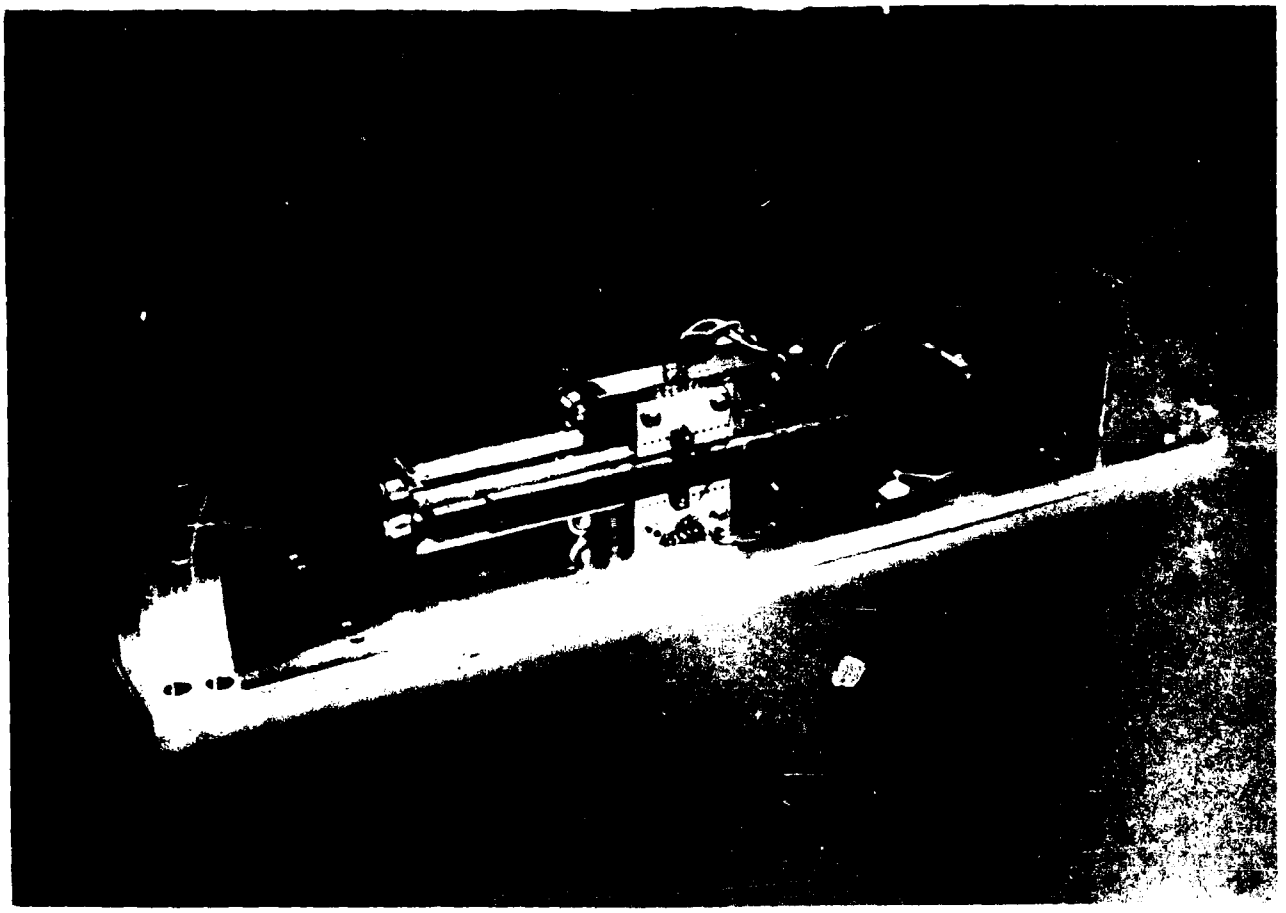

LDCM MOTOR COMPENSATION

The LDCMs are compensated to provide full access to the capabilities of the device while ensuring that they operate within their force and stroke limitations.

The compensation is designed such that the secondary relative position tracks input commands to approximately 1.0 Hz. A transition occurs at this frequency, and for frequencies above 1.0 Hz the actuator output force tracks the input command. Transfer functions for force/command, relative position/command and force/primary velocity (x ω) are shown below. (Here ω is the circular frequency.) The latter transfer function indicates the interaction between the LDCM and the beam. If the real part of this transfer function is negative the interaction is potentially destabilizing, while if it is positive, it adds damping. the objective is to keep this interaction positive but as small as possible so that little damping is added to the beam.

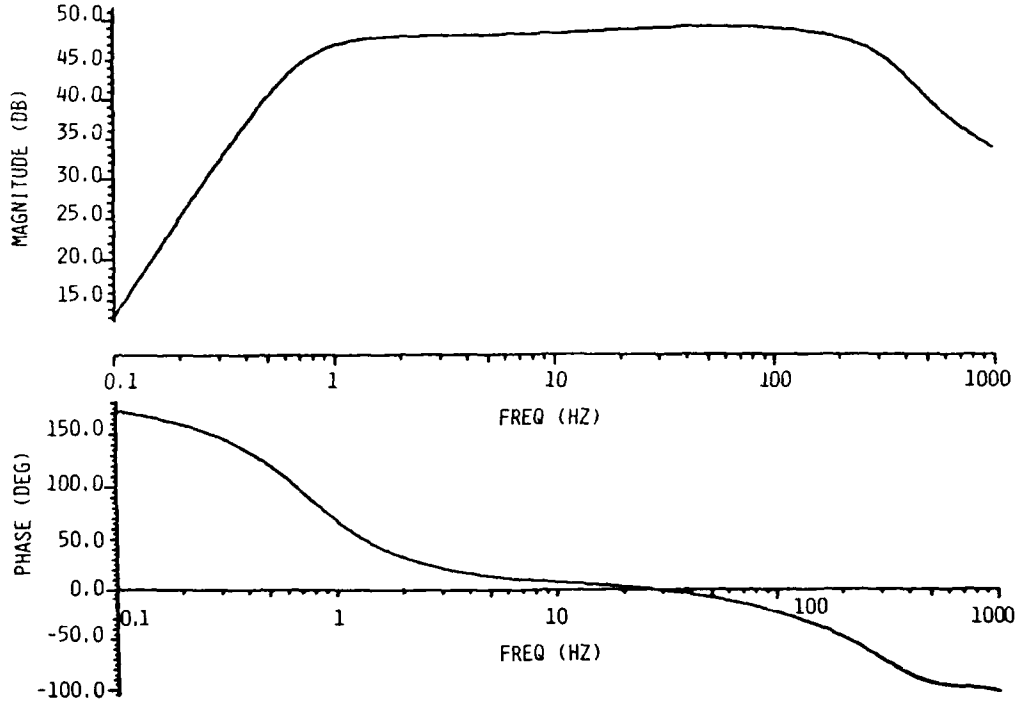

TRANSFER FUNCTION: OUTPUT FORCE/COMMAND

TYPE I LDCM TRANSFER FUNCTIONS (CONT'D)

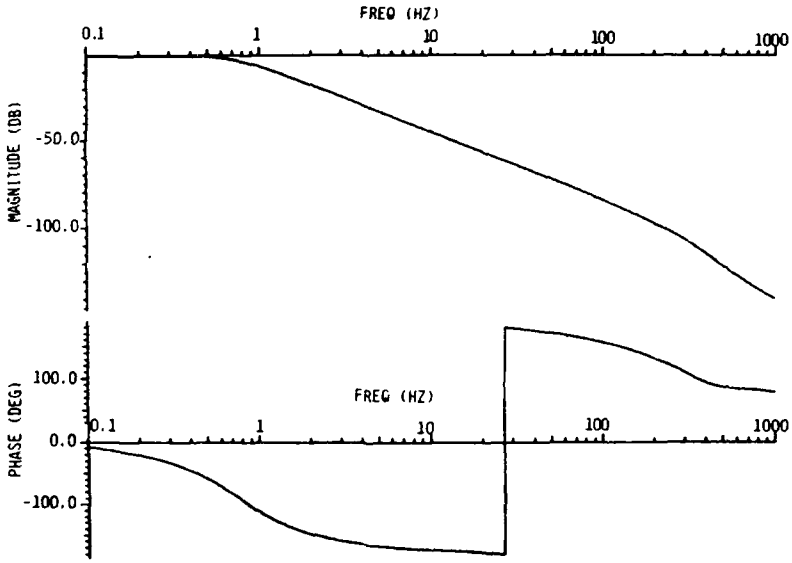

TRANSFER FUNCTION: RELATIVE DISPLACEMENT/COMMAND

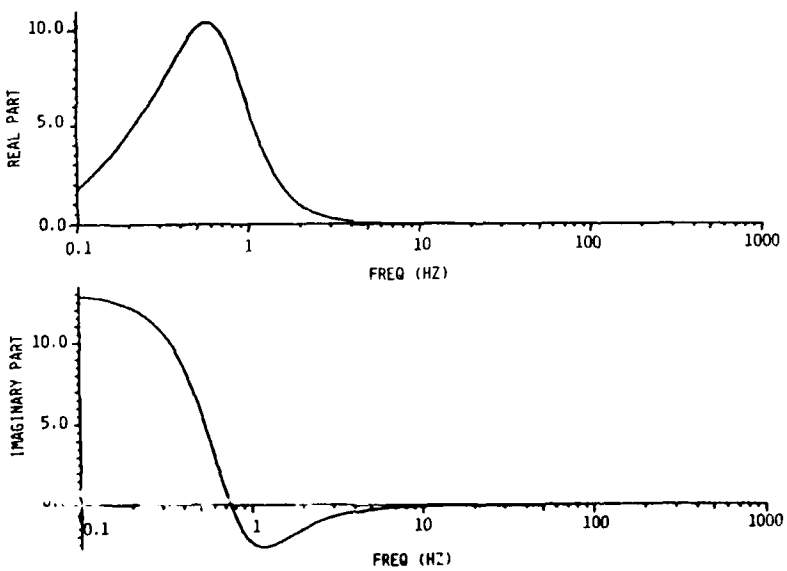

TRANSFER FUNCTION: OUTPUT FORCE/ (ω x PRIMARY VELOCITY)

LDCM PERFORMANCE

Overall specifications for both LDCM types are shown below. The user has access to relative position and secondary acceleration data at the EDS computer.

SECONDARY MASS	TYPE I TYPE II	11.0 KG 7.0 KG
BANDWIDTH	0.10 TO 150.0 HZ	
PEAK FORCE:	TYPE I	30 N
	TYPE II	15 N
STROKE : (DOUBLE AMPLITUDE)	TYPE I :	30.0 cm
	TYPE II :	14.0 cm
FORCE ERROR	rms = 0.08 N, 0.0 - 20.0 Hz	
	rms = 1.6 N, 0.0 - 200.0 Hz	
COMMAND LINEARITY	The command to displacement and command to force transfer functions shall be linear in form with a measured deviation from linearity of less than 0.5 %.	
CROSS-AXIS EXCITATION	0.0 -50.0 Hz, 0.05 % of commanded force.	
BASE MOTION INTERACTION	The LDCM shall be capable of operating without saturating in force or displacement when disturbed in the nonimal orbiter environments	
INADVERTENT DAMPING	The inadvertent damping added to the beam modes by the system of LDCM's shall be less than 1.0 % in the bending modes and less than 2.0 % in the torsional modes. In no event shall the inadvertent damping add to the beam damping in a negative manner in magnitude greater than 0.1 %.	

COMPOUND PENDULUM TEST RESULTS

To evaluate LDCM performance a test bed was developed which simulates the first two modes of the beam using a compound pendulum. Both the generalized masses and frequencies of the two pendulum modes approximate the first and second Mast modes in one plane. The response shown below indicates excitation and damping of the first pendulum mode (approximately 0.2 hz). The damping algorithm was implemented using a Harris MCX-5 computer. Details of the implementation (e.g. sample rate etc.) correspond to the Mast Flight System design.

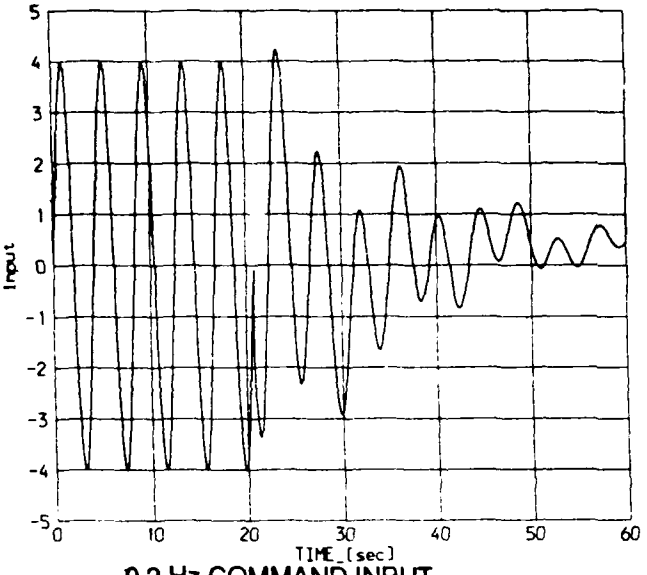

0.2 Hz COMMAND INPUT

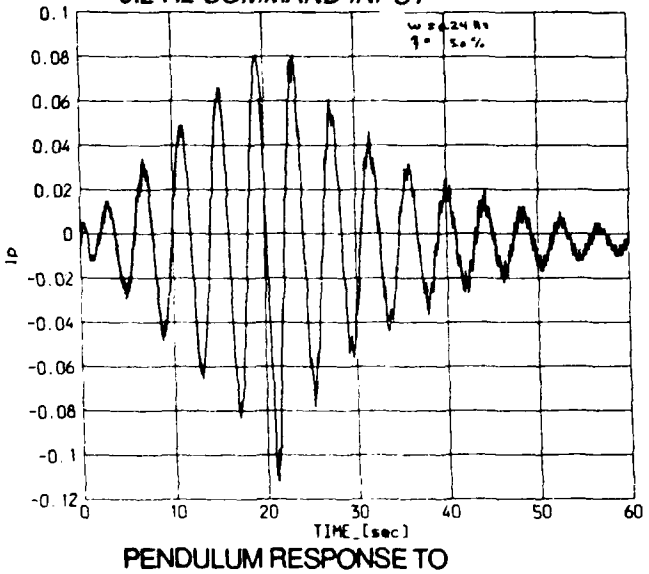

PENDULUM RESPONSE TO COMMAND DAMPING SWITCHED ON AT END OF EXCITATION

COMPOUND PENDULUM TEST SETUP

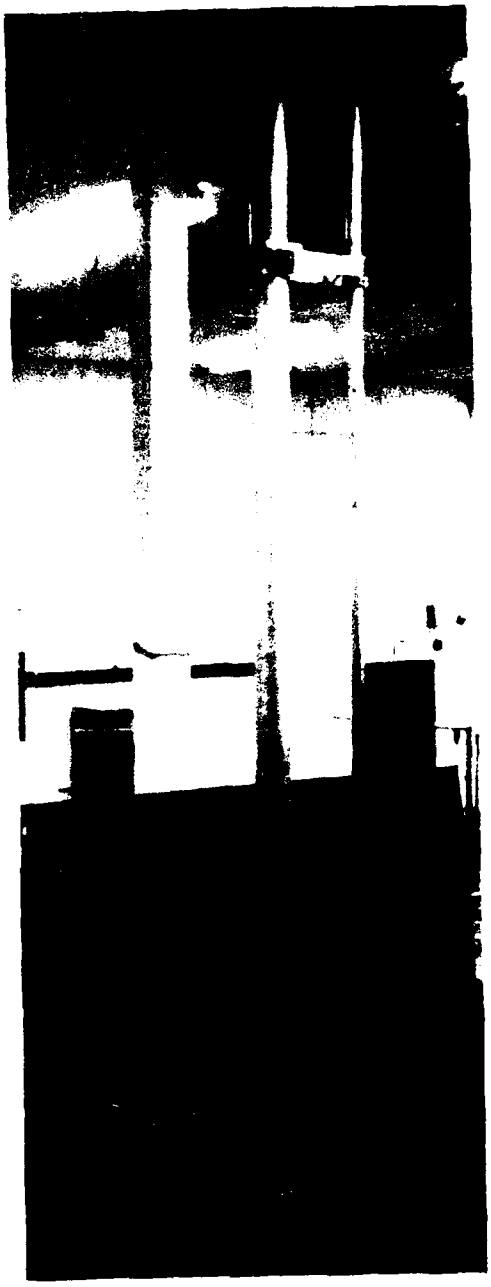

MDIS BLOCK DIAGRAM

All experimental data are controlled by the Modular Distributed Information Subsystem (MDIS) which functions as the bus controller. The MDIS includes two 1750A computers to provide redundant safing. The block diagram shown here indicates command and data flow with in the system. The MDIS interfaces the pallet and Oribter through the SFMDM/DDCU and HRM. All experiment commands including beam deployment, retraction, excitation and control are executed by the mission specilist through the DDCU interface.

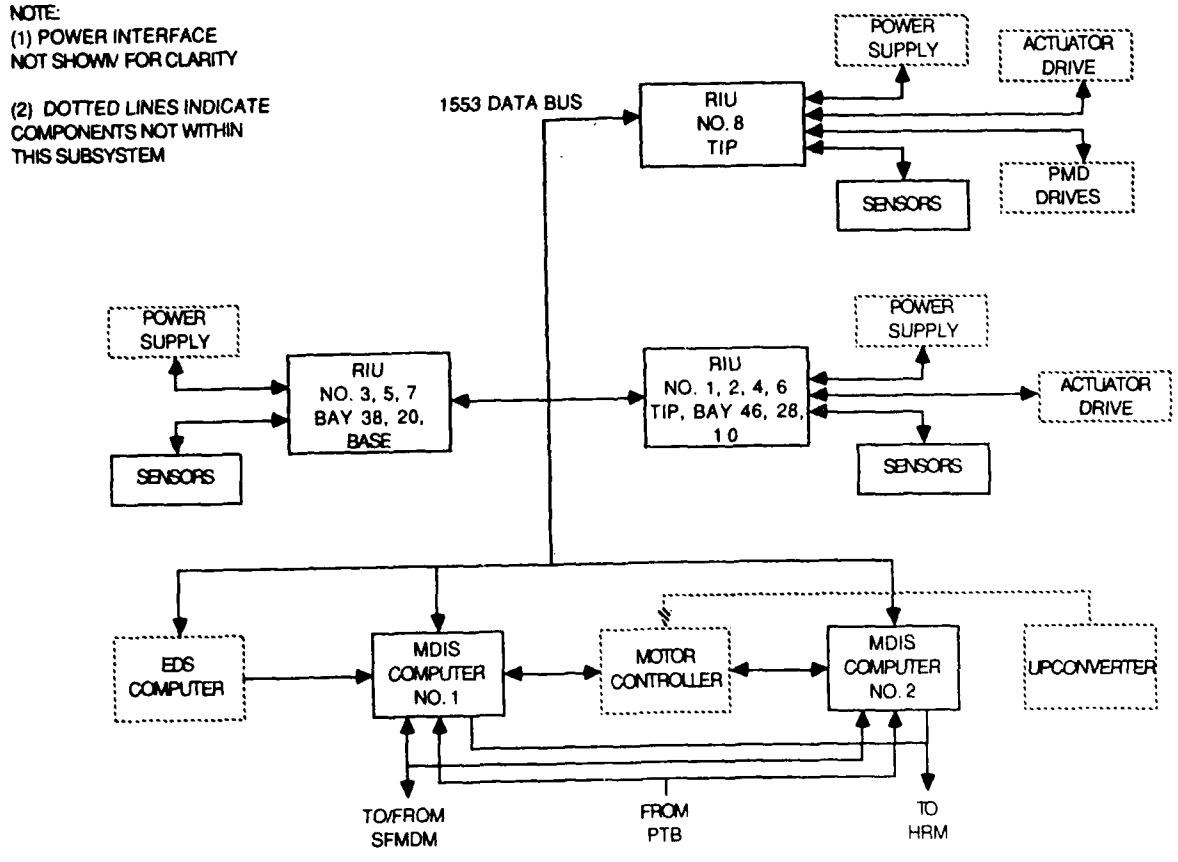

EDS BLOCK DIAGRAM

Excitation and control algorithms reside in the Excitation and Damping Subsystem (EDS) computer which is available to the experimenter. This computer is a dual 1750A CPU computer with an array processor. The computer has the capicity for large order algorithms for control and systems ID. A number of utilities will be available to the experimenter. These include a baseline damping algorithm, which is to be used for checkout and for damping between experiment modes, and basic commands such as sine excitation, random excitation, PMD position and experiment setup.

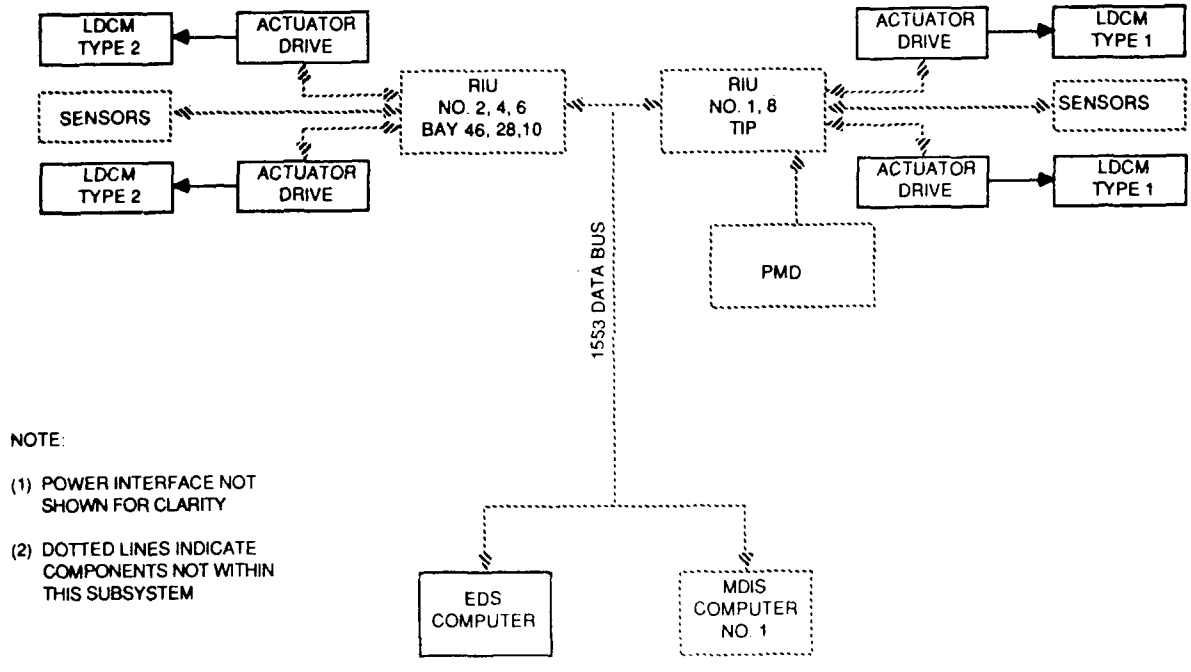

NOTE:

(1) POWER INTERFACE NOT SHOWN FOR CLARITY

(2) DOTTED LINES INDICATE COMPONENTS NOT WITHIN THIS SUBSYSTEM

BASELINE DAMPING ALGORITHM

Harris has developed a baseline control algorithm which damps the first 10 modes of the mast reliably. It achieves the goal of 5.0% damping in these modes while not destabilizing higher order modes. The algorithm uses a decentralized approach.

The pole shift for the first ten modes (shown below) reflects the algorithm performance. Transfer functions for the three types of decentralized controllers, which include LDCM motor compensation, and sample delays for the MDIS and EDS computers, are shown on the next page. Since the sensor/actuator pairs are colocated, the ith mode damping augmentation by the controllers may be computed approximately by multiplying the real part of the transfer function by the square of the modal influence coefficient at the actuator stations. The slightly negative values on the order of .2 to .7 percent, which occur at high frequency because of sample delays, must be offset by the structural natural damping in the higher frequency modes.

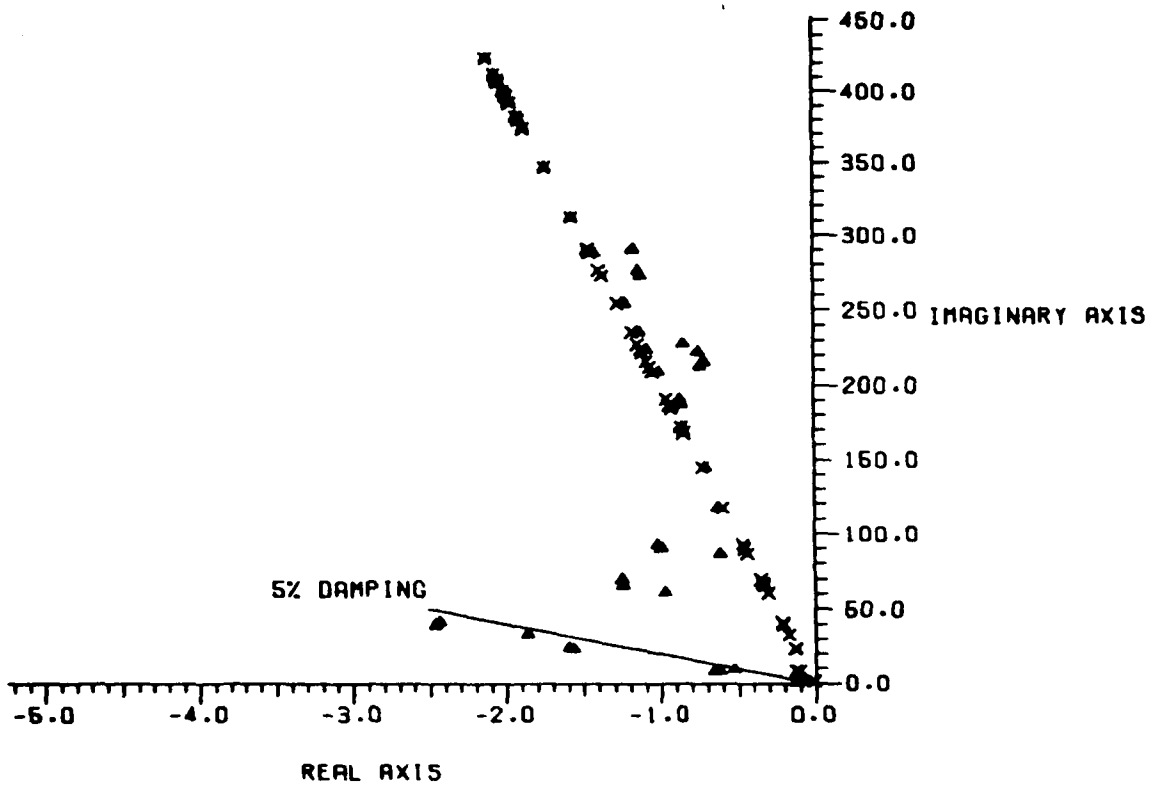

POLE SHIFTS FOR BASELINE DAMPING ALGORITHM DESIGN

BASELINE CONTROLLER TRANSFER FUNCTIONS

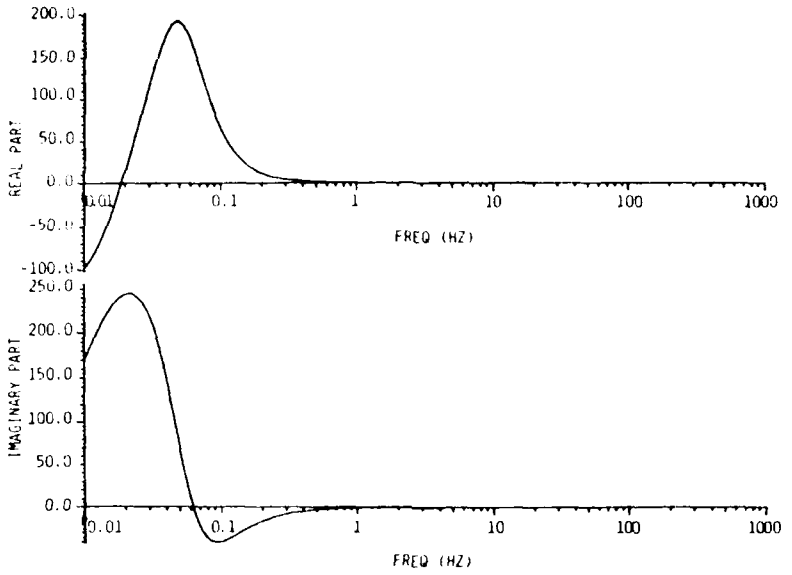

TIP BENDING CONTROLLER TRANSFER FUNCTION: OUTPUT FORCE/ (ω x PRIMARY VELOCITY)

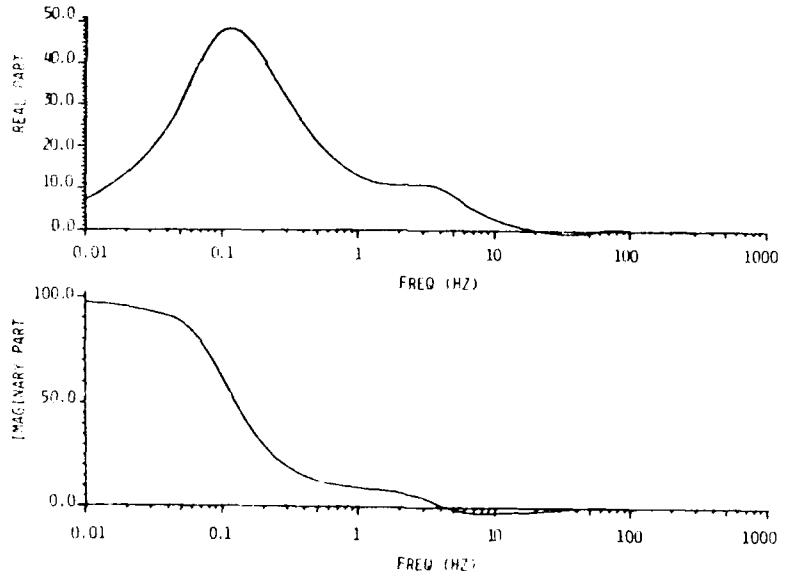

TIP TORSION CONTROLLER TRANSFER FUNCTION: OUTPUT FORCE/ (ω x PRIMARY VELOCITY)

BASELINE CONTROLLER TRANSFER FUNCTIONS (CONT'D)

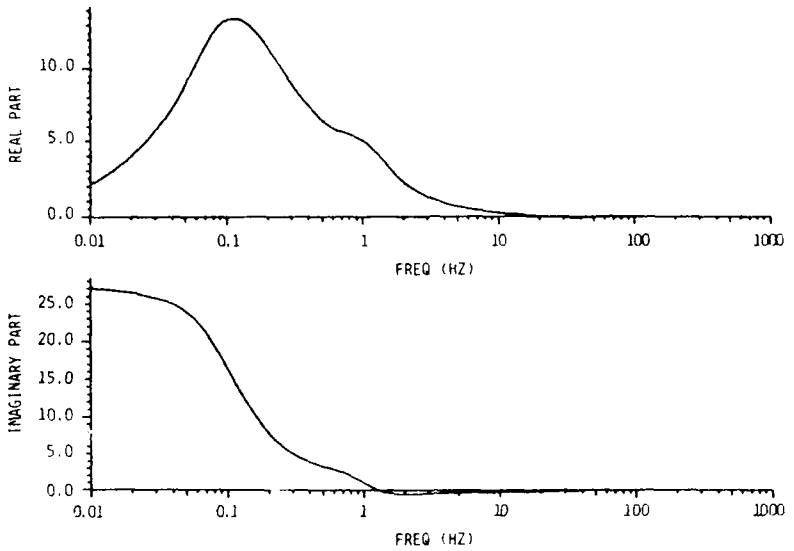

INTERMEDIATE BAY CONTROLLER TRANSFER FUNCTION:
OUTPUT FORCE/ (ω x PRIMARY VELOCITY)

SYSTEM SIMULATION

A detailed simulation is being developed for the Mast Flight System. It includes the system structural dynamic model, LDCM models which include motor compensation and stroke and force limits, noise sources such as LDCM bearing friction, accelerometer noise, the discrete position sensor for the LDCM secondary and the effects of finite word-length and sample delay in the sample data system. Also, the crew motion and several other disturbance sources are available in the simulation. Typical simulation outputs are shown below. In this case five cycles of sine excitation at the fourth X-Z bending mode frequency are input at bays 10 and 46 followed by turn on of the baseline damping algorithms at all stations. Also, the crew motion disturbance is present. This appears as low frequency drift in the response data.

FOURTH BENDING MODE EXCITATION SIMULATION OUTPUT

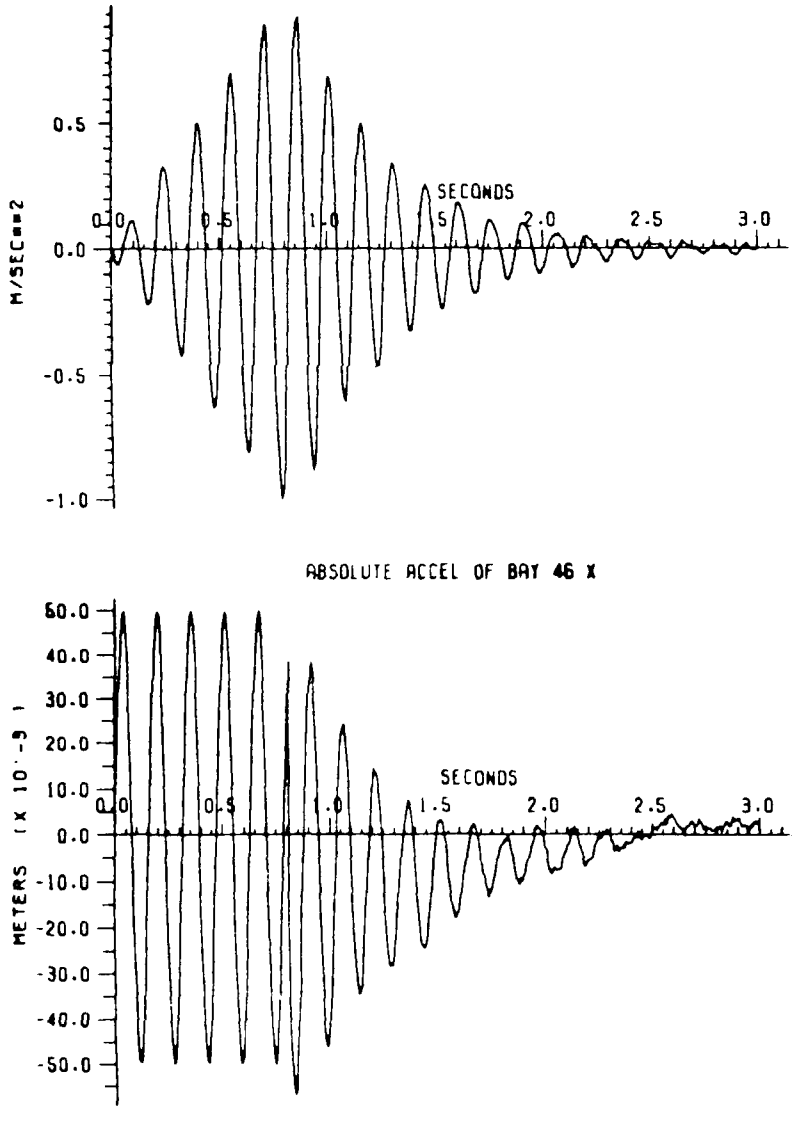

FOURTH BENDING MODE EXCITATION SIMULATION OUTPUT (CONT'D)

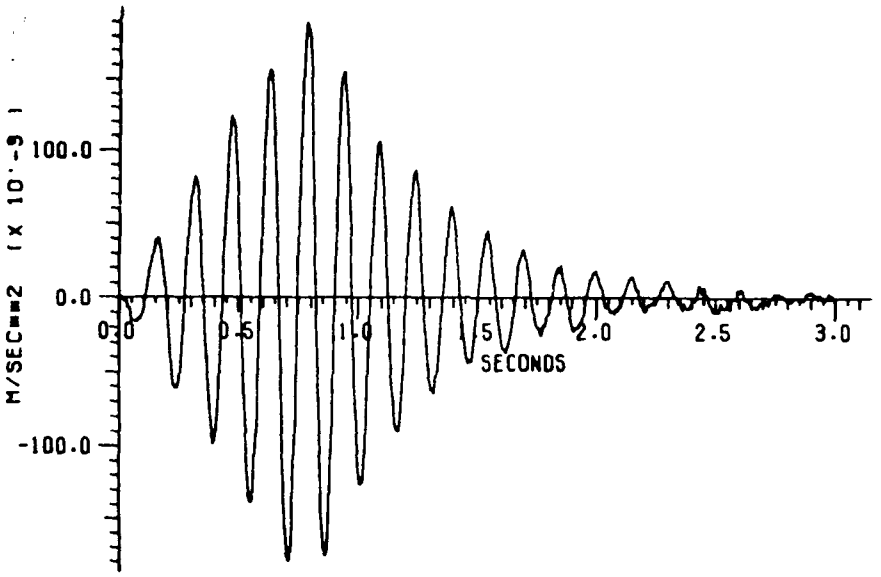

ABSOLUTE ACCEL OF TIP X

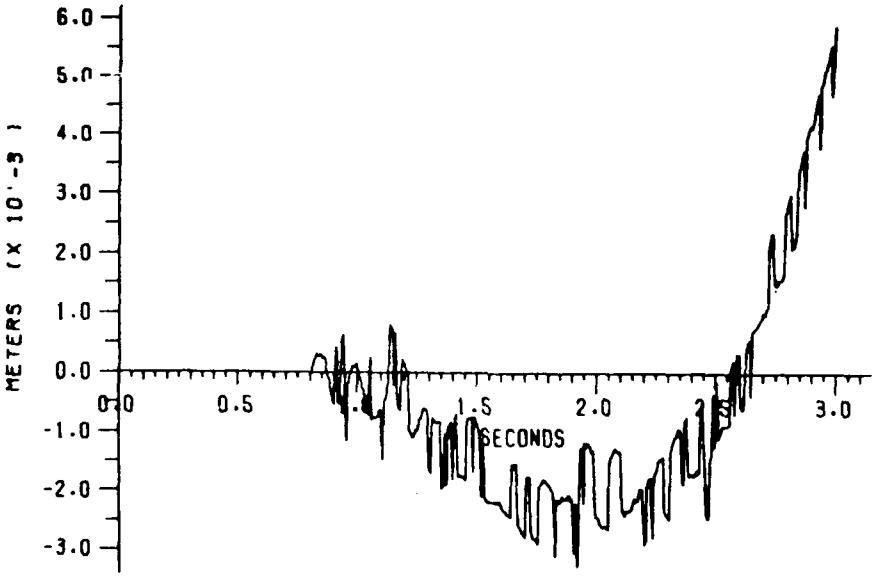

COMMANDED INPUT TIP X

MAST RELATED TEST AND ANALYSIS RESEARCH

Garnett C. Horner

Nancy A. Nimmo

NASA Langley Research Center
Hampton, VA

Second NASA/DOD Control Structure Interaction Conference
Colorado Springs, CO
November 17-19, 1987

Control of Flexible Structures Program

The Control of Flexible Structures Program (COFS) is a funded program in NASA to validate controls/structures technology through ground tests and on-orbit experiments. Some of the objectives of the ground test program are listed below. These objectives will be accomplished with hardware consisting of components, subassemblies, scale models, pathfinder model, and the flight hardware.

Ground test hardware

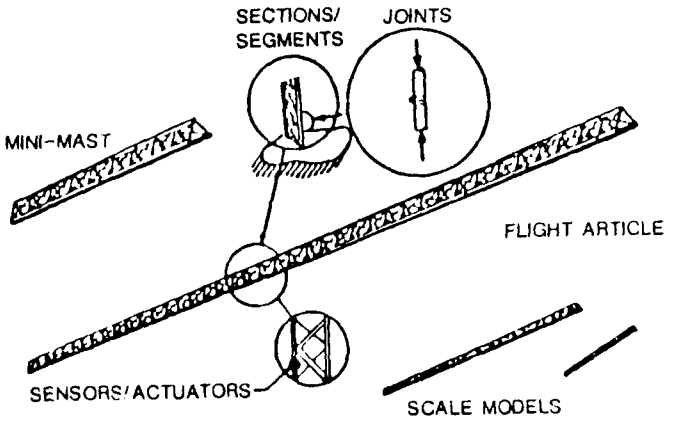

Objectives

- DEVELOP GROUND TEST METHODS AND CAPABLITY
- EVALUATE CONTROLS INSTRUMENTS
- VALIDATE CONTROL STRUCTURES ANALYSES
- EVALUATE SCALING METHODS
- EVALUATE JOINTS/DAMPING EFFECTS
- EVALUATE DISTRIBUTED CONTROL TECHNIQUES

Model Validation Process

The model validation process, shown schematically below, is a process that updates selected parameters in analytical models so that measured performance matches the predicted performance. This process is being used within the Mini-Mast program. The SM (System Modification) processor in the EAL finite element program has the capability to change selected parameters such as tube modulus. These changes are such that the difference between the measured and predicted performance is minimized in a least squares sense.

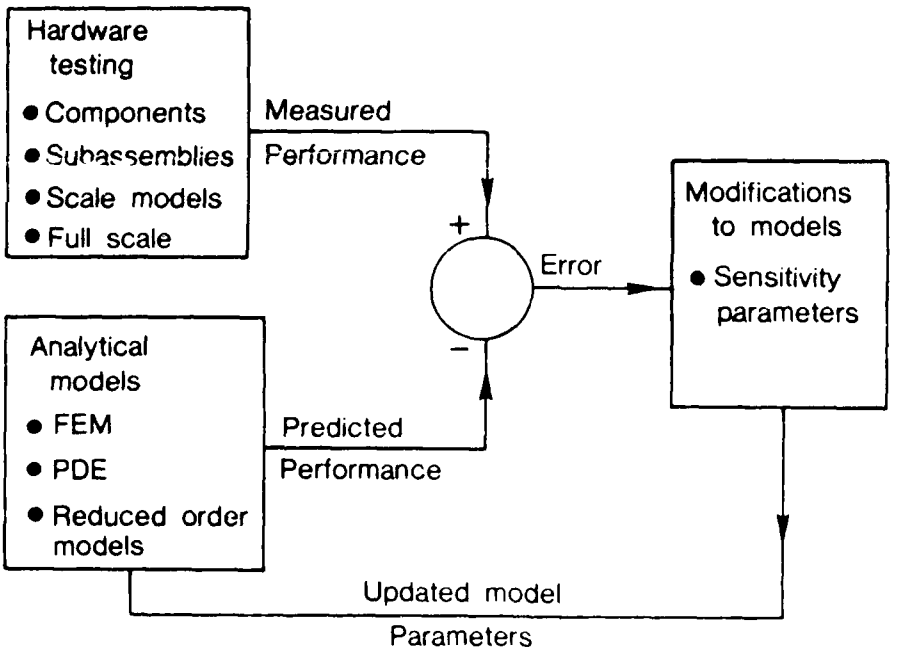

Diagonal Hinge Test

The Mini-Mast diagonal hinge is shown in a test machine. The objective of the test is to measure the axial stiffness of this joint. Rectangular blocks are attached to the tube on either side of the hinge and extensometers are attached on opposite sides. When an axial load is applied to the hinge, the hinge rotates about a hinge pin. Two extensometers are required to separate the rotation from the extension.

Solid Body Model of Diagonal Hinge

Using detailed drawings of the diagonal hinge, a solid body model was developed with the I-DEAS GEOMOD software. Models of the individual parts are shown below. A NASTRAN finite element model of the hinge was generated by I-DEAS software. A point with six degrees-of-freedom at each end of the hinge was used as a reference. Each degree-of-freedom at each end was given a unit displacement and NASTRAN calculated the forces required to constrain the remaining degree-of-freedom to be zero. The result of this analysis is a 12 x 12 stiffness matrix relating the displacements at each degree-of-freedom to the corresponding forces.

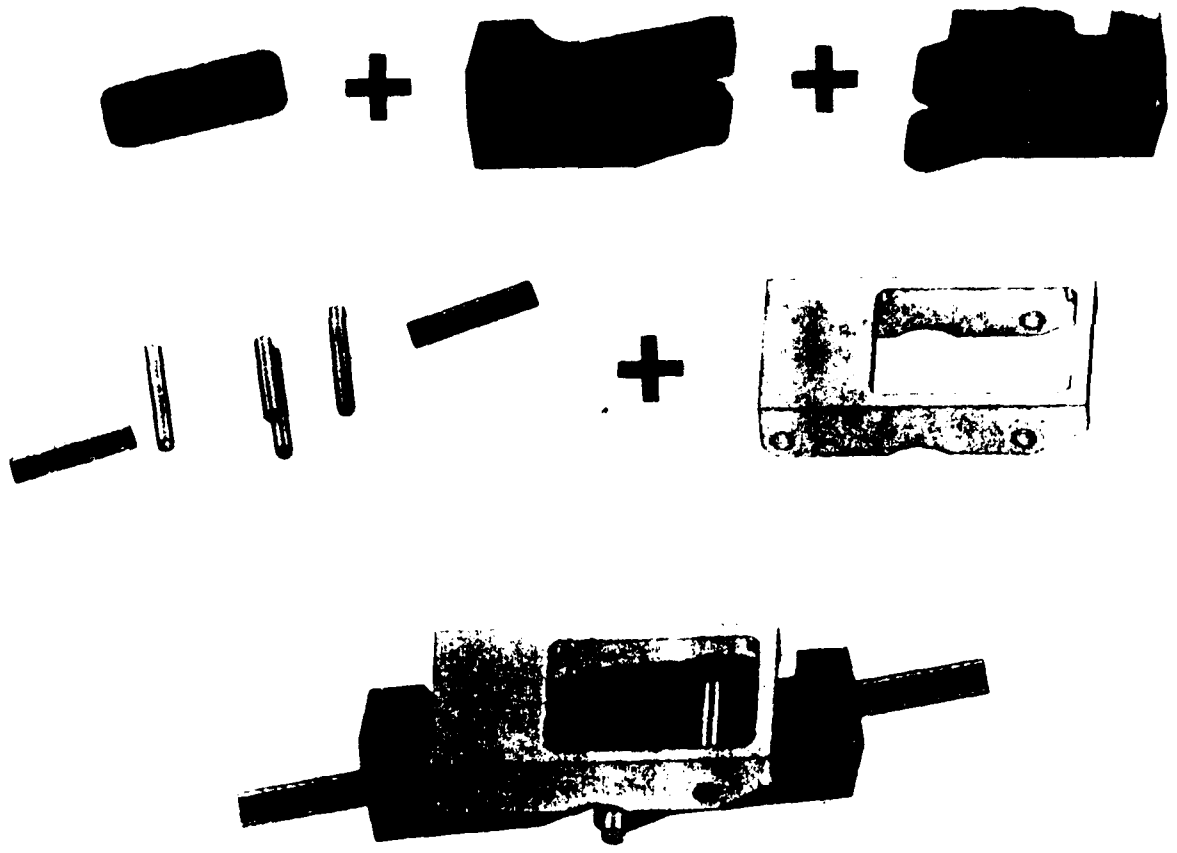

Axial Stiffness of Diagonal Hinge Joint

The results of the experimental measurement of the axial stiffness is compared to the results obtained from a finite element model. These results indicate the analytical model is stiffer than the actual hardware. This trend is to be expected since the finite element model represents the hinge as a "welded" joint.

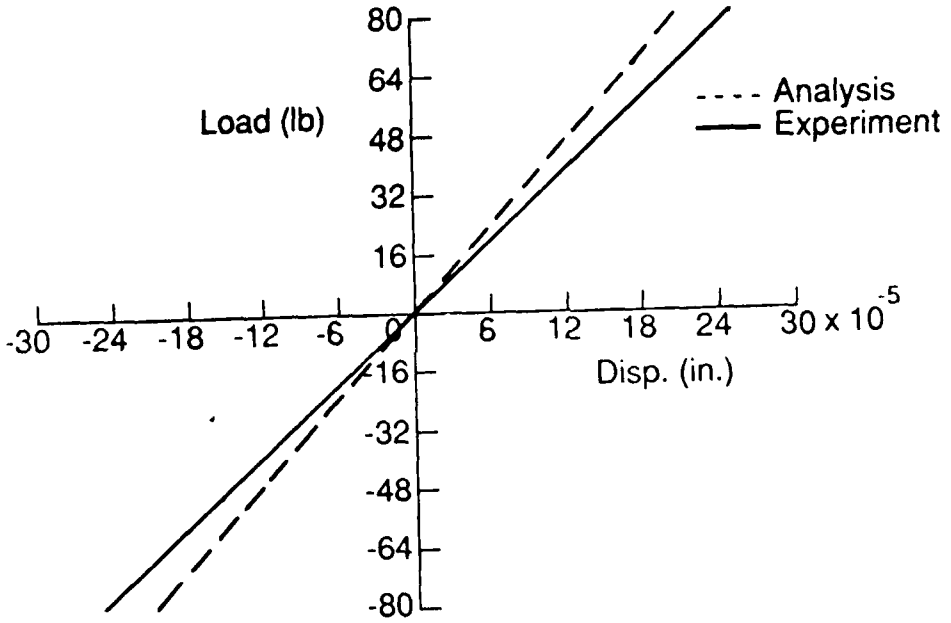

Static Torsional Stiffness Of Mini-Mast

Preliminary test results of the static torsional stiffness of the tip of Mini-Mast are shown in the figure below. These test results indicate the presence of a loss mechanism in the structure as indicated by the area inside the curve. Also, the finite element model over-estimates the torsional stiffness by approximately twenty percent.

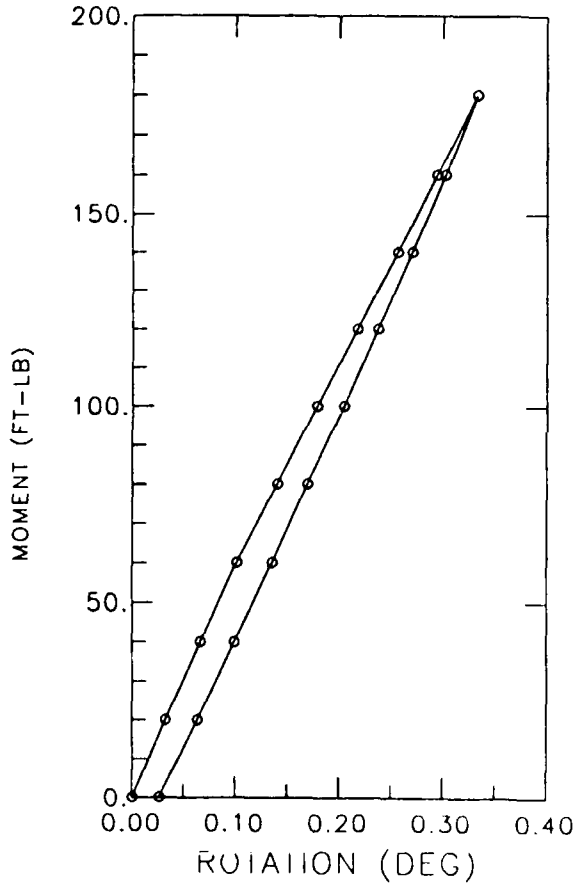

STIFFNESS

TEST **590 FT-LB/DEG**

ANALYSIS **712 FT-LB/DEG**

Mini-Mast Vibration Frequencies

The current level of refinement of the finite element model of Mini-Mast predicts the first three vibration frequencies as shown below. These frequencies are in very good agreement with the measured frequencies. The finite element model does not include any nonconservative elements.

	ANALYSIS		TEST	
	FREQ. (HZ)	DAMPING (%)	FREQ. (HZ)	DAMPING (%)
1st BENDING	1.42	•	1.42	0.6
1st TORSION	8.55	•	8.58	0.4
2nd BENDING	9.50	•	9.52	0.5

Summary

The status of the Mini-Mast program is summarized in the three bullets below.

- VIBRATION FREQUENCIES FROM TEST AND ANALYSIS SHOW GOOD AGREEMENT
- STATIC TORSIONAL STIFFNESS OF MINI-MAST FROM ANALYSIS OVERESTIMATES THE TEST RESULT BY 20%
- ESTIMATION OF STATIC STIFFNESSES OF COMPLEX JOINTS USING SOLID BODY MODELING TECHNIQUES SHOWS GOOD PROMISE

ASTRO 1750A COMPUTER SYSTEM

By James McKelvy and Harold Tinsley

SCI TECHNOLOGY, INC.

ABSTRACT

In addressing the many structures processing applications, a flexible computer is needed which can be tailored in processing power to match the problem. SCI's approach to providing this flexibility is the Astro 1750 Computer, which deviates from the fixed single processors that currently exist. The modular approach of the Astro Computer allows the computing power to be matched to the application requirements.

The small size and low power of the latest 1750A microprocessors, combined with high density solid state memory and the integration of complex logic into Application Specific Integrated Circuits provide the basis for design of a powerful, high throughput, reconfigurable, multi-processor, general purpose space qualified computer system.

The computer system is designed to provide the capability for data collection, data storage, high speed data processing, output control and communication, with each other, and with standard space shuttle and experiment interfaces.

The computer system provides a multiprocessor environment structured around fully compliant MIL-STD-1750A processor boards. The system may contain up to eight processor boards, each operating in parallel, independently or in association with each other, via a unique bus architecture, thus achieving a higher system throughput. The key to the development of the bus interface was to provide structured management of the multi-processor environment.

The computer system provides various ancilary functions such as RAM/EPROM memory, multi-channel analog and digital I/O, communication interfaces and high speed floating point array processors. The array processor is specifically designed to manipulate large matrices as would be encountered in algorithms associated with control of flexible structures.

A NEW APPROACH TO INCREASING THROUGHPUT

The latest generation of integrated circuit MIL-STD-1750A microprocessors lack sufficient speed for a number of system applications for which the SCI Technology, Inc. Data Acquisition and Control System (DACS) could be applied. The classic co-processor and bus interface techniques do not provide an efficient approach to increasing throughput in these applications. However, the small size and low power of the latest 1750A microprocessors combined with the high density of memories now available and the integration of complex logic into a gate array, can reduce to a small single board, a processor of mini-computer capability. A number of these processors in a single system operating in parallel can produce a powerful

computer that can be fully radiation hardened for space applications.

SCI's objective was to determine how to best utilize this new low power, high density technology. The parallel processors would each require onboard memory and I/O resources to operate in parallel at their maximum rate. Yet, these localized resources would have to be shared along with sharing mass memory and system I/O interfaces via the system bus. This bus interface would need to be flexible, modular, fault tolerant, and include convenient methods for intra-communications so that the parallel processing and data flow would occur in harmony using straight forward management techniques.

SCI's development of a bus interface to meet the requirements described above has been implemented in gate array designs. The gate arrays include all the basic processor support functions as well as the unique bus interface and arbitration logic and error detection and correction on bus transfers. The bus interface technique allows all memory and I/O distributed on each processor board to be accessible via a cycle steal concept from any processor. Thus, all local memory combines with mass memory to form the total accessible system memory. The capability to access I/O allows other processors, or a designated management processor, to setup and monitor functions for coordinated system operation. A "hold" technique is included in the interface for system master override or for redundancy management. Status reporting between processors, and the capability to generate as well as respond to interrupts by the processors, is combined with a flexible data flow for rapid communications. To aid software development and system integration the processor includes a flexible console interface and onboard debugger gate array. The debugger combines a flexible 62-bit breakpoint comparator and 1K-word by 64-bit trace buffer with the standard microprocessor breakpoint features.

For applications that have an intensive use of floating point and/or matrix solutions, the Astro 1750 Computer can include one or more Array Processors that extend the throughput to tens of megaflops.

The SCI DACS was developed in 1977 for space applications and has been upgraded as advances in IC technology have occurred. The latest design yields a unit with massive computing power extending its application beyond just data acquisition and control. Its power is derived from a new concept of paralleling processors using a bus architecture that provides system management as a feature rather than an after thought that would be difficult to control with software.

SYSTEM CONCEPT

The concern for system throughput has pushed the speed of processors ever upwards and forced creative processor architectures to gain maximum efficiency in executing instructions. While limits have not yet been reached, the speeds have already extended into the tens of Mega Hertz. This complicates the design of interfaces and often generates a complexity in thermal design to dissipate the increased power that is a byproduct of higher speed. Increasing speed will eventually reach a limit, but even now a concern exists because often the associated disadvantages of higher clock rates impose system constraints which devalue much of the gain faster clock rates provide to increase throughput.

An analogy between the computer and the human mind is often made to demonstrate processing capability. As the size and complexity of jobs increase the boss will search for the most intelligent and efficient employee to perform the most difficult jobs. There is a price that must be paid for this quality and that is also true when faster processors are required. Like the limitations of the processors of today, there is a limit to tasks that an individual is capable of executing. There is a parallel to this analogy in the development of hardware technology when pressing the limits of existing component technology.

The complexity of the world has long since passed the level of tasks a single individual could perform. Multiple workers, each with specific and shared resources, under the direction of a skilled manager, perform in parallel to execute the more complex tasks. This structure has almost limitless bounds. So why push processing speeds beyond that level where cost, power and technology impose other constraints that limit the value of the gains?

Various techniques have been employed to parallel the processing requirements such as co-processors, distributed processing, specialized processors, slave processors, local area networks, etc. These were based on existing processor interface concepts and all have various limitations.

A true parallel processing approach must be based on each processor having adequate local resources (memory and I/O) as well as sharing the total system resources in an efficient way that avoids conflicts by employing a well founded management structure. The key to such a management structure is in the design of the interface and reporting structure. Advances in memory technology and the integration of complex interfaces into gate array designs now provide adequate local resources that will provide extensive processing capability within reasonable size, weight, power and cost.

While the speed of these processors is still important to the system, just as intelligent and efficient workers are to the successful manager, the system throughput or productivity of a group, is no longer restricted by the speed of an individual processor or worker. Efficient interfacing through structured management now becomes the focal point of the overall task size and the success with which a task can be performed. The concept is not new, just its application in processor design is new.

This fundamental everyday concept has been applied to the conceptual design of the Astro 1750 Processor to be described in this paper. The basic processor design is straight forward; it is the interface and reporting structure that is unique. In order to realize actual hardware for existing programs, available component technology and the present DACS mechanical design are utilized in the Astro 1750 Computer.

THE BASIC SYSTEM COMPONENT

The basic system component is the ASTRO 1750 Processor Board. This board utilizes the MDC281 MIL-STD-1750A Microprocessor operating at 10, 15 or 20 MHZ. The MDC281 was chosen because it is fabricated in CMOS-SOS technology offering a high level of radiation hardness.

The board was designed to operate with a number of memory types and technologies in order to provide functional flexibility as well as radiation hardness where applications dictate. Standard memories may be utilized when greater memory density and speed is the primary application requirement.

The MDC281 performs all the mandatory 1750A functions and includes many of the optional 1750A features. Other optional 1750A features, such as memory management and block protection combined with global memory protection and radiation event upset protection, are included with the specialized interface and basic processor interface functions in the gate array designs. The gate arrays are implemented in the latest Harris Corporation DLMRH 2+2 (2 micron drawn channel length double metal layer) radiation hardened standard cell technology.

By integrating the memory management into the CPU gate array it is possible to access the Page RAM from the CPU Bus during the address phase of the bus cycle to achieve the speed needed for the table look-up to translate the logical address to the physical address. During the data phase of the bus cycle the Page RAM can be accessed from the Internal Bus for loading and verification. Since another processor may access the Internal Bus via the Bus Controller and Astro Bus, this allows another processor, such as a system manager, to set up the tables for all processors in the system. I/O instructions can also select one of four look-up tables stored in the Page RAM. This decreases the time to switch between multiple modes of operation since these tables can be set up at initialization and do not need to be loaded and reloaded for each mode change. Being able to accomplish these administrative tasks for the processor designated as the system manager is a feature built into the processor to efficiently manage a multiple processor system.

The board houses up to 64K words of both PROM as start-up memory and RAM as run memory. The flexibility of mixing the two in 16K segments for a total on board addressable 64K of run memory is provided. When the total 128K of memory is installed the two 64K blocks overlay each other. The start-up and run modes are program selectable and when this feature is combined with the "Move Multiple Word" instruction, access is provided to the total 128K following initialization. This memory is addressed from the internal bus as Block 0 in the total system physical addressable 16 blocks (1 Mega Word). Memory words are 16 bits or 22 bits to include check bits for Error Detection and Correction (EDAC). If radiation hardening is not required the PROM can also be UV-EPROM or EEPROM, depending on the application. This is in addition to the options of memory size, mixing types and speed, and the inclusion of EDAC check bits.

EDAC checks bus transfers, not just memory or specific functions. Modes have been included to test the EDAC functions or to disable them. In all there are 12 detectable error types which capture 49 bits of information. This combines with the console and debug features to provide a powerful system analysis capability.

Other basic features of the board include an RS422 Serial Port, flexible console interface, programmable discrete inputs and outputs, various status and control discretes, hardware and software resets, general purpose programmable timers and a watch dog timer, full status

reporting on errors for failure analysis, programmable control features for test analysis or redundancy override, response to a variety of fault and interrupt inputs as well as the generation of interrupts to other porcessors via program control or error conditions. Various application specific configuration straps are combined with the memory options and programmable features to provide application flexibility. The board also houses a debugger gate array and 2K X 32-bit memory to provide function compare recognition with a trace buffer to support software development and system integration.

SYSTEM ARCHITECTURE

Processors communicate with their local resources via an internal bus. The processors communicate with each other via a systems bus referred to as the Astro Bus in reference to off-card access. A Bus Interface Gate Array has been designed to interface all units to the Astro Bus. This gate array has two functions: (1) A Bus Controller which interfaces those devices which must arbitrate for the bus for the purpose of gaining access to the bus to transfer data or control to some other unit. (2) A Bus Responder which interfaces those devices that only respond to a device having a bus controller.

Figure 1, "Astro 1750 Computer Bus Concept," illustrates the system architecture with units interfacing to the Astro Bus via a bus controller or bus responder. The design allows for addressing a maximum of eight bus controller units on the bus and up to sixteen units interfaced to the bus via a bus responder. The bus responder control is unidirectional from the Astro Bus to the board functions and is bi-directional for data flow. The bus controller is bi-directional for control and data. The relationship of the Bus Controller to the Processor Internal Bus and the Astro Bus is shown in Figure 2, "Astro 1750 Processor Board Block Diagram."

The bus controller arbitrates for the Astro Bus based on a priority which is programmable. Once gaining access to the Astro Bus it communicates directly with the addressed bus responder without further delay. The bus controller provides for bi-directional control so that once a bus controller has gained access to the Astro Bus it can also gain access to another unit's internal bus via its bus controller. This allows the internal busses of two units to be tied together via the Astro Bus to share local resources with other system resources, ie. one processor can read or write to another processor's memory or I/O function. This is illustrated in figure 3, "Astro 1750 Processor System Interface Concept." This is important to system management so that a processor designated as the system manager can initialize all units, redirect their functions and/or service their data or control needs. It also reduces by 50% the number of Astro Bus accesses when data flow is processor to processor and maximizes system resources for minimum power and size considerations.

The DMA control feature of the MDC281 is used when access from the Astro Bus to a processor's internal bus is via its bus controller. Once the accessing processor has arbitrated for and gained access to the Astro Bus it then addresses the bus controller of the processor to be accessed. If that processor is not inhibiting such an access by having generated a DMA Enable, its bus controller will issue a DMA

Request to the processor. Upon completion of the current machine cycle the processor issues a DMA Acknowledge and tri-states its internal bus giving control to the bus controller. The bus controller couples the internal bus to the Astro Bus and the accessing processor performs the bus cycle for the addressed function. The bus cycle is completed when the accessed function generates the READY signal back to the processor. This also terminates the DMA access by removing the DMA Request, returning control back to the processor. The effect is that of a cycle steal.

Should the processor to be accessed not desire another processor to access its internal bus it removes the DMA Enable. An attempt to perform an access when this condition exists inhibits the transaction. In this case a READY signal is immediately generated to terminate the bus cycle and an interrupt issued to the requesting processor so that it can take action on the function that was not performed.

An override for this block-out exists which also is a means to manage redundant processors in systems that require such a feature. This is another extremely important feature for system management. This override uses the HOLD interface signals of the MDC281. The bus controller contains a HOLD and DTIMER latch that can be set or reset from the Astro Bus by another processor. Setting the HOLD latch will issue the HOLD signal to the MDC281 and it will respond with HOLD Acknowledge, tri-stating the internal bus when it completes the current executing instruction. It will remain in that mode until the HOLD latch is reset. While in the hold mode the internal bus of the processor is immediately coupled to the Astro Bus by the bus controller when any function on that internal bus is addressed. The DTIMER signal to the MDC281 suspends the internal timers specified as options by MIL-STD-1750A. By setting a third latch called the BROADCAST latch, will allow one processor to write to multiple processors with a single I/O write. This is a valuable time saver when setting up common tables and functions.

The address to which the bus controller responds to the Astro Bus is a board location address set at initialization or an address that has been programmed via a processor (system manager). This address will be one of the fifteen block addresses other than block 0. For memory accesses this is the most significant four bits of the 20 bit physical address. For the special I/O functions on the processors internal bus it is that same block address that must be issued by the requesting processor. System I/O functions reside in the normal sixteen bit address as defined by the top two spare areas designated by MIL-STD-1750A.

For small system applications where only one processor is required this architecture does not impose a penalty. In this case the board address is set to block 0 and the internal bus is directly coupled to the Astro Bus so that no arbitration is required or time added to a bus transaction. In such applications the processor resident memory may be all that is necessary and no additional memory boards required in the system. Also the processor has limited external I/O features that can be used for the system application.

BUS INTERFACE GATE ARRAY - BUS RESPONDER

The Bus Responder is not employed on the processor board but is an important function in the system. It is used to interface all system components that must respond to a request from a device having a bus controller. For this reason a brief review of its capability will help clarify the concept of how the bus architecture functions. The Bus Responder is designed to interface memory and I/O functions to the Astro Bus. Its purpose is to minimize discrete logic on those boards by providing in one IC all common functions such designs would require.

The Bus Responder provides a variety of decoded strobes to activate board functions and enable signals to extend the strobe functions with a minimum of board circuitry. The variety of features provided by the Bus Responder, including its memory-I/O application modes, are programmable. The board is setup via software control and can be functionally altered as the system requires. Complete internal gate array status along with enable/disable features allows software controlled self test.

The Bus Responder includes a four bit coded input so that up to sixteen boards can reside on the Astro Bus with each responding to its own unique address. Thus a number of identical boards having the same functional addresses can reside on the bus. Should there be a system need for memory to exceed one mega word, a software board enable/disable bit allows identical memory mapped boards, which overlay each other, to be included and extend the available memory beyond that limit.

The Bus Responder has the capability to perform error detection and correction on data derived from the Astro Bus and the board functional units. It can also generate check bits for data sent via the bus or the on-board functions.

Three programmable wait states are provided with select and override controls that extend the board functions timing needs for any application. A variety of buffered controls and clocks are provided to simplify the memory or I/O functional designs. The IC also includes an eight input interrupt controller, five bit fault controller, eight discrete outputs and eight discrete inputs. These can be used by functions on the board or for general system application, ie. as an example, a memory board having little I/O interface could also be the interrupt controller for an function external to the unit.

OTHER ASTRO BOARDS

In addition to the Astro 1750 Processor board and Power Supply, the following boards are in development: Array Processor, Mass Memory, Serial I/O, Buffered I/O, AMUX/ADC, High Rate Mux and 1553 Interface Board.

The Array Processor is a microcode driven floating point processor designed specifically to efficiently process large matrices as would be encountered in structural dynamics applications. The processor is built around the Analog Devices 3200 series 32/64 bit chip set which conforms to IEE standard 754 for floating point

operations. With a clock speed of 8 MHZ, the maximum theoritical throughput is 16 Megaflops. The time required to multiply two 40 X 40 matrices is typically 9 milliseconds. A [40 X 40][40 X 1] multiplication requires typically 237 microseconds. The microcode memory is 2K X 96 and there are dual 16K X 32 bit data memories. A network of four 32-bit busses moves data between functional units and data memory. Sixteen registers are accessible via the Astro Bus to the data and microcode memories in the Array Processor.

The basic operating speed of the Astro 1750 Processor with a 20MHZ clock operating with zero wait states based on the DAIS Mix is 610 KIPS. The following is an example to show the speed potential of using an Array Processor in the system. Including an Array Processor to execute the floating point operations of the DAIS Mix, the Astro Processor throughput goes up to approximately 1.1 MIPS with the floating point instructions removed. One Array Processor can easily handle the floating point operations of the DAIS Mix that would be equivalent to five Astro Processors.

The Mass Memory Board may be configured for RAM or EPROM, or a combination of the two. The board provides up to 256K words of memory in increments of 64K. Word width is either 16 bits when not utilizing EDAC memory or 22 bits when EDAC memory is present. The Mass Memory Board interfaces to the Astro Bus via a Bus Responder which includes EDAC a well as other features. These other features include 8 external interrupts, 4 external fault inputs, 8 external discrete inputs and 8 external discrete outputs. Additionally when the Mass Memory Board is configured with EPROM it may be programmed through the bus responder eliminating sockets or unsoldering the devices.

The Analog Board provides 64 single-ended or 32 differential, multiplexed, overvoltage protected inputs. The Analog Board is designed around a high accuracy 12 bit A to D converter. Input voltage range and resolution are programmable. Accuracy over environmental extremes is assured by auto-calibration circuitry which utilizes highly accurate and stable on-board calibration sources. In keeping with the goal of the Asto Computer to provide high system throughput capability, the Analog Board provides 3 different modes of operation. Mode 1 is the conventional directed sample mode, requiring a system bus write and then a system bus read for each sample. Mode 2 is a self-scanning mode in which the Processor Board writes to the Analog Board, a sequence of channels to be sampled. The board then continuously samples the channels in the sequence written, storing each converted value in a channel unique onboard memory location. In this mode, after initialization, the Astro Processor can obtain continuously updated data samples with 1/2 the System Bus overhead required in the directed sample mode. Mode 3 is identical to mode 2 except the the sequence is scanned once and stops until commanded to scan again. A directed sample may be taken at any time in any mode without disrupting operation.

The Buffered I/O Board provides 72 discrete interface lines. These lines may be configured in groups of 8 as inputs or outputs. All inputs are overvoltage protected and have selectable thresholds. Outputs are open collector TTL with high current sink capability. At the users option, 32 of the output lines can provide an onboard pull-up resistor. Additionally each output is "wrapped-around" for output

verification.

The Serial I/O Board is a half-duplex communication board designed to interface to the Space Shuttle's SFMDM. It provides a 1 MBPS Manchester encoded serial link with handshakes. Message integrity is maintained through use of on-board error detecting logic which interrupts the Processor Board should an error occur. Transmit and receive data buffers are provided to store in excess of the 32 words per message required.

The High Rate Multiplexer Board provides a serial data stream compatible with the Space Shuttle's HRM interface. This interface is used to both record experiment data and to provide input for a telemetry downlink from the shuttle. The HRM board provides programmable bit rates up to 2 MBPS and programmable minor frame lengths up to 1K words in addition to complete programmability of minor frame format. An IRIG-B compatible GMT decoder is provided. The GMT output may be included in the HRM serial data output stream or may be read by the Astro CPU board.

The 1553 Interface Board is a communications board that is fully compliant with MIL-STD-1553A/B. This board is designed around an SCI developed chip set and provides Bus Controller, Remote Terminal and Bus Analyzer modes. Mode selection is under program control and may be changed at any time. The board additionally provides extensive error checking and Built In Test capability.

The above boards are the first of the many DACS interface boards being adapted to the new Astro Bus architectrue.

CONCLUSIONS

This paper has attempted to present in some detail those features that are important to the parallel processing concept. It should show that this architecture does have a structure that can increase throughput in relation to the number and types of processors operating in parallel. That, however, is of little value if such a system cannot be properly managed in a way that will not generate a programmers nightmare. That factor was considered in the design of the hardware. The architecture from a hardware viewpoint is efficient in speed and in the sharing of system resources. Considerable effort was directed to make a processor that is flexible for a variety of applications. While future advances in 1750A microprocessors and the speeds and densities of memories and gate arrays will enhance processing throughput, this design uses the application of present IC technology. The concept that this design was based on is not restricted to any specific technology or clock rate and should in the future grow in value as advances in IC technology occur. However, the most important aspect of this concept is that throughput is no longer solely dependent upon speed and IC technology advances.

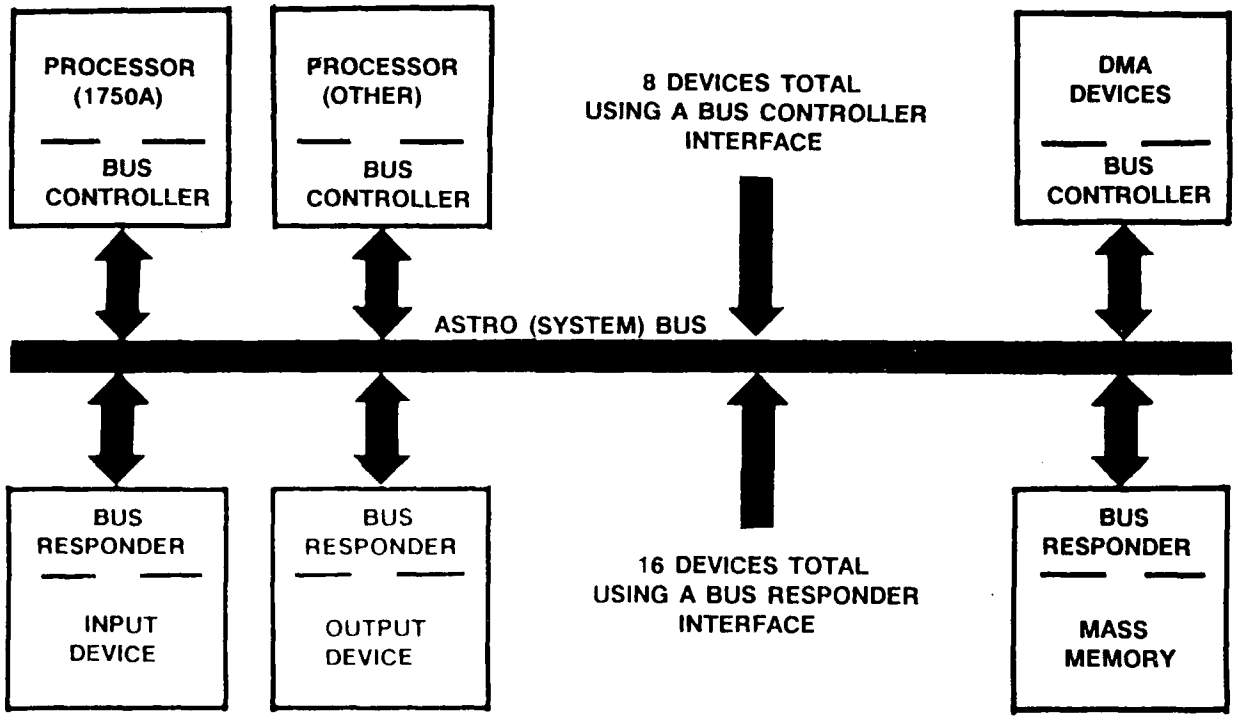

FIGURE 1 - ASTRO 1750 COMPUTER BUS CONCEPT

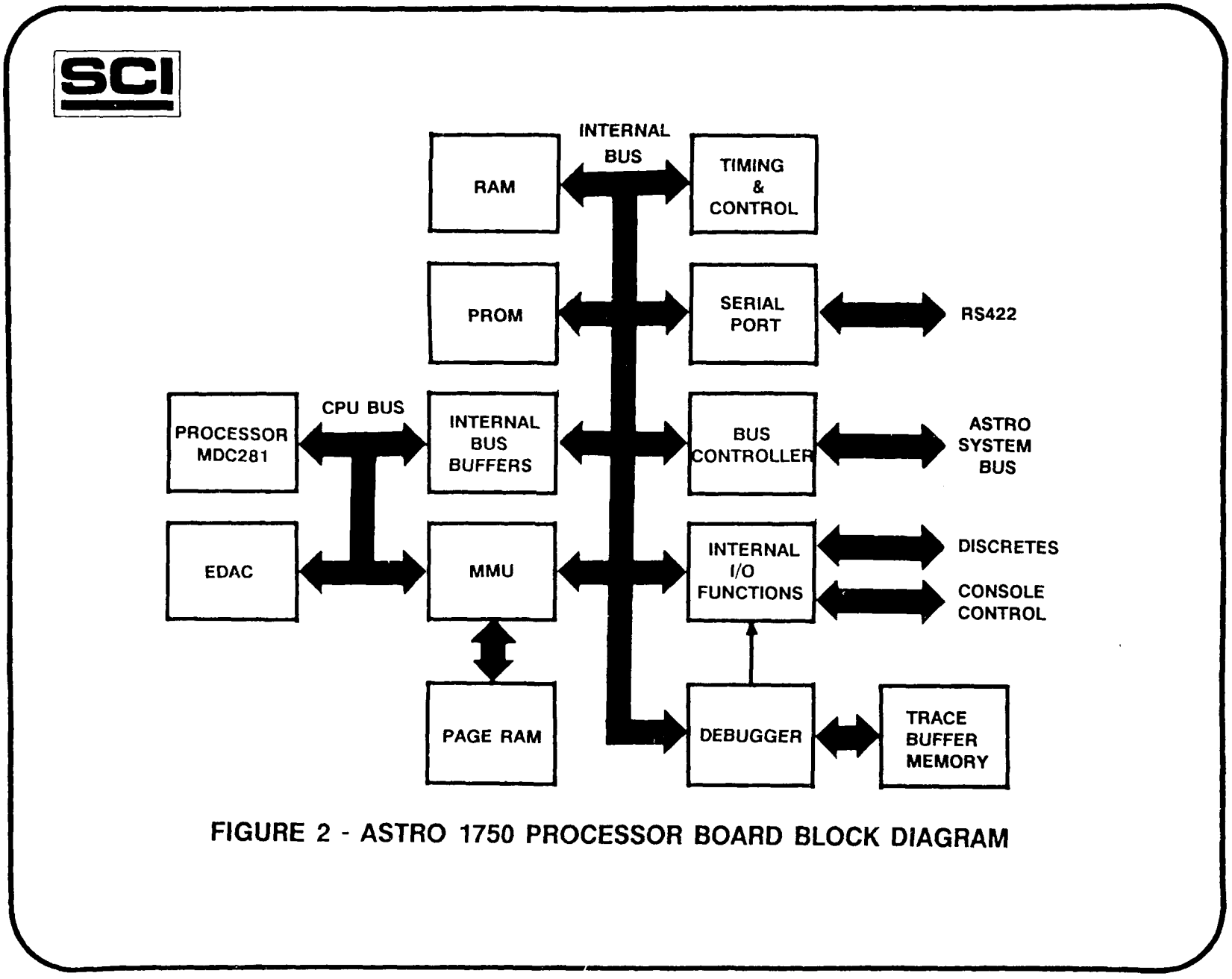

FIGURE 2 - ASTRO 1750 PROCESSOR BOARD BLOCK DIAGRAM

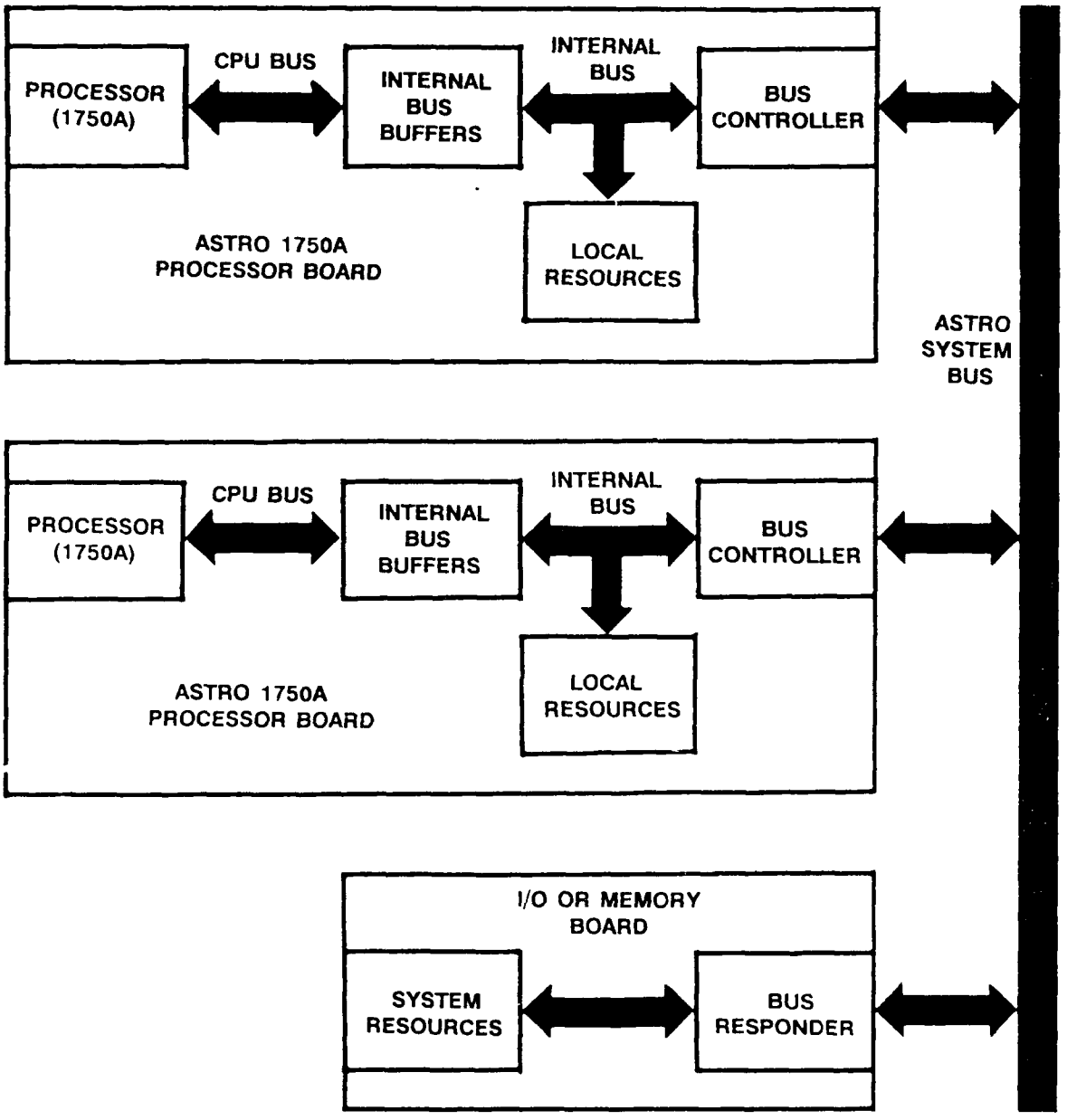

FIGURE 3 - ASTRO 1750 PROCESSOR SYSTEM INTERFACE CONCEPT

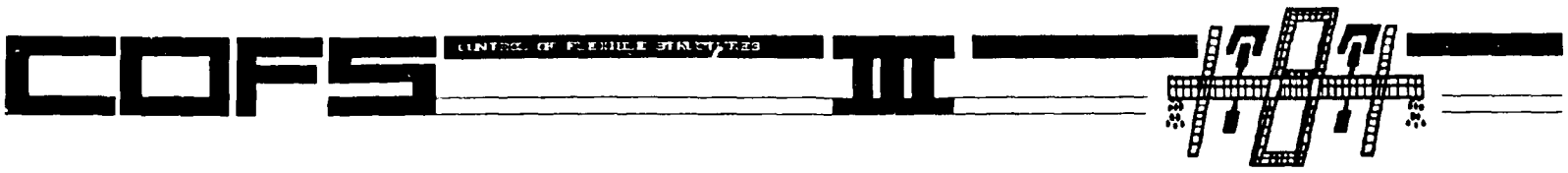

CONCEPTUAL DESIGN OF A SPACE STATION DYNAMIC SCALE MODEL

by

ROBERT LETCHWORTH
PAUL E. McGOWAN
NASA LANGLEY RESEARCH CENTER

MARC J. GRONET
LOCKHEED MISSILES & SPACE COMPANY

DR. EDWARD F. CRAWLEY
MASSACHUSETTS INSTITUTE OF TECHNOLOGY

Presented at the

SECOND NASA/DOD CSI TECHNOLOGY CONFERENCE
COLORADO SPRINGS, COLORADO
NOVEMBER 17, 1987

RLWORS3.PCX
11/9/87

COFS III OBJECTIVE AND TECHNICAL APPROACH

COFS III is a research and technology program which has as its objective the development of a capability for structural dynamic prediction and vibration control of large, multibodied, joint dominated, articulated, flexible space structures. Due to the size and weight of the next generation of large space structures, dynamic ground testing of fully mated systems will be impractical if not impossible. Thus another method is needed for determining the dynamics of these structures. One approach is to use the results of ground tests of dynamically scaled precision models of the specific configuration of interest combined with theoretical analyses to predict the full-scale, on-orbit dynamics. This is the approach being pursued within COFS III. Such a method will also provide a credible means for investigating vibration control methods and techniques.

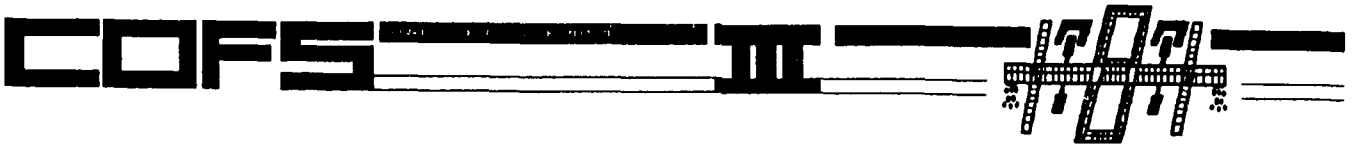

OBJECTIVE:

- **VERIFIED CAPABILITY FOR STRUCTURAL DYNAMICS PREDICTION AND VIBRATION CONTROL OF**

  LARGE MULTIBODIED, JOINT DOMINATED ARTICULATED, FLEXIBLE SPACE STRUCTURES

TECHNICAL APPROACH:

- **DYNAMICALLY SCALED MODEL TESTS**

  PLUS

- **THEORETICAL DYNAMICS ANALYSIS**

→ **PREDICTION OF FULL-SCALE DYNAMICS & VIBRATION CONTROL**

PROGRAM FOCUS

The focus for COFS III is Space Station since it will be a real structure typical of the structures of interest, and will provide the first opportunity to obtain full-scale component and subassembly ground test data resulting from the Space Station development and verification activities as well as on-orbit flight data gathered during the assembly and operations in space. Finally, having a precisely scaled dynamic model of the Space Station provides the means for developing technology for growth versions of Space Station and for future Space Station experiments.

FOCUS:

SPACE STATION

- **Real Structure**
- **Typical of Structures of Interest**
- **First Opportunity to Obtain Full-Scale Data for Correlation**
  - **Ground Test of Key Subassemblies**
  - **On-Orbit Flight Data**
- **Means for Developing Technology for Growth Station**

COFS III SCALE MODEL ASSEMBLY DUPLICATES SPACE STATION ASSEMBLY

The modular construction of the COFS III model will allow it to be assembled and tested in the same configurations as the Space Station assembly sequence.

COFS III

COFS III MODEL ASSEMBLY DUPLICATES SPACE STATION ASSEMBLY

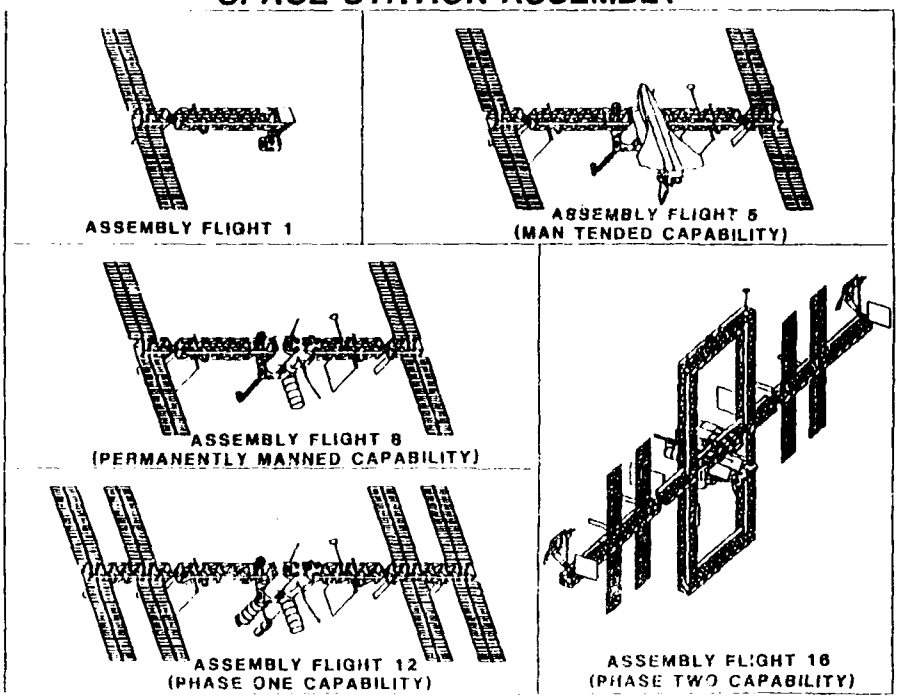

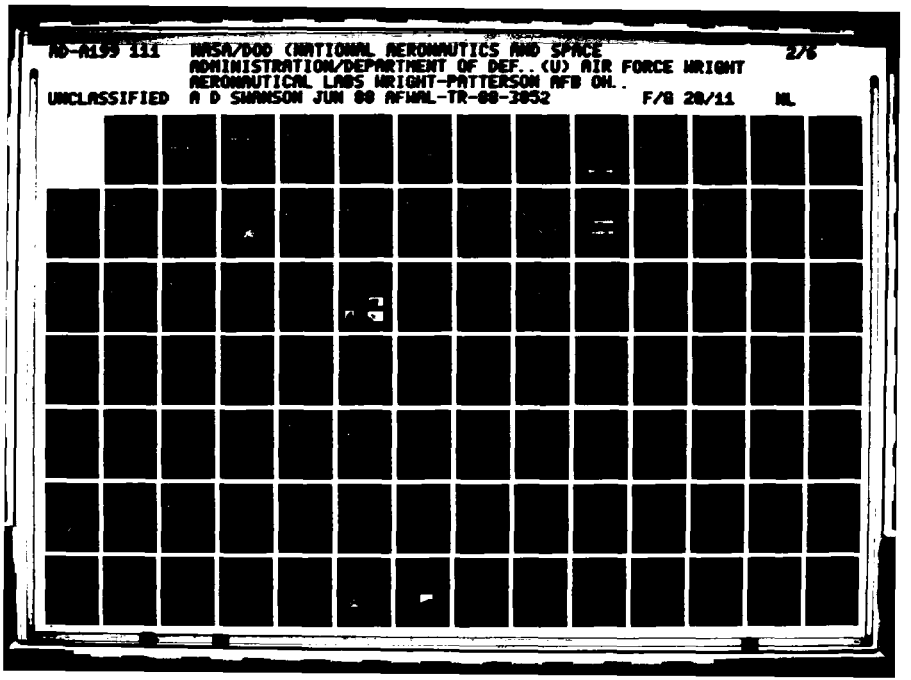
AD-A199 111 NASA/DOD (NATIONAL AERONAUTICS AND SPACE ADMINISTRATION/DEPARTMENT OF DEF..(U) AIR FORCE WRIGHT AERONAUTICAL LABS WRIGHT-PATTERSON AFB OH..
2/6
UNCLASSIFIED A D SWANSON JUN 88 AFWAL-TR-88-3052 F/G 20/11 NL

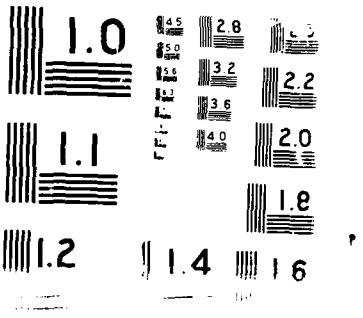
1.0
1.1
1.2
1.4
1.6
1.8
2.0
2.2
2.8
3.2
3.6
4.0
4.5
5.0
5.6

COFS III SCHEDULE

The schedule reveals that since last year, COFS III has been re-structured into three phases: a Studies Phase, a Pathfinder Phase, and a Primary Phase. Last year we reported on the activities within the Studies Phase which included in-house results on the effects of scaling on representative Space Station joints, composite tubes, and truss elements; and the results of a model definition study conducted under contract by the Lockheed Missiles & Space Company.

The Pathfinder Phase is now underway. The purpose of this phase is to develop the test techniques and suspension methods required to test large complex multibodied space structures. It will feature the development and testing of a hybrid-scale Pathfinder model. This hybrid-scale model will be small enough to fit in existing Langley facilities but will be designed to behave in a fashion similar to the larger Primary Phase replica model. The concept of hybrid scaling and a report on the conceptual design of the Pathfinder model will be discussed later.

Once the model suspension and testing technologies are in hand, we plan to proceed with the Primary Phase which will develop a detailed ground test database using a high-fidelity, near-replica model of the Space Station. These model test results will be correlated with analyses, and methods will be developed for predicting the on-orbit dynamic behavior of the Space Station. Ultimately, the model ground test results and the full-scale predictions will be correlated with the flight data obtained from the orbiting Space Station.

MULTI-BODY DYNAMICS & CONTROL TECHNOLOGY

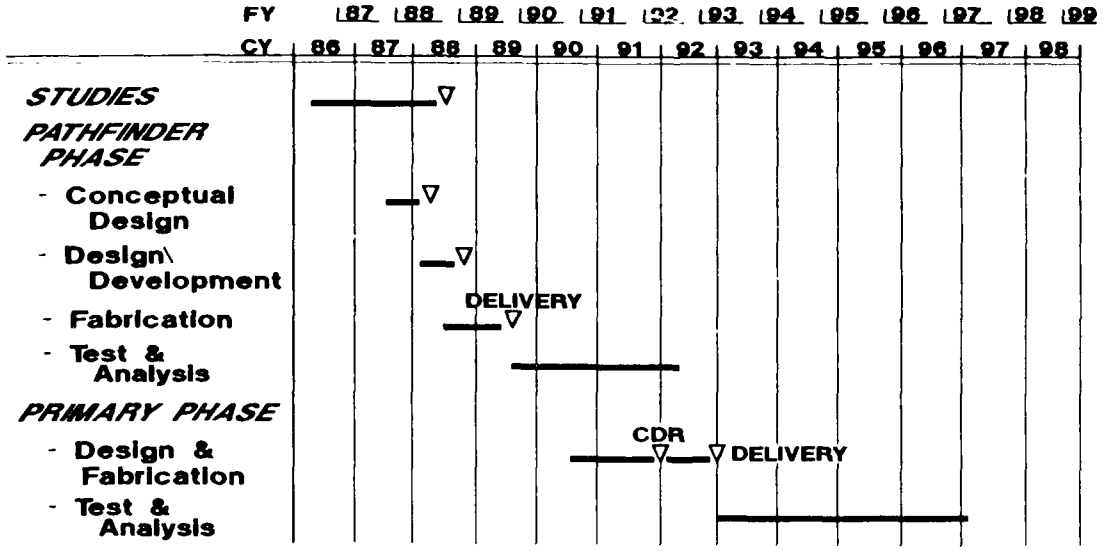

THE PATHFINDER PHASE

The Pathfinder Phase, the conceptual design of which is the subject of this paper, is focused on developing a small hybrid-scale dynamic model, a model suspension system, and a set of analytical tools. Once developed, the model will be used in the development of test techniques and suspension methods that will be required during the Primary Phase and for testing scale models of other truss-type space structures. The conceptual design, design/development, and fabrication of the hybrid-scale model and suspension system will be conducted under contract by the Lockheed Missiles & Space Company, while the testing will be conducted in-house at Langley.

The remainder of this presentation will focus on the conceptual design of the hybrid-scale pathfinder model.

PATHFINDER PHASE HYBRID MODEL - SUMMARY

- DEVELOPMENT OF TEST TECHNIQUES & SUSPENSION METHODS FOR TESTING REPLICA MODEL
- SIMULATES REPLICA MODEL DYNAMICS WHILE USING REALISTIC HARDWARE
- DESIGN DRIVEN BY
  - SIZE OF EXISTING TEST FACILITIES
  - MODEL COMPONENT MANUFACTURING FEASIBILITY/COST
- HYBRID MODEL PROVIDES ACCEPTABLE COMPROMISE
  - SMALLER TRUSS BAY SIZE (~1/10 SIZE)
  - REPRESENTATIVE JOINT HARDWARE (~1/4 SCALE)
  - DISTORTION OF TRUSS MEMBERS STIFFNESS AND MASS LOADING SIMULATES REPLICA MODEL DYNAMICS

PATHFINDER TEAM

The Pathfinder model is the third model in a logical progression of scale models proposed by NASA/LaRC, each characterized by increased fidelity. The first two smaller scale models are part of the research effort at NASA/LaRC to investigate scaling, testing, suspension behavior, etc. This related work at NASA/LaRC is described in a paper by McGowan, Edighoffer, and Ting entitled "Structural Dynamics Research on Scale Model Spacecraft Trusses" (see Session IV of this conference).

The work described in the remainder of this paper was performed by the team of companies and individuals shown below. Lockheed Missiles & Space Co. is the prime contractor. The task items listed under each company are indicative of the scope of activity during the Conceptual Design Phase.

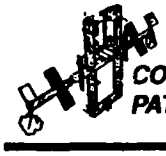

PATHFINDER TEAM

Lockheed

o NASA/LaRC Activities

See Paper by McGowan, et al, Session IV

o Lockheed Missiles & Space Co.

Domenic Sicoli, Marc Gronet, Earl Pinson, Larry Weisstein:
Project Management, Systems Engineering, Similarity Scaling,
Dynamic Modeling & Analysis, Suspension Analyses

o AEC-Able Engineering

Max Benton, Michael Everman:
Prototype Joint Design, Joint Fabrication, Component Design

o CSA Engineering

David Kienholz, Bradley Allen, Kevin Smith:
Joint Testing, Pre-Modal Test Analyses, Suspension Device Design

o Ed Crawley (MIT)

Consultant: Hybrid Scaling, Suspension Device Survey, Device Design

CONCEPTUAL DESIGN TASKS

The tasks performed during the first five months of the Pathfinder Conceptual Design Phase are listed below. The first set of tasks are directed toward the development of system-level requirements and the forecasting of the large space structure challenges that are likely to be encountered during the course of the Pathfinder project. Once identified, these challenges can be addressed early in the upcoming Design and Development Phase. The second set of tasks are directed toward hardware development. Previous studies at NASA/LaRC and Lockheed (1) have indicated that the cost of joint hardware is a large fraction of the total cost of a Space Station scale model. For this reason, a task was included to design, build, and test three 1/5-scale, low-cost, simulated Space Station joints.

CONCEPTUAL DESIGN TASKS

Lockheed

- **INVESTIGATE EXPECTED CHALLENGES**
  - **Hybrid Scaling**
  - **Hybrid-Scale Component Design**
  - **Model Assembly and Modal Testing**
  - **Suspension System Interactions**
  - **Soft Suspension Devices**
- **PROTOTYPE HARDWARE**
  - **Design, Build, and Test Simulated Joints**

CONFIGURATIONS SELECTED FOR STUDY
COFS III PATHFINDER PHASE

The figure below illustrates the Option 1 Phase 1 and Option 2 Enhanced configurations selected for study during the Conceptual Design Phase of the Pathfinder project. These two configurations were selected from a group of four that were initially baselined by NASA for the Space Station Phase C/D proposal effort. The COFS III Pathfinder model assembly and testing effort is intended to duplicate the Space Station flight assembly sequence. Other buildup stages will be studied in a later phase of the Pathfinder effort.

The lower portion of the figure lists data for a hybrid 1/5:1/10-scale model of these configurations. Both configurations will fit in the LaRC Building 1293A test facility. The scale model weight is on the order of 3,000 to 4,000 lbs. The frequency range of the first 10 system modes is 1 - 8 Hz, while the local appendage modes have frequencies as low as 0.5 Hz. Note that both configurations can be characterized as a large number of rigid masses that are connected by a lightweight truss structure. In other words, the flexible portions of the model (solar arrays, radiators, truss structure, etc.), make up about 10% of the total weight.

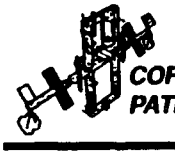

CONFIGURATIONS SELECTED FOR STUDY
COFS III PATHFINDER PHASE

Lockheed

OPTION 1 PHASE 1

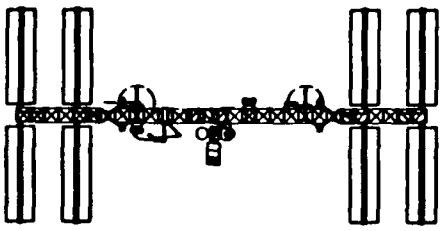

OPTION 2 ENHANCED

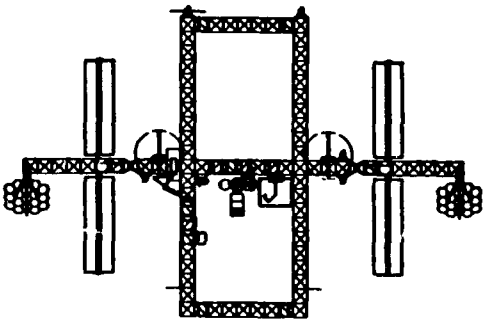

Dimensions* (ft)	**49.8 X 24.4**	**55.2 X 34.5**
Weight (lbs)	**3,422**	**4,202**
Frequency Range (1st 10 modes, Hz)	**1 - 7.4**	**1 - 8.2**
% Rigid Mass	**92%**	**89%**

***Values Shown Are for Hybrid 1/5:1/10-Scale**

HYBRID SCALING RATIONALE

A hybrid-scale model concept was proposed by NASA/LaRC to develop a low-cost research tool within three practical constraints. First, existing facilities can accomodate at most a 1/10-scale model. Second, compatibility with the Primary Phase of COFS III requires that the model have 1/4 or 1/5-scale dynamic properties. Finally, previous studies have shown that cost and manufacturing issues limit the practical joint scale factor to approximately 1/5-scale or larger.

In order to meet these requirements, a hybrid scaling approach (2,3) was proposed to design a research testbed that is 1/10-scale in overall size, has 1/5-scale joints, and exhibits 1/5-scale overall dynamic characteristics. While a replica scale model is desirable from a fidelity standpoint, most scale models do not replicate every detail of the full-scale article. Typically, only the degree of replication necessary to satisfy the relevant similarity laws for the behavior of interest is employed. For the case of the Pathfinder Space Station scale model, the predominant similarity laws are upheld.

HYBRID SCALING RATIONALE

Lockheed

- **Goal: Low-Cost Research Tool**
- **Pathfinder Practical Constraints**
  - **1/10-Scale Overall Size (Existing Facility)**
  - **1/4 or 1/5-Scale Dynamics (Primary Phase)**
  - **1/4 or 1/5-Scale Joints (Cost, Manufacturing)**
- **Replica Models Are The Exception, Not the Rule**
- **It Works**

SIMILARITY SCALING

There are many different ways to scale a pinned element truss, shown here with pin-pin boundary conditions. The intent here is to show that different scaling methods can yield properly scaled frequencies and mode shapes. The frequency, displacement, and mode shape of the full-scale truss is shown at right. One could construct a replica scale model of this truss that incorporates exact geometric and dynamic similarity. The frequency, displacement, and mode shape of the first mode of this replica 1/5-scale truss are shown. As shown in the third row, properly scaled frequencies, displacements, and mode shapes can also be obtained from a similarity-scaled truss model that has 1/5-scale mass and stiffness properties, but is 1/10-scale in size. In the last row, the hybrid-scale truss exhibits overall dynamic behavior that is identical to the similarity-scaled truss, using hybrid-scale truss struts. These hybrid-scale struts are identical to the struts used in the similarity-scaled model, except that the joints are 1/5-scale in size instead of 1/10-scale. The coefficent "c" accounts for the fore-shortening of the truss strut tube required to accomodate the longer joint in the same size strut. More precisely, the last truss model shown at the bottom of the chart is a similarity-scaled truss composed of hybrid-scale truss struts. In summary, all of these scale model trusses exhibit overall dynamic behavior that can be traced back to the behavior of the full-scale article.

SIMILARITY SCALING

Lockheed

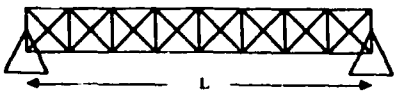	Full-Scale	Full-Scale	ω A $\sin(i\pi x/L)$
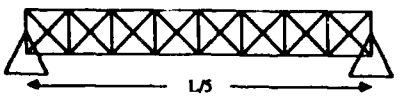	Replica-Scale Exact Geometric & Dynamic Similarity	Geometry 1/5 Dynamics 1/5 Joints 1/5, c = 1.	5ω A/5 $\sin(i\pi x/L)$
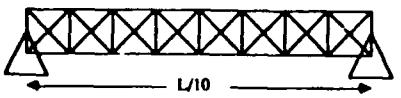	Geometric & Dynamic Similarity (Mass-Loaded)	Geometry 1/10 Dynamics 1/5 Joints 1/10, c = 1.	5ω A/5 $\sin(i\pi x/L)$
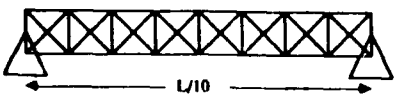	Hybrid Dynamic Similarity	Geometry 1/10 Dynamics 1/5 Joints 1/5, c = .91	5ω A/5 $\sin(i\pi x/L)$

WHY SO MUCH FREEDOM?

The previous chart indicated that one has considerable freedom in scaling a pinned-element truss. The key to proper scaling is to satisfy the similarity laws for the behavior of interest. For the case of the pinned-element truss, the overall dynamic behavior is based only on the axial behavior of the truss struts. The dynamic similarity laws for the axial behavior of a truss strut require that the strain energy distribution in the structure remains constant. This condition was used to derive the equations shown on the chart. To achieve stiffness similarity, one can vary the E, A, and L of the joint and tube as long as the stiffness ratio remains constant. In the hybrid-scale truss example on the previous chart, the E, A, and Lj of the joint are all 1/5-scale, and the joint has 1/5-scale stiffness. The total strut length (Lt + Lj) is 1/10-scale, making the scale factor for the strut tube length c times 1/10-scale, where the correction factor c is defined below. Finally, the E and A of the strut tube are sized so that the strut tube stiffness is 1/5-scale. Mass similarity is achieved by verifying that both the joint and strut tube have 1/5-scale mass properties. Note that this requirement can result in a change in material, as the EA and ρA of the tube are prescribed independently.

In summary, all of the scaling concepts shown on the previous chart exhibit overall 1/5-scale dynamic behavior because the components in each concept are designed to satisfy the relevant similarity scaling laws.

$$0.1(Lt + Lj) = 0.2(Lj) + 0.1c(Lt)$$

for Lt = 181.35", Lj = 15.5", c = 0.9145

WHY SO MUCH FREEDOM? Lockheed

- **Scaling: Satisfy Similarity Laws**
- **Global Truss Behavior Based on Axial Strut Behavior**
- **Dynamic Similarity Laws Require Axial Strain Energy Distribution Remain Constant**

Stiffness Similarity

$$\frac{K_{JOINT}}{K_{TUBE}} = \frac{(EA/L)_{JOINT}}{(EA/L)_{TUBE}} = \text{Constant}$$

Mass Similarity

$$M_{JOINT}/M_{TUBE} = \text{Constant}$$

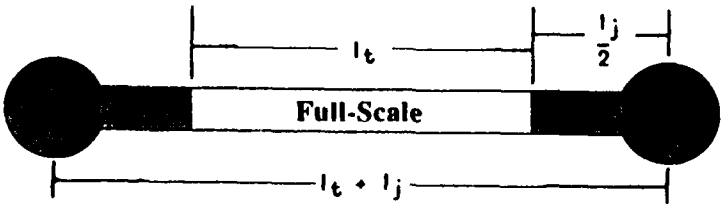

SIMILARITY LAWS

One can investigate a problem that is a step up in scaling complexity by examining a pinned-element truss with lumped masses and inertias which is subjected to combined axial, shear, bending, and torsion loads. One method of deriving the similarity laws for this example involves writing the equations of motion, assigning arbitrary scale factors to each quantity, and developing compatibility relationships between the scale factors (3). The compatibility relationships for scaling are derived in the same manner as those for units - the units for each term on the left-hand side of an equation are required to match the units for each term on the right-hand side. In order for the equations of motion for the behavior of interest to be satisfied, the compatibility relationships, or similarity laws, must be upheld. The similarity laws for the given truss example are shown below. They include many intuitive relationships such as F = MA, f = (K/M)**1/2, and T = FL. In order to construct a proper similarity-scaled model, the scale factors present in the similarity laws must be expressed in terms of the scale factor for the dynamics (λ = 1/5), and the scale factor for overall geometry (λ_l = 1/10). In addition, the design of the hybrid-scale truss struts must satisfy the similarity laws shown on the previous chart.

θ = rotation of truss	x = translation of truss	l = length of truss bay
E = truss strut modulus	A = truss strut area	F = force
t = time	M = mass	T = torque
I = mass inertia	$\ddot{x}$ = linear acceleration	$\ddot{\theta}$ = rotational acceleration

SIMILARITY LAWS

Lockheed

Truss with Lumped Masses and Inertias, Combined Axial, Shear, Bending, Torsion Loads

λ = 1/5 (Dynamics) λ_l = 1/10 (Overall Geometry)

$$\lambda_\theta = \lambda_x/\lambda_l \qquad \lambda_E\lambda_A\lambda_\theta = \lambda_F \qquad \lambda_t^{-2} = \lambda_E\lambda_A/(\lambda_M\lambda_l)$$

$$\lambda_T = \lambda_F\lambda_l \qquad \lambda_I = \lambda_M\lambda_l^2 \qquad \lambda_M\lambda_{\ddot{x}} = \lambda_F \qquad \lambda_I\lambda_{\ddot{\theta}} = \lambda_T$$

Solve for These Scale Factors in Terms of λ, λ_l

COMPARISON OF REPLICA AND HYBRID SCALING OF A TRUSS

This chart lists some of the scale factors satisfying the similarity laws for a pinned-element truss with masses and inertias under combined loading. The replica scale factors (functions of $\lambda = 1/5$) are compared with the hybrid scale factors (functions of $\lambda = 1/5$, $\lambda_l = 1/10$, and $c = .9145$).

The hybrid-scale quantities are divided into three groups. The first group includes dynamic quantities which are identical to the replica-scale values. The second group includes quantities that differ from a replica-scale model, but are nonetheless scaled. These similarity-scale factors must be employed in order to satisfy the dynamic similarity laws. The third group includes local scale factors for the truss strut tubes. As a check, note that if one sets $c = 1$, one recovers the similarity scaling laws. Similarly, if one then sets $\lambda_l = \lambda$, the replica scaling laws are recovered. The presence of the factor c in only the third group indicates that the presence of the of hybrid-scale truss struts ($c < 1$) is not reflected in the overall dynamics of the truss. However, the local bending behavior of the individual truss struts is not scaled (see bottom of chart). Fortunately, for the purposes of the Pathfinder model, these quantities are of secondary importance in the overall dynamics (the greater strut tube wall thickness and buckling load are actually preferable), and can be compromised somewhat without impacting the research goals of the Pathfinder project.

The scale factors shown here are for the overall dynamic behavior. Thus, when the Pathfinder scale model is employed as a CSI testbed, the controller variables (force, stroke, frequency, bandwidth, sampling rate, etc.) should be scaled using the factors shown.

COMPARISON OF REPLICA AND HYBRID SCALING OF A TRUSS

Lockheed

QUANTITY	REPLICA	VALUE AT 1/5-SCALE	HYBRID	VALUE AT 1/5:1/10-SCALE
DISPLACEMENT	λ	.20	λ	.20
MASS	λ^3	.008	λ^3	.008
FREQUENCY	λ^{-1}	5	λ^{-1}	5
ACCELERATION	λ^{-1}	5	λ^{-1}	5
FORCES	λ^2	.04	λ^2	.04
BAY LENGTH	λ	.20	λ_l	.10
ROTATION	1	1	λ/λ_l	2
MASS INERTIA	λ^5	.00032	$\lambda^3\lambda_l^2$	.00008
ROTATIONAL ACCEL	λ^{-2}	25	$(\lambda\lambda_l)^{-1}$	50
MOMENTS	λ^3	.008	$\lambda^2\lambda_l$	.004
STRUT LENGTH	λ	.20	$\lambda_l c$	.09145
STRUT EA	λ^2	.04	$\lambda\lambda_l c$	.0182
STRUT ρA	λ^2	.04	$\lambda^3/(\lambda_l c)$	.0875
STRUT E/ρ	1	1	$(\lambda_l c/\lambda)^2$	.2091

	REPLICA VALUE	HYBRID SCALE VALUE
WALL THICKNESS (in)	.0144 (Gr/Ep)	.0226 (AL, 0.4" OD)
STRUT LONGERON Pcr (lbs)	84.3	121.8
STRUT LOCAL/GLOBAL FREQ (Hz)	51.0	83.3
LONGERON SLENDERNESS RATIO	1.37×10^{-5}	4.61×10^{-5}

SCALING COMPROMISES

The next step in terms of complexity is to examine the scaling of the entire Pathfinder model, with its added appendages (solar arrays, radiators, etc.), payloads, modules and other components. In order for the hybrid scaling technique to work, the dynamic response behavior of these components must also be scaled by the factors shown on the previous chart. The approach used in scaling the entire Pathfinder model is the same: overall dynamic fidelity is achieved by preserving the dominant strain energy distribution. Compromises are made in scaling secondary behavior in order to achieve overall 1/5-scale dynamic fidelity in a 1/10-scale model. For the truss struts, local bending behavior is compromised in order to achieve dynamic similarity. For the appendages, axial behavior is compromised in order to get properly scaled bending and torsion modes. For the modules and payloads, local shell behavior is compromised, and these components are treated as rigid masses. Note that if one were constructing a replica model, both primary and secondary dynamic behavior would be properly scaled. The relative importance of these unscaled secondary behaviors is examined in the next chart.

SCALING COMPROMISES

Lockheed

- **Achieve Overall Dynamic Fidelity By Preserving the Dominant Strain Energy Distribution**

Component Scaled	Dominant Behavior	Secondary Behavior
Strut	Axial	Bending
Appendages, Payload Attach	Bending, Torsion	Axial
Modules, Payloads	Rigid	Local Shell Behavior

- **Replica Scaling: No Compromises**

FINITE ELEMENT CHECK OF HYBRID SCALING LAWS

The proper scaling of the hybrid scale Pathfinder model components can be checked using finite element (FE) models. FE models of the full-scale and hybrid-scale Space Station configurations were constructed and analyzed to obtain modal properties. The modes and frequencies of the hybrid-scale Space Station FE model can be post-multiplied by the appropriate scale factors and compared directly with corresponding results from the full-scale Space Station FE model. Two criteria are used to compare the full-scale (ϕ_A) and hybrid-scale (ϕ_B) modes: cross-orthogonality and modal assurance. Cross-orthogonality is a measure of the correlation of the modal mass distribution between the two modes, and modal assurance is a measure of the correlation of the shape between the two modes.

The results check well for both the Option 1 and Option 2 models, confirming that the hybrid and similarity scaling laws were applied properly. For the 75 modes included in each model, the cross-orthogonality and modal assurance values are no less than 0.99, and the frequency errors are no greater than 0.3%. These results confirm, for the configurations studied, that the scaling compromises listed on the previous chart have a secondary effect on the overall dynamics.

FINITE ELEMENT CHECK OF HYBRID SCALING LAWS

Lockheed

CONSTRUCT FEM MODELS
COMPARE FULL-SCALE AND HYBRID-SCALE MODES

Cross-Orthogonality

$$XO = [\phi_A]^T [M] [\phi_B]$$

XO = 1.0, Modes Are Identical
XO = 0.0, Modes Are Mass-Orthogonal

Modal Assurance Criterion

$$MAC = \sqrt{\frac{([\phi_A]^T[\phi_B])^2}{[\phi_A]^T[\phi_A] \cdot [\phi_B]^T[\phi_B]}}$$

MAC = 1.0, Modes Are Identical
MAC = 0.0, Modes Are Shape-Orthogonal

- Results Check Well for Both Option 1 and Option 2:
  - XO and MAC Values Are .99 - 1.0
  - Frequency Error < 0.3%
- Confirms Proper Selection of Dominant Strain Energy

COMPARISON OF 1/4:1/10 AND 1/5:1/10 SPACE STATION SCALE MODELS

Initially, the Pathfinder scale model was baselined with 1/4-scale joints. A study was conducted to investigate the use of 1/5-scale joints. Key comparisons are shown below (the overall model geometry is 1/10-scale in both cases). It is interesting to note that the strut tube material E/ρ for the 1/5:1/10-scale model is coincidentally the same as that for Aluminum, permitting the use of low-cost Aluminum struts. Overall, the 50% reduction in weight afforded by the selection of 1/5:1/10-scale versus 1/4:1/10-scale overshadows the small changes in the other properties. Since the reduction in weight increases safety and the ease of suspending the model, 1/5:1/10-scale was selected as the baseline scale for the Pathfinder model.

COMPARISON OF 1/4:1/10 AND 1/5:1/10 SPACE STATION MODELS

Lockheed

QUANTITY	1/4:1/10-SCALE	1/5:1/10-SCALE
Geometric Scale Factor	0.10	0.10
Option 1 Weight (lbs)	6681	3421
Option 2 Weight (lbs)	8207	4202
Strut Tube E/ρ (in)	6×10^7	1×10^8
Strut Tube Diameter (in)	0.50	0.40
1g Buckling Margin of Safety	X	1.25 X
Displacement Scale Factor	0.25	0.20
Acceleration Scale Factor	4.0	5.0

Conclusion: **Selection of 1/5:1/10-Scale Permits a 50% Reduction in Model Weight That is Offset By Only Small Changes in Other Properties**

WEIGHT AND SIZE OF 1/5:1/10-SCALE MODEL COMPONENTS

Listed in the figure are the scaled sizes and weights of various scale model components. The values range from a typical lab module that weighs 274 lbs and is 4.45 feet long, to a single truss bay, which weighs 4 lbs and is 1.64 feet on a side. Many of these items are small and light enough to be manipulated by hand during the Pathfinder model assembly.

Weight and Size of 1/5:1/10-Scale Model Components

Lockheed

Component	Weight (lbs)	Length (ft)
Module Cluster	**2097**	**15.08**
Lab Module	**274**	**4.45**
Node	**114**	**1.25**
Solar Dynamic Unit	**97**	**7.38**
Servicing Facility	**63**	**9.02**
Pallets	**7 - 46**	**0.64**
Radiator	**16**	**5.63**
Solar Arrays	**11**	**15.97**
Strut Diagonal	**.125**	**2.32**
Full Truss Bay	**4**	**1.64**

HYBRID SCALING CONCLUSIONS

In conclusion, the hybrid scaling method can be used to design a workable research testbed with 1/5-scale overall dynamics and 1/10-scale overall size. This is possible because the relevant similarity laws governing the global dynamic behavior for the space structure under consideration are upheld. The hybrid scaling technique is not completely general in that each of the scale model components must be scaled according to the of dominant strain energy type. All possible types of strain energy cannot always be scaled properly unless one constructs a replica model.

The hybrid scaling technique *results in scale factors for mass, frequency, joint* size, and linear motion quantities (force, displacement, velocity, and acceleration) that are identical to those for a replica 1/5-scale model. If replica 1/5-scale joints are used, the nonlinear axial behavior of these joints can theoretically be replicated (2). This degree of global fidelity is achieved by comprising the fidelity of some of the local bending behavior in the truss struts, the axial behavior in the flexible appendages, and the combined loading, shell-type behavior of the modules. However, these behaviors are of secondary importance to the global dynamics of the Space Station, which has virtually pinned truss struts, solar arrays whose lower modes are bending and torsion, and modules that are virtually rigid. The good cross-orthogonality and frequency checks between the full-scale and hybrid scale finite element model modes substantiate this result.

HYBRID SCALING CONCLUSIONS

Lockheed

- **Hybrid Scaling Laws Validated for Current Option 1 and Option 2 Configurations - Relevant Similarity Laws are Upheld**
- **Scale Model Components Are Properly Classified by Dominant Type of Strain Energy:**
  - **-Axial/Shear for Truss Struts**
  - **-Bending/Torsion for All Beams, Appendages**
  - **-Rigid Models for Modules, Payloads**
- **Mass, Frequency, Joint Size, and Linear Motion Quantities Are Identical to Those for a Replica Model**
- **Local Behavior is Not Scaled Properly, But it is of Secondary Order in the Overall Dynamic Response**

1/5-SCALE SIMULATED SPACE STATION JOINT

Three prototype 1/5-scale simulated Space Station joint sets were designed and fabricated during the Conceptual Design Phase. The design goal was to develop a low-cost, simulated, linear erectable joint. The 1/5-scale stiffness design requirement was based on the target stiffness for the full-scale NASA/LaRC Erectable Space Station joint. The design shown here incorporates standard threads and tolerances and is similar to the full-scale AEC-Able Quick-Connect joint.

COFS III PATHFINDER

1/5-Scale Simulated Space Station Joint

Lockheed

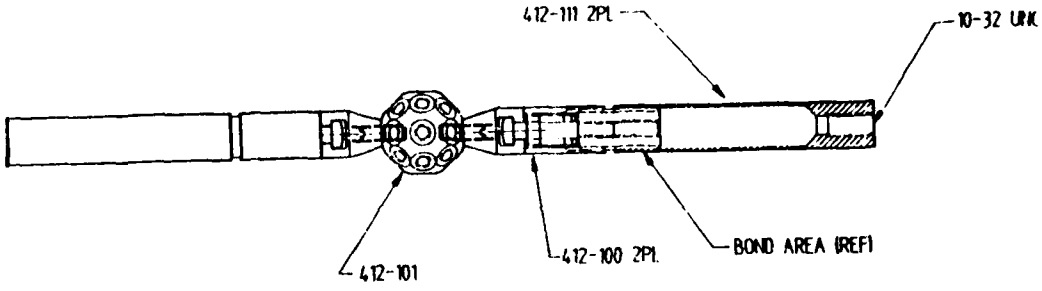

1/5-Scale Joint Design Requirements Are Based on the Target Stiffness of the LaRC Space Station Joint 94,400 lb/in @ 1/5-Scale

Design Goal:
Low Cost, Simulated, Linear, Erectable Joint

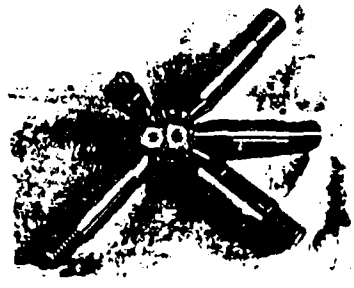

COMPONENT CONCEPTUAL DESIGN CONCLUSIONS

Design trades were conducted to develop design concepts for the scale model components that meet the hybrid-scale size, stiffness, mass, and inertia requirements. Because the hybrid-scale model has 1/5-scale mass properties and 1/10-scale geometric properties, a relative increase in density results. These studies yielded physical designs that meet the requirements. The rigid module design includes a thick shell with a dense tubular insert that is used to achieve the correct mass properties. The hybrid scaling laws for a 1/5:1/10-scale graphite-epoxy strut tube prescribe a material with an E/ρ of 100 million inches, permitting the use of low-cost Aluminum struts. The 1/5-scale simulated joints are not affected by the relative density increase because their mass and geometry are both 1/5-scale. Finally, there are many components that need further design development in the Full-Scale Space Station before sub-scale design requirements can be derived.

COMPONENT CONCEPTUAL DESIGN CONCLUSIONS

Lockheed

- **1/5:1/10 Hybrid Scale Designs Are Physically Realizable**
- **1/5-Scale Prototype Simulated Joints Designed and Fabricated (3) Based on LaRC Joint Target Stiffness**
- **Low-Cost Aluminum Strut Design Baselined**
- **Load-Bearing Thick-Shell Module Cluster Designed**
- **Many Components Need Further Definition in the Full-Scale Space Station Design (Utility Trays, Module-to-Truss Interconnects, Payload Pallets, etc.)**

1/5-SCALE JOINT TESTS

The three prototype joint-node-joint sets were tested for axial stiffness, linearity and damping over the range of expected scaled loads and frequencies. The scaled frequencies shown correspond to full-scale frequencies of 0.2, 1.0, and 5.0 Hz, and the loads correspond to full-scale strut loads of 50, 200, and 1000 lbs. In addition, three different preload torques were used on the locking collar during the joint assembly. The results indicate that the joint stiffness is dependent on on how the joint is assembled. If the joint was assembled loosely, a stiffness of 62,100 lb/in resulted. If the joint was assembled using a tool to provide 6.0 in-lbs of torque, a stiffness of 93,900 lb/in resulted. This is very close to the target stiffness of 94,400 lb/in.

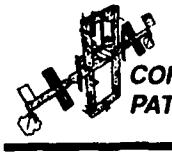

1/5-Scale Joint Tests

Lockheed

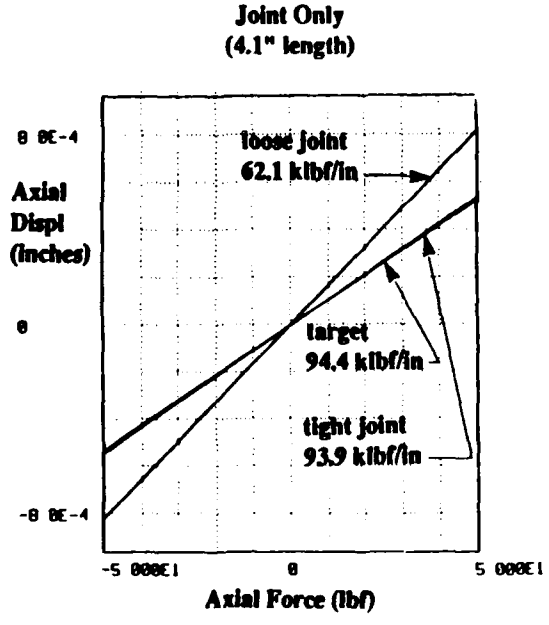

Three Joint-Node-Joint Combinations Tested:

Stiffness
Linearity
Damping
Cyclic Aging Effects

Tests Conducted Over Range of Expected Loads and Freq's:

1, 5, and 25 Hz
2, 8, and 40 lbf
3 Different Preload Torques

CONCLUSIONS: 1/5-SCALE JOINT TESTS

Listed below are the major conclusions from the prototype joint tests. The joint axial stiffness remained linear and nearly constant over the range of expected loads, frequencies, and after sinusoidal cycling. The fact that the damping in this linear joint is very low indicates that the Pathfinder model will be a very lightly-damped structure.

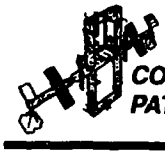

CONCLUSIONS: 1/5-SCALE JOINT TESTS

Lockheed

- **Joints Must Be Tool-Tightened - 6 in-lbs of Torque Required**
- **Joints Are Linear When Properly Assembled**
- **Stiffness Close to Target Value**
- **No Significant Stiffness Variation Over the Expected Range of Loads and Frequencies**
- **Damping is Very Low: $.002 < \eta < .007$**
- **No Significant Stiffness Change after 10^7 Cycles at 2 lbf**

The ideal suspension system for large space structures would permit unrestrained rigid-body motion and would simulate 0-g conditions by off-loading the scale model weight in a manner that produces no internal stresses in the model.

The "real-world" cable suspension system baselined for the Pathfinder model departs from the ideal in that it can potentially interact with and change the free-free modes of interest. Potential suspension system interactions are listed below.

SUSPENSION INTERACTIONS

Lockheed

Ideal Suspension System

- **Permits Unrestrained Rigid-Body Motion**
- **Simulates 0-g: Offloads All Weight**

Baseline Cable Suspension System Interactions

- **Vertical Motion Restrained**
- **Coupling with Pendulum Modes**
- **Cable String Mode Interactions, Damping**
- **Cables, Connectors, etc., add Weight**

Note: Soft (Bungee Cord) Suspension Ruled Out in Previous Study

OPTION 2 TEST CONFIGURATIONS
(LaRC, BUILDING 1293A)

The Option 2 Enhanced Space Station configuration is shown suspended in three orientations in the test facility. The model, building and human figure are shown to scale (the lateral position of the model in the facility is not necessarily as shown). Analyses were conducted to evaluate suspension interactions in all three orientations shown. In these studies, the potential suspension interactions listed on the previous page were incorporated into the finite element models.

The results of the static suspension analyses are summarized at the bottom of the chart. Seventeen to thirty-three cables are required to offload the weight of the larger rigid masses and to prevent static buckling for the Option 1 and Option 2 configurations, respectively. The given set of cable locations results in an average strut preload of 3 lbs (75 lbs full-scale) and a maximum strut preload in a few members of 22 lbs (550 lbs full-scale).

Option II Test Configurations

(LaRC, Bldg. 1293A)

Lockheed

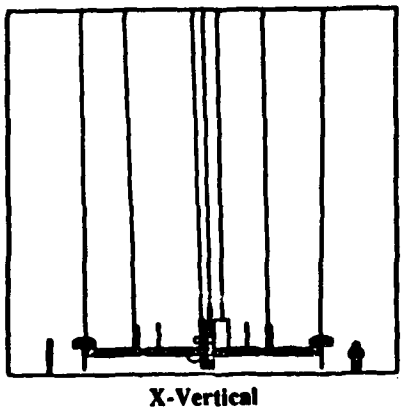

X-Vertical

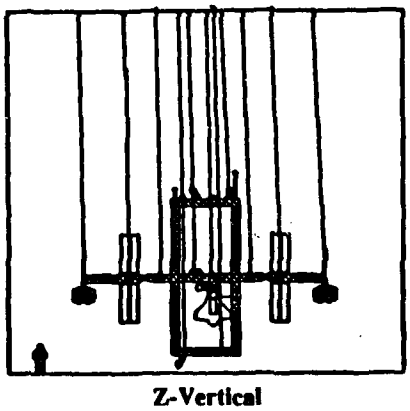

Z-Vertical

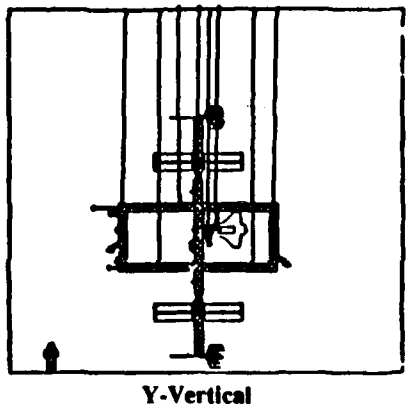

Y-Vertical

17 - 33 Cables Required to Prevent Static Buckling

Average Strut Preload = 3 lbs Maximum Strut Preload = 22 lbs

SUSPENSION INTERACTION SUMMARY

The bar charts below summarize the results of the suspension interaction analyses. The cross-orthogonality, modal assurance, and frequency comparison criteria were used to compare the modes from the free-free model with the modes from the suspended model. Because of the vertical-motion restraint imposed by the cables, modes that tend not to be affected by the suspension system are characteristically planar (i.e. the motion is parallel to the floor). The results indicate that for the Option 1 Space Station, 8 out of the first 10 system modes are relatively planar. Two of the modes are changed by the presence of the suspension system. Similarly, for the Option 2 Enhanced model, 6 out of the first 10 system modes are planar, and 4 modes are changed by the presence of the suspension system. In each case, the primary type of interaction was the vertical restraint imposed by the cables. Note that in order to obtain these results, the model must be assembled and tested in three and five orientations for the Option 1 and Option 2 configurations, respectively.

Suspension Interaction Summary

Lockheed

6 Modes Are Planar
4 F-F Modes Changed By Suspension

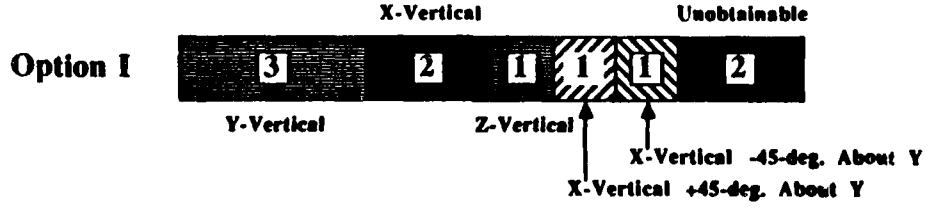

8 Modes Are Planar
2 F-F Modes Changed By Suspension

SOFT SUSPENSION SYSTEM STUDY

Studies were conducted to determine how "soft" the suspension system should be in order to fully simulated free-free vertical boundary conditions for all of the first 10 system modes. The trade shown below compares the cross-orthogonality between the free-free and suspended system modes versus isolator frequency for the Option 1 configuration. The vertical stiffness of each of the 17 isolators was sized so that each isolator would have the same frequency as if it were a single degree-of-freedom system. The isolators are assumed to be in series with an 80 foot pendulum cable, providing a horizontal isolation frequency of approximately 0.1 Hz. The results show that at soft suspension isolator frequencies greater than about 0.2 Hz, the first two system modes (7 & 8) begin to change because of the interactions with the suspension system. Note that the hard cable suspension system examined previously had an equivalent isolator frequency of 8 Hz.

Soft Suspension System Study Lockheed

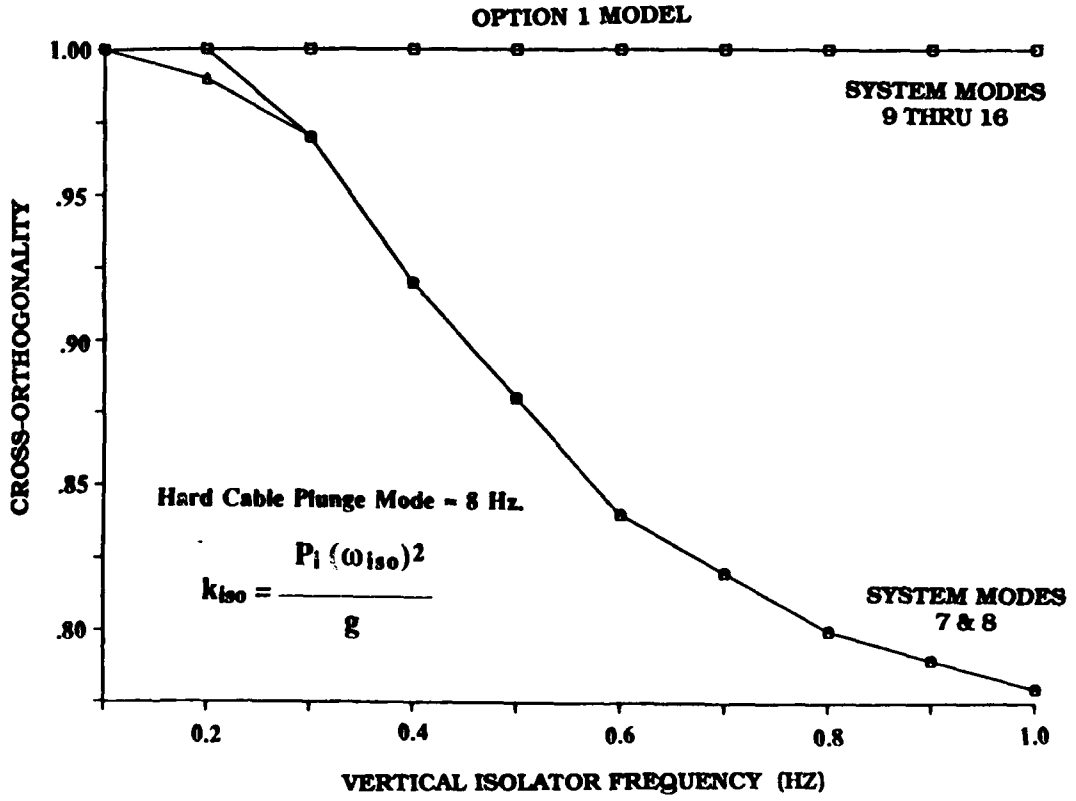

MODEL ASSEMBLY AND SUSPENSION
NASA/LaRC BUILDING 1293A

This figure accompanies the model assembly and suspension procedure described on the next page. The assembly procedure outlined here works best for the suspension orientation that has the x-axis vertical (the plane of the dual keels is parallel to the floor). In this orientation, almost the entire model is within the reach of personnel standing on the floor (components shown are not drawn to scale).

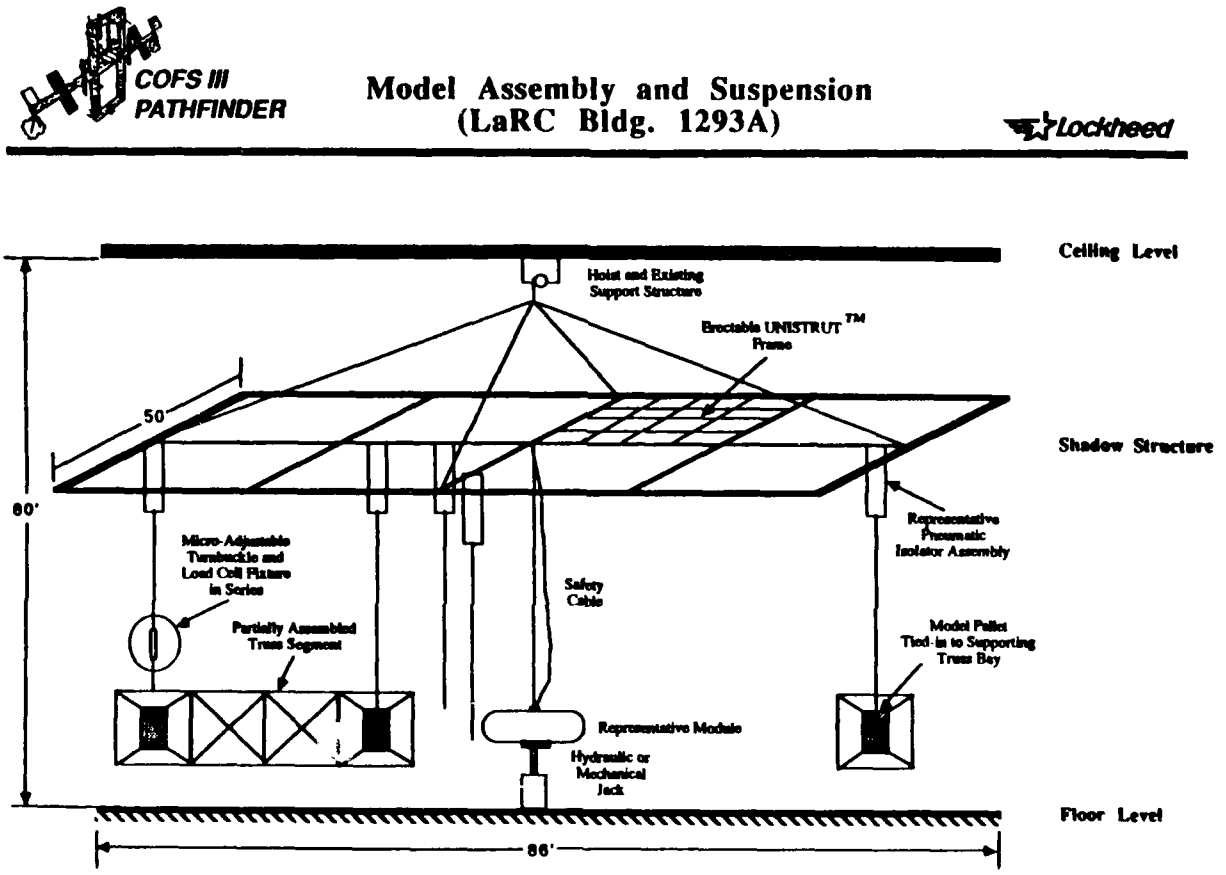

ASSEMBLY SCENARIO

The assembly scenario listed below was devised to maximize safety and access to the Pathfinder scale model. Since the Building 1293A facility was not specifically designed for dynamic testing, a shadow-structure concept was developed to provide structural attachment points for cables near the ceiling. This shadow structure, with the appropriate cables attached, is secured to the ceiling before the model assembly. The large rigid masses are jacked from the floor and attached to the dangling cables. In this way, load is transferred from the floor to the cables in a sequential manner, adjusting the vertical position of each rigid mass individually as a single degree-of-freedom system. When all the rigid masses are adjusted to the correct height above the floor, over 90% of the weight of the scale model is directly off-loaded by the cables. The final step is to assemble the truss structure and the remainder of the model between the rigid mass "pendulums". If the rigid masses are calibrated to the correct height, no further adjustment of the cables is required to produce a level model with a tolerable level of preload (the added 10% of the weight has little effect on the load distribution between the cables). One of the benefits of this procedure is that it does not rely on an unverified analytical model to predict the cable tensions for a statically-indeterminant, flexible space structure. However, the safety of this procedure can be enhanced by monitoring the loads in the cables and in key elements of the scale model during assembly.

ASSEMBLY SCENARIO EMPHASIZES SAFETY, ACCESS

Lockheed

1) Assemble Shadow Structure on Floor and Attach Suspension Cables

2) Hoist Shadow Structure to Ceiling, Secure

3) Jack Rigid Masses from Floor and Attach to Dangling Cables. Adjust Vertical Position. 90% of Model Weight is Now Off-loaded

4) Assemble Structure, etc., Between Rigid Mass Pendulums, Make Micro-Adjustments*

* **If Vertical Position of Rigid Masses is Correct, No Further Adjustment Necessary. (No Reliance on Unverified Math Model)**

CABLE STIFFNESS AND LOCAL MODEL STIFFNESS AFFECT POSITION-ERROR SENSITIVITY

The previous chart showed that further adjustment of the cables is unnecessary if the large rigid masses are aligned correctly. This chart presents the results of a study to evaluate the sensitivity of the gravity preloads in the model to the correct alignment of the large rigid masses. Two cases were examined to bound the problem, both with the Option 1 model suspended in the x-axis vertical orientation. In the first case, the module cluster is out of vertical alignment with rest of the model. In the second case, only the cable attached to the Electrical Power System (EPS) pallet mass at the tip of the transverse boom is out of vertical alignment. The diagram at left shows a spring representing the stiffness of the cable, the rigid mass, and a spring representing the load path through the Pathfinder model. As the offset increases, load is transferred from the cable to the model. The finite element results at right show that a module cluster vertical offset of 0.3 inches transfers enough load from the module cables to the scale model to cause local buckling in some of the truss struts. Similarly, an EPS mass misalignment of 0.5 inches is enough to cause local buckling in the transverse boom. For both of these cases, the cable stiffness was sized to provide a safety factor of 5, resulting in a uniform sag of 0.15 inches. The results of this study indicate that there is a trade between the safety factor for the cables and the safety factor for the model due to misalignment. Softer cables would sag more, providing more margin for error in the alignment of the rigid masses. The results also suggest that it is important to accurately position the large rigid masses before assembling the remainder of the truss structure.

Cable Stiffness and Local Model Stiffness Affect Position Error Sensitivity

Lockheed

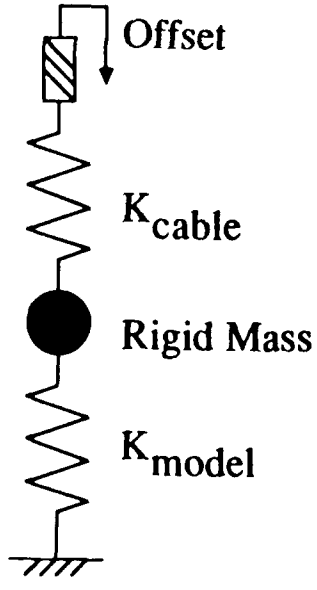

$1/K_{tot} = 1/K_c + 1/K_m$

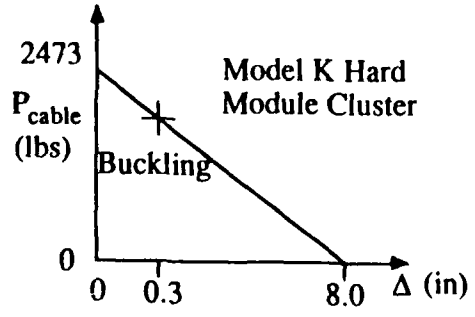

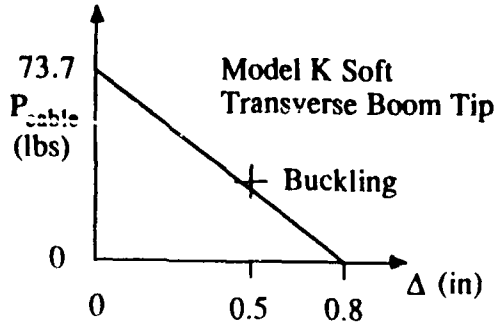

Initial Cable Sag = .15"

CASE FOR SOFT SUSPENSION SYSTEM

The results presented so far suggest strongly that there are many potential benefits associated with the use of soft suspension devices in the testing of large space structures. In addition to providing a better 0-g simulation, these devices could increase safety and access while reducing test time because the model need only be assembled and tested once, in the easily accessible x-vertical configuration. This potential for reduced cost should be traded with the cost of developing and procuring adequate suspension devices. The hard-cable suspension system will serve as a good starting point and backup, since about half of the modes in each configuration are planar.

Case for Soft Suspension System

Lockheed

- **Better 0-g Simulation**
- **Only 1 Suspension Orientation Required**
  - **Increased Access: X-Vertical**
  - **Increased Safety: X-Vertical, Less Assembly**
  - **More Time: Fewer Modal Tests Needed**
- **Potential for Reduced Cost**
- **Keep Hard-Cable Baseline as a Backup**

FIRST-CUT RANKING OF SUSPENSION SYSTEM OPTIONS

This chart presents a survey of candidate soft suspension devices. The first criterion addressed was the fundamental engineering feasibility of each concept. Mechanical Zero Spring Rate Mechanisms (ZSRM's) and pneumatic systems were found to be feasible. Hydraulic systems require fast-acting servo-valves which are at the state of the art. Electric motors with sufficient stall torque capability are, in general, not fast enough. The constant pressure pneumatic system and hydraulic system are more complex and therefore costly, due to the need for active supply and valving. Weight aloft and size are engineering judgement, based on the conceptual work done. The ZSRM and pneumatic "constant" volume systems are reversible, conservative systems, requiring no power addition. The others dissipate power irreversibly and could absorb up to 100 KW in operation. Friction and moving mass are likely to be a problem in the ZSRM and hydraulic systems. Stiffness is difficult to vary in the mechanical ZSRM. The bottom line indicates that by comparison, the hydraulic and electric items are less attractive, and that a "constant" volume pneumatic device has advantages over a constant pressure one. The "constant" volume pneumatic and the ZSRM are therefore the two systems worthy of further development for the Pathfinder project.

First-Cut Ranking of Suspension System Options

Lockheed

CRITERION	ZSRM	PNEUMATIC (V)	PNEUMATIC (P)	HYDRAULIC	ELECTRIC
FEASIBILITY	+	+	+	o	o
COMPLEXITY	+	+	-	-	o
COST	+	+	o	-	o
WEIGHT ALOFT	+	o	o	+	-
SIZE	+	-	o	-	o
POWER	+	+	o	-	-
FRICTION/DAMPING	-	o	o	o	+
MOVING MASS	-	+	+	-	o
STIFFNESS VARIABILITY	-	+	+	o	+
TOTALS*	3	5	2	-4	0

+ = Good o = Neutral - = Bad

*Hybrid Designs Show Promise

SUMMARY

In summary, the conceptual design phase effort has resulted in a basic understanding of hybrid scaling, hybrid-scale component design, 1/5-scale simulated joint design, and the modal testing requirements for the Pathfinder model. The LSS CSI challenges that have been identified include the model assembly and logistics, the strong potential for suspension system interactions, and the need for a low-frequency suspension system. In addition, the very-low damping exhibited by the joints in the Pathfinder model make it an ideal research tool for Control-Structure Interaction damping experiments. Finally, the Pathfinder model can also be used to address the challenges of substructured testing by comparing results from substructured and fully-mated tests. In the particular case of the Space Station structural and controls verification, this comparison would be useful as no fully-assembled tests of the full-scale hardware are planned.

SUMMARY

Lockheed

Basic Understanding

- **Hybrid Scaling of Space Station Model**
- **Hybrid-Scale Component Designs Are Physically Realizable**
- **Prototype Joint Design Meets Requirements**
- **Modal Testing Requirements Not Unusual**

Research Tool for LSS CSI Challenges

- **Model Assembly is A Sensitive Procedure**
- **Low-Frequency Suspension System Enhances Model**
- **Lightly-Damped Space Structure - CSI Testbed**
- **Substructured vs. Fully Assembled Testing**

REFERENCES

1) Gronet, M.J., Pinson, E.D., Voqui, H.L., Crawley, E.F., and Everman, M.R., "Preliminary Design, Analysis, and Costing of a Dynamic Scale Model of the NASA Space Station", NASA CR-4068, July 1987.

2) Crawley, E.F. and Sigler, J.L., "Design and Testing of Linear and Nonlinear Scaled Models of Flexible Space Structures", Presented at the AIAA 28th Structural Dynamics & Materials Conference, 6-8 April 1987, Monterey, CA.

3) Baker, W.E., Westine, P.S., and Dodge, F.T., Similarity Methods in Engineering Dynamics, Hayden Book Co., Inc., Rochelle Park, N.J., 1973, Chapters 1,2 and 11.

OPTIMIZATION OF LARGE SPACE STRUCTURES WITH ACTIVE CONTROLS[1]

A. L. Hale and F. D. Hauser
General Dynamics Space Systems Division

N. S. Khot
Air Force Wright Aeronautical Laboratories (AFWAL/FIBR)

Second NASA/DOD Control/Structures Interaction Technology Conference
Colorado Springs, Colorado

17-19 November 1987

---

[1]Sponsored by Flight Dynamics Laboratory, Air Force Wright Aeronautical Laboratories, Aeronautical Systems Division (AFSC), United States Air Force, Wright-Patterson AFB, Ohio 45433-6553.

INTRODUCTION

The objective herein is to outline the Air Force contract entitled "Optimization of Large Space Structures With Active Controls" (OLSSWAC). The Air Force is interested in large space structures for such missions as atmospheric surveillance, surface target reconnaissance, space vehicle detection and tracking, as well as direct force application. Structures for these types of missions are quite flexible relative to associated requirements for pointing and retargeting, the latter requiring structural vibrations to be suppressed rapidly. To most efficiently satisfy the quite stringent mission requirements, the space structure and its control system must be designed in some optimal manner. Design tradeoffs among structural weight (mass), control force and/or torque, control power, and control robustness, among other things, must be considered. Developing an understanding of these tradeoffs and developing generic software for combined structures and controls design studies are major objectives of the OLSSWAC program.

As shown in the block diagram below, both the structure and the active control system provide feedback control to the fixed parts of the system. Analysis methods and design procedures for structures and controls overlap when viewed in the common context of their feedback effects. Taking a common viewpoint allows adjusting the structural design variables and the control design variables in the same basic way to optimize their combined effects on system performance.

NEW SPACECRAFT STRUCTURES WILL INTERACT SIGNIFICANTLY WITH THEIR CONTROL SYSTEMS. DESIGNING THE BEST COUPLED SYSTEM IS KEY TO ACHIEVING MISSION SUCCESS.

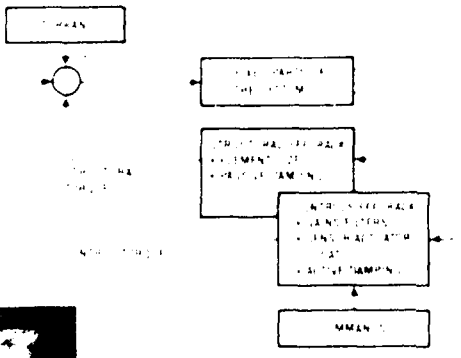

SPACE BASED RADAR ADVANCED

OFFSET COMMUNICATION ANTENNA

LARGE SURVEILLANCE SYSTEM

OLSSWAC PROGRAM OVERVIEW

The objectives, approach, and payoff of the program are listed. The effort, begun in July 1987 and to last 40 months, is an unclassified analytical development, not a system study. The major emphasis of the program is the integration of the structural design and control design instead of treating the two as separate entities. Generic software will be developed for finding an optimal structural and active control design for a given geometry of structure. The software will be able to optimize for specific requirements on slewing, vibration, and pointing, as well as constraints on structural behavior and controlled response. The software product will be a stand alone, non-proprietary computer code written in ANSI standard FORTRAN, which will be ported to, and tested on, a variety of computers from mini- to supercomputers. Six design studies of realistic large space structures will be conducted using the software. The purpose of the design studies is both to demonstrate the software's capabilities and to study tradeoffs between structure and controls.

The technical effort is divided into four tasks. The first task includes reviewing the state-of-the-art and defining the integrated software-system's architecture. The second task is primarily coding of individual engineering modules for structural analysis, control analysis, optimization, and sensitivity analysis. Connecting the modules to form an integrated pilot design system is the objective of the third task. Design studies of realistic space structures will be conducted in the last task.

OPTIMIZATION OF LARGE SPACE STRUCTURES WITH ACTIVE CONTROLS

PROGRAM OVERVIEW

OBJECTIVES

- INTEGRATE THE DESIGN OF SPACE STRUCTURES WITH THE DESIGN OF CONTROL SYSTEMS INSTEAD OF TREATING THE TWO AS SEPARATE ENTITIES
- DEVELOP GENERIC SOFTWARE FOR PERFORMING INTEGRATED STRUCTURAL AND CONTROL DESIGN
- DEMONSTRATE THE SOFTWARE'S CAPABILITIES ON REALISTIC LARGE SPACE STRUCTURES

APPROACH

- REVIEW THE STATE-OF-THE-ART
- DEFINE THE SOFTWARE-SYSTEM ARCHITECTURE
- CODE THE ENGINEERING MODULES
  - STRUCTURAL ANALYSIS
  - OPTIMIZATION
  - CONTROL ANALYSIS
  - SENSITIVITY ANALYSIS
- DEVELOP A PILOT DESIGN SYSTEM
  - ESTABLISH INTERMODULE COMMUNICATON
  - DEFINE AND SOLVE BENCHMARK PROBLEMS
- PERFORM DESIGN STUDIES OF REALISTIC LARGE SPACE STRUCTURES
- DOCUMENT THE STUDIES AND THE SOFTWARE

PAYOFF

ABILITY TO DESIGN A SPACE STRUCTURE AND ITS CONTROL SYSTEM IN AN OPTIMAL MANNER SO THAT MISSION REQUIREMENTS ARE SATISIFIED MOST EFFICIENTLY

372 224 42

APPROACHES TO INTEGRATED STRUCTURAL AND CONTROL OPTIMIZATION

Two approaches to integrating structural design with control design can be distinguished. One approach simply mechanizes the conventional sequential design procedure (below left). The other approach tightly couples the structures and controls design procedures (below right). Examples of both approaches can be found in the research literature on integrated structural and control optimization. The second approach is chosen for this program as it provides the most design flexibility and software extensibility.

TWO APPROACHES TO STRUCTURE – CONTROL DESIGN OPTIMIZATION

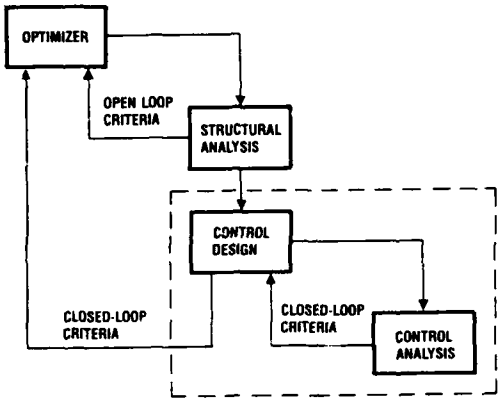

MECHANIZE THE CONVENTIONAL SEQUENTIAL STRUCTURES AND CONTROLS DESIGN PROCEDURE

- **STRAIGHT FORWARD TO IMPLEMENT**
- **TREATS STRUCTURE/CONTROL INTERACTION INDIRECTLY**

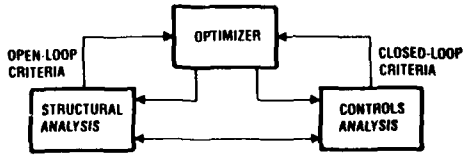

TIGHTLY INTEGRATE BOTH THE STRUCTURES AND CONTROLS DISCIPLINES

CHOSEN BECAUSE:

- **IT IS THE MOST FLEXIBLE**
- **IT IS ALSO THE MOST DIFFICULT TO IMPLEMENT**
- **CONTAINS MECHANIZED SEQUENTIAL DESIGN AS A SPECIAL CASE**

272 224 4

OLSSWAC OPTIMIZATION APPROACH

The optimization approach is that of "mechanized iterative analysis." In any design problem, and particularly in complex structures and controls design problems, an understanding of candidate designs can only be obtained by studying the results of complete analyses. Design changes are made based on the results of the analyses. Once a problem is quantitatively defined, an optimization algorithm can "automate" iterative design changes. However, for complex problems a major difficulty is simply defining the best optimization problem, i.e., quantifying what the constraints are and what the objective of the optimization is. The software will be a tool for making changes in the problem definition quickly and easily. The choice of an objective and of constraints for the optimization can be made from a set of criteria. Thus, an engineer (user) can change the objective and the constraints as the design tradeoffs inherent in the structure and its controller become better understood. The user will thus be able to focus on the meaning of different problem definitions, while extraneous details in going from one optimization problem definition to another will be mechanized.

STRUCTURE/CONTROLLER OPTIMIZATION BY MECHANIZED ITERATIVE ANALYSIS

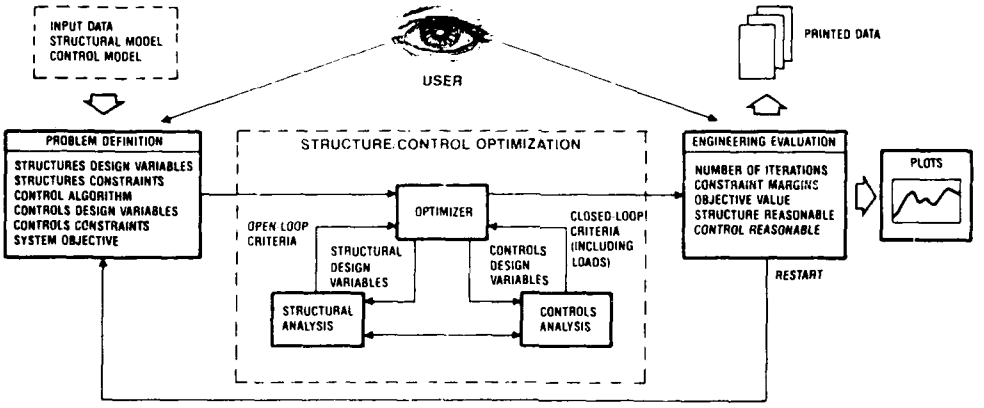

- HUNTING FOR THE PROBLEM, AS WELL AS HUNTING FOR THE ANSWER TO THE PROBLEM, IS KEY
- STRUCTURES AND CONTROLS DESIGN ARE TREATED IN THE SAME FUNDAMENTAL WAY
- THE USER SPECIFIES AN OBJECTIVE FUNCTION AND THE CONSTRAINTS FROM THE SET OF AVAILABLE CRITERIA
- BASED ON THE SPECIFIED OBJECTIVE FUNCTION AND CONSTRAINTS, APPROPRIATE ANALYSES ARE PERFORMED AT EACH ITERATION
- ITERATION-TO-ITERATION MONITORING AND EASY RESTART ARE EMPHASIZED

272-224-5

SOFTWARE ARCHITECTURE

The software system will be modular with user input/output controlled by an executive system. There will be four analysis modules driven by the executive system as shown. Communication among the modules, as well as analysis sequencing, will be controlled by the executive system. Well-structured input and output data and a global data storage system will make the program easy to use. Input data separation will allow a user to deal with logically separate data items. For example, those data associated with model definition are logically separate from those specifying the analyses to be performed. The global data storage system will provide central data storage and will be used as the nucleus of an effective restart mechanism.

SOFTWARE SYSTEM ARCHITECTURE

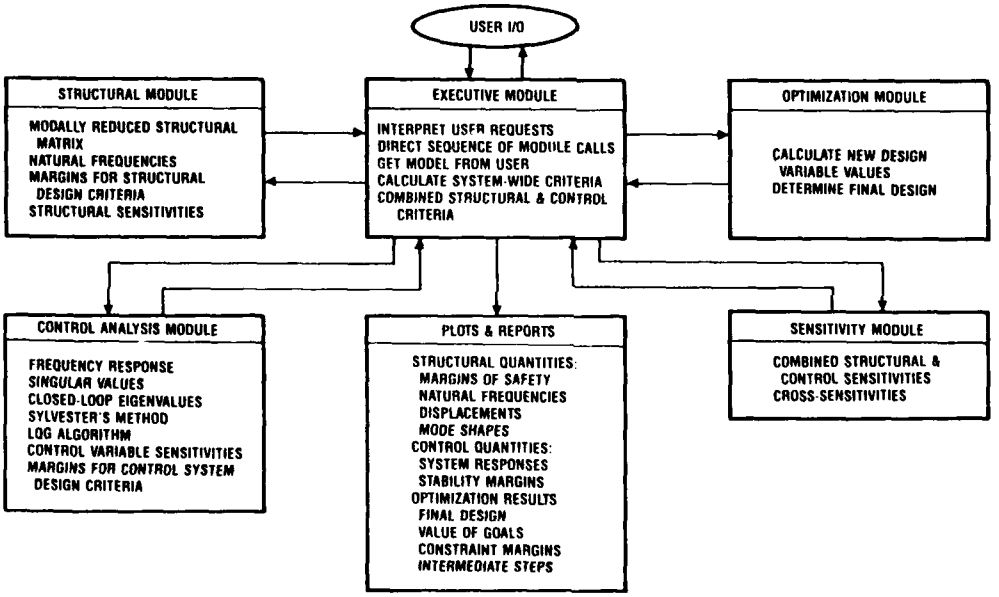

OUR MODULAR SYSTEM WILL TIGHTLY INTEGRATE THE STRUCTURES AND CONTROLS DISCIPLINES FOR EFFICIENT DESIGN OPTIMIZATION

272 224 15

STRUCTURAL ANALYSIS MODULE CAPABILITIES

NASTRAN is a pervasively used finite element structural analysis program with many existing preprocessing programs for preparing structural finite element models and for directly creating NASTRAN bulk data files. For upward compatibility with NASTRAN, the structural analysis module of this program will perform a subset of the analyses of NASTRAN and will use a subset of the input records recognized by NASTRAN. As a minimum, the program will support the NASTRAN bulk data records listed (left column). Note that the finite element library will provide only those elements critical to building models of large space structures. Specifically, spring, damper, point mass, rod, and beam elements will be provided, as will a general element or substructure. The supported analyses are: static analysis due to force and thermal loads, normal modes analysis for natural frequencies and mode shapes, modal transient response analysis, and modal frequency response analysis.

Although NASTRAN input data formats support limited design variable specification for elements, there is a need to permit rod- and bar-element cross sectional dimensions as design variables, a feature not directly supported by NASTRAN. This capability is useful in the case of truss-reflector structures, for example, where the face tubes are of one cross section, the diagonals another, and the back tubes yet another. In such a case, only six design variables, three diameters and three thicknesses, are needed. To support such design variable specification as well as other specifically tailored structural input data, NASTRAN bulk data records will be augmented. Some selected additional record types are listed (right column).

INPUT DATA TO THE STRUCTURAL ANALYSIS MODULE WILL BE SIMILAR TO NASTRAN

Bulk Data Record	Contents
AELIST	Aerodynamic [illegible]
BAR	[illegible]
CELAS1	Scalar spring & damper [illegible]
CONM2	Concentrated mass [illegible]
CROD	Connections for rod element
DMIG	Direct matrix input [illegible]
EIGR	Real eigenvalue extraction data
FORCE	Static load vector
GENEL	General element stiffness [illegible]
GRAV	Gravity vector
GRDSET	Default values for [illegible]
GRID	Locations of grid points
LOAD	Static load combination
MAT1	Isotropic material properties
MOMENT	Static moment vector
PLOAD1	Line load on bar element
PLOTEL	Dummy plotting element
PBAR	Properties of bar elements
PELAS	Scalar spring & damper [illegible]
PROD	Properties of rod elements
RFORCE	Static load due to [illegible]
SEQSET	Grid point sequence [illegible] permutation
SUPPORT	Subpoint [illegible]
TEMP	Grid point temperature
TEMPD	Default grid point temperature
TEMPRB	Rod & bar temperature

THE FORMAT OF MANY NASTRAN BULK DATA RECORDS WILL BE USED

Additional Record Type	Contents
CSECDEF	Cross section variable definition for tube
GROUPEL	Group of elements whose matrices vary together
GROUPEP	Stiffness polynomial for element group variation
GROUPEPD	Damping polynomial for element group variations
GROUPEPM	Mass polynomial for element group variation

THE NASTRAN BULK DATA RECORDS WILL BE AUGMENTED TO PROVIDE EFFICIENT DESIGN VARIABLE CAPABILITIES

STRUCTURAL ANALYSIS MODULE APPROACH

A structural analysis module that is to be used in a design oriented environment must have two characteristics that are not always found in stand alone programs. First, since analyses will be repeated many times as part of an iterative design procedure, only those computations that involve different data from one design to the next need to be repeated. Second, the structural model must be updated efficiently as the design is changed. The design task herein is restricted to changing the member sizes rather than the structural geometry. In this case, the discrete mass and stiffness matrices can be represented in the general form of a summation of invariant matrices, each multiplying a single design variable. Once the finite element model has been created, new designs can easily and efficiently be created by simple scalar multiplications of matrices followed by matrix additions. The same process can be used with design variable linking to create models of varying complexity without the need to return to the finite element assembly module.

It is common practice to reduce the structural dynamic model to those generalized coordinates defined by a number of low frequency normal modes. Here, the normal modes will be computed using the nominal values of the design variables. The invariant matrices will then be transformed by the set of kept normal mode shapes. Further, for at least a certain number of design steps, if not for a complete optimization cycle, the same set of mode shapes will be used. This means that as the design changes the generalized coordinates are defined by merely shape vectors rather than normal modes. Some accuracy in the analysis will be sacrificed, but this is more than offset by the gain in efficiency created by not computing updated mode shapes at each iteration.

FOR EFFICIENCY IN REDESIGN DURING OPTIMIZATION, STRUCTURAL MATRICES WILL BE SPLIT INTO INVARIANT MATRICES MULTIPLYING POLYNOMIAL COEFFICIENTS

STRUCTURAL MATRIX

$$[Z] = [Z_0] + a_1^{h_1} \cdot [Z_1] + a_2^{h_2} \cdot [Z_2] + \ldots$$

VARIABLES	
Z_i	= STRUCTURAL MATRICES (K,B,M)
a_i	= DESIGN VARIABLE
h_i	= EXPONENT

- WE WILL USE A TRUNCATED SET OF NORMAL MODES TO FORM A REDUCED-ORDER STRUCTURAL MODEL
- THE INVARIANT MATRICES WILL BE TRANSFORMED BY THE SET OF KEPT MODES
- THE TRANSFORMATION ARE BE UPDATED PERIODICALLY, BUT NOT AT EACH DESIGN ITERATION

CONTROL ANALYSIS MODULE APPROACH

Turning now to control design methodology, control system analysis and design procedures can be categorized as either direct or indirect. In the direct methods, the procedure varies the gains, filter coefficients, and sensor and actuator locations in a preselected feedback configuration. In indirect methods, the feedback is structured and its coefficients are established by means of an algorithm that centers around an intermediate goal function. The classical controls design procedure and those procedures that mechanize this manual procedure via mathematical optimization are examples of direct methods. The linear quadratic regulator (LQR) and the linear quadratic Gaussian (LQG) procedures, as well as their many variants, are examples of indirect methods.

Common to all of the direct and indirect methods is the use of analysis programs that evaluate the design against particular criteria, e.g., criteria for slewing and pointing performance, vibration control, robustness, and structural and actuator forces. These analysis programs include subroutines that compute closed-loop transient responses, open-loop and closed-loop frequency responses, singular-value frequency responses, root loci, etc.

Selected direct and indirect control design approaches will both be incorporated into the mechanized analysis software of this program. The mechanized analysis approach uses individual analyses as tools for determining the "goodness" of a particular controls design. As shown, whether the design procedure is direct or indirect, design variables are adjusted based on the results of analyses.

THERE ARE TWO BASIC TYPES OF CONTROL DESIGN METHODS

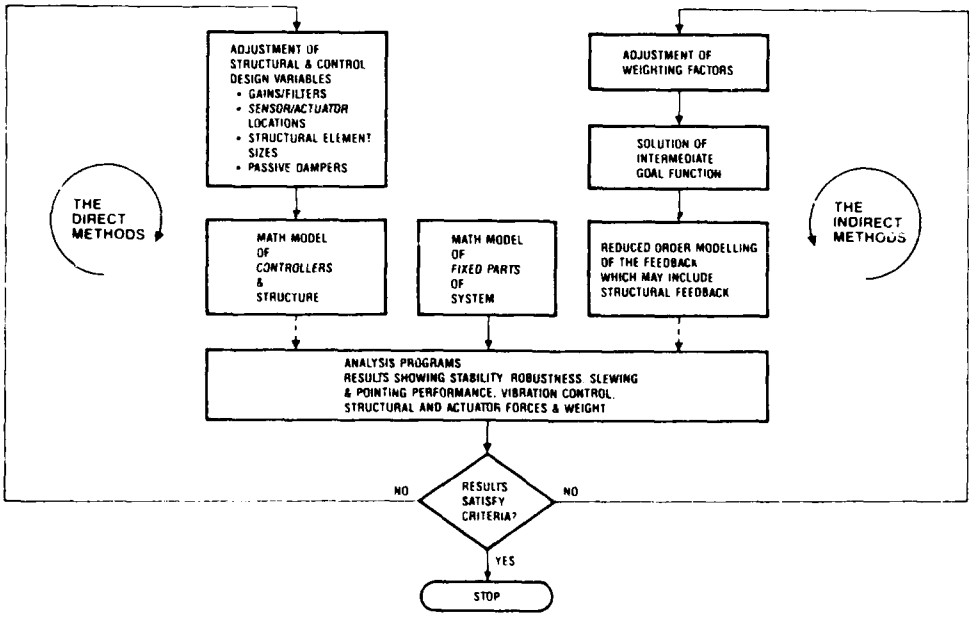

CONTROL ANALYSIS MODULE CAPABILITIES

The control analysis module will include at least the routines listed below. The analysis routines emphasize robustness, which is a key issue in the design of multi-input/multi-output control systems. The modeling routines emphasize model reduction, which is a key issue in designing control systems for large space structures. Finally, the included controller parameterizations encompass the field of control theory, from classical to modern techniques.

THE CONTROL ANALYSIS MODULE WILL INCLUDE THESE ROUTINES

- ANALYSIS ROUTINES EMPHASIZING PERFORMANCE AND STABILITY ROBUSTNESS AND CONTROL FORCE RESPONSE
  - SINGULAR-VALUE FREQUENCY RESPONSE
  - EIGENVALUES, EIGENVECTORS, AND ROOT LOCUS
  - OPEN AND CLOSED-LOOP TRANSFER FUNCTIONS AND FREQUENCY RESPONSE
  - CLOSED-LOOP TRANSIENT RESPONSE
- MODELING ROUTINES
  - STATE-SPACE MODEL GENERATION
  - MODEL REDUCTION BY MODAL COST ANALYSIS
- CONTROL PARAMETERIZATIONS
  - THE DIRECT METHOD (GAINS AND FILTERS)
  - MESS ALGORITHM
  - FREQUENCY SHAPED LQG
  - EIGENSTRUCTURE ASSIGNMENT VIA SYLVESTER'S METHOD

AN ILLUSTRATIVE INTEGRATED DESIGN PROBLEM

As a means for validating and verifying the software product, several benchmark integrated design problems will be formulated. The benchmark problem pictured contains salient features of large space structures, including multiple control loops and low frequency flexible body modes. This problem, with results via a precursor software program, illustrates features of the integrated structures and controls optimization software under development.

The benchmark problem considers roll control of a large, flexible, offset-fed truss-antenna spacecraft. The spacecraft can be modeled (admittedly in a much simplified manner) as two rigid circular disks, one representing the reflector and the other representing the feed platform, connected by a uniform, rather flexible, elastic bar. The cross-sectional area of the connecting bar is the only structural design variable. Note that the total spacecraft mass depends linearly on the area of this bar. Dynamic disturbances due to internal sources occur at the feed. In the presence of these disturbances, the antenna's rigid-body roll attitude must be controlled so as to properly point the solar array. Moreover, the antenna's line of sight must be stabilized by controlling the angular motions of the reflector relative to the feed, i.e., the elastic vibrations of the structure. The absolute roll attitude of both the reflector and the feed are sensed and used in a feedback loop to excite torque actuators at the same two locations. Proportional plus derivative control is used between each sensor and each actuator, making a total of eight control design variables.

EXAMPLE BENCHMARK PROBLEM: ROLL-ATTITUDE CONTROL OF A LARGE ANTENNA SPACERAFT

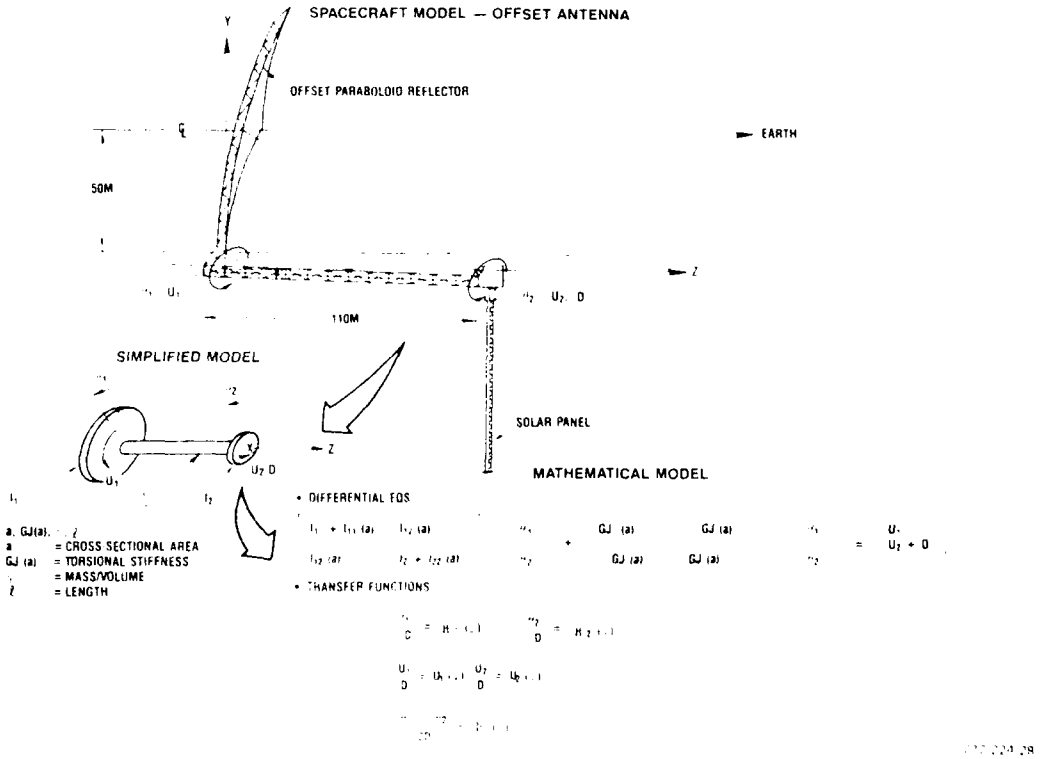

BLOCK-DIAGRAM OF THE ILLUSTRATIVE PROBLEM

A novel way of looking at the benchmark problem is to put it in the block diagram form shown below. In this form, the cross-sectional area of the bar appears as a gain in a structural feedback loop. Both the structure and the active control form feedback loops to control the fixed parts of the system, namely, the two rigid disks representing the reflector and the feed. As discussed earlier, this view of the system allows the structural design variable and the control design variables to be adjusted in the same basic way to optimize their combined effects on the system's performance. The cross sectional area and the values of the eight control system gains can all be changed together to achieve the required pointing command response and the necessary robustness and vibration control, all with minimum total system mass, or with minimum control torques, or with minimum structural internal loads. Note that, in this view, system robustness is assessed for structural and control feedback loops acting on the fixed parts of the system. This is distinguished from the usual assessment of robustness in controls where the control system feedback loop acts on the flexible structure.

Now, what is the specific design problem to be solved? Is it to minimize mass (area) with constraints on internal loads, control torques, and robustness (response and stability in the presence of uncertainty)? Is it to minimize internal loads with constraints on mass, control torques, and robustness? Or is it to maximize robustness with constraints on internal loads, mass, and control torques? Or, is it some other problem?

BOTH STRUCTURE AND CONTROL CAN BE CONSIDERED AS FEEDBACK FOR ROBUSTNESS, SLEWING AND POINTING COMMAND RESPONSE, VIBRATION CONTROL, AND STRUCTURAL LOADS

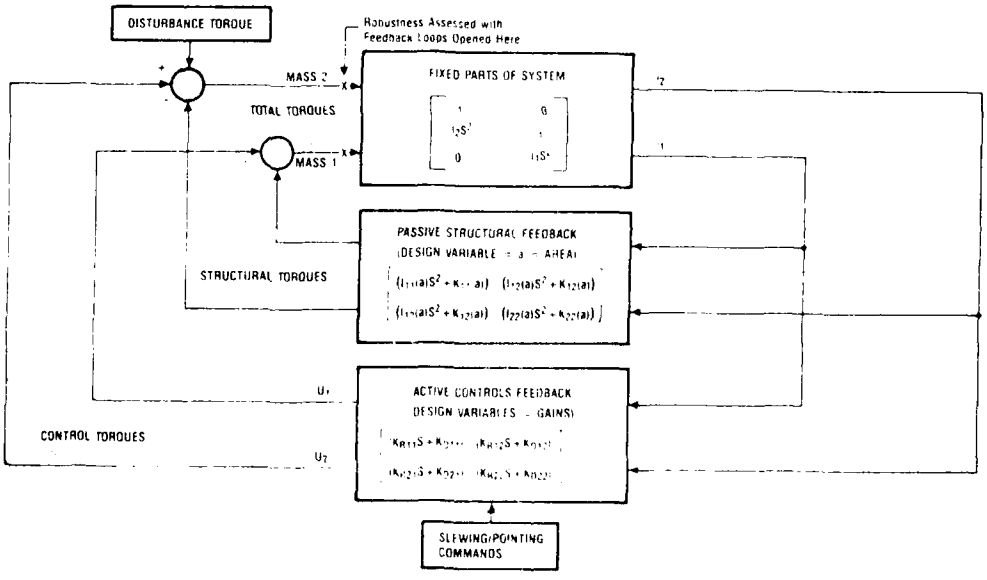

ILLUSTRATIVE DESIGN RESULTS

There are always differing ways to pose the design problem, and the problem as well as its solution can only be found after sensitivity and tradeoff studies, for which the mechanized analysis approach is ideally suited. In other words, as already mentioned, one must hunt for the problem as well as its solution. During this hunt for the problem, the problem is continually re-quantified, and in fact this very act of "quantifying" often leads to the solution.

The figures below show system performance before and after optimization (cross-hatched areas indicate final constraint boundaries). The first three plots (A-C) show the stability of the system. The first plot is the frequency response of the minimum singular value of the return difference matrix. Singular values were computed with the loops broken as indicated in the figure on the preceding page. As the singular values increase, robustness (the degree of stability in the presence of uncertainties) increases. The second plot is a Nichols plot of the system frequency response with the feedback loop opened at θ_1 (the θ_2 loop is closed). The third plot is a Nichols plot with the feedback loop opened at θ_2 with the θ_1 loop closed. These first three plots show marginal stability for initial values of the design variables and robust stability for the final design. The last three plots (D-F) show closed-loop performance of the system. The fourth plot is the closed-loop frequency

(continued on next page)

THESE RESPONSES SHOW STABILITY AND PERFORMANCE BEFORE AND AFTER OPTIMIZATION

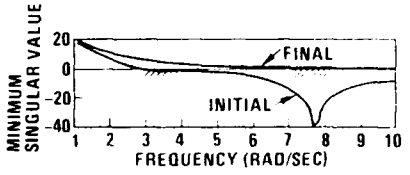

A. MINIMUM SINGULAR VALUE FREQUENCY RESPONSE

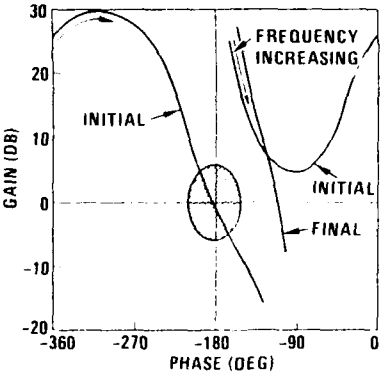

B. OPEN-LOOP FREQUENCY RESPONSE, NICHOLS PLOT WITH θ_1 OPEN, θ_2 CLOSED

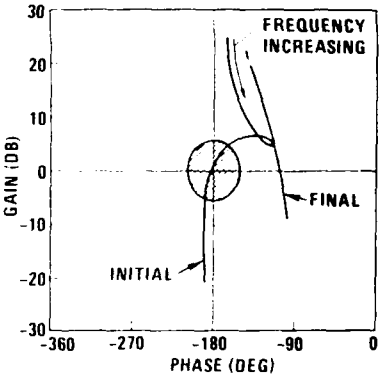

C. OPEN-LOOP FREQUENCY RESPONSE, NICHOLS PLOT WITH θ_2 OPEN, θ_1 CLOSED

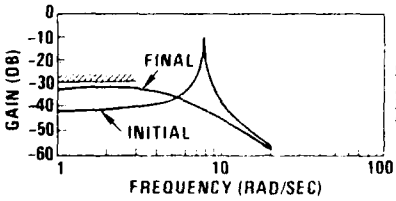

D. CLOSED-LOOP FREQUENCY RESPONSE, MODAL COORDINATE (STRUCTURAL LOAD) DUE TO DISTURBANCE

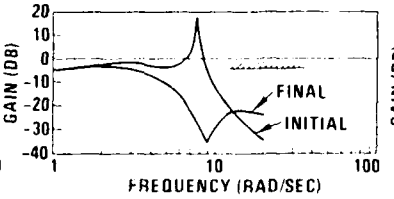

E. CLOSED-LOOP FREQUENCY RESPONSE, CONTROL TORQUE (U_1) DUE TO DISTURBANCE

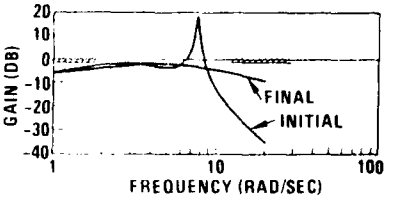

F. CLOSED-LOOP FREQUENCY RESPONSE, CONTROL TORQUE (U_2) DUE TO DISTURBANCE

212 224

response of the internal load due the disturbance, i.e., the load versus the frequency of the disturbance. The fifth and sixth plots are closed-loop frequency responses of the absolute roll angles due to the disturbance, i.e., the angles versus the frequency of the disturbance. These last three plots show unacceptable response for initial values and acceptable response for final values of the design variables.

Initially, the goal of the optimization was to minimize the bar's cross-sectional area, and thus the system total mass. In so doing, it was found that the robustness (singular value) constraint was either binding or not met depending on choices for the other constraints. Therefore, the goal function was changed to maximizing robustness. The final results are the result of maximizing the singular value, while constraining control torque, internal loads, and closed-loop frequency response.

Because the constraint on the U_2 control torque was tight, a sensitivity study was performed on this constraint. The results are plotted below, showing how area (and thus mass) can be reduced and stability robustness increased as more control torque is allowed. In all cases, the closed-loop internal loads constraint was always satisfied. A major strength in using optimization methods to design control systems is illustrated by this example: control magnitude constraints can be made binding, thereby maximizing the use of available control torque.

TRADE STUDY RESULTS

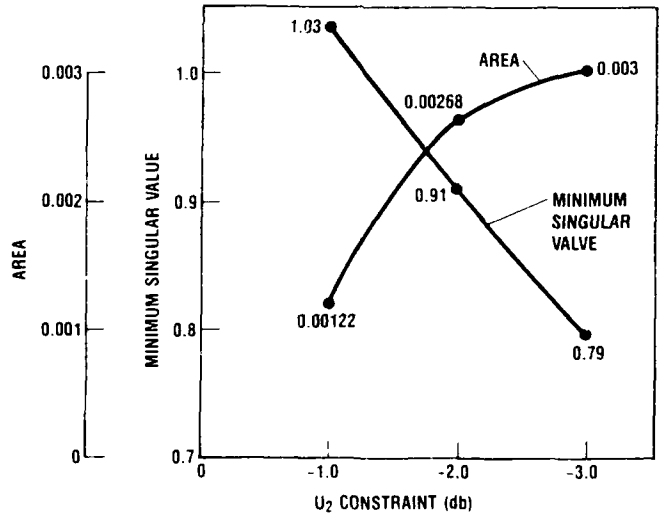

THE BEST VALUES FOR AREA AND ROBUSTNESS-MEASURE VARY AS A FUNCTION OF THE PEAK ALLOWABLE U_2 CONTROL TORQUE

FUTURE OLSSWAC DESIGN STUDIES

The benchmark problem has illustrated the type of optimization problems to be posed and solved in the future design studies with the software under development. Candidate structures for the design studies are listed. After extensive numerical experimentation, the results will be evaluated for weaknesses of various approaches and for practical limitations of the software. Guidelines for using the software will be established with specific attention given to problem size, to efficiency of optimization algorithms, to successes and failures using the software, and to selection of initial values for design variables. Discussion of system limitations will contain, among other things, discussion of the extremes that the system will support, both theoretically and practically.

DESIGN STUDIES

SOW TASK

- SELECT AT LEAST 6 REPRESENTATIVE SPACE STRUCTURES PROBLEMS
  - 2 SHALL BE SELECTED FROM AMONG VCOSS, PACOSS, AND LSPSC PROJECTS
  - PROBLEMS ARE SUBJECT TO AIR FORCE APPROVAL
- ESTABLISH GUIDELINES AND LIMITATIONS ON THE USE OF THE SOFTWARE
- ASSESS HOW THE INTEGRATED OPTIMIZATION TECHNIQUE WORKED

CANDIDATE STRUCTURES

- FROM VCOSS, CSDL MODEL #2 (REVISION #3)
- FROM LSPSC:
  - CENTER-FED ANTENNA
  - OFFSET-FED ANTENNA
- OTHER REPRESENTATIVE SPACE STRUCTURES
  - SYNTHETIC APERTURE RADAR
  - HYBRID BISTATIC RADAR
  - GROUND BASED LASER RELAY MIRROR

EFFICIENT CONTROLLER REDUCTION

FOR

STRUCTURES

H. Öz

DEPARTMENT OF AERONAUTICAL AND ASTRONAUTICAL ENGINEERING

THE OHIO STATE UNIVERSITY

COLUMBUS, OHIO 43210

1. INTRODUCTION

The efficiency concept is recognized and suitably defined in almost every branch of applied engineering sciences as an analysis and design tool (e.g., thermal efficiency, propulsion efficiency, mechanical efficiency, brake efficiency, etc.). Invariably, it is defined as the ratio of two quantities characterizing a realized process and a desired process:

$$\text{EFFICIENCY} = \eta = \frac{\text{REALIZED PROCESS}}{\text{DESIRED PROCESS}}$$

The PROCESS reflects some unique character of the physical nature of the problem.

The concept of controller efficiency has not yet found its way into the structure-control problem. Such a concept is needed and can be defined for structure control (Ref. 1), because

1. The concept has precedence in other engineering disciplines.
2. It makes good engineering sense to design an efficient structure-control system.

Performance indices can be categorized as:

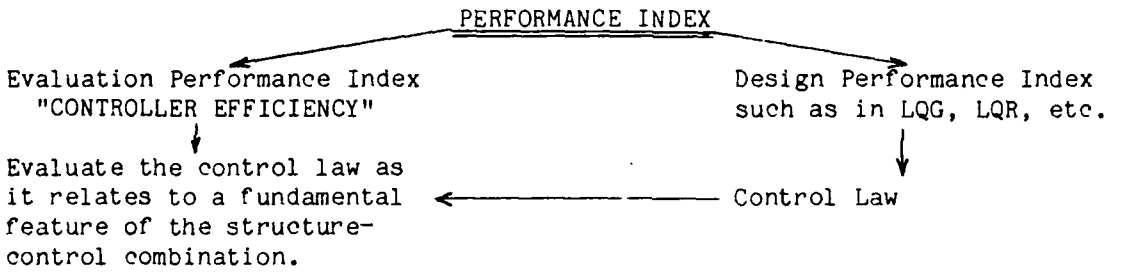

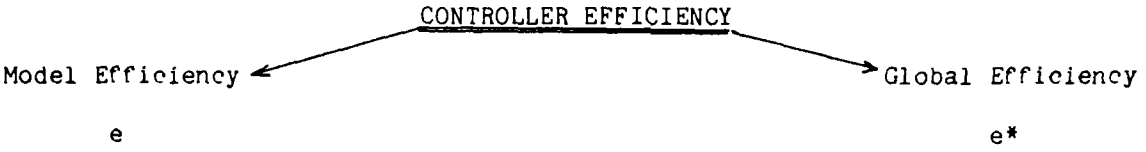

The following presentation considers the model efficiency e only, global efficiency is discussed in Ref. 1.

Definition: $$e = \frac{\text{Control cost expended on the n-Dimensional } (\infty\text{-D}) \text{ design model}}{\text{Control cost expended on the } \infty\text{-Dimensional } (\infty\text{-D}) \text{ DPS (Distributed Parameter System)}}$$

The model efficiency e is the fraction of the total physical control expenditure usefully absorbed by the finite-dimensional design model to satisfy the performance requirements.

Control expenditure on the ∞-D DPS is a function of the finite (n)-dimensional control design model. Consider:

Actual Distributed Parameter System (∞-D DPS)

$$m(p)\ddot{\underline{u}}(p,t) + \mathcal{L}[\underline{u}(p,t)] = \underline{f}(p,t)$$

Control expenditure on the ∞-D DPS $\triangleq S_\infty^R$

$$S_\infty^R = \int_{D(p)} \int_t m^{-1}(p)\underline{f}^T(p,t)\underline{f}(p,t)dtdp$$

regardless of the functional form of the input field f(p,t) and how it is generated numerically. For example, assume one has the DPS input field

$$\underline{f}(p,t) = \sum_{k=1}^{m} \underline{\delta}_k(p)U_k(t) = [\delta(p)]\underline{U}(t)$$

$\underline{\delta}_k(p)$ = local k-th input support functions where $\underline{U}(t)$ are generated from an n-dimensional mathematical control design model (such as an n-mode model of the DPS):

n-Dimensional (n-D) Design Model

$$\dot{x}_n(t) = A_n x(t) + B_n U(t)$$

where B_n is the input projection operator,

$$U(t) = U(x_n(t))$$

or alternatively

$$U(t) = U(x_c(t))$$

where x_c are some finite dimensional compensator states. For simplicity of discussion, take $\{x_c\} = \{x_n\}$.

$$S_\infty^R = \iint m^{-1}(p)\underline{f}^T(p,t)\underline{f}(p,t)dpdt$$

$$\underline{f}(p,t) = [\delta(p)]\underline{U}(t) = [\delta(p)]\underline{U}(x_n(t))$$

$$\therefore \quad S_\infty^R = \int \underline{U}^T(x_n)R_\infty \underline{U}(x_n)dt = \text{Function of the n-D design model}$$

$$R_\infty = \int_p m^{-1}(p)[\delta(p)]^T[\delta(p)]dp = m \times m \text{ Constant matrix for the } \infty\text{-D DPS}$$

Next we note the following property of S_∞^R by recognizing the orthogonality of the modes of the DPS:

Principle of Conservation of Control Expenditure

Control Expenditure on the ∞-D DPS = Control expenditure on the n-D design model + Input expenditure wasted on residual dynamics (due to spillover excitation)

$$S_\infty^R = S_n^M + S_u^M$$

$$S_\infty^R = \sum_{r=1}^{n} \int f_r^2(t)dt + \sum_{n+1}^{\infty} \int f_r^2(t)dt$$

$f_r(t)$ = r-th Modal Input = $\int \underline{\phi}_r^T(p)\underline{f}(p,t)dp$

2. CONTROLLER EFFICIENCY e

Definition:

$$e\% = \frac{S_n^M}{S_\infty^R} \times 100 = \frac{\int U^T(x_n)\ R_n U(x_n)dt}{\int U^T(x_n)\ R_\infty U(x_n)dt} \cdot$$

or

$$e\% = (1 - \underbrace{\frac{S_u^M}{S_\infty^R}}_{\text{Process irreversibility}}) \times 100$$

"Control Effort Wasted on the Residual Dynamics"

$R_n = B_n^T B_n$ = Quadratic input projection matrix onto the n-D design space

$R_\infty = \int m^{-1}(p)[\delta(p)]^T[\delta(p)]dp$ = Quadratic input projection matrix onto the ∞-D DPS

e% = 100% if and only if $S_\infty^R = S_n^M$ (or $S_u^M = 0$, no residual interaction)

Extension of the controller efficiency to spatially discrete equations of motion (such as the finite element models) serving as surrogates to the ∞-D partial differential equations of motion are given in Ref. 1.

- The weighting matrices R_n and R_∞ are not arbitrary, they are uniquely defined to serve the concept of controller efficiency.
- Definition of the controller efficiency e inherently represents the ∞-D of the structure-control system.
- The nondimensional controller efficiency for the ∞-D DPS can always be evaluated on the basis of the n-D design model.

- Definition and use of controller efficiency is independent of the performance requirements by or for which the controller may have been designed.

- Controller efficiency depends on the size of the control design model. Therefore, it can be used to obtain good reduced-order controllers. (See Ref. 1 for other features of e).

3. EFFICIENT CONTROLLER REDUCTION (ECR)

ECR: In the design model, retain states (components) with largest contributions to the controller efficiency.

Controller Reduction via Component Cost Analysis (CCACR) and Efficient Controller Reduction (ECR) can produce entirely opposite results. In other words, it is possible that

{Most significant components of ECR (retained)} = {Least significant components of CCACR (truncated)}

Explanation

First a crucial observation: For any physical control input $\underset{\sim}{U}$ the quadratic control measure $V_c = \int \underset{\sim}{U}^T(x_n)\, R\, \underset{\sim}{U}(x_n)dt$ for any control weighting R other than given above, that is $R \neq R_\infty$, R_∞ is a weighted control measure, not on the finite-dimensional control design model but on the ∞-D DPS regardless of functional (feedback) dependence of $\underset{\sim}{U}$ on x_n!

Then, consider the quadratic control cost:

$$V_c \triangleq \int U^T R_\infty U\, dt = V_\infty = \sum_i^n V_{i\infty} \quad ; \quad V_c = S_\infty^R$$

↑ Controller cost on the ∞-D DPS; ↑ i-th controller component cost

$$V_{i\infty} = V_{in}^M + V_{iu}^M$$

where:

$V_{i\infty}$: Control effort expended on the ∞-D DPS by the i-th controller component.

V_{in}^M: The portion of the i-th component control cost ($V_{i\infty}$) usefully absorbed by the n-D design model.

V_{iu}^M: The portion of the i-th component control cost wasted on residual dynamics as spillover.

The concept of component cost analysis is based on regarding those components with larger costs as dynamically significant and advocates retaining of most costly components in a closed-loop controller reduction.

But, a component cost $V_{i\infty}$ can be large not because it is a good component to retain, but because it may be wasting significant control effort on the residual dynamics as spillover in which case that component would be regarded very inefficient and be truncated according to ECR approach presented herein.

4. APPLICATION OF ECR TO ACOSS-4

Efficiencies of 30 LQR designs which minimize the control design performance index

$$J = \frac{1}{2}\int_0^\infty (x_n^T q\, x_n + U^T r U)dt \ , \quad q=r=1 \ , \quad x_n(0)=1$$

were computed for different size design models, $2 \le n \le 12$ and the number of inputs $1 \le m \le 6$. A 12th order finite element model was considered as the evaluation model (Ref. 1) for the ∞-D DPS. Controller efficiencies of the LQR designs are shown in Fig. 2 and numerical values for $n=2,8$ and $1 \le m \le 6$ are given in Table 1. ECR was applied (and compared to CCACR) to obtain an 8th order reduced design model.

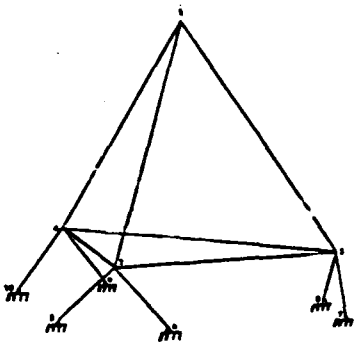

FIG. 1: ACOSS-4 Configuration.

TABLE 1: MODEL EFFICIENCIES FOR n=2,8, m=1 -6

m = # of inputs	η	
	n=2	n=8
1	1.33	56.92
2	1.27	56.82
3	1.86	63.56
4	2.96	69.40
5	3.39	69.00
6	8.68	72.07

n=2, 2 Lowest structural modes

n=8, 8 Lowest structural modes

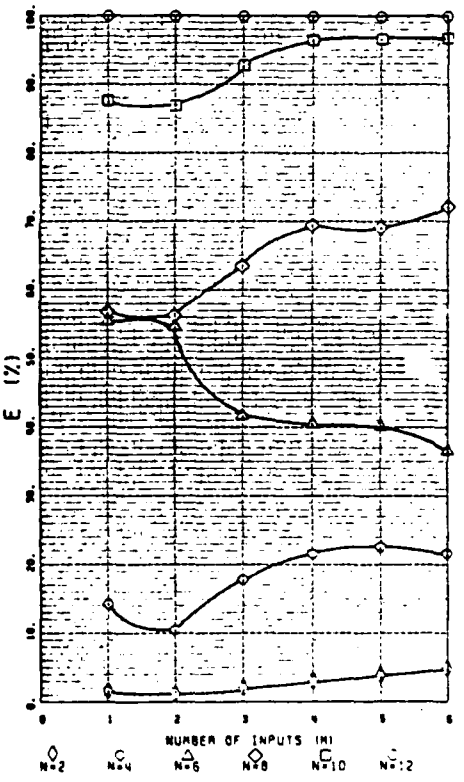

FIG. 2: Efficiencies of Various LQR Designs for ACOSS-4.
N = Order of design model

Actual Component Costs and Efficiencies for the ACOSS-4 Example:

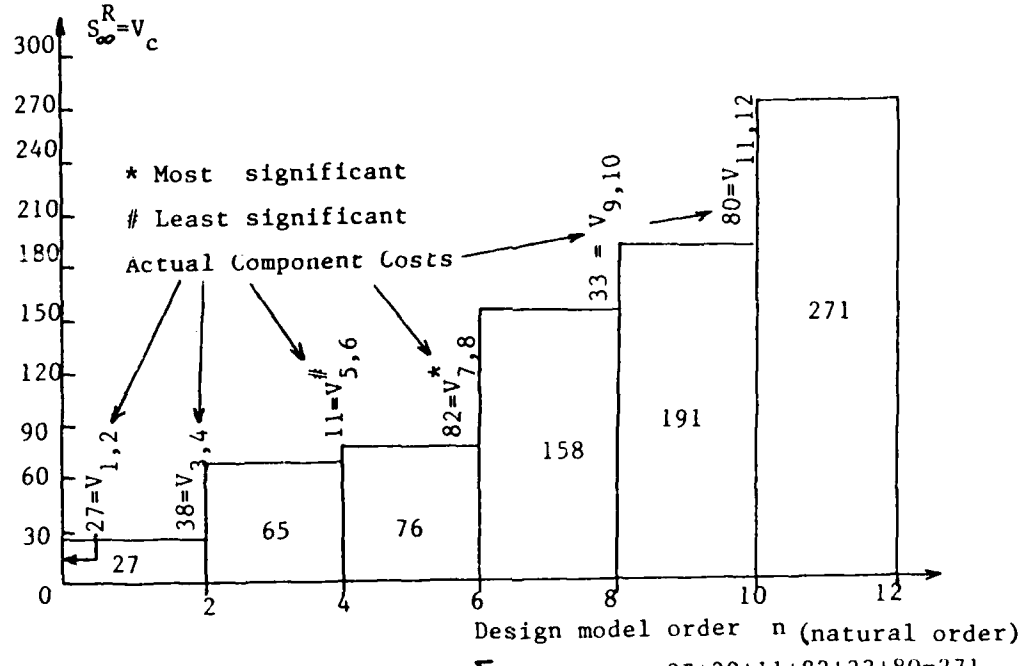

FIG.3a: Actual Component Costs: $V_c=\sum_{\substack{i=1,3\\5,7,9,11}} V_{i,i+1}= 27+38+11+82+33+80=271$

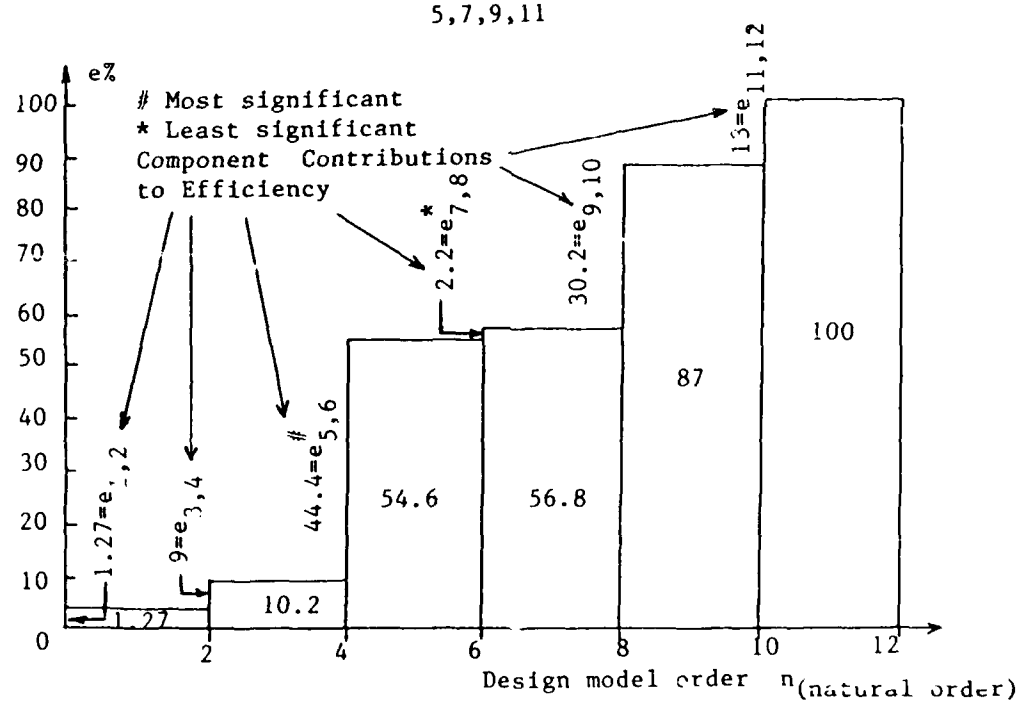

FIG.3b: Component Efficiencies: $e\%=\sum_{\substack{i=1,3,5\\7,9,11}} e_{i,i+1}=1.27+9+44.4+2.2+30.2+13=100\%$

TABLE 2: CONTROL EXPENDITURE (COST) ANALYSIS FOR THE EXAMPLE

{n}	2	4	6	8	10	12	←(Natural order)
S_{∞}^{R}	27.3	65	76	158	191	271	← Total control effort
S_{n}^{M}	0.3	7	41	90	166	271	← Control effort usefully absorbed by the design model
S_{u}^{M}	27	58	35	68	25	0	← Wasted control effort
$V_{n-1,n}$	27	38	11	82	33	80	← Actual Component costs
e%	1.27	10.2	54.6	56.8	87	100	← Efficiencies

Most significant component cost

contributes the largest increment to the wasted control effort

From Fig. 3 and Table 2 we note:

	ECR	CCACR
Most significant modes (retained) :	5,6	7,8
Least significant modes (truncated):	7,8	5,6

∴ For an 8th Order Reduced Model with 2 Inputs:

Modes retained via ECR : 3,4,5,6,9,10,11,12

Modes retained via CCACR: 3,4,7,8,9,10,11,12

Extension

Same observation can also be made for the design of reduced-order compensators of fixed order via the optimal projection approach. The compensator designed to be optimal with respect to its design performance measure is not necessarily going to be optimal with respect to the measure of controller efficiency. In other words, the optimal compensator for the design model can also have large control effort projected onto the residual space and therefore be inefficient.

To see the improvement in the 8th order control design after the application of the ECR concept, the following results are presented:

8th Order Model Before ECR:{n}:1-8 "Natural Order"

$$S^{R} = 158 \ , \quad S_{n}^{M} = 90 \ , \quad S_{u}^{M} = 68$$

% Controller efficiency = e% = 56.8%

8th Order Model After ECR:{n}:3,4,5,6,9,10,11,12

$$S^R = 162 \quad , \quad S_n^M = 156.5 \quad , \quad S_u^M = 5.5$$

$$\% \text{ Controller efficiency} = e\% = 97\%$$

Hence, with mode selection according to ECR a much more efficient combination of the modes for the given actuator configuration (2 inputs) has been identified. Now almost all of the control effort is expended usefully and therefore the residual interaction will be insignificant for all practical purposes.

5. CONCLUSION

Controller efficiency in structure-control systems must also be addressed alongside other performance requirements.

*Acknowledgement: This research is supported under the AFWAL Contract No. F33615-86-R3212.

6. REFERENCES

1. Oz, H., Farag, K., and Venkayya, V. B., "Efficiency of Structure-Control Systems," Proc. of the 6th VPI and SU/AIAA Symposium on Dynamics and Control of Large Structures, Ed: L. Meirovitch, June 1987, Blacksburg, VA.

2. Parry, C. O., and Venkayya, V. B., "Issues of Order Reduction in Active Control System Design," 1986 AIAA Guidance and Control Conference, Williamsburg, VA.

3. Yousuff, A., and Skelton, R., "Controller Reduction by Component Cost Analysis," IEEE Transactions on Aut. Control, Vol. AC-29, No. 6, 1984.

A CONCEPTUAL SYSTEM DESIGN FOR ANTENNA THERMAL AND DYNAMIC DISTORTION COMPENSATION USING A PHASED ARRAY FEED

G. R. Sharp, R. J. Acosta
E. A. Bobinsky, F. J. Shaker

ON-ORBIT THERMAL DISTORTION OF ANTENNA REFLECTORS

Thermal or dynamic distortions of an reflector antenna structural system can affect the Far-Field Antenna power distribution pattern in four ways: 1. The antenna gain is reduced thus delivering less RF power than desired. 2. The main lobe of the antenna can be mis-pointed thus shifting the destination of the delivered power away from the desired location. 3. The main lobe of the antenna pattern can be broadened thus spreading the RF power over a larger area than desired. 4. The antenna pattern side lobes can increase thus increasing the chances of interference among adjacent beams of a multiple beam antenna system or with antenna beams of other satellites.

NASA Lewis Research Center

ON-ORBIT THERMAL DISTORTION OF ANTENNA REFLECTORS

SPACE COMMUNICATIONS DIVISION D 1 - 9

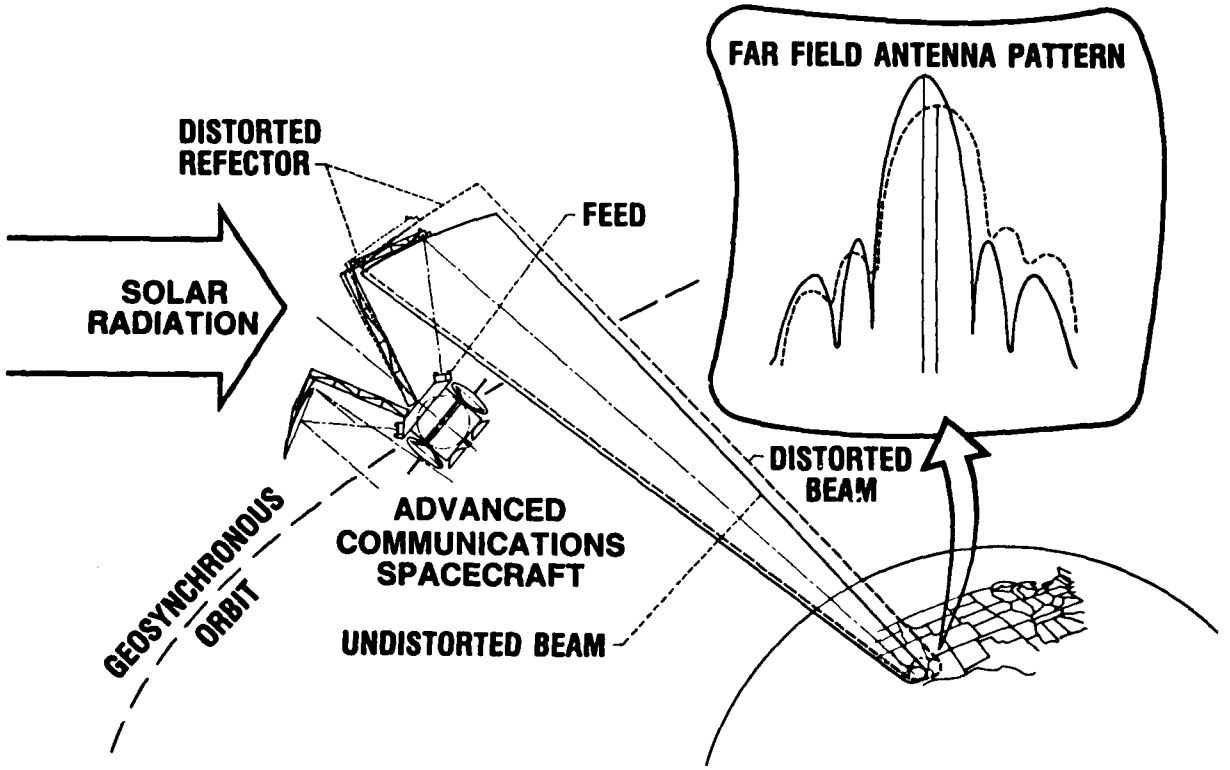

APPROACHES FOR REDUCING IMPACT OF ON-ORBIT THERMAL DISTORTION OF REFLECTORS

Two approaches can be used to at least partially restore antenna performance to the state of an undistorted antenna system. 1. The antenna can be constructed from only the most thermal distortion resistant materials available. It is fortunate that these materials are also usually stiffer and should thus increase the natural frequencies of the system thereby reducing dynamic distortion in most cases. Another possibility would be to go to a more sophisticated thermal control system in order to minimize temperature gradients. 2. A second approach is to use a phased array feed to electronically compensate for distortion by adjusting the phase and amplitude. Thus, the antenna phase front emanating from the antenna feed is shaped to compensate for the distorted antenna reflector or mis-focused antenna structural system.

NASA Lewis Research Center

APPROACHES FOR REDUCING IMPACT OF ON-ORBIT THERMAL DISTORTION OF REFLECTORS

SPACE COMMUNICATIONS DIVISION D 1 - 1 0

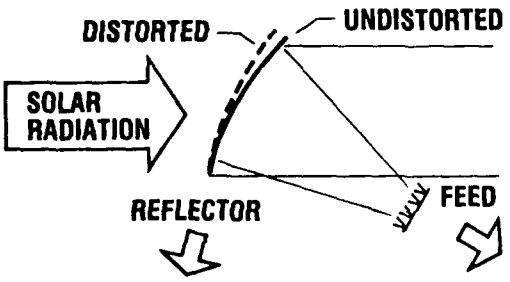

THERMAL/MECHANICAL UPGRADE

- COMPOSITE MATERIAL TECHNOLOGY
- FABRICATION TECHNIQUES
- ACTIVE/PASSIVE THERMAL CONTROL

ACTIVE ARRAY COMPENSATION

- COMPENSATION ALGORITHM
- FEEDBACK MECHANISM
  - REFLECTOR DISTORTION
  - SIGNAL DISTORTION
- CONTINUOUS/PERIODIC UPDATE

RADIATION/THERMAL/MECHANICAL/RF MODEL

CD-86-20525

A CONCEPTUAL SYSTEM DESIGN FOR ANTENNA THERMAL AND DYNAMIC DISTORTION COMPENSTATION USING A PHASED ARRAY FEED

Control of a phased array antenna feed is a complex problem requiring considerable computational power. The on-board computational power necessary for this task is only now becoming practical. However, if the full potential of a phased array to compensate for all known antenna dimensional errors is to be realized, simple methods need to be found to allow these on-board calculations to be made in real time. If accurate and relaible calculations can be made before the launch regarding the expected antenna distortions and necessary phased array corrections, then a look-up table can be created to adjust the phased array to compensate for most of these dimensional errors.

AEROSPACE TECHNOLOGY DIRECTORATE

SPACE ELECTRONICS DIVISION

NASA Lewis Research Center

A CONCEPTUAL SYSTEM DESIGN FOR ANTENNA THERMAL AND DYNAMIC DISTORTION USING A PHASED ARRAY FEED

- OBJECTIVE-TO COMPENSATE FOR REFLECTOR SURFACE ERRORS CAUSED BY EITHER QUASI STATIC THERMAL DISTORTION OR DYNAMIC DISTURBANCES BY ADJUSTING THE PHASE AND AMPLITUDE OF A PHASED ARRAY ANTENNA FEED IN REAL TIME
- APPROACH
  1. DETERMINE THE THERMAL AND DYNAMIC DISTORTION MODE PROFILES
  2. PERFORM PRE-FLIGHT CALCULATIONS TO DETERMINE:
     A. THE OPTIMAL POSITION OF MODAL PARTICIPATION/SEPARATION DETECTORS ON THE ANTENNA
     B. THE REQUIRED PHASED ARRAY CORRECTIONS FOR ALL NECESSARY ANTENNA THERMAL AND DYNAMIC MODE PROFILES
     C. FROM A AND B PREPARE A MODAL PARTICIPATION/PHASED ARRAY LOOK-UP TABLE
  3. DESIGN A SPACECRAFT FLIGHT SYSTEM TO INCLUDE:
     A. LASER OR OTHER MODAL PARTICIPATION DETECTORS OPTIMALLY LOCATED SO AS TO MINIMIZE THEIR NUMBER
     B. AN ON-BOARD COMPUTER FOR IDENTIFYING MODES AND THEIR INTENSITY FROM THE DETECTOR MEASURED DATA
     C. THE PREVIOUSLY CALCULATED MODAL PARTICIPATION/PHASED ARRAY LOOK-UP TABLE
  4. USE THE FLIGHT SYSTEM TO MAKE REAL TIME PHASED ARRAY FEED CORRECTION TO COMPENSATE FOR BOTH THERMAL AND DYNAMIC ANTENNA DISTORTIONS

THERMAL DISTORTION PERFORMANCE ANALYSIS

At Lewis, a series of well established programs (TRASYS, SINDA and NASTRAN) have been combined with interacting programs (SNIP and SPLINE II) to analyze antenna models for thermal distortion. The output of the SPLINE Program results in a mathematical representation of a reflector surface that is piece-wise smooth and differentiable and thus suitable for use with a generalized reflector diffraction analysis program.

AEROSPACE TECHNOLOGY DIRECTORATE

SPACE COMMUNICATIONS DIVISION

NASA Lewis Research Center

THERMAL DISTORTION PERFORMANCE ANALYSIS PROGRAM

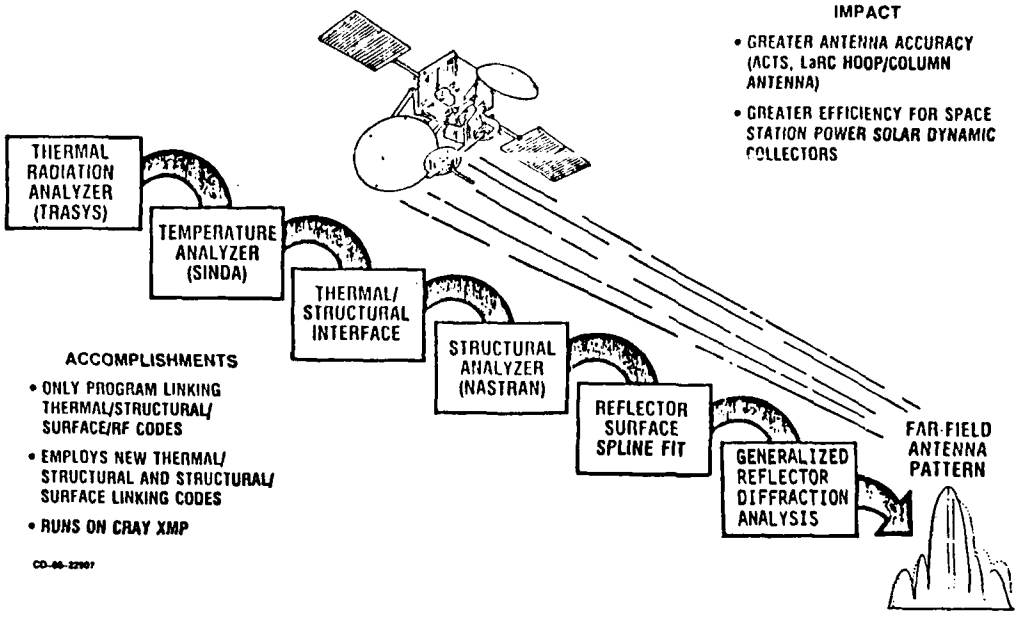

IMPACT

- GREATER ANTENNA ACCURACY (ACTS, LaRC HOOP/COLUMN ANTENNA)
- GREATER EFFICIENCY FOR SPACE STATION POWER SOLAR DYNAMIC COLLECTORS

ACCOMPLISHMENTS

- ONLY PROGRAM LINKING THERMAL/STRUCTURAL/ SURFACE/RF CODES
- EMPLOYS NEW THERMAL/ STRUCTURAL AND STRUCTURAL/ SURFACE LINKING CODES
- RUNS ON CRAY XMP

CD-88-22107

PRESENT PROJECT STATUS

Predictions of the far-field patterns and possible RF interference for the Advanced Communications Technology Satellite (ACTS) multibeam antenna systems has top priority at Lewis Research Center among the thermal distortion analysis projects. First results should be available by 4/88.

The purpose of the accurate antenna reflector flight evaluation is to predict and compare the performance of new antenna reflector designs. A flight version of a laboratory antenna being constructed at Lewis is being used as a base antenna reflector for comparison purposes. It is hoped that this new design will prove less susceptible to thermal distortion than current designs. This effort will also be used to evaluate the long term effects of material dimensional stability on antenna reflector performance for NASA-Langley Research Center. First far-field pattern predictions are expected by 3/88.

The effect of thermal distortions on the RF performance of the Langley hoop-column antenna are also being predicted. Work is expected to start shortly on the SINDA thermal model. The NASTRAN model is being supplied by Langley. First performance predictions are expected by 6/88.

AEROSPACE TECHNOLOGY DIRECTORATE

SPACE ELECTRONICS DIVISION

NASA Lewis Research Center

THERMAL DISTORTION ANALYSIS PRESENT PROJECT STATUS

- ACTS S/C
  - TRASYS MODEL - COMPLETE
  - SINDA MODEL - 90% COMPLETE
  - NASTRAN MODEL - 50% COMPLETE
  - FAR FIELD PATTERN PREDICTIONS BY 4/88
- ACCURATE ANTENNA REFLECTOR FLIGHT EVALUATION
  - TRASYS MODEL - COMPLETE
  - SINDA MODEL - 90% COMPLETE
  - NASTRAN MODEL - 80% COMPLETE
  - FAR FIELD PATTERN PREDICTIONS BY 3/88
- LaRC HOOP-COLUMN ANTENNA REFLECTOR
  - TRASYS MODEL - 90% COMPLETE
  - SINDA MODEL - NOT STARTED
  - NASTRAN MODEL (LaRC) - 90% COMPLETE
  - FAR FIELD PATTERN PREDICTIONS BY 6/88

THERMAL AND DYNAMIC REFLECTOR MODE PROFILE PREDICTIONS AND RF ANALYSIS FOR PRE-FLIGHT CALCULATIONS

With the addition of mass properties, the NASTRAN Program can also be used for dynamic predictions. The NASTRAN dynamic results can then be processed directly by the reflector surface spline fit program to yield dynamically distorted reflector mode profiles for use in the laser modal participation detector optimal location program to follow.

The NASTRAN dynamic results can also be added by superposition to the NASTRAN thermal results for as many combined cases as practical. These results can then be fed into the reflector surface spline fit program and converted into the correct input for the RF analysis program.

All of the desired thermal cases would also be analyzed and separated into distinct modes that can be added together to get the complete thermal profile. The individual thermal modes are needed for the thermally distorted reflector mode profile prediction program that is needed as input to the Laser modal participation detector optimal location program to follow.

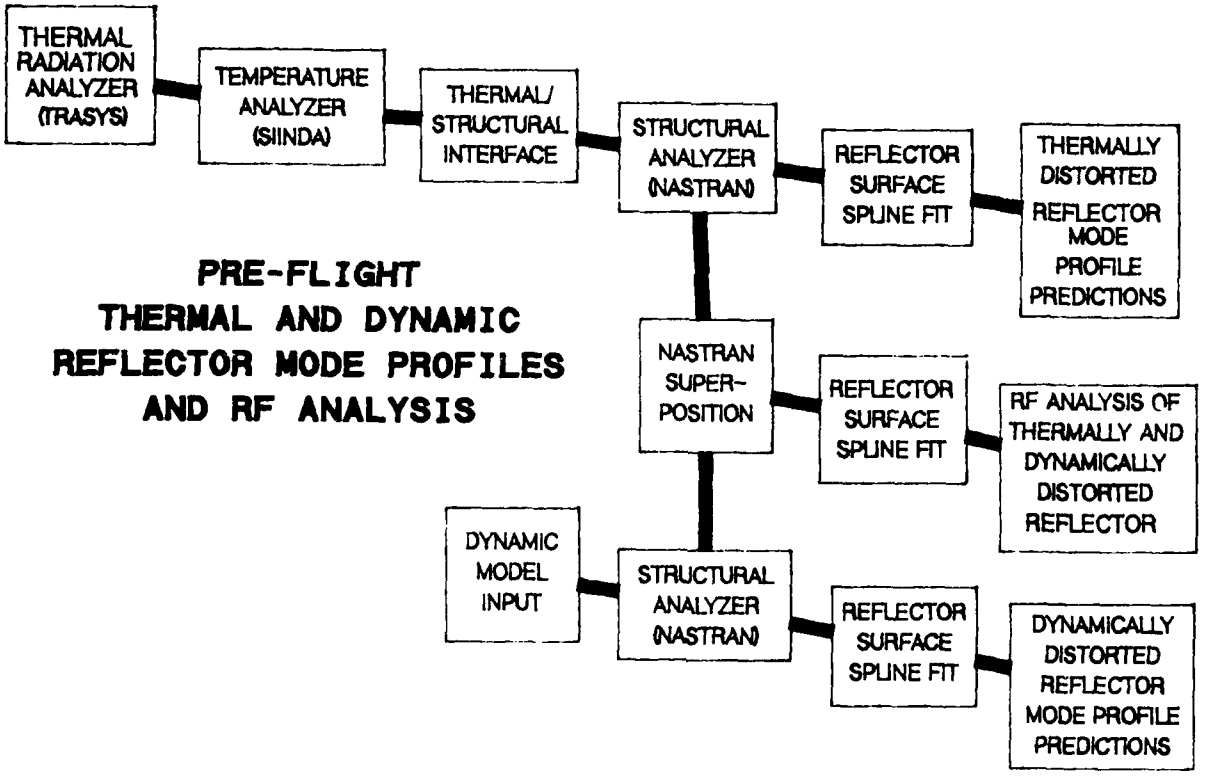

PRE-FLIGHT CALCULATIONS

Here, a block diagram of the routines and programs necessary in the pre-flight preparation of a modal participation/phased array look-up table is shown. On the previous page, two series of programs were used to calculate the dimensional responses of the antenna system to the expected orbital thermal and dynamic disturbances respectively and the NASTRAN outputs of these programs were combined to calculate the RF pattern. These three outputs and the table of the superpositioned mode shapes and amplitudes submitted for RF analysis become the inputs for the block diagram shown here.

First, the dynamic and thermal results are used to find the optimal location and number of sensors necessary to detect and separate the thermal and dynamic mode profiles. This can be done by finding the peaks and nodes of the various modes and then comparing them in order to separate them and establish prime locations for mode sensors. It is very important to minimize coupling with the other modes.

Previously, the thermal and dynamic mode shapes to be considered were combined by superposition to form the cases to be submitted for RF analysis. These results are combined with the optimal detector location program to form a table of correlated detector location position readings that are used as input for the modal participation/phased array look-up table generation.

The RF analysis results are used to prepare a file of the phased array adjustments required to flatten the near-field pattern and thus minimize the side-lobes of the far-field pattern. The RF performance results and the correlated detector reading table are then used to prepare the modal participation/phased array look-up table needed for in-flight phased array corrections.

PRE-FLIGHT CALCULATIONS

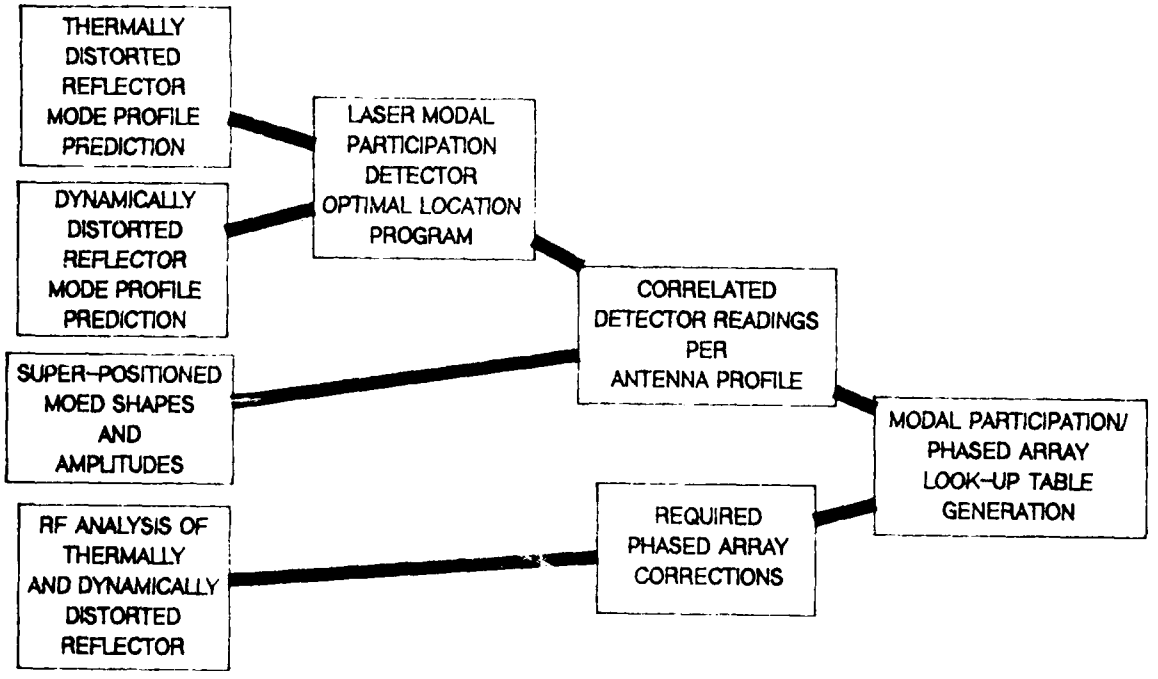

MODAL PARTICIPATION DETECTOR OPTIMAL LOCATION

Dynamic reflector vibration modes can be separated from each other and from the thermal distortion modes if motion detectors can be strategically placed on the reflector. Ideally, the detector of one mode should be placed at the maximum point for that mode and the node or zero motion points of all other modes in order to completely separate modal participation. While this perfect solution is highly improbable, it should be possible to devise a computer program to find primary desired mode detector locations that minimize the modal participation of undesired modes.

The illustration depicts an idealized antenna reflector with perfectly behaved first and second dynamic modes. In such a case it is a simple task to place the first dynamic mode M1 detector at the node point of the second dynamic mode.

MODAL PARTICIPATION DETECTOR OPTIMAL LOCATION

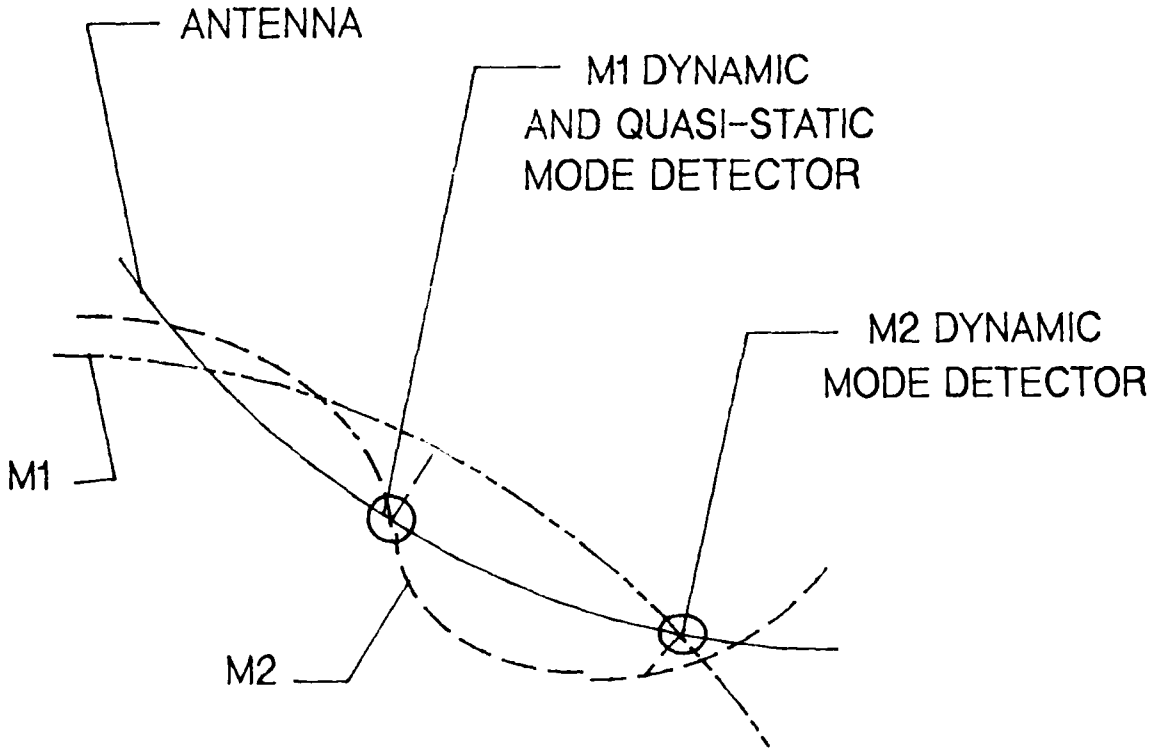

LASER MODAL PARTICIPATION DETECTOR

OPTIMAL LOCATION PROGRAM

Placement of detectors at the highest possible amplitude points of the desired antenna reflector mode and at the nodal points of all the other major quasi-static thermal and dynamic distortion modes requires that the structure be analyzed for all major modes under all assumed conditions.

One possible programmatic approach to this analysis would then be to mathematically "cover" the reflector surface with a sensor or detector grid, solve for the amplitudes of that particular mode, and store the positions of each sensor in a corresponding array. After this process is repeated for all major modes, the sensor position arrays can be compared to determine which sensors have been placed on invariant or semi-invariant points. It should then be straightforward to find the maximum amplitude of a single sensor for the desired mode that is near node lines for all other major modes.

LASER MODAL PARTICIPATION DETECTOR

OPTIMAL LOCATION PROGRAM

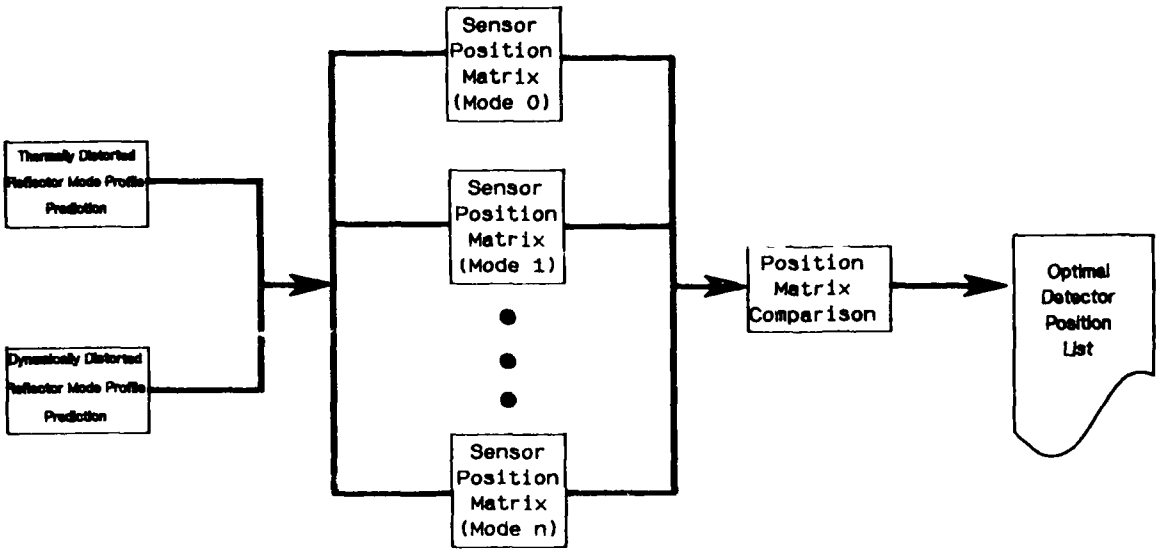

"RF ANALYSIS FOR ESTIMATING THE COMPENSATING FEED ARRAY EXCITATIONS"

The reflector surface may be described by a discrete set of data points (numerically described) or by a generalized polynomial (analytically described). The distorted reflector surface is separated into two surface components; a best fit paraboloid and an error component. The surface error component is expanded into a fourier series (spacial frequency modes). The reflector surface compensation algorithm estimates the focal plane distribution. The feed element excitations are obtained by taking the complex conjugate of the focal plane fields. It is assumed that the locations of the feed element in the focal plane are known. The algorithm for the above process has been developed by R. Acosta (Reference 1).

RF ANALYSIS FOR ESTIMATING THE COMPENSATING FEED ARRAY EXCITATIONS

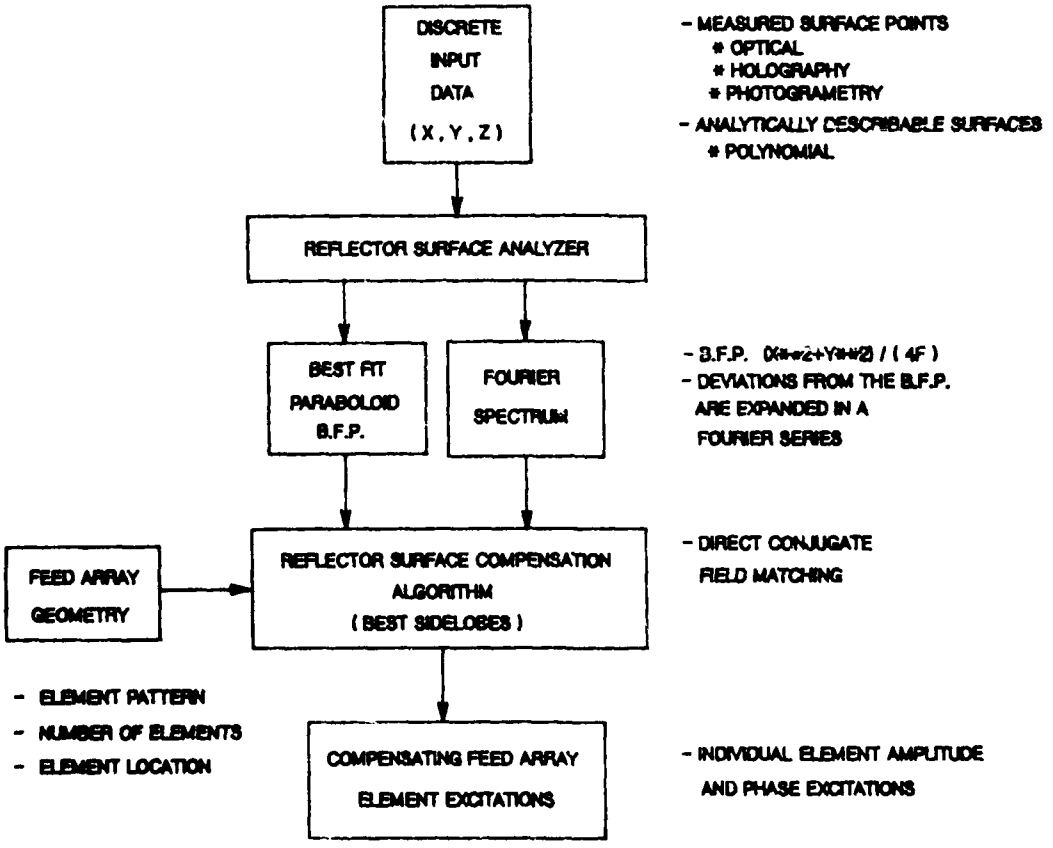

MODAL PARTICIPATION/PHASED ARRAY

LOOK-UP TABLE GENERATION

A look-up table indexed by detector position mode/amplitude sequence and containing bits for the corresponding phase-amplitude correction of the phased array is constructed from computer predictions of in-flight reflector surface profiles. When the system is in actual flight, this table is used to provide the phase-amplitude control information to correct for the effects of the quasi-static thermal and dynamic distortion modes. This table might be stored in an associative (content-addressable) memory structure embedded in a custom-designed associative processing system for fastest possible access time. Alternatively, standard read-only memory and microprocessor hardware might be preferable for reasons of economy or availability.

MODAL PARTICIPATION / PHASED ARRAY
LOOK-UP TABLE GENERATION

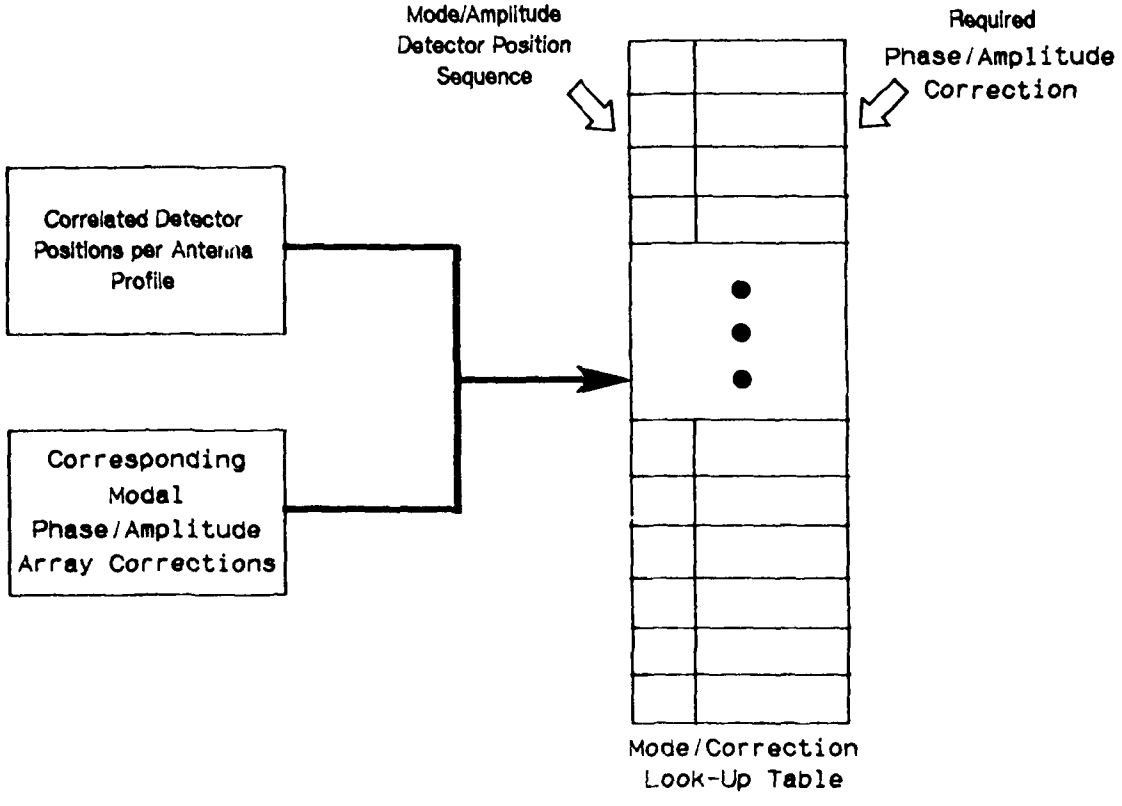

FLIGHT OPERATIONAL SYSTEM

The thermal distortion and dynamic mode profile data base that has been developed by computer modeling is used to simplify the flight system as much as possible. This is accomplished by using the output of strategically placed detectors to produce a particular detector position sequence. This data is then transmitted to the modal participation/phased array look-up table which transmits the corresponding phased array commands to the phase shifters and variable power amplifiers in the phased array for the required corrections.

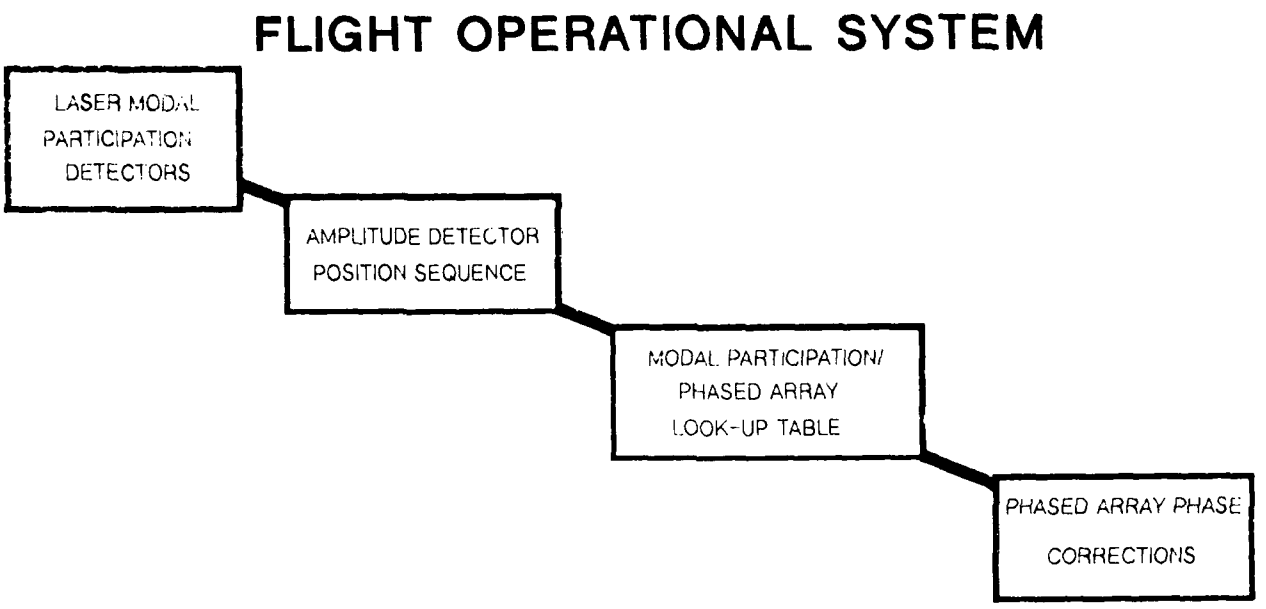

LASER INTERFEROMETER

ANTENNA REFLECTOR POSITION

DETECTION SYSTEM

The illustration shows an off-set fed antenna system geometry with antenna reflector, sub-reflector and phased array feed. However, the proposed detector system could just as easily be configured for other geometries.

Here, laser interferometry is used for position detection. Other position detection systems may work just as well. Hopefully, such a detection system could be configured to detect over-all antenna system distortion so that the phased array could be used to best advantage to correct for all system mis-alignments.

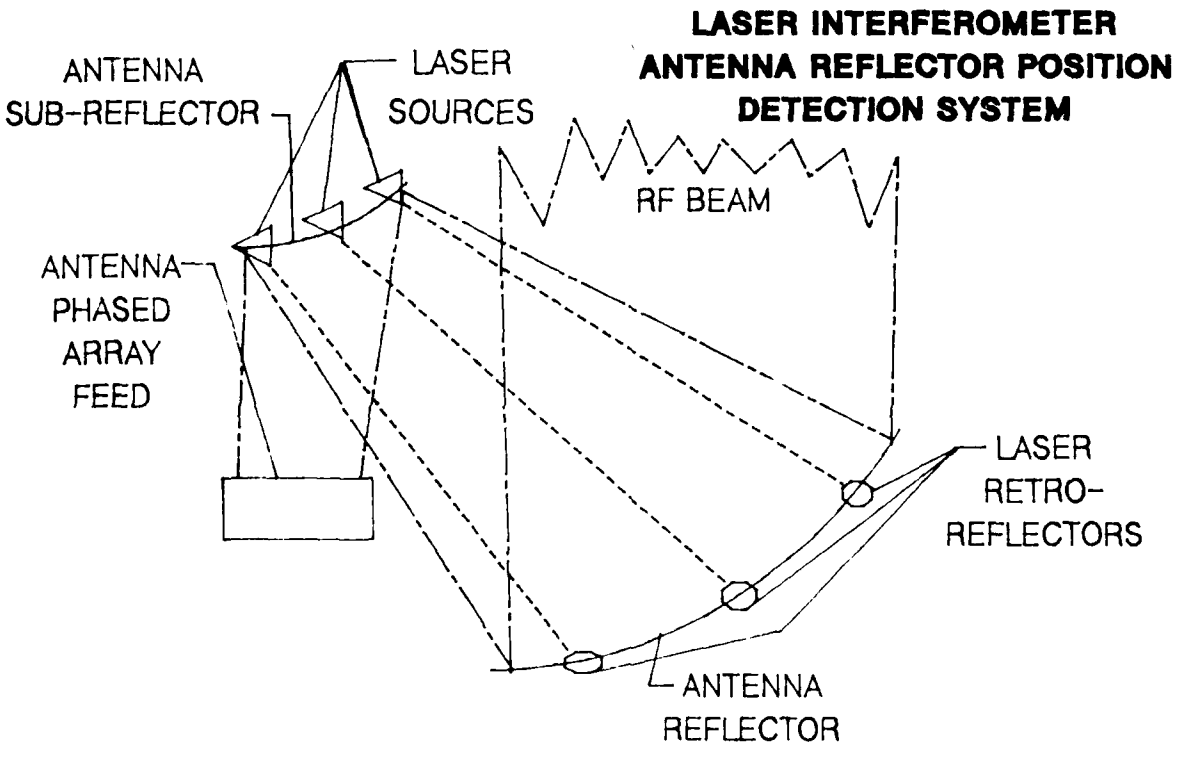

IN-FLIGHT THERMAL AND DYNAMIC MODAL IDENTIFICATION AND PARTICIPATION PROGRAM

An on-board hardware system that can analyze distortion modes and control phase-amplitude characteristics of the phased array requires relatively high speed, substantial memory, and high reliability. Such a system must be able to accept as input the digitally-encoded mode sensor locations, and amplitude sequence and send as output the necessary corrections to the phased-array control circuitry. Preliminary considerations indicate that such a system could be constructed with existing, high-speed microprocessor and memory hardware. It may be desirable, however, to custom-build an associative processing system for faster performance.

IN-FLIGHT THERMAL AND DYNAMIC MODAL IDENTIFICATION AND PARTICIPATION PROGRAM

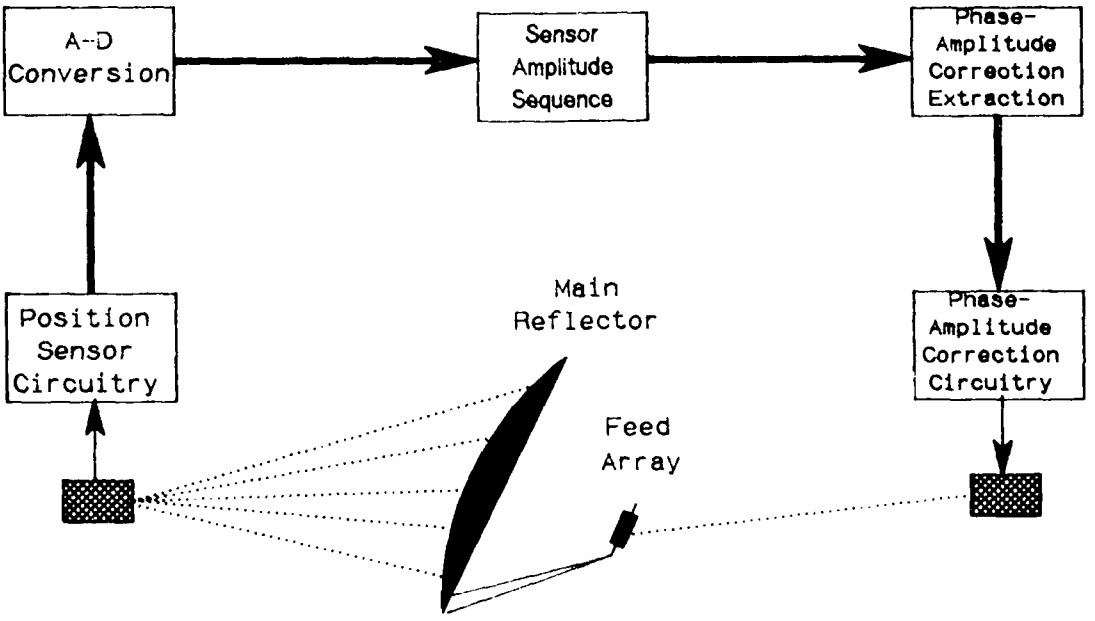

CONCEPTUAL SYSTEM DESIGN

In order to see the problems and trade-offs that might be involved a conceptual system design is shown here for feasibility demonstration purposes. For this illustration, a realitively simple phased array has been chosen. A total of eight modes with four amplitudes per mode is used for position sequencing purposes. This results in a required memory of approximately 5 M-Bits. Since memories much larger than this are in development, it makes sense that a flight phased array feed compensation system should be configured to take advantage of the largest possible memory available at the time. This should allow either the number of phased array elements or the number of modes handled to grow substantially in size. A very complete study will be needed to determine the trade-offs between array size and number of modes handled in order to maximize corrective performance.

AEROSPACE TECHNOLOGY DIRECTORATE

SPACE ELECTRONICS DIVISION

NASA Lewis Research Center

CONCEPTUAL SYSTEM DESIGN

.o ASSUMPTIONS

A. Phased Array

1. 63 elements
2. 4 bit phase shifter per element
3. 3 bit amplitude control per element

B. Modal Participation/Phased Array Look-Up Table

1. Use first three dynamic modes with four amplitudes per mode
2. Use five thermal modes with four amplitudes per mode
3. Use two Laser Interferometer Sensors per dynamic or thermal mode

o OPERATIONAL ESTIMATES

A. Phased Array

Need 4x3x63 = 756 bits per phased array configuration

B. Modal Participation/Phased Array Look-Up Table

Have $(4)^{(3+5)}$ = 65,536 Modal Participation Combinations

C. Required Memory

M=756 x 65,536 = 4.95 M bits or 194 250K bit chips

D. Response Time

1. Phased array typically sec whereas antenna reflector motions are typically in sec. or m sec. for first three dynamic modes

o CONCLUSION

System is feasible pending extensive further study

CONCLUSIONS

The development of large-scale computer memory combined with the demonstrated feasibility of phased array compensation techniques has allowed consideration of real-time corrections to the far-field pattern for thermal and dynamic disturbances to RF transmitting or receiving spacecraft. What now needs to be done is to first demonstrate the feasibility of such a system using dynamic computer modeling and then determine the applicability to existing and proposed spacecraft systems. If the lower mode natural frequencies of such spacecraft are low enough and these modes can be adequately separated and the phased array corrections can be implemented quickly enough, such a real-time system should be feasible. All these questionable areas are candidates for detailed study.

AEROSPACE TECHNOLOGY DIRECTORATE

SPACE ELECTRONICS DIVISION

NASA Lewis Research Center

CONCLUSIONS

- ANTENNA THERMAL AND DYNAMIC DISTORTION COMPENSATION USING A PHASED ARRAY FEED IS FEASIBLE
- FUTURE STUDIES WILL NEED TO CONCENTRATE ON:
  1. MEMORY SIZE AND ADDRESSABILITY
  2. ADEQUACY OF MODAL DESCRIPTION
  3. ERROR ANALYSIS OF OPERATIONAL SYSTEM
  4. DETAILED GROUND PREDICTIONS AND FLIGHT SOFTWARE REQUIREMENT
  5. SYSTEM TIME SEQUENCING
  6. ENABLING TECHNOLOGY
     a. DETECTOR SYSTEM - CANDIDATE DESIGNS

REFERENCES

1. Acosta, Roberto J.: Compensation of Reflector Surface Distortions Using Conjugate Field Matching. NASA TM 87198, 1986.

2. Lam, P. T.; Lee, S. W.; Chung, C.; Acosta, R.: Strategy for Reflector Pattern Calculation: Let the Computer Do The Work. NASA TM 87137, 1985.

3. Acosta, Roberto J.: Secondary Pattern Computation of an Offset Reflector Antenna. NASA TM 87160, 1985.

4. Lam, P. T.; Lee, S. W.; Acosta, R.: Secondary Pattern Computation of an Arbitrarily Shaped Main Reflector. NASA TM 87162, 1985.

5. Lee, R. Q.; Acosta, R.: A Numerical Method for Approximating Antenna Surfaces Defined by Discrete Surface Points. NASA TM 87125, 1985.

6. Steinbach, Russell E.; Winegar, Steven R.: Interdisciplinary Design Analysis of a Precision Spacecraft Antenna. AIAA/ASME/ASCE/AHS, 26th Structures, Structural Dynamics and Materials Conference, 1985.

7. Winegar, Steven R.: SINDA-NASTRAN Interfacing Program Theoretical Description and User's Manual. NASA Technical Memorandum 100158, 1987.

ADAPTIVE STRUCTURES

B. WADA
J. GARBA
J. FANSON
J. CHEN
G-S CHEN

JET PROPULSION LABORATORY
CALIFORNIA INSTITUTE OF TECHNOLOGY

SECOND NASA/DOD CSI CONFERENCE
NOVEMBER 18, 1987
COLORADO SPRINGS, COLORADO

OUTLINE

- MOTIVATION
- ADAPTIVE STRUCTURES
- DEVELOPMENTS
- FUTURE EFFORT
- SUMMARY

MOTIVATION
NEED

Proposed spacecraft/space payload missions are placing stringent requirements on the structure itself, such as the precision required on the geometric accuracy of large structures in both a quasi-static and dynamic environment. Large Space Structures in this presentation are defined as structures with performance requirements that cannot be verified by ground tests. This definition emcompasses structures that are relatively small and stiff with high accuracy requirements to very large and flexible structures.

Many of the proposed structures fall into the class defined as large space structures. Thus validation of the performance of the hardware by ground test is very difficult and in some cases almost impossible based upon the state-of-the-art ground test methods. Since almost all space systems flown to date, in which structural performance is important, have been validated by ground tests, the authors believe Program Managers will not adopt structural concepts that cannot be validated by ground tests.

Some argue that the advances in analysis methods and computers will negate the need for ground tests of structural systems. The authors disagree.

The on-orbit performance requirements for some of the future large space structures are so stringent that even if the structure could be built, adjusted and tested on the ground to the desired requirements, the structure will not be reproduceable to the degree required after disassembly or retraction, launch, and then assembly or deployment.

Adaptive structures will enable some of the proposed missions by relaxing the current ground test requirements and by providing the flexibility to adjust the structure to meet the performance requirements in space.

MOTIVATION
NEED

- **LARGE SPACE STRUCTURES ----> FUTURE**
  - **DEFINITION OF**
- **DIFFICULT TO VALIDATE HARDWARE**
  - **GROUND TEST**
- **MOST STRUCTURES ----> TESTED**
- **ANALYSIS**
- **ENABLE MISSIONS**
  - **DIFFERENT GROUND TEST APPROACH**
  - **PERFORMANCE**

MOTIVATION
LSS

Several years ago, a sector of a 55 meter diameter Wrapped Rib Antenna was built by LMSC under contract to JPL. Two of the objectives were to evaluate potential ground test methods to validate the structural characteristics of the structure and to evaluate ground test and adjustment methods to assure the surface accuracy would meet the requirements in space. The conclusions by the authors were that the state-of-the-art ground test methods and facilities were not adequate to experimentally determine the antenna's structural characteristics and surface accuracy requirements in space could only be assured through adjustments in space.

MOTIVATION
LSS

- **LOCKHEED WRAPPED RIB ANTENNA**
- **OTHERS .....**

MOTIVATION
STATE-OF-THE-ART

During our effort on the Galileo and the Centaur we had the opportunity to evaluate the state-of-the-art of modal test methods. The evaluation gave us an insight to the possible extension of the modal test approaches to large space structures. The data from the modal test on a "well behaved linear" Galilec structure were provided to five organizations responsible for the development of the latest state-of-the-art modal test and identification procedures. Selected comparison of the results are presented.

Similarly the data from the Centaur modal test were used by four organizations for analysis using the latest modal analysis methods. Unlike the Galileo structure, the Centaur structure was supported through trunions during the test. Selected results from the Centaur test are presented. All the work on Centaur was performed for LeRC and the majority of the test was conducted by GDCA.

A comparison of the modal analysis results indicated a wider dispersion of the test results than was anticipated. For many large structures, current ground test approaches are inadequate.

MOTIVATION
STATE-OF-THE-ART

- GLL MODAL TEST
- CENTAUR MODAL TEST

ADAPTIVE STRUCTURES

The objective in Adaptive Structures is to strive to design "ideal structures" that meet the requirements of future space missions. An "ideal structure" is defined as an efficient structure that maintains the required geometric precision in the anticipated space environment and has the desired structural characteristic (stiffness, damping, etc.) during the various expected or unexpected events during its mission. Also the "ideal structure's" performance in space must capable of being validated by ground tests and measurements.

The concept of adaptive structures is to replace a physical element in the load and/or displacement path with an Adaptive Element which can be adjusted in space to achieve the desired structural performance. Thus the parameters of interest are relative displacements and forces between the structural nodes. Note that the internal forces cannot excite the rigid body motions of the spacecraft, thus the action of the Adaptive Elements are uncoupled from the rigid body motion.

The Adaptive Elements are then used to adjust the geometry of the structure, and change the structural parameters by modifying and stiffness and/or damping. Since adverse motions are transmitted through the structure, the adaptive members directly or indirectly senses the force transmission and can provide the proper corrective excitation into the structural system.

ADAPTIVE STRUCTURES

- **IDEAL STRUCTURE**

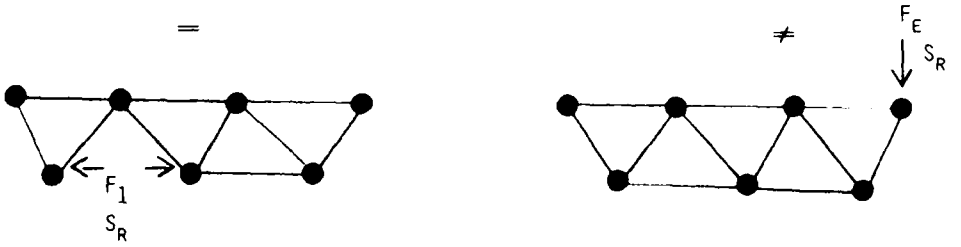

- **RELATIVE DISPLACEMENT** — **RIGID BODY MOTION**
- **INTERNAL FORCES** — **EXTERNAL FORCES**
- **"ELASTIC" DYNAMIC CHARACTERISTIC**

ADAPTIVE STRUCTURES
GROUND TEST APPROACH

The objective of the ground test program for passive structures is to accurately determine the experimental structural characteristics of the structure which is used to validate the structure and/or its mathematical model. As indicated, the state-of-the-art ground test approaches will not meet the accuracy required by future large space structures.

Since Adaptive Structures provides for adjustment of the structure in space, the objective of the ground test program can be modified to establish whether the structure is within the design bounds. The design bounds of the structure is established by the range of structural modifications possible through the Adaptive Elements and its interaction with the structure.

The structure in orbit can then be adjusted to the initial desire structural characteristics or be adjusted to other optimal values based upon flight data. The structure can be optimized to improve its performance for each of the various events in the overall mission.

ADAPTIVE STRUCTURES
GROUND TEST APPROACH

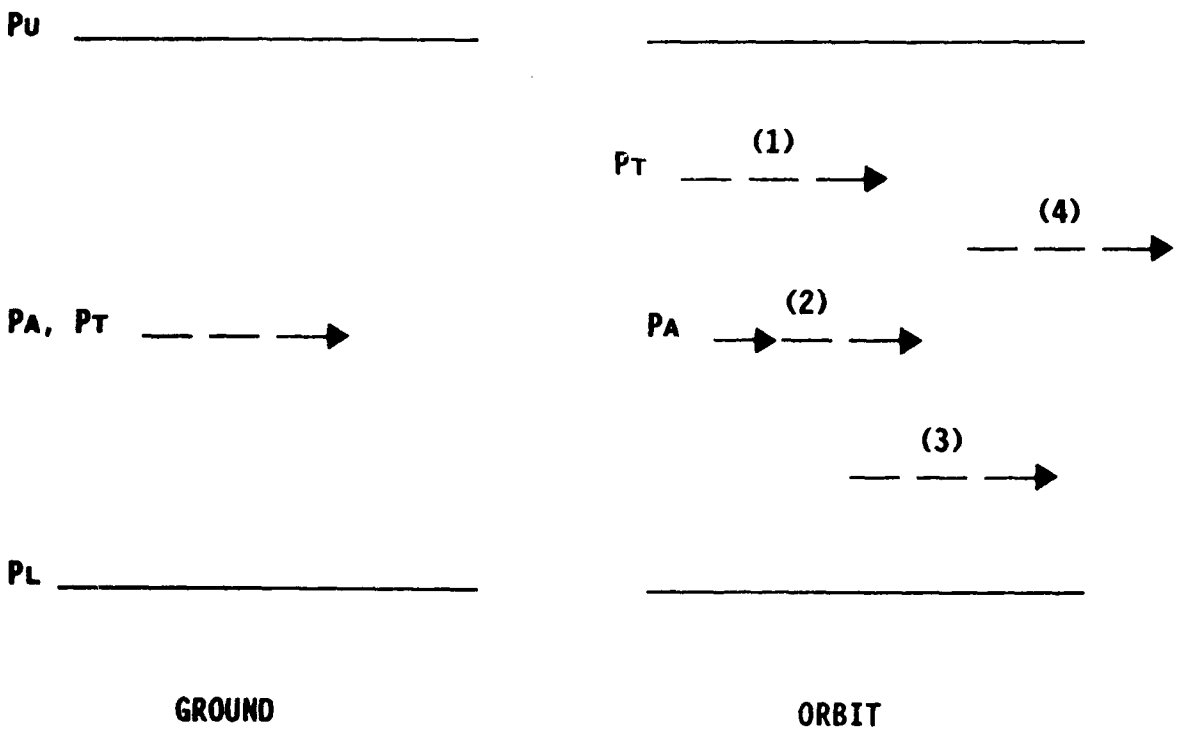

ADAPTIVE STRUCTURE
PERFORMANCE

Adaptive structure will enable missions which require precision in its structural system. For example, if relative position of the structure is required to be in the micron range, adjustments can be made through relative motion between structural joints. Relative displacement sensors exists with measurement fidelity of .01-.1 microns, thermal expansion of members are in the micron range, and the relative displacement of elements when subjected to relatively low stresses are in the micron range. Thus an appropriate place to adjust the structure when subjected to small displacements is through the structure itself. Absolute displacement measurements such as accelerometers are not sufficiently sensitive to small motions. As an example, if a one micron motion is to sensed at one Hz., a 4*E-06g acceleration must be sensed. The requirement is pushing the state-of-the-art in accelerometers. If structural adjustments are made by external forces, small errors in the geometric location of the external forces or in the magnitude and phase of the forces will induce rigid body motions; the rigid body motions will most likely be greater than the magnitude of the desired structural adjustments.

ADAPTIVE STRUCTURES PERFORMANCE

- **ACCURATE TOLERANCES**

ADAPTIVE STRUCTURE

- **RELATIVE DISPLACEMENT SENSORS = (.01 - .1) MICRON**
- $S_R/\Delta T = \alpha L = 10^{-6} * 10 = .25$ MIC.
- $S_R = \epsilon L = \frac{\sigma L}{E} = \frac{1000*10}{30*10^6}$

  = 8 MICRONS

EXTERNAL FORCES

"1 MICRON"

FREQ. (Hz)	ACCEL. (G)
1	$4*10^{-6}$
5	$100*10^{-6}$

ADAPTIVE DAMPING CONCEPTS

An example of an adaptive element is a damping element whose damping characteristics can be altered in space by adjusting the temperature of the damping material. The idea was motivated when observing that most materials used for damping treatment of structures were highly sensitive to temperature. Thus the effectivity of the damping treatment was subject to uncertainties associated with the temperature distribution of the space structure. In order to optimize the structural damping required for on-orbit performance, the concept is to utilize temperature as a control variable to achieve the damping desired in space.

The use of composite structures for space application allows a large degree of flexibility not previously available. To demostrate the concept, a heater, thermocouple, and damping material were imbedded together within a composite beam. Then experiments were performed to establish whether the value of damping could be controlled by adjusting the temperature of the damping material. Experiments on a cantilevered composite beam demonstrated the damping of the beam can be controlled by temperature.

In most space missions, high damping is only required during specific transient events such as launch transients or maneuvers in space. An application would be to excite the structure prior to the critical maneuver and establish the temperature distribution within the finite number of damping elements to obtain the desired damping values of the critical modes. Once the proper set of temperatures are established, then just prior to the critical nanuevers, local controllers can set the temperatures to the previously established optimal values.

ACTIVE VIBRATION SUPPRESSION

Another adaptive element which has a high frequency bandwidth is to place piezo-electric material in series with the adaptive element undergoing strain. When the structural motion is sensed as strain in an adaptive element, the piezo-electric material is electrically activated to force the structure with the proper phasing to add damping to the structure.

In order to illustrate the concept, a laboratory experiment was performed; excellent results were obtained. The experiment consisted of a cantilevered beam with piezo-electric material attached to both sides of the beam with opposite polarity. An electrical input would impart a moment and a rotation of the beam results in an electrical output. Active damping using piezo-electric material was illustrated.

The extension of the concept which can be incorporated into a truss type structure is to develop an adaptive element which can be used for active vibration suppression. The adaptive element can then be inserted into the appropriate location within the truss structure to add damping to specific modes.

FUTURE EFFORT

The near term planned effort includes the incorporation of the adaptive elements within a linear truss at JPL to demonstrate the applicability and to establish the performance of various adaptive elements. Also planned is an activity to incorporate adaptive elements within a two dimensional truss structure being designed for the Precision Segmented Reflector by LaRC/JPL; the sponsors of the program is Code RM of NASA OAST. Various types of adaptive members will be designed and evaluated to meet the potential needs of future space missions.

The ultimate goal is to develop flight qualified adaptive elements which can effectively utilized on a spaceflight application.

FUTURE EFFORT

- DEVELOP NEW CONCEPTS
- TEST IN LINEAR TRUSS STRUCTURES
- TEST IN PSR TWO-DIM STRUCTURE
- TEST IN OTHER ORGANIZATION'S STRUCTURES
- DEVELOP FLIGHT QUALIFIED HARDWARE
- SPACEFLIGHT

SUMMARY

ADAPTIVE STRUCTURES

- ALLEVIATES GROUND TEST
- ALLEVIATES ANALYTICAL PRECISION
- ENABLES MISSION
- IMPROVES SYSTEM PERFORMANCE

REFERENCES

1.0 Wada, Edberg, and Smith,"Adaptive Damping for Spacecraft by Temperature Control," The Role of Damping in Vibration and Noise Control , ASME, DE-Vol. 5 , Sept. 27-30,1987.

2.0 J. L. Fanson, and J-C Chen, "Positive Position Feedback Control for Large Space Structures," Presented at the AIAA Dynamics Specialists Conference, Monterey, CA, Apr. 9-10,1987.

3.0 J. L. Fanson, and J-C Chen, "Structural Control by the Use of Piezo-electric Active-Members," First NASA DOD Control Structures Interaction Technology Conference, Norfolk, VA, Nov. 18-21,1986.

4.0 J. L. Fanson and J-C Chen, "Vibration Suppression by Stiffness Control," Proceedings of the Workshop on Structural Dynamic and Control Interaction of Flexible Structures," NASA Conf. Pub. CP-2447, 1986.

5.0 J. L. Fanson, J-C Chen, and T. K. Caughey, "Stiffness Control of Large Space Structures," JPL Publication 85-29, April 1, 1985.

6.0 J-C Chen, "Response of Large Space Structures with Stiffness Control," J. Spacecr. Rockets, vol. 21, no. 5, Sept.-Oct.,1084.

METHODS RESEARCH USING EIGENSYSTEM ANALYSIS

Jer-Nan Juang
Structural Dynamics Branch
NASA Langley Research Center
Hampton, VA 23665

Richard W. Longman
Department of Mechanical Engineering
Columbia University
New York, NY 10027

John L. Junkins
Department of Aerospace Engineering
Texas A&M University
College Station, TX 77843

Second NASA/DOD
Control/Structures Interaction Technology Conference
Red Lion Inn
Colorado Springs, Colorado
November 17-19, 1987

OUTLINE

Recent progress at the Structural Dynamics Branch of the NASA Langley Research Center in the area of structural dynamics and control for large space structures is reviewed. Topics include system identification, reliable controller designs and learning controller designs for flexible structures. Promising data analysis procedures for system identification using time domain as well as frequency domain responses are described briefly along with recent applications to both laboratory models and flight hardware. Correlation of several modal testing methods for modal parameter identification via system realization theory is shown. The achievement of a reliable design for control and vibration suppression of space structures is becoming more difficult due to the desires for large spacecraft size and better performance. Current work on controller designs for reliable maneuvers of a system with modeling errors is described. A novel algorithm is presented for eigenvalue placement using Singular Value Decomposition (SVD) for state or output feedback, which is insensitive to the system uncertainties. In some spacecraft applications, the spacecraft or some portion of a spacecraft is commanded to perform the same slewing maneuver repeatedly. In such cases, it is desired to develop a learning controller which uses experience to learn to perform better and better each time it performs a maneuver. A general framework for learning control is developed and described briefly.

OUTLINE

- System identification
- Reliable (robust) controller design
- Learning controller design

NEW EIGENSYSTEM REALIZATION ALGORITHM (ERA) SUCCESSFULLY USED FOR GALILEO MODAL PARAMETER IDENTIFICATION

The Eigensystem Realization Algorithm (ERA) (Refs. 1-4), developed at the NASA Langley Research Center, is an extended version of the Ho-Kalman system realization theory from controls field. It is a procedure for constructing an analytical model, or realization, of a structure (or other dynamic system) from measurements. From the realization, the modal parameters of the structure can be calculated. If sufficient measurements are made, a dynamic model of the structure is obtained, based directly on the test results, from which a vibration control system could also be designed. The ERA method is being applied to data from a variety of laboratory experiments to understand its advantages and limitations. One particularly challenging set of data was from the modal survey test of the Galileo spacecraft, conducted at the Jet Propulsion Laboratory (JPL) in 1983. The figure shows a photo of the test article and typical analysis results. This study contributed to a JPL-coordinated project to compare the performance of various contemporary modal identification techniques. The ERA results compared favorably with those of four other industry teams, but used considerably less test and data analysis time. The right hand side of the figure shows a typical comparison from the Galileo data analysis. The reconstruction result, the smoother of the two lines in the FFT plots, is seen to closely follow the original data in both amplitude and phase.

NEW FREQUENCY-DOMAIN EIGENSYSTEM REALIZATION ALGORITHM (ERA-FD) IMPROVES MODAL PARAMETER IDENTIFICATION

The frequency domain eigensystem realization algorithm (ERA-FD) (Ref. 5), via transfer functions, is developed using a known procedure formulated for the time domain Eigensystem Realization Algorithm (ERA), via free decay measurement data. The objective is to provide proof of concept for an identification technique in the frequency domain for large flexible structures, and to expose the close conceptual connection between time domain and frequency domain approaches to identification of modal parameters for linear dynamic systems. As part of ERA-FD, accuracy indicators, namely, output modal amplitude coherence and modal spectrum coherence are developed. Important features in the frequency domain analysis include overlap averaging and windowing. The overlap averaging is used to smooth the transfer function for the complex block matrix, while the windowing is used to concentrate the analysis on the frequency range of interest. For illustration of the algorithm, examples are shown using simulated data and experimental data from a truss structure. The test article, shown in the figure, is a 26.25 ft by 3.75 ft flexible truss structure. Three-dimensional spectra of these measurements are shown in the lower part of the figure. Each spectral peak represents one or more modes of the structure. The ERA-FD requires much less computation and storage than time domain techniques. The method is very promising for use in orbit measurements with a small flight computer.

NEW FREQUENCY-DOMAIN EIGENSYSTEM REALIZATION ALGORITHM (ERA-FD) IMPROVES MODAL PARAMETER IDENTIFICATION

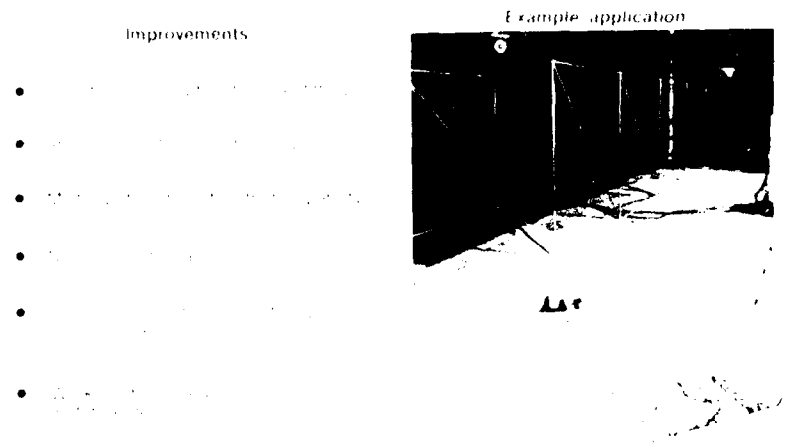

AN EIGENSYSTEM REALIZATION ALGORITHM USING DATA CORRELATIONS (ERA/DC)

A common drawback of time domain methods for system identification is that they produce biased estimates when noise is present and the true model order used. There are various approaches used in the system identification field for reducing bias. Among them, the overspecification principle is used in some of the common time domain modal testing techniques including the ERA. It is possible to reduce bias by overspecification of the model order used in the solution but additional spurious results are generated and need to be rejected via some criteria. The Correlation Fit method, which is non-iterative and does not rely upon model overspecification, is potentially suitable for modal testing and has been proven to compare favorably to other approaches. It eliminates or minimizes the effect of the terms that cause bias. Here, the ERA and Correlation Fit philosophies have been combined to produce the Eigensystem Realization Algorithm using Data Correlations (ERA/DC), to study whether the identification obtained using the ERA can be improved upon. This new method, the (ERA/DC) (Ref. 7), reduces bias errors due to noise corruption significantly without the need for model overspecification. It is found that, when model overspecification is permitted and a minimum order solution obtained via singular value truncation, the results from the two methods are of similar quality.

AN EIGENSYSTEM REALIZATION ALGORITHM USING DATA CORRELATIONS (ERA/DC)

- Objective: To reduce bias error associated with least squares estimation for modal parameters of flexible structures when measurement noise is present

- Approach: Combine system realization and data correlation philosophies

- Results: The ERA/DC can reduce bias without model overspecification

RECURSIVE EIGENSYSTEM REALIZATION ALGORITHM

An algorithm is developed for recursively calculating the minimum realization of a linear system from sampled impulse response data (Ref. 6). The Gram-Schmidt orthonormalization technique is used to generate an orthonormal basis for factorization of the data matrix. The system matrix thus identified is in upper Hessenberg form, which has advantages for the identification of modal parameters including damping coefficients, frequencies, mode shapes and modal participation factors. The recursive algorithm developed here allows one to build up to the proper order, in contrast to the standard version of the Eigensystem Realization Algorithm which creates a large dimensional order and then truncates to the appropriate dimension. Recursive procedures may require more computation than their non-recursive counterparts. However, this algorithm has no loss in computational efficiency, because, once the matrix elements of a realization have been computed, they will never be altered in the following recursive steps. The recursive form will produce the results somewhat quicker than the non-recursive version. Future work will be directed toward the recursive identification with arbitrary forcing inputs and consider recursion in both columns and rows.

RECURSIVE EIGENSYSTEM REALIZATION ALGORITHM

- Recursive in time
- Computational efficiency and lower storage
- Special Hessenberg structure of the system matrix for easy computation of modal parameters
- Build up to a proper order for a system
- Work as good as time-domain ERA for low order systems

NEW DEVELOPMENTS ADD VERSATILITY TO SYSTEM IDENTIFICATION BY EIGENSYSTEM REALIZATION ALGORITHM (ERA)

The first objective of this research is to develop improved methods for analyzing measured dynamic data to estimate dynamic properties, i.e. modal parameters, such as damping, natural frequencies, mode shapes and modal participation factors. The second objective is to develop a unified mathematical framework to treat modal parameter identification so as to achieve an integrated understanding of the field of modal testing. The solid theoretical and methodological foundations of modern controls analysis is combined with the extensive experimental knowledge from the modal testing field. Several variations of the ERA method for modal parameter identification, shown in the chart, have been derived using system realization theory (Ref. 8). Transfer functions are the basic elements for the frequency-domain ERA, whereas the other methods use the free decay responses. The choice of methods can be made largely on the basis of the final purpose of the identification, such as mathematical model improvement or on-line control of flexible structures. All methods have been shown to work well on simulated and test data. There are a number of different important features for each method. The relations between different techniques have been explained and well correlated using system realization theory, providing a basis and insight for comparison and evaluation. Through combing technology from the fields of control and structural dynamics, the diverse field of modal parameter identification is moving towards more unification. A common basis, via system realization theory, is found to explain and to select from the myraid of possible techniques.

NEW DEVELOPMENTS ADD VERSATILITY TO SYSTEM IDENTIFICATION BY EIGENSYSTEM REALIZATION ALGORITHM (ERA)

Application* / Algorithm	Free Decay	Forced Response	Small Computer	On-line	Rapid Analysis	High Accuracy
Original ERA	X				X	X
Frequency domain ERA		X	X			X
Recursive ERA	X			X	X	
Data correlation ERA	X		X			X

*Assumes noisy data

NEW TOOLS FOR USE IN ERA

The identification of modal parameters from experimental test data is affected by noise in the data. Assume that the statistical properties of the measurement noise can be obtained from known properties of the sensors or from certain experimental tests. Mathematical expressions are developed based on perturbation theory to predict the variance of each of the identified modal parameters resulting from these measurement noise, when using the ERA algorithm. This serves as a statement of how confident the user should be in the identification results. It also tells the user which modes are identified well enough to be included in the mathematical model. Explicit interpretation of the variance information is given in terms of confidence intervals which explicitly state how likely the modal parameters are to lie within any chosen interval around the identification results. Previoulsy, this type of variance information was only available by using very time consuming Monte Carlo computer runs. The perturbation results obtained here give still more information. Use of a large amount of data can decrease the variance, due to noise in data, but can also increase the bias in the estimate. Furthermore, both variance and bias are influenced by the choice of which data points are included in the identification. The new tools developed here give mathematical estimates for the bias (Ref. 9) as well as the variance, and hence not only tells the ERA user how good his results are but also guides him in choosing how much data and which data points give best results.

NEW TOOLS FOR USE IN ERA

- New accuracy indicators developed for each modal parameter
  - variance
  - quadratic bias
  - truncation bias
  - confidence intervals for desired confidence level
- Bias and scattering for each modal parameter estimated without Monte Carlo analysis
- Accuracy of identified mathematical model estimated

RELIABLE EIGENSYSTEM ASSIGNMENT

An improved method is developed for eigenvalues and eigenvectors placement of a closed-loop control system using either state or output feedback (Refs 10 - 11). The method basically consists of three steps. First, the singular value or QR decomposition is used to generate an orthornormal basis that spans admissible eigenvector space corresponding to each assigned eigenvalue. Secondly, given a unitary matrix, the eigenvector set which best approximates the given matrix in the least-square sense and still satisfy eigenvalue constraints is determined. Thirdly, a unitary matrix is sought to minimize the error between the unitary matrix and the assignable eigenvector matrix. For use as the desired eigenvector set, two matrices, namely, the open-loop eigenvector matrix and its closest unitary matrix are proposed. The latter matrix generally encourages both minimum conditioning and control gains. In addition, the algorithm is formulated in real arithmetic for efficient implementation. Numerical examples provide some indication of the simplicity and usefulness of the approach and in particular, the advantage of using the open-loop eigenvector matrix or its closest unitary matrix as the desired eigenvector matrix. However, it is clear that the results outlined here is by no means complete and in particular, further work is needed to address the stability problem related to the unassigned eigenvalues for the direct output feedback.

RELIABLE EIGENSYSTEM ASSIGNMENT

- **Problem:** Find insensitive, small control gains that assign closed loop eigenvalues

- **Approach:**
  - Use SVD to compute assignable eigenvalues
  - Compute assignable set closest to apriori orthogonal matrix
  - Choose orthogonal matrix that minimizes projection error

- **Result :** Numerically reliable real algorithm to obtain control gains for state and output feedback

The reason for this particular choice is twofold. First, it is intuitively obvious that the control gains will be close to zero if the desired eigenvector is similar to the open-loop eigenvector when the desired eigenvalues are close to the open-loop eigenvalues. Secondly, the open-loop eigenvector may not be unitary, i.e. not perfectly conditioned, so that the closest unitary neighbor would encourage the selection of a well-conditioned achievable set. The choice of open-loop eigenvector and its closest unitary matrix, as proposed, is believed to be suitable for the purpose of generating well-conditioned eigensystem with small control gains (Refs. 10 -11).

AD-HOC OPTIMAL CHOICE OF DESIRED EIGENVECTORS

- A reasonably good choice of Q is the unitary matrix closest to open-loop eigenvector matrix

$$Q = UV^T$$

where $\Psi_{OL} = U\Sigma V^T$ = open-loop eigenvector matrix

- Heuristic reasons for choice:

(1) control gain $\longrightarrow$ 0 as desired *eigenvectors* $\longrightarrow$ open-loop eigenvectors

if desired eigenvalues $\approx$ open-loop eigenvalues

(2) open-loop eigenvectors are not unitary in general

- Above choice generally produces well-conditioning and small control gains non-iteratively

MAXIMUM PROJECTION CORRELATION

For a given set of orthogonal column vectors, the resulting condition number and the norm of gain matrix depend on the choice of the vector to be used for each mode. For problems with closely spaced modes, as is common in flexible space structures, the correlation between open-loop modes and subspaces of admissible eigenvectors may not be obvious. This is also evident for unitary matrices which do not have direct physical meaning. The approach taken here to resolve the above correlation problem is to search for the mode with the maximum orthogonal projection among the given set of desired eigenvectors into each admissible eigenvector subspace (Ref. 10). The observability plays an important role in determining the correlation of desired eigenvectors with the subspaces of admissible closed-loop eigenvectors. Maximum projection is meaningless if the eigenvector is unobservable!

MAXIMUM PROJECTION CORRELATION

- Correlation between a desired set of eigenvectors and subspace of achievable eigenvectors
- Improved correlation ⟶ minimizes gains and condition number achievable
- Given Q, search for the vector with maximum orthogonal projection into each achievable eigenvector subspace $\bar{v}$

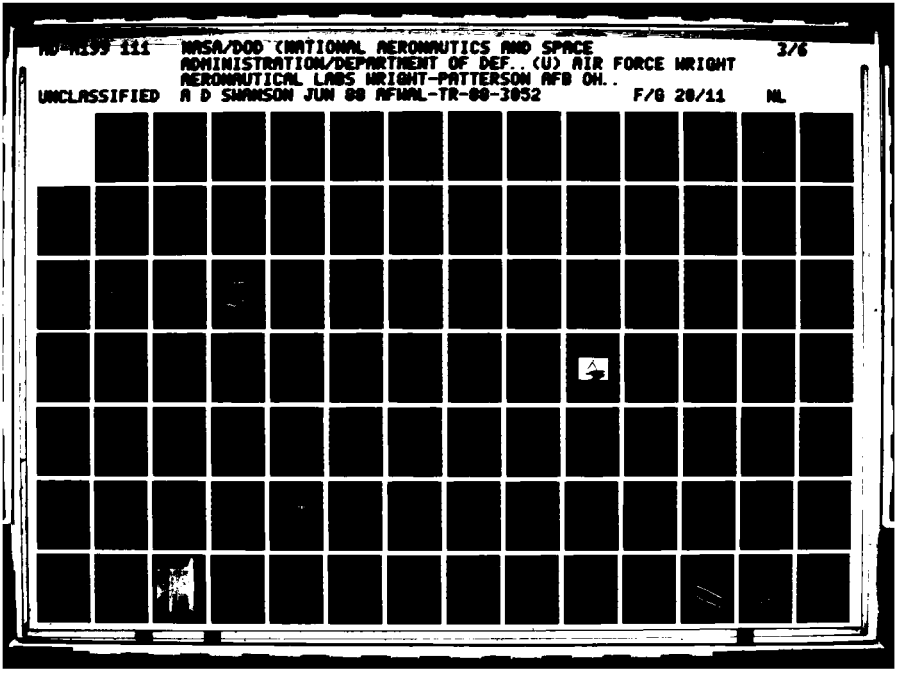
AD-A159 111 NASA/DOD (NATIONAL AERONAUTICS AND SPACE ADMINISTRATION/DEPARTMENT OF DEF..(U) AIR FORCE WRIGHT AERONAUTICAL LABS WRIGHT-PATTERSON AFB OH..
3/6
UNCLASSIFIED A D SWANSON JUN 80 AFWAL-TR-80-3052 F/G 20/11 NL

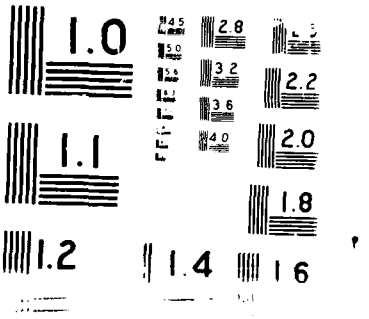
1.0
1.1
1.2
1.4
1.6
1.8
2.0
2.2
2.8
3.2
3.6
4.0

EIGENSYSTEM ASSIGNMENT FOR COFS 1 CONFIGURATION

The system investigated is a reduced order finite element model of the MAST truss beam structure (Ref. 10). The model includes the deployer retractor assembly, Shuttle inertia properties, and rigid platforms for sensors and actuators allocation. The reduced order model consists of 92 first order equations and it includes actuator/sensor dynamics and six rigid body degrees of freedom in addition to elastic deformation. A total of 10 actuators using 20 output measurements (out of which 19 was found to be linearly independent) are used to increase the damping ratio of a selected set of elastic modes to 5%. Although nineteen eigenvalues are assignable, only nine pairs of complex eigenvalues (corresponding to elastic modes) are assigned. The corresponding frequencies and damping values are shown in the Table. Since not all eigenvalues can be assigned, due to the limitation of the number of measurements or the actuator, the remaining eigenvalues are not guaranteed to remain stable. Further research is needed to alleviate the stability problem for direct output feedback.

EIGENSYSTEM ASSIGNMENT FOR COFS 1 CONFIGURATION

OBJECTIVE: Increase damping factor of a selected set of elastic modes to 5%

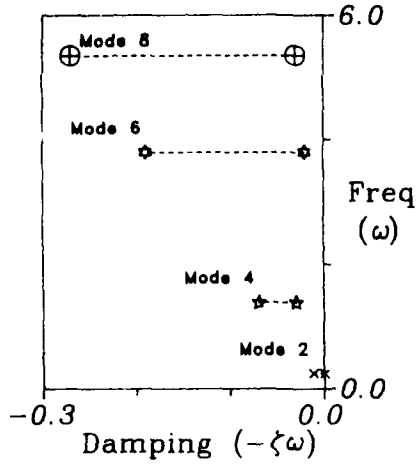

Mode No.	Open-loop		Closed-loop	
	ω^0 (Hz)	ζ^0	ω (Hz)	ζ
1	.183	.004	.183	.050
2	.241	.004	.241	.050
3	1.330	.023	1.330	.050
4	1.387	.022	1.387	.050
5	1.554	.021	1.554	.050
6	3.791	.006	3.791	.050
7	3.969	.006	3.969	.050
8	5.348	.005	5.348	.050
9	6.650	.005	6.650	.050

LEARNING CONTROLLER DESIGN
(Features)

A learning or self-teaching controller learns to do a better job of controlling a system each time it repeats a specific operation or maneuver. Using normal control methods, a controller will repeat the same "mistakes" (or error history) every time it performs a specific maneuver. Learning control reduces the need for exact system modelling and for accurate tuning of the controller. The method can be considered for improving the performance of any type of controller. Implementation is often easy, by simply adding the learning signal to the control signal present in the system.

LEARNING CONTROLLER DESIGN
(Features)

- Perform better and better each time a maneuver is repeated
- Reduce the need for accurate system modelling and controller tuning
- Improve the performance of any type of controller
- Easy implementation: simply add learning signal to system control signal

LEARNING CONTROLLER DESIGN
(Applications)

In some satellite applications, the satellite or some portion of a satellite is commanded to perform the same slewing maneuver repeatedly. An important application is in the slewing of flexible antennas in which the antenna is scanning. In such cases one wants to maintain the shape of the antenna from start to finish in the scan in spite of initial transients. In space station assembly, repetitive motion in building truss structures may be required. The learning controller can increase accuracy by learning from past performance. The space manipulators such as the shuttle remote manipulator tend to be large in size and light weight. This implies that the flexibility effect is important. The learning control can learn to account for the flexibility effect. For nonrepetitive operations, the learning is accomplished in computer simulations, and the learning signal then transmitted to the controller -- very general applications.

LEARNING CONTROLLER DESIGN (Applications)

- Repetative slewing or scanning maneuvers of spacecraft
- Repetative robot motions in space or on earth
- Nonrepetative operations
  - Generate learning signal by computer simulations
  - Transmit learning signal to the controller

LEARNING CONTROLLER DESIGN
(Progress)

A great deal of progress has been made in this area. The existing method which is referred to as p-integrators is studied on various types of simulation problems to learn its characteristics. A very general framework is developed for learning control which contains p-integrators and other currently known learning control laws as special cases. This general framework has been used very effectively to generate very promising control tuning or design methods that select the constants in the learning control law. This is a major contribution, since other general frameworks for learning control in repetitive motions can often prove convergence for a class of controls but has no constructive way to design the controller. Certain mathematical tools are developed to aid in the analysis of learning control systems. One of the major concerns with integral control from classical control theory is that it will give better steady state performance, but has a tendency to destabilize a system. The learning controllers, which usually also contain integration effects in more complicated ways, should have the same property. The stability problem of the learning operation must thus be studied. Pratical implementation of integral control requires some attention to questions of bias in the integrator causing saturation problem. There are various practical methods of handling this difficulty. This problem and its solutions must also be investigated for the learning controllers.

LEARNING CONTROLLER DESIGN
(Progress)

- Start with p-integrator concept (existing method)
- A broad new framework is developed for general learning controller designs, e.g. time optimal operation
- Methods of analyzing the stability of the learning operation are developed
- The effects of control saturation constraints are investigated
- The effects of noise on the learning operation are studied

MANIPULATOR CONFIGURATION AND DESIRED TRAJECTORY

The manipulator configuration simulated is shown in the figure. The simulation includes the following factors: Full coriolis and centrifugal forces, DC motor inductance, resistance and back emf, servo amplifier saturation, ideal gear reductions and friction terms proportional to velocity. The path used involves the end of the robot moving from (x, y, z) = (0.6, 0.2, 0.0) to (1.0, -0.1, -0.3) and back every 2 sec. Thus the end of the robot must move at an average speed of over .58m/sec. The path is essentially constant velocity except near the turning points where the trajectory has been smoothed.

MANIPULATOR CONFIGURATION AND DESIRED TRAJECTORY

configuration

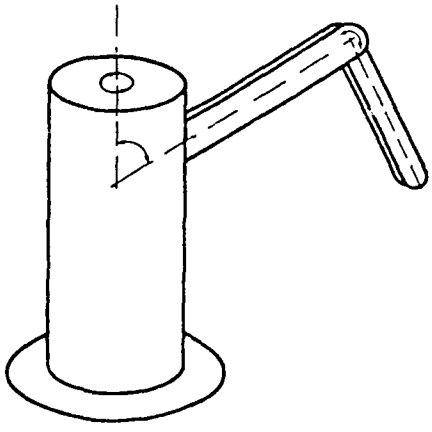

trajectory

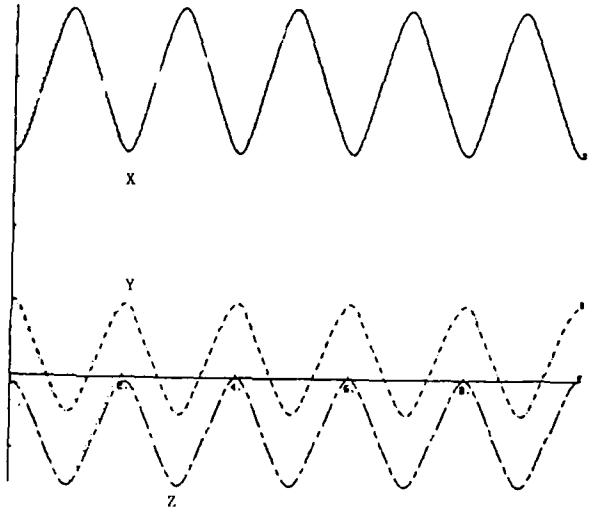

POSITION ERRORS WITH/WITHOUT LEARNING CONTROL

The Proportional Integral Derivatives (PID) controller is a standard classical feedback controller which is usually included in the robot hardware. The PID controller used in the simulation is a simple digital design where the gains are fixed and have been chosen to give a reasonable step response. The digital PID controller is implemented at a sampling period of 20 msec, whereas the learning controller is implemented with a sampling period of 100 msec. The right hand side of the figure shows the results of position errors if the PID control only is used. The steady state error is about 15 mm. This error can only be reduced by increasing the servo gains with consequent reduction in stability and gain margin. The left side of the figure shows the results of position errors when a learning controller is added to the system. The error after the "warm up" period is less than 0.5 mm in any direction. The warm up period is quite short, namely after about two operations of the task the errors are below about 2 mm.

POSITION ERRORS WITH/WITHOUT LEARNING CONTROL

with learning control

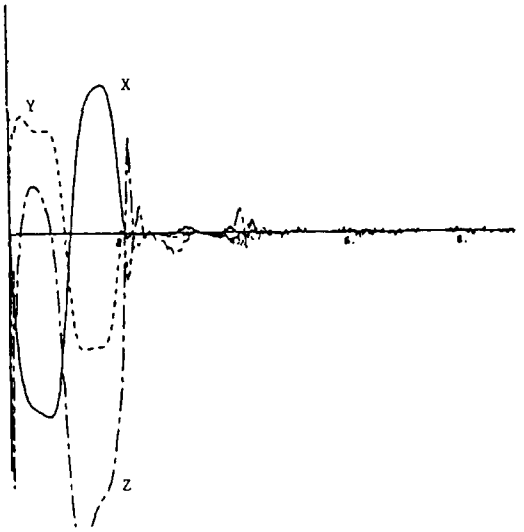

without learning control

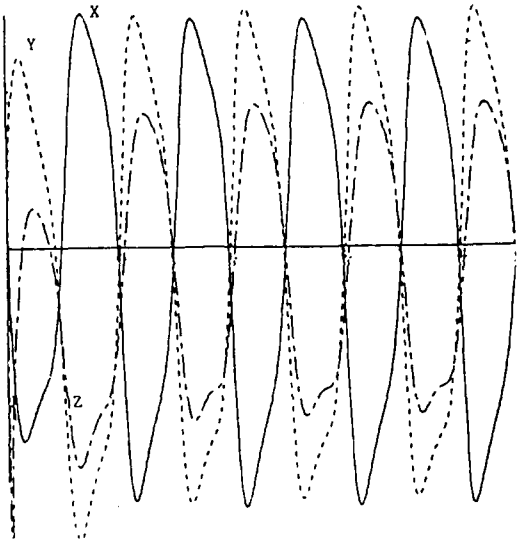

CONCLUDING REMARKS

Several methods for modal parameter identification have been presented and derived using system realization theory. The relations between different techniques are reasonably well understood and the choice of methods can be done largely on the basis of the final purpose of the identification, for example, control of flexible structures. Most methods are claimed to work well on simulated and test data. In spite of a large literature on identification, there are few papers which compare different techniques using experimental data. Unfortunately, conclusive results have not been obtained. It is hoped and expected, through the interaction of control and structure fields, that the field of modal parameter identification is moving towards more unification and that there will be more comparisions of different methods. A novel algorithm using real arithmetic is presented for eigenvalue placement using Singular Value Decomposition (SVD) for state or output feedback. Numerical examples provide some indication of the simplicity and usefulness of the approach and in particular, the advantage of using the open-loop eigenvector matrix or its closest unitary matrix as the desired eigenvector matrix. However, it is clear that the results outlined here is by no means complete and in particular, further work is needed to address the stability problem related to the unassigned eigenvalues for the direct output feedback. The research discussed above on the learning controller design constitutes most of theoretical issues with computer simulations as support. The next step is to demonstrate the effectiveness of the ideas in experiments.

CONCLUDING REMARKS

- System identification methods are presented
  - time domain, frequency domain, recursive, and data correlation ERA
  - techniques developed for correlations of existing modal testing methods
- Reliable (robust) controller designs are presented
  - closed-loop eigenvalue placements
  - closed-loop eigenvector placements
- Learning controller designs are presented

REFERENCES

1. Juang, J. N., and Pappa, R. S.: "An Eigensystem Realization Algorithm for Modal Parameter Identification and Model Reduction," Journal of Guidance, Control and Dynamics, Vol. 8, No. 5, Sept.-Oct. 1985, pp. 620-627.

2. Pappa, R. S. and Juang, J. N.: "Galileo Spacecraft Modal Identification Using an Eigensystem Realization Algorithm," The Journal of the Astronautical Sciences, Vol. 33, No. 1, Jan.-Mar., 1985, pp. 15-33.

3. Juang, J. N. and Pappa, R. S.: "Effect of Noise on Modal Parameters Identified by the Eigensystem Realization Algorithm," Journal of Guidance, Control, and Dynamics, Vol. 9, No. 3, May-June 1986, pp. 294-303.

4. Pappa, R. S. and Juang, J. N., "Studies of Modal Identification Performance Using Hybrid Data," International Journal of Analytical and Experimental Modal Analysis, April 1987.

5. Juang, J. N. and Suzuki, H., "An Eigensystem Realization Algorithm in Frequency Domain for Modal Parameter Identification," Journal of Vibration, Acoustics, Stress and Reliability in Design, to appear in 1988.

6. Longman, R. W. and Juang, J. N. "A Recursive Form of the Eigensystem Realization Algorithm," Journal of Guidance, Control and Dynamics, to appear in 1988.

7. Juang, J. N., Cooper, J. E. and Wright, J. R., "An Eigensystem Realization Algorithm Using Data Correlations (ERA/DC) for Modal Parameter Identification," A special issue on Control in Space Technology, Journal of Control Theory and Advanced Technology, Japan, to appear in 1988.

8. Juang, J. N., "Mathematical Correlation of Modal Parameter Identification Methods Via System Realization Theory," International Journal of Analytical and Experimental Modal Analysis, Vol. 2, No. 1, Jan. 1987, pp. 1-18.

9. Longman, R. W. and Juang, J. N., "A Variance Based Confidence Criterion For ERA Identified Modal Parameters," Paper No. AAS 87-454, Presented at the AAS/AIAA Astrodynamics Conference, Cavanaugh Motor Inn, Glacier National Park, Kalispell, Montana, Aug. 10-13, 1987.

10. Juang, J. N. Lim, K. B. and Junkins, J. L., "Robust Eigensystem Assignment for Flexible Structures," Journal of Guidance, Control and Dynamics, to appear in 1988.

11. Rew, D. W., Junkins, J. L. and Juang, J. N., "Robust Eigenstructure Assignment by a Projection Method," Journal of Guidance, Control and Dynamics, to appear in 1988.

COMMENTS ON LDCM ACTUATORS

Douglas K. Lindner
Bradley Department of Electrical Engineering
Virginia Polytechnic Institute and State University
Blacksburg, Virginia

Jeff L. Sulla
PRC Kentron
Hampton, Virginia

Eric Ide
Bradley Department of Electrical Engineering
Virginia Polytechnic Institute and State University
Blacksburg, Virginia

Second NASA/DOD CSI Technology Conference
Colorado Springs, Colorado
November 16-19, 1987

Presentation Outline

A Linear DC Motor (LDCM) has been proposed as an actuator for the COFS I Mast and the COFS program ground test article Mini-Mast. This talk will review the basic principals of operation of the LDCM as an actuator for vibration suppression in large flexible structures. After a brief description of the actuator, the force limitations imposed by the actuator will be discussed. Next, a model of the actuator plus Mast is developed including the control loops for stabilizing the actuator. Finally, sample simulations are presented.

Presentation Outline

- INTRODUCTION
- BASIC MODEL
- LIMITATIONS
- ACTUATOR CONTROL
- SIMULATION RESULTS
- CONCLUSION

Typical LDCM Actuator

This figure shows the geometry of the actuator. The base is attached to the Mast. A force is applied to the reaction mass via coil windings in the base. Of course, an equal and opposite force is applied to the base (and so the Mast).

The LDCM actuator is being built in two sizes. A type I actuator has a 11.6 kilogram reaction mass and a 15 centimeter stroke. Four of these actuators will be located at the tip of the Mast.

A Type II actuator has a 6.8 kilogram reaction mass and a 7 centimeter stroke. Six of these actuators will be located along the length of the Mast.

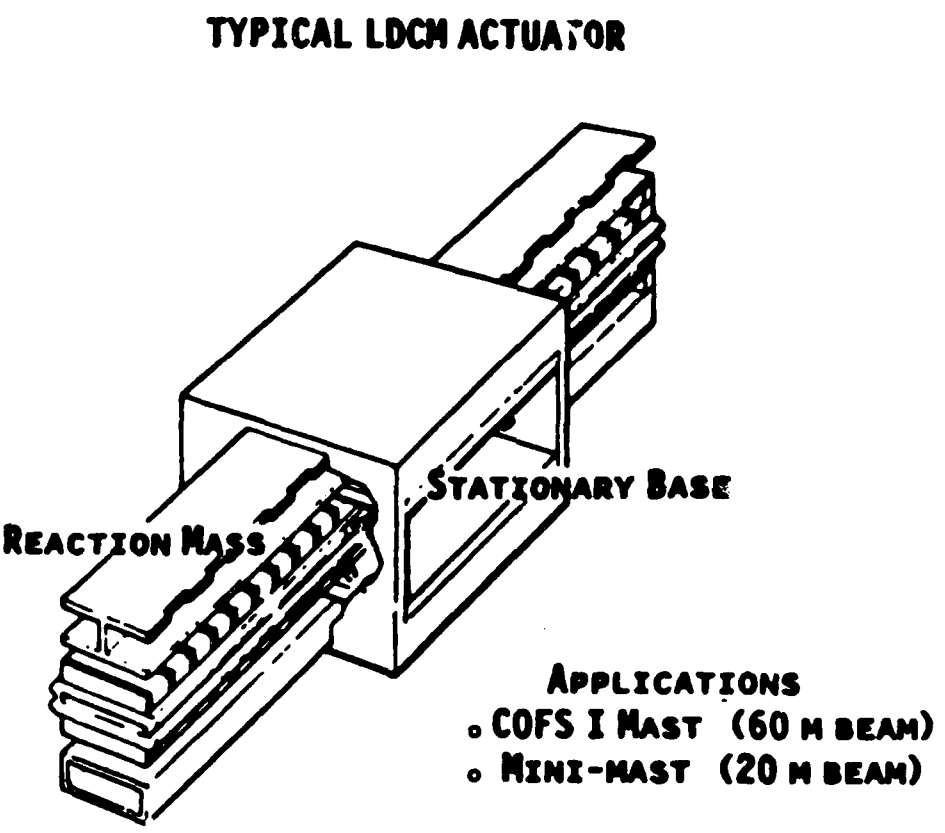

Maximum Force Output of the LDCM Actuator

The force limitations of this actuator are derived from two sources. First, the maximum force achievable is limited by the stroke of the reaction mass. Secondly, the maximum force is limited by the power delivered by the electronics. The first limitation is active at low frequencies while the second limitation is active at high frequencies as shown in the figure below. Note that the first ten flexible modes of the Mast are under 7 Hz.

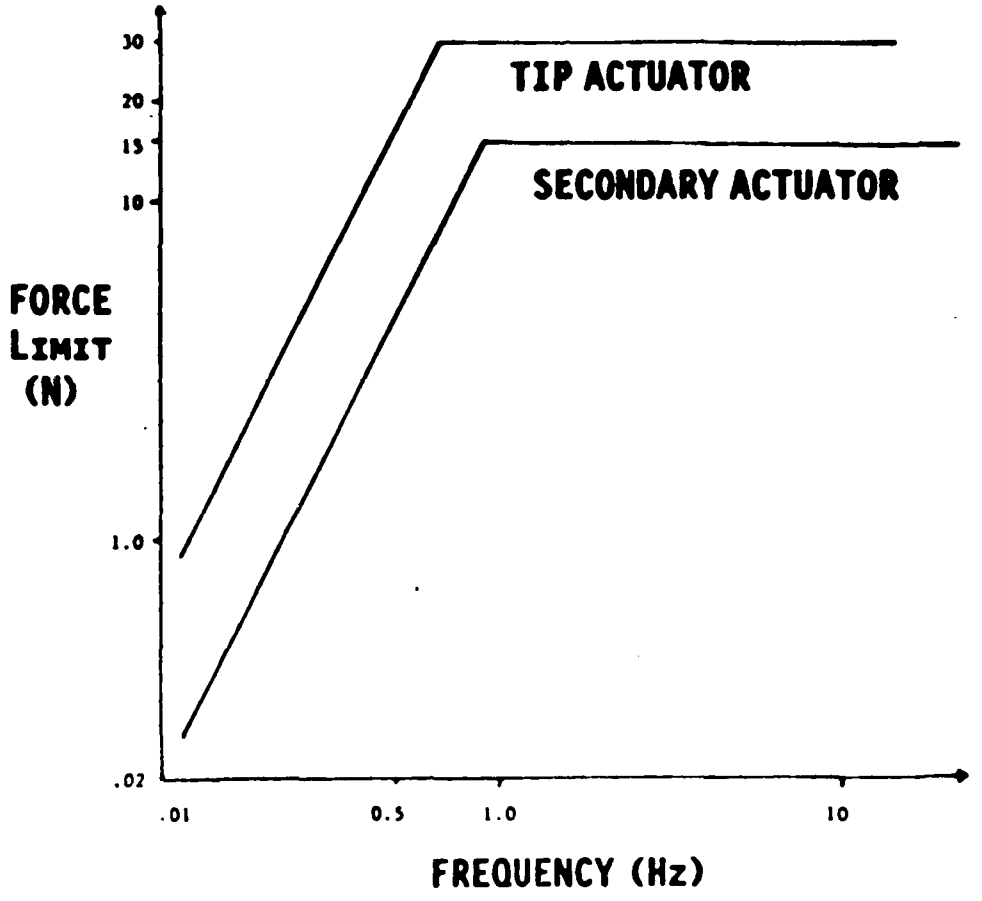

Next we investigate the performance of the actuator on the Mast. We can write a simple model for the actuator on the Mast by summing forces on the reaction mass. This model assumes a standard finite element model of the Mast.

SYSTEM MODEL

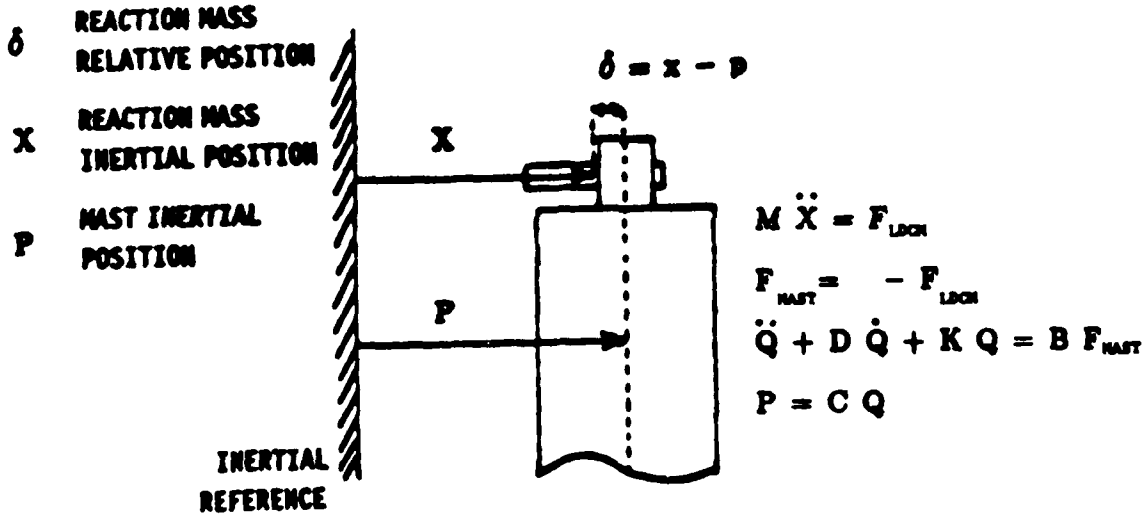

Uncontrolled LDCM Actuator

A block diagram of an uncontrolled LDCM actuator is shown below. F_{ldcm} is essentially the current input to the actuator. This figure clearly shows that in this configuraton, the actuator is unstable. Hence, actuator stabilization loops are required.

UNCONTROLLED LDCM ACTUATOR

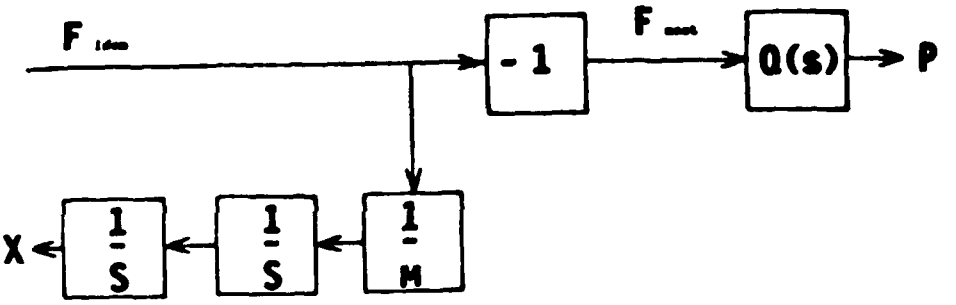

Example LDCM Controller

This figure shows one possible concept for stabilizing the actuator. It is essentially position and velocity feedback. Note, however, that the only position measurement (digital) available is relative position. Hence, the actuator control loops couple the actuator to the structure in a feedback configuration rather than the usual cascade configuration of plant plus actuator.

Also note that the digital position measurement results in force spiking. Thus, a "clean" force is not applied to the structure. The simulations shown next take into account this digital measurement and the force limits imposed by the electronics.

EXAMPLE LDCM LOCAL CONTROLLER

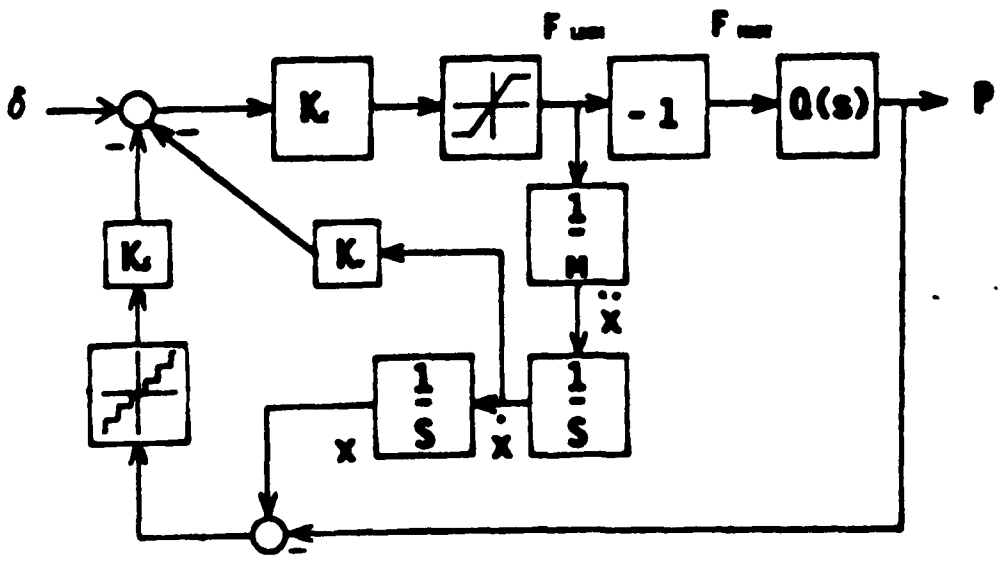

F FORCE APPLIED ON REACTION MASS
x REACTION MASS INERTIAL POSITION
P MAST INERTIAL POSITION
δ POSITION COMMAND INPUT

The simulation model included all ten actuators with non-linearities coupled to a 16 mode Mast & Shuttle model (6 rigid body plus 10 flexible modes). The system was excited by applying a sinusoidal relative position command with frequency corresponding to the second bending mode in the x-direction to those actuators which would be most effective in exciting that mode. All other actuators were given a zero relative position command.

SIMULATION MODEL

16 MODE MAST & SHUTTLE MODEL

6 RIGID BODY MODES

10 FLEXIBLE MODES

10 ACTUATORS

DIGITAL POSITION MEASUREMENT

SATURATION NONLINEARITY

INPUT COMMAND

0.05 sin wt, $w = 2\pi$ (1.36)
5 CYCLES AT BAY 44 X-DIRECTION ACTUATOR

ALL OTHER ACTUATORS COMMANDED TO BE ZERO

This figure shows the displacement of the Mast in the x-direction at the actuator location where excitation occured. The simulation model included a small amount of inherent damping. The actuators increased this damping.

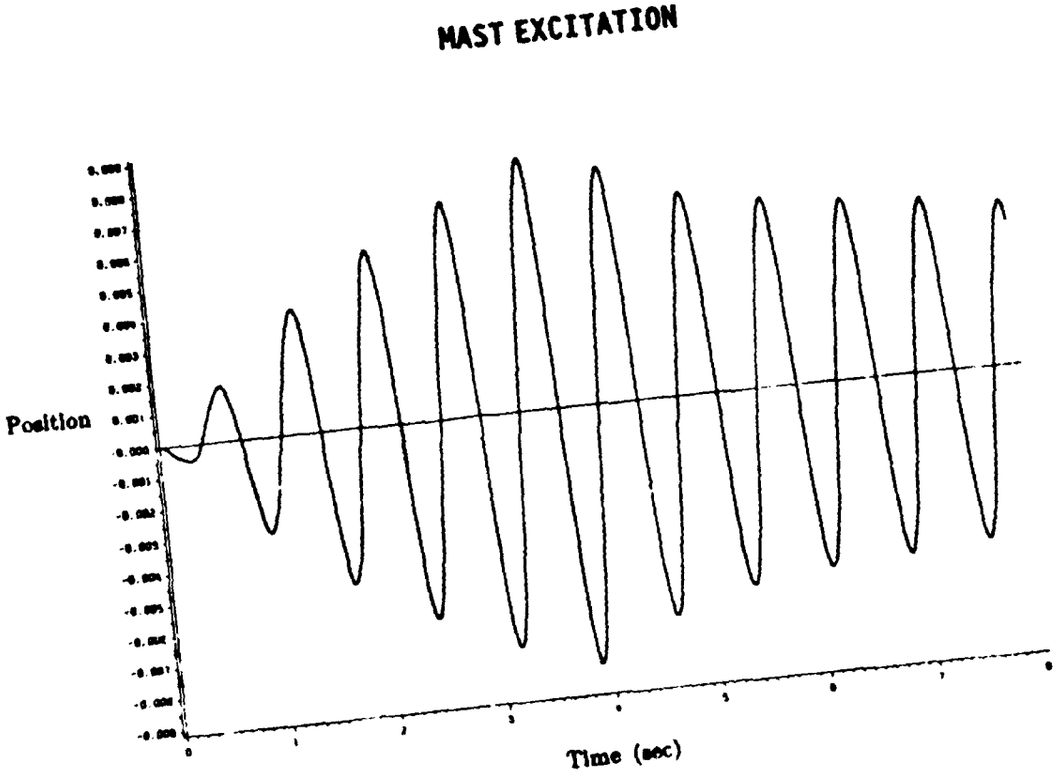

Force Output of Actuator

This figure shows the force generated by the actuator in response to the command signal. Note that the actuator continues to generate an output force after the command signal has been turned off. A similar effect occurs at the other actuators during the excitation phase.

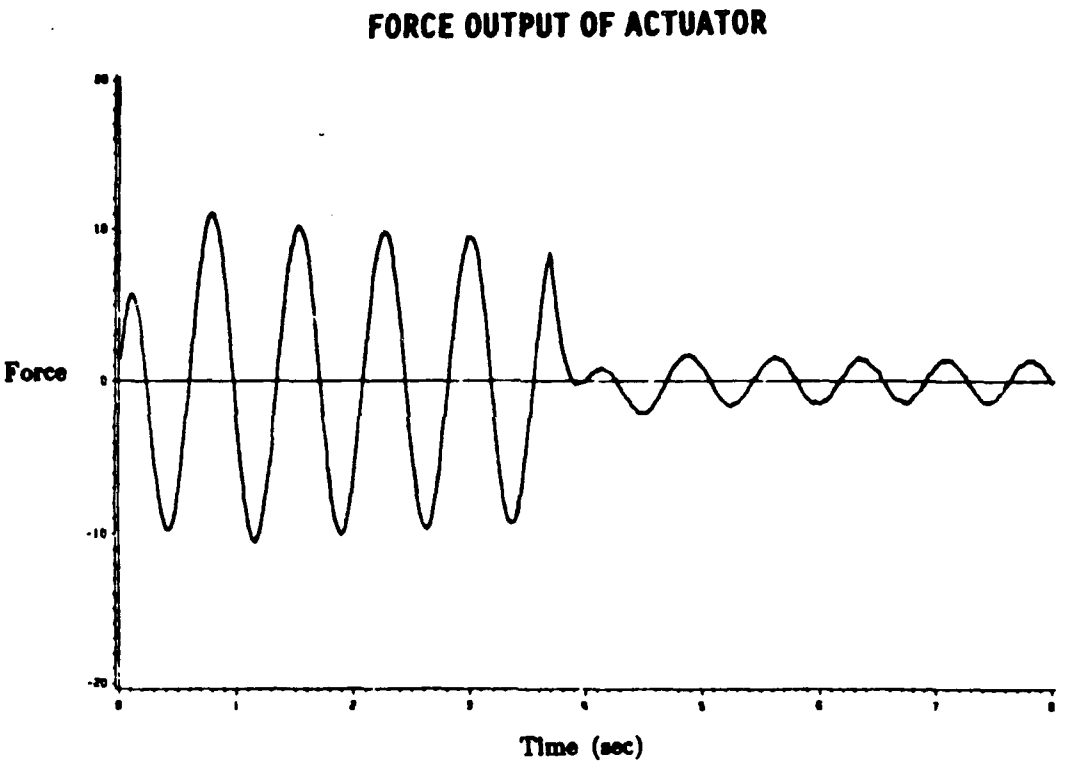

PSD of the Force Output During Excitation

The digital relative position measurement introduces force spiking in the output of the actuator. This figure shows the power spectral density of the force output of the LDCM in the last figure during the excitation phase.

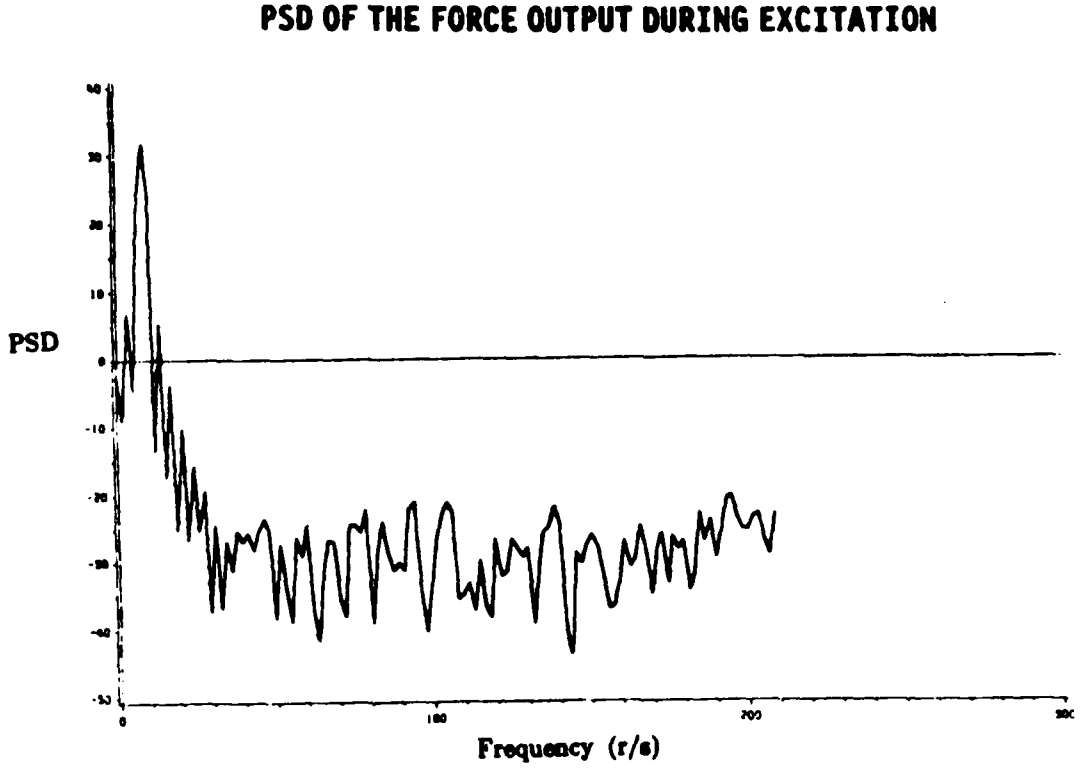

PSD of the Force Output During Free Decay

This figure shows the power spectral density of the force output of the LDCM after the excitation has been turned off. This level of noise is representative of the noise introduced into the mast by the actuators not used for excitation.

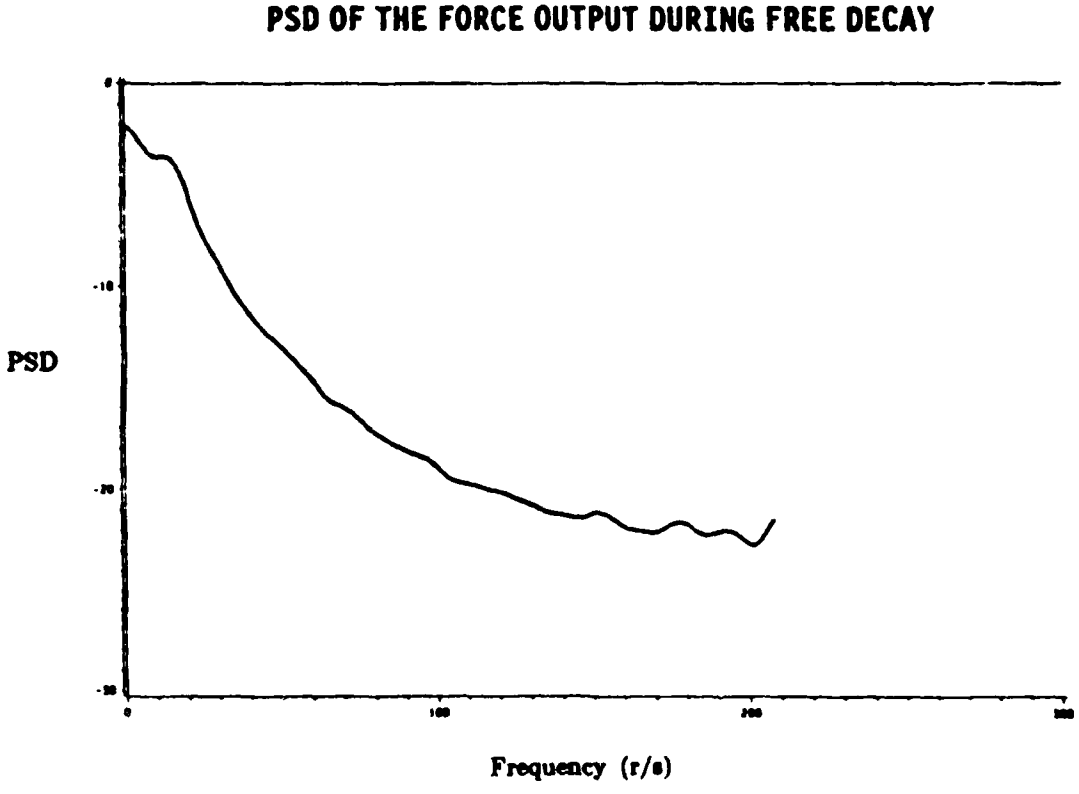

In this talk we have outlined the use of the LDCM actuator for vibration damping on flexible structures. The stroke length and power electronics limit the maximum force generated by the actuator. Because of the need to stabilize the actuator, the Mast-actuator model results in a nonstandard configuration. Selected simulations showed the excitation capability of the actuator. It should be noted that the performance of the delivered actuator will depend on the design of the actuator control loops which have not been finalized at this writing. The qualitative performance will be similar.

CONCLUSIONS

- **FORCE LIMITATIONS**
- **FEEDBACK CONFIGURATION OF THE ACTUATOR - MAST MODEL**
- **SIMULATIONS SHOW EXCITATION CAPABILITY AND FORCE CORRUPTION**

METHODOLOGY FOR OPTIMAL SENSOR LOCATIONS IN DYNAMIC SYSTEMS

Firdaus E. Udwadia
Professor of Mechanical Engineering,
Civil Engineering & Decision Systems
University of Southern California
Los Angeles
California, CA 90089-1114

OPTIMAL SENSOR LOCATIONS FOR SYSTEM IDENTIFICATION

PURPOSE:

1. OBTAIN BEST PARAMETER ESTIMATES
2. MINIMIZE COST OF INSTRUMENTATION
3. MINIMIZE COST OF DATA HANDLING
4. MINIMIZE COST OF DATA PROCESSING
5. EFFICIENTLY DETECT STRUCTURAL CHANGES
6. EARLY FAULT DETECTION

PAST EFFORTS: (1970-1977)

- POSITION SENSORS IN SYSTEM
- USE A SPECIFIC ESTIMATOR
- DO SYSTEM IDENTIFICATION USING DIFFERENT SENSORS
- OBTAIN A SET OF LOCATIONS FOR 'BEST' SYSTEM ID
- REPEAT PROCESS WITH OTHER ESTIMATORS

DRAWBACKS:

- LOCATIONS ARE DEPENDENT ON ESTIMATES
- ESTIMATES ARE DEPENDENT ON ESTIMATOR
  - → OSLP DEPENDENT ON ESTIMATOR
- EXHAUSTIVE SEARCH NEEDED
- OPTIMIZATION & IDENTIFICATION PROBLEMS COUPLED

1978: A METHODOLOGY FOR OPTIMAL SENSOR LOCATIONS FOR IDENTIFICATION OF DYNAMIC SYSTEMS, by P. Shah and F. Udwadia, Journal of Applied Mechanics, Vol. 45, 1978

DRAWBACKS:

- LITTLE PHYSICAL INSIGHT INTO THE OPTIMAL SENSOR LOCATION PROBLEM
- COMPUTATIONALLY VERY INTENSIVE
- DIFFICULT TO USE FOR LARGE STRUCTURAL SYSTEMS

PRESENT METHODOLOGY:

Consider the system

$$M\ddot{x} + C\dot{x} + Kx = f(t), \qquad x(0) = x_0, \qquad \dot{x}(0) = \dot{x}$$

M, K, C, are NxN matrices; $\underline{x}$ is Nx1.

- PROBLEM STATEMENT:

  NEED TO LOCATE SENSORS IN THE SYSTEM IN SUCH A WAY THAT THE MEASUREMENTS OBTAINED ARE MOST INFORMATIVE ABOUT THE PARAMETERS TO BE IDENTIFIED

- COLLECT THE UNKNOWN PARAMETERS IN THE MATRICES M,K,C INTO A VECTOR θ.

- NEED TO LOCATE m LOCATIONS ($m < N$) SO THAT COVARIANCE OF THE ESTIMATE OF θ IS MINIMUM.

- DATA IS ACQUIRED IN A NOISY ENVIRONMENT. NOISE IS MODELLED AS ZERO MEAN, NONSTATIONAY & WHITE.

METHOD:

$$Z = g(x) + w(t) \quad , \quad Z \text{ is } nx1$$

$$Y = Sz \quad , \quad Y \text{ is } mx1$$

$$Y = SRX + v(t)$$

S = selection matrix, R = sensor gain matrix.

COVARIANCE IS "MINIMUM" IF SUITABLE NORM OF

$$Q(T) = \sum_{k=1}^{m} \int_0^T \frac{X_\theta^T \; r s_k^T \; r s_k \; X_\theta \; dt}{\psi^2(t)} \quad \text{is maximum.}$$

$$X_\theta = \partial x_i / \partial \theta_j$$

$$\text{Max} \; \| Q[T; s_1, s_2, \ldots s_m; \mathscr{P}_0, I] \|$$

$$[s_k \in (1, N)]$$

DOES THIS MAKE SENSE?

- ONE SENSOR
- ONE PARAMETER
- $\psi^2(t) = \psi_0$
- Q IS A SCALAR

$$Q = \int_0^T \left(\frac{\partial x_{s_k}}{\partial \theta} \right) dt$$

Find s_k such that Q is maximum.

EXAMPLE:

SYSTEM SHOWN BELOW WITH

- $K_1 = K_2 = 100$, $K_3 = 75$
  $K_4 = K_5 = 50$
- $m_1 = m_2 = 2$
  $m_3 = m_4 = 1$
- $\alpha = .002$, $\beta = .08$, $C = \alpha M + \beta K$

Application of Impulse of magnitude 10 units

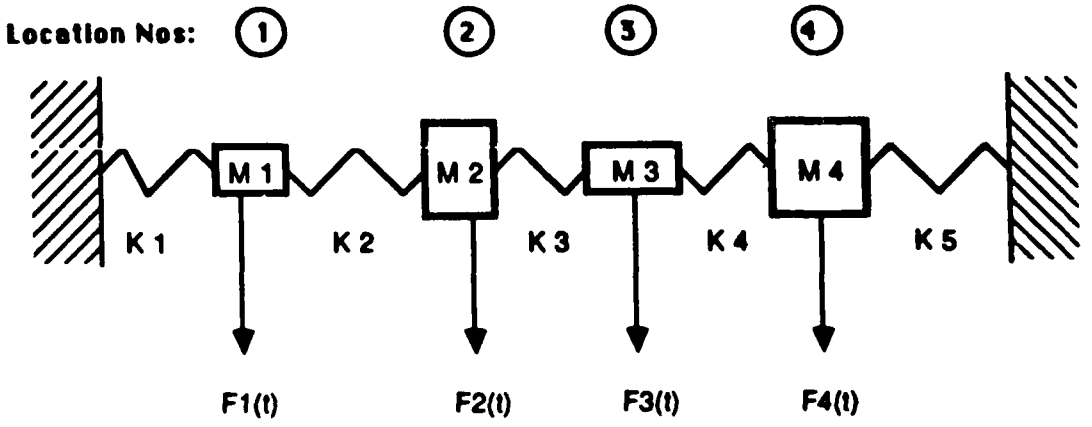

- TYPES OF QUESTIONS THE METHODOLOGY CAN ANSWER:

1. IF THE IMPULSIVE FORCE DESCRIBED ABOVE IS APPLIED TO ONE OF THE MASSES, SAY MASS m_j, $j\epsilon$ (1,4), THEN WHERE SHOULD WE LOCATE A SENSOR TO BEST IDENTIFY ONE OF THE STIFFNESSES k_i, $i\epsilon(1,5)$?

2. WERE WE REQUIRED TO PLACE MORE THAN ONE SENSOR TO IDENTIFY k_i HOW WOULD WE FIND THE OPTIMAL LOCATIONS? COULD WE RANK ORDER THE LOCATIONS 1,2,3,4 INDICATING THE ORDER IN WHICH THEY SHOULD BE POPULATED BY SENSORS SO AS TO BEST IDENTIFY k_i?

3. CAN WE GET AN IDEA REGARDING THE INFORMATION GAINED (OR REDUCED) BY PLACING A SENSOR AT LOCATION r AS OPPOSED TO LOCATION $k(r,k\epsilon(1,4))$?

4. GIVEN THAT WE WANT TO IDENTIFY k_i USING AN IMPULSIVE FORCE WHICH CAN BE APPLIED AT ONE OF THE MASSES, AT WHICH MASS SHOULD IT BE APPLIED AND AT WHICH LOCATIONS SHOULD THE CORRESPONDING RESPONSES BE MEASURED FOR BEST IDENTIFICATION?

5. WHAT ARE THE ANSWERS TO QUESTIONS (1) THROUGH (4) ABOVE IF WE WANT TO IDENTIFY NOT JUST ONE STIFFNESS k_i BUT A GROUP OF THEM, SAY k_1 and k_5?

FIGURES (A) AND (B) SHOW THE INFORMATION AS A FUNCTION OF TIME FOR SENSORS LOCATED AT VARIOUS LOCATIONS. NOTE: (1) INFORMATION ABOUT k_1 FROM DATA OBTAINED AT LOCATION 2 IS ABOUT 4 TIMES THAT OBTAINED FROM LOCATION 4, IF IMPULSE IS APPLIED AT MASS m_1; (2) INDENTIFICATION OF k_2 WOULD NOT BE AS GOOD AS k_1 IN A NOISY MEASUREMENT ENVIRONMENT.

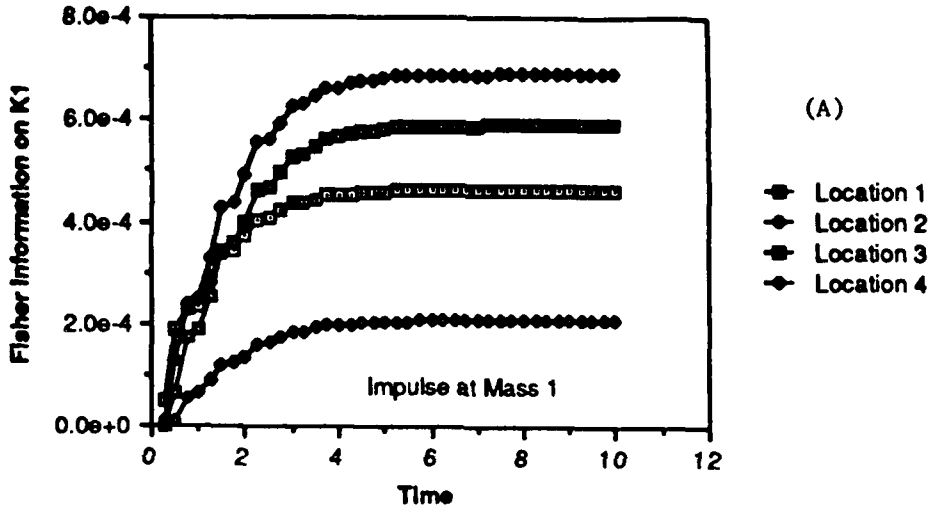

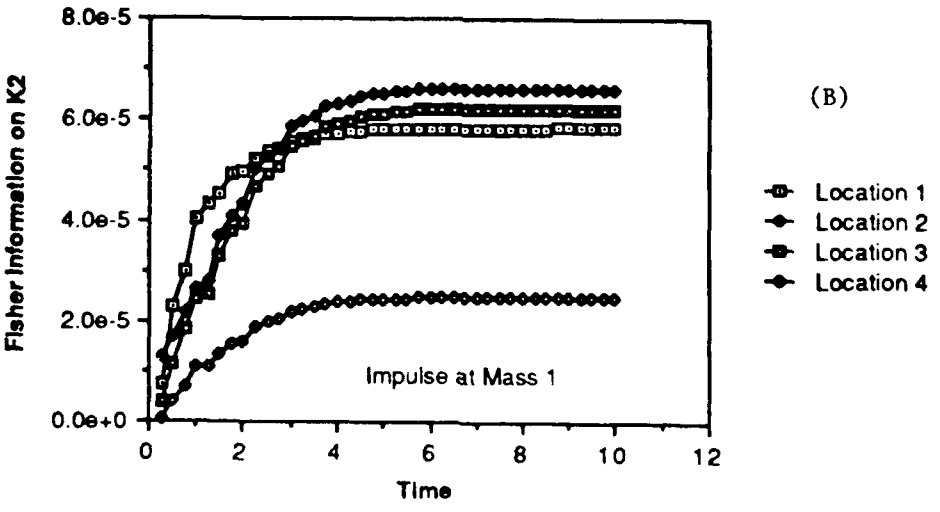

FIGURE SHOWS THAT LOCATION 4 IS SUPERIOR TO LOCATION 3 IN IDENTIFICATION OF k_4 USING AN IMPULSIVE FORCE APPLIED TO MASS 4.

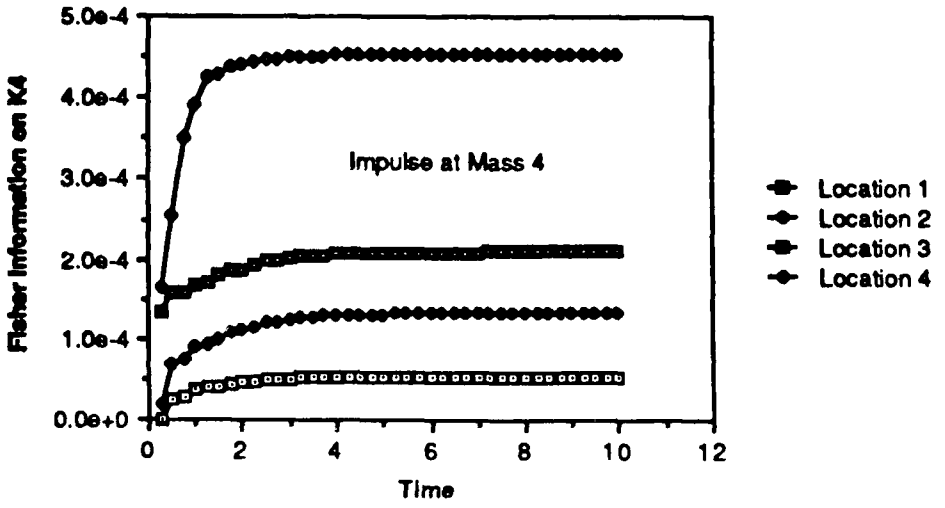

RESULTS ON IDENTIFICATION OF k_4 USING NOISY DATA COLLECTED AT LOCATION 4 AND LOCATION 3. CORRECT VALUE OF $k_4 = 50$. NOTE THAT AS N/S RATIO INCREASES, IDENTIFICATION OF k_4 USING DATA OBTAINED AT LOCATION 3 CAUSES THE ESTIMATES TO DIVERGE. THIS SHOWS THAT LOCATING SENSORS OPTIMALLY MAY HAVE A DRAMATIC INFLUENCE IN OUR ABILITY TO IDENTIFY THE SYSTEM PARAMETERS.

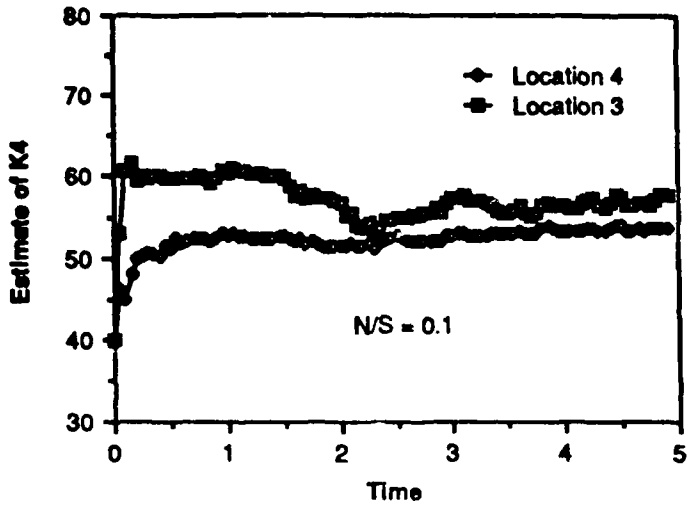

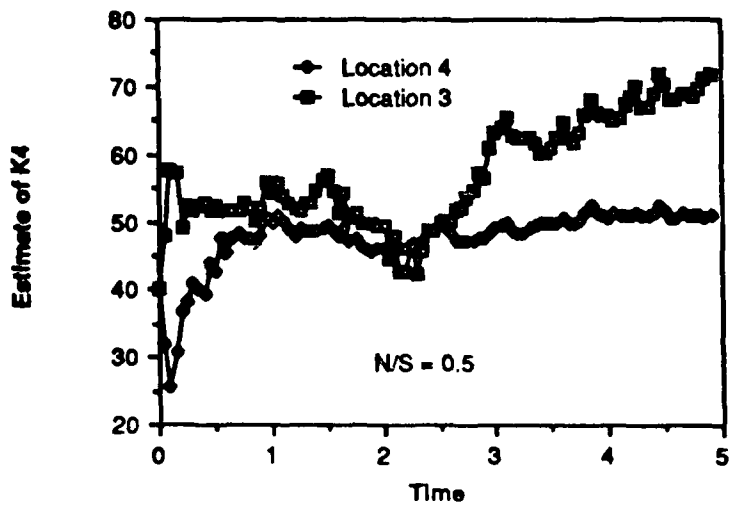

SUMMARY

1. A METHODOLOGY FOR OPTIMALLY LOCATING SENSORS HAS BEEN DEVELOPED.

2. OSL DEPEND ON:

   * NATURE OF SYSTEM
   * SPECIFIC PARAMETERS TO BE IDENTIFIED
   * NUMBER OF SENSORS
   * DURATION OF TIME OVER WHICH ID IS TO BE DONE
   * NATURE AND LOCATION OF INPUTS

3. A COMPUTATIONALLY EFFICIENT ALGORITHM IS DEVELOPED.

4. METHODOLOGY IS APPLIED TO MDOF SYSTEM.

5. METHODOLOGY IS VALIDATED BY USING MEASUREMENTS AT VARIOUS LOCATIONS AND SHOWING THAT THE OSL DO INDEED PROVIDE THE BEST PARAMETER IDENTIFICATION.

6. THE RESULTS OBTAINED USING THE KINETIC ENERGY CRITERION ARE, IN GENERAL, NOT CORRECT.

ACKNOWLEDGMENT

This work was funded by the Air Force Astronautics Laboratory. Edwards AFB. CA.

ROBUSTNESS AND POSITIVITY FOR STRUCTURAL CONTROL SYSTEMS

G.L. SLATER

UNIVERSITY OF CINCINNATI

INTRODUCTION

The intent of this presentation is to show some recent results on how the use of unstructured singular value robustness concepts can complement and expand the guaranteed stability margins provided through positivity designs. By combining these two methodologies we can guarantee stability for structural systems with significant modal uncertainty in frequencies and mode shapes, as well as uncertainties caused by sensor and actuator dynamics.

THE LSS CONTROL PROBLEM

Control System design for large flexible space structures is a difficult problem for many reasons. One is the high order of the system dynamics and the fact that many of the poorly damped lowest frequency modes are within the control bandwidth. Second there is considerable uncertainty about the dynamic model. Estimates of frequency, damping ratio, and mode shape can have significant errors due to modeling problems with the typical structure. Most significantly, the structure can never be adequately tested before being placed in orbit since the 1g environment (and the atmosphere) on Earth prevent a realistic test from taking place. Since the structure must be constructed in space and may evolve with time, modal characteristics may not remain static but may change. Finally for a system to perform in space we must recognize that component failures will take place, and that repair and/or replacement may not be feasible within any short time frame. Hence the system must continue to operate and degrade 'gracefully' with component failures.

CONTROL SYSTEM REQUIREMENTS

- INITIAL DESIGN MUST BE STABLE
- DESIGN MUST ALLOW FOR GROWTH/ ADAPTATION
- SYSTEM MUST BE FAULT TOLERANT
- CONTROLS MUST BE ROBUST TO UNKNOWN PARAMETER VARIATIONS

POSITIVE REAL CONTROLS

The use of positivity is motivated by the strong stability theorems applicable for positive real controls. In its simplest terms the pertinent stability result can be summarized as: A system with transfer matrix G(s) and feedback matrix H(s) is always stable if G(s) and H(s) are (strictly)positive real transfer matrices. The application to LSS comes from the fact that the transfer matrix between colocated sensor-activator pairs is positive real; hence any positive real matrix H(s) will yield a stable closed loop system. This is independent of unmodeled modes (spillover), or erroneous modal information. McLaren (1) also showed how the positive real model, can provide protection from multiple sensor/actuator failures.

The problem with the positivity model is that it requires you to neglect sensor and actuator dynamics - a realistic physical model can not meet the conditions of the positive real theorem. The point of this paper is to show however that use of a singular value stability analysis can provide the extra tools needed to apply the positivity model to a realistic LSS problem.

POSITIVITY MODEL

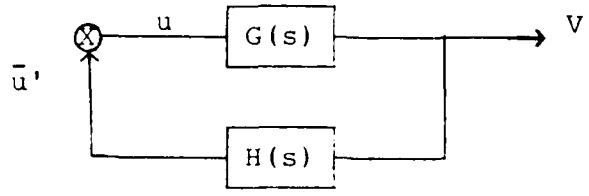

SYSTEM MODEL G(s) IS POSITIVE REAL FOR COLOCATED SENSOR/ACTUATORS

∴ CONSTRUCTION OF POSITIVE REAL H(s) CAN GUARANTEE STABILITY

- o IN PRESENCE OF UNMODELED MODES
- o UNCERTAIN MODAL CHARACTERISTICS
- o SENSOR/ACTUATOR FAILURES

PROBLEM AREAS

- o POSITIVE REAL MODEL IS TOO RESTRICTIVE MATHEMATICALLY
- o CAN NOT INCLUDE SENSORS/ACTUATORS AND EXTRANEOUS DYNAMICS

SINGULAR VALUE ANALYSIS CAN HELP HERE

ROBUSTNESS

A number of different control schemes have been proposed for the LSS control problem. Most or all of these control design algorithms are adequate so long as the actual controlled plant agrees with the control design model. This of course can never happen, which is precisely why after numerous years of research and hundreds of papers on the subject, we are still discussing the LSS control problem. The system design model can never be a true representation of the actual system dynamics. While feedback tends to reduce sensitivity to plant variations, ensuring stability and performance for the actual system continues to be a problem of supreme interest. The advantage of the positivity approach is that it can guarantee stability even in the presence of significant modeling errors in the modal model. (It can not of course guarantee performance). To now add the effect of sensor/actuator dynamics and to determine if performance goals can be met we must consider singular value bounds on the controller.

CONTROL ROBUSTNESS

SYSTEM MODEL IS NOT REALITY

PERTURBED SYSTEM - EXTRA DISTURBANCES, UNCERTAIN PARAMETERS, UNMODELED MODES, SENSORS AND ACTUATOR DYNAMICS.

ROBUSTNESS QUESTIONS

STABILITY ROBUSTNESS - DOES PERTURBED SYSTEM REMAIN STABLE?

PERFORMANCE ROBUSTNESS - DOES PERTURBED SYSTEM CONTINUE TO MEET PERFORMANCE REQUIREMENTS?

ANALYSIS TOOLS

- o POSITIVITY
- o SINGULAR VALUE ANALYSIS

SINGULAR VALUE BOUNDS

Using a multiplicative perturbation model, the singular value analysis can be used to establish sufficiency conditions for stability in the presence of modeling error. To utilize this test the perturbation matrix L(s) must be categorized in terms of its maximum singular value

$$\bar{\sigma}\,[L(j\omega)] = Lm(\omega)$$

Given the modeled plant G(s) and the controller matrix H(s), a sufficiency test for stability in the presence of all perturbation matrices $L(j\omega)$, bounded by the maximum singular value bound $Lm(\omega)$ is given below (see Ref. 2).

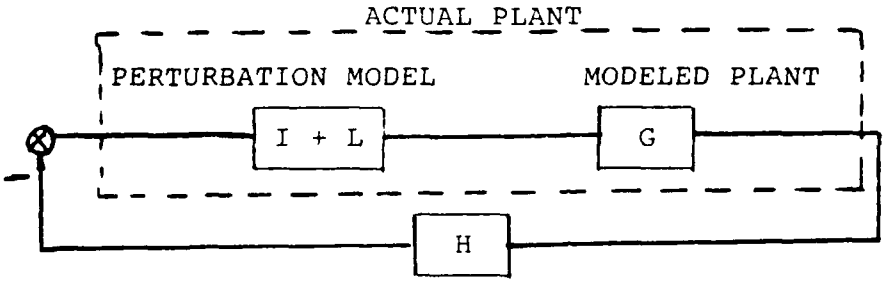

FEEDBACK CONTROLLER

L ~ MULTIPLICATIVE PERTURBATION IN CONTROLLED PLANT

$$\underline{\sigma}\,[(I + HG)(HG)^{-1}] > Lm(\omega)$$

OR

$$\bar{\sigma}\,[HG(I + HG)^{-1}] < \frac{1}{Lm(\omega)}$$

SINGULAR VALUES FOR LSS

These singular value bounds are extremely useful to prove stability when perturbation occurs above the bandwidth of the nominal plant. The typical model problem with unmodeled perturbations in damping ratio and frequency do not lend themselves to this type of analysis.

APPLICATION TO LSS CONTROL

- LOW FREQUENCY CHANGES IN MODES - S.V.'s CAN NOT PROVIDE USEFUL BOUNDS FOR MODE CHANGES
- S.V.'s ARE APPLICABLE TO HIGH FREQUENCY ACTUATOR AND SENSOR DYNAMICS $\Rightarrow$ PROVIDE BOUNDS ON ALLOWABLE VARIATIONS

APPLICATION TO LSS CONTROL

The key to analyzing this and other perturbation models is to use the strong robustness results of the positive real controller to guarantee stability for an unknown positive real model and to regard the perturbation matrix L only as that perturbation from the positive real model. Using this approach for the previous (DRAPER I) perturbation, L = 0 since the perturbed model retains the positive real condition. We may concentrate then not on the modal uncertainties but on the additional dynamics.

APPLICATION FOR LSS CONTROL

$$(G_{ACT}) = (I + L)\ G$$

G ~ POSITIVE REAL MODEL - INCLUDE ALL MODE VARIATIONS

L ~ DEVIATION FROM POSITIVITY

AN AEROELASTIC EXAMPLE

Consider the following example which shows the (scalar) frequency response for an aero elastic model including aerodynamics lags and actuator dynamics. The frequency response on the left shows that the basic input-output response nearly satisfies the positive real condition. The effect of additional actuation dynamics is shown on the right and clearly violates the positive real condition due to the actuator phase shift.

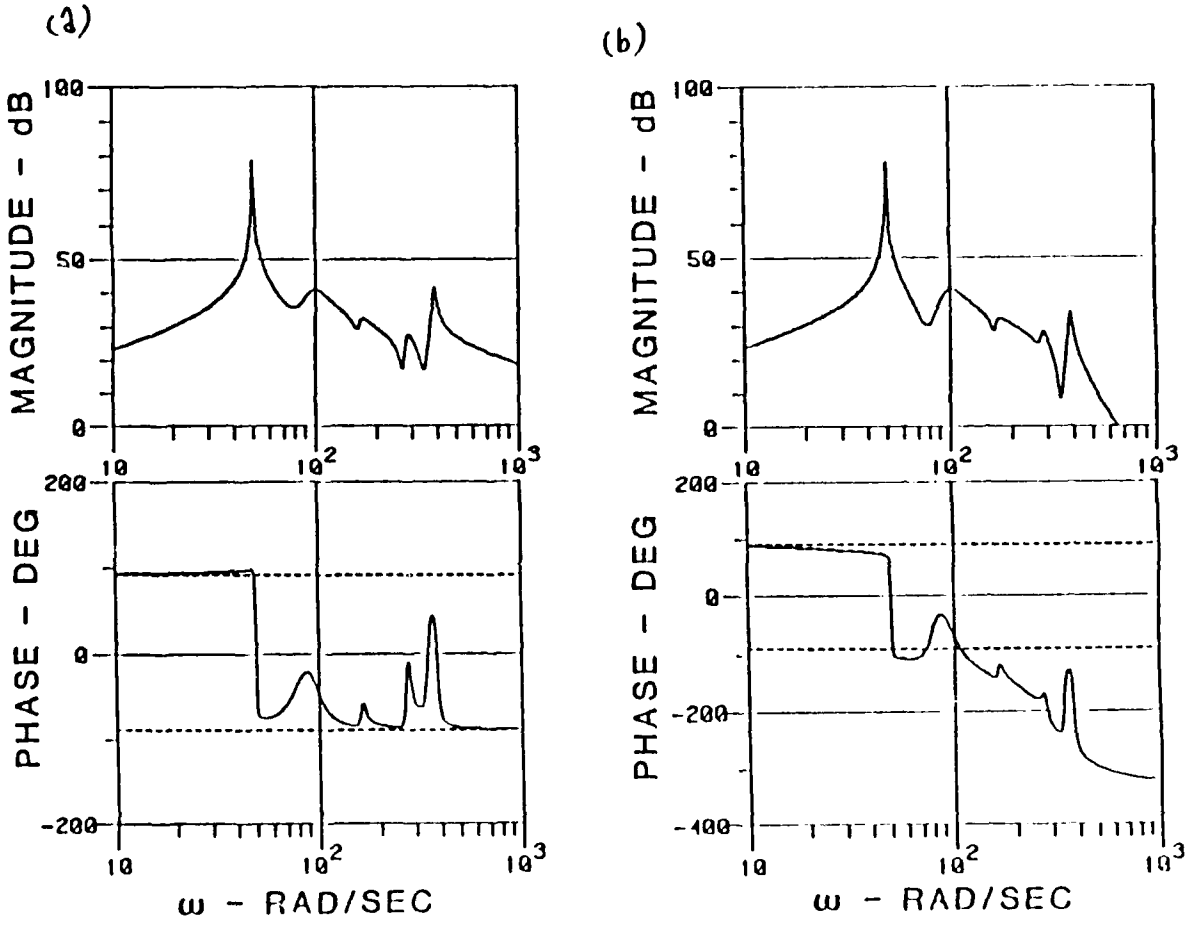

STABLE CONTROL WITH POSITIVITY & ROBUSTNESS

In the previous study, Takahashi (ref. 3) designed a positive real control using a positive real methodology but had no guaranteed stability for the actual system with actuator. Nevertheless simulations showed that this controller was stable and in fact worked quite well. To prove stability consider the extra phase shift in the actuator model as representing the deviation in from the positive real model. If the transfer function has the additional phase shift ϕ, then for the perturbation we have

$$Lm = 2\left|\sin(\frac{\phi}{2})\right|$$

Using the previous singular value test we can now in fact guarantee that this controller does yield a stable closed loop system.

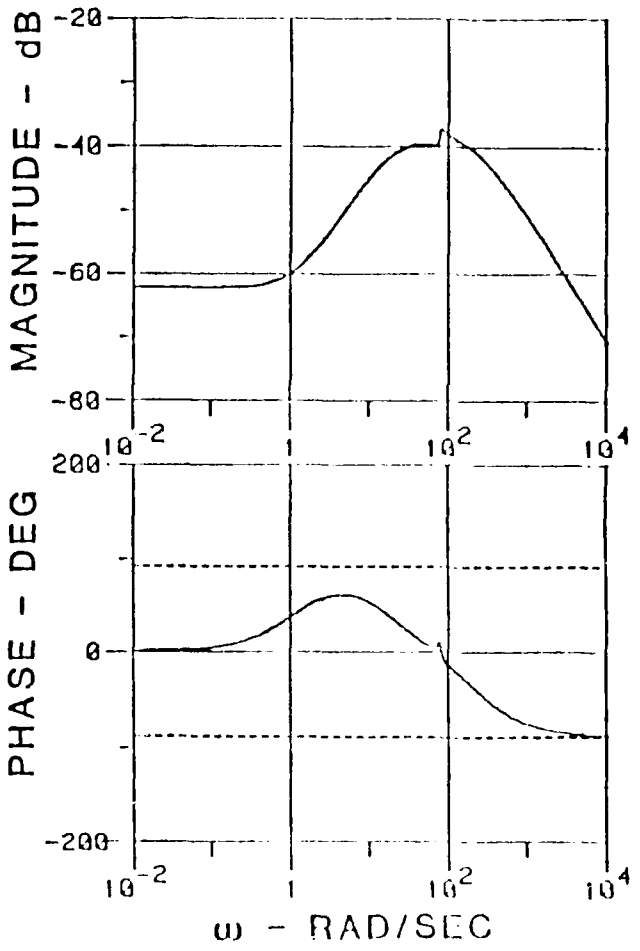

SINGULAR VALUES FOR DRAPER I

For example, the following plot shows the singular value bound $Lm(\omega)$ for a particular perturbation of the DRAPER I, tetrahedral truss structure. The system is 24th order with six inputs and six outputs. The perturbation model was formed by randomly perturbing the area of the truss members and the fixed masses by amounts less than about 5%. The modal model was fixed at 0.2% damping in each mode. Each peak in the plot corresponds to a displaced frequency. Note each shifted mode (or zero) gives two peaks. the exact location of the peak will move with the perturbation model, so only a general bounding function can be found. Clearly for this type of singular value bound, the conventional stability robustness test is of little value.

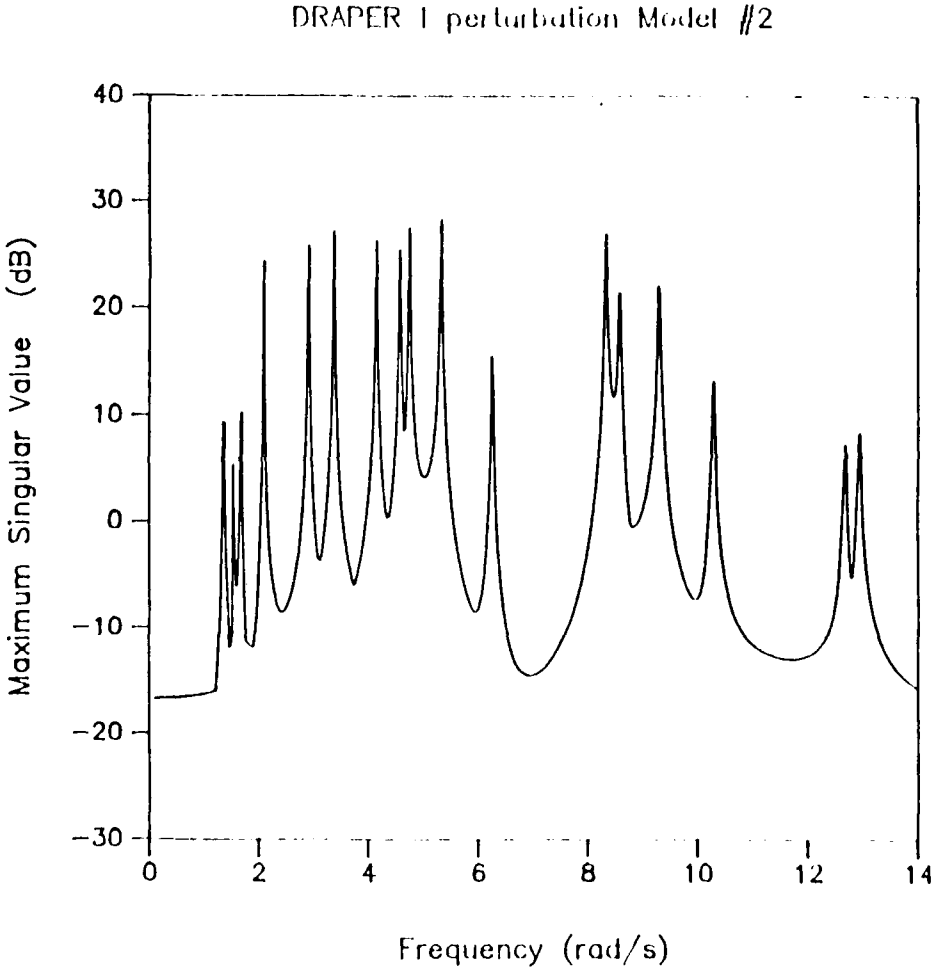

ACTUATOR MODEL FOR THE DRAPER I STRUCTURE

To verify what happens for a space structure model consider a hypothetical second order actuator and let us test for stability of a DRAPER I Controller. The Lm function shown results from the actuator model only. Any modal uncertainties can be ignored.

DRAPER I EXAMPLE

CONSIDER SECOND ORDER ACTUATOR

$$\left[\frac{\omega_n^2 + 2\zeta\omega_n s}{\omega_n^2 + 2\zeta\omega_n s + s^2}\right]$$

IS PERTURBED SYSTEM STABLE?

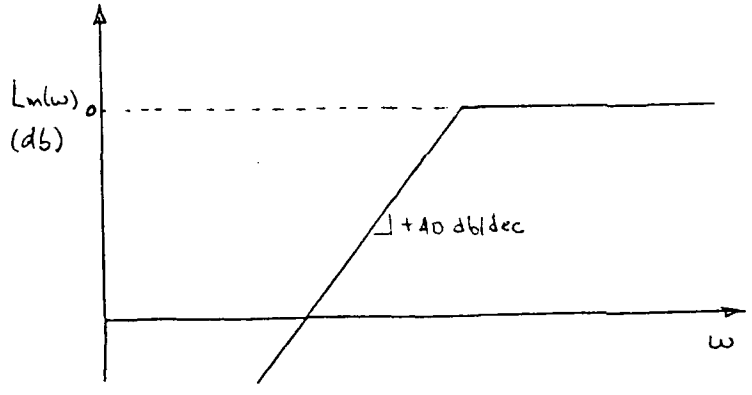

STABLE CONTROLLER DESIGN FOR THE DRAPER I

We now apply this to a reduced order controller designed using positivity (see McLaren). The nominal closed loop transfer function matrix (6x6) has the maximum singular value plot as shown. The feedback matrix H(s) is an estimator based design using a three mode reduced order model of the Draper structure. Again for this simple model it is straight forward to show that the closed loop system is now guaranteed stable for the actuator perturbation in combination with rather arbitrary modal perturbations of the type shown on the previous graph.

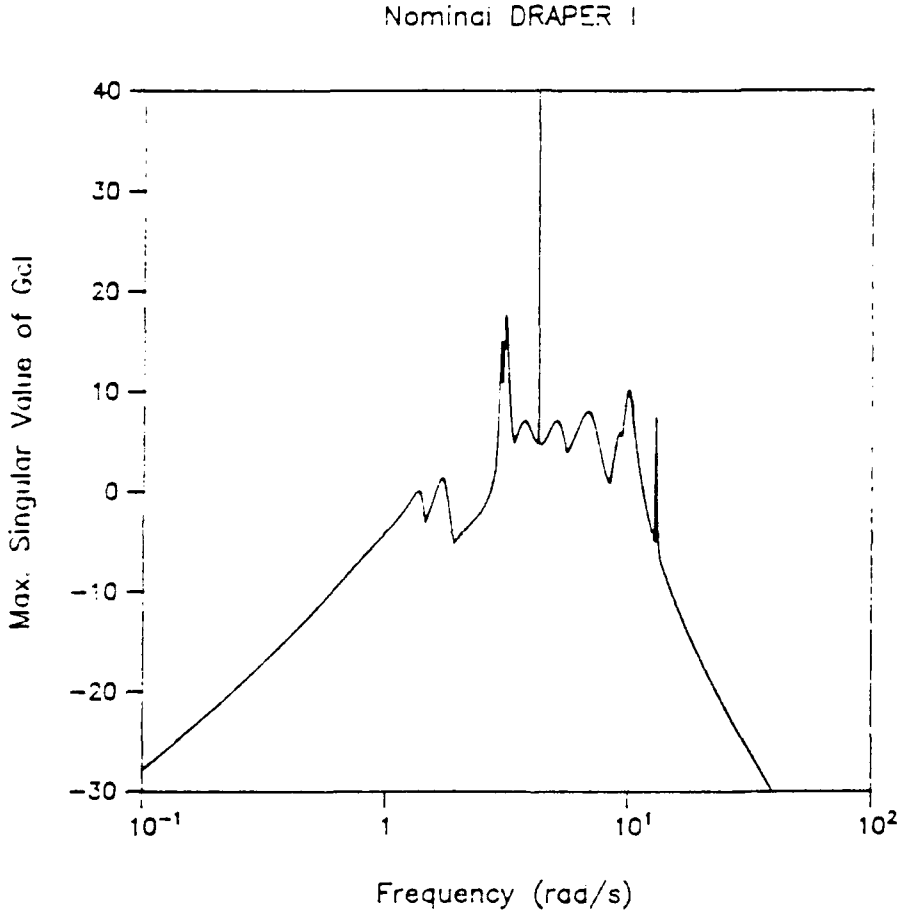

TIME RESPONSE WITH ACTUATOR DYNAMICS

To confirm our analysis we show a typical time response for the system with the actuator mode. This response is for the system with nominal dynamics; however, the stability is assured (and has been demonstrated) even for significant perturbations in the finite element model of the DRAPER I structure.

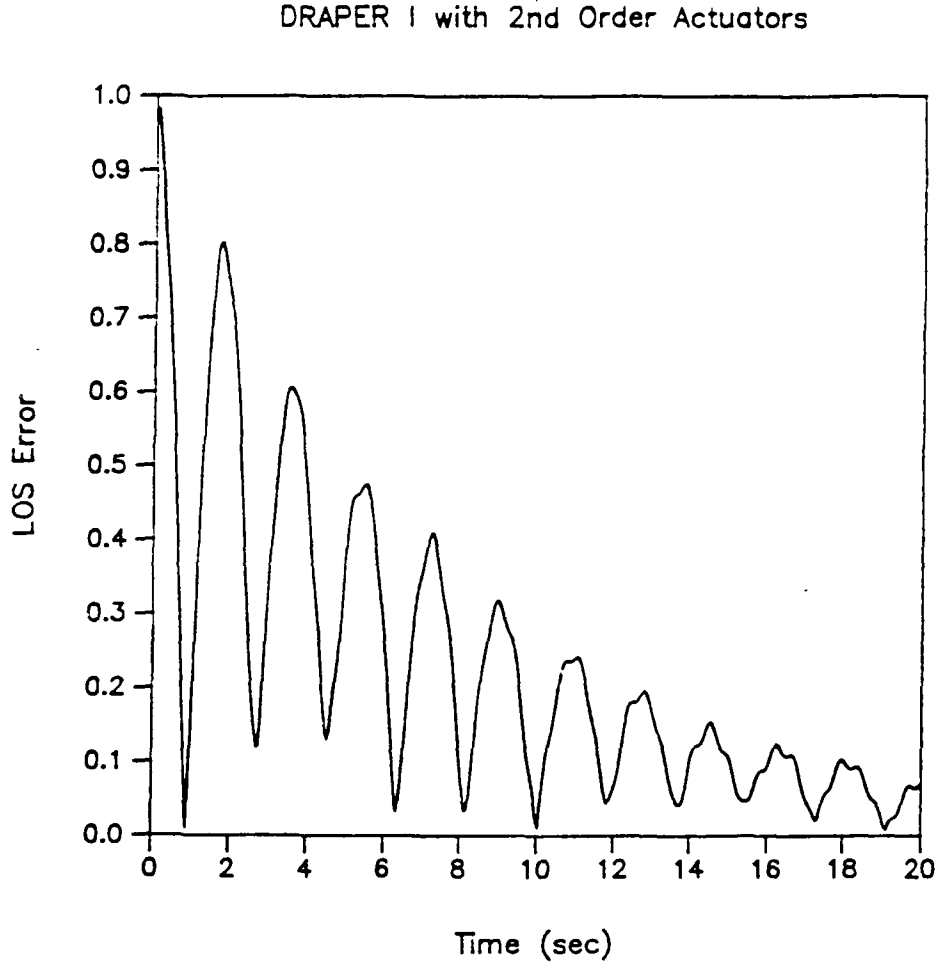

SUMMARY

In summary, we do feel this is a useful approach for guaranteed stability of LSS designs. We need to continue this work to refine the mathematical analysis and to reduce the inherent conservatism of the singular value bounds. For more complicated systems we need to have better ways to define the perturbation bounds but this problem is shared with all who use the unstructured singular value analysis.

REFERENCES

1. McLaren, M., Slater, G.L., "Robust Multivariable Control of Large Space Structures Using Positivity", J. Guidance, Control, and Dynamics, vol. 10, #4, July-August 1987, pp. 393-400.
2. Doyle, J., "Multivariable Design Techniques Based on Singular Value Generalizations of Classical Control", AGARD Lecture Series 117 Multivariable Analysis and Design Techniques, Sept. 1981.
3. Takahashi, M.D., Slater, G.L., "Design of a Flutter Mode Controller Using Positive Real Feedback", J. Guidance, Control, and Dynamics, vol. 9, #3, May-June 1986, pp. 339-345.

RETARGETING CONTROL OF FIGHTING MIRRORS

Steven Ginter

Gunter Stein

Honeywell Systems and Research Center
3660 Technology Drive
Minneapolis, MN 55418

This work was conducted for the Air Force Astronautical Laboratory on the Slew Actuator System Requirements Study, Contract No. F04611-86-C-0101

ABSTRACT

This paper examines control requirements for accurate retargeting and pointing of the fighting mirror spacecraft in a ground based directed energy system. While the spacecraft beam director must be quickly and accurately retargeted, the beam collapser must maintain precise, stable pointing. The paper focuses on robust pointing performance - that is, maintaining performance in the presence of system uncertainty. The structure pointing accuracy attainable is quantified as a function of uncertainty and feedback control bandwidth. The results indicate that current control and structure technologies are close to handling the anticipated fighting mirror retargeting objectives. This conclusion is based on a reasonable allocation of pointing performance between the optical system and the structure. Structure pointing accuracy at the mrad level is achievable. Resonances of representative beam director structures are sufficiently high in frequency to reduce the structure - control interaction problem to one of minor importance.

RETARGETING OBJECTIVES

In a ground based directed energy system a fighting mirror spacecraft is needed to receive the high energy beam and redirect it quickly and accurately from one target to another. Beam retargeting over angles of several degrees in time intervals of seconds are anticipated. Fundamentals of electromagnetic propagation suggest that beam pointing accuracy at retarget completion must be at the nrad level to accomplish mission objectives. Retargeting the spacecraft beam director to that pointing accuracy is an extremely ambitious, if at all possible, objective for any reasonable extrapolation of today's structure and control technologies. In order to accomplish the mission, active optical systems are needed to ultimately achieve the necessary beam pointing performance. Optical steering over a range of mrad is anticipated. Thus, a more reasonable pointing objective for the beam director structure is at the mrad level, an objective which is nearly feasible with existing technology.

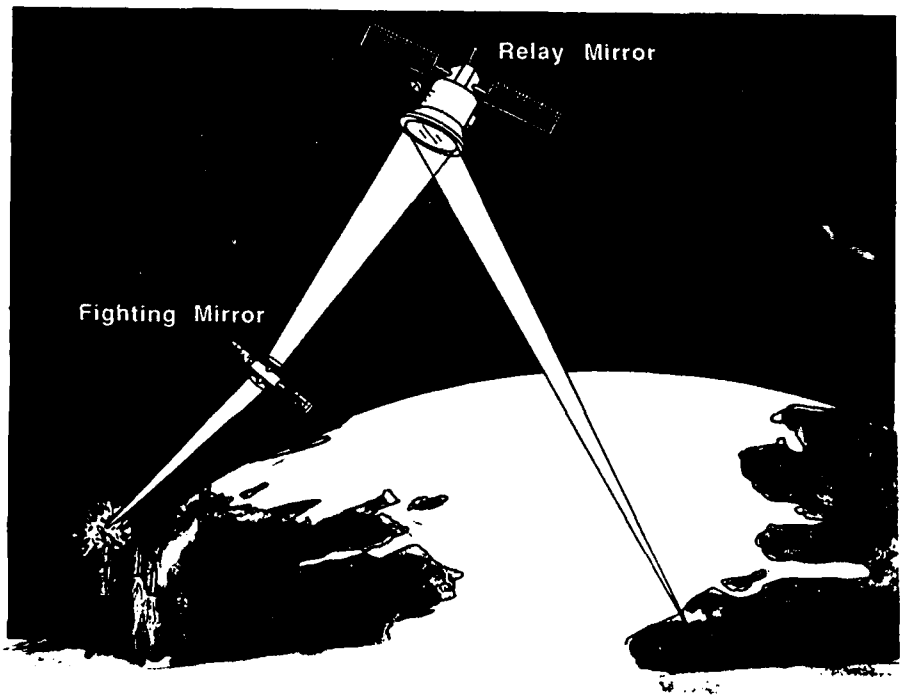

MUTLIBODY SPACECRAFT

Current fighting mirror concepts involve a bi-focal optical arrangement based on a multibody spacecraft configuration. The spacecraft beam collapser receives the high energy beam and reduces its size for transfer to the spacecraft beam director which expands and targets the beam. The beam collapser and director are mechanically supported from the spacecraft central body. The fighting mirror model used in this analysis is based on a generic space based laser model [1]. Although the model is not optimal for a fighting mirror configuration, the body inertias and the structural flexibility in the collapser and director are representative of a fighting mirror spacecraft. The director central moments of inertia are approximately 300,000 kg-m^2 and the first structural resonance occurs around 11 Hz.

In retargeting, the variables of prime importance are the beam director and collapser line of sight angles γ_1 and γ_2. While the director line of sight is quickly and accurately retargeted, the collapser line of sight must maintain precise pointing. Of lesser importance is the central body attitude angle ϕ_A. During retargeting the central body is free to move. Attitude positioning of the central body is used to maintain the interbody suspension systems adequately within mechanical limits. Follow-up positioning on a slower time frame than retargeting is adequate, thereby reducing the spacecraft torques required. Considering planar motion, five general torques are available to control the three variables γ_1, γ_2, and ϕ_A. The torques consist of three direct body torques T_A, T_1, and T_2 and two interbody suspension system torques T_{S_1} and T_{S_2}.

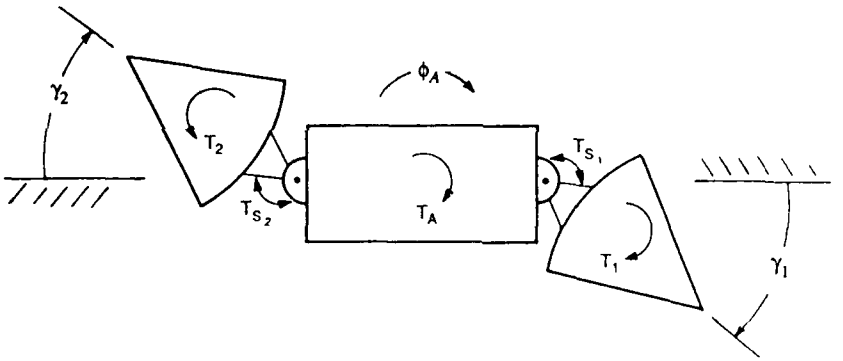

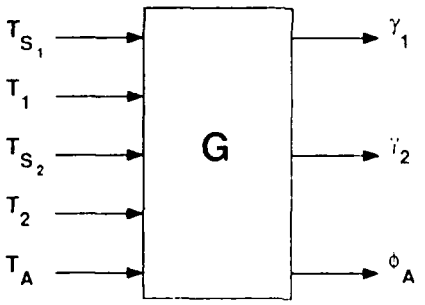

TORQUE ALLOCATION

The key to reducing the torque required from any one actuation device is to use the multiple torques available in concert. The rigid body transfer function from the five spacecraft torques T to the three variables γ is naturally characterized by double integration

$$G(s) = \frac{B}{s^2}, \quad B \equiv \begin{bmatrix} b_1^T \\ b_2^T \\ b_3^T \end{bmatrix}. \tag{1}$$

Three generalized torques u_1, u_2, and u_A are introduced to control the variables γ_1, γ_2, and ϕ_A, respectively. The generalized torques are allocated among the five spacecraft torques according to

$$T = [\, a_1 \;\; a_2 \;\; a_3 \,] \begin{bmatrix} u_1 \\ u_2 \\ u_A \end{bmatrix} \equiv Au. \tag{2}$$

The allocation matrix A is determined to maximize the torque available for retargeting, isolate the beam director and collapser from each other and from the central body, and provide adequate torque for slowly positioning the central body.

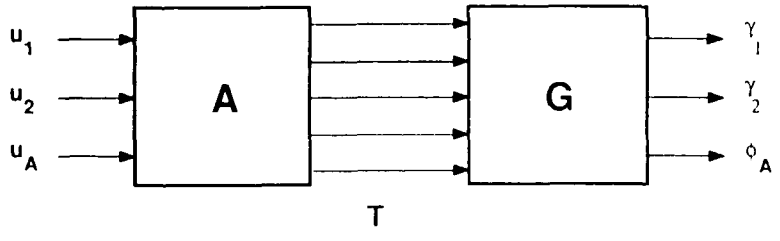

- MAXIMIZE TORQUE AVAILABLE FOR RETARGETING
- ISOLATE BEAM DIRECTOR AND COLLAPSER FROM EACH OTHER AND FROM THE CENTRAL BODY
- PROVID ADEQUATE TORQUE FOR POSITIONING THE CENTRAL BODY

LINEAR PROGRAMING SOLUTION

The torque allocation matrix is obtained as the solution of a linear programing problem:

$$\text{Maximize:} \quad b_1^T a_1 \qquad b_2^T a_2 \qquad b_3^T a_3 \tag{3a}$$

$$\text{Subject to:} \quad b_2^T a_1 = 0 \qquad b_1^T a_2 = 0 \qquad b_k^T a_3 = 0 \quad k = 1, 2 \tag{3b}$$

$$|a_{i1}| \leq c_{i1} \qquad |a_{i2}| \leq c_{i2} \qquad |a_{i3}| \leq c_{i3} \quad i = 1, \ldots, 5 \tag{3c}$$

$$|c_{i1}| \leq 1 \qquad |c_{i2}| \leq 1 \qquad |c_{i3}| \leq 1 \tag{3d}$$

The maximizations in Eq. (3a) indicate that the generalized torques u are to be used in the most effective manner to control the variables γ. The equality constraints in Eq. (3b) provide isolation of the beam director and collapser from each other and from the central body and the inequality constraints in Eq. (3c) specify the relative allocation of the generalized torques to the spacecraft torques T. The resulting transfer function from the generalized torques to the controlled variables has the form

$$G'(s) = \begin{bmatrix} \frac{k_1}{s^2} & 0 & 0 \\ 0 & \frac{k_2}{s^2} & 0 \\ * & * & \frac{k_A}{s^2} \end{bmatrix}, \tag{4}$$

the *'s indicating the dynamic coupling of the director and collapser motions into the central body motion.

CONTROL STRUCTURE

The control structure for retargeting involves both feedforward and feedback. Commanded acceleration profiles for the line of sight variables are fed forward thru the control compensation $F(s)$ and the allocation matrix A to produce direct spacecraft torque commands. The acceleration feedforward supplies the muscle necessary for quick retargeting. Commanded line of sight profiles are compared with the line of sight responses to form feedback pointing error signals e. Based on the pointing errors, the feedback compensation $K(s)$ produces additional spacecraft torque commands. The feedback is necessary to provide pointing accuracy in the presence of system uncertainty. Feedback control of the central body attitude is used on a much slower time frame to regulate the suspension system angles within mechanical limits as discussed previously. The closed loop error sensitivity function to commanded acceleration is

$$e = (I + GAK)^{-1}\left(\frac{I}{s^2} - GAF\right)\alpha_c \equiv S(s)\alpha_c. \tag{5}$$

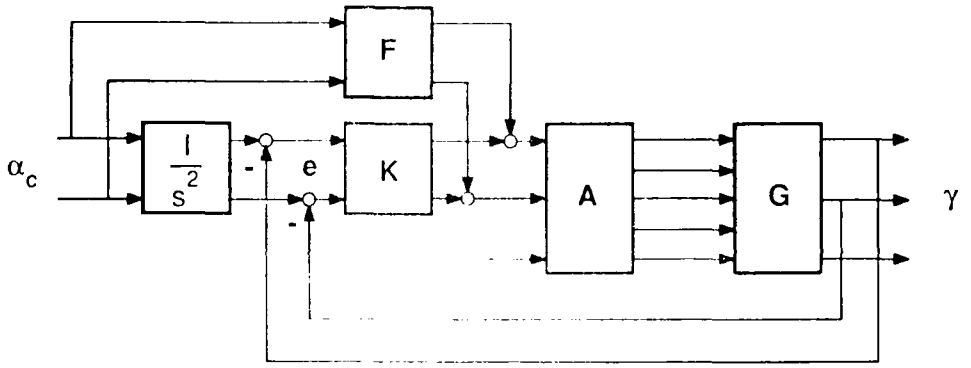

- FEEDFORWARD PROVIDES MUSCLE
- FEEDBACK PROVIDES PERFORMANCE IN THE PRESENCE OF UNCERTAINTY

CONTROL COMPENSATION

The torque allocation solution enables single loop control designs for the line of sight variables. The feedforward compensation F is determined to provide good nominal pointing performance. Based on Eq. (5), the two diagonal elements of F are chosen as approximate low frequency inverses of the corresponding diagonal elements in G':

$$F_i(s) = \frac{1}{k_i} \frac{1+2\tau s}{1+\tau s} \tag{6}$$

where τ is included as a phase approximation for the actuators and structural flexibility. For representative beam director structures and existing control moment gyros $\tau \approx 0.008$ s. The accuracy in the feedforward compensation need be no greater than the accuracy of the actuation torques. The feedback compensation K is determined to provide performance in the presence of system uncertainty. The two diagonal elements of K consist of a basic lead-lag compensator, two notch filters $n_1(s)$ and $n_2(s)$ for flexibility, and a lag for high frequency roll-off:

$$K_i(s) = \sqrt{18}\,\frac{\omega_c^2}{k_i}\,\frac{s+\omega_c/\sqrt{18}}{s+\omega_c\sqrt{18}}\,\frac{200}{s+200}\,n_1(s)\,n_2(s) \tag{7}$$

where ω_c sets the feedback bandwidth. The two notches are at frequencies of 73 and 146 rad/s. The depth of the notches cannot be too great before incurring unacceptable phase loss.

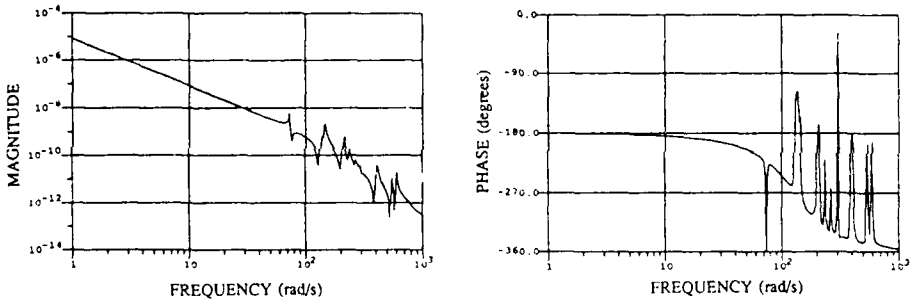

$\frac{\gamma_1}{u_1}$ FREQUENCY RESPONSE

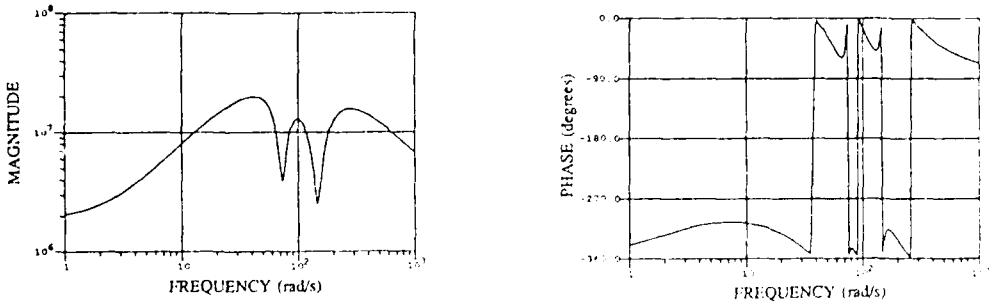

$K_1(s)$ FREQUENCY RESPONSE

PERFORMANCE REQUIREMENTS

Pointing error requirements are specified with respect to a given set of acceleration commands. For analysis, the requirements are translated into frequency domain constraints on the error sensitivity function. Typical acceleration commands are based on a doublet or smoothed doublet profile. Hence, the profile frequency content rolls off at least as fast as $1/s$ at frequencies above $\omega_r = 2\pi/T_r$, where T_r is the retarget time interval.

At low frequency pointing performance is dictated by the requirement to achieve good command tracking during a retarget maneuver. Tracking performance is only required up to frequencies ω_o slightly greater than ω_r. The ideal line of sight response to a commanded acceleration exhibits a $1/s^2$ characteristic. If x denotes the required tracking error as a percentage of the commanded line of sight, then the pointing error requirement is $|e/\alpha_c| = |S(s)| \leq 0.01x/s^2$.

At high frequencies ($> \omega_o$), the pointing error response becomes dominated by induced structural vibrations. The pointing requirement then becomes one of maintaining pointing errors less than a specified level ε: $|e| \leq \varepsilon$. Since typical acceleration profiles roll-off as $1/s$, the pointing error requirement at high frequency is $|S(s)| \leq \varepsilon s$.

- **TYPICAL COMMANDS**

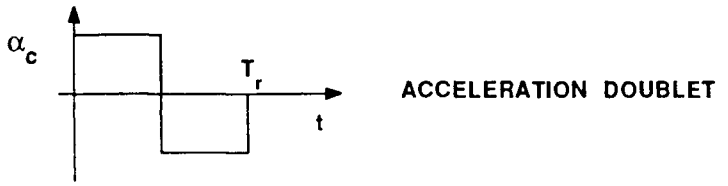

- **SENSITIVITY CONSTRAINTS**

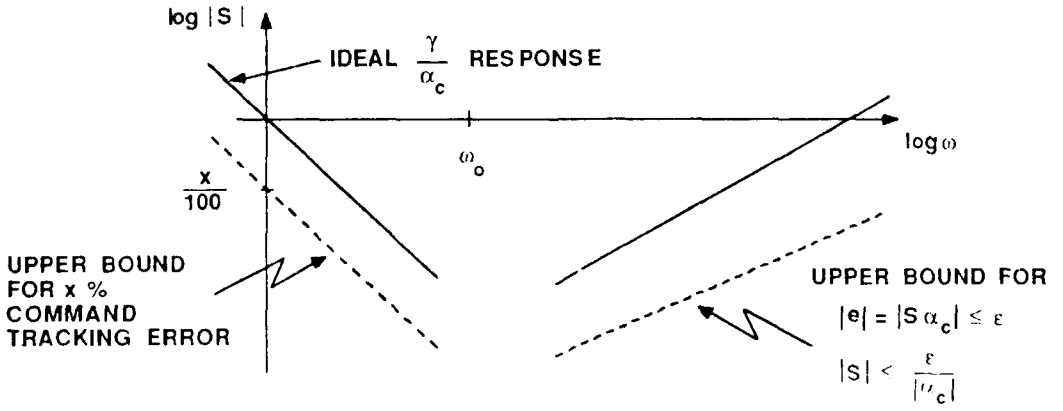

PERFORMANCE OF NOMINAL DESIGN

The pointing performance of a nominal control design is indicated by the magnitude of the error sensitivity function $S(s)$ over frequency. Since $S(s)$ is a matrix transfer function, its magnitude is measured by its maximum singular value. The maximum singular value of $S(s)$ as a function of frequency is illustrated for a 10 rad/s bandwidth design. Also shown is the performance requirement for a retarget time interval of T_r = 1 second with x = 5% and ε = 0.001 - that is, a 5% tracking error during retarget and a pointing error of 0.001 rad at the retarget completion. Performance of the nominal design is achieved with some margin to spare.

BW 10 rad/s x = 5% ε = 0.001 ω_o = 8 rad/s

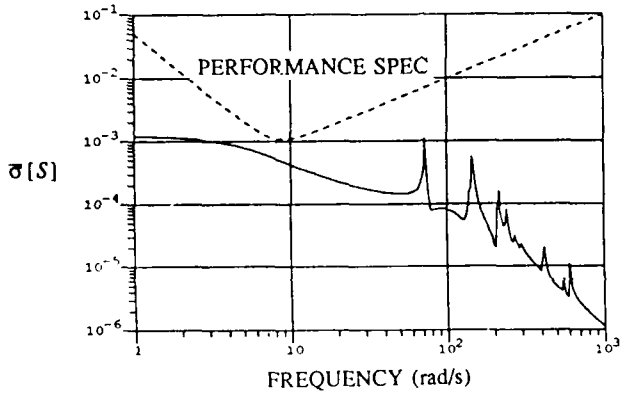

KEY ISSUE – PERFORMANCE IN THE PRESENCE OF UNCERTAINTY (ROBUST PERFORMANCE)

Pointing errors must meet specification in the face of system uncertainty - in particular uncertainty in all five spacecraft torque channels. The uncertainty includes dc errors in the actuation devices, misalignment of the actuator's output axes with the spacecraft control axes, errors in the spacecraft moments of inertia, and dynamic uncertainties at higher frequency in the actuators and the spacecraft's structural characteristics. Analytical tools have been developed over the last few years to specifically assess robust performance. These tools provide a means for quantitatively measuring the level of attainable performance for a given characterization of uncertainty.

- **dc UNCERTAINTY**

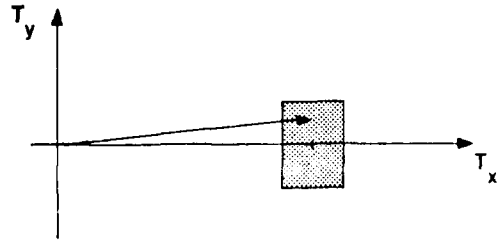

- dc ACTUATOR ERRORS
- ACTUATOR MISALIGNMENTS
- INERTIA ERRORS

- **DYNAMIC UNCERTAINTY**

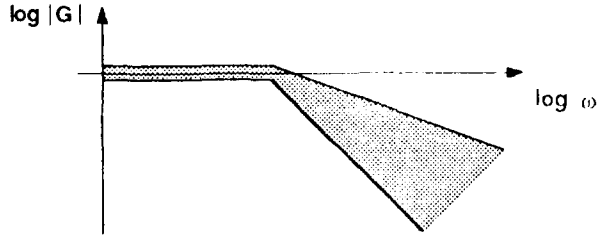

- STRUCTURAL FLEXIBILITY
- ACTUATOR ERRORS

ANALYSIS TOOL – Mu

The structured singular value μ [2] is a quantitative measure of the system performance robustness with respect to a specified class of uncertainty. To effectively utilize the tool the system performance and the uncertainty class must be characterized. The system performance specification is characterized as a frequency dependent weighting W_e. The previous discussion concerning performance requirements illustrated a typical performance weighting. The system torque uncertainty is represented as a percentage of the spacecraft nominal transfer function. The specific class of uncertainty is defined by a an arbitrary, but bounded, perturbation $|\Delta'| \leq 1$ and a frequency dependent weighting W_z. At low frequency W_z is flat with magnitude less than one. The dc value of the weighting represents the percentage level of uncertainty against which performance is measured. Robust performance is achieved for a given level of uncertainty if and only if $\mu[M(i\omega)] < 1$ for all frequency.

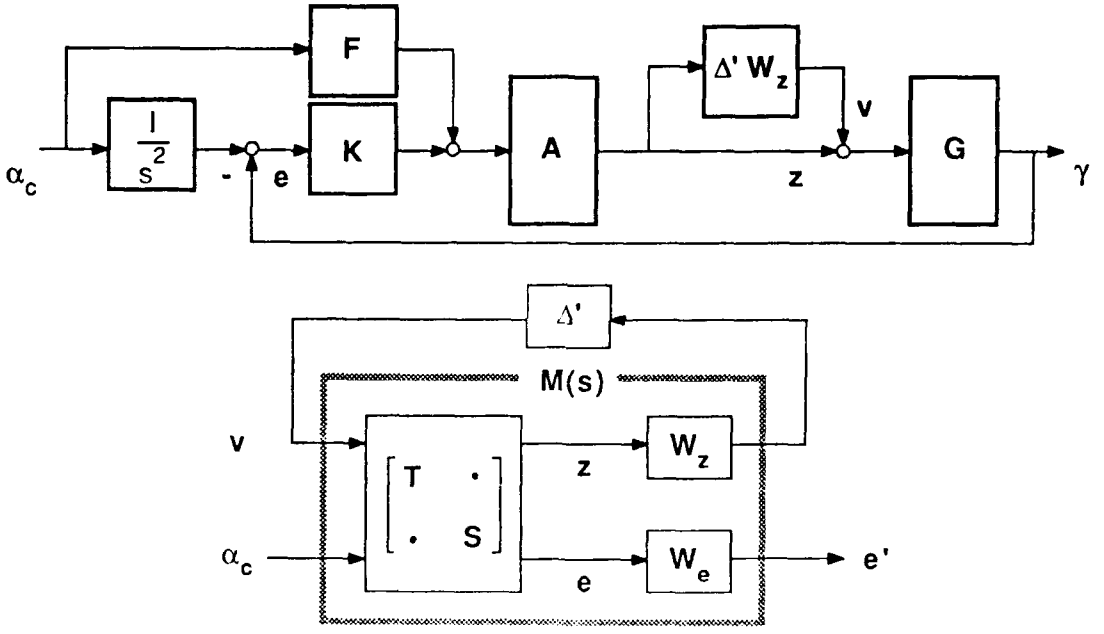

ROBUST PERFORMANCE $\leftrightarrow \frac{|e'|}{|\alpha_c|} < 1 \leftrightarrow \mu[M(j\omega)] < 1$

ANALYSIS RESULT

A frequency plot of $\mu[M(i\omega)]$ is illustrated for a 10 rad/s bandwidth with tracking performance of $x = 5\%$, pointing performance of $\epsilon = 0.001$, and an uncertainty level of 3%. Again, a retarget time interval of 1 second is considered. Robust performance is not quite achieved. Slightly less pointing accuracy could be achieved at uncertainty levels up to 3%, or the specified pointing accuracy could be achieved for uncertainty levels slightly less than 3%. The most difficulty in achieving robust performance occurs in the frequency region where $\mu \geq 1$. In this case, that region is in the vicinity of the retarget frequency $\omega_r = 2\pi$, not at the frequency of structural resonances. Thus, performance is not impacted by structural vibrations induced from the maneuver.

BW 10 rad/s x = 5% ϵ = 0.001 ω_o = 8 rad/s

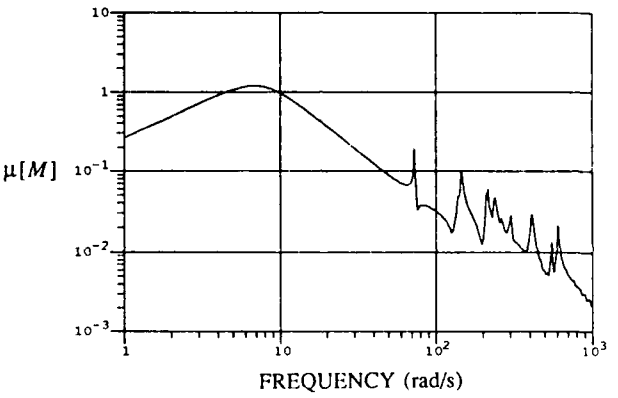

ROBUST POINTING PERFORMANCE

The level of robust pointing performance is governed by the level of uncertainty and the feedback control bandwidth. Increasing the bandwidth improves low frequency performance desensitization. Bandwidth is limited, however, by actuator capabilities and large uncertainty at higher frequency. In particular, structural flexibility uncertainty is an important factor limiting feedback bandwidth. The relationship between performance, uncertainty, and bandwidth is quantified in the figure. The pointing error performance is expressed as the percent tracking error x and the system uncertainty as a dc percentage. The figure pertains to a retarget time interval of T_r = 1 second.

The figure indicates the attainable robust pointing performance for a given level of uncertainty and bandwidth. A 30 rad/s bandwidth provides a pointing accuracy of 2% for uncertainty levels up to 3% and an accuracy of 5% for uncertainty levels up to 10%. A 10 rad/s bandwidth provides a pointing accuracy of 6% for uncertainty levels up to 3% and an accuracy of 11% for uncertainty levels up to 10%. With on-orbit system calibration, it is reasonable to expect that uncertainty levels of 3% to 5% can be attained. Assuming an uncertainty of 3%, consider a retarget maneuver of 1° in 1 second. A 30 rad/s bandwidth will deliver a pointing accuracy of 0.3 mrad and a 10 rad/s bandwidth will deliver a pointing accuracy of 1 mrad.

ω_o = 8 rad/s

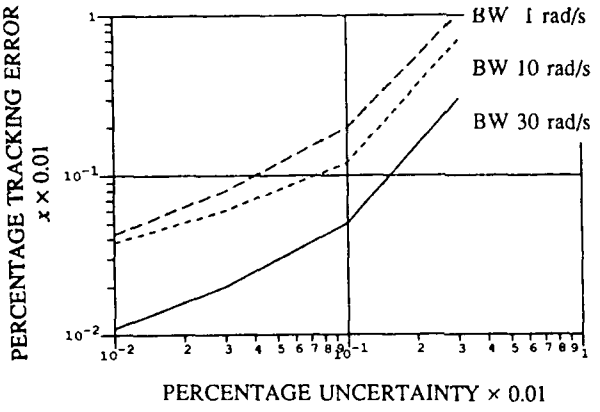

CONCLUSIONS

The results presented indicate that current control and structure technologies are close to handling the anticipated fighting mirror retargeting objectives. This conclusion is based on a reasonable pointing performance allocation between the structure and the optical system. Structure pointing accuracy at the mrad level is achievable, leaving the optical system to achieve beam pointing accuracy down to the necessary nrad level. Resonances of proposed beam director structures are sufficiently high in frequency to reduce the structure - control interaction problem to one of minor importance.

A bandwidth of 30 rad/s represents the practical limit achievable for the class of fighting mirror spacecraft considered. The limit is due to an actuator bandwidth of 125 rad/s, which is representative of current control moment gyro practice, and structural flexibility. In order to achieve this bandwidth, notch filters must be employed in the feedback compensation to provide stability. The phase loss from the filters and the actuator is too great to achieve good feedback crossover characteristics at bandwidths greater than 30 rad/s.

The performance results obtained are not based on the use of structure augmentation. That is, the use of either passive or active means to increase inherent structural damping or stiffness. Modal damping ratios of 0.005 were employed in the model. The use of structure augmentation would ease the need to use notch filters in the control compensation. The benefit would be to improve robust stability and performance by reducing phase loss and hence amplification in the crossover region. The performance improvement, however, would only be minor due to the 125 rad/s actuator bandwidth. Significant improvements could only be achieved with actuator bandwidths approaching 1000 rad/s. The actuation devices must also be capable of generating the large retarget torques needed. Such actuation devices are considerably beyond existing practice.

REFERENCES

[1] Space Based Laser (SBL) Structures Final Report and Dynamic Model, R&D Associates and Cambridge Research, AFWL/ARHB Subtask 02-05/02 F29601-85-C-0025, October 1985.

[2] Doyle, J.C. *Analysis of Feedback Systems with Structured Uncertainties*, IEE Proceedings, Vol. 129, Part D, No. 6, pp 242-250, November 1982

COST EFFECTIVE DEVELOPMENT OF A NATIONAL TEST BED

Dr. Henry B. Waites
NASA/MSFC

Victoria L. Jones
Dr. Sherman M. Seltzer
Control Dynamics Company

ABSTRACT

The MSFC has pursued for several years the coordinated development of a Large Space Structures (LSS) National Test Bed for the investigation of numerous technical issues involved in the use of LSS in space. This paper describes the origins of this development, the current status of the various test facilities and the plans laid down for the next five years' activities. Particular emphasis on the control and structural interaction issues has been paid so far; however, immediately emerging are user applications (such as the proposed pinhole occulter facility). In the immediate future, such emerging technologies as smart robots and multibody interactions will be studied. These areas are covered in this paper.

INTRODUCTION

The LSS GTF (Large Space Structure Ground Test Facility) is a facility which is being developed to investigate the controls and dynamics issues associated with LSS. The NASA/MSFC (Marshall Space Flight Center) initiated the LSS GTF to meet the desired objectives of complex space projects, by investigating the topics of control development and synthesis, dynamics verification, dynamic modeling, and hardware flight systems for space structures. The overall goal of the LSS GTF is to become a national test bed for investigations in dynamics and controls.

Spacecraft structures have become more complex and LSS requirements have become more stringent due to an increased use of space for Earth sciences, solar physics, astrophysics, material sciences, and defense. With the increase in spacecraft complexity, the experiments have become more ambitious and multifaceted (i.e., Space Station, Advanced Solar Observatory, etc...) Many of these missions require high performance from the LSS, such as extremely accurate pointing of optical elements and the attainment of vibration free observation image planes. The LSS GTF provides the ground test capability necessary to experiment with large beams, LSS components, and even full-size LSS.

The LSS GTF has been developed over the past four years in a very cost-effective manner. The cost-efficiency has been "enabled" by using components from past projects and by assembling a team able to develop and operate the facility. The development of the LSS GTF required a multi-discipline team, since the LSS issues cover a wide range of technical disciplines. The team includes members expert in the areas of control, structures, optics, sensors and actuators, propulsion, computer hardware and software, electronics, and materials. The team members include MSFC, Control Dynamics, and DYNACS personnel.

OBJECTIVES

The goals of the LSS GTF are to automate as many LSS technical disciplines as possible and to integrate where possible, these disciplines into a user friendly analysis methodology. The LSS GTF is utilized to experimentally test and evaluate the dynamics and control of realistic space structures. The LSS GTF is a non-proprietary installation in which guest investigators are encouraged to implement and validate control and structural methodologies. The objectives of the LSS GTF are as follows:

1. Investigate control and dynamics issues on a single space structure. Develop a laboratory where control methodologies, dynamic modeling, and data reduction techniques can be evaluated.

2. Develop a laboratory for ground testing a possible flight experiment.

3. Develop and validate a computer tool which allows efficient simulation and analysis of connected flexible structures.

4. Investigate control and dynamics issues on complex multi-body structures. Study the disturbances induced by a robotic system on precision pointing experiments.

5. Investigate the use of novel sensors and effectors whose weights and geometries are relatively negligible compared to those of the flexible structure to be controlled. Examine the sensing and actuating capabilities of piezo-electric materials.

The expected outputs of the LSS GTF Team are as follows:

1. A national test bed capable of implementing and evaluating LSS control methodologies.
2. An LSS ground test facility capable of applying and validating structural modeling techniques.
3. A facility in which real time testing procedures for space systems can be examined.
4. A multibody modeling computer analysis tool which is experimentally verified.

GROUND TEST FACILITIES

The current LSS GTF consists of the Single Structure Control (SSC) Laboratory. The GTF will be expanded to include the Pinhole Occulter Facility (POF), the Multi-Payload Pointing Mount (MPPM) Laboratory, and the Unobtrusive Sensor and Effector (USE) Laboratory. The Robot Enhancement Laboratory and a number of Thermal and Thermal/Vacuum Chambers will be incorporated into the overall LSS GTF. The POF design is proceeding presently, and initial testing is underway in the USE Laboratory. These future expansions are described in the section entitled Future LSS Activities.

Single Structure Control (SSC) Laboratory

The objectives of the SSC Lab are to apply and implement control design techniques on a realistic LSS, and to evaluate performance of LSS controllers. The control methodologies already implemented include the pole placement, FAMESS, HAC/LAC, and Positivity control algorithms. Comparison between these LSS control methodologies is presently nearing completion (see section on ACES Program). A model of the SSC test article has been developed and validated using modal testing and transfer function testing.

The SSC Laboratory (Figure 1) is located at NASA/MSFC in a high bay building. The laboratory contains a flexible test structure, a Base Excitation Table (BET) for inducing prescribed vibrations and disturbances into the structure, a gimbal system for producing controller rotations of the test article, Linear Momentum Exchange Devices (LMEDs) for damping beam vibrations, a payload mounting plate, assorted sensors (accelerometers, rate gyroscopes) at several structure locations, an Image Motion Compensation (IMC) system for optical pointing, and a computer/telemetry system.

1. Base Excitation Table
2. 3 Axis Base Accelerometers
3. 3 Axis Gimbal System
4. 3 Axis Base Rate Gyros and Counterweight
5. 3 Axis Tip Accelerometers
6. 3 Axis Tip Rate Gyros
7. Optical Detector
8. Mirrors
9. Laser
10. 2 Axis Pointing Gimbal System
11. LMED System

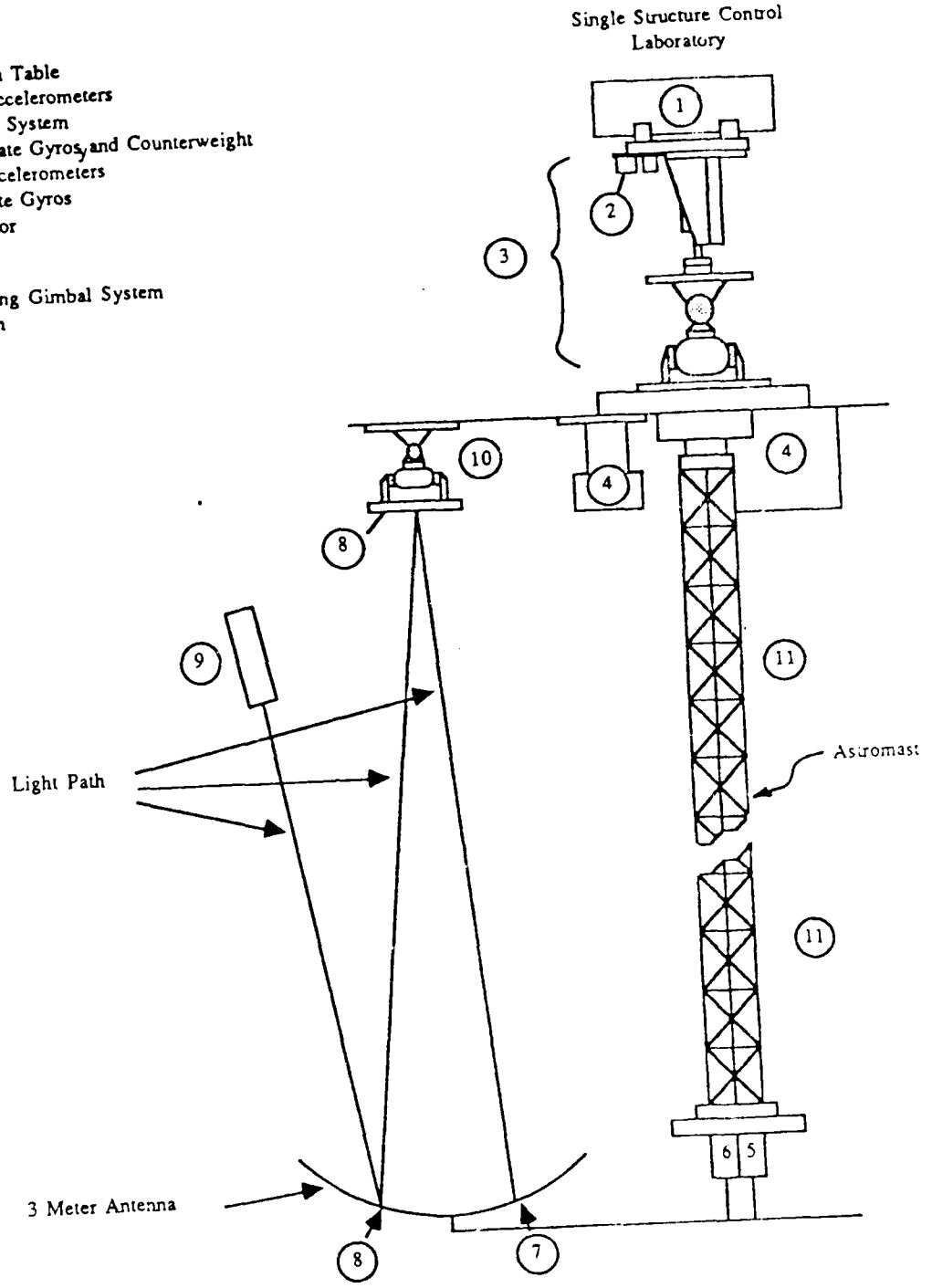

Figure 1. Single Structure Control (SSC) Laboratory.

The evolution of the SSC Laboratory over the past four years is depicted in Figure 2. Various sensors and actuators have been incorporated for different configurations. The basic test article has also been modified through the addition/replacement of tip appendages (i.e. cruciform, antenna structure).

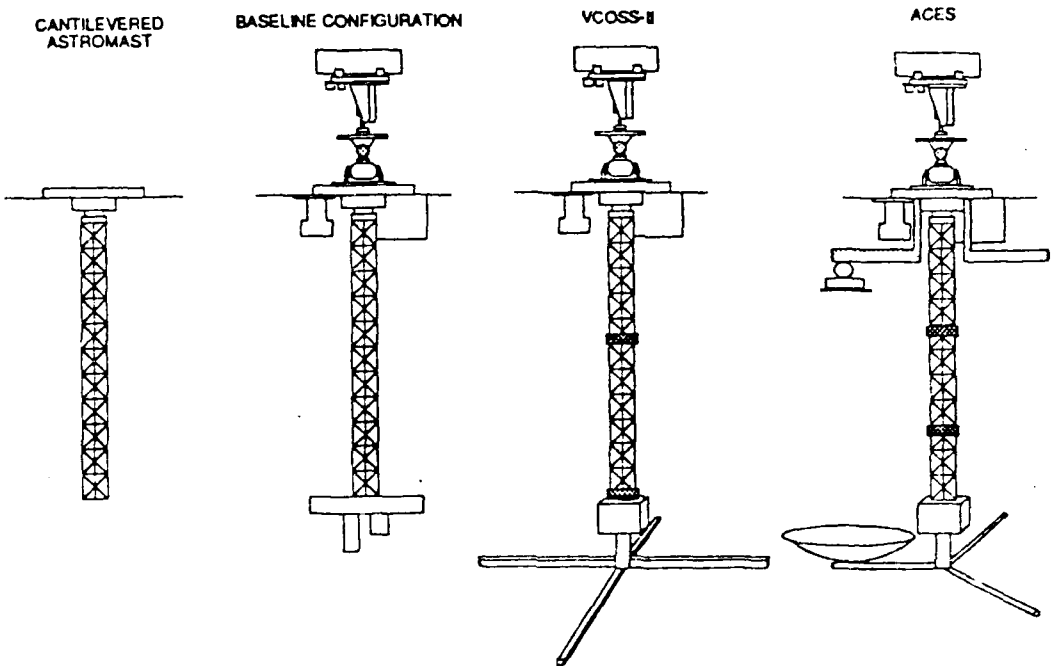

Figure 2. SSC Laboratory Evolution.

COST EFFECTIVE DEVELOPMENT OF THE LSS GTF

The development of the LSS GTF has proceeded in a very cost-effective manner. This cost-efficiency stemmed from the following two factors:

1) Ability to obtain and update useful laboratory components from past projects
2) Availability of LSS GTF Team members who are capable of developing integrating, maintaining, updating, and operating all facility components.

The first factor is examined in Table 1, which compares the actual cost (to the LSS GTF Program) with the estimated (or actual) development cost of each component.

Table 1. Actual versus Development Cost of LSS GTF Components.

Component	Actual Cost ($K)	Development Cost ($K)
Beam	0.6	225.
Gimbal System (AGS)	0.4	2500.
Roll Motor	0.0	2.
Computer System Hardware	70.0	110.
Computer System Software	0.0	125.
Base Excitation Table (BET)	5.0	20.
Tip Gyros (KARS)	50.0	75.
Base Gyros (ATM)	0.0	50.
Accelerometers	0.0	50.
IMC System	17.0	2000.
LMEDs	7.0	150.
Linear Thrusters	28.0	130.
SAFE-I	0.0	4500.
Robot Arm	0.0	100.
Solar Optical Telescope	95.0	95.
Roll Tip Motor	7.0	7.
Sum	280.0	10,139.

An experienced intra-structure of personnel was necessary to successfully develop and integrate the LSS GTF. The following discipline areas are presently assembled: controls, structural modeling, electronics, computer systems and programming, fabrication, sensors and actuators, optics, simulation, facility operation, propulsion, and program management. The vast experience assembled on the LSS GTF Team is indicated in Table 2. It should be emphasized that, even if one had $10 Million to invest in the LSS ground test facility components, it would be impossible to develop the facility without an established multidiscipline team having vast experience. The assembly and training of such a team would require another substantial investment. In addition, the actual implementation and development of the facility (i.e. hardware integration, software development, component modifications, interface definition, development, maintenance, etc...) would require an investment several times the initial component investment.

Table 2. LSS GTF Team Member Experience.

Discipline	Number of Members	Experience (Years)
Controls	6	80
Dynamic Testing	5	60
Structural Modeling	4	50
Computer Systems and Programming	5	55
Electronics	3	50
Simulation	6	55
Sensors and Actuators	7	100
Optics	3	50
Propulsion	2	20
Program Management	4	80

DYNAMIC MODELING

One of the more time consuming areas of LSS control verification is the development of the structural model. In many space projects, the data is presented to the control designer one substructure at a time. In addition, the substructure models are usually defined for a fixed substructure orientation. Most LSS have flexible substructures which change their orientation; this implies that a multitude of structural models are required to effect an LSS control verification. This scenario is not only time consuming, but it also contains many possible sources of error.

A user friendly computer analysis tool (CONTOPS) was developed to eliminate the aforementioned problems of time consumption and error generation. The tool works within the constraints of the system, such as model definition via substructures and different orientations. The significant features of the CONTOPS (Closed Tree Topology) are as follows:

1. Modular concept allows for rapid reconfiguration.
2. Models large angle rotations and angular rates for any module.
3. Allows for chain, tree, and ring topologies of flexible bodies.
4. A variety of control modules are available, including pole placement and quadratic minimum techniques.
5. Allows equality and inequality constraints between any two or more elements of the substructures.

The ring topology of flexible bodies is the latest feature that has been added to CONTOPS. The ring joints for each substructure have either equality or inequality constraints. The equality constraints consist of kinematic conditions Inequality constraints are conditions such as:

1. Hard stops.
2. Coulomb dampers.
3. Velocity squared dampers.
4. Solid dampers.
5. Displacement squared springs.

The ring topology with joint constraints models and simulates many LSS, but future enhancements are required to upgrade the disturbance models, selection of critical structural modes, and the modeling of effectors with momentum. The enhancements for the nonlinear modeling and simulation program will be:

1. Gravity Gradient model.
2. Atmospheric model.
3. Magnetic model.
4. Modal selection methods.
5. Momentum effector model.
6. Geometric Stiffness.

With these additions, very complex structures can be modeled and simulated using various control options. The system model objectives, which were relative ease and reasonable times to model LSS, were achieved with the development and use of CONTOPS.

LSS CONTROL SYNTHESIS

The SSC Laboratory provides a realistic LSS on which LSS control methodologies can be experimentally implemented and evaluated. Several control techniques have been applied to each configuration.

The preliminary control technique demonstrated at the SSC on the cruciform configuration was a centralized pole placement technique. The cruciform configuration had 15 modes below 2.5 Hz and these modes had damping of 1.5 percent or less. The fundamental mode was at 0.5 Hz. An Orbiter thruster-like disturbance at the BET was applied to demonstrate the controller effectiveness. The open and closed loop rate gyro responses to the same stimuli are shown in Figure 3.

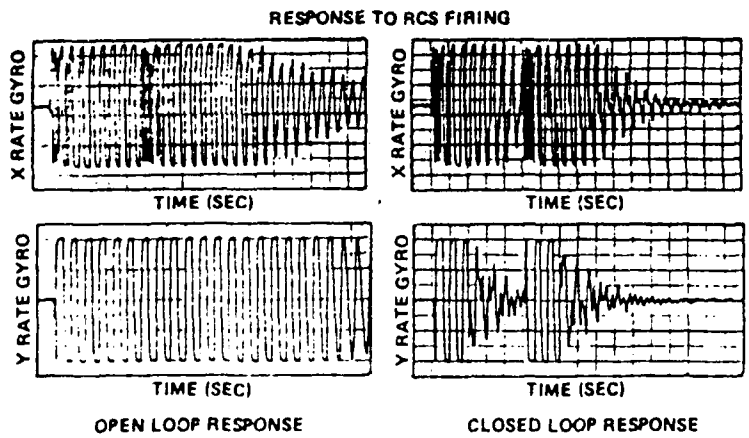

Figure 3. Open and Closed Loop Responses at SSC Lab (Cruciform Configuration).

The SSC Laboratory evolved into the VCOSS-II configuration from the cruciform configuration through the addition of the LMEDs (Linear Momentum Exchange Devices). The LMED provides a colocated sensor/actuator pair which applies a force and measures the resulting acceleration. Each LMED package contains two LMEDs having orthogonal axes, two accelerometers, and two LVDTs (Linear Variable Displacement Transducers). The two LMED packages are positioned at intermediate points along the Astromast, where these points were selected to maximize the actuation capability. A control loop was designed for the LMEDs and was able to significantly damp a mode at 5 Hz.

Active Control Evaluation of Spacecraft (ACES) Program

The ACES Program was a joint AFWAL (Air Force Wright Aeronautical Laboratories) MSFC venture which was implemented at the SSC Laboratory (ACES configuration) in 1986-1987. The purpose of the ACES Program was to investigate the implementation of the three primary ACOSS (Active Control Of Space Structures) LSS control techniques: FAMESS (Filter Accommodated Model Error Sensitivity Suppression), HAC/LAC (High Authority Control/Low Authority Control), and Positivity.

The ACES configuration evolved by incorporating the IMC (Image Motion Compensation) system, the antenna system, and the arm system to the VCOSS-II configuration. The IMC system consists of the laser, two mirrors, a two-axis detector, a set of two-axis pointing gimbals, and electronics to interface both the detector and gimbals to the computer. The laser is fixed to the facility, the mirrors are located at the tip and base of the Astromast, and the detector is at the base of the antenna. The arms are located at the base of the mast. The pointing gimbals are attached to the tip of one of the flexible arms; the other arm acts as a counterweight. The arms are purposely very flexible to increase the complexity of the control problem. The antenna system consists of the antenna, the antenna arm, and the two counterweight legs appended to the tip of the Astromast. The ACES configuration contains many closely spaced, low frequency modes (43 modes under 8 Hz), which are lightly damped (<2%).

The goals of the controller are:

1) to reduce the IMC (Image Motion Compensation) LOS (Line Of Sight) error due to three representative disturbances,
2) to ensure that the controller has a practical size (order), and
3) to attempt to ensure that the controller is tolerant of model limitations.

The primary performance criterion is the RMS LOS error. The controllers' effectiveness as structural vibration suppressors was investigated. The ACES Program has been recently been completed, and the final report is being written.

FUTURE LSS GTF ACTIVITIES

Future activities to be implemented in the LSS GTF include numerous programs, such as the ACES-II and ACES-III, COT (Control of Optical Train), and MMV (Multibody Modeling Verification) programs. Future laboratories to be developed include the POF (Pinhole Occulter Facility), MPPM (Multi-Payload Pointing Mount) lab, and the USE (Unobtrusive Sensors and Effectors) lab.

SSC Laboratory (ACES-II Program)

The SSC Laboratory will be used for the ACES-II program, which is a follow-on to the current ACES program. Additional promising candidate control techniques will be identified, implemented, and assessed. Several control techniques, such as Harris' MEOP (Maximum Entropy Optimal Projection), Control Dynamics' 1-CAT (One Controller At a Time), the various H-infinity techniques, and Johnson's DAC (Disturbance Accommodating Control) will be among those techniques under consideration. The ACES-II program is to be performed in 1988.

SSC Laboratory (ACES-III Program)

This follow-on to the ACES programs will modify the SSC Laboratory through the incorporation of a tip roll gimbal motor and a set of bi-directional linear thrusters. Letters of Invitation will be sent to interested candidate Guest Investigators from industry, universities, and other Government installations. Guest Investigators will propose additional utilization and/or modification of the LSS GTF. Selected Guest Investigators will implement their proposed ideas within the ACES-III program. The ACES-III is scheduled for 1989.

Pinhole Occulter Facility (POF)

The POF will consist of several configurations; the Primitive POF (PPOF) is the first configuration and will be followed by the POF. The PPOF (Figure 4) is presently under development and will consist of the vertical suspension of the 105 foot SAFE-I boom from a tripod air bearing. Two sets of AMEDs (Angular Momentum Exchange Devices) are being developed and a set of BLTs (Bi-directional Linear Thrusters) are being tested and developed for use as control actuators. The PPOF is planned to be operational in 1988. The POF configuration will be a modification of the PPOF by incorporating a set of control gimbals. Eventually, the POF will evolve to the omega-POF, through the application of USE technology to the boom.

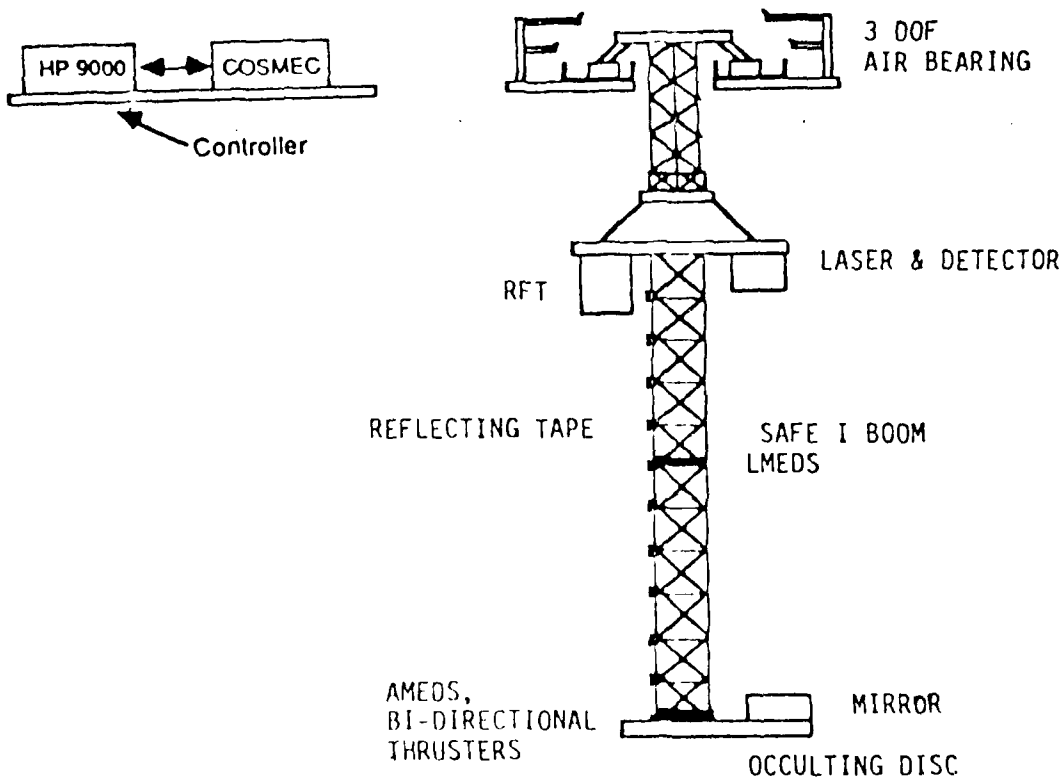

Figure 4. PPOF Configuration.

Multi-Payload Pointing Mount (MPPM) Laboratory

The purpose of the MPPM Laboratory (Figure 5) is to investigate the dynamic interaction between two or three pointing experiments that are mounted on the same structure and are operating simultaneously. Several configurations are to be examined, including components such as the SAFE-I boom, Solar Optical Telescope (SOT), and a Robot Arm.

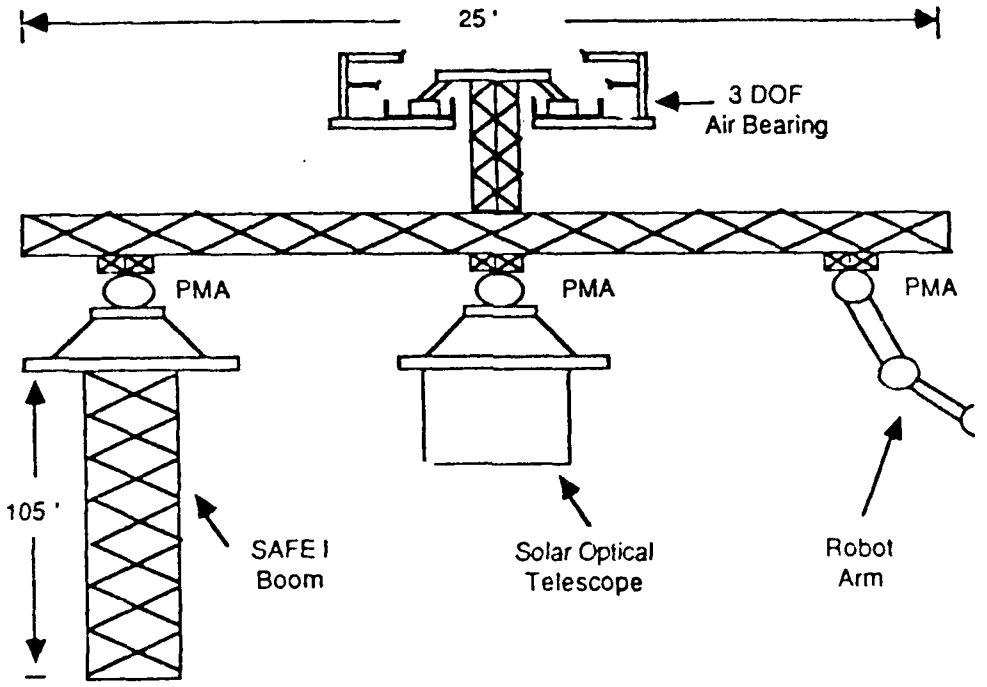

Figure 5. MPPM Laboratory.

Unobtrusive Sensor and Effector (USE) Laboratory

The USE Laboratory is to investigate the use of sensors and actuators which are lightweight and have unobtrusive geometries. Testing of piezo-electric materials is presently underway; a small scale experiment has been developed which demonstrates the actuation capabilities of a piezo material. The experimental open and closed loop responses (Figure 6) to an initial disturbance show the active damping capabilities induced by the piezo control loop. The USE lab will be expanded to accommodate the robot arm, which will be augmented with an end-effector having active fingers (to communicate with the piezo-electric sensors and effectors).

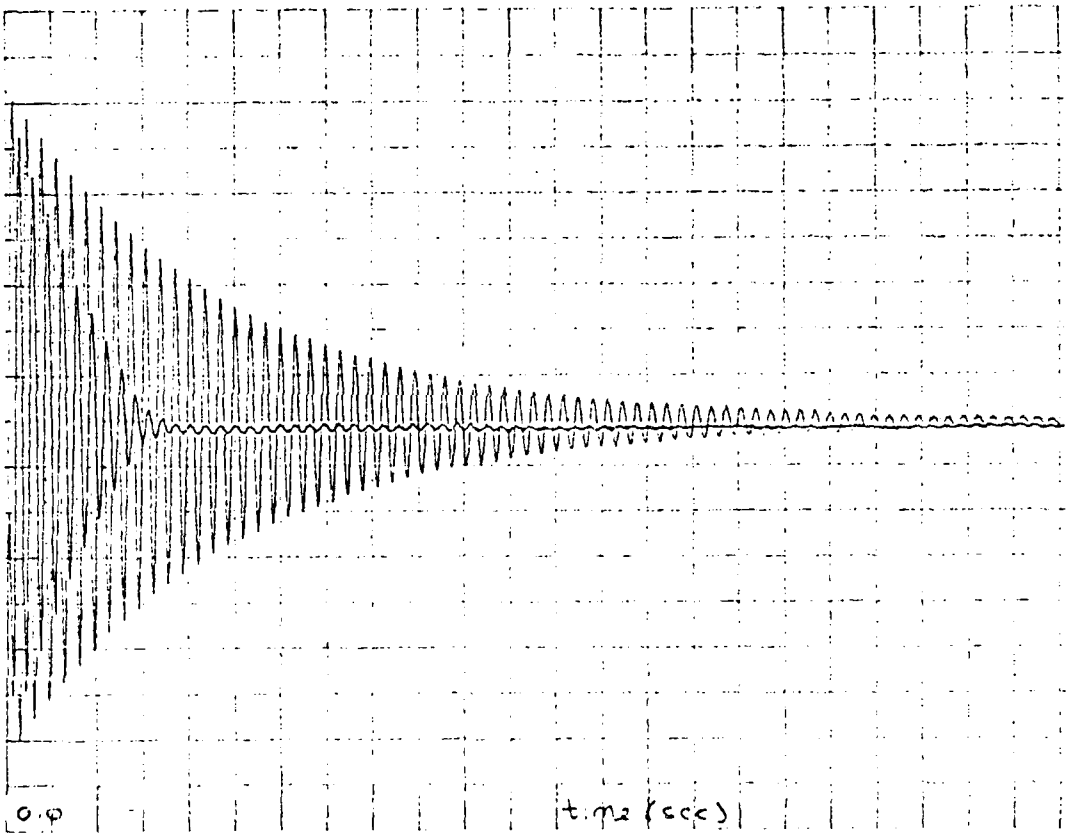

Figure 6. Piezo-electric Actuation Experimental Open/Closed Loop Responses.

Control of Optical Train (COT) Program

The COT Program will be designed and developed for the purpose of investigating the dynamics of future programs which will utilize precisely pointed, stabilized, folded optics. Figure 7 shows the proposed experimental configuration of the COT.

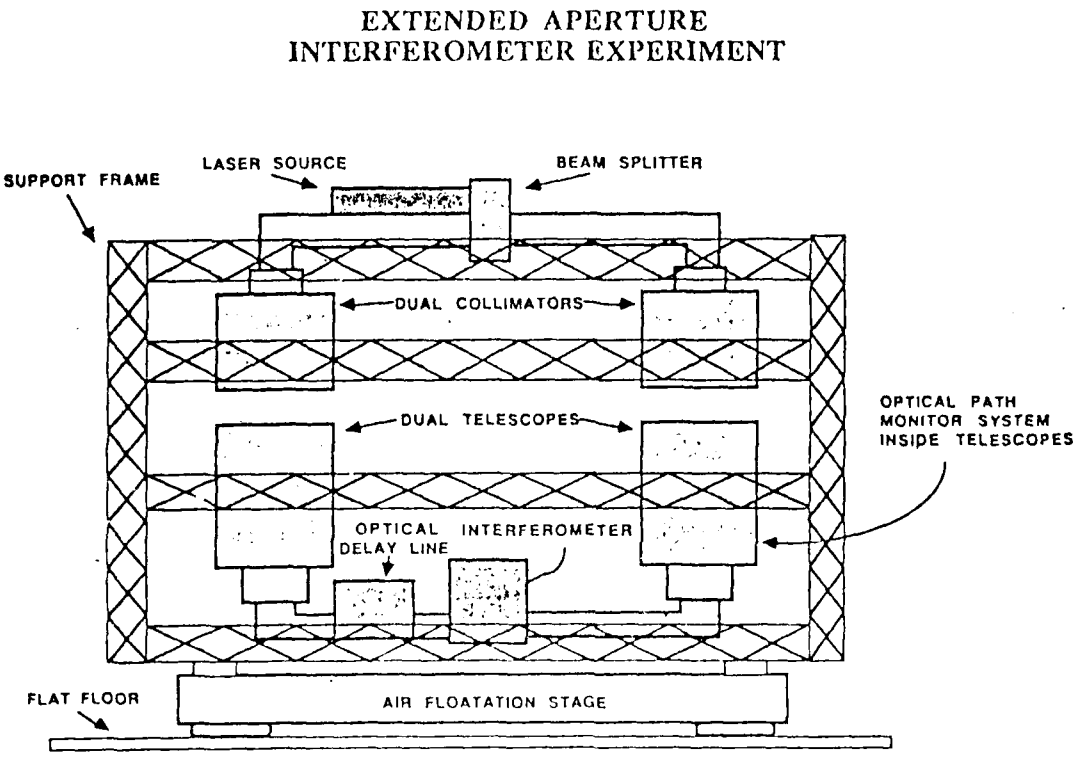

Figure 7. Control of Optical Train (COT) Configuration.

Multibody Modeling Verification (MMV) Program

The main objectives of the MMV Program are to improve the user friendly multibody modeling computer tool (CONTOPS) and to experimentally verify component modal synthesis methods. CONTOPS has the capability to effect component modal synthesis for a chain, tree, or ring topology of flexible bodies which can undergo large angular motions. The modal component synthesis methods are to be verified on a series of test articles. These test articles will be able to be reconfigured and will have the capability to experience large angular and translational displacements. One of the test articles is shown in Figure 8 in several of its configurations.

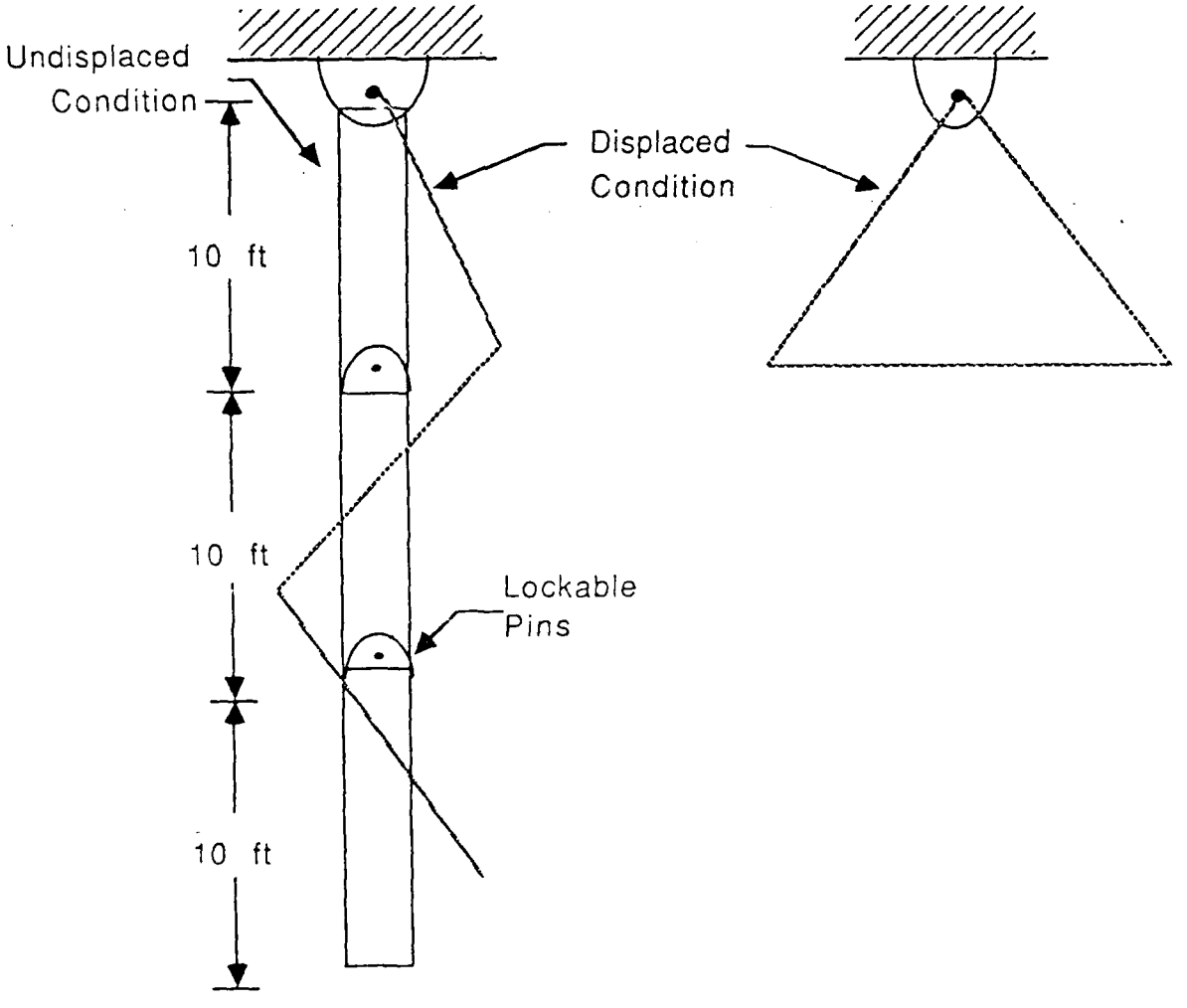

Figure 8. Multibody Modeling Verification Test Article.

CONCLUSION

The NASA/MSFC LSS GTF is one of the most complete LSS ground test facilities in the United States. The topics of control development and synthesis, dynamics verification, dynamic modeling, and hardware flight systems for space structures are being addressed. The present and future activities will enable the LSS GTF to become a national test bed for investigations in dynamics and controls.

The SSC Laboratory has been successfully developed and several significant experimental LSS programs have been completed. The SSC Laboratory contains a structure which is representative of LSS, with many lightly damped, closely spaced, low frequency modes. The ACES program is the first direct experimental comparison of the ACOSS LSS control methodologies.

The future activities include many investigations which will validate present control and dynamics methodologies and which will hopefully lead to the development of promising technologies. The application of unobtrusive sensors and effectors is presently underway; a small scale piezo-electric material experiment has been developed. The design and development of the Primitive Pinhole Occulter Facility is also currently proceeding. The multibody modeling computer tool (CONTOPS) is being improved. A plan is being developed for a facility in which validation of multibody modeling algorithms will be effected. Eventually, the complex control problems dealing with multi-payload pointing experiments will also be addressed.

Recent Laboratory Results on the Control of Flexible Structures

P. C. Hughes,
Cockburn Professor

and

T. Hong,
Graduate Student

Institute for Aerospace Studies
University of Toronto

Scope of this Presentation

This presentation is not a "paper" in the normal achive-journal sense--with experimental results, a crafty theory, and a convincing demonstration of good agreement between the two. It is more of a "report on research in progress." Particular attention has been paid to generating the "laboratory results." At the time of this conference, the accompanying theory, which will provide a framework for understanding these results in detail, has been well started but is not yet in a form suitable for presentation, due partly to unforeseen electronics difficulties with the facility.

The two main purposes of this presentation are:

1. To bring to the attention of the CSI community the existence of the Daisy facility; and
2. To present some recent laboratory results on the effects of computer time delays on the performance of flexible-structure control systems.

The "Daisy" Facility

Approximately five years ago, the (Canadian) Department of Communications and the (Canadian) Natural Sciences and Engineering Research Council began to fund the design and construction of the "Daisy" facility, including a structure suitable for carrying out laboratory experiments on the control of flexible structures. Now completed, the Daisy structure has three rigid and 20 elastic degrees of freedom, very low frequencies ($\approx$ 0.1 Hz), very low damping ($\approx$ 0.6%), "clustered" modes, and the potential to study both attitude control, shape control, parameter identification (modal testing), and sensor and actuator hardware. Sensors include digital encoders for "attitude" measurements, and accelerometers; actuators include three reaction wheels, and thrusters.

To achieve these goals, the Daisy structure is capable of mimicking the following characteristics, usually regarded as the salient ones for large space structure control:

- large dimensions;
- structural frequencies within the controller passband;
- vibration mode "clusters";
- very light structural damping;
- tight pointing requirements;
- shape control studies possible;
- sensors & actuators distributed over the spacecraft;
- modern (multivariable) control theory a necessity;
- new sensors and actuators can be developed;
- on-board signal processing, requiring microprocessors;
- opportunity for modal testing studies.

The most visible component of the Daisy facility is the Daisy test structure, whose current form is illustrated in Figure 1.

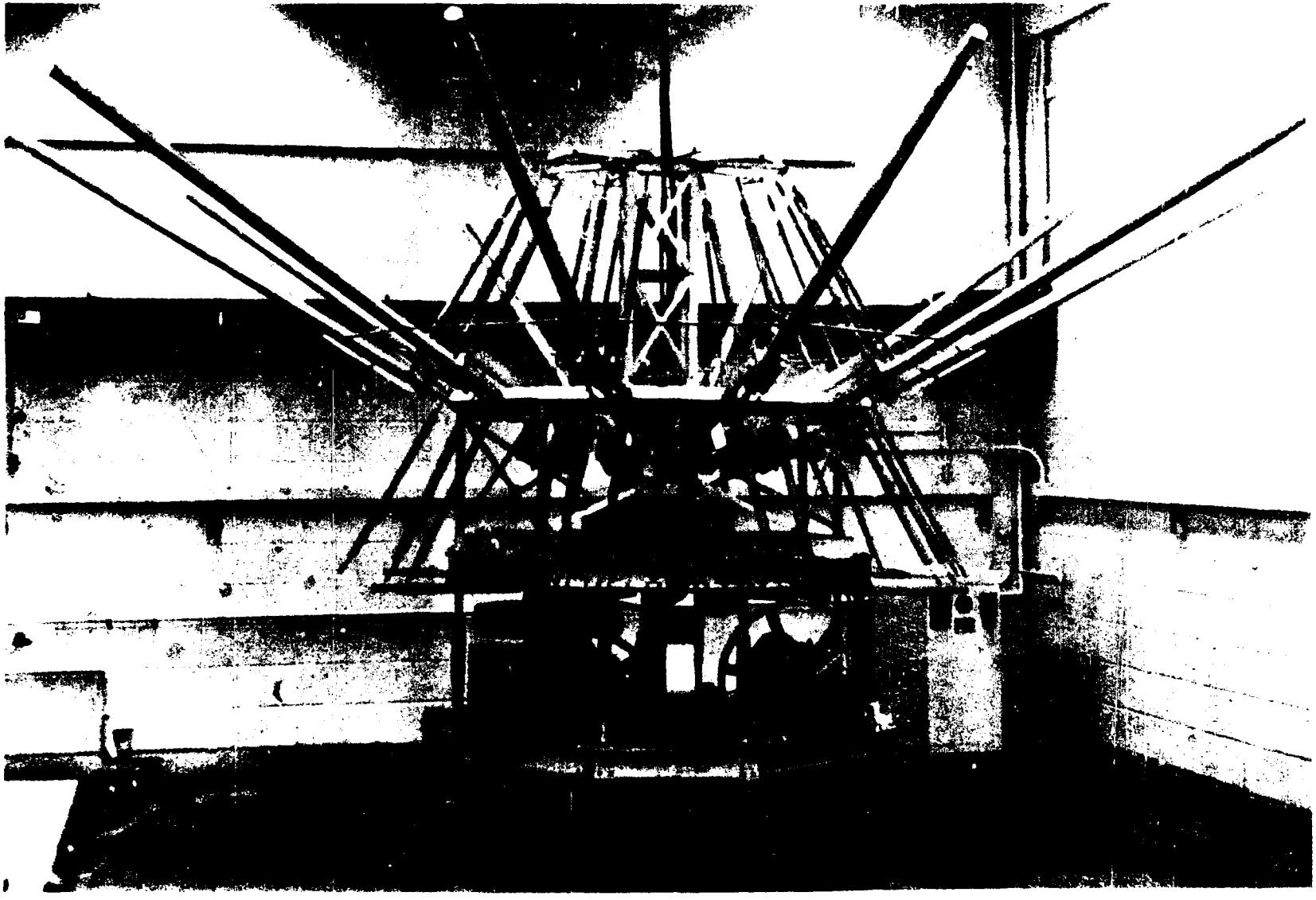

The Daisy Structure -- Designed To Study The Control Of Flexible Space Structures

The Daisy Structure

The Daisy structure, whose planform is shown below, has already been shown capable of accommodating most of the target requirements, with the remaining requirements requiring feasible upgrades. The Daisy structure consists of a central rigid hub to which ten counterbalanced ribs are attached. The rigid hub contributes three rigid degrees of freedom. Furthermore, since each of the ten attached (rigid) ribs has two flexible degrees of freedom, there are a total of 20 flexible modes. It is important to note that *although the flexibility in the Daisy structure is at discrete locations, it is capable of representing spacecraft that have distributed flexibility.* This is because the essential requirements for dynamic emulation—as stated on page 2—have been met.

Summary of Structural Characteristics

In summary, then, the Daisy structure has

- 3 "rigid" rotational modes, and 20 flexible modes;
- low frequencies of vibration ($\omega_1 = 0.1$ Hz);
- very light damping ($\zeta_1 = 0.006$);
- "clustered" frequencies.

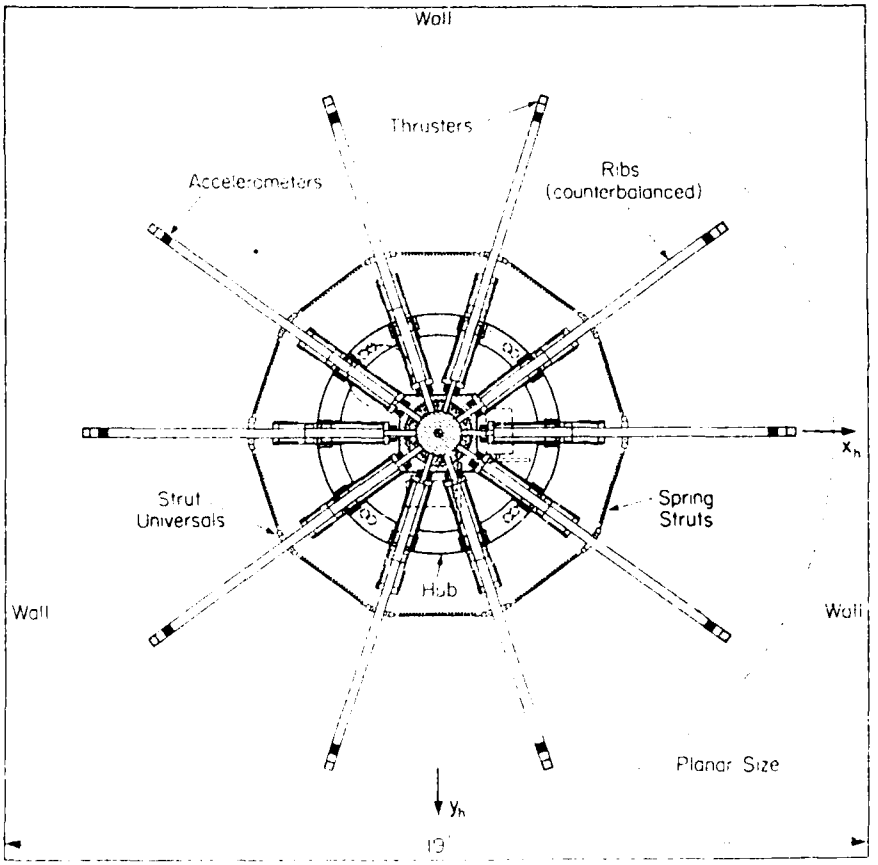

Modal Model

The basic linear structural model is of the form:

$$M\ddot{\mathbf{q}} + D\dot{\mathbf{q}} + K\mathbf{q} = B\mathbf{u}(t)$$

Rigid-Elastic Partitioning

Partition as follows:

$$\mathbf{q} = \begin{bmatrix} \mathbf{q}_r \\ \mathbf{q}_e \end{bmatrix} \quad , \quad B = \begin{bmatrix} B_r \\ B_e \end{bmatrix}$$

$$M = \begin{bmatrix} M_{rr} & M_{re} \\ M_{re}^T & M_{ee} \end{bmatrix} \quad , \quad D = \begin{bmatrix} \mathbf{O} & \mathbf{O} \\ \mathbf{O} & D_{ee} \end{bmatrix} \quad , \quad K = \begin{bmatrix} \mathbf{O} & \mathbf{O} \\ \mathbf{O} & K_{ee} \end{bmatrix}$$

Modal Coordinates

We set

$$\mathbf{q}_r = \mathcal{E}_{rr}\boldsymbol{\eta}_r + \mathcal{E}_{re}\boldsymbol{\eta}_e \quad , \quad \mathbf{q}_e = \mathcal{E}_{ee}\boldsymbol{\eta}_e$$

where $\boldsymbol{\eta}_r$ are the 'rigid' modal coordinates and $\boldsymbol{\eta}_e$ are the 'elastic' modal coordinates. (It is assumed above, and in the sequel, that the physical coordinates $\mathbf{q}_e$ are *relative* coordinates.) The rigid eigenvectors are

$$\begin{bmatrix} \mathcal{E}_{rr} \\ \mathbf{O} \end{bmatrix}_{\text{columns 1,2,3,}}$$

and the elastic eigenvectors are

$$\begin{bmatrix} \mathcal{E}_{re} \\ \mathcal{E}_{ee} \end{bmatrix}_{\text{columns 1,2,...}}$$

Modal Form of Structural Model

With appropriate orthogonality and normality conditions, the resulting structural model in *modal form* is

$$\ddot{\boldsymbol{\eta}}_r = \tilde{B}_r\mathbf{u}(t)$$

$$\ddot{\boldsymbol{\eta}}_e + \tilde{D}_{ee}\dot{\boldsymbol{\eta}}_e + \Omega^2\boldsymbol{\eta}_e = \tilde{B}_e\mathbf{u}(t)$$

where

$$\tilde{B}_r \triangleq \mathcal{E}_{rr}^T B_r \quad , \quad \tilde{B}_e \triangleq \mathcal{E}_{re}^T B_r + \mathcal{E}_{ee}^T B_e$$

$$\tilde{D}_{ee} \triangleq \mathcal{E}_{ee}^T D_{ee}\mathcal{E}_{ee} \quad , \quad \Omega^2 \triangleq \mathcal{E}_{ee}^T K_{ee}\mathcal{E}_{ee}$$

Baseline Control System

The "baseline" control law is of the form

$$\mathbf{u}(t) = -\mathbf{K}_P\mathbf{y}(t) - \mathbf{K}_D\dot{\mathbf{y}}(t)$$

where $\mathbf{K}_P$ and $\mathbf{K}_D$ are the "proportional" and "rate" gain matrices, and $\mathbf{y}(t) \equiv \boldsymbol{\theta}(t)$ represents the measurements to be fed back. Note that $\boldsymbol{\theta}(t)$ is {roll, pitch, yaw} of the hub, and that these angles and their rates are independently measured. Thus,

$$\mathbf{u}(t) = -\mathbf{K}_P\boldsymbol{\theta}(t) - \mathbf{K}_D\dot{\boldsymbol{\theta}}(t)$$

Closed-Loop System Equations, with Spillover

It follows that the closed-loop control of the rigid coordinates obeys the system equations

$$\ddot{\boldsymbol{\eta}}_r + 2\mathbf{Z}_c\boldsymbol{\Omega}_c\dot{\boldsymbol{\eta}}_r + \boldsymbol{\Omega}_c^2\boldsymbol{\eta}_r = \underbrace{-\tilde{\boldsymbol{\mathcal{B}}}_r\mathbf{K}_P\boldsymbol{\mathcal{E}}_{re}\boldsymbol{\eta}_e - \tilde{\boldsymbol{\mathcal{B}}}_r\mathbf{K}_D\boldsymbol{\mathcal{E}}_{re}\dot{\boldsymbol{\eta}}_e}_{\text{spillover}}$$

provided the gain matrices are chosen thus:

$$\mathbf{K}_P = \boldsymbol{\mathcal{B}}_r^{-1}\boldsymbol{\mathcal{E}}_{rr}^{-T}\boldsymbol{\Omega}_c^2\boldsymbol{\mathcal{E}}_{rr}^{-1} \quad , \qquad \mathbf{K}_D = 2\boldsymbol{\mathcal{B}}_r^{-1}\boldsymbol{\mathcal{E}}_{rr}^{-T}\mathbf{Z}_c\boldsymbol{\Omega}_c\boldsymbol{\mathcal{E}}_{rr}^{-1}$$

with $\boldsymbol{\Omega}_c$ being a diagonal matrix of desired natural frequencies for the rigid modal coordinates, and $\mathbf{Z}_c$ being a diagonal matrix of desired damping factors. Note that, for Daisy, $\boldsymbol{\mathcal{B}}_r$ is an invertible 3×3 matrix.

To complete the system equations, we note that the elastic modal coordinates satisfy the following system equations:

$$\ddot{\boldsymbol{\eta}}_e + \left(\tilde{\boldsymbol{\mathcal{D}}}_{ee} + \underbrace{\tilde{\boldsymbol{\mathcal{B}}}_e\mathbf{K}_D\boldsymbol{\mathcal{E}}_{re}}_{\text{spillover}}\right)\dot{\boldsymbol{\eta}}_e + \left(\boldsymbol{\Omega}^2 + \underbrace{\tilde{\boldsymbol{\mathcal{B}}}_e\mathbf{K}_P\boldsymbol{\mathcal{E}}_{re}}_{\text{spillover}}\right)\boldsymbol{\eta}_e = \underbrace{-\tilde{\boldsymbol{\mathcal{B}}}_e\left(\mathbf{K}_P\boldsymbol{\mathcal{E}}_{rr}\boldsymbol{\eta}_r + \mathbf{K}_D\boldsymbol{\mathcal{E}}_{rr}\dot{\boldsymbol{\eta}}_r\right)}_{\text{more spillover (from rigid modes)}}$$

First: A Typical Rigid, Controlled Response

The figure below shows the chart-recorded response of the Daisy structure when the ribs are locked—i.e., when the structure is rigid and possesses only rigid modes. The baseline control system is active. The response shown is for the roll angle, but the pitch and yaw responses are very similar.

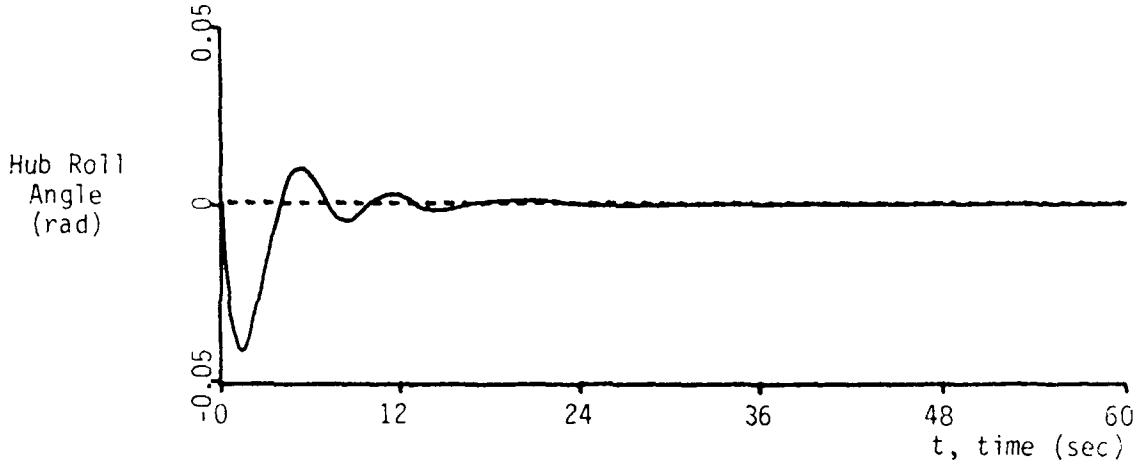

Figure 3: Typical Rigid, Controlled Response

Effect of Computer Time Delays on the Rigid Response

Prior to showing results for the flexible case, the rigid results for computer time delays are useful for reference purposes. Shown below in Figures 4 and 5 are the rigid controlled responses for additional computer time delays of $\Delta T = 12$ and 32 units. The (additional) time delay is denoted by ΔT rather that T because even the baseline control system has an irreducible time delay. These results should be compared with the $\Delta T = 0$ results (Figure 3).

With $\Delta T = 12$, the performance is already severely compromised, and with $\Delta T = 32$, the closed-loop system is clearly unstable. (Theoreticians please note: there are hardware limitations to providing an arbitrary torque, whether stabilizing or destabilizing.)

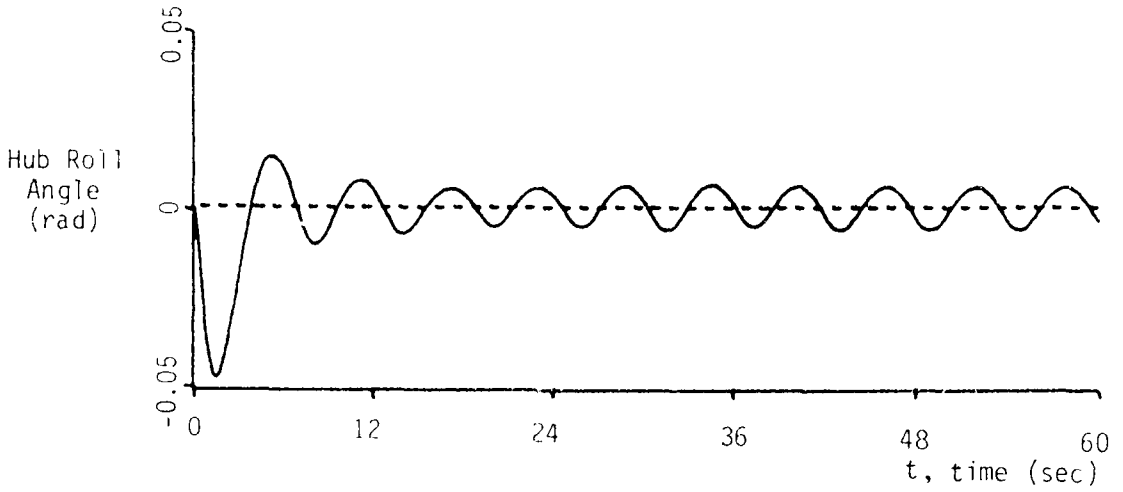

Figure 4: Rigid, Controlled Response wih ΔT = 12 units.

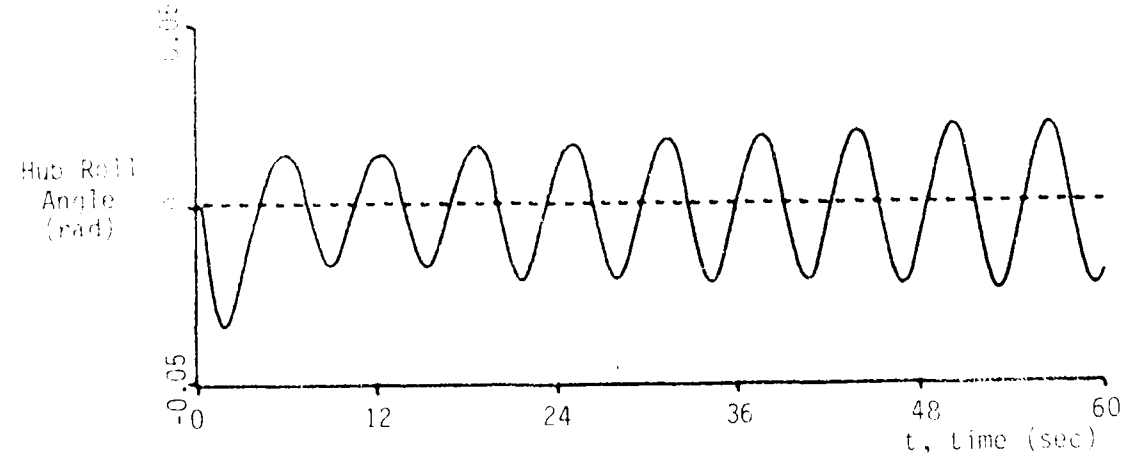

Figure 5: Rigid, Controlled Respense with ΔT = 32 units.

Effect of Gain Magnitude on the Rigid Response

Again prior to showing results for the flexible case, the rigid results for variations in gain magnitude are also useful for reference purposes. Shown below in Figures 6 and 7 are the rigid controlled responses for the gains at, respectively, $\frac{1}{3}$ and 3 *times their nominal values. In* both cases, the computer time delays are $\Delta T = 12$ units. These results should be compared with the nominal-gain results (Figure 4). (Watch out for changed scales!)

Evidently, and as expected, the lower the controller gain (i.e., the lower the controller bandwidth) the less the impact of a time delay. Generally speaking, it is $\omega_{BW} \cdot T$, the product of a typical control bandwidth with the computer time delay, that matters.

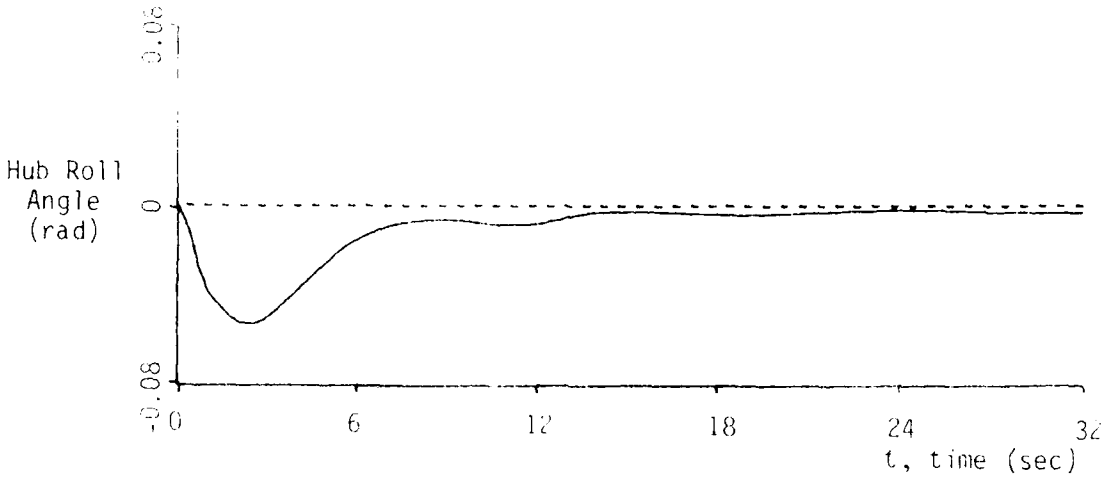

Figure 6: Rigid, Controlled Response with Gains Reduced by 3

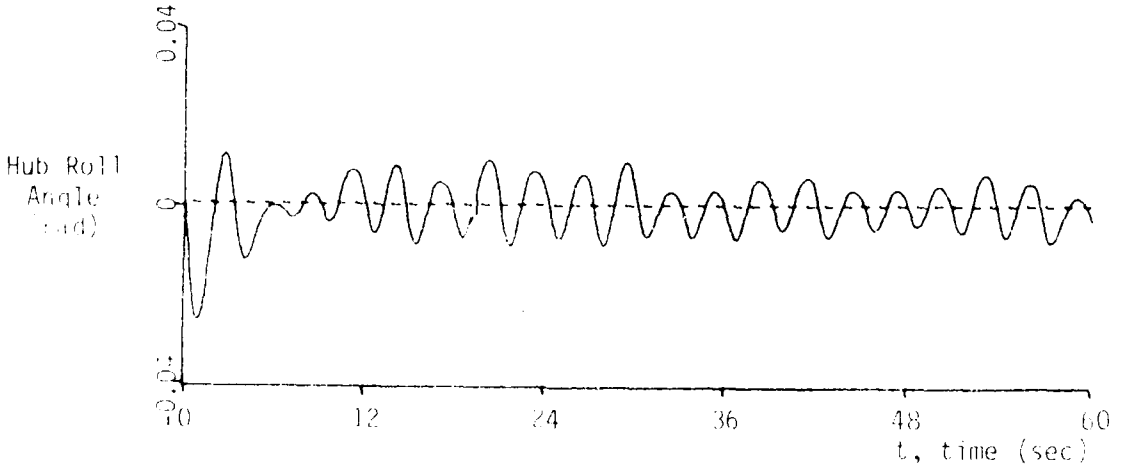

Figure 7: Rigid, Controlled Response with Gains Trebled

Typical Flexible, Controlled Response

Finally, we come to the results for the *flexible* Daisy structure, with the ribs unlocked. Figure 8 below shows a typical response plot for the flexible case. The gains are nominal, and no extra computer delay ΔT has been added.

This figure should be compared with Figure 3.

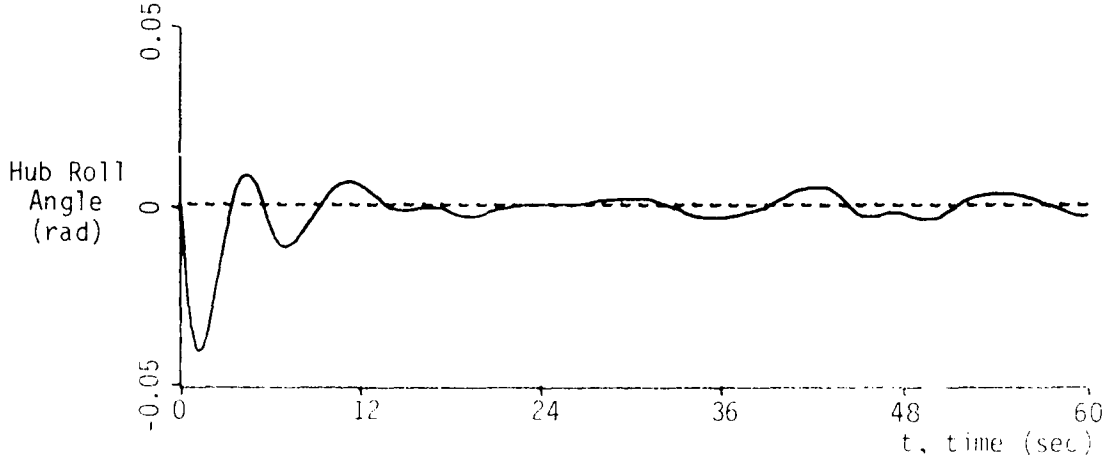

Figure 8: Typical Flexible, Controlled Response
(Nominal Gains, $\Delta T = 0$)

Effects of Computer Time Delays

If the case discussed on the preceding page has computer time delays added as well, the results are as shown in Figures 9 and 10. Obviously, the performance is severely degraded. Indeed, for $\Delta T = 24$ units, the only things keeping matters from being even worse are the mechanical limitations in the control actuators.

Figures 9 and 10 should be compared with Figures 4 and 5, respectively.

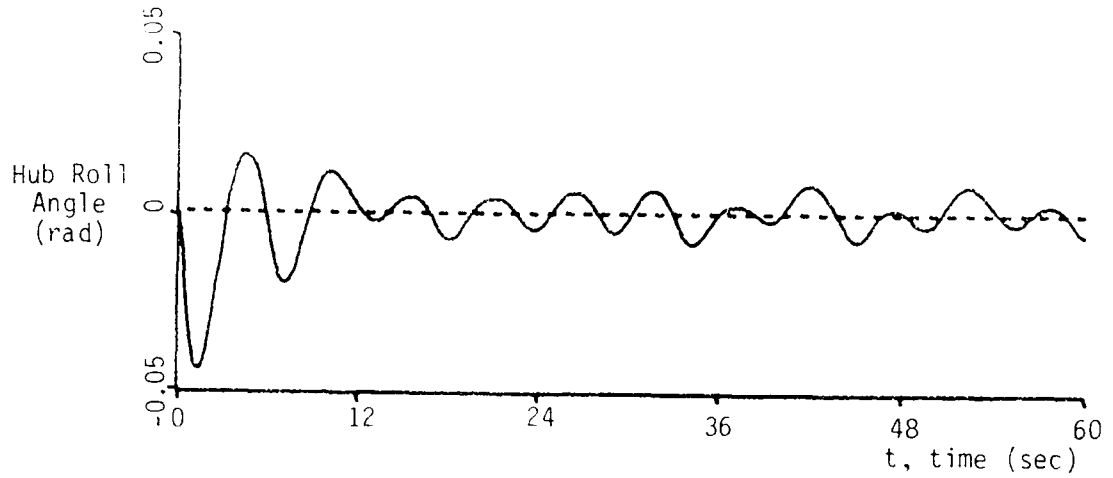

Figure 9: Typical Flexible, Controlled Response (Nominal Gains, ΔT = 12 units)

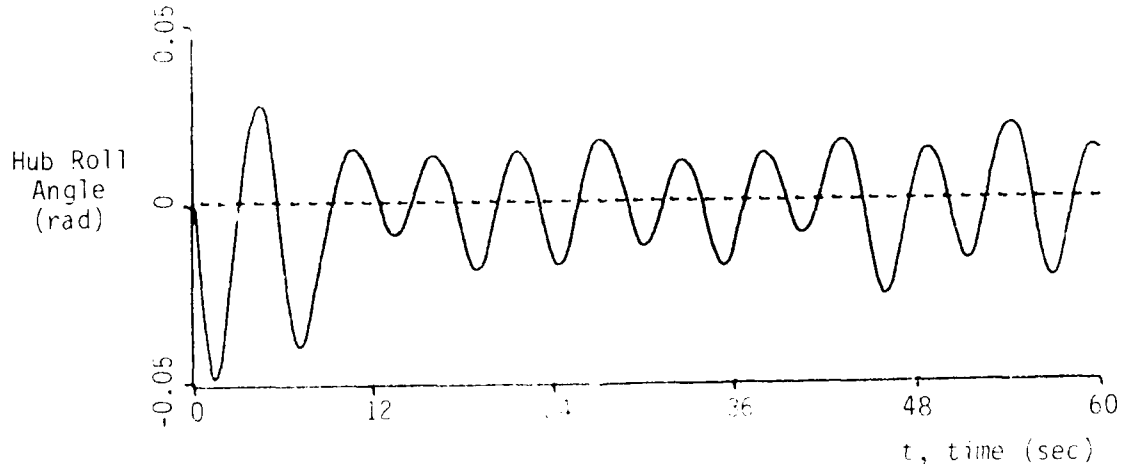

Figure 10: Typical Flexible, Controlled Response (Nominal Gains, ΔT = 24 units)

Imputed Damping Ratios

One of the chief objectives of an active feedback system for a flexible spacecraft is to provide asymptotic stability to the rigid modes. This, in turn, requires rate feedback. Computer time delays erode the effectiveness of this rate feedback, and this can be semi-quantitatively measured from the time plots generated by a laboratory facility like Daisy. This sort of graphical measurement is not "exact," but gives a valid measure of the phenomenon under study. Thus the ideal damping factor ζ is replaced, with computer time delays, by an imputed damping factor, $\zeta_{imp} < \zeta$. Some results for Daisy are shown below. Note that

1. the slopes are negative (the bigger the time delay, the worse its effect);
2. the "flexible" data lie below the "rigid" data (the effect on a flexible spacecraft is worse than the effect on a rigid spacecraft).

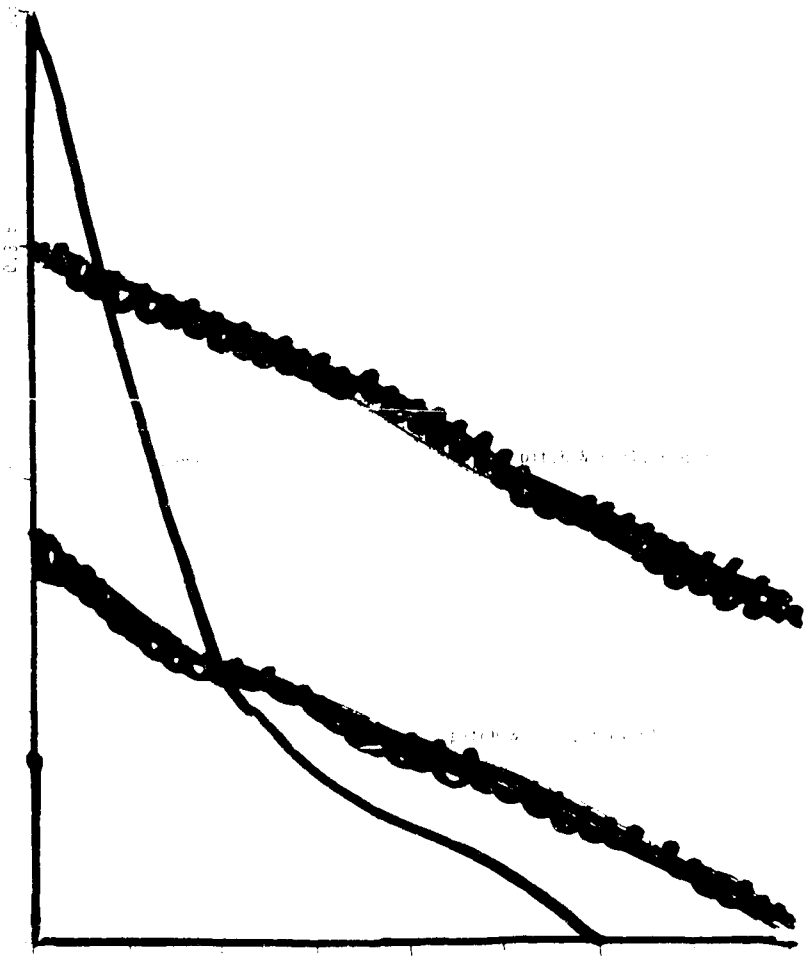

Limit Cycle Widths

Although limit cycles cannot occur within *linear* analysis, they can for *nonlinear* systems. Daisy is nonlinear, the principal nonlinearity residing in the reaction wheel actuators. Thus, as the effectiveness of the rate feedback is increasingly eroded by computer time delays (see Figure 11), the onset of limit cycles can be discerned in the system time responses. Some results for Daisy are shown below. Note that

1. the slopes are positive (the bigger the time delay, the worse its effect);
2. the "flexible" data lie above the "rigid" data (the effect on a flexible spacecraft is worse than the effect on a rigid spacecraft).

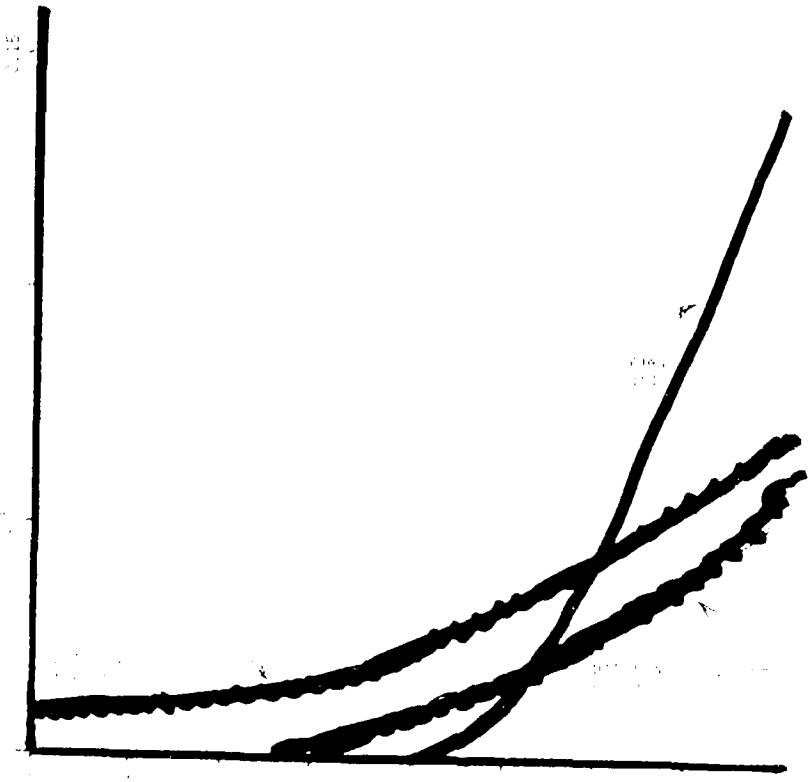

RECENT DEVELOPMENTS ON MBCT

B. WADA
C. P. KUO

JET PROPULSION LABORATORY
CALIFORNIA INSTITUTE OF TECHNOLOGY

SECOND NASA/DOD CSI CONFERENCE
NOVEMBER 18, 1987
COLORADO SPRINGS, COLORADO

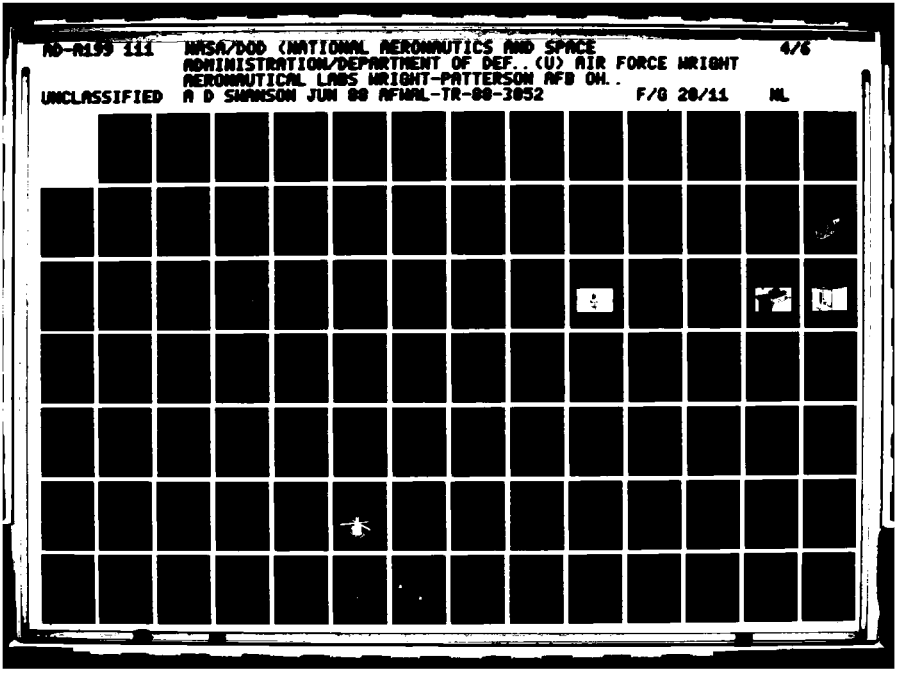
AD-A199 111 NASA/DOD (NATIONAL AERONAUTICS AND SPACE ADMINISTRATION/DEPARTMENT OF DEF..(U) AIR FORCE WRIGHT AERONAUTICAL LABS WRIGHT-PATTERSON AFB OH..
4/6
UNCLASSIFIED A D SWANSON JUN 88 AFWAL-TR-88-3052 F/G 20/11 NL

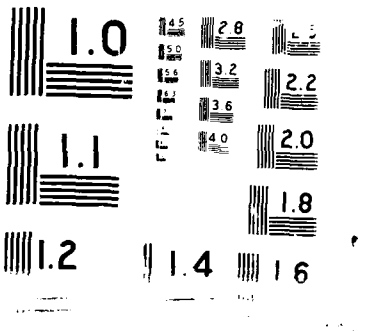
1.0
1.1
1.2
1.4
1.6
2.8
3.2
3.6
4.0
2.2
2.0
1.8

OUTLINE

- MOTIVATION
- BASIC CONCEPT
- WORK TO DATE
- RECENT EFFORTS
- FUTURE PLANS
- SUMMARY

11/18/87

MOTIVATION
NEED

Proposed spacecraft/space payload missions are placing stringent requirements on the structure itself, such as the precision required on the geometric accuracy of large structures in both a quasi-static and dynamic environment. Large Space Structures in this presentation are defined as structures with performance requirements that cannot be verified by ground tests. This definition allows for structures that are relatively small and stiff but has high accuracy requirements to very large and flexible structures.

Many of the proposed structures fall into the class defined as large space structures. Thus validation of the performance of the hardware by ground test is very difficult and in some cases almost impossible based upon the state-of-the-art ground test methods. Since almost all space systems flown to date, in which structural performance is important, have been validated by ground tests, the authors believe Program Managers will not adopt structural concepts that cannot be validated by ground tests.

Some argue that the advances in analysis methods and computers will negate the need for ground tests of structural system. The authors disagree.

Thus in order to meet the challenges of the future, new ground test approaches must be developed in order to validate Large Space Structures. One of the approaches proposed several years ago by the authors is referred to as the Multiple Boundary Condition Test (MBCT). (See references)

The Multiple Boundary Condition Test (MBCT) approach was developed to provide an approach to obtain ground test data to help validate the mathematical models of large flexible space structures that couldn't be ground tested by existing state-of-the-art modal test methods. Testing of large flexible space structures is severely hampered by the adverse ground environment such as gravity and air; thus reliable test data can't be obtained.

The approach is to carefully select artificial boundary conditions for the structure to obtain good ground test results, select a variety of boundary condtions to allow validation of the significant portions of the mathematical model, and to obtain a number of independent test measurements to increase the reliability of the test data.

The theory, results of the analytical simulation, and the available test results will be presented.

MOTIVATION
NEED

- LARGE SPACE STRUCTURES ----> FUTURE
  - DEFINITION OF
- DIFFICULT TO VALIDATE HARDWARE ---->
  - GROUND TEST
- MOST STRUCTURES ----> TESTED
- ANALYSIS
- "NEW" GROUND TEST APPROACH ----> LSS

MOTIVATION
LSS

Several years ago, a sector of a 55 meter diameter Wrapped Rib Antenna was built by LMSC under contract to JPL. One of the objectives of the effort was to evaluate potential ground test methods to validate the structural characteristics of the structure. One of the conclusion by the authors was that the state-of-the-art ground test methods and facilities were not adequate to experimentally determine the antennas structural characteristics.

MOTIVATION
LSS

- **LOCKHEED WRAPPED RIB ANTENNA**
- **OTHERS**

MOTIVATION
STATE-OF-THE-ART

During our effort on the Galileo and the Centaur we had the opportunity to evaluate the state-of-the-art of modal test methods. The evaluation gave us an insight to the possible extension of the modal test approaches to large space structures. The data from the modal test on a "well behaved linear" Galileo structure were provided to five organizations responsible for the development of the latest state-of-the-art modal test and identification procedures. Selected comparison of the results are presented.

Similarly the data from the Centaur modal test were used by 4 organizations for analysis using the latest modal analysis methods. Unlike the Galileo structure, the Centaur structure was supported through trunions during the test. Selected results from the Centaur test is presented. All the work on Centaur was performed for LeRC and the majority of the test was conducted by GDCA.

A comparison of the modal analysis results indicated a wider dispersion of test results than was anticipated. For many large structures, current ground test approaches are inadequate. New test approaches are required.

MOTIVATION
STATE-OF-THE-ART

- GLL MODAL TEST
- CENTAUR MODAL TEST

BASIC CONCEPT

The MBCT concept evolved during the activity to establish ground test methods for the LMSC Wrapped Rib Antenna. The method is especially applicable to long or large surface type structures which are contiguous; structures which cannot be conveniently disassembled into subsystems. For example, the antenna rib cannot be cut into segments without destroying the structure itself.

The most effective and accurate results from current modal test/analysis correlation efforts are obtained by testing the most representative hardware with the proper boundary conditions. Thus in order to maximize the test data which are used to modify the large mathematical model, emphasis is placed on obtaining accurate modal data using many accelerometers and obtaining as many modes as possible. In most structures the fidelity of the test data decreases with ascending mode number. Even if good modes (tens) could be measured, the number of parameters in the mathematical model with potential errors (tens of thousands) far exceeded the amount of the test data.

Current state-of-the-art test methods couldn't be used for the Wrapped Rib Antenna due to the influence of gravity and air.

The MBCT approach is not to identify and correct the entire mathematical model with one test but to validate submatrices of the total model which represent portions of the physical structure. The objective is to artificially constrain the physical structure to negate the adverse influence of the terrestrial environment from the modal test results and minimize the coupling between the structure being tested from the other part of the structure. Localization of the test data also focuses the potential error in the model to a much smaller subset of the entire mathematical model. Since the artificial constraint affects the ability to identify certain parameters, the artificial boundary must be moved such that all portions of the mathematical model which required validation is tested. The number of experimental estimates of a mathematical parameter can be increased to any number desired by the engineer by selecting the constraints for various tests to include the structure of interest. The test is simplified since the number of modes acquired for a particular test could be substituted by acquiring a smaller number of modes for a larger number tests with different boundary constraints.

In summary the MBCT is attractive because it can be used to test large space structures on the ground, many simple tests can be used to replace a complex modal test, and a large number of experimental estimates for a structural parameter are possible.

BASIC CONCEPT
SUMMARY

- MANY SIMPLE TESTS
- LARGE NUMBER OF TEST DATA
- ACQUIRED DATA ON HARDWARE

WORK TO DATE

The activity on MBCT reported at the first CSI Meeting included efforts on using analytical simulations to validate the MBCT approach. The examples used in the simulation represented simple beams supported at both ends. The object was to identify errors in the cross-section moment-of-inertia by using MBCT. The successful results to date have encouraged further work on the MBCT.

WORK TO DATE

- THEORY
- BEAM SIMULATIONS

RECENT EFFORTS

Our effort in the past year included the application of MBCT on a laboratory test beam which was similar to the beams used in the analytical simulations. The beam with its end restraints was selected to be severely affected by gravity. The figure shows the large initial deflection due to gravity. The next figure shows the beam supported by an artificial boundary condition used for a modal test to obtain data required by MBCT. The application of the MBCT accurately corrected for large errors in the mathematical model.

In order to demonstrate the applicability of MBCT to a wider class of structures, the next effort was to apply the method on a beam configuration similar to that planned for COFS. In the mathematical simulation, the structural parameters selected to have potential errors were the top and bottom longerons, diagonal, and battens. As noted in the results, errors were accurately detected in the mathematical model.

RECENT EFFORTS

- LABORATORY TEST OF BEAM
- ANALYTICAL SIMULATION OF "MAST"

FUTURE PLAN

The MBCT method has been successful on every application to date. During each application of the MBCT, enhancements and improvements to the method have been and will continue to be made. However the validation of the MBCT approach is possible only by using test data acquired on physical hardware. Since fabrication of hardware to test MBCT is expensive, our objective is to test the MBCT using existing NASA/AF hardware at the NASA or AF facilities containing the hardware and test setup.

Our plans (desires) are to perform ground tests on a Mast type truss, the PSR Backup Structure and any other structure which may be available. Ultimately the plan is to ground test a structure which will be placed and tested in space to validate the MBCT method. Only by flight validation will confidence in the MBCT approach be developed by the Program Managers.

FUTURE PLAN

- CONTINUE DEVELOPMENT
- GROUND TEST "MAST" TYPE BEAM
- GROUND TEST PSR BACKUP STRUCTURE
- VALIDATE -- FLIGHT TEST

SUMMARY

The application of MBCT has been successful to date; however it must be applied to more physical hardware.

Also its applicability to a wider range of structures must be demonstrated. With each application, knowlege of the application of the MBCT has increased to account for test related uncertainties which are not always evident in a mathematical simulation. The ultimate validation is to use the MBCT to ground test a structure which cannot be ground tested by the current state-of-the-art test techniques; then validated by a space flight test.

SUMMARY

- MBCT WORKS
- MORE GROUND TESTS
- IMPROVEMENTS
- FLIGHT TEST VALIDATIONS

REFERENCES

1.0 Wada,Kuo,Glaser,"Extension of Ground-Based Testing for Large Space Structures," Journal of Spacecraft and Rockets, Volume 23, No.2, March-April 1986.

2.0 Wada, Kuo, Glaser,"MBCT Approach to Update Mathematical Models of Large Flexible Structures," SAE Paper No. 851933, Oct. 1985.

3.0 Wada, Kuo,Glaser,"MBCT for Verification of Large Space Structures," AIAA 27th SDM Conference, San Antonio, Texas, 1986.

4.0 Kuo,Wada,"System Identification of a Truss Type Space Structure Using the MBCT Method," AIAA 28th SDM Conference, Monterey, CA., 1987.

QUIET STRUCTURES FOR PRECISION POINTING

P. A. Studer
Magnetic Concepts
Silver Spring, Maryland

H. W. Davis
Ball Aerospace Systems Division
Boulder, Colorado

OVERVIEW OF QUIET STRUCTURES

The objectives of this paper are to establish the need for and demonstrate the feasibility of proceeding immediately with implementation of quiet structures. Quiet structures (also called "smart" structures) are those structural subsystems that maintain their figure or shape and resist disturbance vibrations through the use of active and/or passive damping and control systems. The design of such structural subsystems is interdisciplinary and requires extensive interaction between the structural designer and the control system designer.

Control/structure interaction of the highest order is at the very heart of quiet structures. Complex systems analysis is required to integrate and balance these disciplines. Many difficult challenges face us. For example, determining the proper balance between active and passive damping elements is a complex task. However, none of these challenges exceeds our present technological capabilities.

While much analytical work has been done on the control of flexible structures, demonstration of this technology is still lacking. Most of the planned demonstrations (e.g., COFS) focus specifically on the needs of Space Station and similar "space docks," rather than generic space platforms that can support precision pointing requirements for multiple, coaligned payloads. We should be proceeding at this time toward on-orbit demonstrations of quiet structures for generic platform applications.

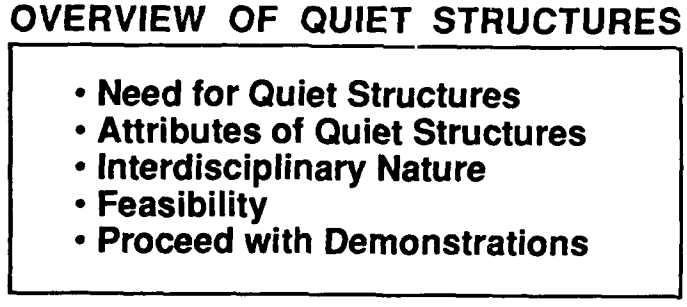

SPACE COMPETITION INCREASES

The need for technological improvements in spacecraft design was given increased emphasis recently by the report of the Sally Ride Panel on Space Initiatives (ref. 1). Further motivation was provided by the Soviets when they launched a 15- to 20-ton, "schoolbus-sized" Earth resources/ocean survey spacecraft in July 1987 (ref. 2). The Soviet platform is between 7 and 10 times heavier than the most advanced operational U.S. Earth resources vehicle, and its launch precedes our planned launch of a similar platform by at least 7 years.

The use of large space platforms for Earth observations is advantageous because it results in improved capabilities such as coincident observations, shared resources, serviceability and growth potential. However, large platform structures produce lower mechanical resonance frequencies and structural/dynamic interactions which create severe problems for precision pointed instruments.

The report of the Earth Observing Systems (Eos) Technology Working Group (ref. 3) identified an order of magnitude increase in the number and size of payload instruments planned for the Eos polar orbiting spacecraft. They further recognized that platforms of this size (approximately 60-ft long) can no longer be described or controlled as rigid bodies.

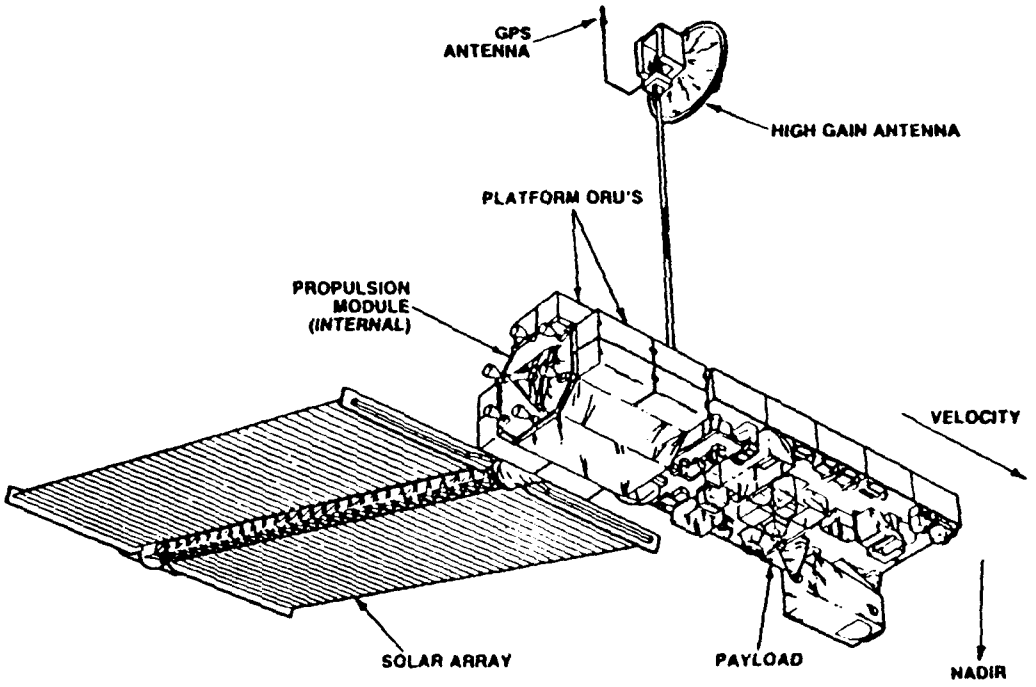

US Polar Platform Concept (ELV configuration)

CHALLENGES TO TRADITIONAL DESIGN APPROACHES

Traditionally, pointing stability has been achieved by using rigid structures that physically hold the instrument in a known attitude relative to the spacecraft's attitude determination system (ADS). Thus the conventional attitude control system (ACS) corrects only rigid body dynamic errors. Deflections of the structure between the instrument and the ADS were assumed to be small and constant. Limited bandwidth and centrally located actuators did not permit control of static deflections or structure-borne vibrations. The cutoff frequency was normally depressed below the resonant modes of the structure.

This approach will not work for future, larger platform structures required by the larger instrument payloads. Spacecraft structures would grow exponentially in mass if the same constraints of deflection were placed on larger platforms. Thus, launch weight constraints preclude the use of such design approaches for future platforms. Additional rigidity in the structure does not reduce distortion due to thermal gradients nor vibration amplitudes if not damped. In fact, it may impede the operation of controllers used to reduce static offsets.

While traditional ACS are perfectly capable of handling the external disturbances produced by the space environment, they are not able to control higher frequency modes produced by onboard disturbances. These disturbances lie in the range between the ACS cutoff (approximately 0.1 Hz) and the region where intrinsic structural damping becomes effective (approximately 100 Hz). Over time, their energy becomes concentrated in a large number of structure resonant modes. Damping can reduce their effect by an order of magnitude. Passive techniques, effective at higher frequencies, become increasingly ineffective at lower frequencies where active control is needed.

TRADITIONAL SPACECRAFT DESIGN APPROACHES ARE BEING OUTPACED BY ADVANCES IN FUTURE POINTING REQUIREMENTS

- **Static deflections are not presently measured**
- **Structural vibrations are outside the ACS bandwidth and cannot be controlled by centrally located ACS actuators**

A/N 8260/MD65.14

SHORTCOMINGS OF FLEXIBLE SPACECRAFT STRUCTURES

In the past, spacecraft structures were designed for strength, in order to survive the launch environment. Future platforms are expected to be larger (approximately the length of the shuttle bay) and will most likely be designed primarily for the operational environment. Designing for this more benign environment will result in significant weight savings. To accomplish this, however, loads from the heavier instruments must be supported directly (i.e., structurally connected to the STS tie points with releasable fittings). A structure of this size will be flexible to a marked degree.

Flexibility in large spacecraft structures creates some significant problems in structural behavior and resultant pointing capabilities. For example:

- Alignment measurements made prior to launch in one "g" do not accurately reflect the zero-"g" shape of the structure.
- Distortions and deflections will occur due to inertial and thermal effects, resulting in pointing accuracy degradation.
- Flexible structures have lower-frequency mechanical resonances; therefore, instruments and other subsystems can more easily excite the structure and thereby disturb instruments' pointing. These effects are compounded by resonant behavior.

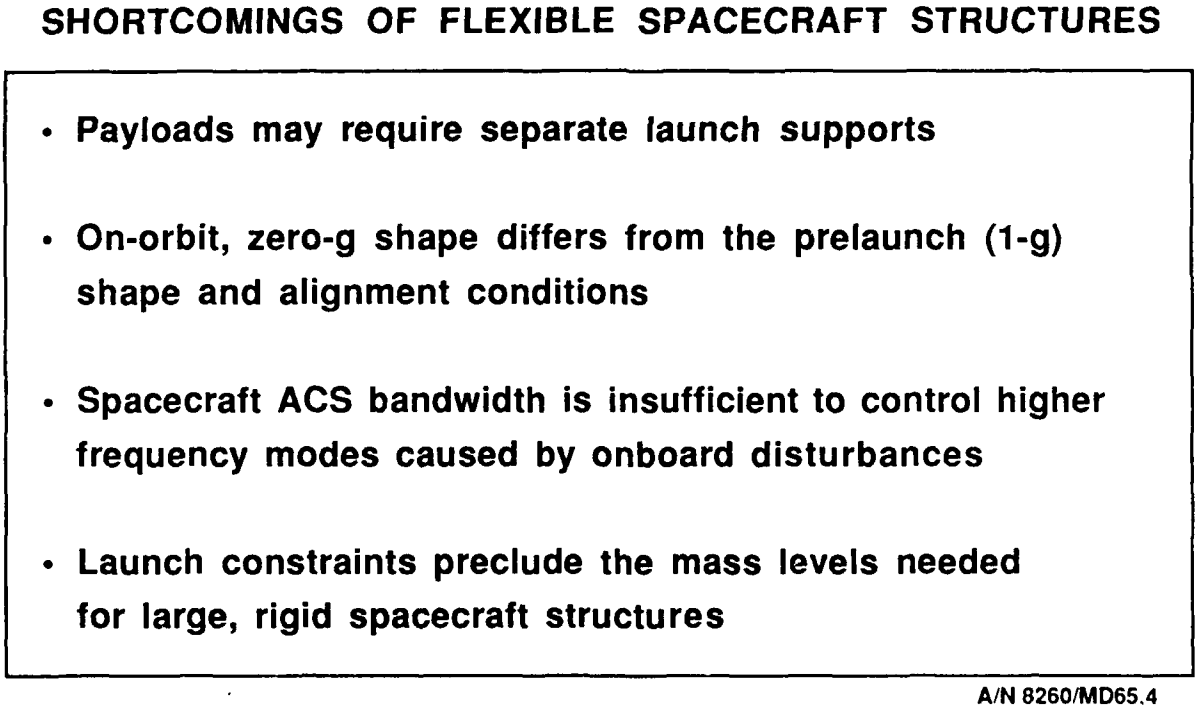

APPROACHES TO DISTURBANCE COMPENSATION

Control systems for inertially pointed instruments must account for and remove the effects of orbital motion and other attitude variations. They must also counteract the effects of base motion disturbances on the instrument's pointing capability. The control system relies on the ADS for reference data and assumes no structural distortion between the instrument and the ADS.

Pointing stability can be achieved in one of several ways:

1) By imposing on each instrument the requirement for image motion compensation and isolation

2) By imposing strict momentum and vibration limits on each active subsystem element and instrument

3) By allowing for large data flows and ground processing loads to correlate data and remove jitter

These approaches are all expansive, redundant, and custom-tailored solutions to the disturbance compensation problem. A better approach is the use of active and/or passive structural control of the platform structure on a systems level to counteract disturbances and prevent structural distortion. This approach appears to be less complex and less costly, and will be increasingly superior as platforms get larger and as the number of pointed instruments increases.

The systems approach for structural control offers the additional benefit of accommodating growth with minimum cost. Existing instruments will eventually be replaced by improved versions or by different ones as mission requirements change. Recognizing that these long-life, flexible platforms must accommodate growth needs, those that rely on fixed system dynamics would be less amenable to such changes.

ALTERNATIVES

- **Impose on each instrument the requirement of image motion compensation and isolation**
- **Impose strict momentum and vibration limits on each active subsystem element and instrument**
- **Anticipate large data flows and ground processing loads to correlate data and remove jitter**

These are all expansive, redundant, and custom solutions, compared to resolving the problem on a systems basis

A/N 8260/MD65.16

PROGRESS TOWARD QUIET STRUCTURES

Fortunately, the incompatibilities between the higher-resolution prospects for larger mirrors and antennas and the flexibility inherent in large-scale lightweight structures were recognized early. Research efforts are making significant strides in resolving these conflicts. They are going beyond the individual instrument isolation and image motion compensation techniques to address the issue on a systems level, i.e., to make large platforms behave like the stable observing platform we would like to see. Investigations have proceeded along many fronts with good progress in the analytical, simulation, and modeling efforts being reported annually at VPI, Waterloo, SPIE, and these CSI conferences.

Precision pointing is a generic spacecraft need shared by many types of payloads, including scientific payloads, applications missions (such as imaging), military instruments for reconnaissance and targeting, and by future communication systems as frequencies move into the optical regime. Space is often viewed as the quietest observing post. This perception is a valid one until we complicate the spacecraft with devices that communicate, collect power, and control the platform, in addition to the mechanical complexity of facility-class instruments.

Recent progress toward quiet structures has been achieved through recognition of the following inevitable spacecraft needs:

- Larger platforms which result in lower resonant frequencies and greater structural deflections
- Larger, more complex payloads resulting in greater disturbances and the need for growth accommodation
- More advanced instruments that possess higher angular sensitivity and increase coalignment requirements

PROGRESS TOWARD QUIET STRUCTURES

Larger platforms	**= Lower frequencies, greater deflections**
Varied payloads	**= More disturbances, growth is planned**
Advanced instruments	**= Higher angle sensitivity, more coalignment requirements**

A/N 8260/MD65.5

TIME TO PROCEED WITH DEMONSTRATIONS

Extensive investigations (both theoretical and experimental) have been conducted recently at various government, industrial, and university laboratories, all seeking ways to implement shape measurement, control, and attenuation of structural dynamic modes of vibration. Progress in the related technologies of semiconductor lasers, low power fast digital processors, a variety of actuator techniques, and composite materials afford practical means to implement a new generation of spacecraft.

It is now time to build and fly a spacecraft representative of the next generation of smart structures. All of the needed technologies have been investigated, evaluated, and shown (at least analytically) to be feasible. The next step toward implementation should be to demonstrate this technology conclusively and collect quantifiable cost and performance data through detailed, realistic simulation followed by on-orbit, full-scale demonstration. The remainder of this paper discusses the features and attributes which such a spacecraft can be expected to possess.

Active structural control techniques are ready to meet the needs of next generation observing platforms

A/N 8260/MD65.6

INTEGRATED SYSTEMS DESIGN

It is important to recognize the interdisciplinary nature of the proposed approach to next-generation spacecraft structures. The integrated, cooperative efforts of materials, structures, controls, and other design areas will be needed to reach an optimal solution. Systems engineering support will be required to accurately evaluate the various approaches against mission requirements and to achieve the best overall solution in terms of mission function.

The next generation of spacecraft can greatly enhance the capability of scientific and application observations. These new observing platforms will not meet their expected potential unless the characteristics inherent in their growth (in both physical size and complexity) are recognized and addressed early in the design process.

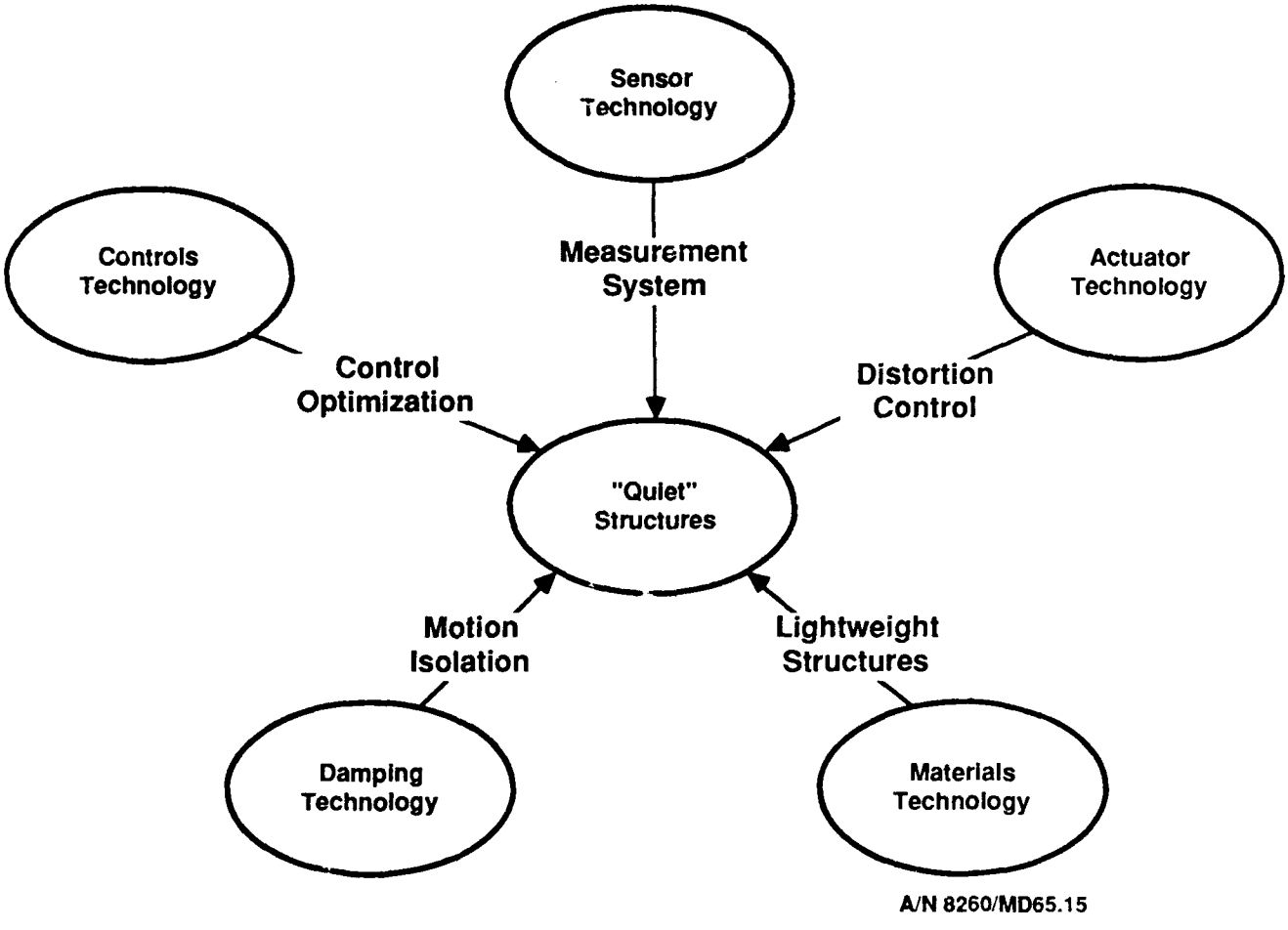

NATURE OF ON-ORBIT DISTURBANCES

Even though the external environment is relatively benign, the platform structure has imposed on it many sources of vibrational excitation. These stem from active onboard systems such as steerable antennas, solar array drives, and even the attitude control system itself. In addition to spacecraft support systems, larger and more complex payload/instrument complements will typically include scanners, active mechanical coolers, filter wheels and doors, and high-torque fine pointing systems.

The disturbances span a broad range of frequencies, well beyond the control bandwidth of the attitude control system, up to frequencies as high as 100 Hz. At higher frequencies, disturbances are attributable primarily to mechanical and thermal subsystems. At the lower frequencies, static distortions of the structure are produced by the on-orbit changes to tne prelaunch (one "g") shape of the structure and by orbital changes in thermal loads. Pre-launch alignment measurements, no matter how carefully made, cannot remove these sources of error. Once in orbit, changing thermal conditions can produce significant deflections as a spacecraft goes from sunlight to darkness and back.

Measurements of the dynamic behavior of spacecraft on-orbit have been reported by Sudey and Schulman (ref. 5). Similar on-orbit studies of manned vehicles (ref. 6) have been made on the Shuttle orbiter. In both cases, despite obvious differences in the sources and magnitudes of the disturbances, a broad spectrum of vibration clearly existed which affected pointing accuracy and "g" sensitive experiments.

The response of the platform structure to these disturbance sources is predominantly determined by the degree of damping. The momentary effects of impact, such as a door closure, can persist over an extended period of time and generate vibrations at any frequency at which an undamped structural resonance is found. Small repetitive disturbances, such as those that are generated by stepper motors, over time can cause large amplitude vibrations if the energy is not removed by damping.

Typical Spacecraft Disturbance Factors

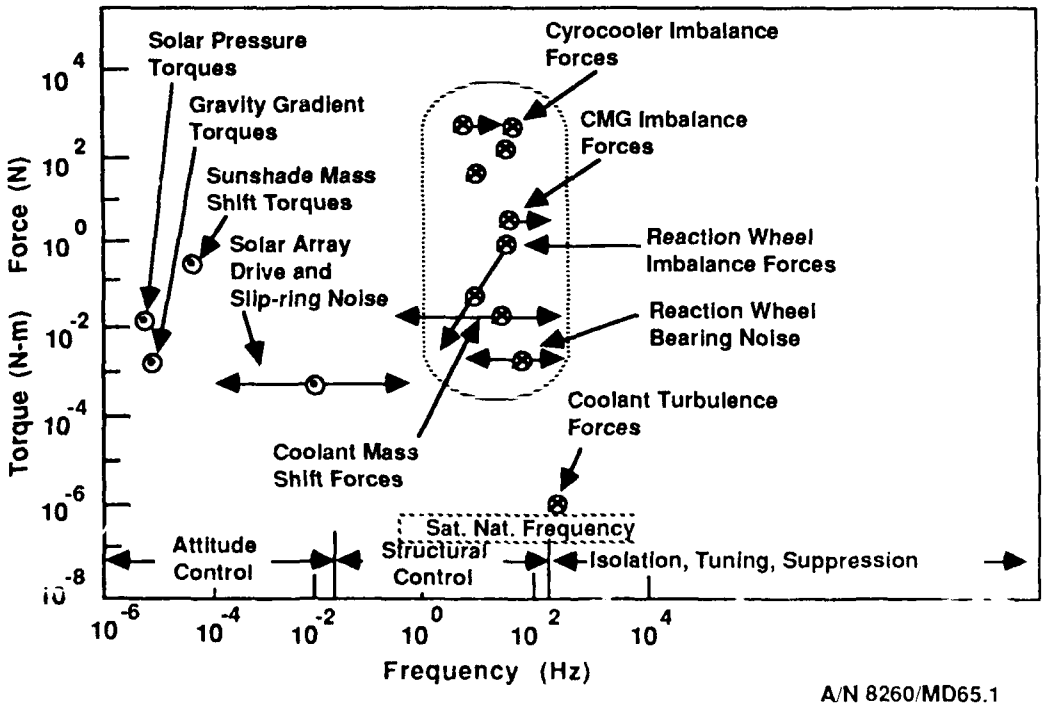

A/N 8260/MD65.1

ATTRIBUTES OF QUIET STRUCTURES

The quiet structure system must provide both distortion control (low frequency shape control) and dynamic control (higher frequency vibration isolation) to accommodate the wide range of disturbance frequencies due to a variety of sources. The essential elements of a quiet structure system must have sufficient dynamic range to satisfy performance requirements over the entire spectrum of disturbance frequencies and amplitudes. The functional attributes of quiet structures are listed below, viewed in terms of both distortion control and dynamic control.

The essential elements of quiet structures include alignment sensors, actuators, structural design concepts, advanced materials, enhanced simulation techniques, advanced algorithm development, and state-of-the-art processor capabilities. Each of these technology areas is vital to the successful implementation of a quiet structure system. The recent progress described in the following summary reports supports our recommendation to proceed with on-orbit demonstration of quiet structure systems.

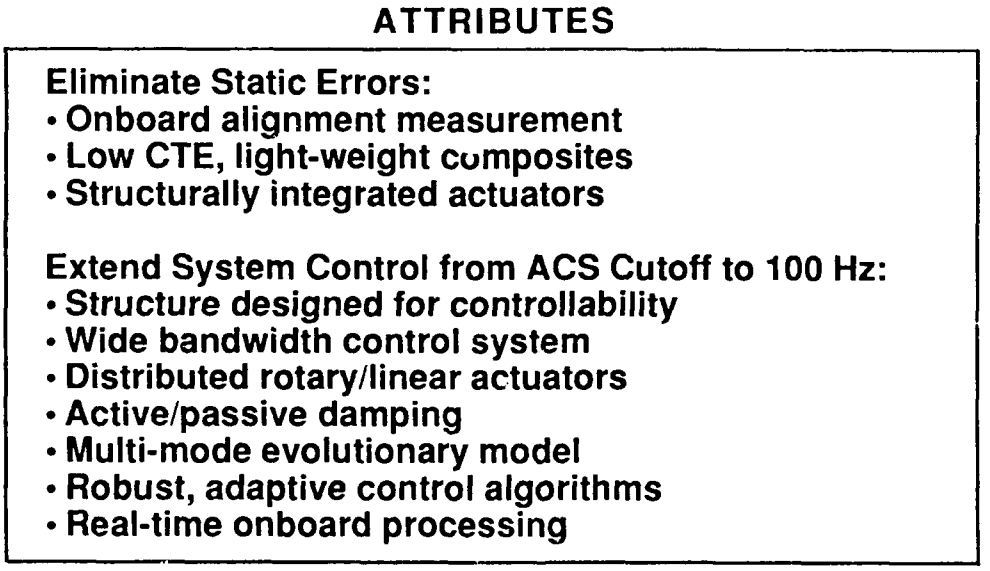

SENSORS

A wide variety of sensors is available to measure the predicted vibration levels. The primary problem in selecting a sensor is the wide dynamic range which must be encompassed. Deflections can range from a fraction of an inch down to a microinch, and "g" levels are expected to vary from one "g" to a micro "g". To accommodate this entire dynamic range, more than one type of sensor may be required.

Optical sensors are capable of resolving the smallest expected displacements, as demonstrated by Kollodge and Pace (ref. 7), Denner (ref. 8), and Burkehalter and Gloeckner (ref. 9). As a point of reference, Kollodge and Pace defined optical sensors based on charge-coupled device (CCD) technology with the capability of measuring angular misalignments of one-tenth arcsecond with update rates of 1 KHz for each of 100 separate targets. This update rate is sufficient to support active control of a platform structure with disturbances up to 150 Hz.

Piezo-electric and electrodynamic sensors become more viable at higher displacement levels. The sensors also have the advantage of being able to simultaneously extract energy (i.e., provide damping) from the system and provide output signals that are directly proportional to the rate of displacement change.

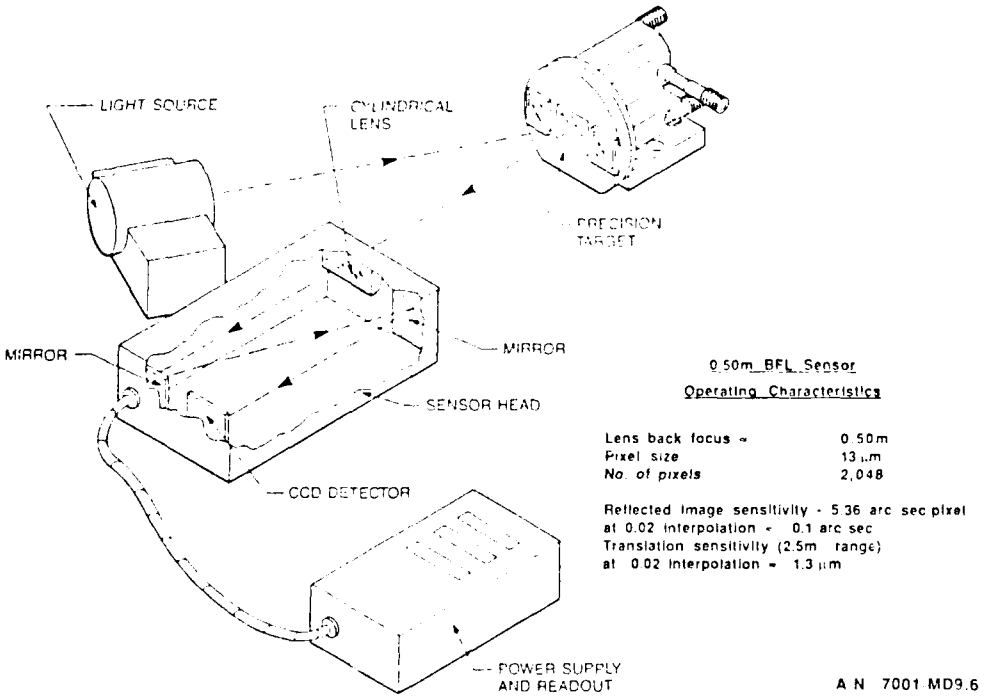

ACTUATORS

If a mass can be made to move at 90 degrees phase-shifted with respect to its point of attachment, energy will be extracted from the structure and resonant build-up of the amplitude will be prevented. This would appear to be a relatively straightforward solution were it not for the fact that vibrations occur simultaneously in all six degrees of freedom and the vibration absorber must not respond to cross-axis vibration in a resonant manner. In addition, the suspension must be designed with a minimum of stiction and hysteresis or its behavior will become nonlinear and lack sensitivity at low levels. The fact that it can both sense and control vibration makes the electrodynamic actuator an attractive localized control element (ref. 10).

The location of both the sensor and actuator is critical to their effectiveness (ref. 11). This ideal location for maximum effectiveness depends on the modal frequency to be controlled. Because broad-band damping is required, a nodal point for one frequency may be an anti-node at another frequency. This situation may be resolved if the actuator is capable of both rotary and linear motion, because an anti-node for translation is a node for rotation (ref. 12). A pair of rotary devices with unbalanced rotors can be controlled to produce both linear forces and torquing moments. The characteristic performance of each actuator can be described in terms of its response versus amplitude and frequency, the power required, saturation levels of amplitude and force, and "breakaway" or minimum response thresholds.

The most promising candidate for structural distortion control is the piezo-electric actuator. A key virtue of the piezo-electric technique is its high electrical impedance. This equates to low power consumption when their primary function is to adjust and maintain a fixed displacement. Piezo-electrics are available in both polymeric and ceramic form, the former are very light weight. Research on actuators of this type has been conducted by Crowley (ref. 13) at MIT, by Baz (ref. 14) at CUA, and by Fanson and Chen at JPL as well as other locations.

Actuators

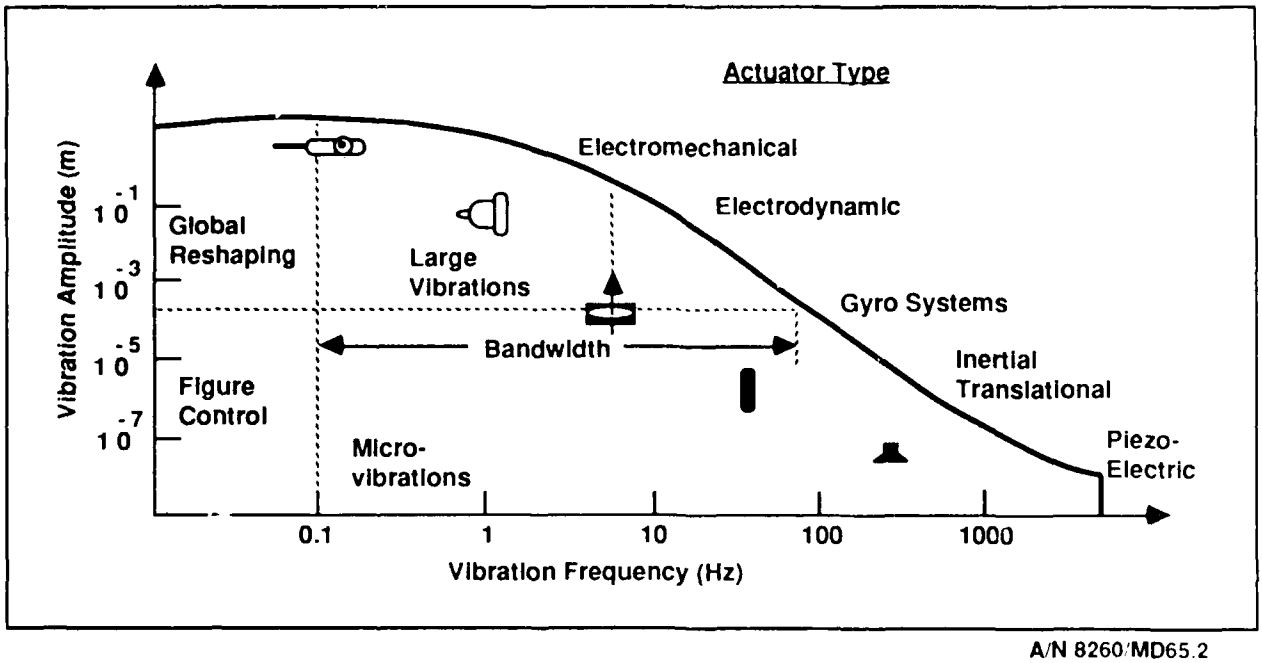

A/N 8260/MD65.2

STRUCTURE DESIGN

Ideally, the structure should be made from materials with high intrinsic damping. This, however, is inconsistent with the objective of lightweight, rigid, dimensionally stable material. The use of composites offer some improvement over metal structures; however, in the microstrain region, damping ratios of one hundredth are to be expected. This implies high transmissibility and resonant amplification with the vibrational energy focused in many resonant peaks over a broad range of frequencies. Some means of introducing active damping must be used to make the platform the stable observing base which is desired.

Given the ability to measure and correct for post-injection structural distortions, the structural designer's task is greatly simplified. The advanced composite materials now available can provide a very substantial weight savings for the structure. Geodesic designs offer versatility of shape, redundant load carrying elements, and a high degree of rigidity.

The need for an interdisciplinary team to successfully implement future structural designs is perhaps best illustrated by the need to integrate the structural elements of quiet structure systems. For distortion control to be effective, the actuators must be integrated into the structure itself. If piezo-electric or electrodynamic sensors are used, these also must be integrated into the structural elements. In a similar fashion, the optical alignment system must be considered in the initial layout stage of structural design to assure that observable views of critical points of structure are preserved.

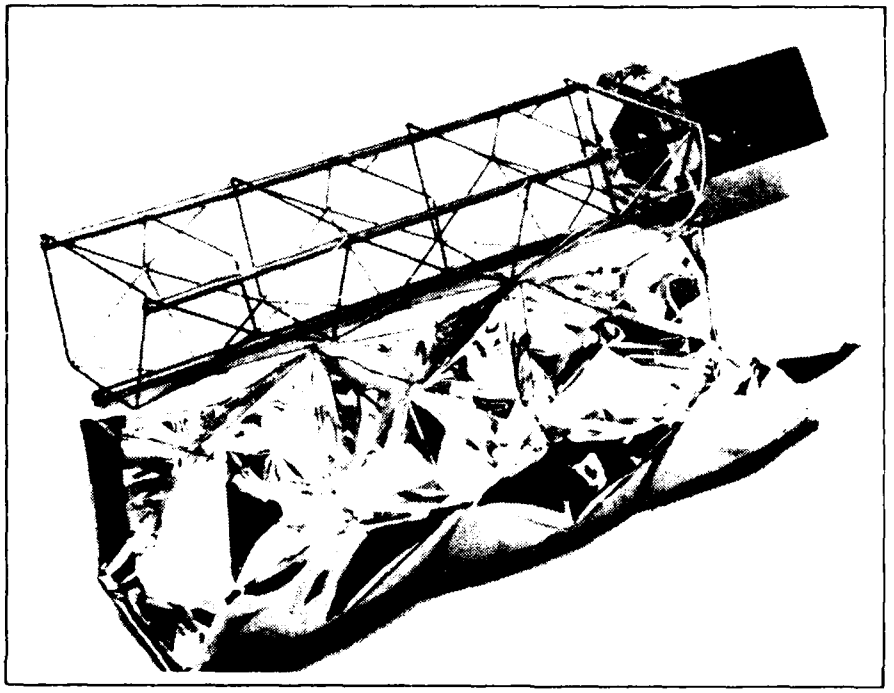

ADVANCED MATERIALS

Early structures made of composites were inhibited by the need for machined metal fittings to produce satisfactory joints. In addition to the weight and cost impact, the low coefficient of thermal expansion (CTE) of the composite element was often lost when combined with high CTE metallic fittings. Recent advances in thermoplastic forming techniques will apparently allow consideration of clamped lap joints and full-length continuous fiber elements. These features will contribute to the design of large-scale structures with near-zero temperature coefficients.

Resin matrix composites have been used in structural applications requiring low weight, high strength, high stiffness, and low CTE. However, these materials exhibited shortcomings in the form of moisture susceptibility and undesired outgassing. Advanced graphite fiber-reinforced glass matrix composites appear to offer the advantages of resin matrix composites without the above-mentioned shortcomings and, in addition, offer the desired thermoplastic properties.

The nature of composite material fabrication permits us to tailor the structural properties by varying the choice of fiber and matrix material, and by adjusting other factors such as fiber volume, fiber orientation, and fiber form. The thermoplastic property means it can be heat formed after initial fabrication and hot pressed into a variety of shapes. Recent NASA-sponsored investigations conducted by United Technologies Research Center (ref. 16) have evaluated composite formulations, fabrication techniques, and joint designs, all with promising results.

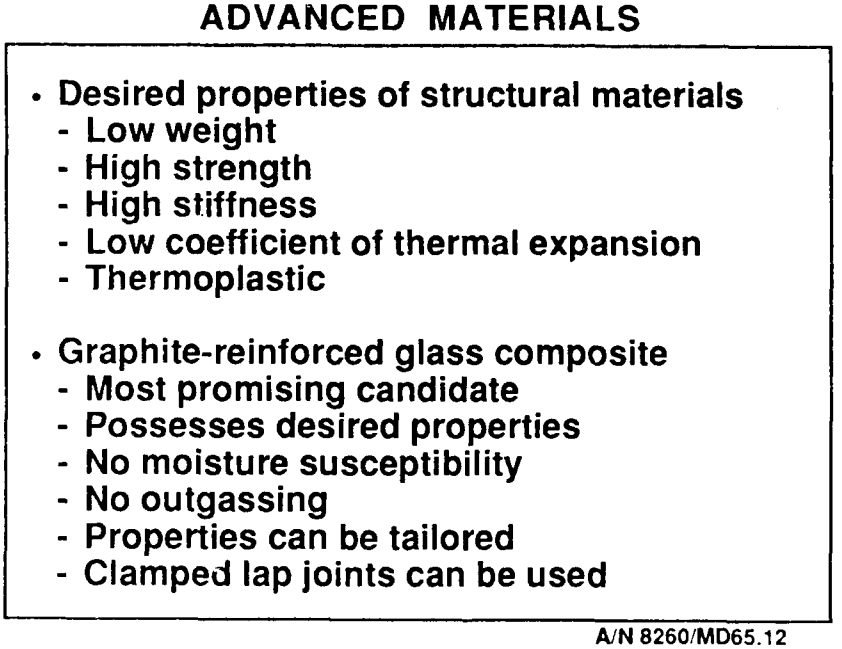

SIMULATIONS

Based on the work of L. Meierovitch (ref. 17) at Virginia Tech, modal analysis by computerized simulation can determine the characteristic response of a projected structure. Baz has extended this work (ref. 18) to include the effects of uncontrolled higher order modes. The behavior of complex structures with a very large number of degrees of freedom can be simulated and the response with a network of active and passive dynamic control devices can be evaluated. This provides a tool with which to minimize the number of control devices by selective location and orientation. The model evolves concurrently as specific payload elements are selected, and provides specific information about the stability and motion spectrum of the instrument mounting surfaces. Thus, the effects of platform dynamics can be evaluated and compared to the desired pointing accuracy of the instrument. In this manner, operational performance can be verified prior to launch. It can form the basis for flight software which will contain a model of the platform, updatable as growth additions are made and payload changeouts occur. In all likelihood, the system will be adaptive. By automatically adjusting parameters to minimize measured disturbances, it will save power and provide fault tolerance. A key benefit is that such a system does not require perfect alignment of the platform and its payload complement prior to launch.

SIMULATIONS

- Modal analysis of proposed structures
  - Accommodates very large number of states
  - Incorporates network of active and passive control devices
  - Includes effects of uncontrolled higher order modes
- Structural design tool
  - Minimizes number of control devices
  - Used in location selection
  - Used in orientation determination
  - Evaluates platform stability and motion spectrum
  - Permits payload performance verification

A/N 8260/MD65.11

CONTROL ALGORITHMS

Control system modeling relies on accurate prediction of the flight dynamic conditions to be experienced by the spacecraft. Unfortunately, modal frequencies, mode shapes, and other dynamic behavior may deviate from design values by margins of 100 percent or more (ref. 19). Inability to reliably predict flight dynamics conditions may seriously degrade the mission.

The goal is to develop robust, adaptive control systems for large flexible structures. Robust control provides control laws that are insensitive to large parameter variations. Adaptive control provides the capability to identify these parameters and make necessary adjustments within the control system. Adaptive control also permits system modification or growth without the need to completely revamp the control system design.

Baz (ref. 20) has been investigating active control schemes and the influence of sensor and actuator locations on controllability. He has developed active control algorithms for computing optimal controller gains and optimal placement of a minimum number of actuators to effect vibration control within the structure. He has also addressed the spillover problem in which unwanted excitation of other structural modes occurs as a direct result of controller or sensor behavior.

Other related algorithm development efforts deal with adaptation of the dynamic equations of motion to the geodesic structure; the optimal force and stroke characteristics of actuators and sensors; and the interaction of passive damping in an actively controlled structure.

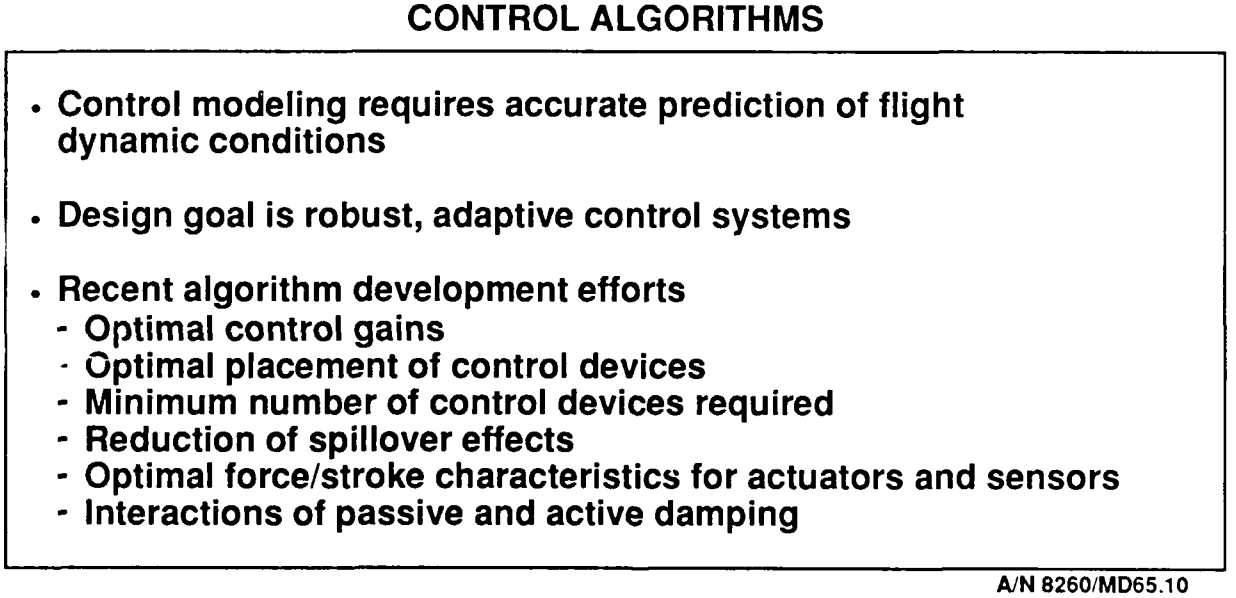

PROCESSORS

Active control of a large platform will require a large array of physically distributed actuators. The need for coordinated action and the advantages of localized control must be evaluated before partitioning of the controller can be defined for distortion control. However, for real-time, multi-axis vibration control, it is evident that the signal processing requirements will require the closing of numerous loops locally. The demands of growth and fault-tolerance warrant consideration of all digital control. This opens up dramatic new possibilities of adaptive techniques which will permit standardization of hardware while accommodating actual on-orbit conditions without hardware changes.

Only recently, precision multi-axis, real-time control was beyond the capability of microcontrollers. A six-axis, 10-Hz controller (circa. 1978) required a multiple-chip bit-slice processor approach on three boards using 40W. This same system is now available in CMOS with power requirements comparable to analog loops. Computational speed has increased by one hundredfold since that time. A number of digital signal processor (DSP) chips originally designed for image processing applications are now found to be ideal for real-time control. These are capable of tens of millions of floating point operations per second and easily able to perform many channel digital control algorithms at electromechanical frequencies. Gallium arsenide offers another factor of ten improvement.

At this pace of development, digital control hardware will be available to implement the control requirements of large complex structures. Coordination of an array of actuators, robust control, fault tolerance, and sufficient flexibility to accommodate growth will require diligent efforts to make effective use of the hardware becoming available.

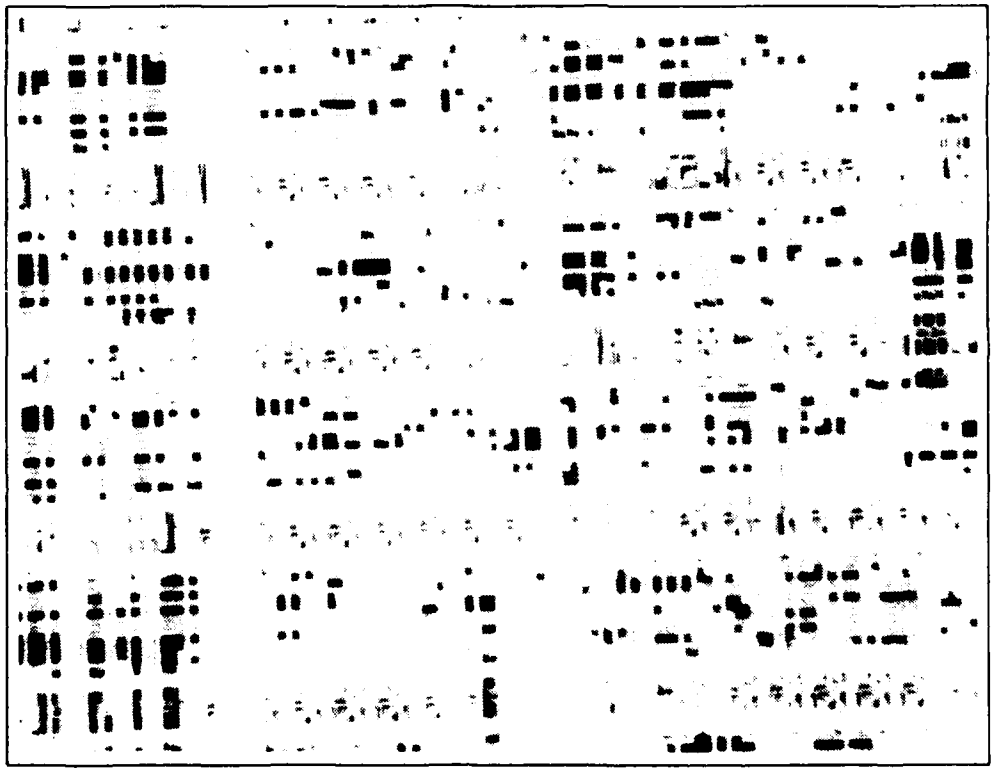

SUMMARY

As on-orbit payloads get larger and heavier, it is evident that traditional, rigid platform construction methods are no longer adequate to meet increased requirements for pointing precision. It is also becoming increasingly clear that some form of active and passive structural control system will be required to provide the necessary degree of distortion control and dynamic control.

Theoretically, the degree of pointing precision achievable is limited only by the ability to sense and to measure (ref. 21). Advancements in the development of improved sensors and actuators have been both impressive and encouraging. Added to the progress exhibited in the areas of materials, algorithm development, modeling, and adaptive processing, there is now confidence that active control systems for spaceborne pointing platforms are both feasible and necessary.

Now is the time to begin the vital demonstration tasks needed to verify these concepts in space. The technology is sufficiently mature in all essential areas. If begun now, quiet structures could be developed early enough to use on the Earth Observing System and other observation platforms of the 1990s. Now is the time to design and build a platform that is truly a quiet, stable observing base for future mission operations.

SUMMARY

Now is the time to design and build a platform which is truly a quiet, stable observing base for future mission operations

A/N 8260/MD65.7

REFERENCES

1. Covault, Craig: Ride Panel Will Urge Lunar Base, Earth Science As New Space Goals. AW&ST, vol. 127, no. 2, July 13, 1987, pp. 16-18.

2. Covault, Craig: Soviets Launch Massive Earth Survey Platform. AW&ST, vol. 127, no. 5, August 3, 1987, pp. 27-28.

3. Report on Technology For The Eos Polar Orbiting Mission (Draft). Eos Technology Working Group, NASA, March 1986.

4. Studer, P.; Baz, A.; Sharma, R.: Actuators For Actively Controlled Space Structures. SPIE Acquisition, Tracking, and Pointing Conference, vol. 641, 1986.

5. Sudey, J.; Schulman, J.R.: In Orbit Measurements of LANDSAT-4, Thematic Mapper Dynamic Disturbances. ACTA Astronautica, vol. 12, no. 7/8, pp. 485-503, 1985.

6. Davis, H.: Payload Accommodations Studies. Ball Aerospace Systems Division, IR&D Project 4828, Final Report, January 1987.

7. Kollodge, J.; Pace, D.: System Analysis of Onboard Instrument Alignment and Coalignment. BASD Report F86-03, Ball Aerospace Systems Division, 1 March 1986.

8. Denner, William: Electro-Optical Spin Measurement System Study. Report No. FT-07-741-86-RP-183, Grumman Aerospace Corporation, 17 January 1986.

9. Burkhalter, James; Gloeckner, P.: An Alignment Sensor For Adaptive Optics. Final Report, Coleman Research Corporation, April 1987.

10. Bronowicki, Allen J.; Lukich, Michael S.; Kuritz, Steven P.: Application of Physical Parameter Identification to Finite Element Models. NASA/DOD Control/Structures Interaction Technology Conference (Norfolk, VA), November 1986.

11. Burdisso, R.; Haftka, R.: Optimal Location of Actuators For Correcting Distortions Due to Manufacturing Errors in Large Truss Structures. Sixth VPI&SU/AIAA Symposium on Dynamics and Control of Large Structures (Blacksburg, VA), 29 June - 1 July 1987.

12. Damaren, C.J.; D'Eleuterio, M.T.: Optimal Control of Large Flexible Space Structures Using Distributed Gyricity. Sixth VPI&SU/AIAA Symposium on Dynamics and Control of Large Structures (Blacksburg, VA), 29 June - 1 July 1987.

13. Crowley, E.F.; deLuis, J.: Use of Piezo-Ceramics as Distributed Actuators in Large Space Structure. Proceedings of the 26th Structures, Dynamics and Materials Conference, AIAA (Orlando, FL), April 1985.

14. Baz, A.; Poh, S.: Optimum Vibration Control of Flexible Beams by Piezo-Electric Actuators. NASA Technical Report No. NTIS HC A04/MF A01, March 1987.

15. Fanson, J.L.; Chen, J.C.: Structural Control by the Use of Piezo-Electric Active Members. NASA/DOD Control/Structures Interaction Technology Conference (Norfolk, VA), November 1986.

16. Studer, P.: Advanced Earth-Orbital Spacecraft Systems Technology. NASA/OAST, Status Report, RTOP 506-49-21, pp. 39-43, May 1987.

17. Meierovitch, L.; Baruh, H.; Oz, H.: Comparison of Control Techniques For Large Flexible Systems. Journal of Guidance & Control, vol. 6, no. 4, pp. 302-310, 1983.

18. Baz, A.; Poh, S.; Studer, P.: Modified Independent Modal Space Control Method For Active Control of Flexible Systems. Sixth VIP&SU/AIAA Symposium on Dynamics and Control of Large Structures (Blacksburg, VA), 29 June - 1 July 1987.

19. Mackison, D.: Model Reference Adaptive Control of a Flexible Space Structure. Unpublished paper. October, 1986.

20. Studer, P.: Advanced Earth-Orbital Spacecraft Systems Technology. NASA/OAST, Status Report, RTOP 506-49-21, pp. 46-55 and pp. 60-69, May 1987.

A FACILITY FOR CONTROL STRUCTURE INTERACTION TECHNOLOGY VALIDATION

D. Eldred
H. Vivian

Jet Propulsion Laboratory
Pasadena, California

SECOND NASA/DOD CSI TECHNOLOGY CONFERENCE
COLORADO SPRINGS, COLORADO
NOVEMBER 17-19, 1987

INTRODUCTION

Extensive research has been conducted over the past decade in the methodologies associated with the control of large flexible space structures. Validation by means of experimental confirmation of performance estimates is an important part of this research. In recognition of this need, an advanced, general utility laboratory test structure has been developed which duplicates, to a reasonable extent in a gravity and atmospheric environment, many of the important characteristics of a large flexible space structure. These include having many low frequency modes, densely packed modes, low structural damping, and complex interactions among structural components.

The experiment structure was developed in conjunction with the development of a long-range technology demonstration plan to ensure that it would satisfy the validation needs of control technology research programs for five or more years. The technologies selected for initial demonstration include: dynamic control of a distributed parameter system; adaptive control of a system with poorly known parameters; static shape control; and parameter identification. Demonstration of a recently developed remote sensing device, SHAPES, was also adopted as a program objective.

This paper describes the experiment structure and the results of the dynamic control and adaptive control experiments.

EXPERIMENTAL VALIDATION OVERVIEW

- OBJECTIVE
  - DEVELOP A LABORATORY EXPERIMENT TO CONDUCT GROUND-BASED EVALUATION OF LARGE SPACE STRUCTURE CONTROL TECHNOLOGIES
- CANDIDATE TECHNOLOGIES
  - DISTRIBUTED PARAMETER SYSTEM CONTROL
  - AUTONOMOUS ADAPTIVE CONTROL
  - OPEN/CLOSED LOOP PARAMETER IDENTIFICATION
  - DISTURBANCE DETECTION AND TIME HISTORY IDENTIFICATION
  - STATIC FIGURE DETERMINATION AND CONTROL
  - SENSOR TECHNOLOGY (SHAPES)

Figure 1. Experimental Validation Overview

DEMONSTRATION SYSTEM

The experiment structure is shown below in Figure 2. The main component of the apparatus consists of a central hub to which 12 ribs are rigidly attached. The overall diameter of the structure is nearly 19 feet. Each rib is suspended by two levitators to prevent excessive sag from gravity. A levitator consists of a counterweight attached to the rib by a thin wire which passes over a low friction pulley. The ribs themselves are linked to one another by coupling wires, which incorporate compliant springs to maintain nearly constant tension. The hub is supported by flex-joint bearings in a gimbal arrangement, with the two pivot axes lying in the horizontal plane. A flexible boom hangs downward from the hub, and a weight is attached at its lower end.

The backup structure, which is also visible in the figure, is a truss assembly whose function is to provide a rigid base on which to mount the levitators and the inner gimbal ring.

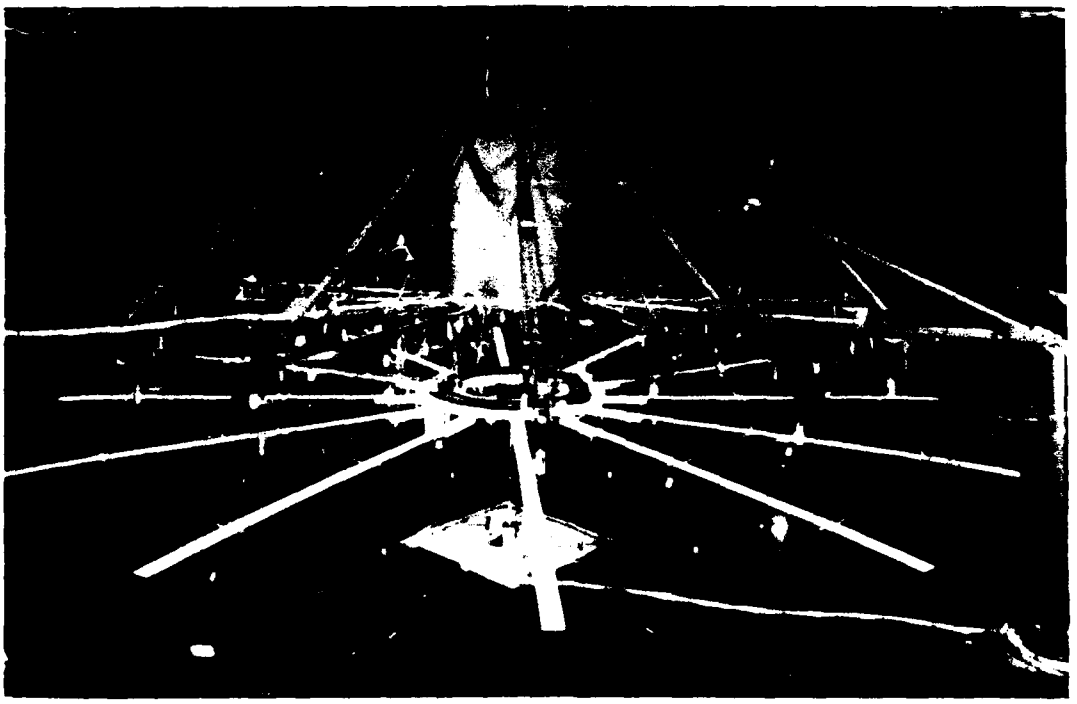

Figure 2. Experiment Structure

SENSORS AND ACTUATORS

There are a total of 30 sensors and 14 actuators mounted on the experiment structure, not including the SHAPES sensor which is described later. Their locations are shown below in Figure 3.

Actuation is as follows. Each rib can be forced individually by a rib-root actuator. These are custom-made permanent magnet devices which have a solenoid design. These actuators react against the hub by pushing against a lever arm which is rigidly fixed to the hub. The hub can be torqued about its two gimbal axes by hub torquers. These are linear force actuators which act directly on the hub and react against the backup structure. They produce torque by virtue of the lever arm between the gimbal axes and the point where the force is applied. The hub torquers use a knife configuration in which a flat air core armature coil passes between the poles of a large permenent magnet. This configuration is required to obtain an adequate range of motion.

Sensing is as follows. First, all of the 24 levitators are equipped with incremental optical encoders which measure the relative angles of the levitator pulleys. These sensors thus provide, in an indirect manner, measurements of the vertical motion of the ribs at the levitator positions. Second, rotary variable differential transformers (RVDT's) are mounted at both of the hub gimbal bearings to provide hub angle measurements. And finally, four of the ribs are equipped with linear variable differential transformers (LVDT's) which provide measurements of the rib positions at locations collocated with rib-root actuators.

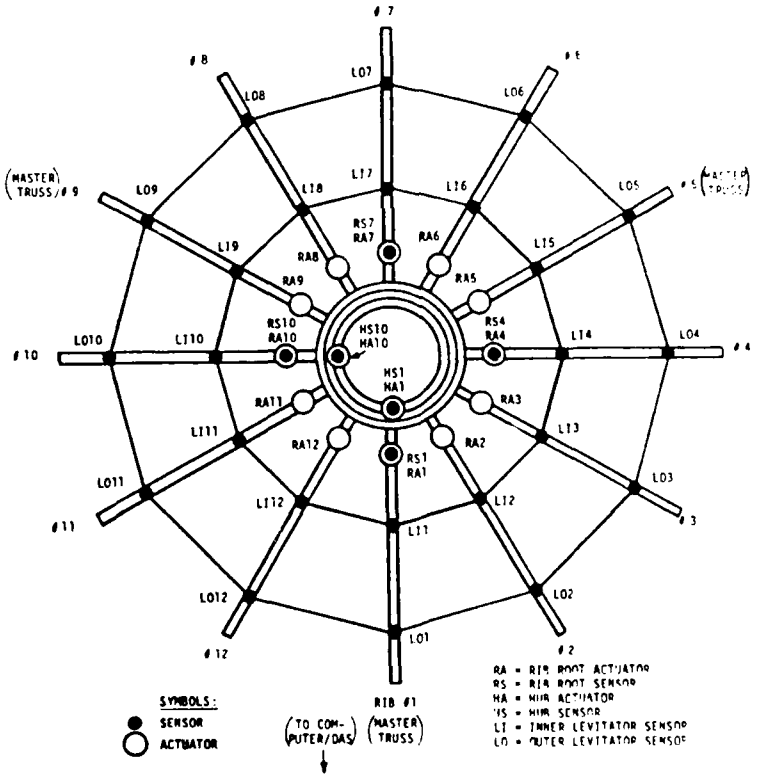

Figure 3. Sensor and Actuator Locations

SHAPES SENSOR

The Spatial, High-Accuracy, Position-Encoding Sensor (SHAPES) is an optoelectronic range sensor which is capable of simultaneously ranging multiple moving targets with sub-millimeter accuracy. SHAPES makes use of laser diodes, a streak tube camera, a charge coupled device (CCD) detector, and custom electronics to determine the time of flight of short optical pulses which are returned from retroreflector targets. In its present configuration, SHAPES is capable of obtaining and transmitting range data from 16 targets at a data update rate of 10 Hz.

Each rib of the experiment structure has 9 equally spaced holes drilled to accept the retroreflectors, which are corner cube reflectors. If a retroreflector is not used at a given location, a dummy weight is placed there instead so that the system dynamics are not changed. As shown in Figure 4, mirrors on the ground mounted in adjustable fixtures direct the optical paths of the laser diodes to the retroreflectors attached to the ribs.

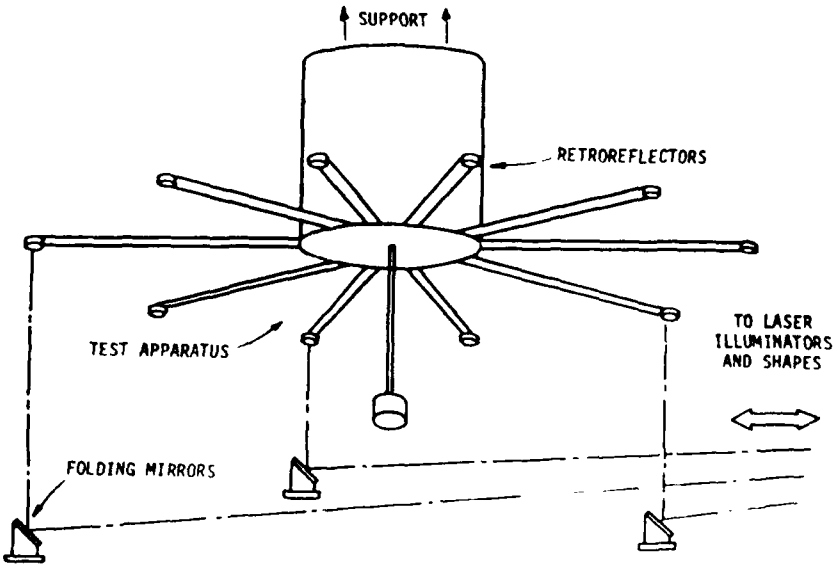

Figure 4. Optical Routing for SHAPES Sensor

COMPUTER HARDWARE AND SOFTWARE

A DEC VAXstation II computer system with 5 megabytes of memory and a floating point processor was selected for conducting the experiments because of its speed and software capabilities. Additional hardware includes a 71 megabyte hard disk, a cartridge tape system, a floppy disk drive, a bit-mapped video graphics monitor, and a high-resolution dot-matrix printer.

The system software provides the experimenters with a user-friendly menu-based interface for testing the system, conducting experiments, and processing data. By making appropriate selections, a user can choose and run an experiment, change parameters, select variables for real-time or off-line graphical display, and save experiment data for future analysis. It also provides the routines necessary for communicating with the sensors and actuators, maintaining correct timing, and reporting errors.

The majority of the system software is written in Ada. A main task executes a real-time loop, which includes all the functions which are time critical. These include the individual experiment algorithms, which are coded as FORTRAN subroutines. A secondary task, which is assigned a lower priority than the main task, handles all of the user input and output.

Figure 5. Computer system

DATA ACQUISITION SYSTEM

The Data Acquisition System (DAS) is a separate enclosure housing the power supplies and interface electronics for the sensors and actuators. These include the optical encoder cards for the levitators, the analog-to-digital interfaces for the LVDT's and RVDT's, and the power supplies and digital-to-analog interfaces for the actuators. Communication with the control computer is via a high-speed parallel interface. Upon receipt of a command sent by the computer, the DAS will either sample all of the sensors and pass these data back to the computer, or send appropriate drive signals to the actuators.

The DAS is based on a STD bus and uses an 8088 microprocessor to coordinate its actions. All subsystem electronics are assembled on boards that slide into card cages which are installed in a custom designed rack. Individual cables connect each sensor and actuator to the DAS. All cables and connectors are labeled to make an incorrect connection unlikely, and transducers of different type use incompatible connectors.

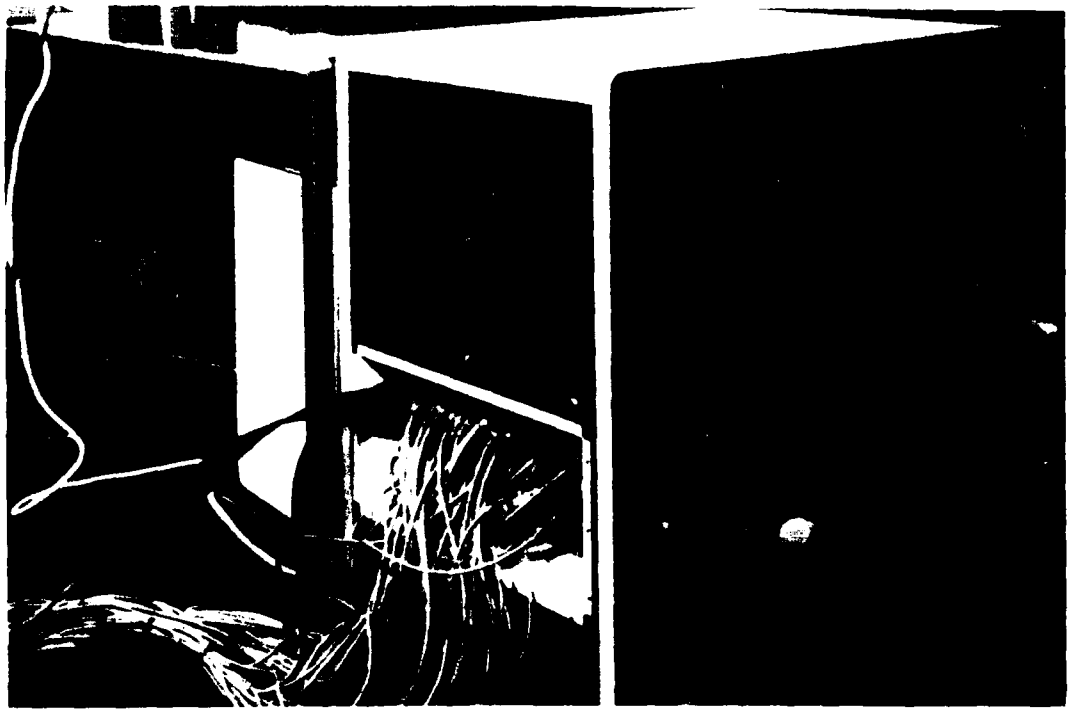

Figure 6. Data Acquisition System

SYSTEM MODEL

A finite element model using beam-type elements is used to obtain the normal modes of the system. The displacement and slope at each of 154 nodes constitute the 308 degrees of freedom. Once the mass and stiffness matrices are assembled, the normal modes are obtained by solving a generalized matrix eigenvalue problem.

Using the cyclic symmetry of the structure, it is possible to perform a transformation which reduces the order of the eigenvalue problem nearly twelve-fold. Furthermore, the matrices in the reduced order problem are tightly banded. A modified power method using Schmidt orthogonalization is used to solve the eigensystem because this algorithm can be coded to take advantage of the banded structure. The resulting eigenvalues are listed below in Figure 7. The significance of the variable k, the circular wave number for a mode, is discussed below.

Freq(Hz)	k	Freq(Hz)	k
0.091	1	2.577	1
0.091	1	2.682	1
0.210	0	4.656	0
0.253	2	4.658	2
0.253	2	4.658	2
0.290	3	4.660	3
0.290	3	4.660	3
0.322	4	4.661	4
0.322	4	4.661	4
0.344	5	4.662	5
0.344	5	4.662	5
0.351	6	4.663	6
0.616	1	4.858	1
0.628	1	4.897	1
1.517	0	9.474	0
1.533	2	9.474	2
1.533	2	9.474	2
1.550	3	9.474	3
1.550	3	9.474	3
1.566	4	9.474	4
1.566	4	9.474	4
1.578	5	9.475	5
1.578	5	9.475	5
1.583	6	9.475	6
1.685	1	9.822	1
1.687	1	9.822	1

Figure 7. Modal Frequencies

MODE SHAPES

The circular wave number k defines the angular dependence of a given mode. k can take on values from 0 to 6. Modes in which k = 0,2,3,4,5, or 6 are symmetric with respect to the reaction forces on the hub caused by the ribs, and hence neither the hub nor the boom participates in such modes. These are called the dish modes. For k = 2,3,4 or 5, the dish modes are two-fold degenerate.

When k=1, the reaction forces on the hub are assymetric, and hence both the hub and boom participate in such modes. These modes are called the boom-dish modes. These modes are not quite two-fold degenerate because of slight differences in the principal moments of inertia of the hub.

Figure 8 shows representative boom-dish and dish modes.

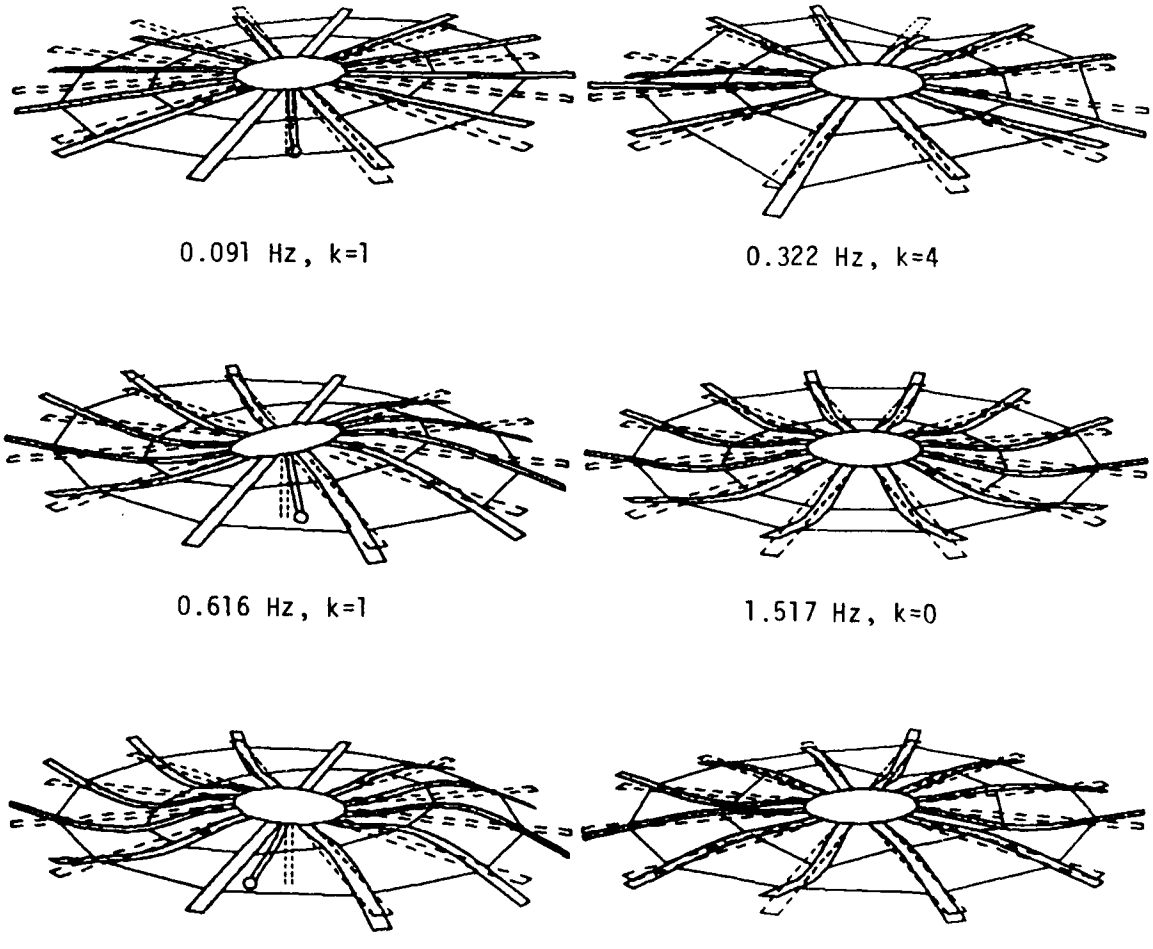

0.091 Hz, k=1

0.322 Hz, k=4

0.616 Hz, k=1

1.517 Hz, k=0

1.685 Hz, k=1

1.566 Hz, k=4

(a) Boom-dish modes

(b) Dish modes

Figure 8. Mode Shapes

DYNAMIC CONTROL EXPERIMENT

This experiment in the dynamic control of a distributed parameter system demonstrates the application of linear quadratic gaussian (LQG) design methodology to achieve transient regulation. Initially a low gain compensator based on the a priori model is implemented to establish a baseline performance level. Via manipulation of the LQG design parameters, the gain or bandwidth of this compensator is increased until the controller goes unstable. The model is subsequently improved using a least squares algorithm in the frequency domain. When the control process is repeated, improved transient response is seen. Finally, a robustness enhancement modification is applied to yield yet further improvement.

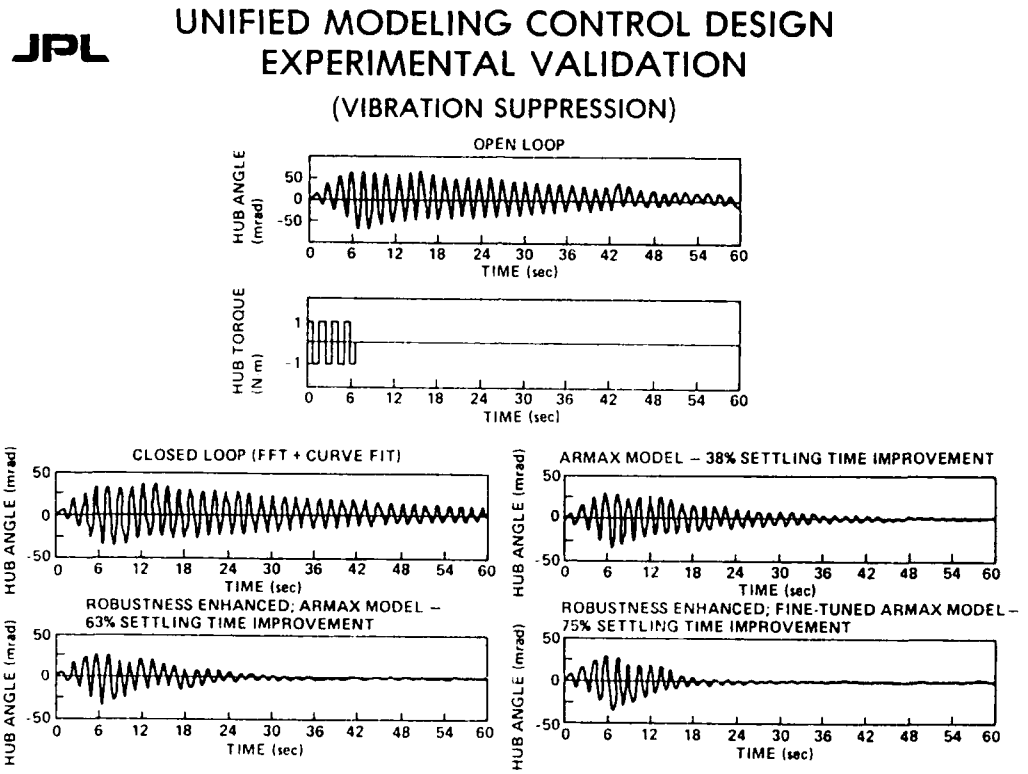

Figure 9. Dynamic Control Experiment

ADAPTIVE CONTROL EXPERIMENT

This experiment demonstrates autonomous Model Reference Adaptive Control (MRAC) methodology. First, a low-order reference model is specified which has a desired output. Then an algorithm utilizing adaptive rate and position feedback is designed which forces the system to follow this model.

The algorithm requires rate measurements, which are unavailable on the experiment structure. Instead, rate estimates are obtained from a state estimator and fed to the adaptive control algorithm. Sensor noise can create difficulties but these are reduced by the addition of a branch filter to the algorithm.

FY'87 ACCOMPLISHMENTS (CONT'D)
INITIAL DEFLECTION REGULATION EXPERIMENT

- PLANT OUTPUT TRACKED HIGHLY DAMPED REFERENCE MODEL OUTPUT AND CONVERGED RAPIDLY
- ACHIEVED 400% IMPROVEMENT OVER OPEN-LOOP SETTLING TIME

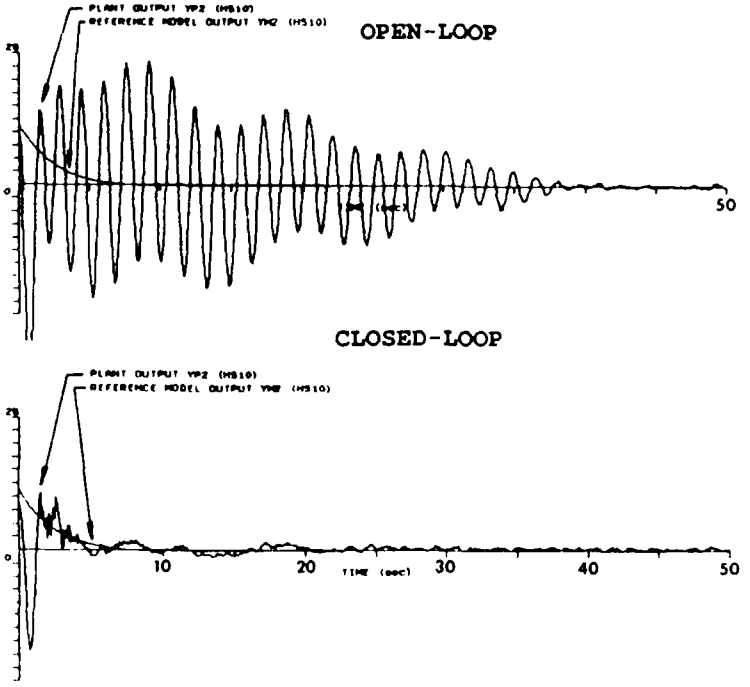

Figure 10. Adaptive Control Experiment

SUMMARY AND CONCLUSIONS

This paper describes a laboratory experiment which is being used to demonstrate technologies associated with the identification and control of large flexible space systems. The experiment structure is fully operational and has been used to conduct initial experiments in dynamic control, adaptive control, and static shape control. Future experiments will use more sensors and actuators and will estimate and control many more modes than the current experiments. Model integrity, algorithm organization and computation speed will become critical issues.

° SUMMARY

- EXPERIMENT IS FULLY OPERATIONAL
- INITIAL RESULTS HAVE BEEN OBTAINED
- FUTURE EXPERIMENTS WILL PRESENT A CHALLENGE

Figure 11. Summary

REFERENCES

1. Rodriguez, G. and R.E. Scheid, Jr., "An Integrated Approach to Modeling, Identification, Estimation and Control for Static Distributed Systems", Fourth IFAC Symposium on the Control of Distributed Parameter Systems, Los Angeles, CA, June 1986.

2. Bayard, D.S., C.C. Ih, and S.J. Wang, "Adaptive Control for Flexible Space Structures with Measurement Noise", Proc. of 1987 American Control Conference, June 10-12, 1987, Minneapolis, Minnesota.

3. Kwakernaak, H. and R. Sivan, Linear Optimal Control Systems, John Wiley, New York, 1972.

4. Eldred, D., Y. Yam, D. Boussalis and S.J. Wang, "Large Flexible Structure Control Technology Experiment and Facility Design", Fourth IFAC Symposium on Control of Distributed Parameter Systems, Los Angeles, CA, June 1986.

5. Gibson, J.S., D.L. Mingori, A. Adamian, and F. Jabbari, "Approximation of Optimal Infinite Dimensional Computations for Flexible Structures", Proc. of Workshop on Identification and Control of Flexible Space Structures, Jet Propulsion Laboratory Publication 85-29, April 1, 1985.

6. McLauchlan, J., W. Goss and E. Tubbs, "SHAPES: a Spatial High Accuracy, Position-Encoding Sensor for Space-System Control Applications", American Astronautical Society Publication 82-032, January 20, 1982.

EMULATING A FLEXIBLE SPACE STRUCTURE: MODELING

S. C. Rice
V. L. Jones
Control Dynamics Company
Huntsville, Alabama

Dr. H. B. Waites
Marshall Space Flight Center
Huntsville, Alabama

Abstract

Control Dynamics, in conjunction with Marshall Space Flight Center, has participated in the modeling and testing of Flexible Space Structures for the past several years. Through the series of configurations tested and the many techniques used for collecting, analyzing, and modeling the data; many valuable insights have been gained and important lessons learned. This paper discusses the background of the Large Space Structure program, Control Dynamics' involvement in testing and modeling of the configurations (especially the ACES configuration), the results from these two processes, and insights gained from this work.

Introduction

Control Dynamics, in conjunction with Marshall Space Flight Center (MSFC), has participated in the modeling and testing of Flexible Space Structures for the past several years. Many valuable insights have been gained and important lessons learned through the many configurations tested and the many techniques used for collecting, analyzing, and modeling the data. The following sections discuss the background of the Large Space Structure program, Control Dynamics' involvement in testing and modeling, and the results from these two processes.

Structural Background

MSFC has developed a facility in which dynamic behavior and closed-loop control of Large Space Structures (LSSs) can be demonstrated and verified. Figure 1 depicts the evolution of the test configurations since the conception of the facility.

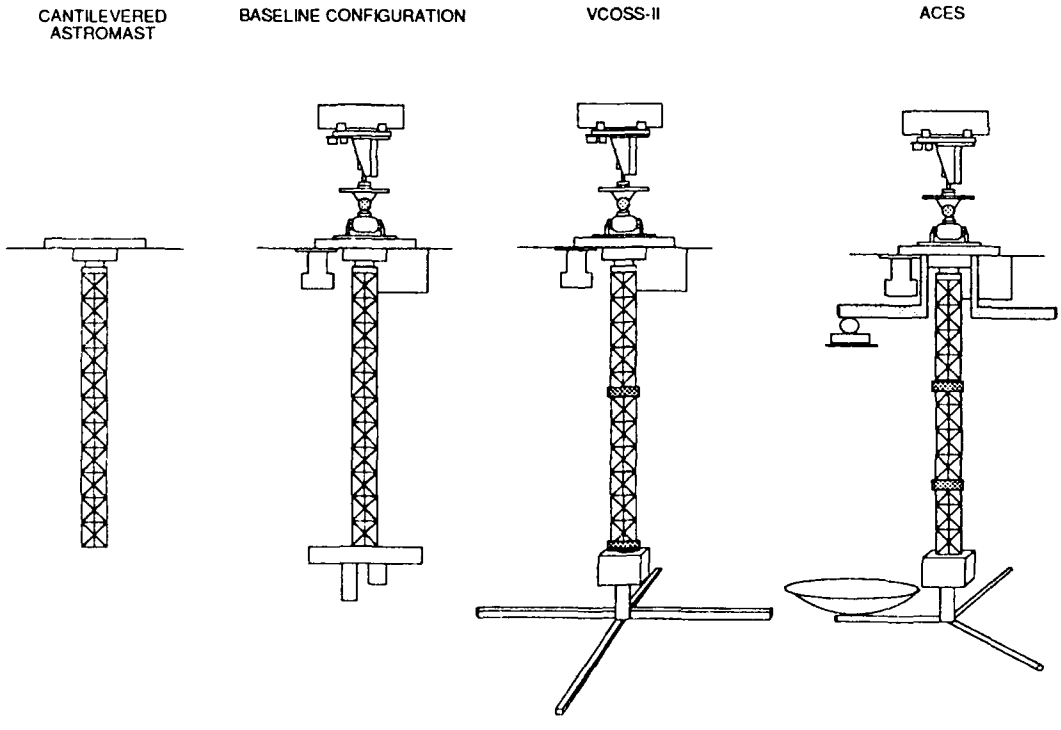

Figure 1. Configuration History

In 1983, the first set of modal tests was initiated, by MSFC, on the spare 13 meter Voyager Magnetometer Boom (ASTROMAST) hung in a cantilevered state. The structure was excited using impact testing techniques. Frequencies and modeshapes were obtained and an analytical model was tuned to correspond to the test data. The beam's stiffness values were the main variables to be adjusted as they were not initially well known. After tuning the model, analytical frequencies within 10 percent of experimental values were obtained and the mode shapes agreed well. The testing revealed that the ASTROMAST behaved as a linear beam. This enabled the analytical model to be fairly simple, four consistent beam elements which would minimize the number of Degrees of Freedom (DOFs). The beam itself did not exhibit a typical LSS characteristic such as densely packed modes.

In 1984, a baseline set of sensors and actuators was incorporated into the LSS laboratory. The baseline set of sensors and actuators included the Base Excitation Table (BET) for two-axis translational disturbance at the base of the structure, the augmented Advanced Gimbal System (AGS) at the base for control in the three rotational axes, and a three axis set of gyros and accelerometers at both the base and the tip of the mast for measurements. These hardware components were modeled using their mass properties and were assumed to be rigid. Gravity effects were accounted for in the model by adding in geometric stiffness elements. Each of these elements is a function of the load seen at the point of interest. The analytical model yielded frequencies within 20 percent of experimental values and good mode shape agreement. It was not realized at this time that the load on the mast changes the beam's inherent stiffness values. The model and the structure showed that the structural differences in each axis (shake table masses, tip and base inertias, rotational moment arms for each gimbal) tended to separate the bending pair frequencies. This second configuration also did not exhibit densely packed modes.

In 1986, the VCOSS-II configuration was obtained by adding a cruciform and additional pairs of sensors/actuators. This configuration produced the desired LSS characteristics with the addition of an unsymmetric cruciform attached to the tip instrument package. The ASTROMAST retained its basic properties and the addition of the four 'legs' induced some structural interaction between the components to introduce more modes at the lower frequency range. The sensor/actuator pairs introduced were the Linear Momentum Exchange Devices (LMEDs) produced under the VCOSS (Vibration Control of Space Structures) program; these

were later modified by Control Dynamics to diminish the stiction and hysteresis effects. The VCOSS-II configuration was the first structure to have independent transfer function testing beyond the modal testing conducted by MSFC personnel. The LMEDs were not utilized during the transfer function testing as they were in the process of being modified. Dummy masses were attached to the structure to represent the LMEDs.

The model for the VCOSS-II configuration compared well with the modal test data except for one pair of modes. One of these pair was later determined to contain some invalid data and was eliminated from the modal data set. Transfer function testing was then performed to further quantify the amount of difference between the model and experimental results. This led to recalculations of the tip package and roll gimbal inertias, as well as a change in the beam's stiffness characteristics. Thus it was realized that the ASTROMAST's stiffness values vary under different load conditions. An increased load starts to untwist the mast causing its structural characteristics to change. With these modifications model frequencies within 12 percent of the experimental values were generated. And again, there was good modeshape correspondence.

These previous configurations have evolved into the ACES-I (Active Control Technique Evaluation for Spacecraft) configuration which is the main configuration examined in the paper. Using everything which has been learned from the previous configurations, MSFC and Control Dynamics have produced an extensive amount of accurate experimental data and a valid analytical model which was used in control design.

ACES Testing: Modal and Transfer Function Tests

The ACES configuration (Figure 2) underwent the most rigorous testing of any configuration. Modal testing of the structure was conducted over a series of frequency ranges. In addition, a full complement of sensor/actuator transfer functions were generated to aid in final model development and control system design and analysis.

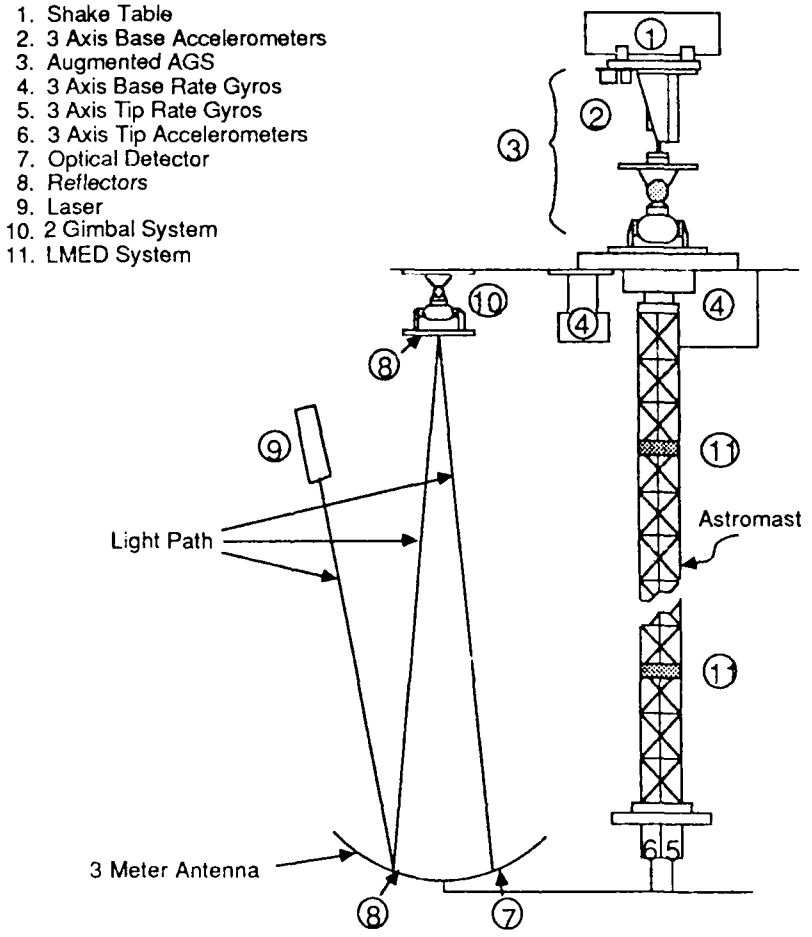

Figure 2. ACES Configuration

MSFC has conducted extensive modal tests on the preliminary ACES configuration in order to obtain a reliable set of test data. The preliminary ACES structure had the BET and augmented AGS turned off, the LMEDs locked in place, and dummy masses for the Image Motion Compensation (IMC) equipment. Single and multi-point random techniques were used to obtain the modal data. This data was stored and manipulated on a GenRad 2515 Structural Dynamics Analyzer from which frequencies, modeshapes, and damping values were obtained. From these tests, the frequencies and modeshape descriptions given in Table 1 were obtained. For a detailed report on the modal testing contact ET53 at MSFC and reference report number TCF DEV-ET86-040.

A second means of verifying the model was through the use of transfer function tests which were effected by Control Dynamics personnel. Dummy masses were still on the structure representing the pointing gimbals, mirrors, and detector. These tests had the roll gimbal and LMEDs operational. A set of tests was also run with the LMEDs locked in order to readily compare with the modal test data.

All control actuators and sensors were utilized in the transfer function tests. Tables 2 and 3 list the possible excitation and response locations. The blocks which do not contain an 'X' had a minimal response for the associated input-output combination. The transfer functions for the boxes with an 'X' were saved on tape, plotted, and used to compare with those transfer functions from the analytical model.

The transfer functions were generated utilizing the control actuators and sensors. An input excitation was applied to the structure through each control actuator. Each output response was measured by each of the control sensors. The actuator input signal and the sensor output signal were transmitted to the HP5423 structural analyzer to calculated the transfer function.

Table 1
SUMMARY OF MODAL TEST RESULTS

TEST NO.	FREQUENCY (HZ)	DAMPING (%)	DESCRIPTION
TSS-002	0.637	1.13	2nd Bnd Y
	0.752	1.07	2nd Bnd X
	0.826	1.03	3rd Bnd Y
	1.04	0.65	3rd Bnd X
	1.405	0.68	Antenna Torsion, Upper Balance Arms Bnd
	1.702	0.36	Antenna Rocking About X, Lower Balance Arms Bnd X, Mast Bnd Y
	1.752	0.41	Antenna Torsion, and Rocking About Y Mast Bnd X, Upper Balance Arms Bnd X, Power Balance Arms B Z
	1.92	0.51	Antenna Torsion and Rocking About X, Mast Bnd Y, Upper Balance Arms Bnd XZ, Lower Balance Arms Bnd XZ
TSS-003	2.0	0.37	Antenna Torsion, Mast Bnd XY, Upper Balance Arms Bnd X, Lower Balance Arms BndX
	2.356	0.76	Antenna Torsion, Mast Bnd XY, Upper Balance Arms Bnd X, Lower Balance Arms Bnd X) Same Motion A 2.0Hz Mode but out of Phase)
	2.494	0.63	Mast Bnd Y, Upper Balance Arms and AGS Plate Bnd Z, Antenna Rolling About Y
TSS-004	4.196	0.54	Mast Bnd XY (3rd Bnd), Antenna Rolling About Y, Lower Balance Arms Bnd Z
	7.023	1.44	AGS Adapter Plate and Upper Balance Arms Torsion
	7.261	0.91	Mast Bnd XY
TSS-005	1.36	0.2	Lower Balance Arms Bnd 2
	1.47	0.56	Antenna Torsion

NOTE: Three system modes, a first bending pair at approximately 0.14Hz and a first torsion at approximately 0.03Hz were observed in the PRF's but mode shapes were not obtainable.

Table 2
Transfer Functions with LMEDs Locked

INPUT \ OUTPUT	BASE ACCEL x	BASE ACCEL y	BASE GYRO x	BASE GYRO y	BASE GYRO z	LMED1 x	LMED1 y	LMED2 x	LMED2 y	TIP ACCEL x	TIP ACCEL y	TIP ACCEL z	TIP GYRO x	TIP GYRO y	TIP GYRO z	ANTENNA BASE x	ANTENNA BASE y	ANTENNA BASE z	GIMBAL ARM x	GIMBAL ARM y	GIMBAL ARM z
BET x																					
BET y																					
AGS x			X	X		X		X	X			X	X				X			X	X
AGS y			X	X		X	X	X	X			X	X			X			X		X
ROLL z																					

Table 3
Transfer Functions with LMEDs Unlocked

INPUT \ OUTPUT	BASE ACCEL x	BASE ACCEL y	BASE GYRO x	BASE GYRO y	BASE GYRO z	LMED1 x	LMED1 y	LMED2 x	LMED2 y	TIP ACCEL x	TIP ACCEL y	TIP ACCEL z	TIP GYRO x	TIP GYRO y	TIP GYRO z	ANTENNA BASE x	ANTENNA BASE y	ANTENNA BASE z	GIMBAL ARM x	GIMBAL ARM y	GIMBAL ARM z
BET x																					
BET y																					
AGS x			X	X		X	X	X	X				X	X							
AGS y			X	X		X	X	X					X	X							
ROLL z					X																
LMED1 x				X		X															
LMED1 y			X						X				X	X							
LMED2 x						X		X					X	X							
LMED2 y									X				X	X							

Judicious selection of the input excitation improves the accuracy of the transfer function over the frequency range of interest. The coherence function was examined to determine the reliability of each transfer function. Figure 3 illustrates the input excitation chosen to generate the transfer functions. The protracted pulse is of length 5 times the sample period, where the length is chosen such that its frequency response zero does not interfere with the transfer function. The amplitude of the input is maximized; this maximization is limited by sensor saturation. Ten averages were collected for each final transfer function. An 8 Hz bandwidth was used as it accommodates the significant modes and corresponds to an analyzer sampling time of close to 20 msec. An exponential window was applied to force the response to zero.

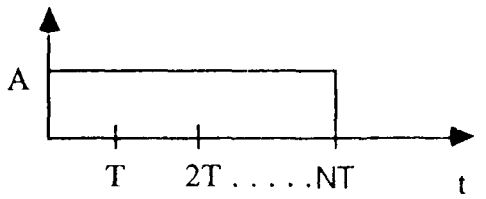

Figure 3. Transfer Function Excitation

ACES Model

The ACES model was the most complex model developed. It was developed in stages as the actual hardware became available. A pre-test model was developed to aid the modal test team in determining the testing ranges. As the modal test data and transfer function data became available, this model became the preliminary model. With all the data correlated, the control model evolved from the preliminary model. The control model is the one provided to the control designers working on Positivity, FAMESS, and HAC/LAC designs.

Process

The present configuration is the ACES configuration, which has undergone the most extensive testing and analysis of any configuration. The cruciform was removed from the tip of the VCOSS-II model and a tri-element figure was added. The one 'leg' contains an antenna structure with a mirror and detector at its center. There was originally a covering on the antenna frame, but this produced an extensive amount of damping in the tip movement and was removed. There are also two counterbalance 'legs' at the tip of the structure to keep the center of mass along the vertical axis. Near the base of the structure two 'arms' were also added. One 'arm' reaches over the antenna and has attached to its end a two-axis gimballed mirror; the second 'arm' functions as a counterweight to the first 'arm'. The gimbals on the 'arm' provide a new actuating location and the detector provides a new sensing location. All in all, the simple cantilevered ASTROMAST has become a very complex control structure. The new appendages have succeeded in making this configuration conform to the definition of LSSs; lightly damped, densely packed, coupled low frequency modes.

Comparison with Test Results

A comparison of the preliminary analytical model with the modal test data shows that the antenna model contributed a significant number of frequencies in the 0 - 8 Hz range. These modes were not measured in the modal tests. It was decided to simplify the antenna model by eliminating many localized modes of the antenna and to become more consistent with the actual structure. The original antenna model was fairly complex with more detail than was required. The antenna modes still did not correspond well with the measured antenna behavior, but since these modes do not

effect any sensor/actuator behavior it was decided that it was more important to tune the behavior of the ASTROMAST, 'arms', and 'legs' than the local antenna motion.

During the transfer function testing it became apparent that the roll gimbal and the BET could move even when turned off. At this point it was decided to unlock the DOFs corresponding to the X and Y translations of the BET and the rotation about Z of the roll gimbal. For modeling purposes only, stiffness values were implemented to model the break-away friction for the equipment. This was done in an attempt to better match the modal test conditions. Stiffness values were chosen so that key modal frequencies matched. In the control model, these DOFs are freed (no associated stiffness values) in order to agree with the ACES configuration which has the equipment fully operational.

The problems matching the measured torsional modes with the preliminary model were alleviated through the utilization of the torsion spring. Freeing the roll gimbal DOF and inserting the torsional spring helped immensely, as the modes could not occur with the roll gimbal locked. This allowed the shapes to match, but the frequencies were still not within an allowable range. The E (Young's Modulus) value for the 'arms' was then adjusted for stiffness purposes. It could not be adjusted dramatically as the 'arm' behavior for the bending modes would be effected. It was adjusted in coordination with the torsional spring and the ASTROMAST G (torsional modulus) value to match the torsional frequencies and to not disrupt the bending frequencies.

The modal testing and transfer function testing revealed a great deal more cross coupling than seen in the model. Actual location measurements were then made on the structure and it was observed that the components were not lined up as assumed. When the misalignments were added to the model the coupling did increase, but the magnitude of the cross coupling was still below the measured behavior.

Based upon the results of the modal and transfer function testing, a tuned model was developed incorporating the updates previously discussed. The results from this tuned model and its comparison with the modal data is given in Table 4. The analytical frequencies are all within 20 percent except for the first torsional mode. Looking at this frequency numerically, it is only off by 0.04 Hz. In the testing, this mode could be seen but is difficult to

Table 4. Tuned Preliminary Model Mode Descriptions

Model Frequency (Hz)	Experimental Freq. (Hz)	Percent Error	Description
.07	0.03	-133%	Torsion
.14	0.14	-	X-Bending
.14	0.14	-	Y-Bending
.53	0.637	17%	Y-Bending
.59			X + Antenna
.59			Y + Antenna
.60			Torsion + Antenna
.70			X + Legs + Ant.
.71			X + Legs + Ant.
.73	0.752	3%	X + Ant. + Arms
.95			Antenna
.95			Antenna
.95	0.826	-15%	Y + Legs + Ant.
1.00	1.042	4%	X + Legs + Ant. + Arms
1.20	1.405	15%	Torsion + Arms
1.34			Arms
	1.357		Legs
	1.466		Antenna Torsion
1.70	1.702	-	X + Y + Legs
1.73	1.752	1%	X + Y + Legs + Arms
1.84			Y + Legs + Ant.
1.92			Antenna
1.92			Antenna
2.12	1.920	-10%	Y + Antenna
2.20	2.000	-10%	X + Arms
2.53	2.356	-7%	X + Legs + Ant.
2.55	2.494	-2%	Y + Ant. + Arms
3.31			Antenna
3.31			Antenna
3.80			Torsion
4.29	4.196	-2%	X + Legs + Ant.
4.71			Antenna
4.71			Antenna
5.35			Antenna
5.45			Y + Legs + Ant.
6.73			Y + Z + Legs
6.87	7.023	2%	Torsion + Arms
6.97	7.261	4%	Torsion

measure due to its extremely low frequency; the transfer function testing located this mode at 0.045 Hz.

There are also two modes obtained in the modal testing which do not appear in the model. They were both obtained during the torsion testing, which had its own difficulties. As neither mode appeared in the transfer function tests and these modes did not appear from the modal testing to have a great deal of action at the sensor/actuator complement, it was decided not to try and force the model to yield these behaviors.

The remaining experimental and analytical modeshapes agreed well. The basic characteristics which appeared in the modal testing appeared in the model. See Figures 4 and 5 for example modeshape comparisons. Since the model is linear and the structure is not, discrepancies are bound to occur. These differences involve 'arm' motion and some 'leg' motion. Some of the nonlinearities include non-rigid joint connections, friction, and damping.

While the modal testing helped in matching frequencies and modeshapes, the transfer function testing aided in matching the system coupling and mode dominance. Because the torsional measurements were limited by equipment and measurement locations, the transfer function results are only useful for transverse vibrations. Figures 6 and 7 depict two comparisons of the measured and modeled behavior. The analytical transfer functions basically have the same behavior as the experimental ones. Discrepancies between the two sets do exist however; the major differences involve the magnitudes of the peaks, the model peaks are generally lower than their experimental counterparts. The phases are difficult to compare as the experimental plots contain lags due to the computational delays in the computer system.

The control model has utilized all that has been learned in the previous configurations, especially from the results of the preliminary model. The modal testing and transfer function testing have contributed a significant amount of knowledge about the structure which previously was not available. The following changes have been made to update the preliminary model to the control model form. The characteristics of the actual equipment have been implemented: pointing gimbal assembly, mirrors, detector, and any counterweight updates. The stiffness values for the BET and roll gimbal have been removed as the equipment is operational

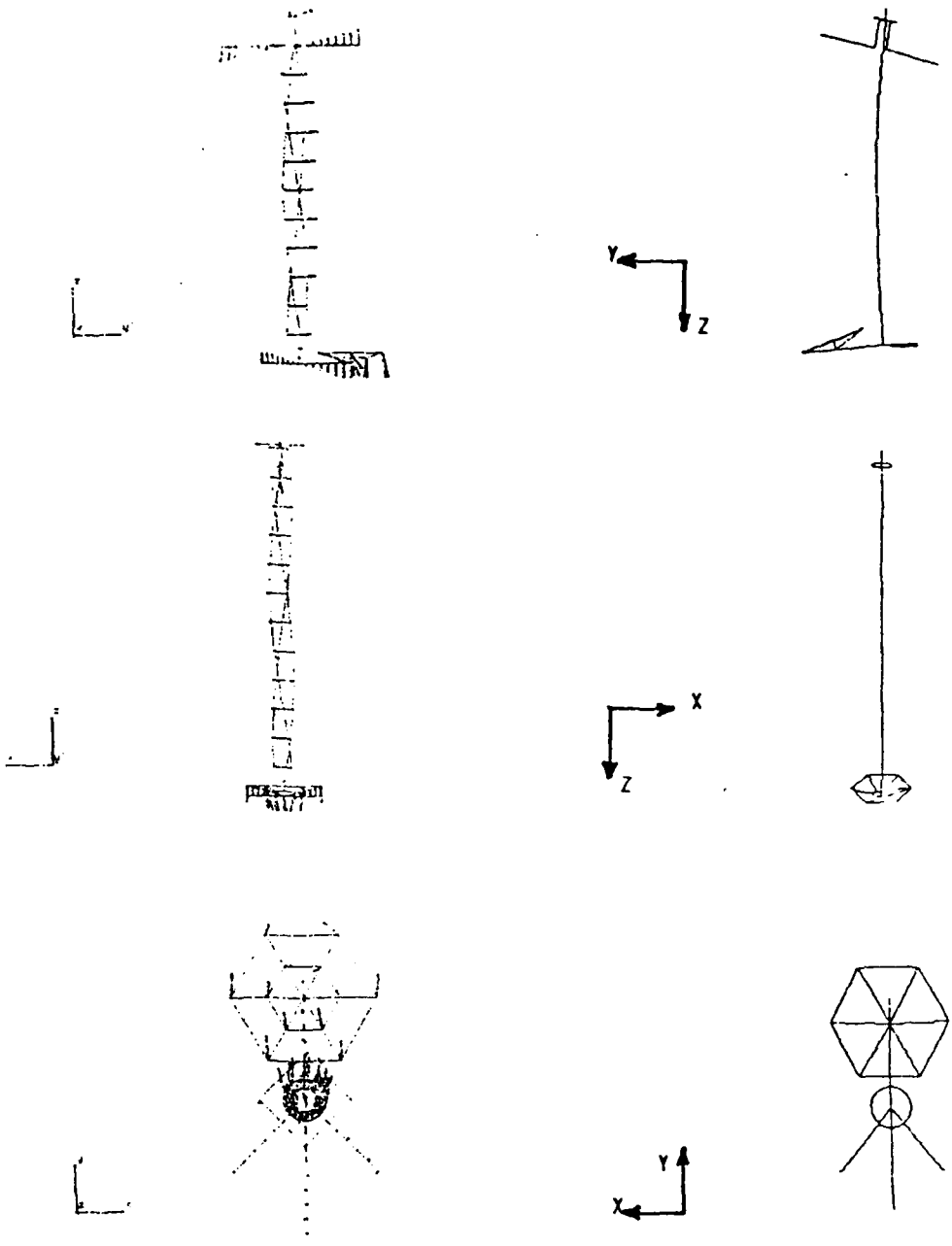

Experimental Mode, 0.637 Hz

Analytical Mode #4, 0.53 Hz

Figure 4. Y-Bending

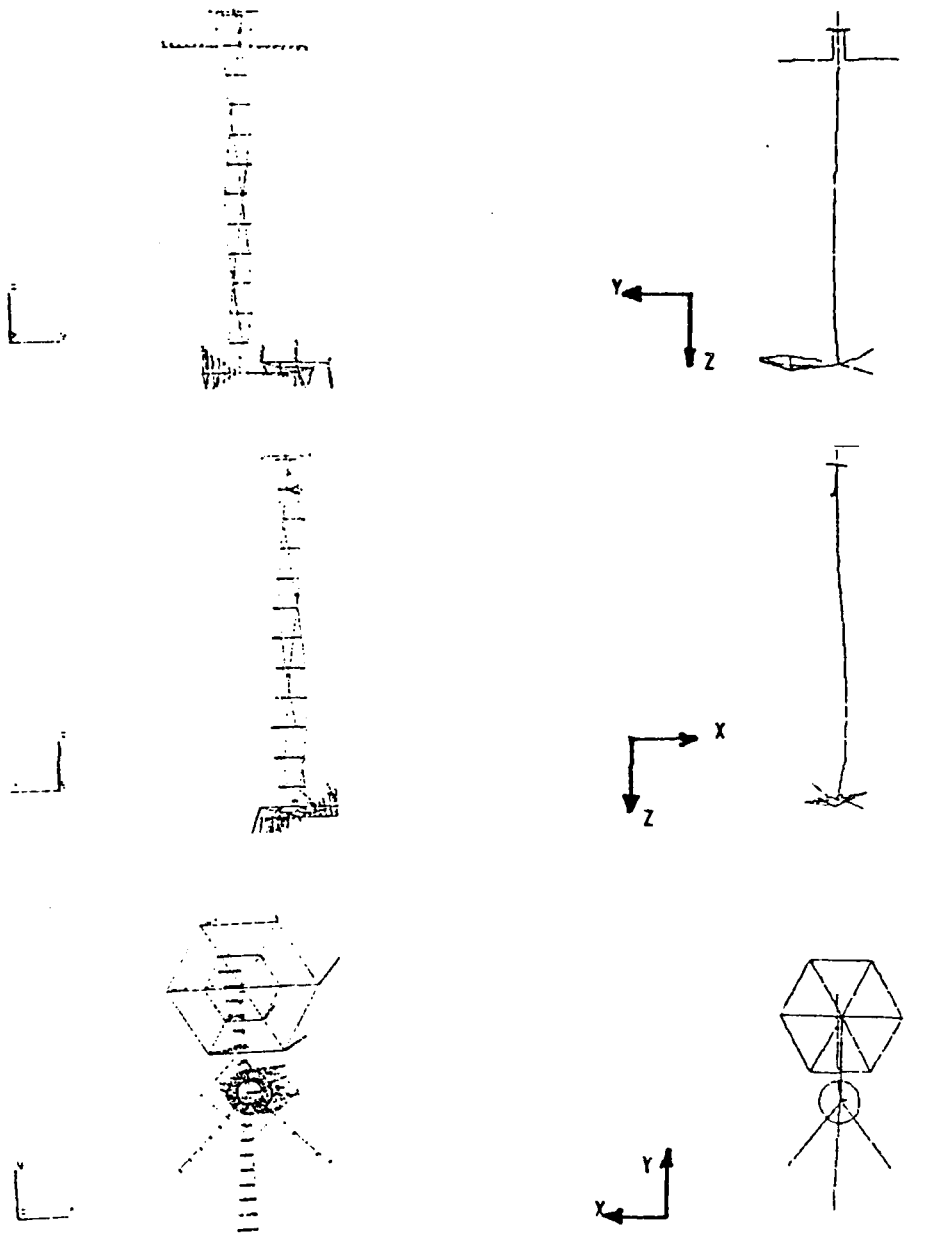

Experimental Mode, 1.042 Hz

Analytical Mode #14, 1.00 Hz

Figure 5. X-Bending

AGS-Y to BASE GYRO-Y

Model TF #10

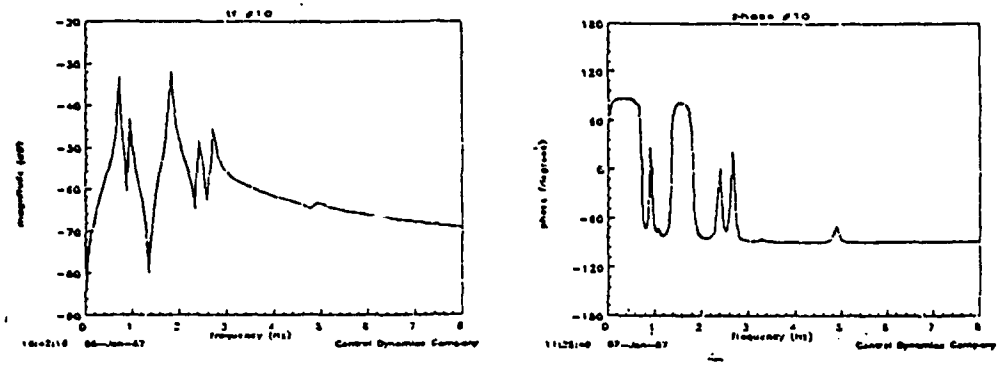

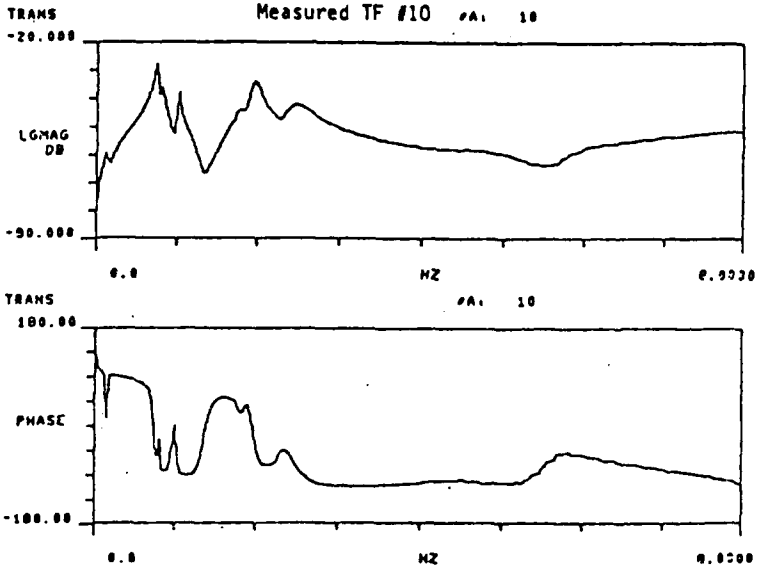

	Analytical	Experimental
.75Hz	-33dB	-28dB
.83Hz		-35dB
1.0 Hz	-44dB	-38dB
1.8 Hz	-32dB	-42dB
2.0 Hz	-48dB	-32dB
2.5 Hz	-45dB	-40dB

Figure 6. Transfer Function

AGS-Y to LMED1-X

Model TF #46

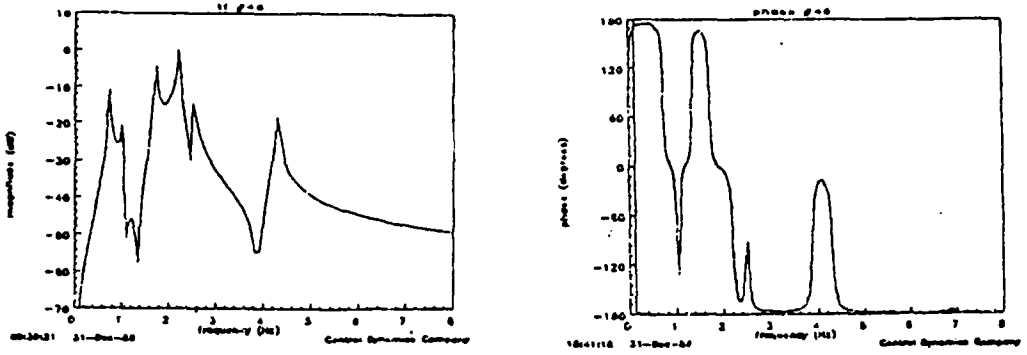

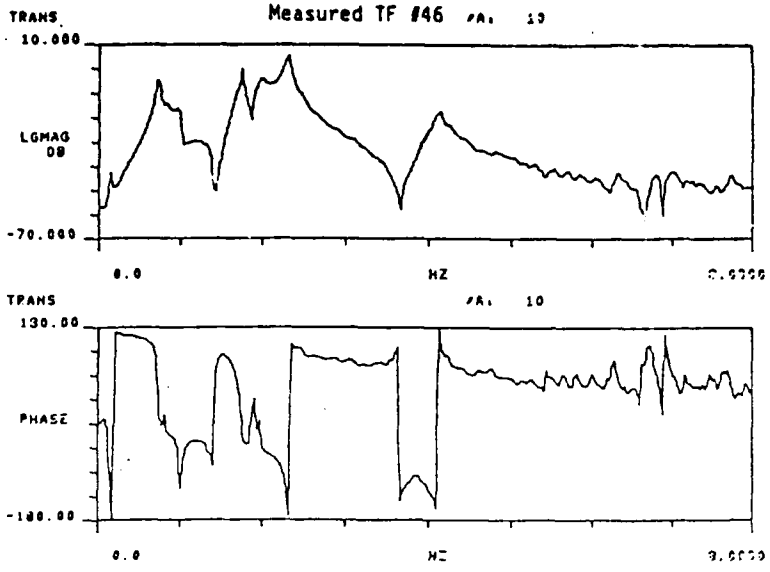

	Analytical	Experimental
.75Hz	-10dB	-5dB
1.0 Hz	-21dB	-15dB
1.75Hz	-4dB	0dB
2.0 Hz	0dB	-5dB
2.3 Hz	-15dB	5dB
4.2 Hz	-18dB	-20dB

Figure 7. Transfer Function

for control and disturbance purposes. Table 5 gives the frequencies and modeshape descriptions for the control model.

Line-Of-Sight (LOS) errors were calculated, for each mode, for the two mirrors and the detector. The LOS errors were calculated utilizing the structure's geometry (Figure 8) and the modal gains for each frequency. The geometry relating the laser source, mirrors, and detector for a static condition is input and transformed from the laboratory reference frame to local detector and mirror frames. For the static case, this produces a 0.0 LOS error in the plane of the mirrors and detector. When the modal gains are included in the LOS equations, an X and Y error are calculated for each mirror and the detector. The detector local coordinate system is calculated to be parallel to the global system as the detector was originally in the horizontal plane and there are only small angle perturbations at the detector location in the analytical model. Again, these are the two LOS error components in the plane of a mirror or detector, and the values are the distance of the laser beam from the center point in meters.

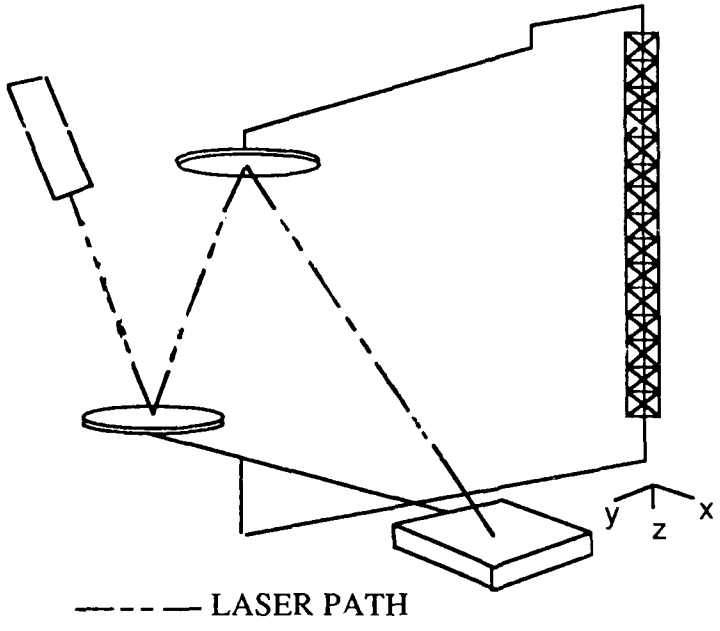

Figure 8. LOS Geometry

Table 5

Final ACES Model	
Mode	Frequency (Hz)
Rigid Body, Torsion + X-Bending	0.00
Rigid Body, Torsion + X-Bending	0.00
Rigid Body, Y-Bending	0.00
Torsion + Legs + Antenna + Arms + Gimbals	0.09
Y-Bending + Antenna + Gimbals + LMEDs	0.50
X-Bending + Antenna	0.59
Antenna	0.59
Torsion + Antenna	0.60
X-Bending + Legs + Antenna + Arms + Gimbals + LMEDs	0.69
X-Bending + Y Bending + Legs + Antenna	0.70
X-Bending + Legs + Antenna + LMEDs	0.71
Y-Bending + Legs + Antenna + LMEDs	0.92
Antenna	0.95
Antenna	0.95
X-Bending + Legs + Arms + Gimbals + LMEDs	0.96
X-Bending + Y-Bending + LMEDs	1.17
X-Bending + Y-Bending + LMEDs	1.18
X-Bending + Y-Bending + Legs + LMEDs	1.23
X-Bending + Y-Bending + Legs + LMEDs	1.24
Arms + Gimbals	1.25
Gimbals	1.51
X-Bending + Arms + Gimbals + LMEDs	1.67
Y-Bending + Legs + Antenna + Gimbals + LMEDs	1.76
Y-Bending + Legs + Antenna + Gimbals	1.85
Antenna	1.92
Antenna	1.93
X-Bending + Gimbals	2.08
Y-Bending + Antenna + Arms + Gimbals + LMEDs	2.18
X-Bending + Antenna + Gimbals	2.34
X-Bending + Legs + Antenna + Gimbals	2.58
Y-Bending + Antenna + LMEDs	2.67
Torsion + Arms + Gimbals	3.31
Antenna	3.31
Antenna	3.31
X-Bending + Y-Bending + Torsion + Legs + Antenna	4.58
Torsion + Antenna	4.71
Antenna	4.71
Torsion	4.71
Antenna	5.34
Y-Bending + Legs + Antenna	5.84
Y-Bending + Z + Legs	6.92
Torsion	8.77
Gimbal Arm	8.82

Modal gains and frequencies were provided for use in the control designs. Gains at the following specific locations were provided:

1) BET translations,
2) translations at the base accelerometers,
3) translations at the tip accelerometers,
4) translations at the antenna base,
5) translations at LMED1 and LMED2 pairs,
6) LMED1 - mast and LMED2 - mast relative translations,
7) AGS rotations,
8) rotations at the base gyros,
9) rotations at the tip gyros,
10) rotations at the tip base,
11) pointing gimbal rotations,
12) AGS relative rotations,
13) pointing gimbal rotations,
14) LOS error for mirror1, mirror2, and the detector.

Table 6 shows an example table of data provided to the controls designers. The data was provided in the form of modal gains since two of the control techniques used the state-space form and could not directly utilize the transfer function data.

TABLE 6

Mode Number	Translational Gains				
	BET		Base Accelerometers		
	X	Y	X	Y	Z
1	.2874E-01	-.9650E-03	.2874E-01	-.9650E-03	.1672E-09
2	-.2381E-01	.1694E-02	-.2381E-01	.1694E-02	-.1188E-09
3	-.1978E-02	-.3455E-01	-.1978E-02	-.3455E-01	-.1053E-10
4	-.3925E-02	-.3710E-04	-.3925E-02	-.3710E-04	-.3284E-10
5	-.1111E-03	.4255E-02	-.1111E-03	.4255E-02	.5111E-11
.	.	.	.	.	.
.	.	.	.	.	.
.	.	.	.	.	.
42	-.1865E-05	.2609E-07	-.1865E-05	.2609E-07	-.3482E-12
43	.7512E-03	.8661E-08	.7512E-03	.8661E-08	-.8268E-11

The control model has not been verified against experimental data, but Control Dynamics feels it is a good model based upon the preliminary model tuned with the modal test data and the transfer function data. For a more thorough explanation of the model, model results, and test results refer to the ACES Report on the Finite Element Model prepared by Control Dynamics.

Closing Comments

Some valuable lessons have been learned from the ACES program and the configurations which have preceded it at the MSFC Ground Test Facility, and much has been learned about the development of a large flexible structure with the associated characteristics in a 1g environment. The realization that appendages are necessary to reduce the structural frequencies led to the pointing/antenna ACES configuration. There have been difficulties in measuring the structure's behavior as the structure became more complex. The torsional behavior is especially difficult to measure since there needs to be a tremendous amount of energy to excite this motion. The structures have been modeled using fairly simple approaches and element types, and the models represent the structures well. Other more complex techniques are available, but when a simple approach works, as it does here, there is no need to spend extra time developing extremely detailed models. An important asset here was the in-house ability to perform transfer function testing on the structure. These tests provided valuable insights to the world of testing and about the structure itself. Some characteristics which may not have shown up in the modal testing were shown in the transfer function testing and vice versa.

It has been a great learning experience for Control Dynamics to have been involved with MSFC in the LSS arena. Dealing with the problems in modeling, testing, analysis, and hardware has left a sense of accomplishment as they have been overcome. This facility also directly applies the CSI goals: from the structural model development and tuning with test data, to the interaction with control engineers to provide them with the data they need, to the design and implementation of the latest control design techniques. Control Dynamics has been proud to have been involved in this effort and plans to continue working with MSFC and WPAFB in the LSS area.

SLEWING AND VIBRATION SUPPRESSION FOR FLEXIBLE STRUCTURES

P. MADDEN

The Charles Stark Draper Laboratory
Cambridge, Massachusetts

INTRODUCTION

A number of future DOD spacecraft such as space based radar will be not only an order of magnitude larger in dimension than current spacecraft, but will exhibit extreme structural flexibility with very low structural vibration frequencies. Another class of spacecraft such as space defense platforms will combine large physical size with extremely precise pointing requirements. Such problems require a total departure from the traditional methods of modeling and control system design of spacecraft where structural flexibility is treated as a secondary effect (ref. 1).

With these problems in mind, the Air Force Astronautics Laboratory (AFAL) initiated a technology development project at Charles Stark Draper Laboratory (CSDL) to investigate methods for designing control systems for slewing flexible spacecraft using on-off thrusters. As a follow on to this project, AFAL initiated two new projects to investigate the design of control systems employing linear actuators for vibration control in large flexible structures. The objectives of these three projects are listed in figure 1. This paper summarizes the completed and ongoing work in the three projects.

VERIFICATION OF RCS CONTROLLER METHODS FOR FLEXIBLE SPACECRAFT

Generalize the theory for flexible spacecraft RCS controller design methods.
Demonstrate the application of this RCS controller design methodology through analysis and simulation.
Verify the RCS controller design with a simple ground-based experiment.

VERIFCATION OF CONTROLLER DESIGN METHODS EMPLOYING RCS AND LINEARLY DISTRIBUTED PIEZOELECTRIC POLYMER FILM FOR FLEXIBLE SPACECRAFT CONTROL

Develop control theory which employs distributed piezoelectric linear actuation devices for controlling structural vibration modes in large space structures.
Verify the application of these controller designs through analysis and simulation.
Demonstrate the controller designs on the AFAL/CSDL test structure.

VERIFICATION OF CONTROLLER DESIGN METHODS EMPLOYING RCS AND LINEAR ACTUATION DEVICES FOR FLEXIBLE SPACECRAFT CONTROL

Develop the control theory required for using linear actuation devices such as proof-mass actuators and CMG's, to control structural vibration modes in large space structures.
Verify the application of these controller designs through analysis and simulation.
Demonstrate the controller designs on the AFAL/CSDL test structure.

Figure 1

NEED FOR SLEW CONTROL USING ON-OFF THRUSTERS

Several future DOD space systems, particularly space defense platforms, will require rapid slewing (retargeting) of the spacecraft. Ideally, control-moment-gyro's (CMG's) would be used for slewing these systems, but the large moment of inertia of such spacecraft coupled with the rapid retargeting requirement results in a slew torque requirement which is beyond the reach of state of the art control-moment-gyro's (CMG's). Figure 2 shows the gap between the current state of the art and system requirements (ref. 1).

Because CMG's are inadequate RCS thruster control systems must be used. Although thruster based control systems are capable of meeting the torque requirements, their use poses other problems. The majority of control techniques developed for large flexible structures are not directly applicable when using on-off actuators such as thrusters. The use of on-off thrusters also tends to excite a wide range of vibratory modes within a structure. Methods for implementing slew control systems using on-off thrusters are needed which minimize the excitation of vibratory modes of the structure. Controller designs which can suppress vibrations which do arise due to use of thrusters are also needed.

TORQUE/MOMENTUM CAPABILITIES AND REQUIREMENTS

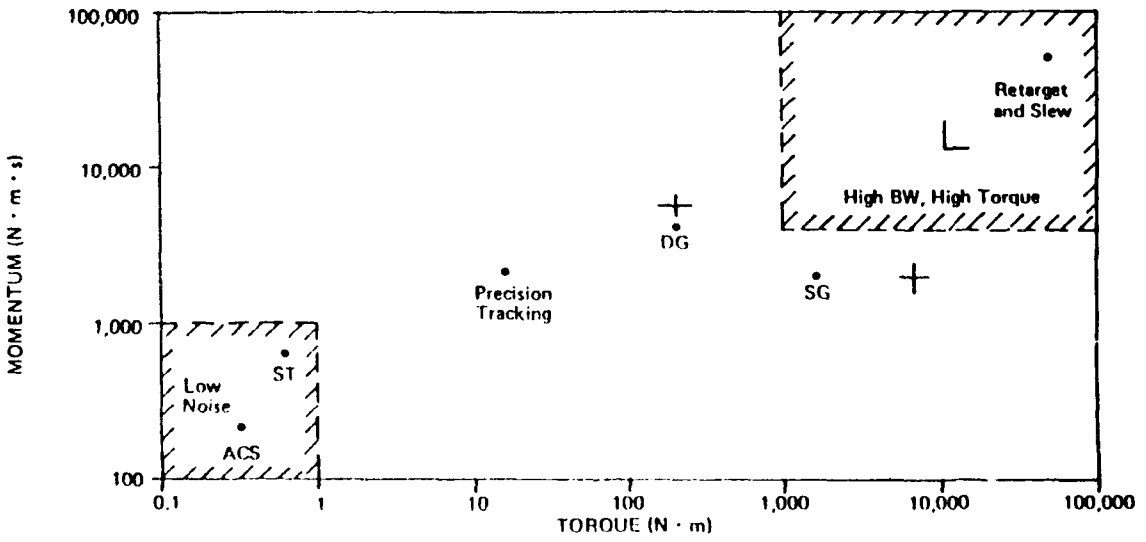

Technology Development Required

NOTES: (1) ST = Space Telescope Reaction Wheel
(2) ACS = Attitude Control System
(3) DG = Double Gimbal Control Momentum Gyro
(4) SG = Single Gimbal Control Momentum Gyro

Figure 2

RCS THRUSTER CONTROLLER DESIGN METHODS FOR FLEXIBLE SPACECRAFT

The initial AFAL sponsored project in the area of slew and vibration suppression for large structures focused heavily on the generalization of controller design methods for RCS thruster control systems for flexible spacecraft. Much work had been done prior to this project on designing control systems for flexible structures, but this work was not directly applicable when using on-off thrusters. These new RCS controller design methods were to be validated using simulation software and then demonstrated on a simple proof-of-concept testbed.

Necessary to the successful completion of this project was the development of the controller design methods, the simulation codes, and a ground based experiment. A breakdown of the specific tasks completed is shown in figure 3.

RCS THRUSTER CONTROL STUDY
MAJOR TASKS

Design and fabricate a single axis flexible test structure supported by an air bearing

Develop finite element model and dynamic equations of motion for the test structure

Develop a simulation of the experimental structure and controller

Develop control theory (Vander Velde and Floyd controllers)

Develop identification algorithms

Develop digital controller for implementing control and identification algorithms and data collection

Perform test and evaluation on uncontrolled structure to verify modal characteristics

Perform test and evaluation on controlled structure to determine closed loop slewing performance

Figure 3

FLEXIBLE STRUCTURE SLEW TESTBED

A key aspect of the RCS controller design project was the implementation of the methods on a physical system. A testbed where slew and vibration suppression experiments could be performed was needed. This testbed was designed and constructed at Charles Stark Draper Laboratory. Figure 4 shows the fully assembled structure.

The testbed consists of four flexible appendages extending radially outward at 90 degree intervals from a rigid hub. The appendages are 4' long, 6" wide, 1/8" thick aluminum, and each has a tip mass. The tip masses are nominally 5 pounds but can be varied. The rigid hub rests on an air bearing table, allowing it to rotate freely about a vertical axis. Actuators on the testbed include four half pound nitrogen gas thrusters mounted in opposing pairs on two of the four appendages. Sensors include an accelerometer at the tip of each appendage, and an angle resolver on the rigid hub.

With minimum tip masses (3.5 lb) the structure's first and second vibration modes are 0.8 Hz and 1.3 Hz respectively. The time necessary to complete a 15 degree slew starting from rest is 2.1 seconds. The maximum tip deflection during that slew maneuver is 3.9 inches (ref. 1).

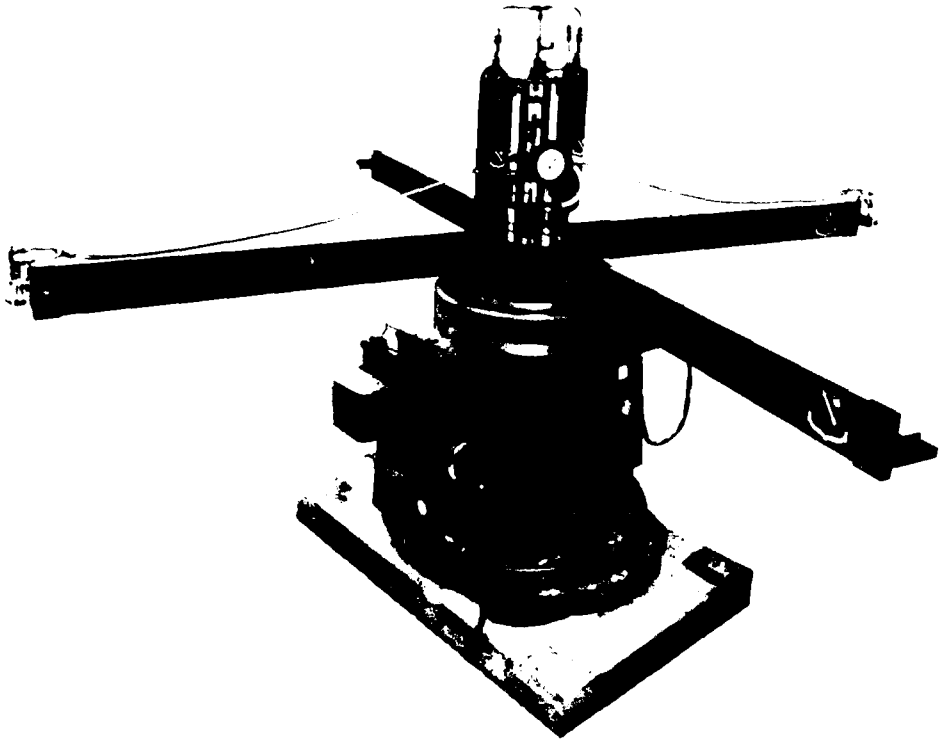

Figure 4

CONTROLLER DESIGN

Two different control laws were tested on the experiment. Vander Velde's approach was to set up a minimum time and fuel optimization problem, using a cost function which represented the trade-off between fast response and minimum fuel usage. This controller is relatively easy to synthesize, but is characterized by frequent thruster switchings. This increases the frequency content of the controller, causing control spillover (ref. 1).

Floyd's approach was to set up a "single step" optimal control problem, using a cost function which attempts to minimize a quadratic form in the state at the following time step while minimizing necessary control. This controller uses control switchings relatively infrequently, minimizing the likelihood of control spillover. It is also able to accomodate different types of actuators simultaneously, although the computational burden increases quadratically with the number of actuators (ref. 1, 2 and 3).

Figure 5 shows the results of experiments implementing the Vander Velde (top row) and Floyd (bottom row) controllers on the slew testbed (figure 4). The solid lines show the simulated response and the squares are the actual sensor measurements.

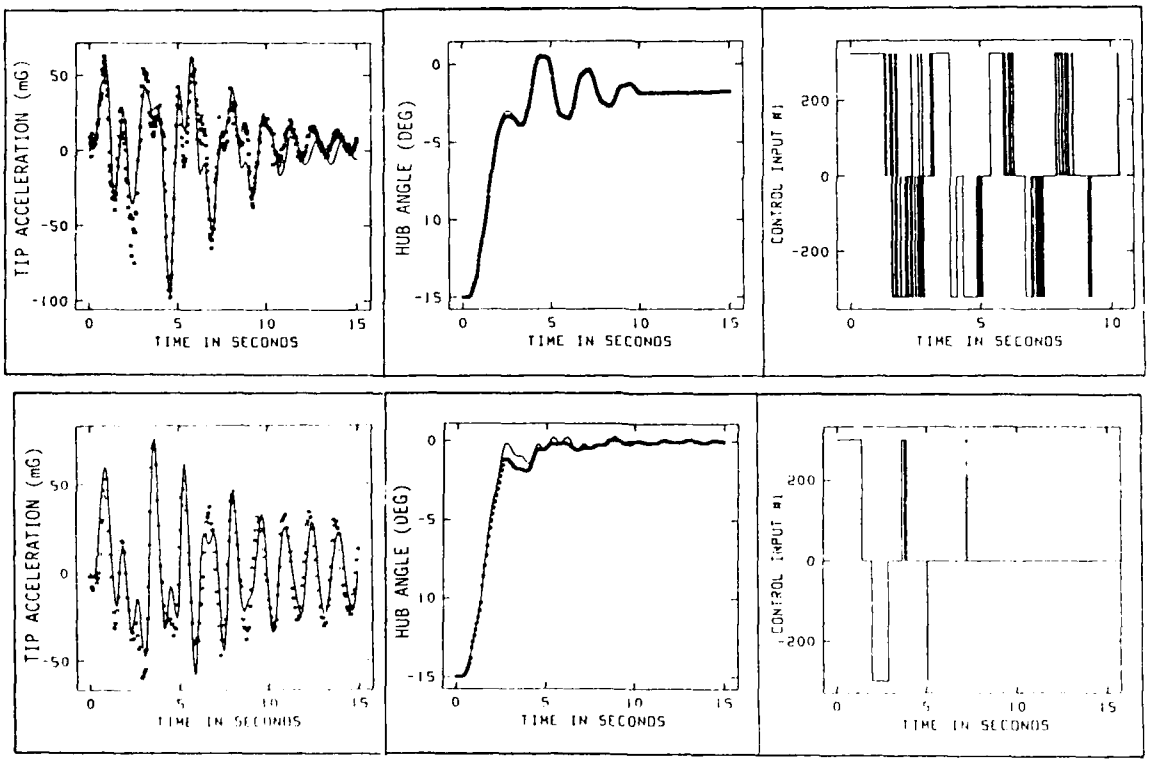

Figure 5

SIMULATION RESULTS

The main thrust of the RCS thruster control design project was the experimental demonstration of control algorithms. To test these control algorithms prior to physical implementatin, a real-time simulation was developed. The simulation allowed the control algorithms to be tested using configurations not available on the experimental setup.

Figure 6 compares the results of two simulations. The first simulation (left column) uses only the on-off thrusters. The second simulation (right column) utilizes a linear actuator with one-tenth the force capability of the thrusters in combination with the thrusters. This relatively weak actuator is placed at the tip of the passive appendages. The plots show that in the configuration utilizing the weak linear actuators, the flexible modes are driven to zero much more quickly than in the configuration using only the on-off thrusters (ref. 1).

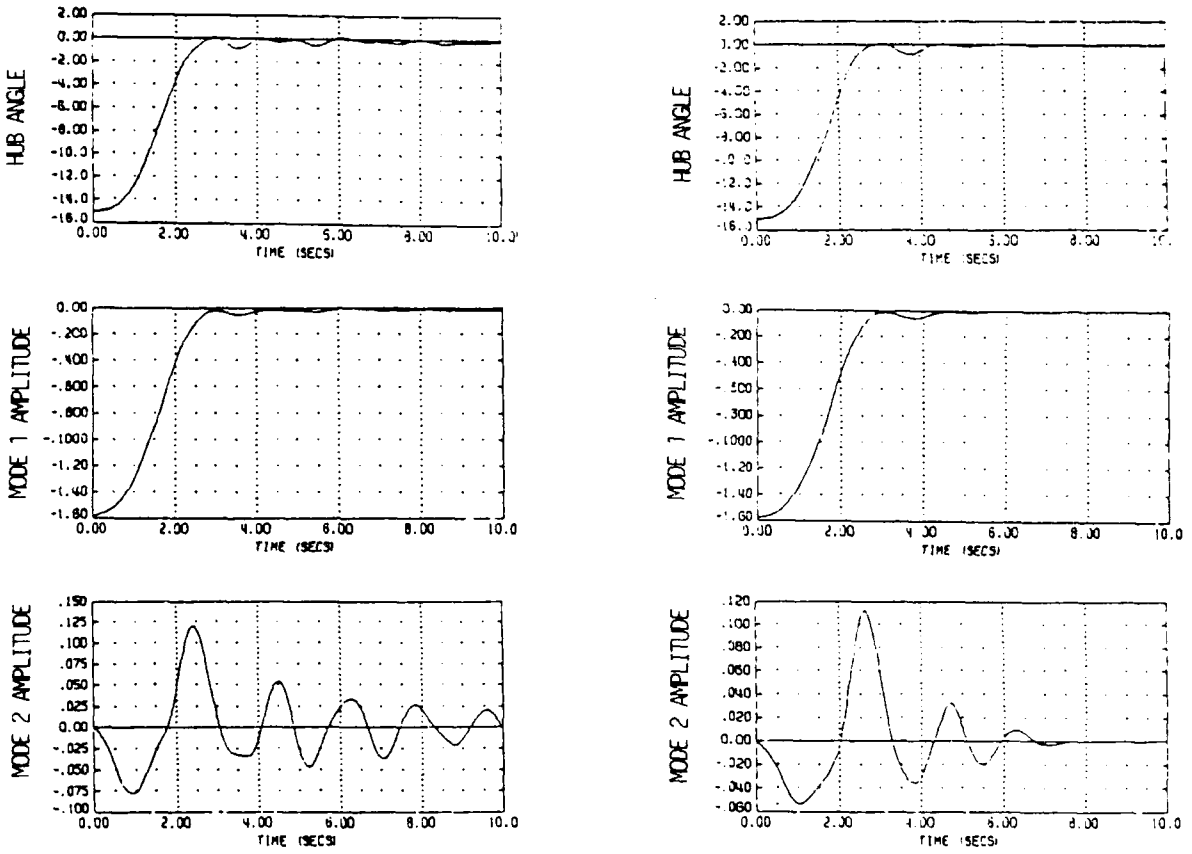

Figure 6

PIEZOELECTRIC DISTRIBUTED ACTUATOR

Several of the active control simulations performed at CSDL indicated that gains in vibration suppression performance could be obtained by combining RCS thrusters with relativley weak linear actuators. One of the most promising actuators being considered is a piezoelectric film. The film contracts or elongates in a predetermined direction when a voltage is applied across its thickness. The strain occurs over the entire length of the film, making it a truly distributed actuator. Theoretically this type of actuator could control all vibratory modes of a structure, avoiding the problem associated with spillover of uncontrolled modes.

Preliminary testing of this concept was done on a 15cm long cantilevered beam. Figure 7 compares the performance of two different active controllers with the uncontrolled decay of vibration. For large vibrations, the controlled system displayed twice the damping of the uncontrolled system. For smaller vibrations the controlled system damping ratio was as much as 40 times that of the uncontrolled system (ref. 4).

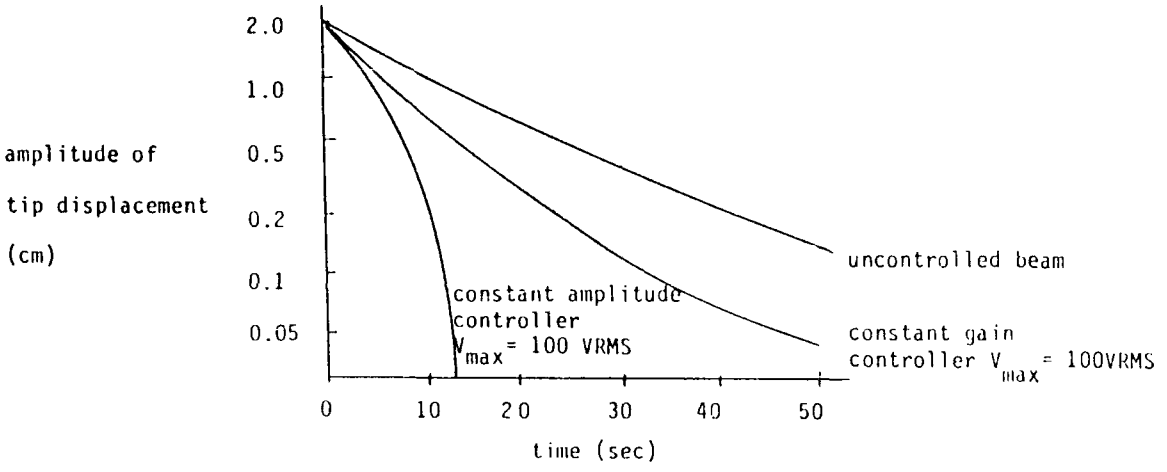

Decay Factor (1st mode)

	Large Vibrations	Small Vibrations
Free Decay	0.003	0.001
Constant Gain Controller	0.006	0.002
Constant Amplitude Controller	0.006	0.04

Figure 7

PIEZOELECTRIC DISTRIBUTED ACTUATOR

To investigate the use of distributed actuators for vibration suppression in large flexible structures, AFAL initiated a project at CSDL to incorporate piezoelectric film as an actuator on the AFAL/CSDL slew testbed. The major emphasis of this effort was to design a controller which could employ a distributed actuator for performing vibration suppression during the terminal phase of a rapid slew maneuver. The slew maneuver was to be accomplished using the existing RCS thruster system and a linear torquer motor placed in the air bearing table.

The experimental demonstration of this controller required that several major modifications be made to the existing testbed. The most significant of these was the coating of the four appendages with piezoelectric film. Presently, all necessary modifications have been made and demonstrations are ready to begin.

MAJOR TASKS

Develop control algorithms for combined structural damping augmentation and modern modal control

Modify the testbed model to account for new sensors and actuators

Perform simulation and evaluation of controller

Perform experiments using on-off thrusters for slew and distributed actuator for vibration suppression

Perform experiments using on-off thusters and CMG for slew and distributed actuator for vibration suppression

Figure 8

CONTROLLER DESIGN FOR LINEAR ACTUATION DEVICES

To investigate the use of linear actuation devices such as control moment gyro's (CMG's) and proof-mass-actuators for vibration suppression in large flexible structures, AFAL initiated a project at CSDL to incorporate a linear torquer actuator and four proof mass actuators on the AFAL/CSDL slew testbed. The major emphasis of this effort was to design a controller which could employ several linear discrete actuators for performing vibration suppression during the transient and terminal phases of a rapid slew maneuver. The slew maneuver was to be accomplished using the existing RCS thruster system and the linear torquer motor placed in the air bearing table.

The experimental demonstration of this controller required that several major modifications be made to the existing testbed. The most significant of these was the placement of a proof mass actuator at the tip of each of the four appendages, and the installation of a linear torquer motor in the air bearing table. Presently, all necessary modifications have been made and demonstrations are ready to begin.

MAJOR TASKS

Update model of testbed to account for new sensors and actuators

Perform simulation and evaluation of controller performance

Perform controls experiments with on-off thrusters for slew and proof-mass-actuators for vibration control

Perform experiments with on-off thrusters for slew and CMG for fine pointing and tracking

Figure 9

REFERENCES

1. Vander Velde, Wallace E.; and He, Jun: Design of Space Structure Control Systems Using On-Off Thrusters. AIAA Guidance and Control Conference (Albequerque, New Mexico) August 1891.

2. Floyd, M. A.; and Vander Velde, W. E.: Verification of RCS Controller Design Methods for Flexible Spacecraft. Air Force Rocket Propulsion Laboratory, Edwards CA, AFRPL TR-84-092, December 1984.

3. Floyd, M. A.: Single-Step Optimal Control of Large Space Structures Model. Department of Aeronautics and Astronautics MIT, Sc.D. Thesis, June 1984.

4. Bailey, Thomas: Distributed Parameter Active Vibration Control of a Cantilevered Beam Using a Distributed Parameter Actuator. Massachusetts Institute of Technology, MS/BS Thesis, September 1984.

ASTREX - A FACILITY FOR INTEGRATED STRUCTURES AND CONTROL RESEARCH

RICHARD QUARTARARO

AND

JAMES HARRIS

SPARTA, INC.
LAGUNA HILLS, CALIFORNIA

OUTLINE

The Advanced Space Structures Technology Research Experiments (ASTREX) Laboratory was conceived by the Air Force Astronautics Laboratory (AFAL) to provide the control/structure interaction community with a versatile research facility. Under the direction of Mr. Kevin Slimak and Dr. Alok Das, ASTREX was envisioned as a laboratory for demonstrating advanced structures and control technologies on realistic models of high performance spacecraft.

This paper summarizes a contracted effort to develop a conceptual design for ASTREX.

- **STRUCTURE/CONTROL TEST FACILITY NEEDS**
- **ASTREX DESIGN CONCEPT**
- **FACILITY OPERATION PLAN**
- **SUMMARY**

STRUCTURE/CONTROL DEVELOPMENT IS REQUIRED

A review of future SDI and AF spacecraft identified several that will benefit from new integrated structures and control technology: Space Based Laser (SBL), the mission mirror for a Ground Based Laser (GBL) system, Neutral Particle Beam (NPB), Electromechanical Launcher (EML), Space Surveillance and Tracking System (SSTS) and Space Based Radar (SBR). SBL and GBL structure/control issues have been characterized in a number of analytical studies. Their need to obtain precise performance from large optics, which must be rapidly retargeted and operated in the presence of severe onboard vibration disturbances, causes the most demanding structure/control issues. NPB and EML are long beam-like spacecraft that must maintain critical alignments while subjected to disturbances from slewing maneuvers and onboard equipment. SSTS spacecraft designed to satisfy mid-term SDI requirements are characterized by two or three agile gimballed sensors, at least one of which is large. Design studies have not completely defined the structure/control issues for these spacecraft. Many recent studies of advanced SBR spacecraft have selected phased array radar, thereby eliminating the need for rapid attitude maneuvers. However, the shape of phased arrays must be maintained accurately, and unacceptable vibration disturbances might be caused by rapid evasive maneuvers.

	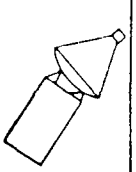 SBL	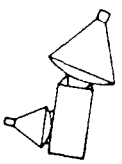 GBL	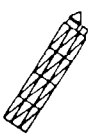 NPB	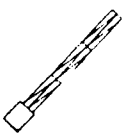 EML	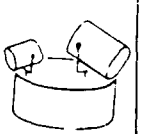 SSTS	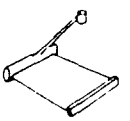 SBR
• RETARGETING	X	X	X	X	X	
• VIBRATION SUPPRESSION	X	X	X	X	?	?
• SHAPE/ALIGNMENT	X	X	X	X		X
• CONTROL/STRUCTURE INTERACTION	X	X	?		?	
• INTER-BODY POINTING DISTURBANCE		X			X	
• PERFORMANCE VALIDATION	X	X	X	X		X

CURRENT SDI TEST FACILITIES DO NOT ADDRESS ALL STRUCTURE/CONTROL ISSUES

The few existing government facilities for structure/control R&D either (i) do not directly address the foregoing space systems or (ii) deal with a subset of a system's issues. Facilities in the first category include the Draper/AFAL Slew Laboratory, NASA COFS Laboratories, the AFWAL/MSFC VCOSS Laboratory and the JPL/AFAL Antenna Control Laboratory. They are excellent facilities for developing basic concepts but do not address configuration-specific issues for the spacecraft listed above. Facilities in the second category include the AFWL Aluminum Beam Expander Structure (ABES), which is planned to be replaced by the System Pointing Integrated Control Experiment (SPICE), and the Martin/SDI Rapid Retargeting and Precision Pointing (R2P2) Laboratory. Each addresses a subset of the SBL structure/control technology issues.

- **NO GOVERNMENT FACILITIES FOR NPB, EML, SSTS, SBR**
- **SOME GBL ISSUES ARE ADDRESSED IN SBL FACILITIES**
- **LIMITED SBL TEST FACILITIES DO NOT:**
  - ***ADDRESS ALL ISSUES***
  - ***PROVIDE A GENERAL CAPABILITY FOR DEMONSTRATING NEW HARDWARE AND ALGORITHMS***

ASTREX WILL PROVIDE A NEEDED STRUCTURE/CONTROL TEST FACILITY

The ASTREX Laboratory objectives established by AFAL are intended to define a facility for performing a broad range of integrated structures and control experiments on scale model spacecraft.

OBJECTIVES

- **VERSATILE FACILITY TO:**
  - **Address Integrated Controls and Structures Issues**
  - **Demonstrate New Actuators, Sensors, Algorithms, Structures**
- **RESULTS SCALABLE TO SDI WEAPON AND SURVEILLANCE SPACECRAFT**
- **RAPID CHECKOUT OF NEW CONCEPTS**

ASTREX INITIAL CONFIGURATION

A series of design trade studies were performed to define a conceptual design for ASTREX. The Laboratory consists of five major elements:

- o Test Article -- An SBL is shown, although a wide variety of test articles could be accommodated.
- o Real Time Computing -- The control algorithms and other functions are implemented on the Control/Display Computer, which communicates with the Test Article through the Interface Electronics (input/output processor).
- o Experiment Control and Data Handling -- An Ethernet connection enables the Real Time Computers to communicate with one of AFAL's existing general purpose computers (VAX 8600). Data storage, terminals and strip chart recorders are also provided.
- o Orbit Simulation -- Free fall is simulated by supporting the Test Article at its c.g. on a spherical air bearing, providing at least + 20 degrees of free motion in each rotational axis.
- o Facility and Support Equipment -- The Test Article is contained in a 40 ft x 40 ft x 40 ft laboratory with a connecting office/control room. An overhead crane helps to move equipment into and out of the laboratory. Regulated power and dry air are supplied to the laboratory to run test equipment and the air bearing.

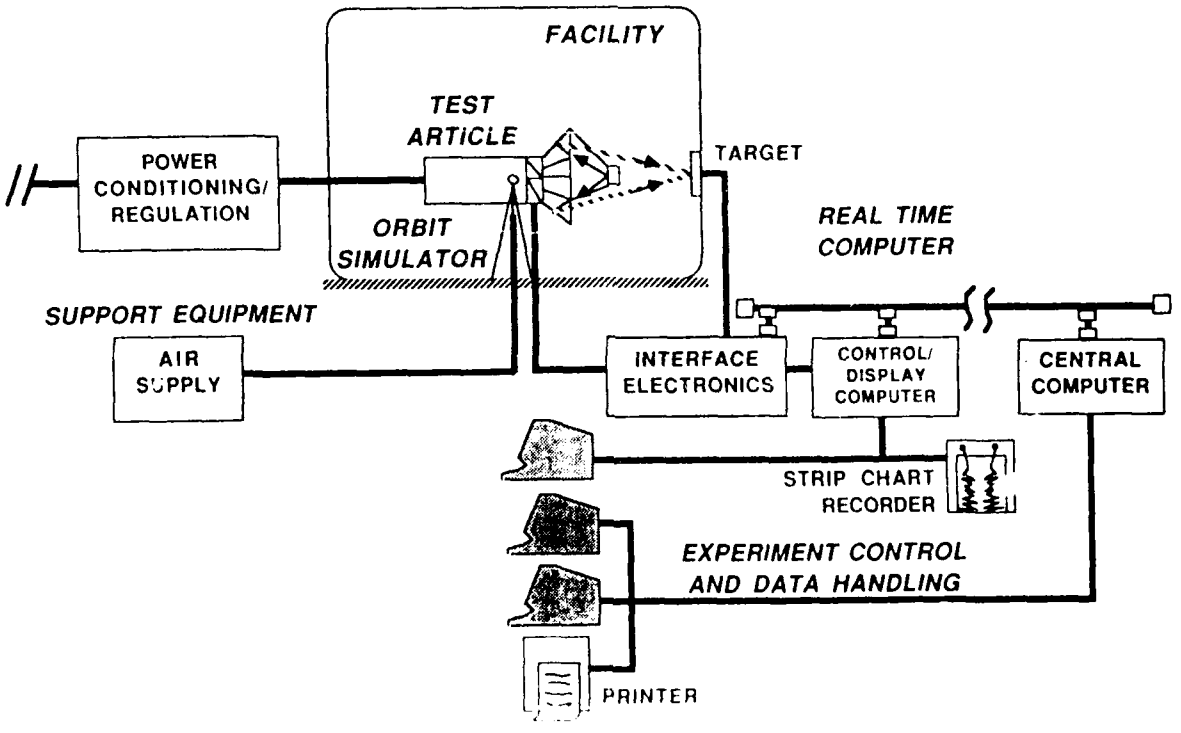

INITIAL TEST ARTICLE

The ASTREX facility design concept has been selected to accommodate a wide variety of test articles that may be of interest to the structures/ control R&D community and/or spacecraft hardware development programs. The question of which test article should be included in the initial facility was the subject of a trade study which identified the NPB and SBL as the best choices. The selection was based on usefulness, cost and legacy criteria.

The selected test article is a Space Based Laser spacecraft with a dynamically scaled structure. Lengths and transverse dimensions of structural elements are scaled by a factor of approximately four, and structural element stiffness is scaled to match operational modal frequencies and shapes.

- NPB AND SBL ARE APPROPRIATE TEST ARTICLES
- SBL SELECTED BECAUSE TECHNOLOGY ISSUES ARE BETTER DEFINED

STRUCTURE

- OVERALL LENGTH < 10M
- WEIGHT APPROX. 2,300 LBS
- NON-ARTICULATED, FLEXIBLE AFT BODY
- TEST ARTICLE MODES ~ OPERATIONAL MODES

ACTUATORS

- 6 HIGH LEVEL COLD GAS THRUSTERS
- 6 LOW LEVEL COLD GAS THRUSTERS
- PROVISIONS FOR 2 OR 3 SINGLE AXIS CMGS (TO BE ADDED LATER)
- 6 OR MORE PROOF MASS ACTUATORS

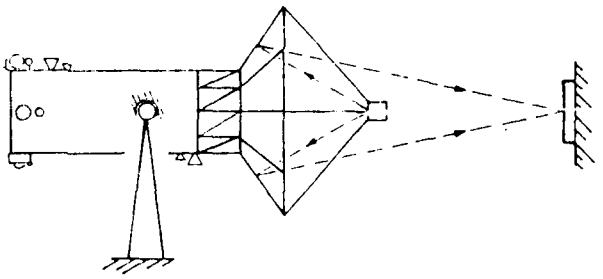

SENSORS

- 3 RATE INTEGRATING GYROS
- 6 OR MORE ACCELEROMETERS
- OTHERS (TBD)

AIR BEARING

- SPHERICAL (3 D.O.F.)
- ± 20° ALL AXES
- 5K - 10K LB CAPACITY

PERFORMANCE DEMONSTRATION SENSOR

- ONBOARD LASER
- EXTERNAL TARGET

COMPUTER AND DATA HANDLING SOFTWARE DEVELOPMENT MODE

Development of experiment software will be accomplished with the real time computers connected to an AFAL central computer, a VAX 8600. Programs will be developed at software development stations connected directly to the VAX 8600 acting as a host computer. The Control/Display Computer, a MicroVAX III using VAXELN, and the Interface Electronics, a 68020-based input/output processor, will both be programmed in this mode. For real time debugging, the software will be downloaded via Ethernet to the target computer. VAX code will be debugged in a dual mode, with the programmer using this workstation to control the execution. 68020 code will be developed in a more traditional cross compiler environment.

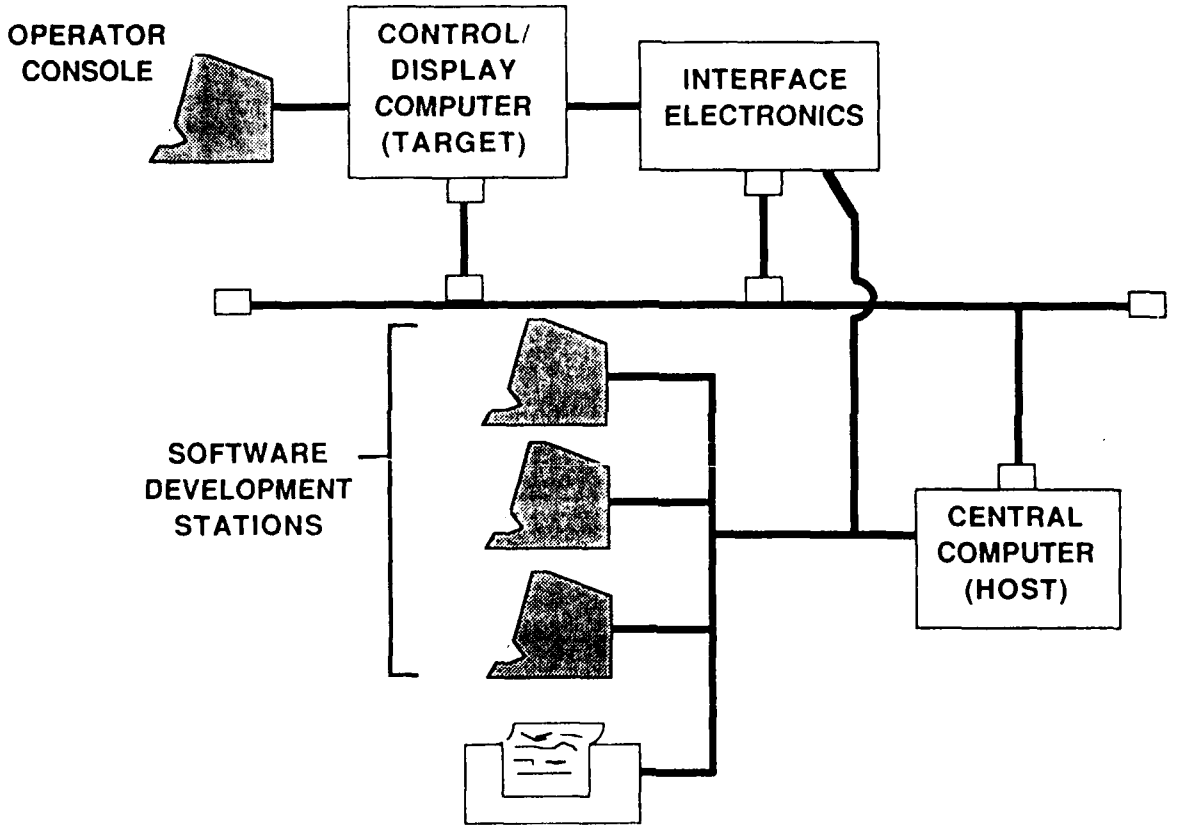

COMPUTER AND DATA HANDLING EXPERIMENT MODE

This chart illustrates the computer and data handling configuration during an experiment. Programs for the Control/Display Computer and Interface Electronics will be downloaded via Ethernet from the host VAX 8600. An operator console tied to the Control/Display Computer will allow the experimenter to set up the experiment, execute, and monitor certain status data. Strip chart recorders will be used to display important parameters in real time, while the experiment data will be stored in the control/display computer's memory for download to disk and post processing. The Interface Electronics and it's custom I/O processor will provide the only interface between the Test Article and the ASTREX computers.

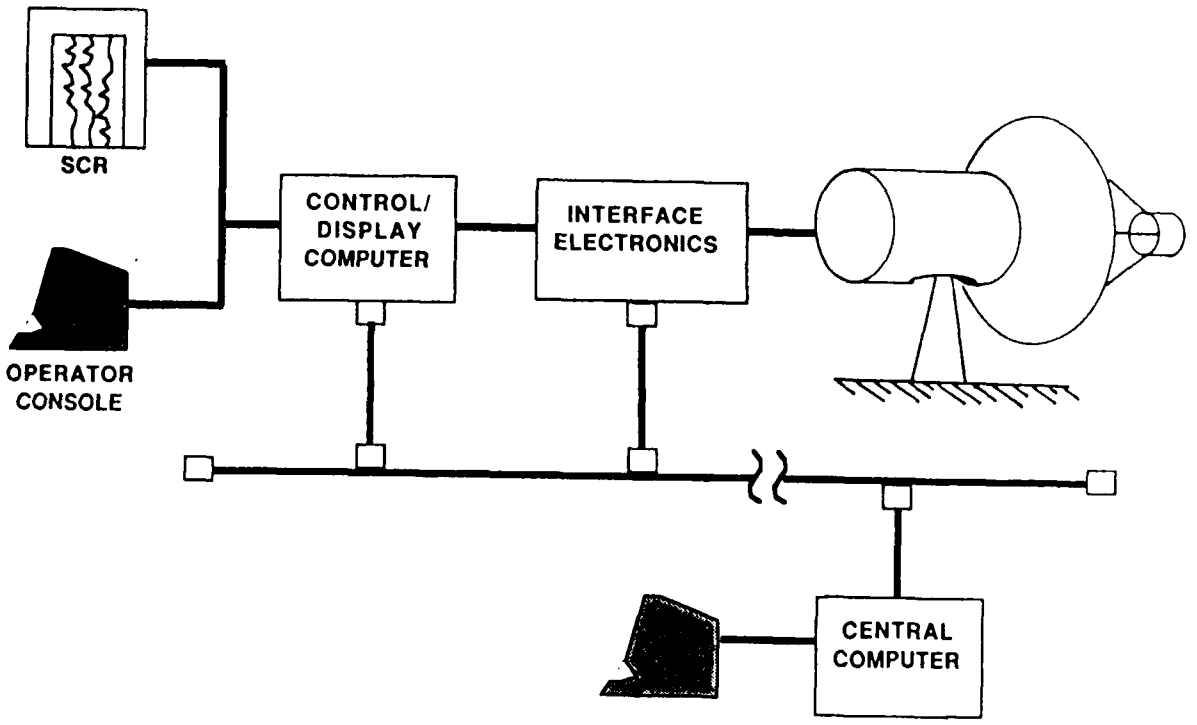

ASTREX IS ADAPTABLE

An important feature of the ASTREX design is its ability to handle a wide variety of test articles. This adaptability is achieved through the general purpose laboratory infrastructure and the use of test article equipment and orbit simulator components on multiple test structures.

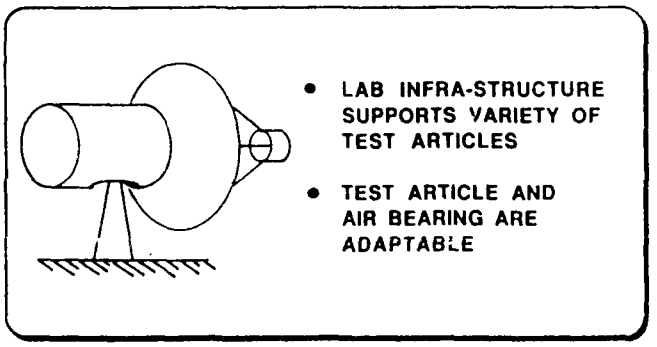

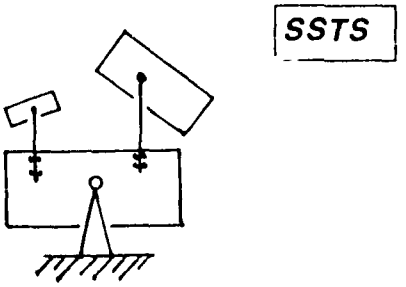

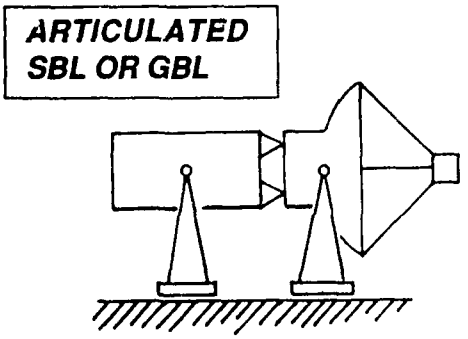

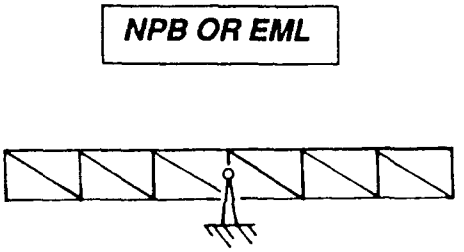

FACILITY OPERATION PLAN

Structures/control researchers will be provided with information and support to facilitate their use of the ASTREX Laboratory. Experimenters wishing to check out new control or system identification algorithms will be able to code in either C or FORTRAN.

AFTER FACILITY ASSEMBLY AND CHECKOUT:

- **USER'S GUIDE WILL BE PUBLISHED**
  - PHYSICAL DESCRIPTION OF FACILITY
  - DATA ACQUISITION SYSTEM AND CONTROLLER SPECIFICATIONS
  - SENSOR AND ACTUATOR SPECIFICATIONS
  - PHYSICAL DESCRIPTION OF TEST ARTICLE
  - PRELIMINARY MATH MODEL
  - SOFTWARE DEVELOPMENT GUIDELINES
- **USERS WORKSHOP WILL BE CONDUCTED AT AFAL**
  - FAMILIARIZE POTENTIAL USERS WITH FACILITY
  - PERFORM PRELIMINARY DEMONSTRATIONS
  - DESCRIBE CONTRACTUAL VEHICLES FOR FUNDING FACILITY USERS

ASTREX FACILITY WILL BE OPERATED BY AFAL DESIGNATED PERSONNEL

USERS WILL INTERFACE WITH FACILITY OPERATOR PRIOR TO AND DURING EXPERIMENTS

- **USERS WILL BE ENCOURAGED TO USE FACILITIES AT AFAL FOR SOFTWARE DEVELOPMENT AND TO PARTICIPATE IN EXPERIMENT SETUP**
- **USERS WILL NOT RUN EXPERIMENT**

SUMMARY

The ASTREX facility will be useful to both the structures/control research community and spacecraft hardware development programs. Its development will be paced by funding availability; the laboratory could be operational within one year.

ASTREX PROVIDES:

- **A FACILITY FOR DEMONSTRATING SOLUTIONS TO STRUCTURE/CONTROL PROBLEMS FOR SDI WEAPON AND SURVEILLANCE SPACECRAFT**
- **A RAPID-RESPONSE RESOURCE AVAILABLE TO SDI/ USAF SPACECRAFT PROGRAMS AND STRUCTURE/ CONTROL RESEARCH COMMUNITY**
- **UNIQUE FEATURES**
  - EQUIPMENT AND PERSONNEL INFRASTRUCTURE + BUILDING BLOCK APPROACH = VERSATILITY
  - LARGE ANGLE MOTION OF FLEXIBLE SPACECRAFT
  - GROUND TEST METHODS TO BE ADDRESSED

ASTREX CAN BE OPERATIONAL IN FY88

ACKNOWLEDGEMENT

This work was funded by the Air Force Astronautics Laboratory at Edwards Air Force Base, California.

ACTUATOR STRUCTURE INTERACTIONS

D.C. Zimmerman
Assistant Professor
Department of Engineering Science
University of Florida
Gainesville, FL 32611

D.J. Inman
Professor
Department of Mechanical & Aerospace Engineering
State University of New York at Buffalo
Buffalo, NY 14260

Second NASA/DOD Control/Structure
Interaction Technology Conference
17-19 November 1987
Colorado Springs, CO

This work supported in part by NASA Grant numbers NGT 33183801 and NAG 1785 through the Structural Dynamics Branch at NASA Langley Research Center and AFOSR Grant numbers F49620-86-6-0111 and AFOSR 85-0220 through the Mathematics and Information Sciences Program.

INTRODUCTION

This paper presents an analysis of the interaction between a structure and an actuator used to control the structure. The control device is the NASA/UVA/UB proof mass actuator (PMA). Two structures are used in this study. One is a simple cantilivered beam made of a quasi-isotropic composite used for experimental tests. The second is a two element (statically reduced) model of the COFS I flight article. Figure 1 illustrates a simple idealized mechanical model for the combined structure/PMA system (ref. 1) ,the equations of motion (ref. 2) and a preliminary look at the effect of increase in rate feedback gain on modal damping ratios (ref. 3).

Structure/Actuator Dynamic Model

o Idealized Mechanical Model

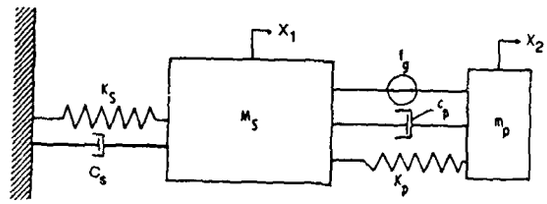

o Equations of Motion

$$\begin{bmatrix} M_s & 0 \\ 0 & m_p \end{bmatrix}\begin{bmatrix} x_1 \\ x_2 \end{bmatrix} + \begin{bmatrix} C_s + c_p & -c_p \\ -c_p & c_p \end{bmatrix}\begin{bmatrix} x_1 \\ x_2 \end{bmatrix} + \begin{bmatrix} K_s + k_p & -k_p \\ -k_p & k_p \end{bmatrix}\begin{bmatrix} x_1 \\ x_2 \end{bmatrix} = \begin{bmatrix} -f_g \\ f_g \end{bmatrix}$$

o Effect of Rate- Feedback Gain on Modal Damping

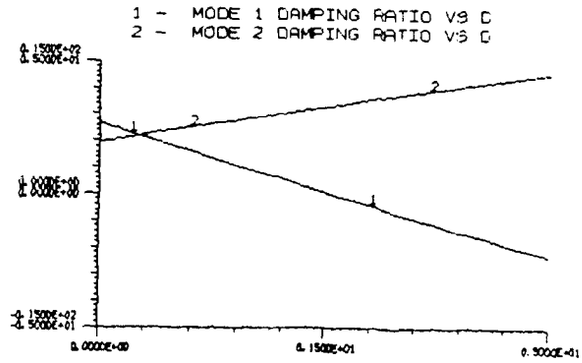

$\Rightarrow$ Actuator Dynamics Can Not be Neglected

FIGURE 1

PMA DETAILS

The PMA is a space realizable actuator causing minimal parasitic dynamic effects when attached to a flexible structure. The actuator system is comprised of a movable proof mass, a fixed coil, two collocated sensors, a digital microcontroller, and a power amplifier. All of the components are mounted as a single unit with power lines being the only external cables required by the actuator system to operate. When attached to a structure, the actuator can be ideally modeled as a single degree of freedom untuned vibration absorber with a force generator acting between the structure and the absorber mass. The transfer function for the actuator is given in figure 2.

$$\frac{F(s)}{V(s)} = \frac{G_1 G_2 m_p s^2}{m_p s^2 + G_1 G_2 c_p s + G_1 G_2 k_p}$$

FIGURE 2

MEASURED FREQUENCY RESPONSE

Figure 3 shows the measured frequency response of the actuator/composite beam system in both the uncontrolled (actuator off and stripped) and the controlled (actuator on) states. Note that the uncontrolled transfer function shows two definite modes of vibration (3.49 and 29 Hz) and that the controlled (closed loop) transfer function shows three clear modes (3.19, 4.03 and 28 Hz, clear from circle fits). The appearance of the third mode is due to the PMA dynamics and is referred to as the actuator mode. The actuator mode is the sharp narrow spike at 3.19 Hz. The first structural mode is shifted up to 4.03 Hz and is heavily damped by the actuator.

Measured Frequency Response

o Uncontrolled Structure

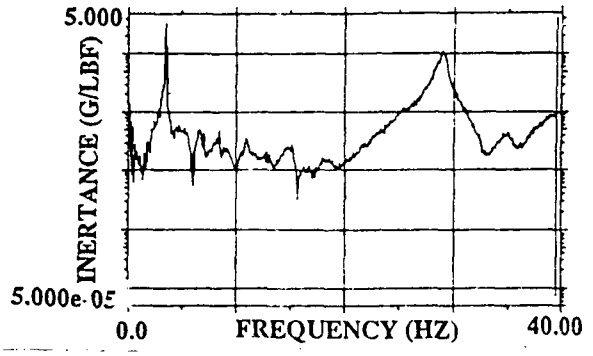

Measured Inertance Frequency Response - Uncontrolled Structure

o Controlled Structure

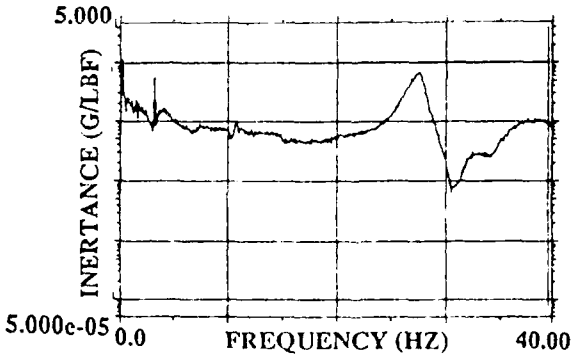

Measured Inertance Frequency Response - Controlled Structure

FIGURE 3

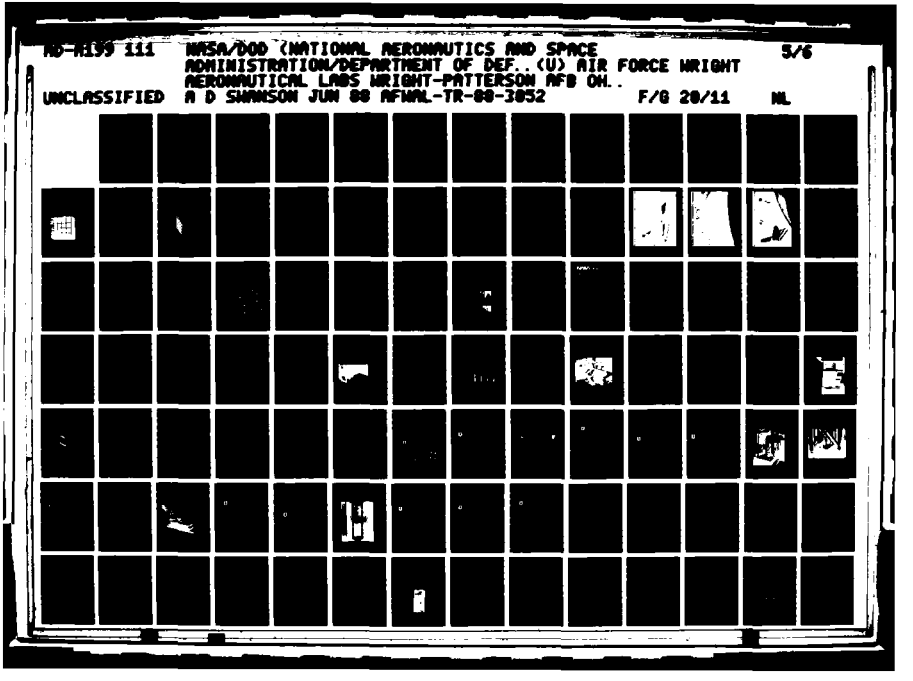
AD-A199 111 NASA/DOD (NATIONAL AERONAUTICS AND SPACE ADMINISTRATION/DEPARTMENT OF DEF..(U) AIR FORCE WRIGHT AERONAUTICAL LABS WRIGHT-PATTERSON AFB OH..
5/6
UNCLASSIFIED A D SWANSON JUN 88 AFWAL-TR-88-3052 F/G 20/11 NL

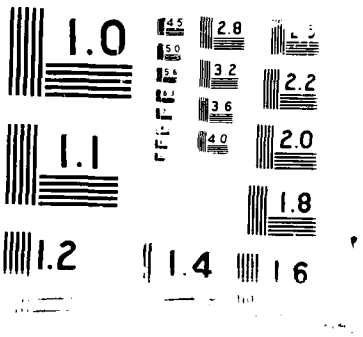
1.0
1.1
1.2
1.4
1.6
1.8
2.0
2.2
2.8
3.2
3.6
4.0

MEASURED TIME RESPONSE

The acceleration of the tip of the beam was measured in both controlled and uncontrolled states as illustrated in figure 4. Note that the uncontrolled structural response is very lightly damped whereas the controlled structural modes are heavily damped dying out in less then two seconds. The actuator dominated mode however, persists for long periods of time. In this experiment, the addition of digital quantization error also reduces the damping of the actuator dominated mode (ref. 3). The results show the degradation of system performance due to actuator dynamics.

Measured Tip Acceleration

o Uncontrolled Structure

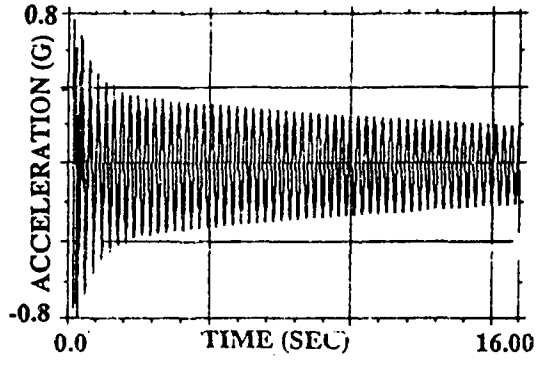

o Controlled Structure

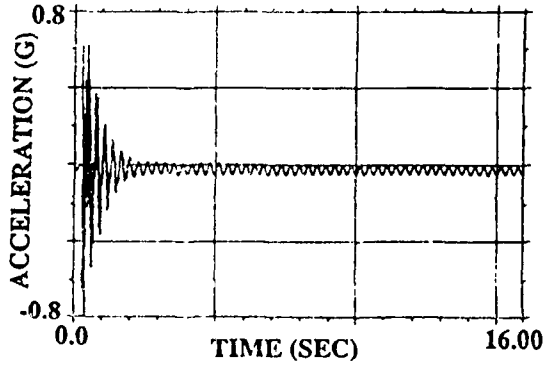

FIGURE 4

SIMPLE COFS I MODEL

The COFS I structure was modeled using a two element finite element model with vibration in the x-z plane only. The lumped masses along the beam were ignored. The lumped mass at the tip of the beam was included. Appropriate translations and rotations were included. Static condensation techniques were then utilized to obtain the 2x2 stiffness matrix, and rotational mass was ignored to obtain the 2x2 mass matrix (with concentrated tip mass). The dynamic model of the proof-mass actuator was then added to the model (at the tip of the beam), the resulting dynamic model is then a 3 DOF system. The mass of the proof-mass was taken to be the sum of the proof-mass of the tip actuators that counteract vibration in the x-z plane (2 actuators @ 11kg/actuator = 22kg; this is only 7% of the structural mass). The spring -rate of the actuators were varied to obtain the different frequency cases. The back-emf damping was adjusted per case (except case #5 where we are adjusting it) so that the actuator damping ratio (just m_p, c_p,k_p alone was 5%.

IDEAL ACTUATOR

Figure 5 shows the effect of the rate-feedback control law on the structures damping using an ideal actuator for control law implementation. That is, the actuator applied a force that directly opposes the tip velocity (a damper connected to ground). The control greatly increases the damping of mode 1; mode 2 is only slightly affected due to the location of the actuator.

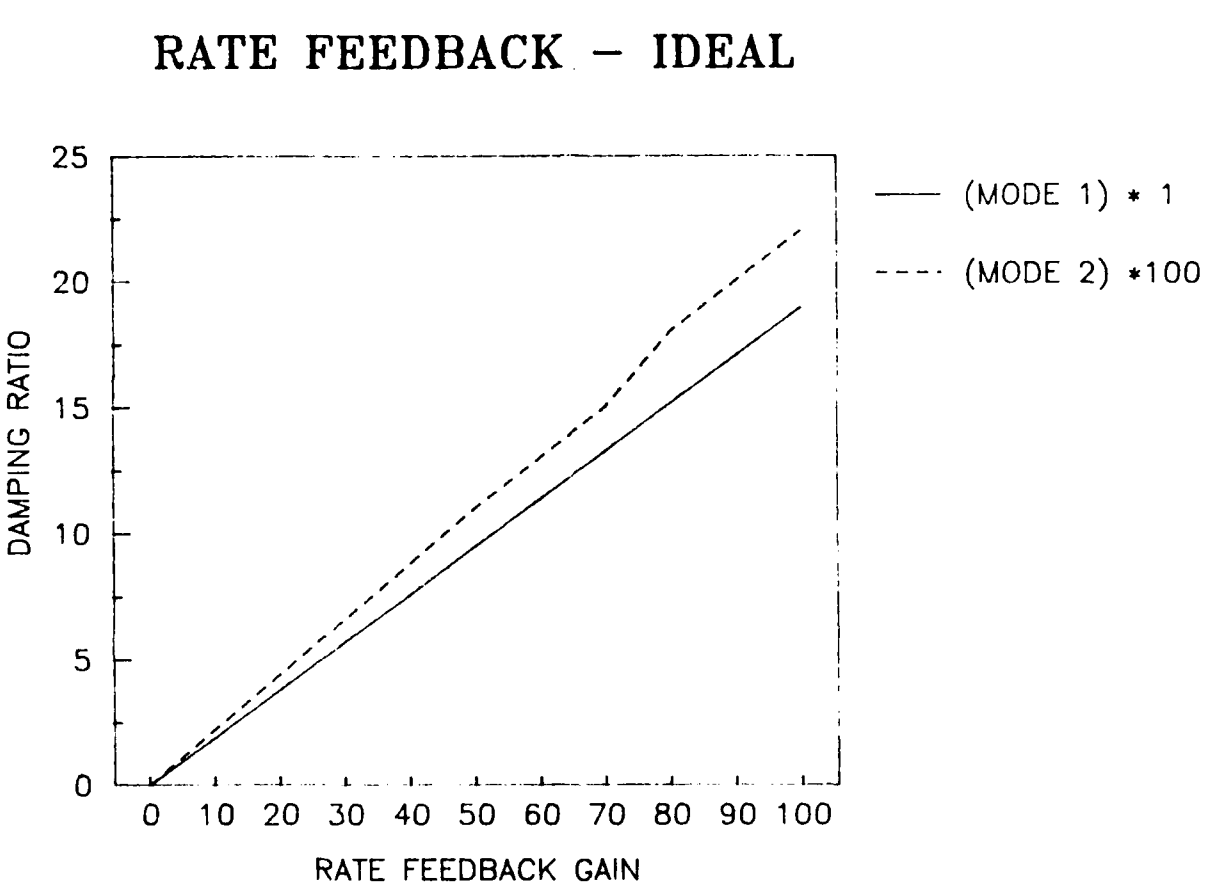

FIGURE 5, CASE 1

PMA PROPERLY CHOSEN

Figure 6 shows the effect of the rate feedback control law on the structures damping using a proof-mass actuator for control law implementation. The break frequency (sqrt (k_p/m_p)) of the actuator has been set to be lower than either of the structural modes of vibration (the actuator will be stroke-length limited). Therefore, with the proper sign for the rate feedback gain, the damping will be increased in those two structural modes. Note that the PMA adds an additional DOF to the system, and therefore an additional mode of vibration. The eigenvectors of the system show that the lowest mode of vibration is "actuator dominated," while the other two are "structure dominated". This figure shows that as the rate-feedgack gain is increased, the two structure dominated modes' damping is increased (mode 2 dramatically, mode 3 slightly for the same reason as Case #1), but that the actuator dominated mode damping (mode 1) decreases monotonotically. In fact, there is some point at which the mode is unstable (negative damping), and therefore the total system is unstable. Therefore, there is a "high-gain" limitation on this control law (which would not be seen unless actuator dynamics are modeled).

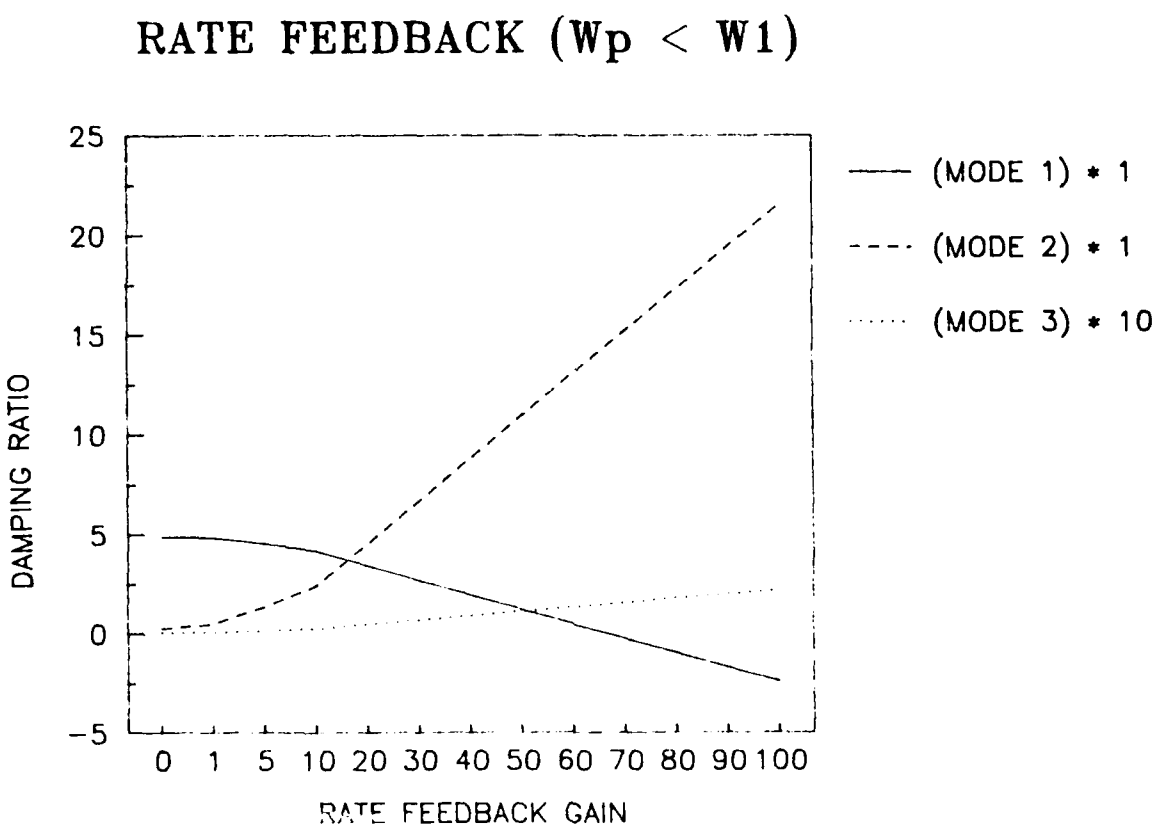

FIGURE 6, CASE 2

ACTUATOR FREQUENCY BETWEEN STRUCTURAL FREQUENCY

In this case, the PMA break frequency was chosen to lie between the two structural modes of vibration. Eigenvectors show that mode 1 is an actuator-structure mode (both play a role), mode 2 is actuator dominated, and mode 3 is structure dominated. From the PMA model, it is known that energy will be dissipated (damping) in one of the structural modes and energy will be added in the other structural mode (ref. #1). Which mode is damped is dependent on the sign of the feedback gain. Figure 7 shows this effect. Even at "small" feedback gains, one of the structural modes is unstable. The "smallness" is dependent on how damped (with a zero feedback gain) the structure is due to the inherent damping of the back-emf damping. The example shows that selecting the break-frequency to lie between structural modes is not feasible (unless additional compensation is used).

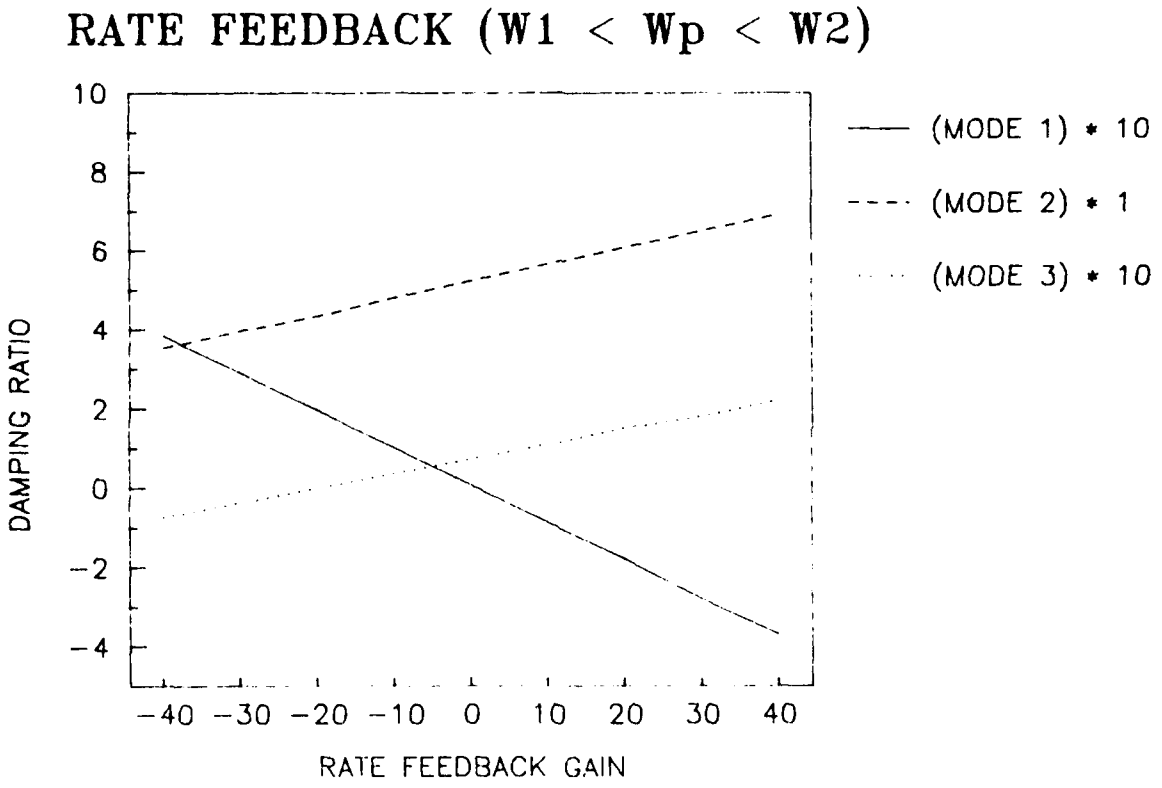

FIGURE 7, CASE 3

ACTUATOR FREQUENCY ABOVE STRUCTURE FREQUENCIES

In this case, the PMA break frequency was chosen to be higher than the structural modes of vibration. Therefore, the actuator will be output force limited (since the force output roles off at 40 dB/dec from the break frequency) (ref. #1,2). This could be done for this 2 DOF structure, what can be done for a structure that has an infinite number of DOF's would require further research. Eigenvector analysis reveals that the actuator plays a big part in each mode, however, mode 3 is clearly actuator dominated. Figure 8 shows that increasing the feedback gain increases the structural damping (to a small extent in comparison to case #2 because of the force output limitation), but that the actuator dominated mode damping decreases and eventually goes unstable. This is again the "high-gain" limitation of the PMA with this control law.

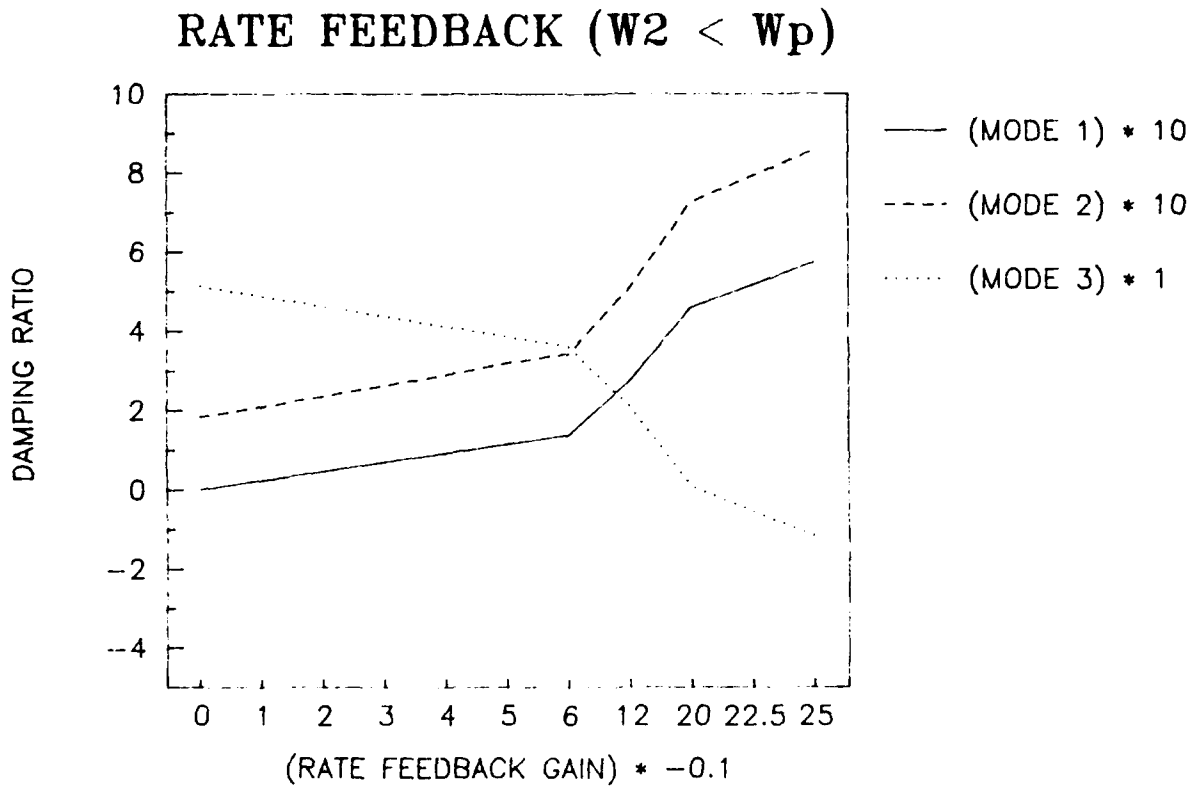

FIGURE 8, CASE 4

WHERE THE DAMPING COMES FROM

It is obvious that the amount of the back-emf damping introduced by the PMA dynamics into the system greatly effects the stability of the controlled structure. Figure 9 shows the effect of the back-emf damping ratio on the "high-gain" limitation and on the achievable damping ratio. Parameters from case #2 were used. The actuator damping ratio was varied from 0% to 10%. The gain at which the actuator dominated mode went unstable was noted, as well as the damping ratio of mode 2 (the first structural mode). The figure shows that at a 0% back-emf dampng ratio, the unstable gain is zero. That is, the control law is unstable for all gains. As the damping ratio is increased, the high gain also increases, as well as the damping ratio of the first structural mode. (as we increase the gain, the increase in damping of the structural modes is "stolen" from the damping of the actuator mode).

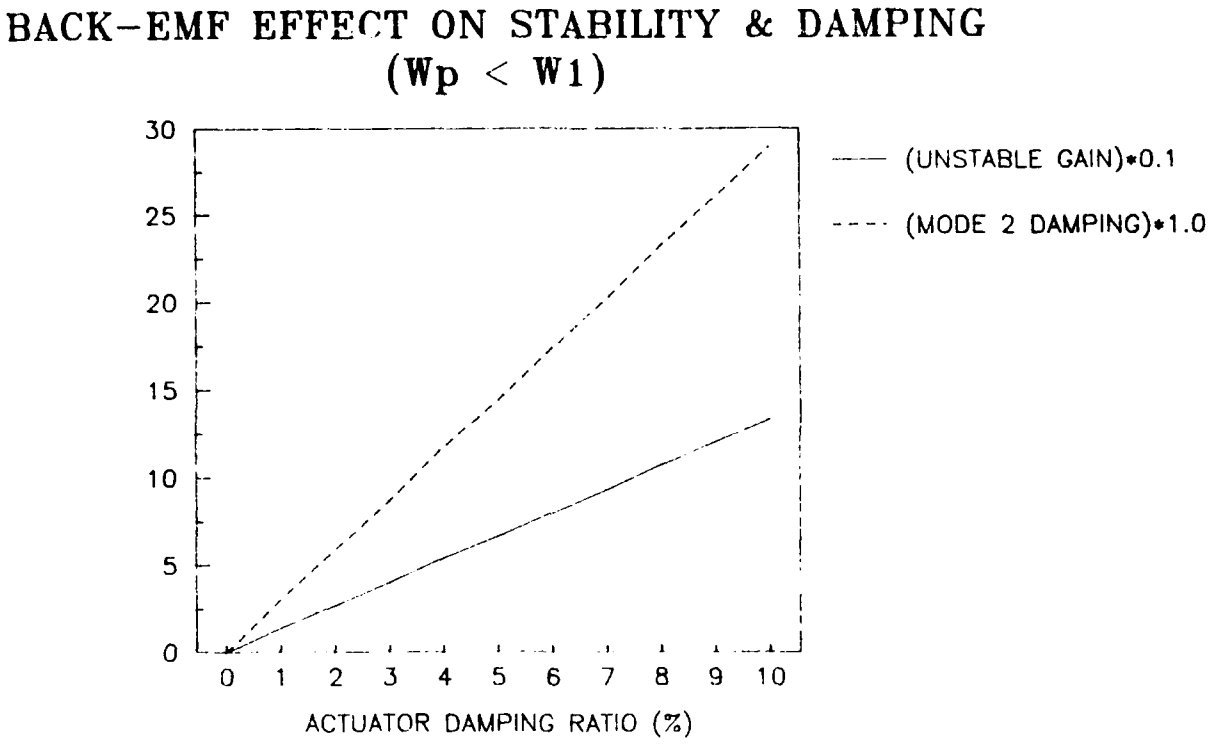

FIGURE 9, CASE 5

SUMMARY

- PMA limited by low frequency at high gain
- actuator back emp is source of increased modal damping and is required for stability
- high gain instability is due to control structure interaction
- proper consideration for control/structure interactions allows for more effective use of PMA as a control device and avoids potential instabilities and/or performance degradation
- proper considerationis are
  - actuator frequency should be below structure frequency for maximum damping
  - compatability between controller design, high gain and back emf is required

REFERENCES

1) Zimmerman, D.C., Horner, G.C. and Inman, D.J. "Microprocessor Controlled Force Actuator," to appear AIAA Journal of Guidance, Control and Dynamics, Jan.-Feb. 1988.

2) Zimmerman, D.C., Dynamic Characterization and Microprocessor Control of the NASA/UVA Proof-Mass Actuator, M.S. Thesis, Department of Mechanical & Aerospace Engineering, State University of New York at Buffalo, June 1984.

3) Zimmerman, D.C. and Cudney, H.H., "Practical Implementation Issues for Active Control of Large Flexible Structures," Proceedings of the 6th VPI&SU/AIAA Symposium on Dynamics and Control of Large Structures, June 29-July 1, 1987, Blacksburg, Virginia.

EXPERIMENT IN MODELING AND PARAMETER ESTIMATION OF FLEXIBLE STRUCTURES

Alok Das
Timothy J . Strange
Waid T. Schlaegel
John M. Ward

Interdisciplinary Space Technology Branch
Air Force Astronautics Laboratory
Edwards AFB, California

Second NASA/DoD CSI Technology Conference
November 17-19, 1987

INTRODUCTION

A number of DoD/NASA space missions proposed for the 1990's and beyond will require orbiting space structures the size of a football field. Such spacecraft fall under two broad categories. The first category of spacecraft, such as the surveillance radars and communication antennas, are being designed to be stowed in a compact form for launch and to unfold to the operational state in orbit. The fact that such structures are incapable of supporting their own weight under 1-g, precludes accurate ground testing. The other class of large space structures is the space defense platforms. Although characterized by relatively stiffer structure, the mission of the space defense platforms requires very precise pointing and vibration control in the presence of on-board disturbances.

Precision control system design requires an accurate mathematical model of the structure; however, the current modeling codes such as NASTRAN are incapable of providing analytical models to the desired precision. The large physical size coupled with gravity loading effects make accurate ground-based system identification impossible. The favored approach is to design a programmable controller based on the "best" ground-based mathematical model, to perform on-orbit parameter estimation and to tune the controller to the new system parameter values. This paper describes an experiment developed at the Air Force Astronautics Laboratory (AFAL) for comparing various modeling and parameter estimation techniques.

NEED: ACCURATE SYSTEM MODEL IS A MUST FOR PRECISE POINTING AND CONTROL OF LARGE SPACE STRUCTURES

- **PROBLEMS IN STRUCTURAL MODELING**
  - **NO INFORMATION ON MODAL DAMPING**
  - **SIGNIFICANT ERROR IN HIGHER MODAL FREQUENCIES**
  - **UNMODELED VARIATIONS IN PHYSICAL AND MATERIAL PROPERTIES**
  - **UNMODELED NONLINEARITIES SUCH AS JOINTS**
- **PROBLEMS IN GROUND TESTING**
  - **DIFFICULT/IMPOSSIBLE TO TEST FLEXIBLE LSS ON GROUND**
  - **GRAVITY BIAS**
  - **ATMOSPHERIC EFFECTS**

A SOLUTION : ON-ORBIT SYSTEM IDENTIFICATION

Figure 1

ON-ORBIT SYSTEM IDENTIFICATION

Currently there exists a large body of literature on system identification/parameter estimation methodologies in use in diverse fields such as Aerospace, Civil, and Electrical engineering (Ref. 1). However on-orbit identification of space structures poses new and challenging problems which will require either the development of new identification techniques or major modifications to existing methods before they could be used. For example, some ground modal identification techniques use a large number of sensors and mechanical shakers to determine the mode shapes. On-orbit, one is limited by the availability of hardware, also since special equipment will not be available, it will not be possible to conduct tests with specialized actuation needs. Another consequence of orbital testing is that the location of sensors and actuators cannot be varied. This problem may be partly remedied with the availability of embedded distributed sensors and actuators now under development. Another limiting factor will be the lack of human interaction during tests. Also a number of identification techniques are extremely computationally intensive and would be unsuitable for the limited computational power on board.

FACTORS IN DETERMINING APPROPRIATE IDENTIFICATION TECHNIQUES

- HUMAN INTERACTION REQUIREMENTS
- NUMBER, LOCATION & TYPE OF SENSORS/ACTUATORS
- ON-BOARD COMPUTATIONAL POWER
- CLOSED LOOP VS OPEN LOOP
- TYPE AND DURATION OF TESTS
- SPECIALIZED EQUIPMENT REQUIREMENT

Figure 2

EXPERIMENTAL STRUCTURE

Thus a need was felt at the AFAL to develop a simple ground test-bed to compare and test modeling and system identification techniques for future large flexible structures. It was decided that a generic structure which was simple to model, yet which possessed the basic dynamic characteristics of the future LSS (low fundamental vibration frequency, large number of closely spaced modes, etc.) should be selected. An additional requirement was that the structural vibrations should be visible during testing.

An appropriately sized 2-dimensional aluminium grid structure, cantilevered at one end, was chosen as the experimental structure. The selection was based on a survey of existing LSS experimental facilities and in-house modeling of various candidate test articles.

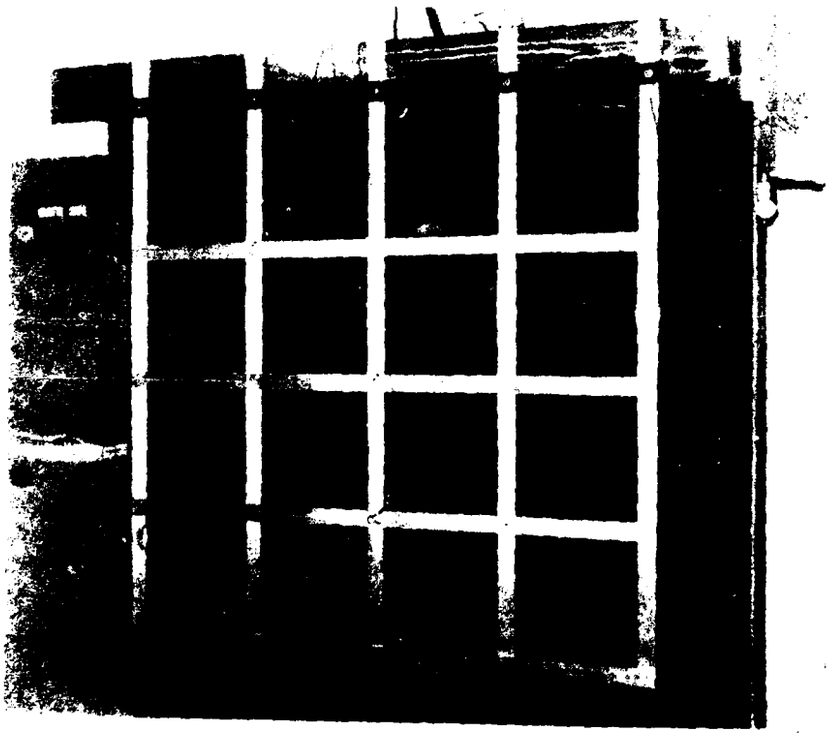

Figure 3

HARDWARE DESCRIPTION

The experimental structure consists of a 5-ft x 5-ft 2-dimensional grid made up of 2-inch wide and 1/8-inch thick 6061-T6 aluminium strips. At every point where the horizontal and vertical strips cross each other, they are connected by four rivets, thus effectively removing any play at the joints. The grid hangs vertically down, being cantilevered at the top to a large I-beam which itself is anchored to a cinder block wall. Directly behind the grid, 20 steel plates (14-inch x 14-inch x 1/4-inch each) are attached to the wall as a base for mounting sensors and actuators such as a mechanical shaker, proximity sensors, etc.

Currently energy is imparted to the structure using either a electrodynamic shaker or a quartz impulse hammer. The structural vibrations are monitored using high sensitivity piezoelectric and low mass piezoelectric accelerometers, and eddy current proximeters.

HIGH SENSITIVITY PIEZOELECTRIC ACCELEROMETERS

Sensitivity - 500 mV/g ; Range - 10 g ; Frequency Response 5% over 0.2 to 100 Hz ; Weight - 64 gram.

LOW MASS PIEZOELECTRIC ACCELEROMETERS

Sensitivity - 10 mV/g ; Range - 500 g ; Frequency Response - 5% over 4 to 15,000 Hz ; Weight 0.4 gram.

QUARTZ PIEZOELECTRIC LOAD CELLS

Range (compression/tension) - 5 lbs ; Sensitivity - 900 mV/lb Rise Time - < 6 micro sec ; Sensitivity - 0.0002 lbs rms.

ELECTRO DYNAMIC MINI SHAKER

Peak Force - 10 N ; Frequency Response - DC to 18 kHz Displacement - 6 mm peak to peak.

QUARTZ IMPULSE HAMMER

Sensitivity - 50 mV/lbf ; Force Range - 100 lbf ; Frequency Range - to 10 kHz.

Figure 4

EXPERIMENTAL SET-UP

The experimental setup is shown in Figure 5. The structure is excited using either an electrodynamic shaker or an impulse hammer. The magnitude and time history of the force imparted to the structure is measured using load cells in series with the actuator. The structural vibrations are picked up using accelerometers and proximeters. The output of the vibration sensors along with the load cells is first conditioned to ensure that it is zero mean with maximum swings limited to 5 Volts (the maximum range of the data acquisition system). The output is then fed to a patching network where up to 16 signals can be selected for data acquisition. Next the selected signals are filtered using 6th order Butterworth filters to reduce the aliasing effect as much as possible. Finally, if necessary, the signals are amplified to the full range of the data acquisition system. Gains of 1, 6, 11 can be selected for each channel individually. The signals are acquired using a digital real-time controller/data acquisition system with a capacity of 16 inputs and 8 outputs (12 bit precision). The controller can be used either to perform real-time system identification or to acquire data for off-line identification. The complete analog electronics, including the filters, were designed, fabricated and tested to be within 1% of their theoretically predicted performance.

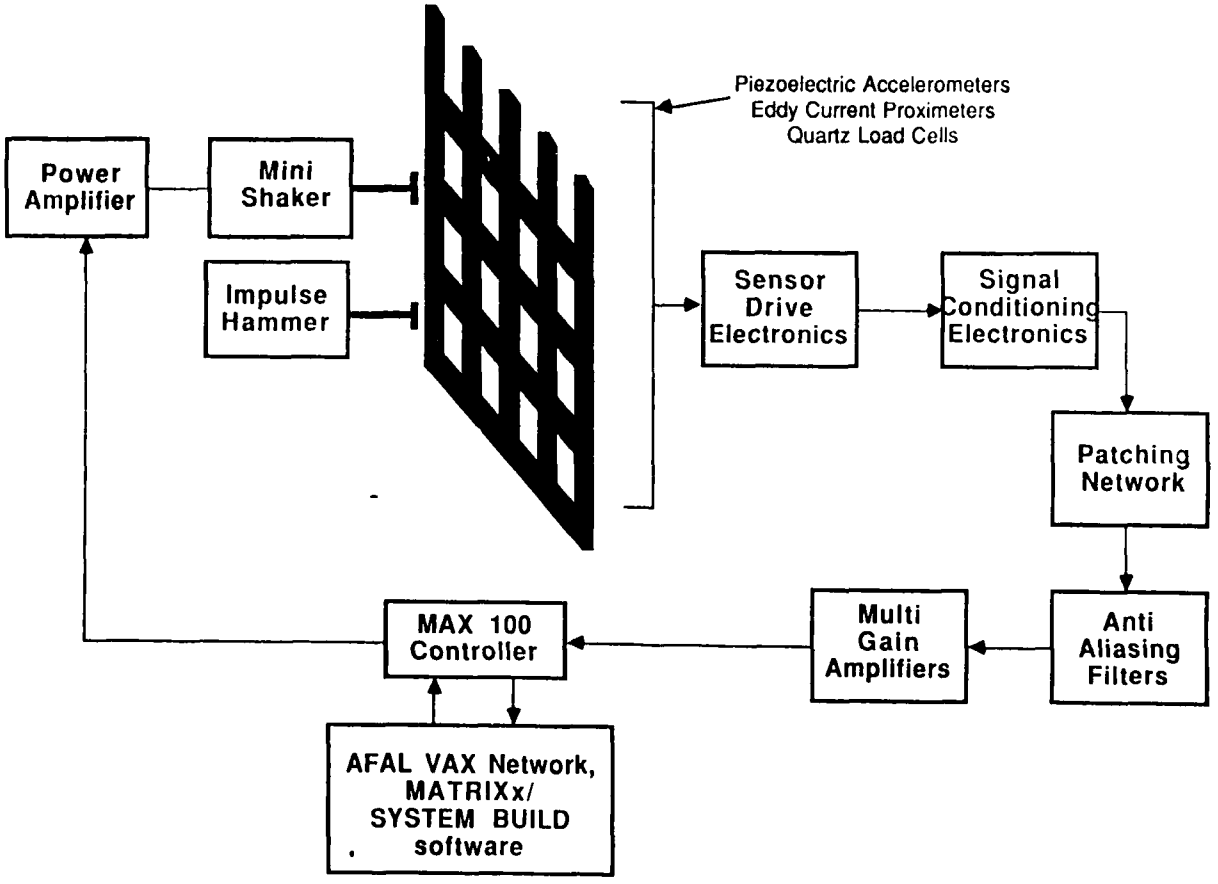

ANTI-ALIASING FILTERS

For proper reproduction of a signal by a sampling system, it is required that signals with frequency higher than half the sampling frequency (fs) should not enter the sampler. Generally a low pass filter is added to sufficiently attenuate signals whose frequency is greater than fs/2, thus reducing the aliasing effect.

The system requirements called for less than 1% attenuation in the pass band of 0-35 Hz with a minimum of 20 db attenuation beyond fs/2 (fs, the sampling frequency, being 150 Hz). A sixth order Butterworth low pass filter (Ref. 2) with a cutoff frequency of 50 Hz was required to meet the specifications. A Butterworth filter was chosen since it exibits a nearly flat response in the passband and rapid attenuation outside the passband. The filter provided an attenuation of 21 db at 75 Hz while limiting the attenuation to under 0.06 db in the pass band. The filter was implemented using operational amplifiers and discrete components. The circuit diagram of the filter is given in Figure 6.

REQUIREMENTS	**SOLUTION**
SAMPLING FREQUENCY - 150 Hz	**BUTTERWORTH FILTER**
< 1% ATTENUATION OVER 0 - 35 Hz	**SIXTH ORDER , LOW PASS**
> 20 db ATTENUATION BEYOND 75 Hz	**< 0.06 db ATTENUATION OVER 0 - 35 db**
	21 db ATTENUATION AT 75 Hz

CIRCUIT DIAGRAM

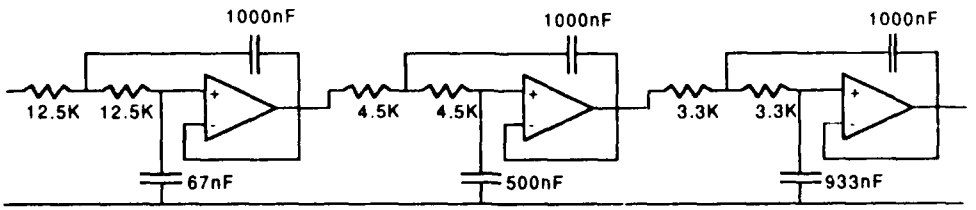

Figure 6

STRUCTURAL MODELING

The grid structure was modeled using the finite element modeling code NASTRAN. Two separate models were developed. In the simpler model, the portion of the aluminium strips between the centers of adjacent joints were modeled as beams. Although this model adequately represented the mass distribution, the stiffness was not properly modeled. The overlap of the strips at the joints significantly stiffens the structure locally. The first model did not take this into account. A second NASTRAN model was developed which accounted for the increased stiffness by in effect replacing the overlaping areas in the first model with thicker elements. With this correction, it was expected that the modal frequencies obtained from NASTRAN would better correspond with those obtained experimentally.

To further study the effect of overlap on the model, another grid structure (with identical overall dimensions) is being acquired. This grid will be milled from a sheet of aluminium, thus eliminating the overlap at the joints.

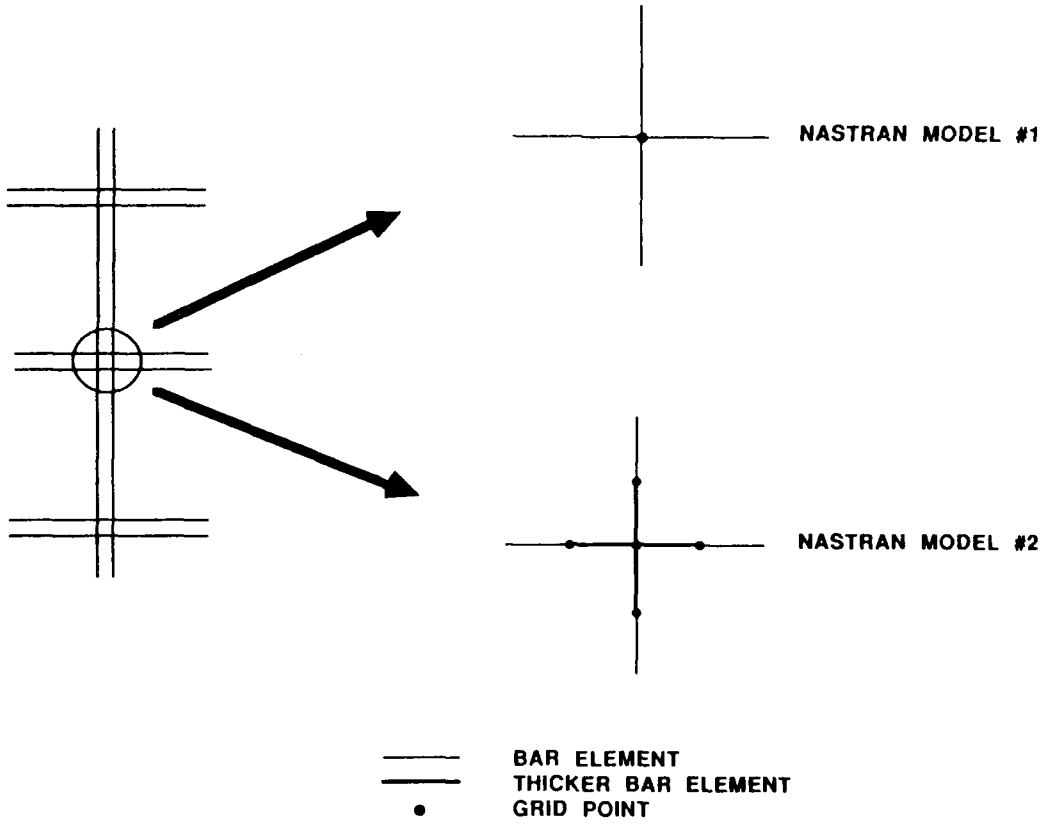

Figure 7

MODE SHAPES

Figure 8 gives the mode shapes for the first six modes of the grid structure. These mode shapes (generated from the first NASTRAN model) compared favorably in a qualitative manner with experimental mode shapes determined by exciting the structure at the modal frequencies using the electrodynamic shaker.

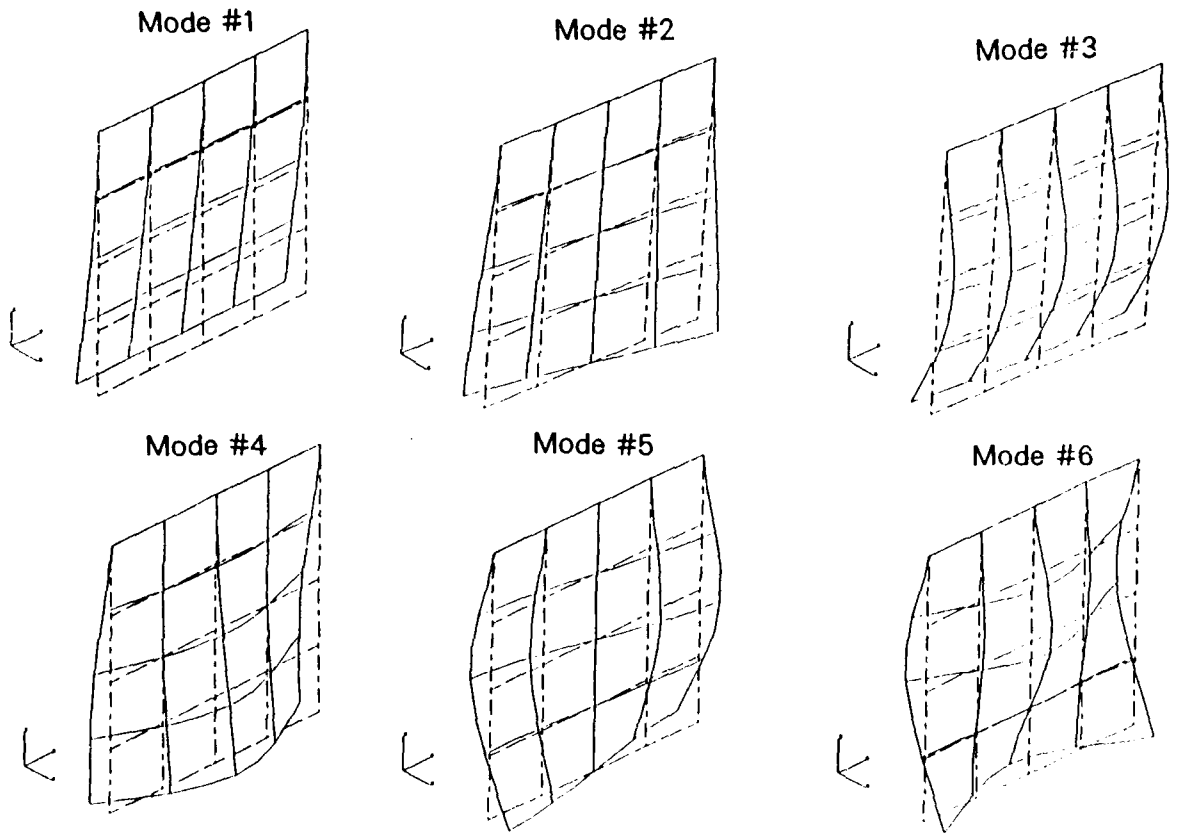

Figure 8

MODAL IDENTIFICATION

Preliminary estimation of the modal frequencies was performed using the Ibrahim Time Domain Technique (ITD, see Ref. 3) and the Eigenvalue Realization Algorithm (ERA, see Ref. 4). Parameter estimation was performed on the impulse response of the structure. Figure 9 gives the first six modal frequencies of the structure as estimated by the two NASTRAN models and compares them with the estimates provided by the ITD and ERA techniques.

Counter to expectation, the first NASTRAN model provided modal frequencies which were closer to those given by the ERA and ITD techniques. The NASTRAN values differed significantly from the experimental values for the first modal frequency only. This is probably due to the effect of 1-g loading on the structure. Although NASTRAN model #2 did raise the frequency of the first mode over that given by model #1, its overall effect on the modal frequencies was undesirable. The impact of different methods of modeling the overlap on the modal frequencies is currently under further study.

Future work will involve testing and comparing a large number of system identification techniques. Also the NASTRAN models will be further refined to provide a better match with the experimental results.

MODE #	NASTRAN MODEL #1	NASTRAN MODEL #2	ERA	ITD
1	0.715 Hz	0.728 Hz	0.836 Hz	0.86 Hz
2	2.119 Hz	2.169 Hz	2.073 Hz	2.13 Hz
3	4.498 Hz	4.686 Hz	4.467 Hz	4.4 Hz
4	5.562 Hz	5.807 Hz	5.500 Hz	5.56 Hz
5	7.170 Hz	7.434 Hz	6.963 Hz	7.04 Hz
6	11.58 Hz	12.17 Hz	11.31 Hz	

Figure 9

CONCLUSION

The modeling and system identification laboratory with the flexible grid structure is a first in a series of laboratories being developed at the Air Force Astronautics Laboratory to address specific dynamics and control issues for future large space systems. The grid provides a simple but effective testbed for comparing and testing various modeling and identification techniques with potential use in the design and operation of future space systems. Also the hands-on laboratory environment coupled with a real-time data acquisition/control hardware provides rapid turn around and thus is ideal for testing new concepts. This fully equipped laboratory is available to industry and faculty to develop and test innovative concepts in modeling, identification and control of space structures.

CONCLUSION

* **FIRST IN A SERIES OF DYNAMICS & CONTROL FACILITIES AT AFAL**
* **SIMPLE AND EFFECTIVE TESTBED FOR LSS**
* **MODELING AND IDENTIFICATION EXPERIMENTS**
* **HANDS-ON LABORATORY ENVIRONMENT**
* **RAPID TURNAROUND**
* **AVAILABLE TO INDUSTRY AND FACULTY**

Figure 10

REFERENCES

1. Denman, E.; et al: Identification of Large Space Structures on Orbit. AFRPL TR-86-054, Air Force Rocket Propulsion Laboratory, Edwards AFB, Ca., Sep. 1986.

2. Van Valkenburg, M. E.: Analog Filter Design. Holt, Rinehart and Winston, 1982, pp 167-179.

3. Ibrahim, S. R.; and Mikulcik, E. C.: A Method for the Direct Identification of Vibration Parameters from the Free Response. Shock and Vibration Bulletin, no. 47, part 4, Sept. 1977, pp 183-198.

4. Longman, R. W.; and Juang, Jer-Nan: A Recursive Form of the Eigensystem Realization Algorithm for System Identification. Proceedings of the AIAA/AAS Astrodynamics Conference, Williamsburg, Va., Aug. 1986.

OAST
IN-SPACE TECHNOLOGY EXPERIMENTS PROGRAM

BY

JON S. PYLE

MANAGER, FLIGHT RESEARCH & TECHNOLOGY PROGRAMS

FLIGHT PROJECTS DIVISION

OFFICE OF AERONAUTICS AND SPACE TECHNOLOGY

NASA HEADQUARTERS

WASHINGTON, DC

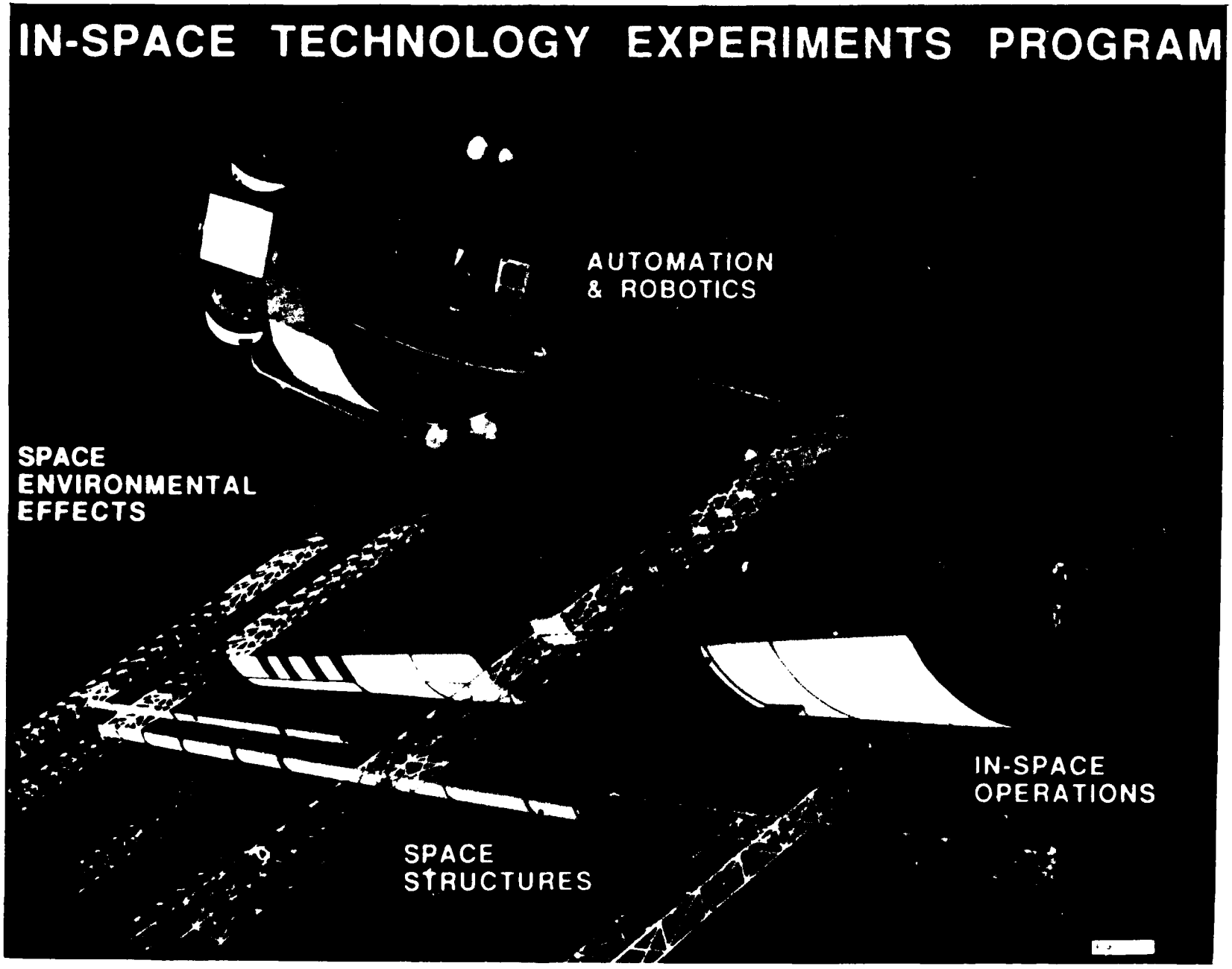
IN-SPACE TECHNOLOGY EXPERIMENTS PROGRAM
AUTOMATION
& ROBOTICS
SPACE
ENVIRONMENTAL
EFFECTS
IN-SPACE
OPERATIONS
SPACE
STRUCTURES

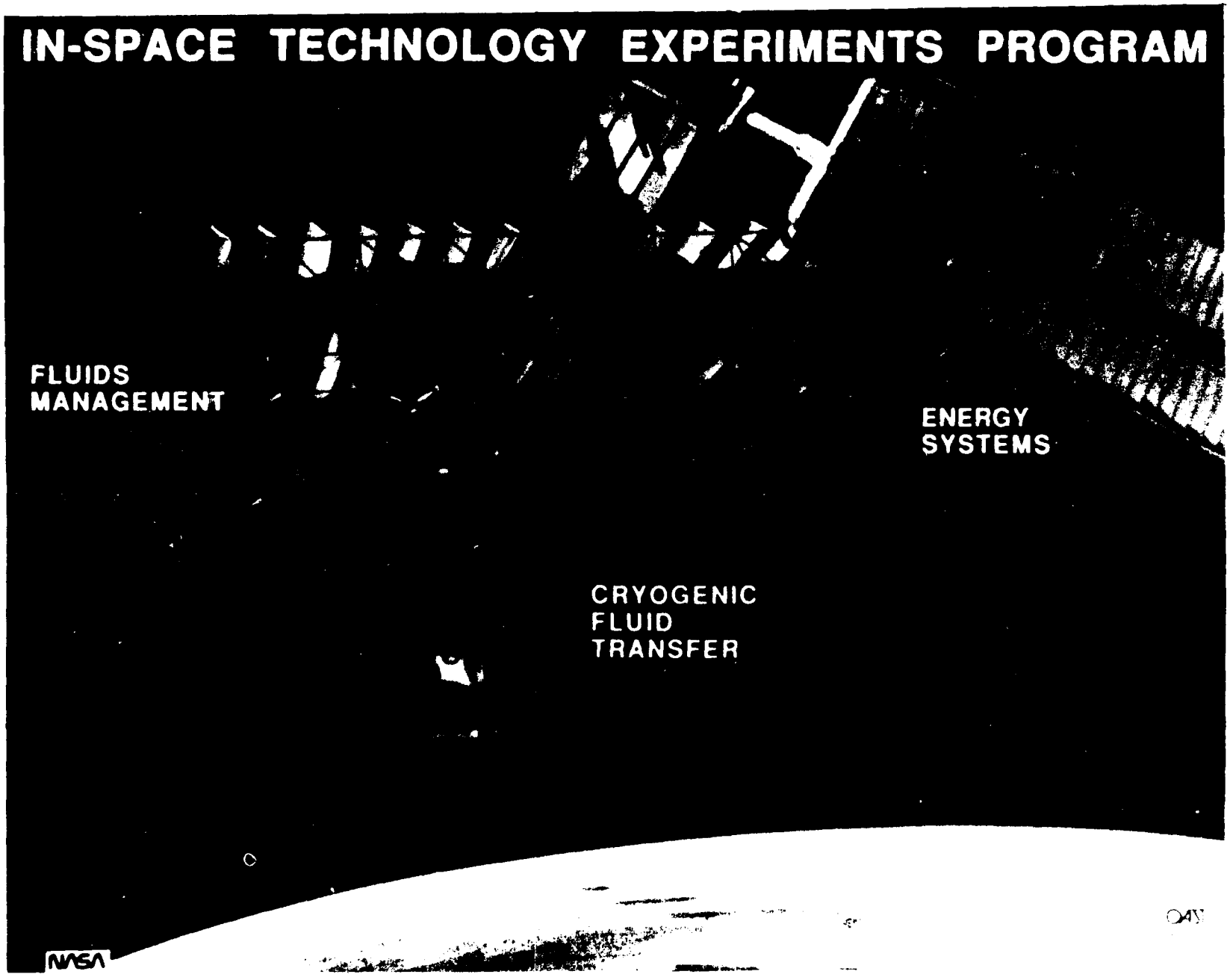
IN-SPACE TECHNOLOGY EXPERIMENTS PROGRAM
FLUIDS MANAGEMENT
ENERGY SYSTEMS
CRYOGENIC FLUID TRANSFER
NASA

IN-SPACE TECHNOLOGY EXPERIMENTS PROGRAM

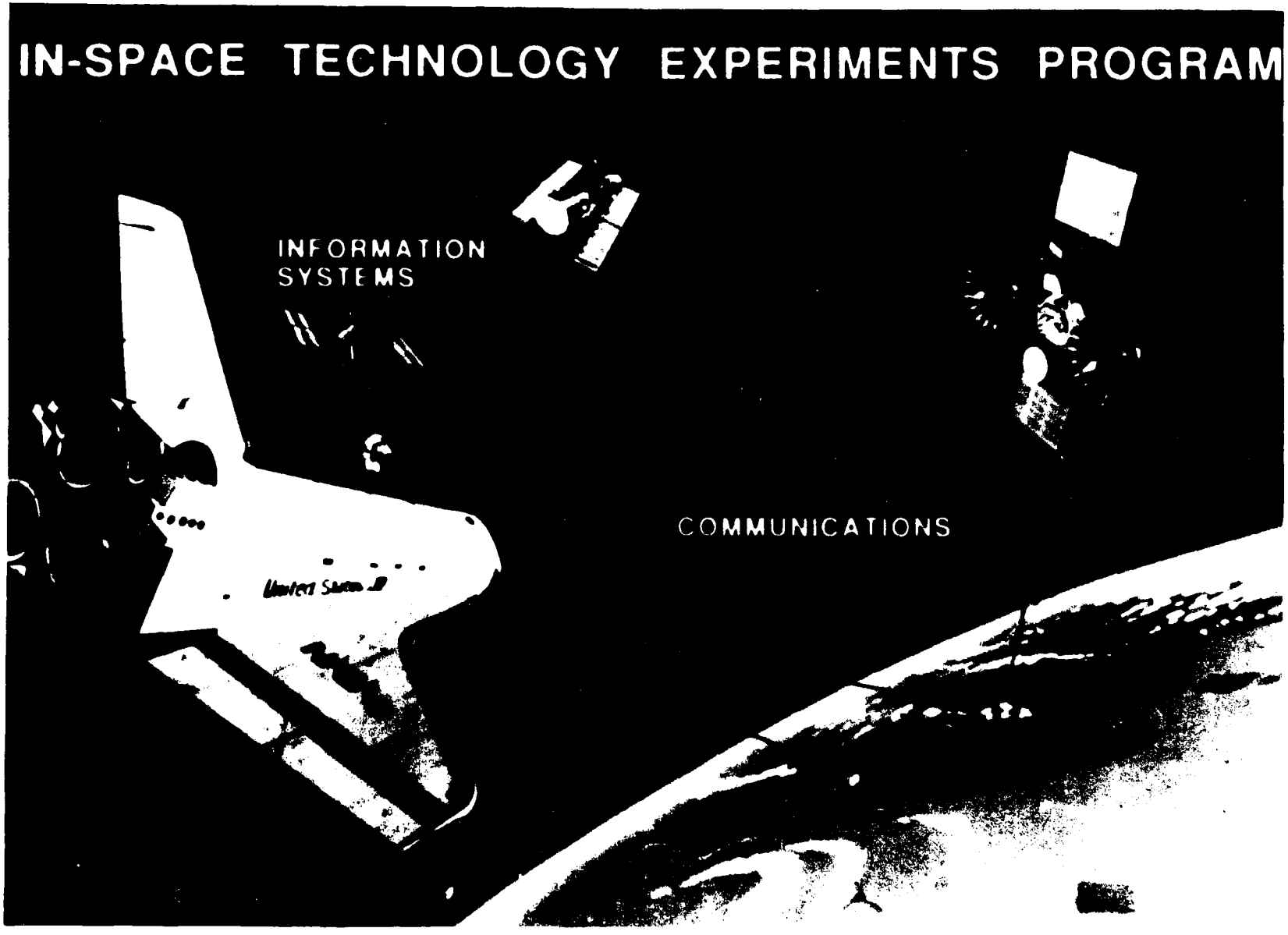

BACKGROUND

The Office of Aeronuautics and Space Technology (OAST) In-Space Technology Experiments program was initiated in response to a recognized need for the continued development of the U.S. space technology capability and to provide the stimulus for the U.S. Industry, Universities and the Department of Defense (DOD) to prepare for the utilization of the Space Station. In 1984, the National Aeronautics and Space Administration (NASA) Administrator issued a policy letter broading the role for space technology and increasing the emphasis of in-space flight experiments in NASA. In May of the following year, a panel of the Aeronautics and Space Engineering Board (ASEB) reviewed the stragetic plans for the NASA Space Station program and recommended strong emphasis be placed on increasing OAST's role in developing and space testing technology payloads. A workshop was held in October 1985 to establish the structure and content of a national in-space RT&E program. As a result of this workshop, proposals for space technology experiments were solicitated from U.S. Industry, Universities and from the NASA research organizations. The results of these solicitations and the future of the OAST's In-Space Technology Experiments program are the subjects of this paper.

BACKGROUND

LETTER FROM NASA ADMINISTRATOR, APRIL 1984

- BROADER ROLE FOR SPACE TECHNOLOGY
- SUPPORT DOD & THE SPACE INDUSTRY THROUGH COOPERATIVE RESEARCH & TECHNOLOGY PROGRAMS

AERONAUTICS & SPACE ENGINEERING BOARD (ASEB), MAY 1985

- NASA / OAST SHOULD UTILIZE SPACE SHUTTLE & SPACE STATION AS NATIONAL FACILITIES SIMILAR TO WIND TUNNELS & RESEARCH AIRCRAFT
- OAST SHOULD ESTABLISH AND FUND A MEANINGFUL RESEARCH & TECHNOLOGY PROGRAM WITH THE AEROSPACE COMMUNITY TO DEVELOP SPACE TECHNOLOGY

IN-SPACE RT&E WORKSHOP - OCTOBER 1985

- AA / OAST ANNOUNCED INITIATION OF PROGRAM TO FOCUS IN-SPACE TECHNOLOGY NEEDS OF INDUSTRY, UNIVERSITIES AND GOVERNMENT

OBJECTIVES

With the successful achievement of a permanent manned Space Station, NASA will dramatically expand its potential for providing facilities for science and technology investigations. NASA/OAST is in the process of expanding its program for the continued utilization of Space Shuttle and, in the next decade the utilization of Space Station as advanced technology test facillities similar to that which currently exists through the collaborative use of the national aeronautical wind tunnel and flight test facilities. The program is designed to incorporate technologies developed by the entire aerospace community for the purpose of advancing the total U.S. technology inventory. The goal of this program is to expand the OAST role beyond supporting technology development for NASA's future space missions, to include a role as the national focal point for in-space technology experimentation. OAST is advocating funds to support this program and to support its internal technology experiment development. OAST also recognizes that it must assist the small businesses, universities and those organizations without sufficient funding to build and test flight experiments and to provide a "value added" service to those organizations which will build and test their own flight hardware and software. This "value added" service must include the coordination and integration of all technology experiments onto appropriate carriers and pallets and provide assurances that these experiments will be flown within a reasonable time frame.

OBJECTIVES

- **ENABLE AEROSPACE COMMUNITY(INDUSTRY/UNIVERSITY NASA/DOD) TO HAVE ACCESS TO SPACE FOR R&T DEVELOPMENT**
- **ESTABLISH OAST AS NATIONAL FOCAL POINT FOR IN-SPACE TECHNOLOGY EXPERIMENTS**
- **PROVIDE FUNDING TO DEFINE AND DEVELOP SPACE TECHNOLOGY EXPERIMENTS**
- **PROVIDE FOR INTEGRATION OF EXPERIMENTS ON SPACE SHUTTLE, SPACE STATION, ELV'S AND FUTURE SPACE VEHICLES**

NASA EXPERIMENTS

In June 1986, the Associate Administrator of OAST requested proposals for space flight experiments from the NASA Centers and the Jet Propulsion Laboratory. In response to the request, fifty-eight (58) proposals were submitted for consideration as flight experiments. The proposals were reviewed and evaluated by the NASA Headquarters organizations. The proposal evaluations were summarized and submitted to a Selection Advisory Board for review and prioritization. Seventeen (17) of the proposals were recommended for selection to the Selecting Official (Deputy Associate Adminsitrator of OAST) of which seven (7) were selected for continued definition and development for flight experiments.

The seven proposals accepted for further definition and development include:

- Laser Communication Terminal
- Space Station Structural Characterization
- Contamination Flight Experiments
- Effect of Exposure on Thin-foil Mirrors
- Predicted Behavior of Thermal Energy Storage Materials
- Debris Collision Warning Sensor
- Laser In-Space Technology Experiment

NASA EXPERIMENTS

- **CENTERS REPRESENTED:**

  ARC, GSFC, JPL, JSC, LaRC, LeRC, MSFC

  58 PROPOSALS SUBMITTED

  7 PROPOSALS SELECTED

- **DISCIPLINES:**

COMMUNICATIONS	**1**
SPACE STRUCTURES	**1**
CONTAMINATION	**2**
THERMAL	**1**
SENSORS	**2**

INDUSTRY / UNIVERSITY EXPERIMENTS

In October 1986, a formal solicitation entitled "Amended Program Solicitation for Industry and University In-Space Technology Experiments" was released from OAST. The purpose of the solicitation was to stimulate the engineering community interested in testing space technology for cooperative participation with NASA to make greater use of space facilities for in-space experimentation. Proposals were requested to inlcude two different phases of maturity: (1)experiment definition, where an innovative concept or unique idea would be defined to assure its feasibility as a flight experiment; and (2)experiment development, where concepts would be transformed into space flight experiments through design, fabrication, assembly and ground testing preparatory to integration on a flight vehicle.

Two hundred and thirty-one proposals were submitted from 140 companies and 91 universities. In many cases, proposals were submitted in teaming efforts to best utilize the facilities and experience from different companies and/or universities. The proposals were submitted in seven different technology theme areas that had been identified at the In-Space RT&E Workshop held in October 1985. Forty-one proposals were accepted, thirty-six for definition and five for development of flight experiments. The contracts for these experiments will be conducted by twenty-eight separate companies and eleven separate universities.

INDUSTRY/UNIVERSITY EXPERIMENTS

231 PROPOSALS SUBMITTED

41 PROPOSALS ACCEPTED

- **DISCIPLINES:**

SPACE STRUCTURE	6	SPACE ENVIRONMENTAL EFFECTS	3
FLUID MANAGEMENT	8	IN-SPACE OPERATIONS	10
INFORMATION SYSTEMS	4	AUTOMATION & ROBOTICS	4
ENERGY SYSTEMS & THERMAL MGMT.	6		

- **PARTICIPATION:**

INDUSTRIES	28
UNIVERSITIES	11

THEME CENTER DESCRIPTION

As a result of the In-Space RT&E Workshop held in October 1985, seven technology theme disciplines were defined to represent the technology areas for the In-Space Technology Experiments program. These theme disciplines provided the basis for evaluation and ranking of the proposals submitted as part of the October 1986 technology experiments solicitation. A chairman from the lead center and members from the supporting NASA field centers and JPL constituted a theme committee. The theme committees were responsible for assuring a comprehensive evaluation of the proposals by the representative technical experts, for summarizing the evaluations, and ranking the proposals based on how well they satisfied the evaluation criteria identified in the solicitation. Advocacy charts were prepared describing the proposed experiment, its strengths and weaknesses, and the justification for conducting the experiment in space. These charts were then presented to the Selection Advisory Committee for prioritization and recommendation for selection.

THEME CENTERS

THEME \ CENTER	ARC	GSFC	JPL	JSC	LaRC	LeRC	MSFC
SPACE STRUCTURE		○	○	○	●		○
FLUID MANAGEMENT	○	○		○		●	○
INFORMATION SYSTEMS	○	●	○	○	○	○	○
ENERGY SYSTEMS/ THERMAL MGMT.		○	○	○		●	○
SPACE ENVIRON-MENTAL EFFECTS		○	●	○	○	○	○
IN-SPACE OPERATIONS	○	○	○	○	○	○	●
AUTOMATION & ROBOTICS	○	○	●	○	○		○

● LEAD ○ SUPPORT

EVALUATION / SELECTION PROCESS

The proposals were sent to NASA Langley Research Center where they were screened into the appropriate theme catagories. They were then distributed to the NASA field centers and the Jet Propulsion Laboratory (JPL) where technical experts provided an evaluation based upon the criteria defined in the solicitation. The evaluations were collected, reviewed, summarized, and ranked by theme committees. The ranking catagories included: high (meeting all the evaluation criteria); medium (meeting some of the evaluation criteria); or low (meeting few of the evaluation criteria). Only the high ranked proposals were presented to the Selection Advisory Committee.

The Selection Advisory Committee included each OAST Discipline Division Director and a representative from each of the NASA field centers. The high ranked proposals were reviewed and prioritized by the advisory committee. The list of proposals recommended for selection was obtained by comparing the prioritized listing with the available contract funds. An accommodation assessment was conducted on the recommended proposals by Johnson Space Center to determine the acceptability of flying the proposed experiments on the Space Shuttle. All proposals were considered acceptable, if adequate early engineering and safety reviews are conducted. The Selecting Official (Deputy Associate Administrator for OAST) conducted a detailed review of the recommended proposals and selected forty-one for definition and development of flight experiments.

EVALUATION/SELECTION PROCESS

(1) PROPOSAL EVALUATIONS:

- **EVALUATED BY NASA TECHNICAL EXPERTS**
- **SUMMARIZED AND RANKED BY DISCIPLINE/ THEME COMMITTEE**

(2) PRIORITIZED BY SELECTION ADVISORY COMMITTEE

(3) SHUTTLE ACCOMMODATION ASSESSMENT

(4) SELECTED BY OAST

"PROPOSED" TECHNOLOGY EXPERIMENT PROCESS

The Technology Experiment Process identifies the proposed procedure by which OAST technology experiments will be defined and developed for space flight. The focused technical planning may occur at workshops, symposium, conferences or through the NASA stragetic planning process with the purpose of identifing high priority technologies which require immediate development. These identified technologies would be used in the next solicitation of definition experiments. A modified selection process is currently under consideration which may improve the time period required for evaluation and selection of future proposals.

A technology experiment could enter the process at any point depending on the maturity of the hardware and software; however, the experiment should be able to pass each of the reviews before proceeding to flight test. The initial study phase would determine the feasibility of the concept and define a preliminary plan for developing the concept into an actual flight experiment. The first review would determine if the concept is technically feasibile, the objectives are acheiveable and the plan is adequately defined. Authorization to proceed to the engineering study would occur through approval by an advisory board or through a new competition. This study should develop an engineering design and define preliminary hardware/software requirements, establish a final development plan and develop accurate estimates of costs and schedules. Authorization by a Engineering Review Board would be required to proceed with the design, fabrication, assembly, and testing of the hardware/software in preparation for integration onto a carrier/pallet for the space flight test. The end product from this process would be the analysis of the flight data and the report of the technology development results.

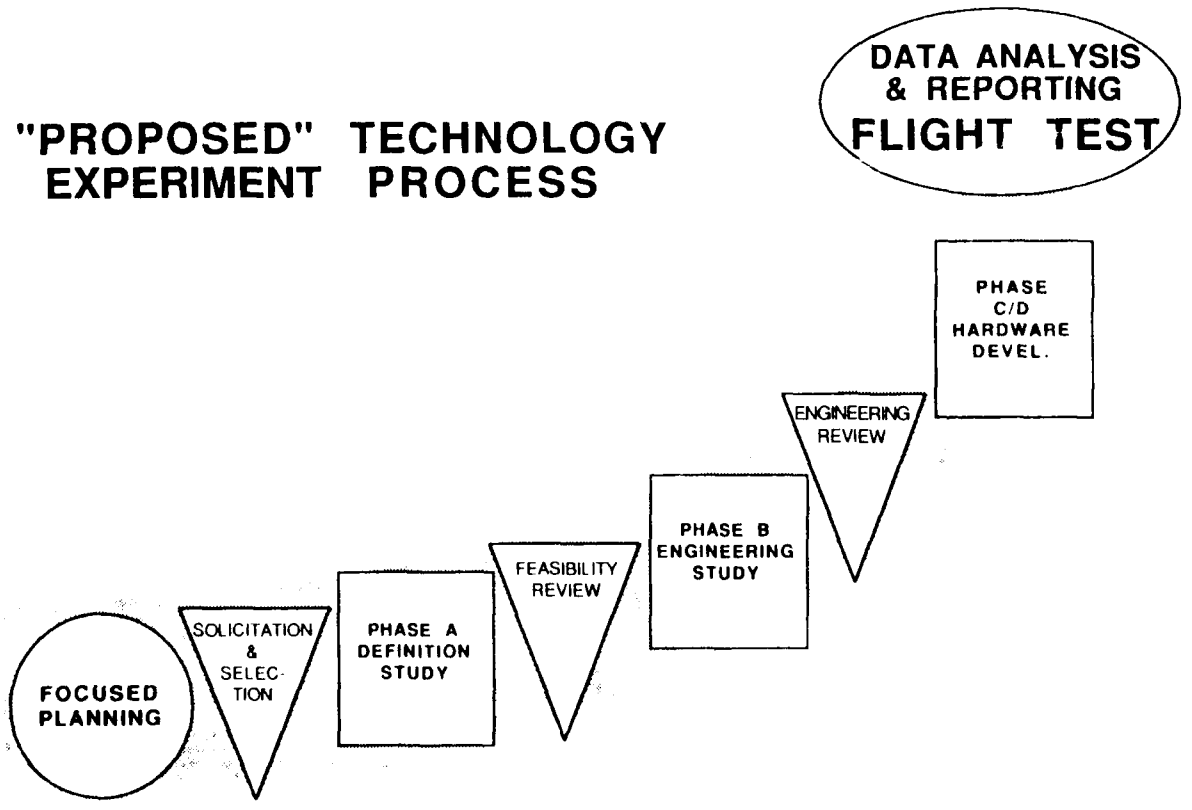

SOLICITATION ROADMAP

The schedule for the conduct of the In-Space Technology Experiments program is conceptualized on the Solicitation Roadmap. The 1987 evaluation and selection of the Phase A and B studies identify the process which has been recently completed. It is expected that the initial definition and engineering studies will be completed in approximately twelve (12) months. At that point, the flight experiments will proceed on somewhat different paths.

The engineering study (Phase B) results will be reviewed by the Engineering Review Board and approval to proceed would allow the experiment to continue without further competition through Phase C/D (design, fabrication, assembly and ground testing) and be flown on the appropriate spacecraft at the earliest possible time.

During the 1989 time period, the experimentors who have accomplished the definition studies (Phase A) would submit proposals to compete for the development of the flight experiment. It should be recognized that only a few experiments may be accepted for continued development. Some concepts will be eliminated due to lack of technical feasibility, high development costs, unavailability of flight opportunities, improper timing for continuation of the technology development, or lack of sufficient program funds to build the flight hardware/software.

A request for proposals is expected to be initiated in late 1988 to identify new technology concepts which may address the high priority technologies identified at a proposed spring workshop. The selected concepts should proceed through the previously described experiment process with a schedule similar to that outlined on the Solicitation Roadmap. Initially, this process is expected to occur on two year cycles.

SOLICITATION ROADMAP

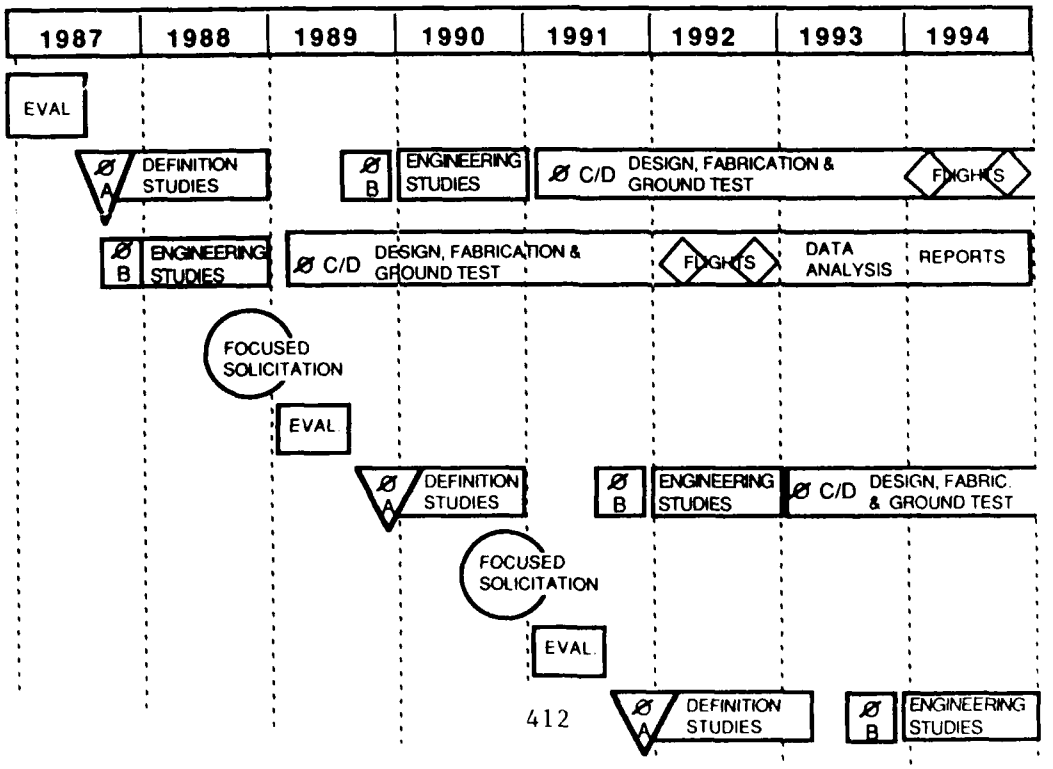

EXPERIMENT ROADMAP

The Experiment Roadmap is a pictorial concept of the planned In-Space Technology Experiments program. The central path indicates the proposed thrust of the OAST experiment program with growth in the number of flight experiments. If Industry or the Department of Defense (DOD) have flight hardware developed with their own funds, the technology experiments utilizing this hardware would enter the program through the separate paths. The OAST path would offer industry and DOD the advantage of utilizing existing carrier/pallet capabilities and manifested flight test opportunities to validate their technologies. The outlets to the Space Shuttle and eventually Expendable Launch Vehicles (ELV's) indicate that an increasing number of flight experiments are expected to be developed and flown on these space facilities provided adequate funding can be obtained. Similarily, the outlets to the Space Station indicate that an increasing number of flight experiments are expected to be developed and flown on that facility. Estimates have indicated that by the year 2000 as many as thirty-five to forty flight technology experiments per year may require flight evaluation on the national space facilities in order to maintain the U.S. leadership in space technology.

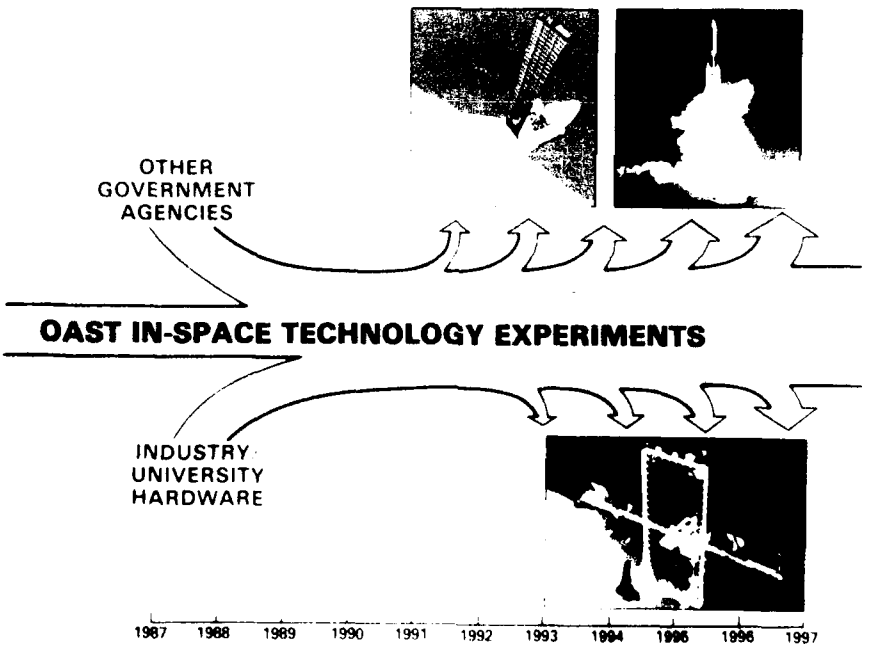

CONCLUSIONS

A new and vital space flight experiments program was announced at the October 1985 In-Space Research, Technology and Engineering Workshop in Williamsburg, Virginia. The Associate Administrator for Aeronautics and Space Technology initiated a NASA/OAST program to focus the needs of industry, universities, and the government for in-space technology experiments and to begin building a strong national user constituency for space research and engineering. The program announcement was followed in June 1986 with a request for proposed flight experiments from NASA researchers and in October 1986 with a solicitation for space technology experiments from the U. S. Industry and Universities. Almost three hundred (300) proposals were submitted and evaluated of which forty-eight (48) experiments have been selected for definition and development. The contracting process for these experiments is currently underway and OAST is identifing opportunities for validating these technologies on available space vehicles.

OAST is agressively pursuing the continued development of in-space technology experiments with the implementation of the current flight experiments and the planning for the next series of experiment solicitations. OAST has requested NASA Langely Research Center to sponsor the second in the series of In-Space Technology Experiments Workshops for the spring of 1988. This workshop will be open to the entire U.S. aerospace community and is intended to identify the high priority space technologies necessary to maintain U.S. space leadership. The next solicitation for the identification of promising flight experiments for developing these high priority technologies is expected to be released in late 1988.

CONCLUSIONS

- **OAST INITIATED THE INDUSTRY / UNIVERSITY IN-SPACE TECHNOLOGY EXPERIMENTS PROGRAM WITH A SOLICITATION RELEASED OCT. 1986**

- **IN-SPACE TECHNOLOGY EXPERIMENTS PROGRAM UNDERWAY**
  - **231 INDUSTRY / UNIVERSITY PROPOSALS EVALUATED, 41 SELECTED**
  - **58 IN-HOUSE NASA PROPOSALS EVALUATED, 7 SELECTED**
  - **CONTRACTING PROCESS UNDERWAY**
  - **MANIFESTING OPPORTUNITIES BEING IDENTIFIED**

- **PLANNING INITIATED FOR PROGRAM CONTINUATION**
  - ***PROPOSED WORKSHOP: SPRING 1988***
  - **NEXT FOCUSED SOLICITATION: LATE 1988**

NASA News

National Aeronautics and
Space Administration

Washington, D.C. 20546
AC 202-453-8400

Les Reinertson
Headquarters, Washington, D.C.
(Phone: 202/453-2754)

For Release:
October 30, 1987

RELEASE: 87-164

NASA SELECTS INDUSTRY/UNIVERSITY IN-SPACE TECHNOLOGY STUDIES

NASA's Office of Aeronautics and Space Technology (OAST) has selected five organizations for development of space flight technology experiments and 36 additional proposals for definition of possible future space flight technology experiments in its Industry/University In-Space Technology Experiments program.

The program was established to stimulate the aerospace engineering community to work with NASA to make greater use of space facilities, such as the Space Shuttle and Space Station, for in-space research, technology and engineering experimentation.

The current NASA/OAST Industry/University In-Space technology program represents a $5 million investment by NASA to extend U.S. leadership in space technology development.

The program is the first in a series of flight experiment solicitations sponsored by OAST.

The five proposals selected for development of space flight technology experiments are:

"Investigation of micro-gravity effects on heat pipe thermal performance and working fluid behavior", Hughes Aircraft Company, Torrance, Cal.

"Tank pressure control experiment", Boeing Aerospace Company, Seattle, Wash.

"An experimental investigation of spacecraft glow", Lockheed Missiles and Space Company, Palo Alto, Calif.

"Middeck 0-gravity dynamics experiment", Massachusetts Institute of Technology, Cambridge, Mass.

- more -

"Development of emulsion chamber technology for cosmic ray and high energy nuclear physics research in the Space Station era", University of Alabama, Huntsville.

The 36 proposals selected for definition studies are:

"Design of a closed loop nutrient solution delivery system for CELSS application", Lockheed Missiles and Space Company, Sunnyvale, Calif.

"Extra-vehicular activity welding experiment" Rockwell International, Rocketdyne Division, Canoga Park, Space & Technology Group, Redondo Beach, Calif.

"Flexible arm controls experiment", Martin Marietta Corporation, Denver.

"Jitter suppression for precision space structures", McDonnell Douglas Astronautics Company, St. Louis.

"Control of flexible robot manipulators in zero gravity", Utah State University, Logan, Utah.

"Measurement of surface reactions in the space environment", Globesat, Inc., Logan, Utah.

"Definition of an in-space experiment on liquid motion in a rotating tank", Southwest Research Institute, San Antonio.

"Vapor crystal growth technology", University of Alabama in Huntsville.

"Liquid encapsulated float zone refining", McDonnell Douglas Astronautics Company, St. Louis.

"Sodium/sulfur battery flight experiment definition", Ford Aerospace & Communication Corporation, Palo Alto, Calif.

"Impact of zero-gravity on water electrolysis operation", Life Systems, Inc., Cleveland.

"Definition of a microbiological monitor for application in space vehicles," University of Alabama, Huntsville.

"Acceleration measurement and management", University of Alabama, Huntsville.

"In-space structural dynamics of a skewed scale space station structure", McDonnell Douglas Astronautics Company, Huntington Beach, Calif.

- more -

"In-space experiments to identify or develop effective microgravity fire suppressants", Battelle, Columbus, Ohio.

"Dexterous manipulator advanced controls experiment, Martin Marietta Corporation, Denver.

"Payload vibration isolation in microgravity environment", Texas A & M Research Foundation, College Station.

"On-orbit electron beam welding experiment definition", Martin Marietta Michoud Aerospace, New Orleans.

"Inflatable solar collector experiment", L'Garde, Inc., Newport Beach, Calif.

"Advanced magnetic suspensions for vibration isolation and fast attitude control of space-based generic pointing mounts", AiResearch Manufacturing Company, Torrance, Calif.

"Verification of moving belt radiator performance characteristics in a low gravity environment", Arthur D. Little, Inc., Cambridge, Mass.

"Liquid drop radiator", Grumman Corporation, Bethpage, N.Y.

"Unitized regenerative fuel cell in-space technology experiment", United Technologies, Hamilton Standard, Windsor Locks, Conn.

"Enhancement of in-space operations using spatial perception auditory referencing", University of California, Irvine.

"Experiment definition phase for measurement and modeling of joint damping in space structures", Utah State University, Logan.

"Integrated Cryogenic Experiment-A (microsphere insulation investigation)", Lockheed Missile and Space Company, Palo Alto, Calif.

"Passive damping augmentation for space manipulators", Old Dominion University Research Foundation, Norfolk, Va.

"Infrared focal plane performance in the South Atlantic anomaly", Lockheed Missile and Space Company, Palo Alto, Calif.

"Optical properties monitor experiment," John M. Cockerham and Associates, Inc., Huntsville, Ala.

- more -

"Dynamic spacecraft attitude determination with GPS," Mayflower Communications Company, Inc., Wakefield, Mass.

"In-Space experiment on thermoacoustic convection heat transfer phenomenon," University of Tennessee, Knoxville.

"Study of in-space plasma arc welding," University of California, Berkeley.

"Laser welding technology in space," University of Alabama in Huntsville.

"Construction and in-space performance evaluation of high stability hydrogen maser clocks," Smithsonian Institution Astrophysical Observatory, Cambridge, Mass.

"Risk-based fire safety experiment definition," University of California, Los Angeles.

- end -

STRUCTURAL DYNAMICS RESEARCH ON SCALE MODEL SPACECRAFT TRUSSES

Paul E. McGowan
NASA Langley Research Center
Hampton, VA 23665

Harold H. Edighoffer
AS&M, Inc.
Hampton, VA 23665

and

Joseph M. Ting
Massachusetts Institute of Technology
Cambridge, MA 02139

Second NASA/DOD CSI Technology Conference
Colorado Springs, Colorado
November 17-19, 1987

TALK OUTLINE

The paper discusses ongoing research in the Structural Dynamics Branch at the Langley Research Center related to testing and analysis of scale model structures. These studies are being done in preparation for the COFS III Space Station Pathfinder Scale Model Project (ref. 1). Included are descriptions of various types of scale model hardware and their relation to the COFS III structure. Plans for a fully mated test of a dual keel truss structure which simulates Space Station dynamics are discussed along with a model test support system. Results of static tests of truss sections with different truss member lacing patterns are presented. Predictions of finite element models which have member properties based on the results of truss element component tests are compared to static test results. Bi-directional coupling evident in the various truss configurations is compared. The sensitivity of modeling key interfaces on the dynamics of a dual keel frame structure are investigated.

TALK OUTLINE

- Objective and approach
- Relationship w/ COFS III activities
- Space Station scale model hardware
  - Elements (joints, tubes . . .)
  - Phenomena model
  - Generic truss model
- Truss member lacing configurations
- Static test results
- Effects of interface flexibilities
- Initial dynamic test results

STRUCTURAL DYNAMICS RESEARCH ON SCALE MODEL SPACECRAFT TRUSSES

The objective of this research is to develop test and analysis techniques for conducting ground tests on a fully mated dual keel Space Station scale model. Space Station is the focus for this program since it is the first complex, three-dimensional structure to be assembled on-orbit (ref. 2). It also provides an opportunity to obtain flight data for correlation with ground tests and analytical predictions. Previous studies (refs. 3-5) have identified significant challenges involved with such a program. These challenges include the development of minimum-restraint suspension systems and our ability to analytically model them, the fabrication and modeling of scale model joints, and the effects of subassembly and component interfaces on the overall station dynamic response.

The technical approach involves a test and anlysis program using a series of scale model structures representative of various build-up stages, subassemblies, and the fully mated Space Station. In this way substructure synthesis predictions can be compared to the results obtained from the fully mated configuration to assess the importance of accurately identifying interface properties.

STRUCTURAL DYNAMICS RESEARCH ON SCALE MODEL SPACECRAFT TRUSSES

Objective: Develop test techniques, analysis methods, and logistics approaches to conduct valid dynamics ground tests on large truss structures.

Approach: Utilize a series of realistic and increasingly complex scale model structures which:

1) allow a variety of test configurations and analysis techniques to be investigated
2) lead to dynamics test of a fully mated dual keel truss structure

CURRENT AND ANTICIPATED SPACE STATION SCALE MODEL HARDWARE

The figure depicts the steps leading to the ground test of a fully mated near-replica scale Space Station model. Each step uses a model with increased complexity so that the technical challenges can be addressed in a progressive fashion. All of the models are scaled to simulate the dynamics of Space Station. The phenomena model is a table-top size structure useful for studies of suspension systems and subassembly interfaces. The generic and pathfinder models are both the same size (approx. 35'x50' planform) and represent the first opportunity to obtain data on a mated dual keel configuration. The generic model is an artificially stiff structure useful for developing assembly and test logistics methods. On the other hand, the pathfinder model uses realistic Space Station hardware including flexible appendages and interfaces. Finally, the primary model will provide the best fidelity of all and will be used for Space Station on-orbit predictions and studies of growth configurations.

CURRENT AND ANTICIPATED SPACE STATION SCALE MODEL HARDWARE

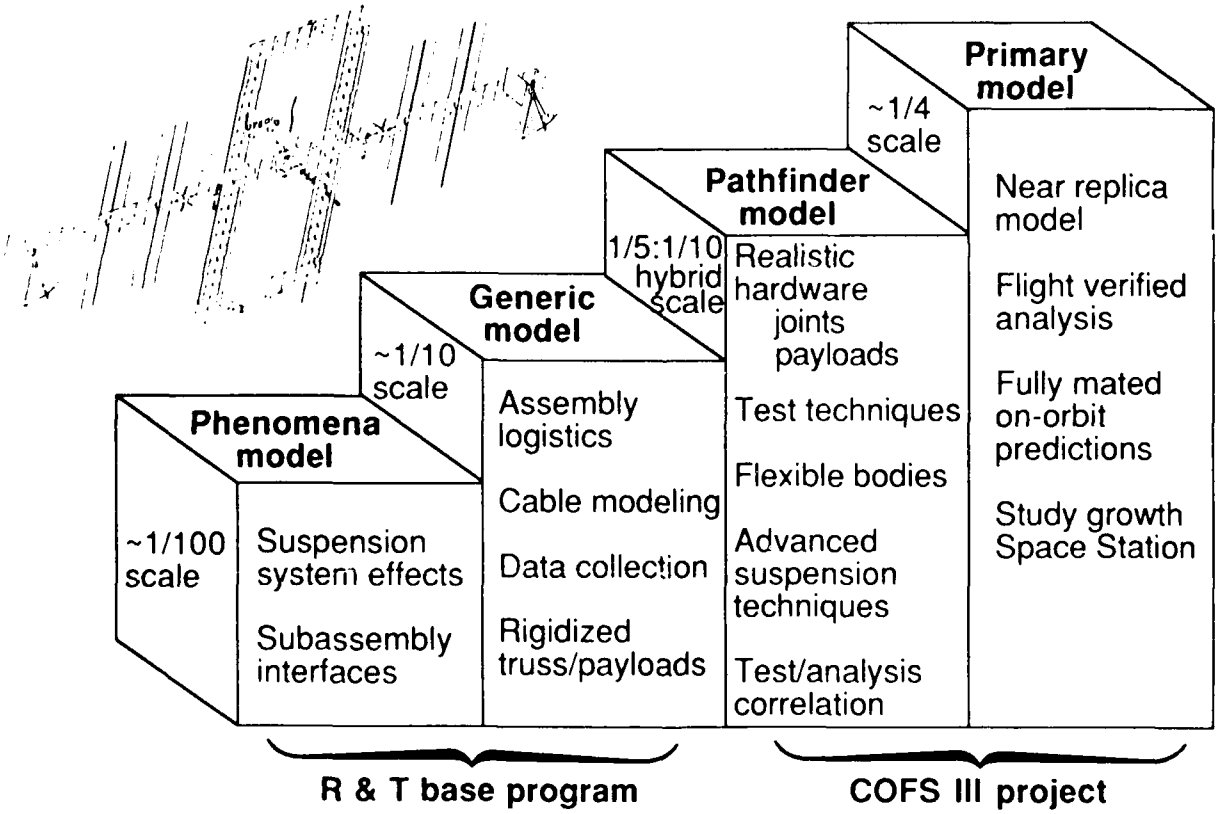

COMPARISON OF FREQUENCY SPECTRUM OF FULL SCALE DUAL KEEL SPACE STATION WITH VARIOUS SCALE MODELS

The dynamic characteristics of a properly scaled model can be related to those of the full-scale prototype structure by various scaling laws. Often times, the vibration frequency of the scale model is related to the full scale value by the inverse of the length scale factor. Although scale models are often designed only to simulate the dynamics of the prototype, it is also desirable to retain similar modal density. To illustrate this, the figure shows the frequency spectrums of various size structures. The abscissa reflects the appropriate scale factors to permit direct comparison. Note that the phenomena model has a fundamental frequency of approximately 20 Hz, whereas the hybrid scale and replica models have fundamental frequencies of approximately 1 Hz.

COMPARISON OF FREQUENCY SPECTRUM OF FULL SCALE DUAL KEEL SPACE STATION W/ VARIOUS SCALE MODELS

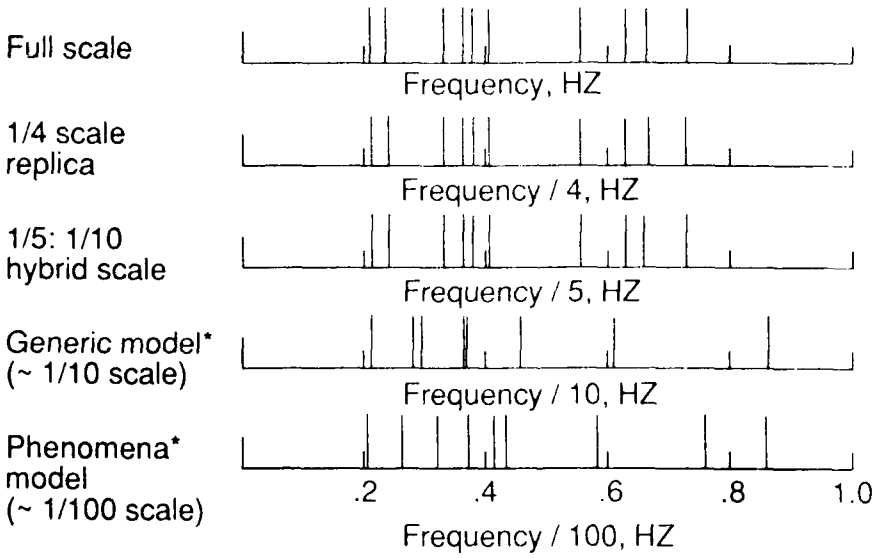

*Payloads/subsystems modeled as lumped masses

GENERIC MODEL HARDWARE DESCRIPTION

The generic model is a commercially available truss structure which is functionally similar to that proposed for the Space Station. Each bay length is 1/10 that of the 5 meter Space Station truss, thus it has the same overall dimensions as the COFS III Pathfinder model. The truss joints and members, however, are not to scale since they are too stiff and heavy compared to their length dimension. When fully assembled and mass loaded the truss yields a good 1/10 scale model simulator. This truss hardware accomodates the anticipated Space Station build-up sequences from first element launch through the fully mated dual keel structure. When fully assembled into the dual keel structure, the model will consist of approximately 400 joints and 1100 members. A "shadow structure" suspension system is being developed which allows the model to be suspended and dynamically tested in any of three orthogonal configurations (transverse boom and dual keels horizontal, transverse boom horizontal and dual keel vertical, and transverse boom vertical).

GENERIC MODEL HARDWARE DESCRIPTION

- Same overall dimensions as COFS III Pathfinder model
- Commercially available truss structure ("Meroform")*
  - Joint design accomodates SS build-up stages
  - Truss member x-section & joint fittings not to scale

$$K_{\substack{\text{generic}\\\text{model}}} / K_{\substack{\text{1/10 scale}\\\text{model}}} \simeq 11 \,, \; M_{\substack{\text{generic}\\\text{model}}} / M_{\substack{\text{1/10 scale}\\\text{model}}} \simeq 10$$

- Mass loaded frequencies simulate 1/10 scale dynamics

$$f_1 = 2.1 \text{ HZ}$$

- Shadow structure concept accomodates various model test orientations

*Trade name of MERO corporation

GENERIC SPACE STATION TRUSS HARDWARE

Shown in the figure is a ten bay test section of the generic truss hardware cantilevered from a backstop with a tip mass plate. Each bay of the truss is a cube 1.64 feet on a side, and weighs approximately 7 lbs. The nodal joint design allows the anticipated Space Station truss layup configurations to be achieved.

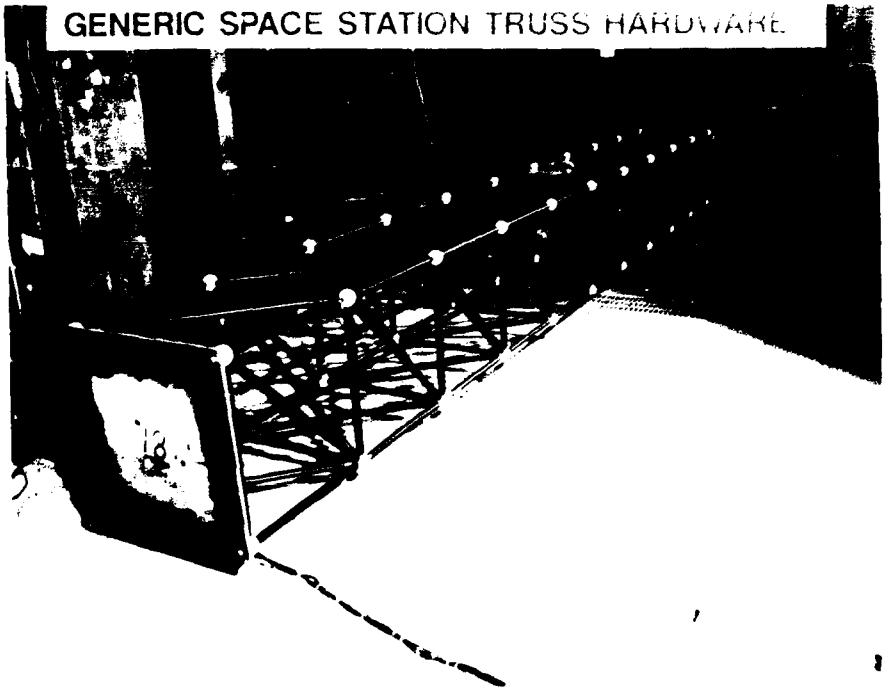

SPACE STATION TRUSS MEMBER LACING CONFIGURATIONS

An important factor which, as of this paper, has not been established for the Space Station is the lacing configuration for the truss. For this study four truss configurations were examined; Orthogonal, Warren, and two types of Inverted Warren. Some of the factors to consider in selecting a truss configuration include: 1) the unobstructed area inside the truss for payloads, 2) the ease of astronaut assembly and repair, 3) the degradation in structural performance due to a damaged or removed truss member, and 4) the amount of coupling present due to various types of loading. Static tests have been performed on the truss configurations to compare some of the above factors.

SS TRUSS MEMBER LACING CONFIGURATIONS

- Several lacing patterns considered
  - Orthogonal
  - Warren
  - Inverted Warren type 1
  - Inverted Warren type 2
- Factors considered
  - Payload volume inside truss
  - Astronaut assembly
  - Structural performance
    - w/ full truss
    - w/ member removed
  - Coupling and equivalent beam modeling
- Static tests performed on generic truss hardware to:
  - Update/verify initial analysis based on element tests
  - Compare coupling in each configuration

COMPARISON OF INTERNAL TRUSS PAYLOAD AREA

Each of the four truss configurations is depicted schematically in the figure along with the amount of unobstructed "pass-through" area in three directions along the truss. This "pass-through" area is important since it allows the inner volume of the truss to be exploited for payload placement and servicing. In the Orthogonal truss, all diagonal members on each face are oriented in the same direction such that 50 percent of the truss bay cross-section is clear along the three axes. For the Warren truss the diagonals running along the axial direction and the left, right, top, and bottom faces are in phase yielding the same "pass-through" area as the Orthogonal truss. In both Inverted Warren trusses, the right and left and the top and bottom face diagonals are alternated out of phase. In addition, in the Warren #1 configuration the face diagonals normal to the truss axis are in the same direction, whereas in the Warren #2 configuration those face diagonals are alternated from bay to bay. Therefore, the Inverted Warren trusses yield lower values of the "pass-through" area.

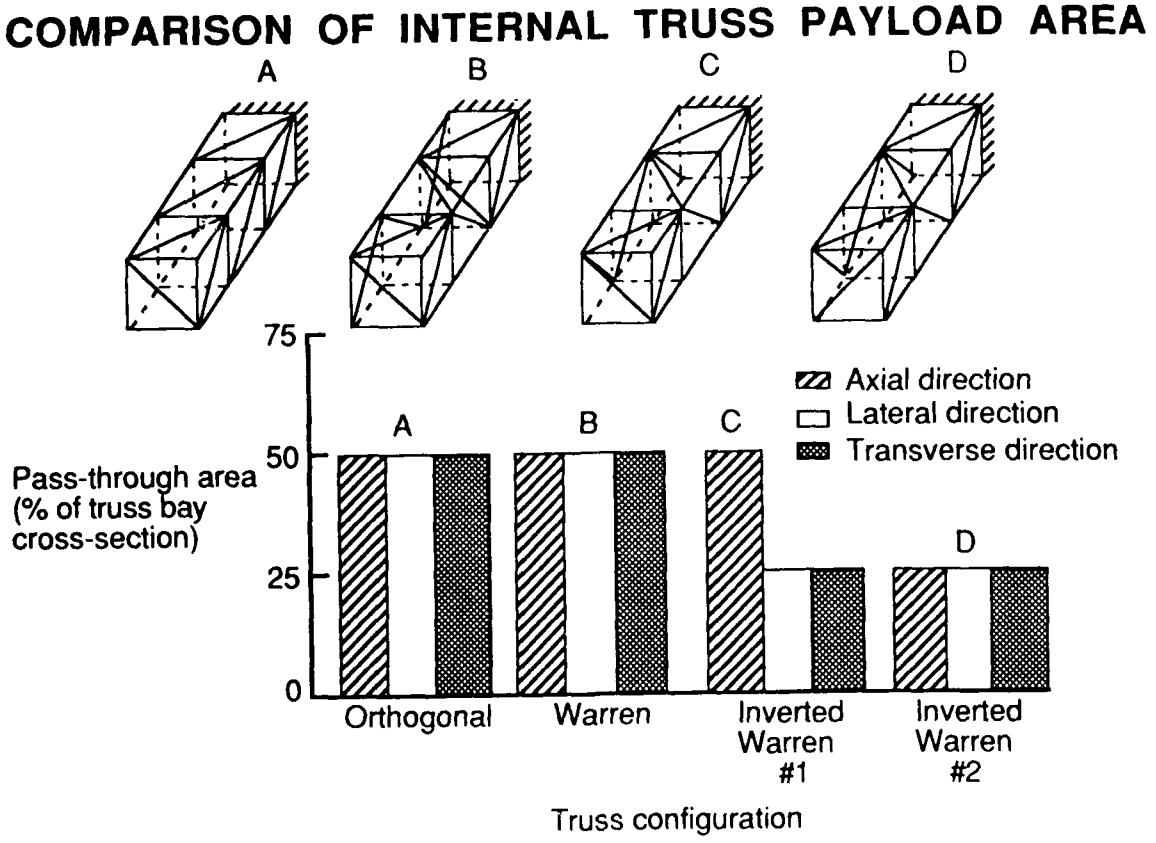

STATIC TEST RESULTS ON GENERIC HARDWARE

Static tests were performed on cantilevered truss sections of the generic hardware. Lateral bending loads were applied at the truss tip, and horizontal and vertical displacements were measured at several stations. A typical test and analysis comparison for a ten bay Orthogonal truss section is shown in the figure. These tests confirm the linearity and predictability of the generic model hardware. The finite element analysis models were based on results obtained from static tests performed on the individual truss elements in reference 6.

STATIC TEST RESULTS ON GENERIC HARDWARE

Typical test/analysis comparison

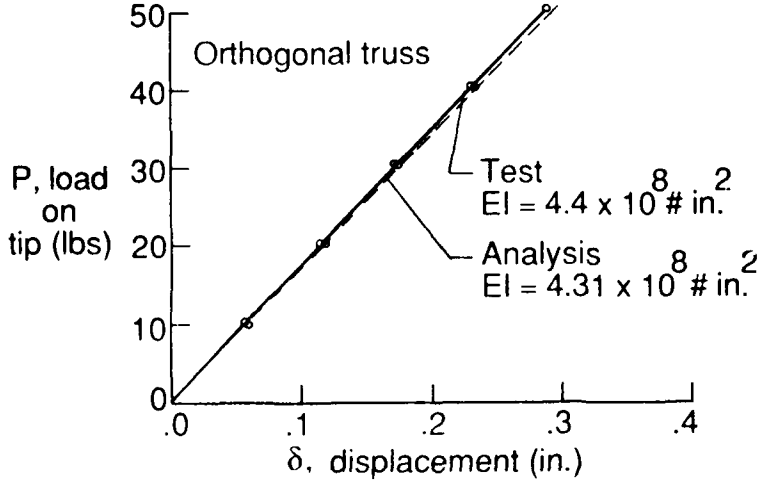

Test set-up schematic

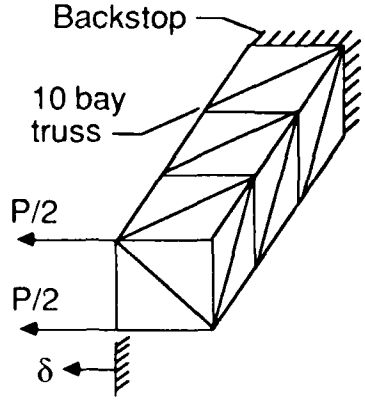

10 BAY CANTILEVER TRUSS WITH TIP MASS TEST SUMMARY

For all truss configurations the test and analysis comparisons for the bending stiffness at the tip of the truss were within 3.5% as shown in the table (due to time constraints the Warren truss configuration was not tested). The analysis predictions all displayed the same trends since they each slightly under-predicted the measured values.

10 BAY TRUSS MODEL STATIC TEST APPARATUS

10 BAY TRUSS MODEL STATIC TEST APPARATUS

Depicted in the figure is the static test set-up at the tip of the 10 bay generic truss hardware. Lateral bending loads were applied horizontally at the tip of the truss by means of two load pans each connected to the truss by cables looped over pulleys. Noncontacting displacement sensors were placed horizontally and vertically at various stations. The tip mass consisted of a steel plate (approximately 68 lbs.) rigidly fixed to tne four node points on the last bay which served to keep the truss cross-section square.

10 BAY CANTILEVER TRUSS W/ TIP MASS TEST SUMMARY

Approximate bending stiffness, EI (# in.^{2})

Truss configuration type	Test	Initial analysis	% difference
Orthogonal	4.399×10^8	4.310×10^8	2.1
Warren	—	4.461×10^8	—
Inverted Warren # 1	4.476×10^8	4.324×10^8	3.5
Inverted Warren # 2	4.420×10^8	4.324×10^8	2.2

COMPARISON OF COUPLING PRESENT IN VARIOUS TRUSS CONFIGURATIONS

Depending on the placement of the truss diagonal face members, static coupling occurs for different types of loading. The figure shows the results of an analytical study of the coupling present in each truss type. The column labeled "coupled dof" indicates the degree-of-freedom which is coupled with the one associated with the direction of applied loading. For example, a transverse bending load P_1 normally produces a bending rotation θ_5. Thus, any torsional rotation about the truss axis, θ_6, due to the load P_1 indicates a coupling between those two degrees-of-freedom. In the Orthogonal truss there exists a significant rotation, θ_6, which is approximately 50 percent that of θ_5. In the case of the Warren truss, this coupling reduces to 5 percent, and is nonexistent for the Inverted Warren trusses. An examination of the tabulated results indicates that the Orthogonal and Warren trusses have high torsional/bending coupling, whereas the coupling present in the two Inverted Warren trusses is minimal.

It is important that a truss configuration have low torsional/bending coupling so that equivalent beam models using standard finite elements can be confidently employed for controls analyses or parameter studies.

COMPARISON OF COUPLING PRESENT IN VARIOUS TRUSS CONFIGURATIONS

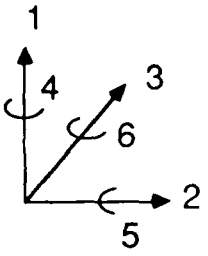

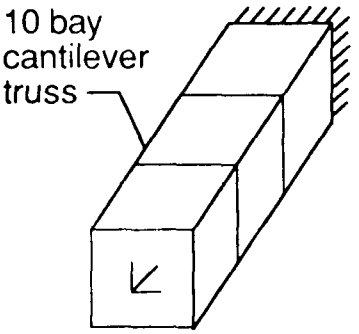

Nomenclature

Bending loads P_1, P_2

Bending moments M_4, M_5

Torque T_6

Rotations θ

Displacement δ

Coupling value (% of value in applied load direction)

Loading case	Coupled DOF	Orthogonal	Warren	Inv. Warren #1	Inv. Warren #2
P_1, P_2	θ_6	49.8	5.1	0.0	0.0
T_6	δ_1	1162.0	316.1	0.0	0.0
M_4, M_5	θ_6	50.2	0.0	0.2	0.0

EFFECTS OF REMOVING TRUSS MEMBER ON STRUCTURAL STIFFNESS

Since the Space Station truss is a four longeron, statically indeterminate structure there exists some margin of safety if an individual element were broken or removed. An experimental and analytical examination of the effects of removing a truss member on the truss bending stiffness was performed. A similar analytical study was performed in reference 7 which focused on an earlier version of the Space Station. Using the finite element analysis as a benchmark, each of the four base longerons was removed individually, and the reduction in truss bending stiffness due to a 50 lb. tip load was calculated. For each truss configuration the worst case scenario was simulated in the laboratory. Excellent agreement was acheived between the predicted and measured values (recall that the Warren truss was not tested). The Orthogonal truss retains approximately 60 percent of its cantilever lateral bending stiffness with a member removed whereas the Inverted Warren #2 retains approximately 70 percent of its stiffness. It should be emphasized that these represent worst case scenarios since the truss member was removed at the location of highest stress.

EFFECTS OF REMOVING TRUSS MEMBER ON STRUCTURAL STIFFNESS

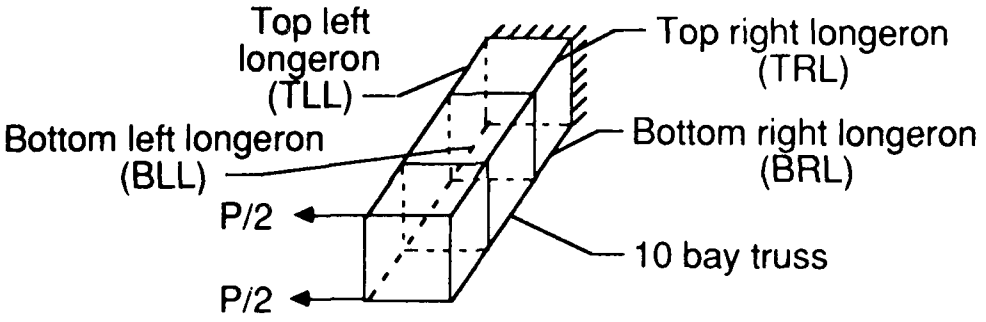

$\frac{EI_{reduced\ truss}}{EI_{full\ truss}}$	Orthogonal minus TRL	Warren minus BLL	Inverted Warren # 1 minus TRL	Inverted Warren # 2 minus TRL
Analysis	.595	.655	.672	.690
Test	.605	—	.674	.701

1/100 SCALE DUAL KEEL PHENOMENA TEST MODEL

A 1/100 scale dual keel test model has been fabricated and is shown in the figure suspended from a "shadow structure" by four steel cables. The overall size of the model is scaled such that cable attachment locations are representative of those anticipated in the larger truss models. This model is constructed of approximately [illegible] in. square Aluminum bar such that the first structural bending mode is [illegible] times that of the Space Station. The shadow structure covers the planform of the model allowing the model to be hung in any orthogonal orientation with cables attached at virtually any location. The interfaces which connect the dual keels with the upper, lower, and transverse booms were designed to be replaceable. In this way, the effects of interface flexibility can be established experimentally by inserting new interfaces with different materials or cross-sectional properties.

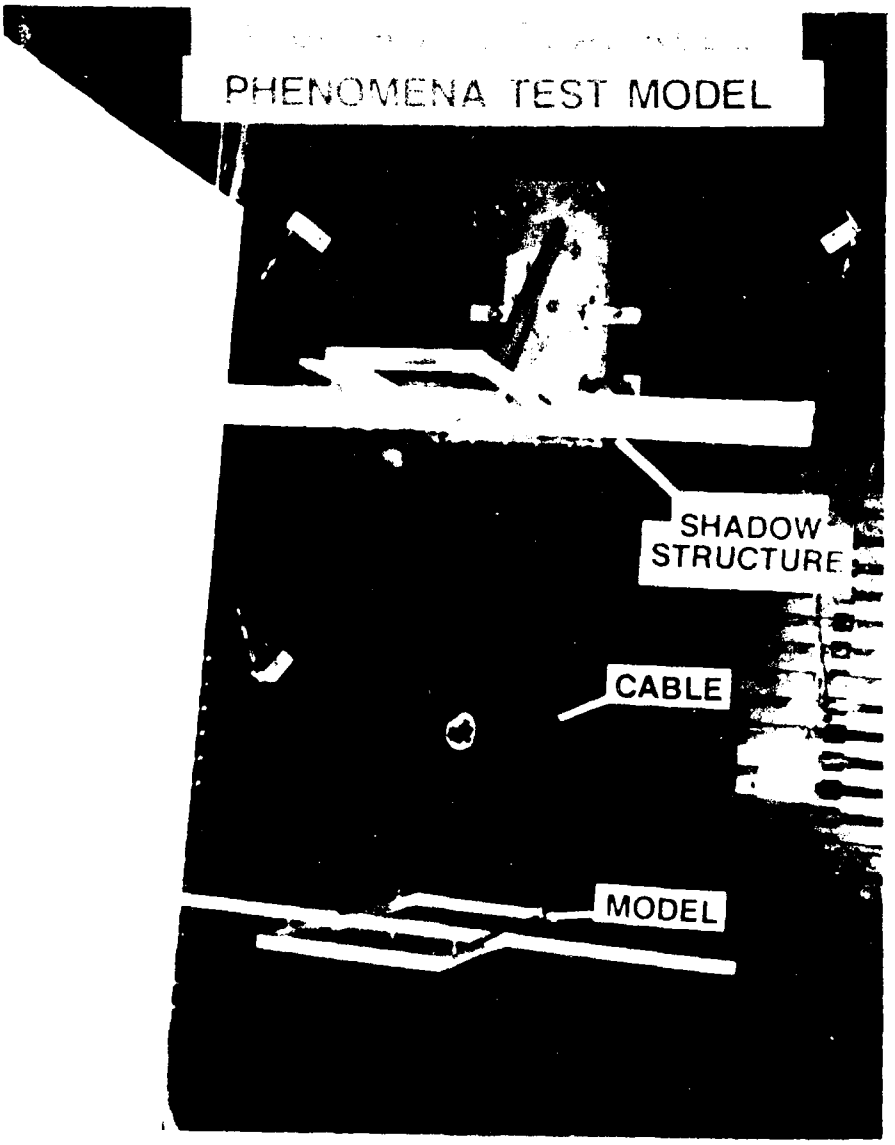

MODELING OF STRUCTURAL INTERFACE FLEXIBILITIES

The effects of interface flexibility was studied analytically. The figure shows a simple spring model of two of the six interfaces. Ignoring the off-axis coupling terms, these springs were used in the finite element model as generalized elements with diagonal stiffness matrices. The spring stiffnesses were varied, individually and collectively, and the variations of the global structural modes were examined.

MODELING OF STRUCTURAL INTERFACE FLEXIBILITIES

Equivalent beam dual keel model

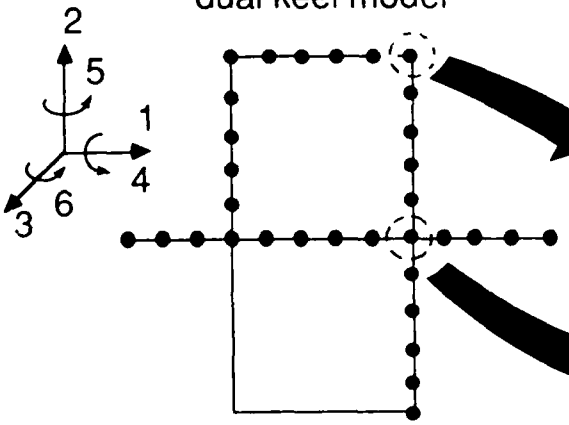

Interface flexibility schematic

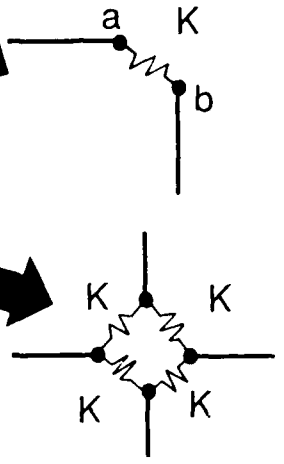

Mathematical representation (coupling terms neglected)

$$K = \begin{bmatrix} K_{11} & & & & & \\ & K_{22} & & \phi & & \\ & & K_{33} & & & \\ & & & K_{44} & & \\ & \phi & & & K_{55} & \\ & & & & & K_{66} \end{bmatrix}$$

Typical force - displacement relation

$$f_{bj} = K(u_{bj} - u_{aj})$$

$j = 1, 2, \ldots, 6$
u = displacements
f = force

EFFECTS OF INTERFACE FLEXIBILITIES ON DUAL KEEL VIBRATION MODE SHAPES

A representative sample of the interface flexibility effects on the vibration mode shapes is shown in the figure. Plotted on the ordinate is the variation in frequency for the first six global modes relative to a nominal value (the nominal value is the frequency obtained when the interface flexibilities are not included). Likewise the abscissa shows the variation of interface spring stiffness in the 4-direction (see previous figure) relative to its nominal value. As the interface becomes softer some frequencies are drastically affected while others which have no components in that direction are unaffected. Furthermore, at certain values of the interface stiffness ratio the ordering of the modes can switch. These results indicate the importance of correctly characterizing the structural properties of key interfaces to faclilitate system identification. One of the advantages of scale model testing is the ability to not only characterize the interfaces at the subassembly level, but also to be able to assemble the fully mated configuration and fine-tune the interface characterizations.

EFFECTS OF INTERFACE FLEXIBILITIES ON DUAL KEEL VIBRATION MODE SHAPES

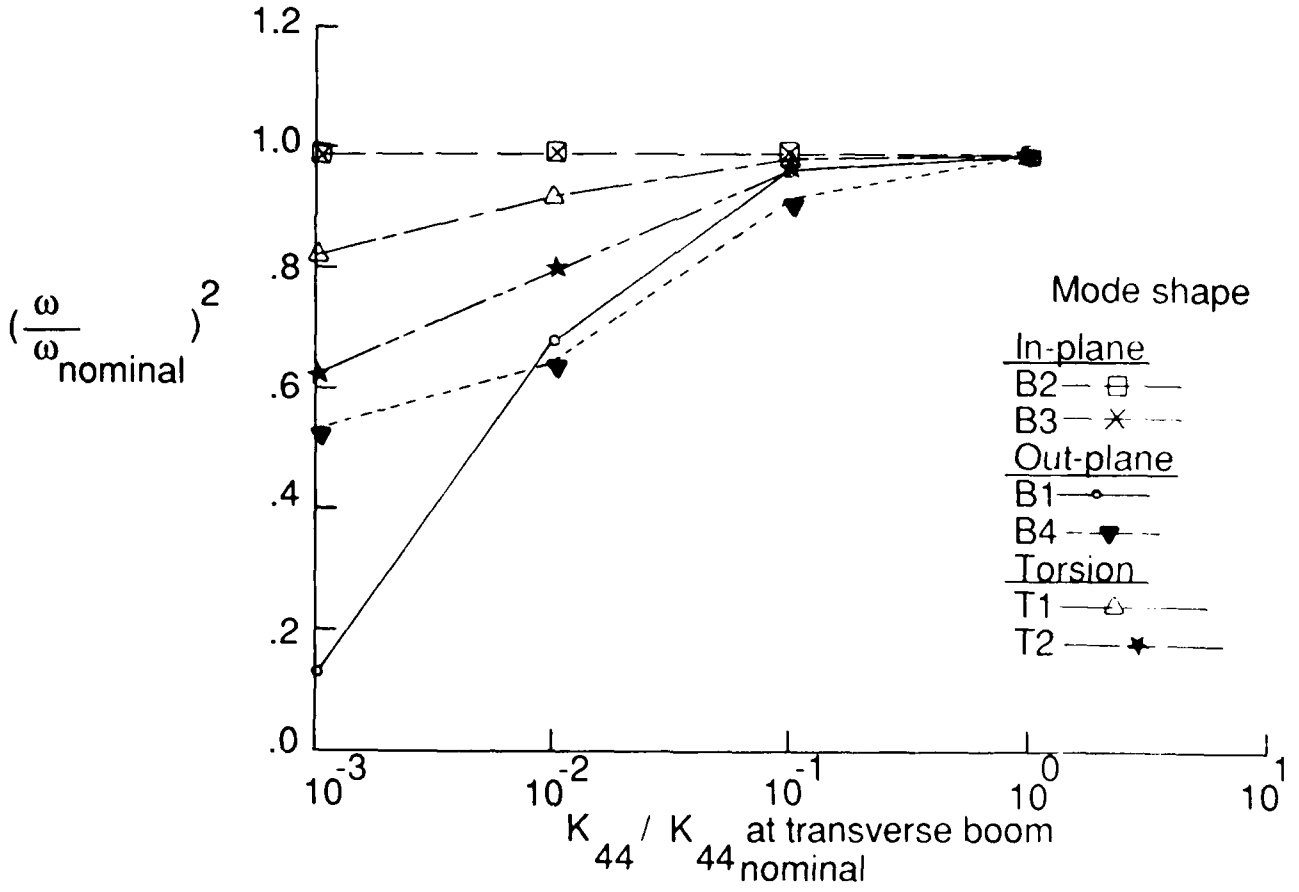

SUMMARY

Ground test and analysis techniques for the COFS III structure are being developed with the aid of a variety of scale model structures. The generic model hardware is functionally similar to that proposed for Space Station and accomodates Space Station build-up stages and key subassemblies. The linearity and predictability of the generic hardware was demonstrated by the excellent agreement between the analysis predictions and static tests. Wide differences in static coupling between the various truss configurations was evident. A 1/100 scale phenomena test model provides early experience with the dual keel structure. Modeling of key interfaces was shown to be important in identifying global vibration modes.

SUMMARY

- Scale model hardware useful for developing ground test and analysis methods on large truss structures
- Generic model accomodates all space station build-up stages and key subassemblies
- Static tests on generic hardware in excellent agreement with analysis
- Truss member lacing patterns exhibit wide differences in coupling
- Phenomena model provides early hands-on experience with dual keel structure
- Truss subassembly interface flexibilities important for accurate modal identification

REFERENCES

1. Letchworth, Robert; McGowan, Paul E.; Gronet, Marc J.; and Crawley, Edward F.: Conceptual Design of a Space Station Scale Model. Presented at the Second NASA/DOD CSI Technology Conference, Colorado Springs, Colorado, November 17-19, 1987.

2. Mikulas, Martin M., Jr.; and Bush, Harold G.: Design, Construction and Utilization of a Space Station Assembled from 5-Meter Erectable Struts. NASA TM-89043, October 1986.

3. McGowan, Paul E.: Considerations in the Design and Development of a Space Station Scale Model. Presented at the Workshop on Structural Dynamics and Control Interaction of Flexible Structures, Marshall Space Flight Center, April 22-24, 1986.

4. Letchworth, Robert; McGowan, Paul E.; and Gronet, Marc J.: COFS III Multibody Dynamics and Control Technology. Presented at the First NASA/DOD CSI Technology Conference, Norfolk, Virginia, November 18-21, 1986.

5. Gronet, Marc J. et al: Preliminary Design, Analysis, and Costing of a Dynamic Scale Model of the NASA Space Station. NASA CR-4068, July 1987.

6. McGowan, David M.; and Lake, Mark S.: Experimental Evaluation of Small-Scale Erectable Truss Hardware. NASA TM-89068, June 1987.

7. Dorsey, John T.: Structural Performance of Space Station Trusses With Missing Members. NASA TM-87715, May 1986.

ACKNOWLEDGEMENTS

The authors gratefully acknowledge the assistance of Mr. James C. Edelen in obtaining and reducing static test data and in generating figures for this paper. In addition, the assistance of Mr. Joseph Laufer and Mr. Richard S. Pappa in performing static and dynamic tests was quite valuable. Finally, the dedication and professionalism shown by Ms. Dawn Erskine, and Messrs. Albert B. Insley, Otto C. Ripley, and Charles E. Brown for general laboratory support is sincerely appreciated.

LARGE SPACE STRUCTURES TECHNOLOGY PROGRAM

Robert Gordon

Structures Division
Air Force Wright Aeronautical Laboratories

Program Introduction

The Structures Division of the Air Force Wright Aeronautical Laboratories Flight Dynamics Laboratory is conducting an inhouse exploratory development program in the dynamics and control of large space structures (LSS). The program, entitle Large Space Structures Technology Program, was initiated in 1985 to investigate several technical areas important to the development of future LSS. These areas include ground suspension and test methods, active vibration control approaches, and sensors and actuators for vibration control. The program is being conducted by the Structural Dynamics Branch and is supported by the Analysis and Optimization Branch and the Structural Test Branch.

Program Plan

The overall objective of the program is to establish a capability in the Structures Division for dynamic analysis and testing of large, flexible structures with active vibration control. The program approach is a series of experiments in the three general areas of active vibration control, sensors and actuators and ground testing. The figure depicts these experiments and their timing. The first controls experiment is the Cantilevered Beam which investigated control of a simple beam in bending using a single electromagnetic shaker as an actuator. The next controls experiment is the Advanced Beam which is also a cantilever beam but with control expanded to two bending axes plus torsion. Proof mass actuators mounted at the free end provide control forces. Following the Advanced Beam, an Active Member Truss experiment is planned to investigate the use of extendable members in providing active vibration control. The long task in the center of the figure depicts continuing sensor and actuator development to support the controls experiments. This task includes evaluation of a video based motion analysis system, development of linear and angular proof mass type actuators, evaluation of mechanical and piezoelectric member actuators, and development of a control computer hardware architecture for conducting ground experiments in a similar manner to flight experiments. In the ground test area the Counterbalance Suspension experiment evaluated a counterbalance technique for ground simulation of zero g. The 12 Meter Truss experiment combines ground test evaluation and active control of two truss beams; one lightly and one heavily damped. The final experiment shown at the right of the figure combines all the previous work in the control demonstration of a representative large, flexible structure.

LSSTP EXPERIMENTS

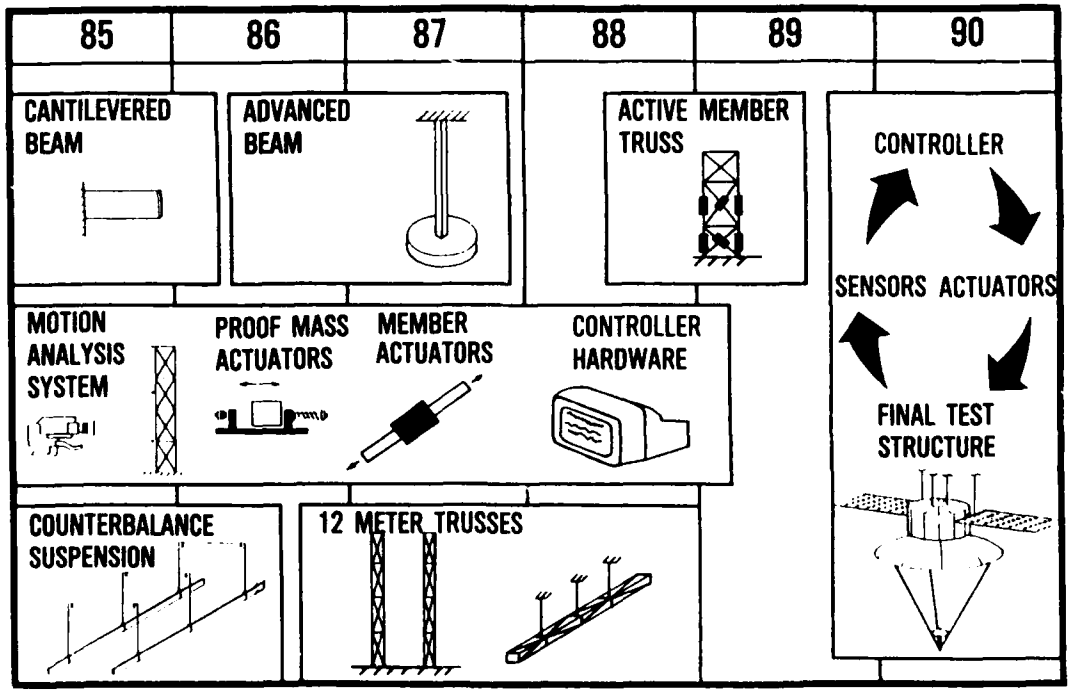

Counterbalance Suspension Development

Effective techniques are needed for supporting LSS during ground testing to remove the effects of gravity. A counterbalance suspension technique has been evaluated in the program to reach this goal. The counterbalance approach is simple. The structure to be tested is attached to an identical structure by means of wires and pulleys as shown in the figure. This approach would appear to provide nearly unrestrained vertical motion while providing pendulum constrained motion in the horizontal plane. Several counterbalanced dynamic systems were analyzed including point masses, rigid dumbells and flexible beams.

COUNTERBALANCE SUSPENSION CONCEPT

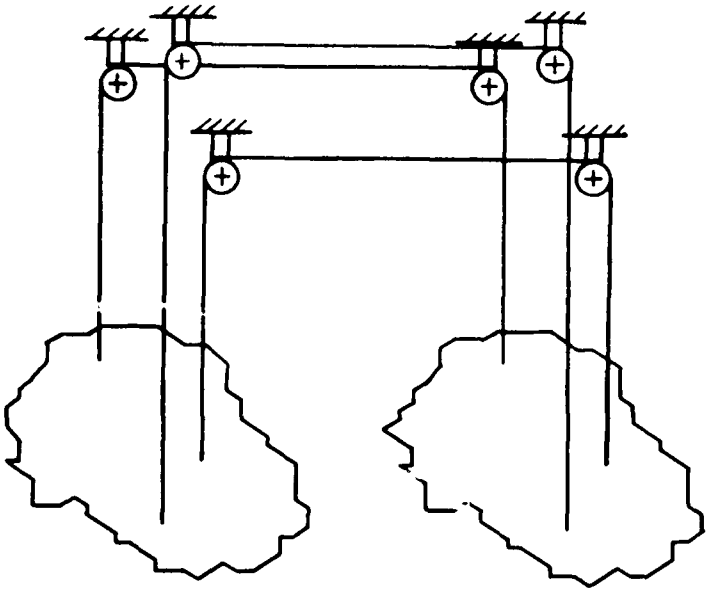

Flexible Beam Analysis

An analysis of counterbalanced flexible beams was conducted to evaluate the effectiveness of the approach in simulating zero g for a ground test. A finite element analysis of the vertical plane dynamic behavior of the two beams was performed. The analysis predicted the presence of two families of modes in the system of two beams. The first family of modes reproduces the frequencies and mode shapes of a single beam with free-free boundary conditions. These modes are independent of suspension parameters. In addition, a family of suspension dominated modes is also predicted which could interfere with the desired beam modes. The suspension modes are dependent on the suspension parameters of wire stiffness, number and attachment location. Additional system parameters including pulley friction, wire lateral modes and pendulum modes can interfere with desired system response.

PREDICTED MODES OF COUNTERBALANCED BEAMS

BEAM MODE

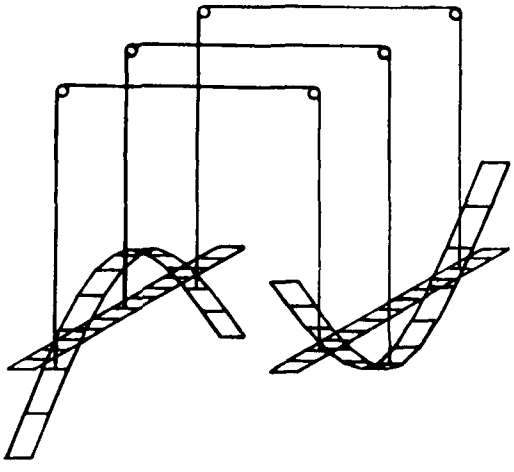

SUSPENSION MODE

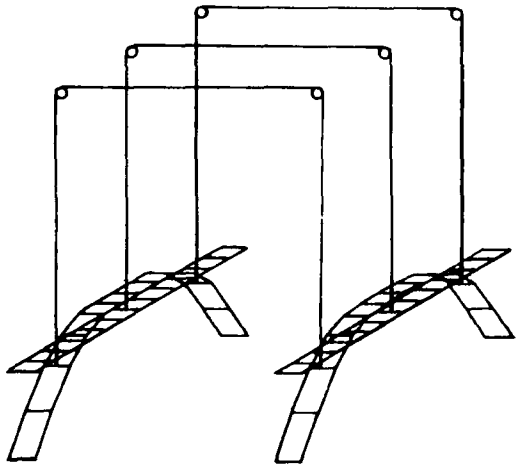

Testing was conducted on two counterbalanced flexible beams to verify the analysis. The beams were .125 inches by 1.5 inches in cross section and were 60 inches long. The beams were suspended on two fine steel wires and small pulleys. Modal testing of the system was done using both instrumented hammer impacts and sine dwell with noncontacting magnetic transducers. Measured frequencies show good agreement with predictions for both the beam and suspension modes.

COUNTERBALANCED BEAMS - TEST RESULTS

BEAM MODES	MEASURED FREQ (HZ)	PREDICTED FREQ (HZ)
1ST BENDING	7.06	7.12
2ND BENDING	19.19	20.09
3RD BENDING	37.60	39.39
SUSPENSION MODES		
1ST	6.81	7.28
2ND	10.25	10.84
3RD	18.06	19.22
4TH	36.44	39.68

Counterbalance Suspension Conclusions

The testing conducted on two flexible beams verifies the analytical prediction that the counterbalance suspension approach works. The system of two suspended beams possesses the identical frequencies and mode shapes as a single beam with free-free boundary conditions. However, a family of suspension modes is predicted which can interfere with the beam modes. Since the suspension mode frequencies are dependent on suspension parameters like wire length and spacing and the beams modes are independent of the suspension, it may be possible to "tune" the suspension modes to a frequency range above the test range of interest. A more serious limitation to the usefulness of the counterbalance approach is the fact that an identical twin of the structure to be tested is needed. This can prove to be expensive for complex structures. In addition, it is practically impossible to have two completely identical structures due to dimensional tolerances and variability in material properties and manufacturing processes. The effects of differences in the dynamic characteristics of the two structures on system response have not been investigated, but they will most certainly not improve the simulation of free-free behavior.

COUNTERBALANCED SUSPENSION CONCLUSIONS

- FREE-FREE BEAM MODES ARE ACCURATELY REPRODUCED
- UNWANTED "SUSPENSION" MODES ALSO OCCUR, BUT CAN BE TUNED
- APPROACH IS NOT PRACTICAL BECAUSE:
  - COST OF A SECOND STRUCTURE
  - IDENTICAL TWIN IS IMPOSSIBLE
- EVALUATE ZERO RATE SPRING DEVICE AS AN ALTERNATIVE

Advanced Beam Experiment Description

The Advanced Beam is a bending-torsion beam active vibration control experiment. The objective is to provide an active control experiment with a simple structure that addresses the LSS control challenges including low frequency, closely spaced modes, low inherent damping, nongrounded actuators and modal coupling. It incorporates a vertically oriented flexible beam cantilevered at the top. Control forces are provided by two pairs of proof mass actuators mounted on a disk at the beam tip. The aluminum alloy beam is .75 inches by 1.0 inches in cross section and 71 inches long. The dimensions of the disk can be altered to vary the torsion mode frequency and to couple the bending and torsion modes. The actuators used are modified versions of the VCOSS design now in use at the NASA Marshall Space Flight Center's facility.

ADVANCED BEAM EXPERIMENT

OBJECTIVE:

- DEMONSTRATE ACTIVE VIBRATION CONTROL OF A 3-DOF BEAM WITH CLOSELY SPACED COUPLED MODES

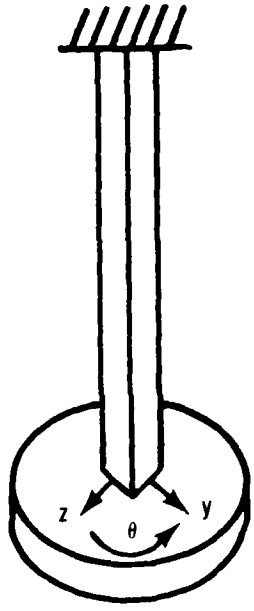

DESIGN FEATURES

- 3 LOW FREQUENCY MODES
- SIMPLE ANALYSIS
- OFFSET CG TO COUPLE MODES
- TIP MASS WITH REALISTIC ACTUATORS
- BENDING MODES CAN BE DAMPED

Advanced Beam Experiment Hardware

The Advanced Beam is shown in the figure suspended from an aluminun support frame. The frame is mounted on a seismic table in the vibration test area at the Flight Dynamics Laboratory.

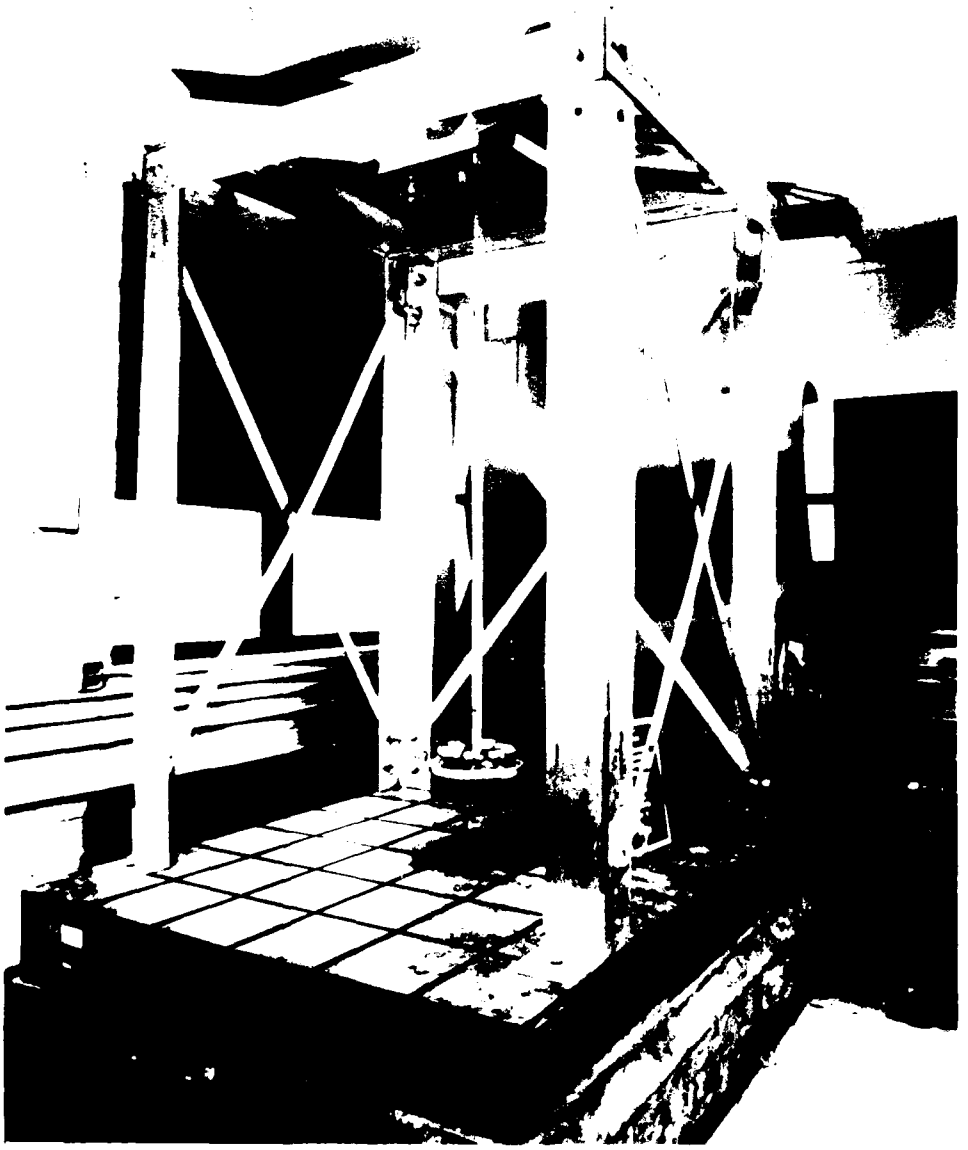

Advanced Beam Experiment Actuator Configuration

The arrangement of the four proof mass actuators at the free end of the Advanced Beam is shown in the figure. The actuators are arranged in two pairs; one pair is used in phase for each bending axis and either pair can be driven out of phase to provide torque for torsion mode control.

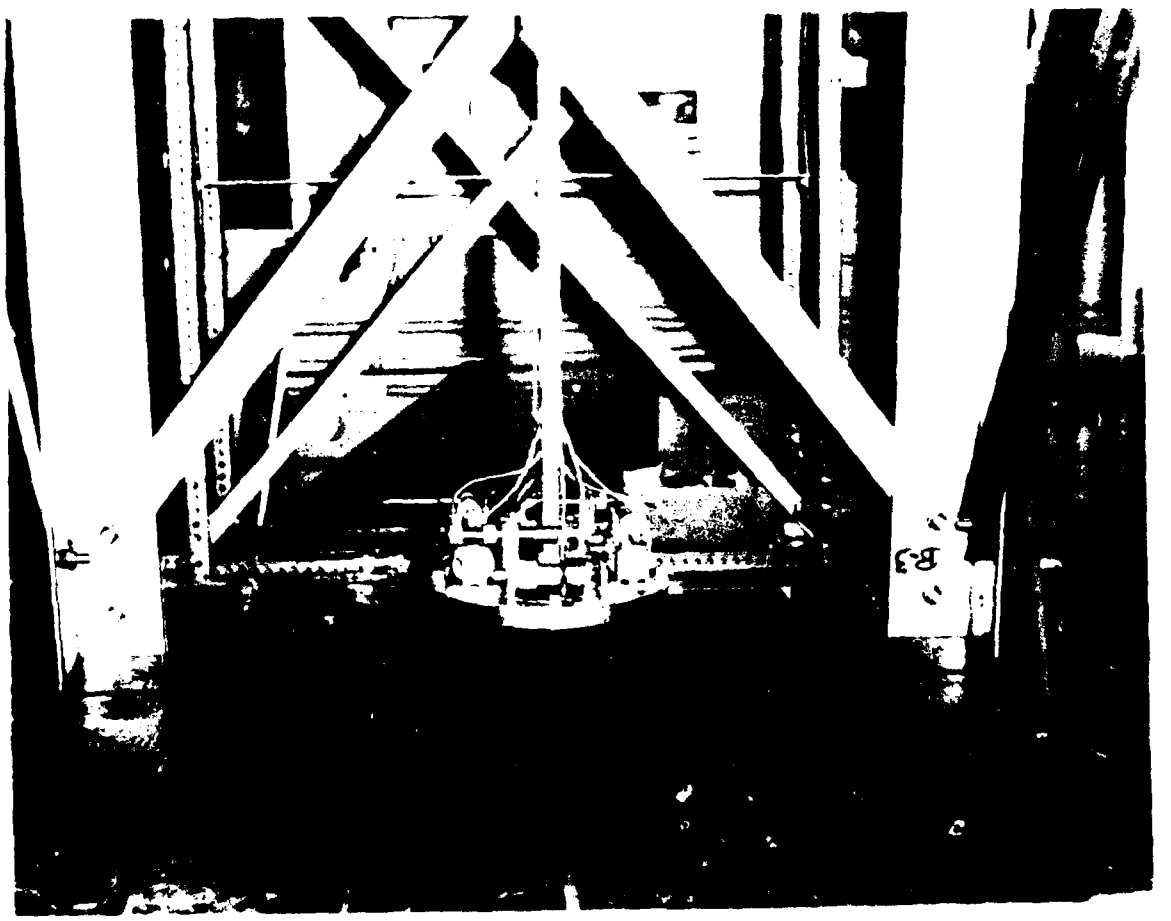

Proof Mass Actuator Development

Four proof mass actuators are used to provide control forces on the Advanced Beam. Each actuators is fabricated from a linear DC motor with the armature held fixed and the field magnets allowed to translate on a shaft supported on linear bearings. This design is based on the one developed by TRW Space and Technology Group on the Vibration Control of Spacecraft (VCOSS II) contract. A feedback compensator is used to improve the performance of the actuator so that actuator dynamics can be left out of the overall active controller. Proof mass acceleration and relative position are fed back to flatten low frequency response and to help center the proof mass on the shaft. Extensive testing has been conducted to characterize actuator response to commands and the degree of coupling between the proof mass and the structure when the actuator is not commanded.

PROOF MASS ACTUATOR DEVELOPMENT

- BASELINE ACTUATOR RESPONSE WAS NOT SATISFACTORY
  - MAGNITUDE & PHASE ERRORS AT LOW FREQUENCY
  - PROOF MASS WON'T STAY CENTERED
  - FRICTION CAUSES PROOF MASS TO COUPLE WITH STRUCTURE
- IMPLEMENT FEEDBACK COMPENSATION
- CONDUCT EXTENSIVE CHARACTERIZATION TESTING

Proof Mass Actuator Performance

The goals of the actuator compensator design effort were to obtain constant magnitude and phase in the frequency range from 1 to 100 hertz, to maintain centering of proof mass motion on the shaft and to minimize coupling between the proof mass and the structure when the actuator is not commanded. The uncompensated actuator adds considerable phase error at low frequencies as can be seen from the figure. But, when the compensator is used this phase error is reduced to just a few degrees at 1 hertz. The magnitude error is also improved significantly. Good proof mass centering has been achieved, but at the expense of some coupling of the proof mass with the structure. A major limitation of proof mass actuators in general was demonstrated during the development effort. The actuator is capable of generating over 4 pounds of force at maximum current. However, at low frequencies, the force output is limited by available proof mass travel. For example, at 1 hertz, the actuator can provide only about .1 pounds of force. This limitation is significant at the 1.3 hertz fundamental bending mode of the beam.

ACTUATOR PERFORMANCE

ACTUATOR TRANSFER FUNCTION

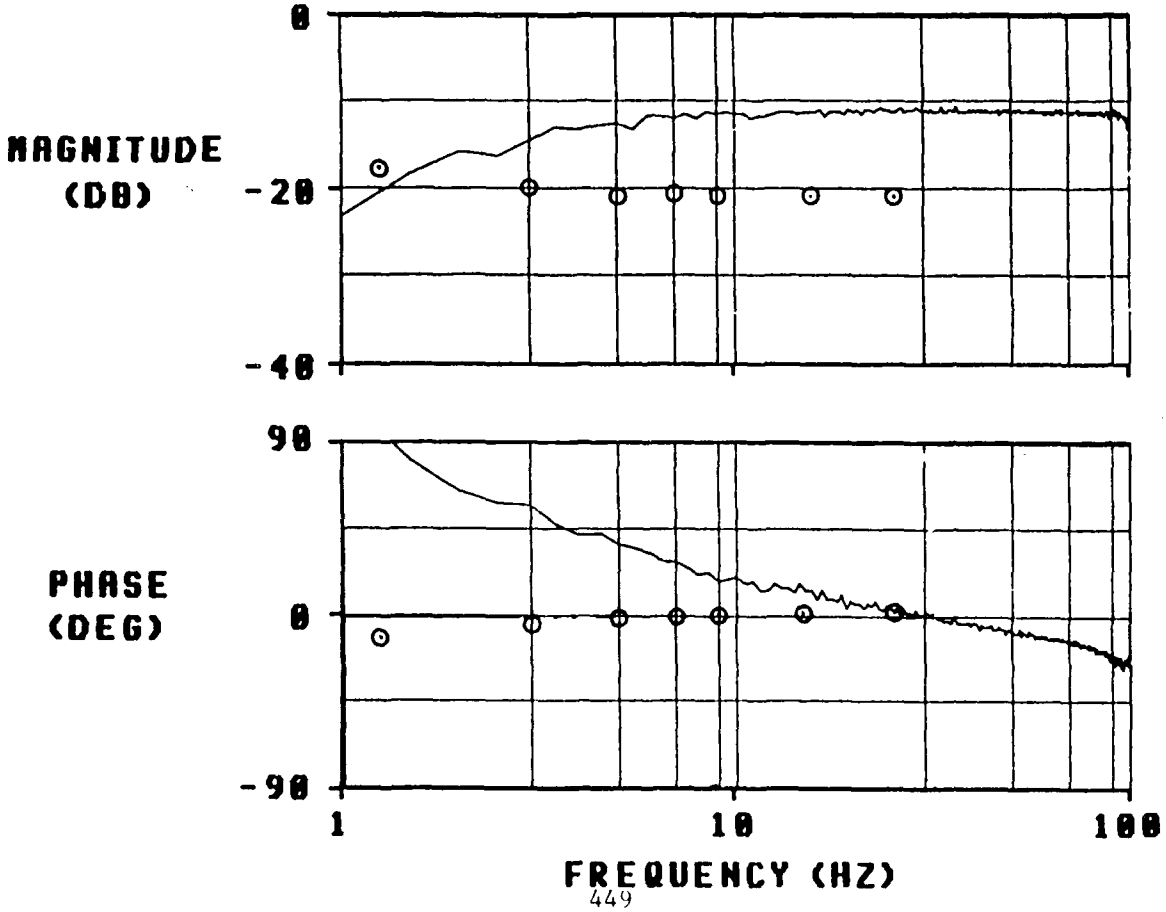

Proof Mass Actuator Testing

The figure shows one of the actuators during characterization testing. The actuator is mounted on a low friction table for direct measurement of force output. The accelerometer and linear variable differential transformer (LVDT) used for proof mass acceleration and relative displacement measurement (respectively) can be seen in the figure.

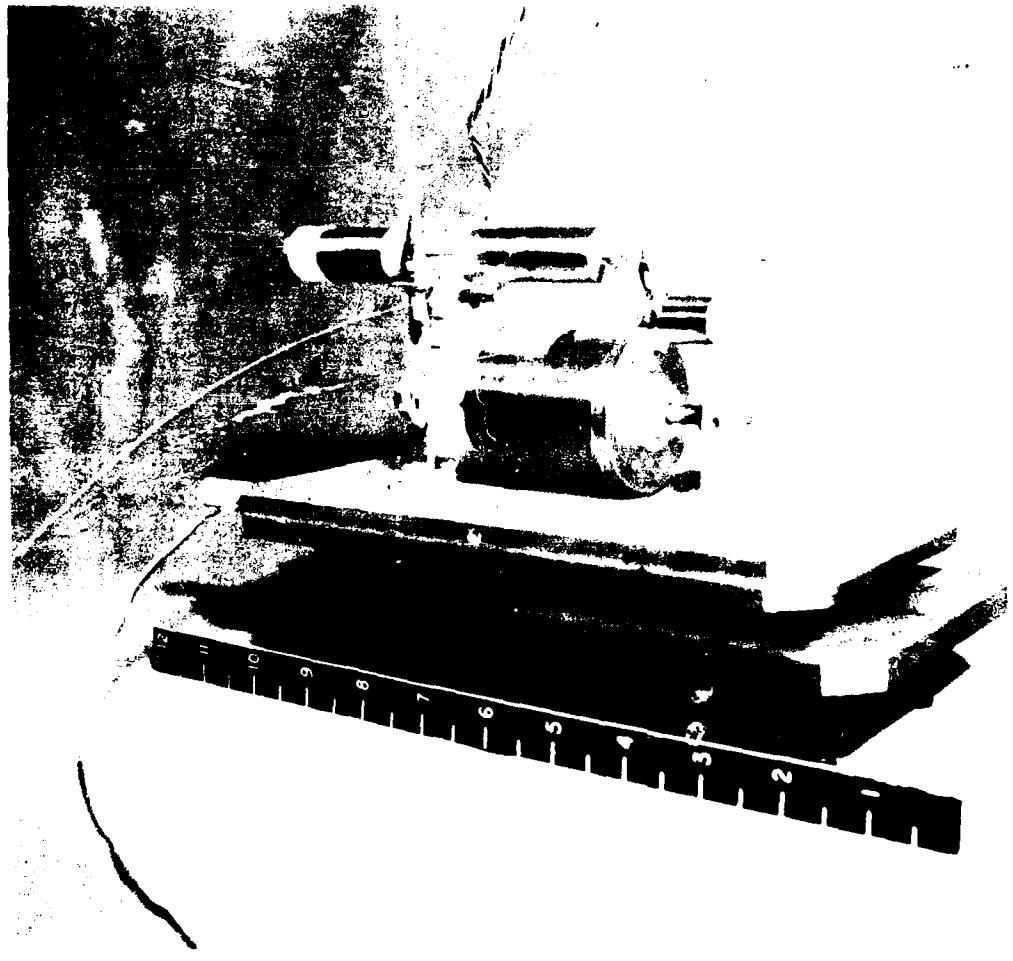

Advanced Beam Experiment Status

The Advanced Beam Experiment is completely set up and is essentially ready for closed loop controls testing. Control approaches for the experiment are being designed under a contract with the Ohio State University Research Foundation. Three control designs will be implemented on the hardware. They are: High Authority Control/Low Authority Control (HAC/LAC), Linear Quadratic Guassian with Loop Transfer Recovery (LQG/LTR) and Model Reference Adaptive Control. The performance of each controller in minimizing beam tip response will be evaluated.

ADVANCED BEAM EXPERIMENT STATUS

- HARDWARE SET UP COMPLETED
- ACTUATOR DEVELOPMENT COMPLETED
- OPEN LOOP MODAL TEST COMPLETED
- CONTROLLER DESIGN IN PROGRESS AT OHIO STATE
  - HAC/LAC
  - LQG/LTR
  - MODEL REFERENCE ADAPTIVE CONTROL
- CONTROL TESTING WILL BEGIN IN DECEMBER

12 Meter Truss Experiment Overview

The 12 Meter Truss Experiment will investigate ground suspension, test methods and active vibration control approaches for truss type structures with integral passive damping. Two 12 meter long truss beams have been fabricated; one with relatively high modal damping while the other is lightly damped. The two beams have identical welded aluminum alloy frames (longerons and horizontal members) with either aluminum or lexan bolt on diagonal members. The damped truss has aluminum diagonals with a viscoelastic damping element built in. The undamped truss has lexan diagonals which provide relative light damping. The aluminum and lexan diagonals are designed to have identical axial stiffness at low frequency so that the two trusses will have nearly identical natural frequencies and mode shapes but significantly different damping. Due to the frequency dependence of the viscoelastic material, stiffness can only be identical at one frequency but differences should be small near the design frequency. The trusses are built in four sections with easy removal of diagonals for convenient "tuning" of desired structural response. The approach to the experiment is to conduct a series of modal tests to completely characterize the structures and then to conduct active vibration control testing.

12 METER TRUSS EXPERIMENT

DESIGN FEATURES

- 12 METER LONG
- MODULAR DESIGN
- FIRST BENDING MODES - 2.6 Hz
- TRUSSES ARE DYNAMICALLY SIMILAR

APPROACH

- MODAL TESTING
- ACTIVE CONTROL

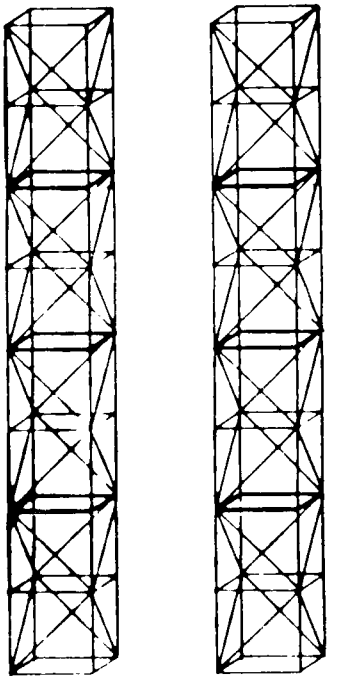

Modal testing will be [illegible] configurations: cantilevered vertically [illegible] (as shown in the figure) and horizontally suspended [illegible] a pseudo free-free condition. Modal parameters [illegible] the finite element model of the truss [illegible] testing. Measured mode shapes [illegible] predictions from the analytical [illegible] will be compared with methods.

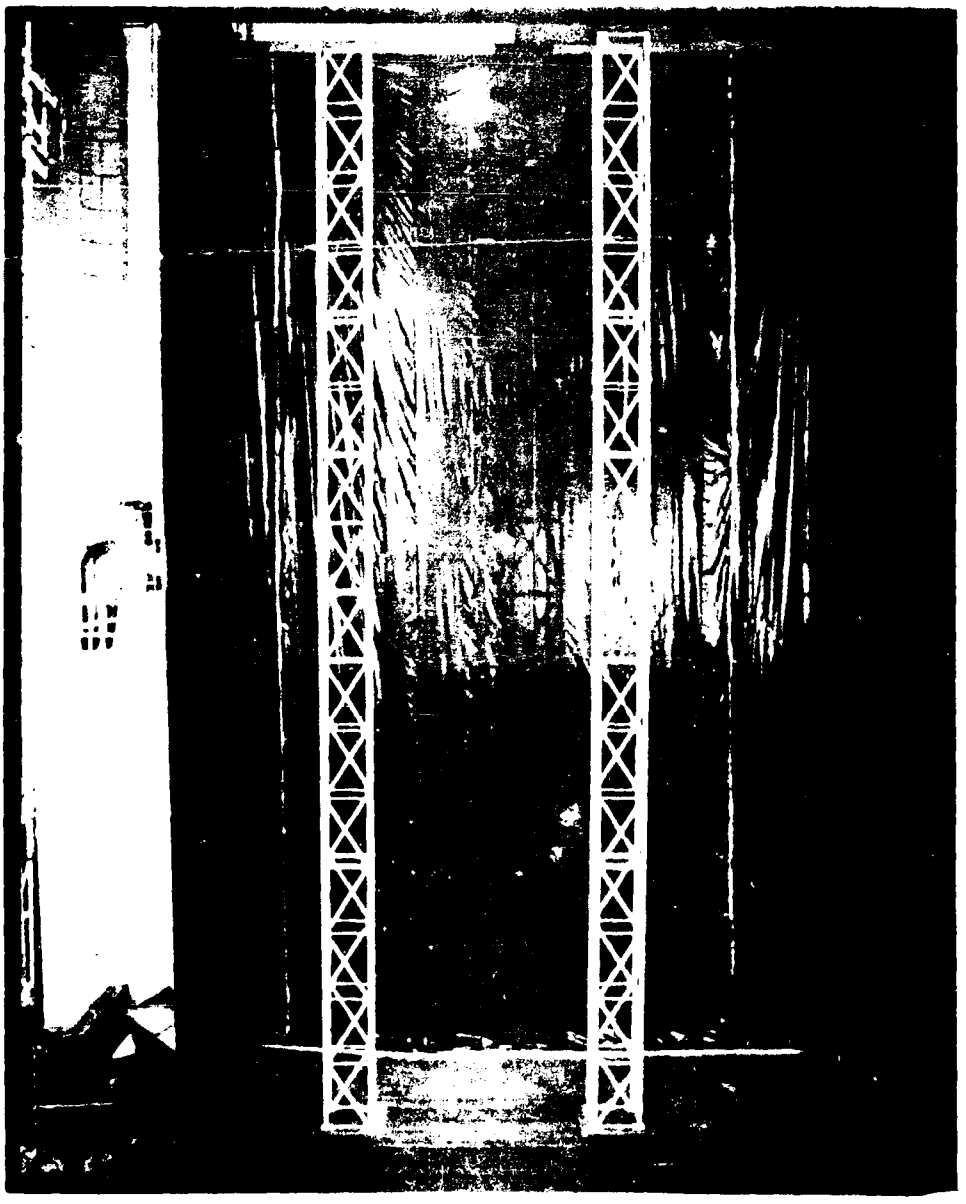

Preliminary Modal Test Results

Preliminarty modal testing of the undamped truss has been completed. Measured frequencies and modal damping are shown in the figure along with predicted frequencies. The agreement between predicted and measured frequencies is poor. This is attributed at least in part to errors in the finite element model which have susequently been identified and are being corrected. The measured modal damping values are low as expected ranging from approximately .1 to .5 percent. Testing is underway to measure detailed mode shapes for the lowest 7 modes. In addition, testing will be conducted to determine the linear range of response of the undamped truss. Testing of the damped truss will begin upon completion of the undamped truss testing.

12 METER TRUSS MODAL TEST UNDAMPED RESULTS

	FREQUENCY (Hz)			DAMPING (%)
MODE	TEST	PREDICTED	ERROR (%)	TEST
1ST X BENDING	2.175	2.606	19.8	.180
2ND X BENDING	10.23	11.14	8.9	.399
1ST Y BENDING	2.225	2.620	17.7	.140
2ND Y BENDING	10.25	11.25	9.8	.328
1ST TORSION	7.031	5.984	14.9	.507

12 Meter Truss Active Vibration Control

A series of active vibration control tests will be conducted on one of the 12 meter trusses after modal testing is completed. Control approaches will be selected and applied by Ohio State University personnel under contract. Both centralized and decentralized control approaches will be investigated. One of the trusses will be suspended horizontally on zero rate spring mechanisms for controls testing. The truss will be configured for several levels of passive damping by selectively applying lexan and damped aluminum diagonals to observe the effect on controller performance. Both linear and angular proof mass type actuators will be used to provide control forces and torques.

12 METER TRUSS ACTIVE VIBRATION CONTROL

- TEST ONE TRUSS BEAM IN FREE-FREE CONFIGURATION
- OHIO STATE WILL DESIGN CONTROLLERS
  - ADVANCED BEAM CONTROLLER
  - DECENTRALIZED CONTROLLERS
- VARY TRUSS PASSIVE DAMPING TO SEE ITS EFFECT ON CONTROLLER PERFORMANCE
- LINEAR AND ANGULAR PROOF MASS ACTUATORS

Program Summary

The Large Space Structures Technology Program at the Flight Dynamics Laboratory's Structures Division is continuing to investigate structural dynamics and control issues for future large space structures. Experiments are being conducted involving active vibration control, ground testing and sensor and actuator hardware. Active control of truss type structures will be developed using both proof mass type (external) and active member type (internal) actuators. The effects of passive damping on controller performance will also be investigated.

PROGRAM SUMMARY

- COUNTERBALANCE SUSPENSION STUDIED
- PROOF MASS ACTUATOR DEVELOPED AND TESTED
- ADVANCED BEAM EXPERIMENT READY FOR CONTROLS TESTING
- 12 METER TRUSS MODAL TESTING IN PROGRESS
- ACTIVE MEMBER TRUSS EXPERIMENT IN PLANNING

EXPERIMENTAL FAILURE DETECTION RESULTS USING THE SCOLE FACILITY

by

Mathieu Mercadal

Student

and

Wallace E. Vander Velde

Professor

Department of Aeronautics and Astronautics

Massachusetts Institute of Technology

Cambridge, Massachusetts

LSS CONTROL SYSTEMS MUST BE DESIGNED FAULT TOLERANT

One of the essential characteristics of control systems for large, flexible spacecraft is that they be able to continue to perform their intended mission in spite of component failures. This is because a large number of sensors and actuators are likely to be needed for some systems to meet their performance requirements, and a long period of operation is expected between visits for maintenance and resupply. For example, if the control system utilizes 100 sensors and 100 actuators (which is small by some estimates) and the component mean time to failure is 100,000 hours (which is long by present standards), then the expected number of component failures in each year of operation is 17. That means, on average, one can expect a component of the control system to fail about every 21 days!

WHY DO WE NEED TO CONSIDER COMPONENT UNRELIABILITY?

- A LARGE, LIGHTWEIGHT STRUCTURE IN SPACE WILL DISPLAY MANY VIBRATORY MODES WHICH MAY HAVE TO BE ACTIVELY DAMPED TO ASSURE MISSION SUCCESS.
- EFFECTIVE CONTROL OF THESE MANY MODES WILL REQUIRE USE OF A LARGE NUMBER OF SENSORS AND ACTUATORS—POSSIBLY HUNDREDS OF THEM.
- EVEN IF THESE CONTROL SYSTEMS ARE SERVICED IN ORBIT, ONE WOULD LIKE THE SERVICE INTERVAL TO BE LONG—AT LEAST ONE YEAR.
- WITH COMPONENT MEAN TIME BETWEEN FAILURES WHICH CAN REASONABLY BE ANTICIPATED, ONE MUST EXPECT MANY OF THE CONTROL SYSTEM COMPONENTS TO FAIL IN THE COURSE OF A YEAR.

PROBLEMS TO CONSIDER IN DESIGNING FOR FAULT TOLERANCE

If a control system is to be designed with the capability to tolerate component faults, there are several problems to be addressed. One of the first that appears in the design process is the decision about how many sensors and actuators to incorporate in the control system and where to locate them on the structure. This decision should be made with full consideration of the sets of failures that are likely to occur during the operating lifetime of the system. A central problem is design of the fault monitoring system which decides when a component has failed during system operation, and which component it is. One must also determine the methodology to be used to reconfigure the control system each time a component has been declared failed. Finally, there is the important matter of evaluating how well the system may be expected to perform - taking account of the usual noises and disturbances, and in addition recognizing the random events of component failures and the actions taken by the redundancy management system.

In this presentation, we will deal only with one approach to the failure detection and isolation problem.

RELIABILITY ISSUES IN ACTIVE CONTROL

OF LARGE FLEXIBLE SPACE STRUCTURES

CONTROL SYSTEMS FOR LSS WILL SUFFER COMPONENT FAILURES DURING SYSTEM OPERATION

ASPECTS OF THE PROBLEM OF DEALING WITH FAILURES

- CHOICE OF NUMBER AND PLACEMENT OF SENSORS AND ACTUATORS - RECOGNIZING THE LIKELIHOOD OF FAILURES
- FAILURE DETECTION AND ISOLATION
- SYSTEM RECONFIGURATION
- EVALUATION OF SYSTEM PERFORMANCE - INCLUDING THE EFFECTS OF REDUNDANCY MANAGEMENT

GENERAL FORM OF A FAILURE DETECTION AND ISOLATION SYSTEM

This Figure shows the general form of a Failure Detection and Isolation (FDI) system. The Residual Generator produces a set of signals, usually called residuals, which under nominal conditions are zero except for noise and other unmodeled effects. The residual becomes significantly nonzero when a failure occurs. The purpose of the Decision Algorithm is to sense the significantly nonzero residual and decide what failure produced it.

In this presentation we will discuss only the Residual Generation function.

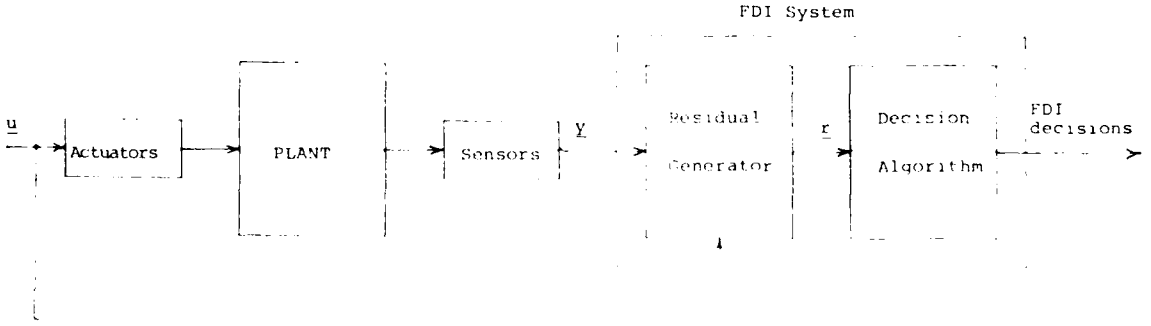

GENERAL FORM OF FDI SYSTEM

THE ROLE OF ANALYTIC REDUNDANCY

The simplest and most robust form of redundancy is direct hardware redundancy where, for example, all sensors might be triplicated. In that case, the outputs of each triplicated set of sensors can be compared directly to see if one sensor fails to conform to the other two.

But if a large space structure control system requires a large number of sensors and actuators to perform its mission, it would be unrealistic to consider triplicating, or even duplicating, all components directly. In such a case, one must use "analytic redundancy" to infer abnormal behavior of a sensor or actuator. Analytic redundancy refers to the use of analytic relations describing the dynamic characteristics of the system to relate the outputs of unlike sensors and the effects of unlike actuators to each other to check for consistency. Unfortunately, when the system dynamic model is used for failure monitoring, the FDI system becomes sensitive to errors in the model of the system dynamics.

THE NEED FOR USE OF ANALYTIC REDUNDANCY

WE ANTICIPATE THAT LARGE SPACE STRUCTURE CONTROL SYSTEMS MAY REQUIRE USE OF A LARGE NUMBER OF SENSORS AND ACTUATORS IN SOME CASES.

IT WOULD BE PROHIBITIVELY COSTLY TO EMPLOY MASSIVE HARDWARE REDUNDANCY - SUCH AS TRIPLICATING EACH COMPONENT.

WITHOUT DIRECT HARDWARE REDUNDANCY, FDI MUST BE BASED ON ANALYTIC REDUNDANCY RELATIONS WHICH DEPEND ON A MODEL OF THE SYSTEM DYNAMICS.

UNFORTUNATELY THIS MAKES THE FDI SYSTEM SENSITIVE TO MODELING ERROR - INCLUDING PARAMETER UNCERTAINTY AND MODEL TRUNCATION.

SUMMARY OF APPROACHES TO COMPONENT FAILURE DETECTION AND ISOLATION

A requirement for most fault tolerant control systems is a means for detecting the event that a component has failed, and identification of the faulty component. This is known as the Failure Detection and Isolation (FDI) function.

Many methods for performing the FDI function have been suggested - mostly in the context of aircraft flight control systems. Some of these methods are applicable only to sensor failures while others are applicable both to sensor and actuator failures.

Summary of FDI Techniques

Applicable to sensors only

- Simple voting
- Midpoint select with threshold test
- Simple parity relations
- Estimate of confidence for sensor outputs
- Filters or observers using partial sets of sensors

Applicable to sensors and actuators

- Failure states included in Kalman filter
- Generalized parity relations
- Estimate probability of jump variable state
- Generalized likelihood ratio
- Multiple hypothesis tests
- Failure detection filter

CHOICE OF FDI METHOD

As noted on the previous slide, some FDI methods are applicable only to sensor failures while others are applicable to both sensor and actuator monitoring. For convenience only, we have chosen to consider only techniques applicable to both sensors and actuators. A more important distinction among FDI methods is that some are designed to detect specific modes of failure. Any hypothesis testing method, for example, looks for a failure signature resulting from a specific type of abnormal behavior - such as a bias shift in a sensor output. We prefer not to have to anticipate all the ways in which a failed component may behave.

Two FDI methods which are applicable to both sensors and actuators, and do not require hypotheses about mode of failure, are generalized parity relations and the failure detection filter. We have worked with the design and simulation of both these types of FDI processors, but the results reported here are based on use of generalized parity relations.

FAILURE DETECTION AND IDENTIFICATION

- MANY APPROACHES TO FDI HAVE BEEN SUGGESTED.
- WILL NOT CONSIDER METHODS WHICH REQUIRE SPECIFICATION OF THE MODE OF FAILURE.
- WILL CONCENTRATE ON METHODS WHICH ARE APPLICABLE TO BOTH SENSOR AND ACTUATOR FAILURES.
- TWO CANDIDATE TECHNIQUES FOR INITIAL CONSIDERATION:

  AN OPEN LOOP METHOD: GENERALIZED PARITY RELATIONS

  A CLOSED LOOP METHOD: FAILURE DETECTION FILTER

GENERALIZED PARITY RELATIONS

The type of failure monitoring residual generator known as a generalized parity relation is a generalization of the simpler notion of a parity relation introduced for failure monitoring in strapdown inertial navigation systems. As one example, if one had a set of four rate gyros mounted on a rigid body, or at essentially one location on a general body, there would be a redundant piece of information since the angular velocity vector has only three components. Thus it must be possible to form a linear combination of the four gyro outputs in such a way that the result is zero under nominal conditions except for noise. This is called a parity relation; it can be used to detect a failure in one of the gyros.

The generalization can be used to monitor the performance of sensors and actuators in dynamic systems without any special form of hardware replication.

GENERALIZED PARITY RELATIONS

The generalized concept of parity relations uses measurements at different points in time, if necessary, to form relations which have null residuals if the system is nominal and we neglect noise.

Discrete system model:

$$\underline{X}_{k+1} = A\underline{X}_k + B\underline{U}_k$$

$$\underline{Y}_k = C\underline{X}_k + D\underline{U}_k$$

The measurement relations are:

$$Y_k = CX_k + DU_k$$

$$Y_{k+1} = CAX_k + CBU_k + DU_{k+1}$$

$$Y_{k+2} = CA^2X_k + CABU_k + CBU_{k+1} + DU_{k+2}$$

etc.

GENERALIZED PARITY RELATIONS (CONTINUED)

There are other ways of constructing generalized parity relations, but the idea can be understood readily from the following description. The discrete time model of the system dynamics is used and expressions are written for the set of measurements produced by the sensors at a number of points in time. Using the discrete time recursion for the system dynamics, the state at any time can be replaced by the state at the time of the first measurement and the actuator commands which were executed after that time. For convenience, all these expressions for the sensor outputs are collected into a single vector.

GENERALIZED PARITY RELATIONS (CONTINUED)

If we define

$$\underline{Y}_k^* = \begin{bmatrix} \underline{Y}_k \\ \underline{Y}_{k+1} \\ \underline{Y}_{k+2} \\ \vdots \end{bmatrix} \qquad C^* = \begin{bmatrix} C \\ CA \\ CA^2 \\ \vdots \end{bmatrix} \qquad \underline{U}_k^* = \begin{bmatrix} \underline{U}_k \\ \underline{U}_{k+1} \\ \underline{U}_{k+2} \\ \vdots \end{bmatrix}$$

$$D^* \quad \begin{bmatrix} D & 0 & 0 & \cdots \\ CB & D & 0 & \cdots \\ CAB & CB & D & \cdots \\ \vdots & \vdots & \vdots & \end{bmatrix}$$

then the measurement relations can be generalized as

$$\underline{Y}_k^* = C^* \underline{Y}_k + D^* \underline{U}_k^*$$

GENERALIZED PARITY RELATIONS (CONCLUDED)

The vector which contains the sensor outputs at a number of points in time is expressed in terms of the state of the system at just one time - the time of the first measurement in the set - and the actuator commands which were issued after that time. If enough time points have been included in the set, and we know that we never need more than n+1 where n is the order of the system dynamics, the matrix which multiplies the state vector has a left null space. The inner product of the vector of measurements with any vector in that left null space forms a scalar quantity which is a generalized parity relation. The state vector does not appear in the expression of that scalar; it depends only on the set of sensor outputs and actuator commands - all available quantities. This scalar is zero under nominal conditions except for noise. It can be used to monitor all of the sensors and actuators which appear in the relation for consistent behavior.

To isolate which component has failed as well as detect that a failure has occurred, one must generate a number of generalized parity relations. Each one must depend on only some of the sensors or some of the actuators. This can be done in such a way that the state of all the relations is sufficient to determine which component is behaving in an off-nominal manner.

GENERALIZED PARITY RELATIONS (CONTINUED)

Any linear combination of the measurements

$$\underline{\ell}^T Y_k^* = \underline{\ell}^T C^* X_k + \underline{\ell}^T D^* U_k^*$$

for which $\underline{\ell}^T C^* = 0$

can be used as a parity relation

$$r = \underline{\ell}^T Y_k^* - \underline{\ell}^T D^* U_k^*$$

Neglecting noise, this residual is zero under nominal conditions

An appropriate set of parity relations is one in which each one depends on different subsets of the measurements. The pattern of the set of zero and non-zero residuals indicates which component.

A COMPLETE FDI SYSTEM USING SINGLE-COMPONENT PARITY RELATIONS

One convenient way to generate generalized parity relations for easy isolation of the failed component is to use single-component parity relations. A single-sensor parity relation is one which depends on only a single sensor - although it generally depends on all the actuators as well. It is readily generated by starting with a vector of measurements taken from only one sensor. It is not so obvious how parity relations which depend on only one actuator can be generated, but it is usually possible to construct such relations as well. In general, they depend on all the sensors.

The FDI system then makes failure decisions based on a complete set of single-component parity relations - one for each sensor and one for each actuator. The logic is simple; if a sensor fails, only one of the sensor parity relations becomes large whereas most or all of the actuator parity relations become large. So the decision logic determines that a single sensor has failed rather than that most or all of the actuators have failed at once.

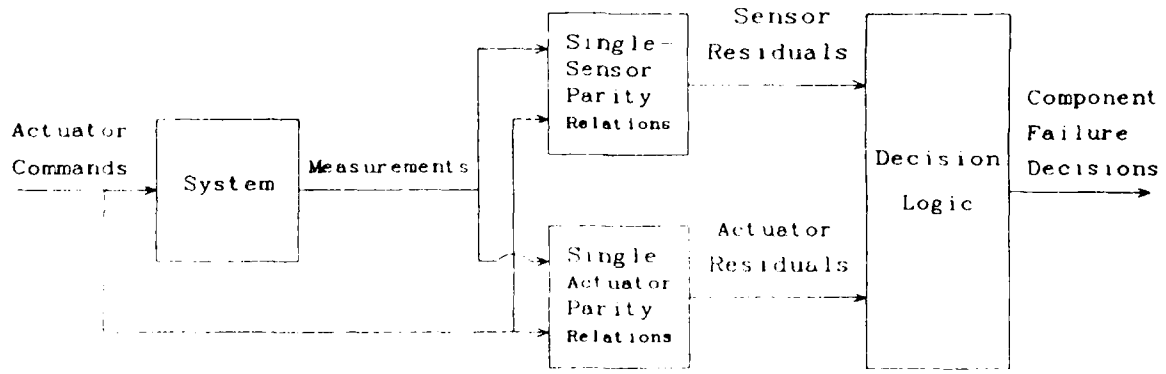

FDI System Based on Single-Component Parity Relations

THE SCOLE FACILITY

The Spacecraft Control Laboratory Experiment (SCOLE) facility, designed and assembled at NASA Langley Research Center, is a testbed for experiments on control of flexible spacecraft and related problems. The configuration resembles that of the COFS II experiment where a reflector at the tip of a long flexible mast is deployed from the Space Shuttle. The Shuttle has been represented with a massive steel plate cut in the general shape of the orbiter. Fully instrumented, it weighs 501 pounds. Attached to the simulated Shuttle is a slender, flexible beam 120 inches long weighing 4.48 pounds. To the end of this mast is attached a simulated reflector which is a hexagonal frame 22 inches long on each side and weighing 4.76 pounds.

The experiment can be operated in two configurations. The pendulous configuration has the Shuttle suspended from the roof girders by a long cable and a universal joint attached near the center of gravity of the assembly. In the cantilever configuration, the Shuttle is lowered to rest on sawhorses with only the flexible mast and reflector free to move. In both configurations the mast points downward.

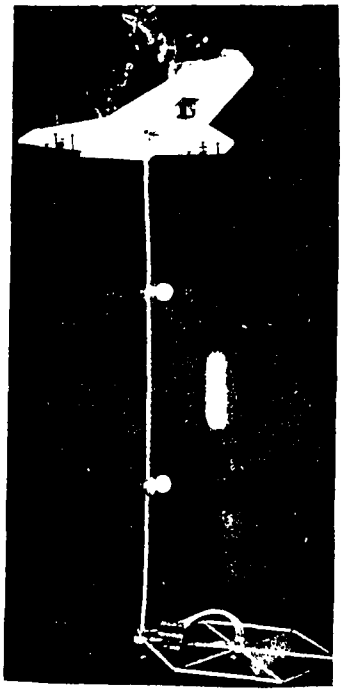

THE SCOLE EXPERIMENT APPARATUS

TEST PROCEDURE

The results presented here were produced by single-component parity relations designed using a 10 mode model of the dynamics of SCOLE. The modes were derived from a finite element model and were not improved by the use of actual experimental data. Some discrepancies were clear; the measured period of the third mode in the cantilever configuration, which is strongly excited in some of the tests, is about 10 percent shorter than that predicted by the model.

The failure detection tests were performed off-line on files of data taken on test runs of the apparatus at an earlier time. These tests were not designed to enhance FDI performance - they were conducted for other reasons. Failures were simulated in the data which was input to the parity relations. Sensor failures were simulated as "off" failures (zero output) while actuator failures of both the "off" and "on" type were simulated.

TEST PROCEDURE

- **Generalized parity relations based on first 10 modes of SCOLE**
- **Modes were obtained from FEM and were not updated based on experimental data**
- **FDI tests performed off-line with failures simulated in data**
- **Data files came from tests conducted for other reasons - not designed to enhance FDI capability**

MINIMUM TIME SLEW MANEUVER

COMMAND TO Y THRUSTER

The first test was conducted with SCOLE in the pendulous configuration - where it is free to rotate in all directions. This is a maneuver about the roll axis in which the apparatus was initially pushed to one side and released, then a minimum time slew logic was engaged to return the system to zero roll angle. This figure shows the bang-bang thrust history typical of minimum time slews. The two thrusting periods are not equal because the angular velocity at initiation was not quite zero.

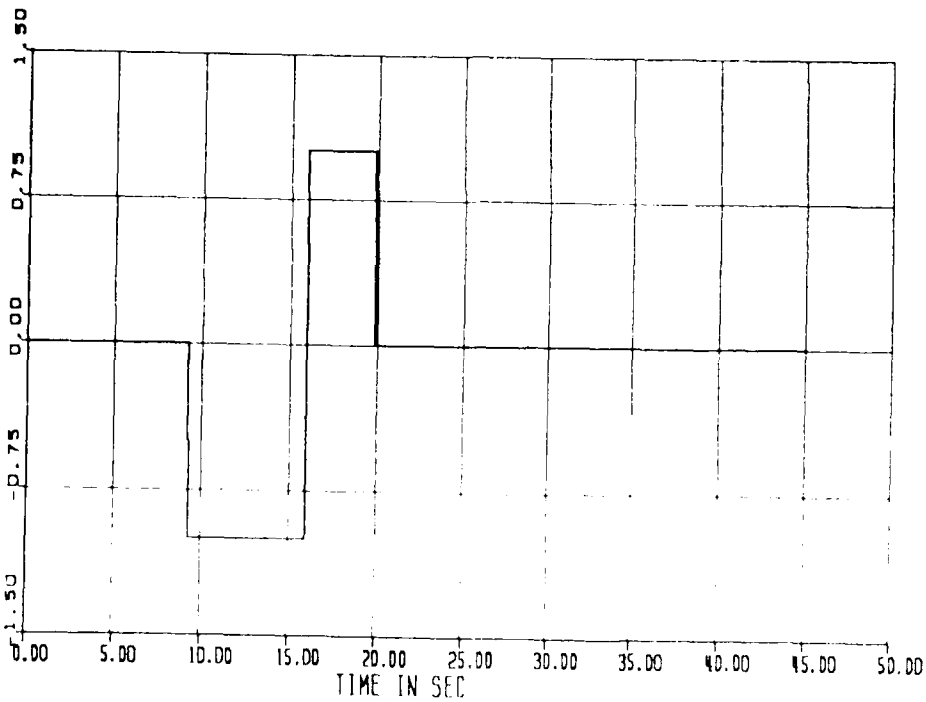

Minimum Time Slew Maneuver: Thrust Command TY History

MINIMUM TIME SLEW MANEUVER

OUTPUT OF Y ACCELEROMETER ON SHUTTLE BODY

This figure shows the output history of the Y accelerometer mounted on the body of the simulated shuttle. This signal is dominated by the component of suspension cable specific force along the y axis of the shuttle. Because of this effect, the Y accelerometer is essentially measuring roll angle. In constructing the generalized parity relations, it is essential to include the effect of the suspension cable in the model of the accelerometer output.

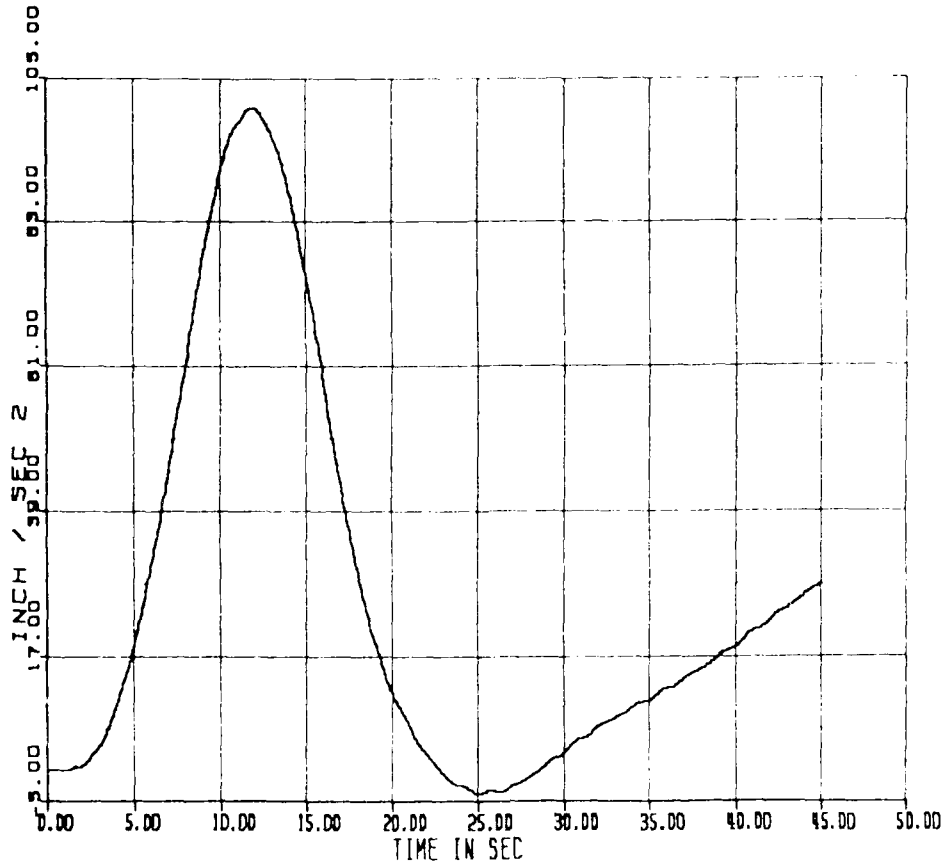

Minimum Time Slew Maneuver: Output SHACCY

MINIMUM TIME SLEW MANEUVER

PARITY RELATION RESIDUAL FOR THE SHUTTLE Y ACCELEROMETER

An "off" failure of the accelerometer was simulated in the time interval 10 to 20 seconds. Notice that the output of the parity relation is quite clean everywhere except near the beginning and end of the failure period. In the middle of the failure period, the residual shows no indication of failure. This is a consequence of the fact that the model of the system has at least one mode with zero frequency. In such a case, tne failure signature for slowly varying signals appears only in the transient period while the memory of the parity relation is being filled or emptied. The failure signature at the beginning of the failure period is much larger than that at the end because the output of the accelerometer is much larger at 10 seconds than it is at 20 seconds. If the actual sensor output were zero, an "off" failure would of course have no signature at all.

So this failure mode of the accelerometer is easily detected. Failures of the gyros on the shuttle body are not well detected because the gyro noise, relative to the typical gyro signals, is much larger than that of the accelerometers.

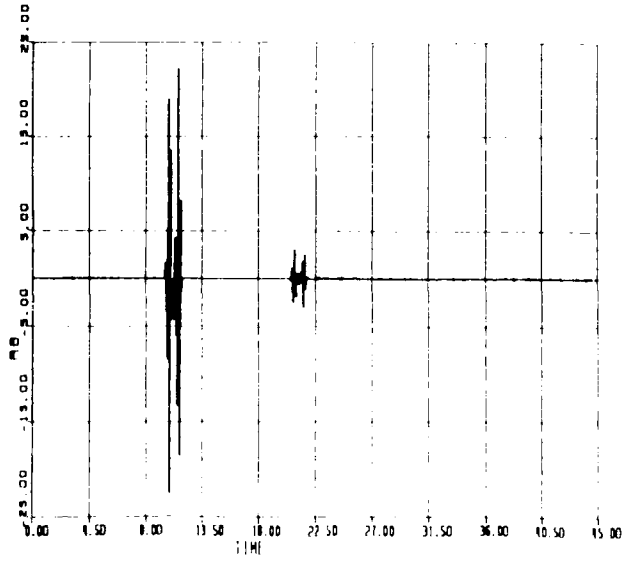

Minimum Time Slew Maneuver -- SHACCY Residual
Interrupted Measurements between t=10 and t=20 seconds

MODE 1 FREE VIBRATIONS

REFLECTOR X ACCELEROMETER OUTPUT

For this and the remaining tests, the SCOLE apparatus was set in the cantilever configuration in which the shuttle body is fixed and the mast and reflector move only because of the flexibility of the mast. In this case, the mast was excited in such a way that the first bending mode dominated the response. The mathematical model for this mode appears to be quite good as the response matches well with that predicted by the model.

This figure shows the output history of the x accelerometer which is mounted on the reflector.

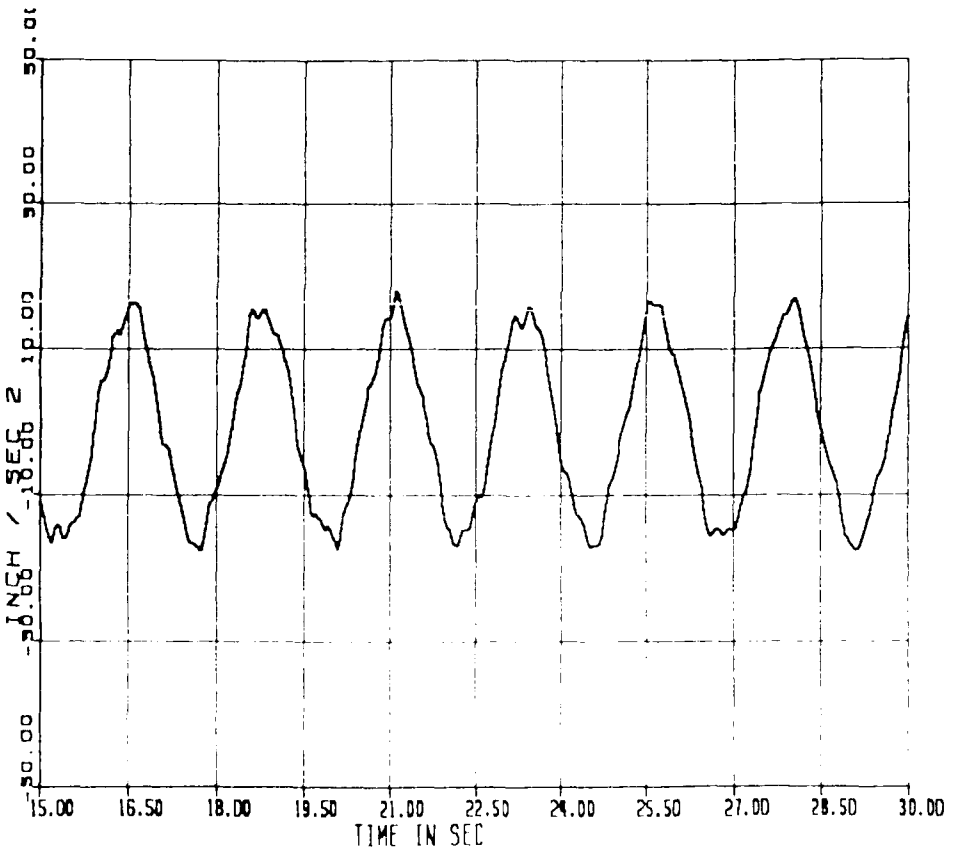

Structural Mode 1: RACCX Output

MODE 1 FREE VIBRATIONS

X THRUSTER PARITY RELATION RESIDUAL

This figure shows the output of the single-actuator parity relation designed for the x thruster on the reflector. It is essentially colocated with the x accelerometer whose response is shown in the preceding figure. There is no actual thrusting activity in this experiment, but the parity relation was given a thrust on command in the interval 20 to 25 seconds. This experiment therefore simulates a failure of the thruster to turn on when commanded.

Actuator failures seem almost universally more difficult to detect than sensor failures. Notice that the failure signature to noise ratio is much smaller in this case than it was for the accelerometer parity relation shown earlier. However, with a properly chosen threshold setting in the decision logic, this might be considered a detectable failure.

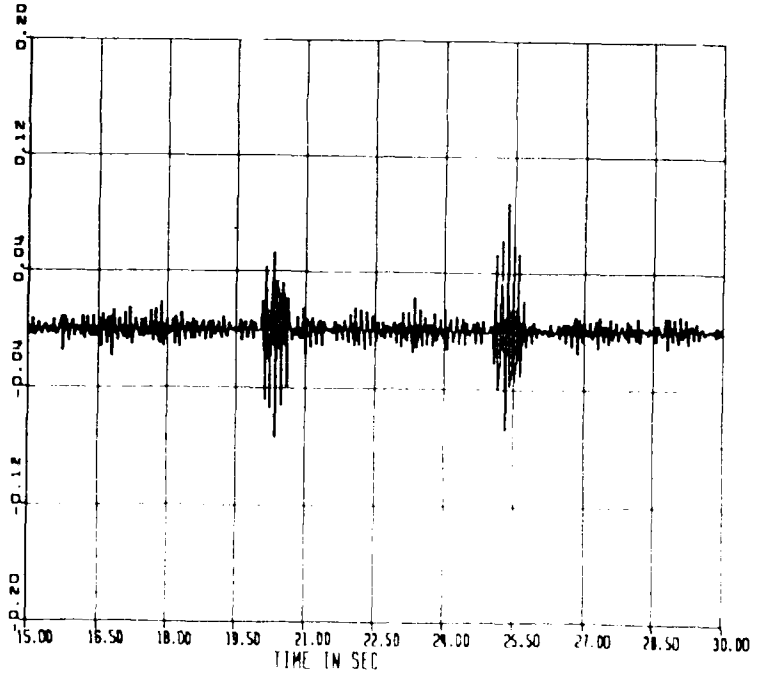

Structural Mode 1 — IX Residual
Failure to Actuate between t 20 and t 25 seconds

MODES 1 AND 2 FREE VIBRATIONS

REFLECTOR X ACCELEROMETER OUTPUT

This test is similar to the previous one except that the system has been excited in such a way that both the first and second modes of the mast appear prominently in the response. The purpose of this test is to see if parity relation performance holds up when a higher ordered mode than the first is excited. We suspect that modeling inaccuracy increases with the order of the mode.

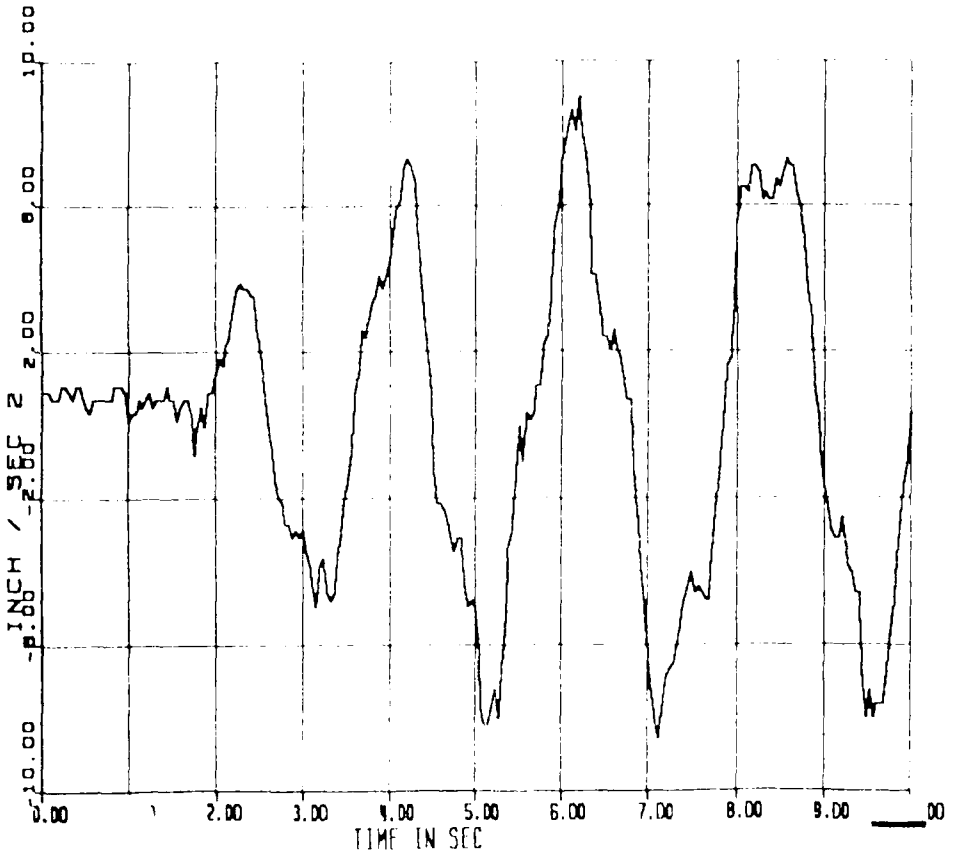

Structural Modes 1 and 2: RACCX Output

AD-A199 111 NASA/DOD (NATIONAL AERONAUTICS AND SPACE ADMINISTRATION/DEPARTMENT OF DEF..(U) AIR FORCE WRIGHT AERONAUTICAL LABS WRIGHT-PATTERSON AFB OH.

UNCLASSIFIED A D SWANSON JUN 88 AFWAL-TR-88-3052 F/G 20/11 NL

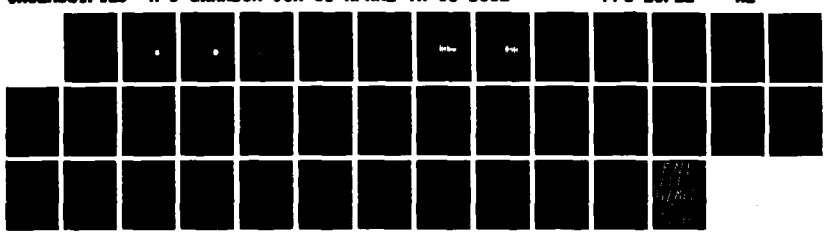

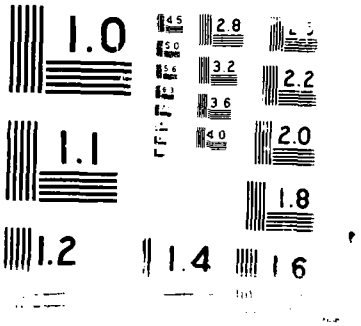
1.0
1.1
1.2
1.4
1.6
1.8
2.0
2.2
2.8
3.2
3.6
4.0

MODES 1 AND 2 FREE VIBRATIONS

THRUSTER X COMMAND HISTORY

This experiment, like the last, tests the ability of the parity relation to detect the failure of the thruster to turn on when commanded. To illustrate the fact that the parity relation residual is strongly dependent on the history of the command which the thruster fails to respond to, two different commands were simulated. They are shown in this figure.

The first is the same command used in the previous test. It is simply a command to turn on; however, the interval is 1 1/2 seconds in this case whereas it was 5 seconds in the previous case. The other command which was issued between 7 and 8 1/2 seconds is an alternating sequence of plus and minus on commands which change at every time step.

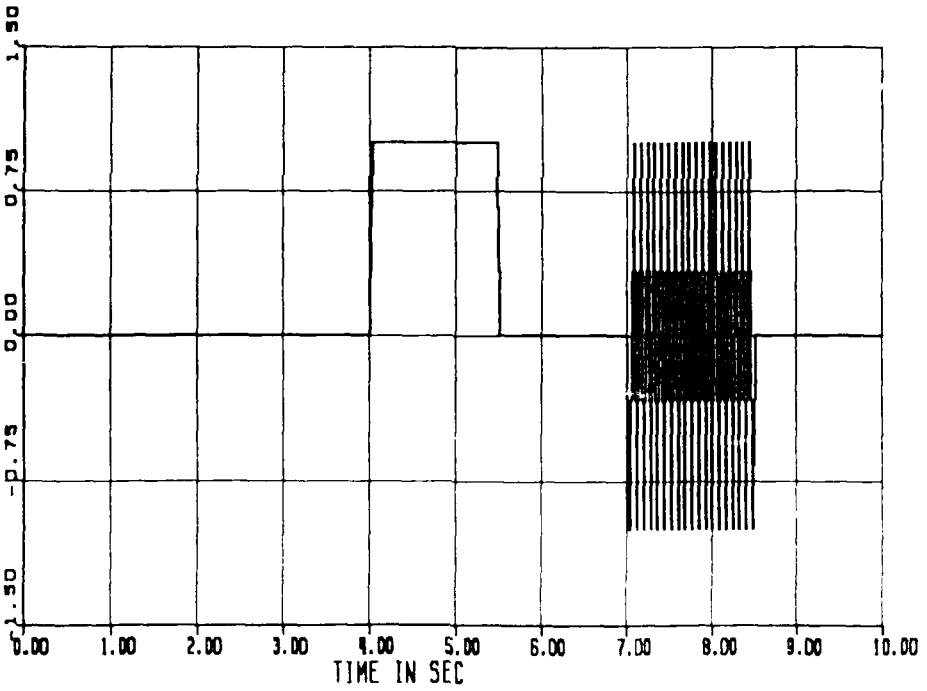

TX Thrust Command History

MODES 1 AND 2 FREE VIBRATIONS

X THRUSTER PARITY RELATION RESIDUAL

The less accurate modeling of the second mode is obvious in this record of the output of the parity relation for the x thruster on the reflector. The signature of the failure to turn on with the steady command between 4 and 5 1/2 seconds is scarcely observable whereas it had been quite clearly distinguishable from the noise when only the first mode was excited.

The strong dependence of the failure signature on the thrust command is illustrated by the response between 7 and 8 1/2 seconds. This large signature results from the alternating sequence of plus and minus commands which is unrealistic but clearly shows the point.

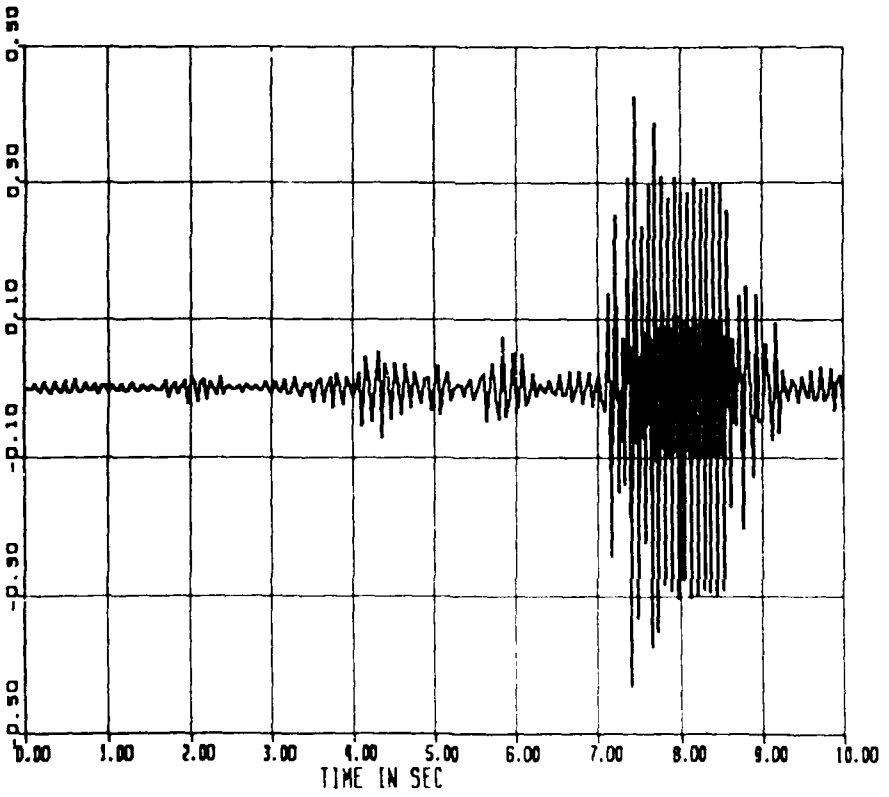

Structural Modes 1 and 2: TX Residual: Failure to Actuate

MODES 1 AND 2 FREE VIBRATIONS

X ACCELEROMETER PARITY RELATION RESIDUAL

The modeling inaccuracy of the higher modes affects sensor parity relation performance as well. This figure shows the output of the single-sensor parity relation designed for the x accelerometer mounted on the reflector. An "off" failure of the sensor (zero output) is simulated beginning at 6 seconds. Recall that the failure signature is a transient which persists only over the memory span of the parity relation. The output over that period is definitely larger than the residual noise which preceeds it, but the signal to noise ratio is not large enough for reliable failure detection.

The clean signal at the end of this test is indicative of the null output of the sensor. However, one could not use a test for null output of the parity relation residual as a general test for failure because that output characteristic is specific to the null output failure mode.

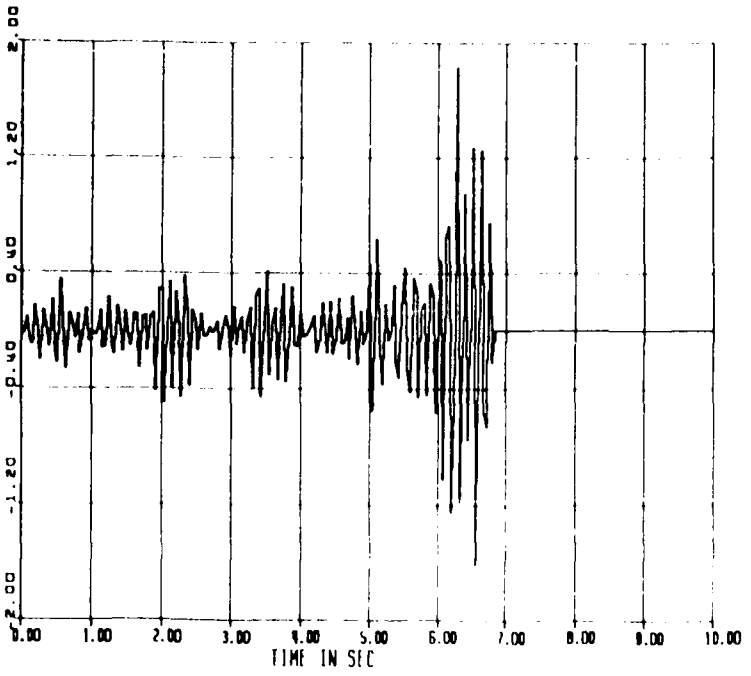

Structural Modes 1 and 2 RACCX Residual
Interrupted Measurements at 6 Seconds

CLOSED LOOP CONTROL MODE

X THRUSTER COMMAND HISTORY

The final experiment to be reported here shows the effect on failure detection performance of actual thrusting activity. The SCOLE apparatus in the cantilever configuration was operated with a closed loop controller functioning to damp bending vibrations. Both x and y channels were engaged, but results will be given only for x axis performance. The behavior of the y channel was very similar.

This figure shows the history of the x thruster. The damping loop was engaged at 16 seconds, and the controller than called for alternating plus and minus thrust commands with a period equal to that of the first bending mode which was the principal mode excited.

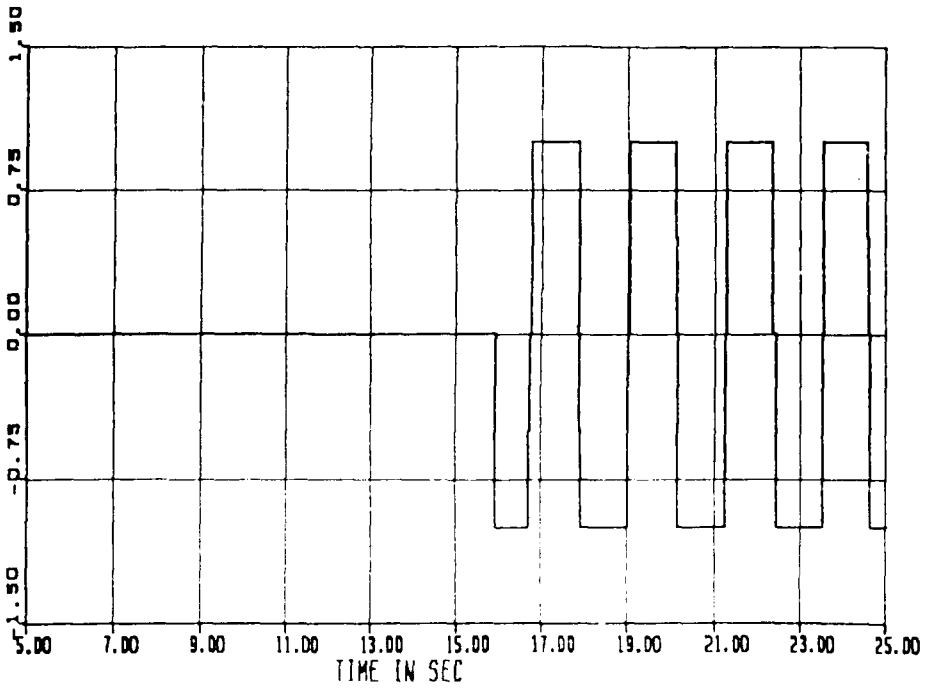

Active Vibration Damping: Thruster Command TX History

CLOSED LOOP CONTROL MODE

REFLECTOR X ACCELEROMETER OUTPUT

This figure shows the response of the structure as indicated by the x accelerometer mounted on the reflector. In the initial part of this record, the structure is being excited by hand. The accelerometer, responding to the gravitational effect, is indicating essentially the pitch angle of the reflector. When the controller is engaged at 16 seconds, and thruster activity begins, the accelerometer output becomes noticeably more noisy. It appears that higher ordered interference is generated, and of course, thruster activity tends to excite higher ordered structural modes as well.

This response characteristic suggests that there will be difficulty detecting component failures using any technique which depends on analytic redundancy. The higher ordered structural modes which are excited by thruster activity are not as well modeled as the lower ordered modes, and any additional interference generated is not modeled at all.

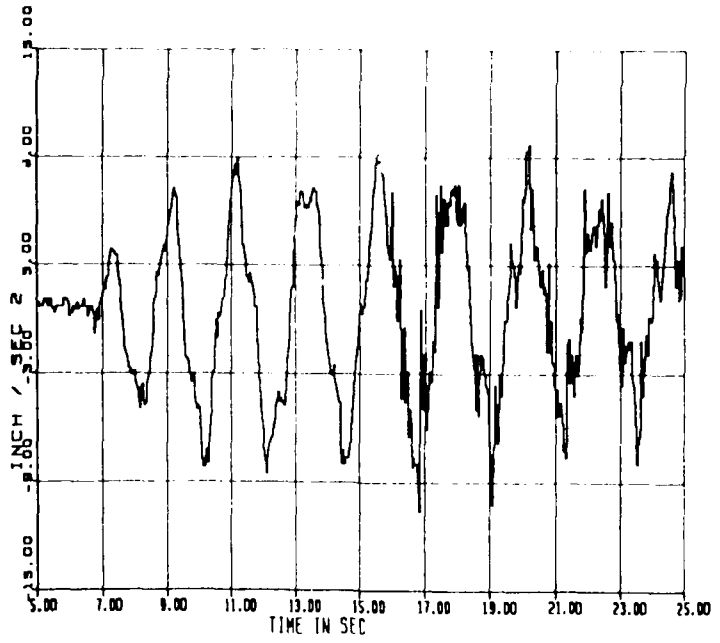

Active Vibration Damping: Output RACCX

CLOSED LOOP CONTROL MODE

X THRUSTER PARITY RELATION RESIDUAL WITHOUT FAILURES

The concern about failure detection system performance is well justified, as is indicated by this figure. This shows the output of the parity relation designed for the x thruster with no failures simulated. The large increase in residual noise when thruster activity begins is obvious. This noise is larger than the signature of a thruster failure, so no failure detection is possible.

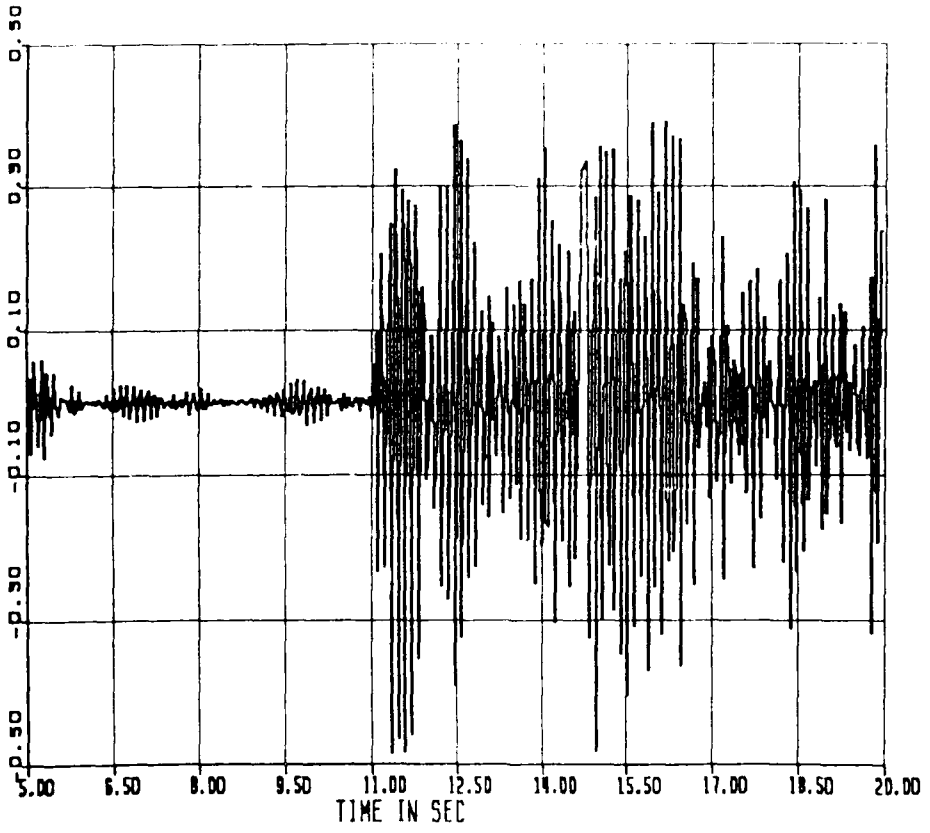

Active Vibration Damping: TX Residual: No Fail

CLOSED LOOP CONTROL MODE

X ACCELEROMETER PARITY RELATION RESIDUAL WITHOUT FAILURES

Sensor failures are generally more observable than actuator failures. However, the poorly modeled effects excited by thruster operation corrupt the accelerometer parity relation significantly as well as the thruster parity relation. The residual noise shown in this figure after thruster activity begins is not as large relative to the failure signature as that of the thruster parity relation, but still is large enough to preclude failure detection.

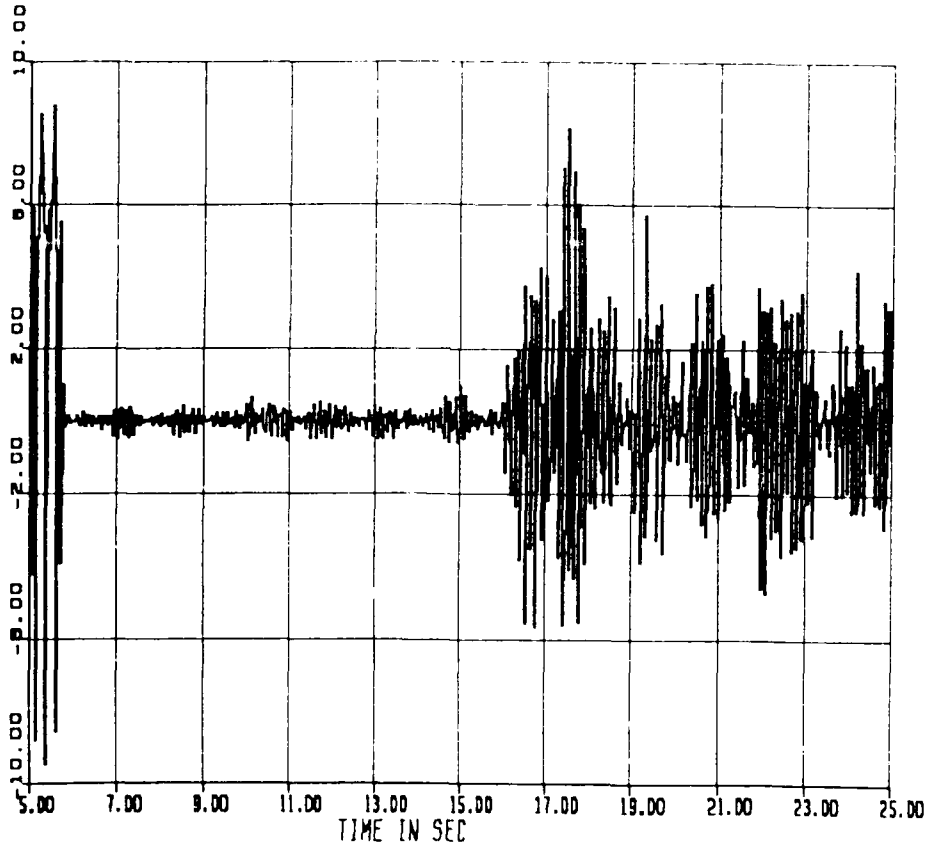

Active Vibration damping: RACCX Residual: NO Fail

CONCLUSIONS

In this series of tests it was seen that failures of the sensors mounted on the simulated shuttle body could be indicated by single-sensor parity relations quite reliably. Very likely it would also be possible to detect failures of actuators mounted on the shuttle body, but this could not be verified as no shuttle-mounted actuators were operational at the time these runs were made. The important effect seems to be that the massive shuttle body is well isolated from the poorly modeled behavior of the mast and the equipment on the reflector.

Failures of the sensors and actuators mounted on the reflector could be detected if there was no thruster activity and mast bending was dominated by the first mode which is well modeled. However, either higher order modal response or thruster activity caused parity relation residual noise of large enough magnitude to deny reliable failure detection for both sensors and actuators. It should be emphasized that it was obvious from the responses that the modeled frequencies for modes higher than the first were in error - but no attempt was made to improve upon the model in the work that is reported here.

CONCLUSIONS

- Experimental results for detection of failures of sensors mounted on the shuttle body have been successful
- It is believed that failures of actuators on the shuttle body could also be detected because the massive shuttle body is isolated from the poorly modeled effects of the mast and the equipment on the reflector
- Detection of failures of sensors and actuators mounted on the reflector has been demonstrated in the case where there is no thruster activity and no significant higher ordered structural bending response
- The structural modes higher than the first are not as well modeled, and if significantly excited, cause considerable degradation of failure detection performance
- Thruster activity excites the higher ordered structural modes and appears to introduce additional interference as well - making failure detection for components mounted on the reflector with the thrusters impossible

Single Step Optimal Control Implemented on the SCOLE

D. Sparks, Jr.
J. P. Williams

NASA Langley Research Center
Hampton, VA

Second NASA/DOD CSI Technology Conference
Colorado Springs, Colorado
November 17-19, 1987

OUTLINE

This paper reports on the current work being performed on the Spacecraft Control Laboratory Experiment (SCOLE), a facility for testing control laws for use on flexible structures. A brief description of the SCOLE apparatus is provided. A more detailed description of the SCOLE program, facility and the various control problems associated with flexible structures can be found in reference 1. In this paper, the problem of vibration suppression using Single Step Optimal Control methods is addressed. Simulation results and a summary conclude the discussion.

OUTLINE

- ⊙ DESCRIPTION OF THE SCOLE APPARATUS
- ⊙ THE PROBLEM OF VIBRATION CONTROL ON SCOLE
- ⊙ SINGLE STEP OPTIMAL CONTROL: THEORY AND DESIGN
- ⊙ SIMULATION AND RESULTS
- ⊙ SUMMARY

THE SCOLE APPARATUS

The SCOLE hardware and software are described in more detail in references 2 and 3. Briefly, the SCOLE apparatus consists of three main parts - a rigid plate representing the shuttle platform, a hexagonal, tubular reflector frame and a flexible tube connecting the reflector to the platform. The platform is suspended by a steel cable via a univerval joint that provides roll, pitch and yaw degrees of freedom. This is illustrated in the schematic below (left).

The complex problems of slew maneuvering and attitude pointing of a flexible spacecraft model can be studied using the SCOLE apparatus. However, this paper regards the control of the flexible motion of the mast and reflector frame. For this purpose, the shuttle platform and suspension cable are clamped.

The schematic below (right), shows a detailed view of the cantilevered mast and reflector and the location of actuators and sensors along the structure. The actuators consist of four jets firing in the $\pm x$ and $\pm y$ directions and three reaction wheels providing torque about the x, y and z axes. The sensors consist of three pairs of linear accelerometers, each pair sensing in the x, y directions, and a three axis rate gyro measuring angular rates about the x,y and z axes.

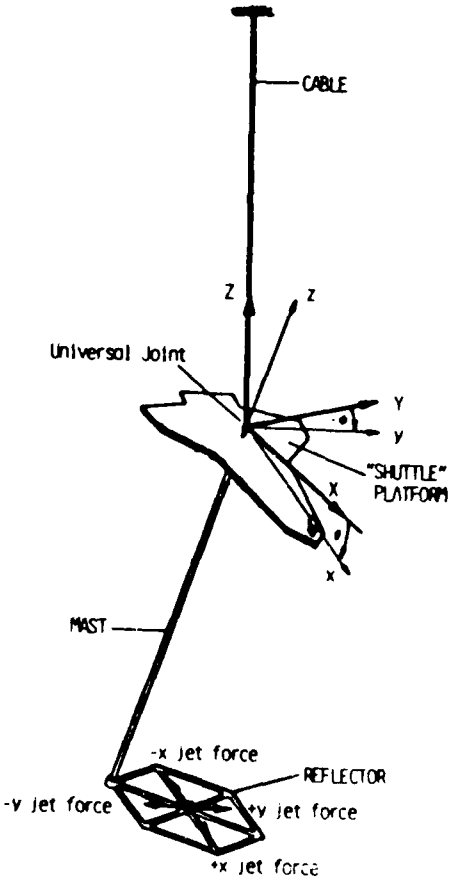

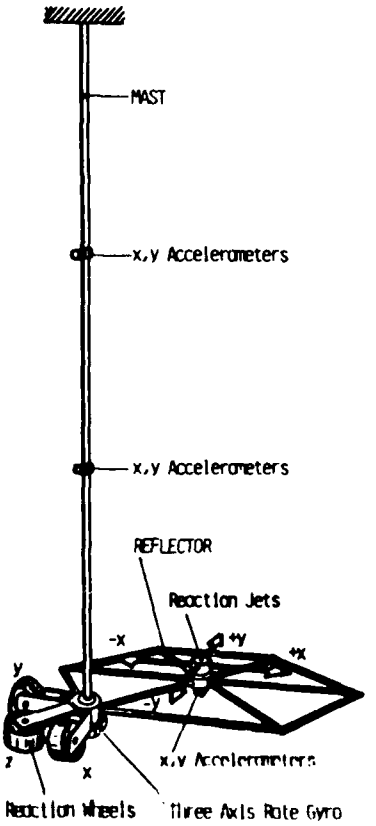

VIBRATIONAL CONTROL ON SCOLE

The problem of suppressing the vibrational motion of the cantilevered mast and reflector frame is presented. The vibrations of the flexible mast are to be damped by blending the actuator inputs of the jet thrusters and the reaction wheels with a minimum of control effort. The chief difficulty of the problem lies with the nature of these actuators. The thrusters are on-off devices and the proportional reaction wheels have saturation limits, thus they are nonlinear and are bounded. Generally, functional optimization methods, like Linear Quadratic Gaussian (LQG) in its basic form, treat only linear, unconstrained inputs.

The approach taken here are the Single Step Optimal Control methods developed by N.R. Tomlinson and M.A. Floyd (references 4 and 5).

VIBRATION CONTROL BLENDING ON-OFF AND PROPORTIONAL DEVICES

⊙ . . . FOR MINIMUM EFFORT CONTROL LAW ON CANTILEVERED SCOLE

⊙ ACTUATORS - COLD GAS JETS AND REACTION WHEELS

⊙ APPROACH - SINGLE STEP OPTIMAL CONTROL METHOD

SINGLE STEP OPTIMAL CONTROL THEORY

Instead of optimizing the controls over the entire time interval as done by LQG, the single step method divides the given time interval into sub-intervals and performs the optimization over each sub-interval. The problem is then one of parameter optimization. A cost function can be defined in terms of the controls and the task is to solve for the controls that minimizes the cost over each interval. By doing so, the bounds on the control inputs can be taken into account by treating them as constraints.

For the vibration suppression problem of the SCOLE, the cost function for the kth time interval is defined in terms of the controls over the interval and the vibrational energy in the next time interval (kth + 1). By substituting the equations of motion into the cost function, the kth cost will only be in terms of the controls. The kth cost can then be minimized with respect to the kth controls.

One advantage to this method is that it works in discrete time, lending itself to digital implementation on a real time computer.

SINGLE STEP OPTIMIZATION

MODEL OF MOTION

$$X_{k+1} = AX_k + BU_k$$

COST FUNCTION IN NEXT STATE & PRESENT CONTROL

$$J_k = X_{k+1}^T PX_{k+1} + U_k^T RU_k$$

SOLVE FOR U_k THAT MINIMIZES J_k

SINGLE STEP OPTIMIZATION BACKGROUND

Two minimum control algorithms based on single step optimization were found in the literature and applied to the SCOLE problem. The first was proposed by Tomlinson. The method involves calculating the unconstrained optimal control values. From this, the control values are divided into those that violate their respective bound limits and those that do not. All the violating control values are replaced by their respective limits and the optimization is repeated over the non-violating controls. This procedure is iterated until all the optimal control values are either below their bounded values or have been replaced by them.

The second algorithm is similar to the first. It was proposed by Floyd. Like Tomlinson's, this method begins by computing the unconstrained optimal control values, but instead of optimizing over a group of controls, it optimizes each control input one at a time. To accomplish this, it is assumed that the actuators can be ordered from the strongest to the weakest, and that the weaker actuators do not influence the control values of the stronger actuators. That is, the ith actuator's optimal control value is assumed to be only a function of the control inputs of the stronger actuators in the hierarchy. This reduces the optimization of each actuator input to a scalar level.

Note that with the above assumptions, both methods do not give the true optimal solution, but a relatively easily computable approximation to it.

SINGLE STEP OPTIMIZATION BACKGROUND

- TOMLINSON (1966)

  PRESENTED ITERATIVE VECTOR ALGORITHM

- FLOYD (1984)

  PRESENTED NON-ITERATIVE SOLUTION

SINGLE STEP OPTIMIZATION DESIGN

A state space model of the cantilevered SCOLE mast was developed from a finite element analysis. The state space model was done in modal coordinates and the first ten modal displacements and velocities were used as state variables. It was assumed that all the modes were decoupled. No actuator dynamics were taken into account; the control inputs were simply taken to be forces or moments acting at their respective actuator locations. The four jets were combined into two jets that fire in the $\pm x$ and $\pm y$ directions. Similarly, no sensor dynamics were included in the model.

A Kalman filter was developed to estimate the states of the system.

Although both Tomlinson's and Floyd's methods were tested, most of the work was concentrated on Floyd's method because of its relative simplicity and the fact that it performed just as well as Tomlinson's more complex method.

SINGLE STEP OPTIMIZATION DESIGN

⊙ MODEL - LINEAR FEM OF SCOLE

- 10 DECOUPLED MODES
- 2 REACTION JETS AND 3 REACTION WHEELS

⊙ DESIGN APPROACH

- STATE ESIIMATION BY KALMAN FILTER
- FLOYD'S METHOD TO CALCULATE CONTROL

SIMULATION

Numerous simulations were made for both the Tomlinson and the Floyd methods. The state space model previously mentioned was used, with previously measured modal damping and sensor noise values included. Most of the vibrational motions were initialized through initial conditions placed on the modal states, both with single modes and multiple modes excited.

SIMULATION

- LINEAR 10 MODE FEM WITH NOISE AND DAMPING
- SIMULATION DONE ON MATRIX$_x$
- INITIAL CONDITIONS ON MODE STATES
  - SINGLE MODE (1ST, 3RD, 4TH)
  - MULTIPLE MODES

RESULTS

A typical simulation result is presented. The first torsional mode (mode 3) was excited by giving it an initial modal displacement. The motion of the mast and reflector for this particular mode is shown below. The natural frequency is about 1.5 Hz and the motion predominantely involves the reflector frame rotating about the mast's longitudinal axis. The axes 1,2 and 3 on the figure represent the x,y and z axes, respectively.

VIBRATIONAL MODE. FREQ (HZ) 1504 X10 +01

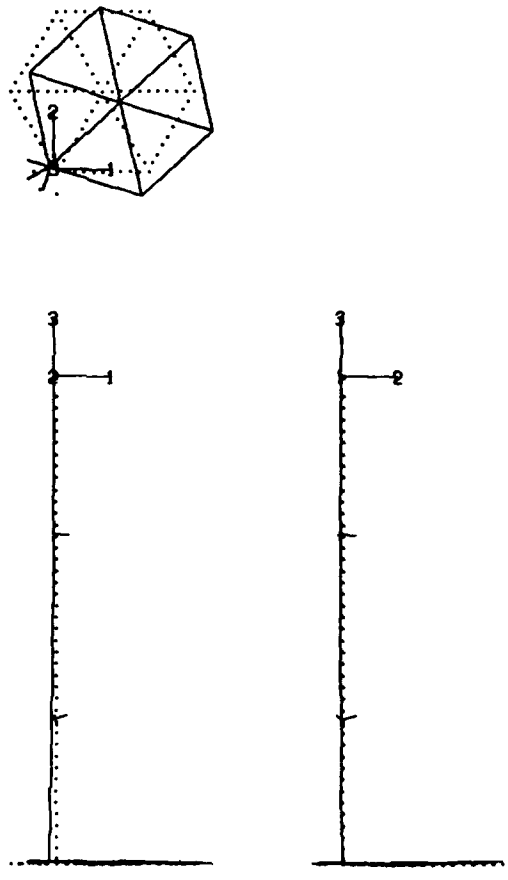

SCALE VIBRATIONAL MODE SHAPE 3

RESULTS

The third mode was given an initial modal displacement of 0.529, the jet thruster levels were ±0.35 lbs and the torque limits for each of the reaction wheels were ±1.875 in-lbs. The sampling rate used in the simulation was 50 Hz. The estimate of the modal amplitude, the x acceleration at the reflector center, the x jet applied force and the torque applied by the z reaction wheel are shown in figures a-d, respectively. The torsional motion was suppressed in 4 seconds, as may be observed in figures a and b. The thruster and torque wheel worked in unison to damp out the vibrations. Near the end of the vibration suppression, in the 3-4 seconds range, the thruster commands were reduced and eventually ended, while the torque wheel became less saturated and operated in its linear region.

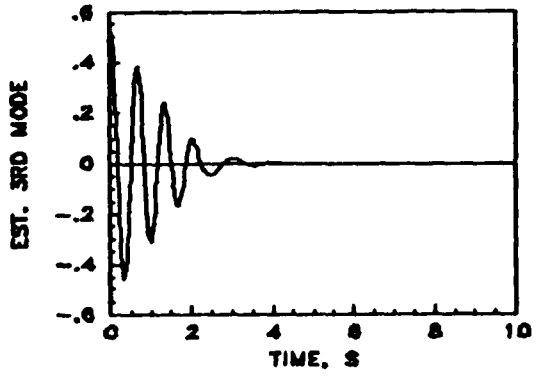

FIG. A ESTIMATE OF 3RD MODE

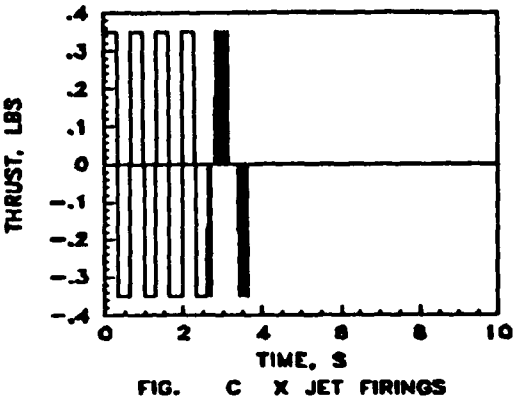

FIG. C X JET FIRINGS

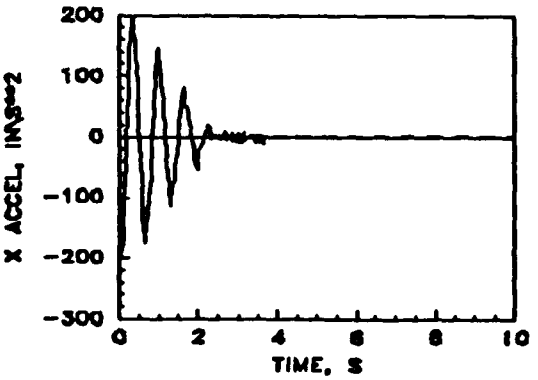

FIG. B X ACCELERATION, REFLECTOR

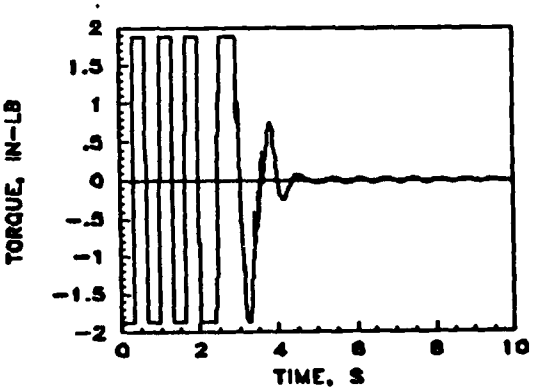

FIG. D Z REACTION WHEEL CMDS

SUMMARY

Two control laws, based upon Single Step Optimal Control theory, were tested on a cantilevered mast model of the SCOLE. Although both algorithms gave good results in vibration suppression, Floyd's algorithm was found to be simpler computationally and thus easier to implement.

Future work will include real time testing of Floyd's algorithm on the cantilevered SCOLE mast in the laboratory.

SUMMARY

SIMULATION TEST USING SINGLE STEP OPTIMAL CONTROL METHOD

ON SCOLE

CODING OF SINGLE STEP OPTIMIZATION ALGORITHM

ON SCOLE, TEST COMPLETION JAN 1988

REFERENCES

1. Taylor, L.W., Jr., and Balakrishnan, A.V., A Laboratory Experiment Used to Evaluate Control Laws for Flexible Spacecraft ... NASA/IEEE Design Challenge. Proceedings of the Fourth VPI&SU Symposium on Dynamics and Control of Large Structures, Blacksburg, VA, June 1983.

2. Williams, J.P. and Rallo, R.A., Description of the Spacecraft Control Laboratory Experiment (SCOLE) Facility. NASA TM-89057, February 1986.

3. Shenhar, J., Sparks, D., Jr., Williams, J.P., and Montgomery, R.C., Attitude Control System Testing on SCOLE. Proceedings of the Sixth VPI&SU/AIAA Symposium on Dynamics and Control of Large Structures, Blacksburg, VA, June 1987.

4. Tomlinson, N.R., Suboptimal Digital Control Systems with Bounded Inputs. Electronic Letters, 1966 #2.

5. Floyd, M.A., Single Step Optimal Control of Large Space Structures. Doctor of Science Thesis, Massachusetts Institute of Technology, April 1984.

Problems Associated with Reaction Mass Actuators used in Conjunction with LQG Control on the Mini-Mast

D. Ghosh
PRC Kentron
303 Butler Farm Road
Hampton VA 23666

R. C. Montgomery
NASA Langley Research Center
Hampton VA 23665

Second NASA/DOD CSI Technology Conference
Colorado Springs, Colorado
November 16-19, 1987

Outline

This paper presents an overview of the work being done at NASA LaRC on developing control laws for the Mini-Mast experimental facility which falls under the COFS I program. Guest Investigators will be selected from government agencies and the industrial and academic communities to conduct research using the facility. Mini-Mast is a truss-beam structure similar to Mast but only 20 meter in length. This facility will have inertial sensors and actuators that are functionally similar to those of the Mast Flight System being developed by Harris Corporation for COFS under a NASA contract. Displacement sensors will also be available on the facility. Inertial sensors are conventional servo-accelerometers and the inertial actuators are linear reaction mass actuators (RMA) and rotary wheel components. Problems arise with use of RMA's because of two fundamental limitations - force and stroke limits. In particular, this paper is concerned with the problems associated with stroke limit.

First, the Mini-Mast system will be described, briefly. This will be followed by the problems associated with the use of reaction mass actuators in conjunction with LQG control, a description of the local controller used herein, a description of the algorithm for converting the force commands of the LQG algorithm into position command for the reaction mass devices, and finally a description of the results of the simulator developed for this work.

- MINI-MAST
  - COFS - I EXPERIMENTAL FACILITY
  - 20 METER LONG TRUSS-BEAM STRUCTURE SIMILAR TO MAST
  - WILL HAVE SERVO-ACCELEROMETERS, DISPLACEMENT SENSORS AND REACTION MASS ACTUATORS
- REACTION MASS ACTUATORS
  - FUNDAMENTAL LIMITATIONS
    1. FORCE LIMIT
    2. STROKE LIMIT
- PAPER DEALS WITH ISSUES ASSOCIATED WITH STROKE LIMIT

Figure 1.

Mini-Mast System

The apparatus consists of a test-article on which there are sensors and actuators that can be controlled by a digital computer in real time. The actuators are all inertial components that could be realized in space operations. However, only the components used in this study will be described herein.

- MINI-MAST STRUCTURE
- DISPLACEMENT SENSORS
- REACTION WHEEL ACTUATORS
- REACTION MASS ACTUATORS

Figure 2

Mini-Mast

The Mini-Mast is a deployable statically determinant, three - longeron, single-laced truss with every other bay repeating. The truss is 20.16 m high and contains 18 bays each 1.12 m high. The longeron corners fall on a 1.4 m diameter circle. The corner joints are machined titanium bars with provisions for the longeron and diagonal members to be hinged with a stainless steel pin. The horizontal member joints are not pinned. The diagonals fold inward by a titanium hinge located near the center of the member. The tubing members are constructed of graphite/epoxy. The mass of the truss-beam structure is 130.93 Kg. The test article is bolted to a base plate at the three lowest joints of the beam. An equipment mounting plate, used for mounting actuators and sensors, is attached to the top of the structure.

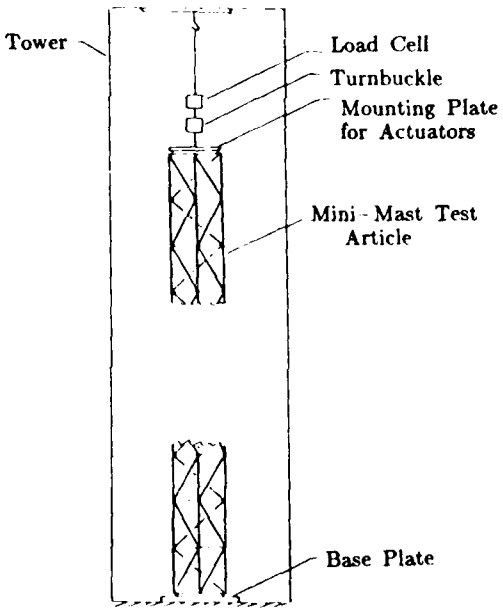

Figure 3. Side View Sketch of the Mini-Mast Test Apparatus

Deflection Measurement System

The deflection measurement system uses noncontacting displacement sensors, probes that measure the distance between the flat face of a joint and the circular face of the sensor (see figure 4). To provide sensor data for the motion of the beam, the cross section of the beam is assumed to be rigid. Thus, three probes are required to obtain the transverse and torsional motion of the beam at any station.

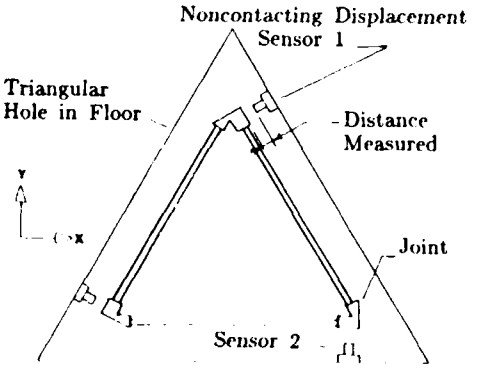

Figure 4. Top View Sketch of the Mini-Mast Test Apparatus Showing the Locations and Orientations of the Position Measurement Devices.

Actuators

Excitation and control forces are exerted on the structure using reaction mass actuators and reaction wheels. These can be driven by commands from a digital computer in real time to test various open-loop excitations and closed-loop control laws. Locations of the actuators on the top equipment plate are illustraced in figure 5.

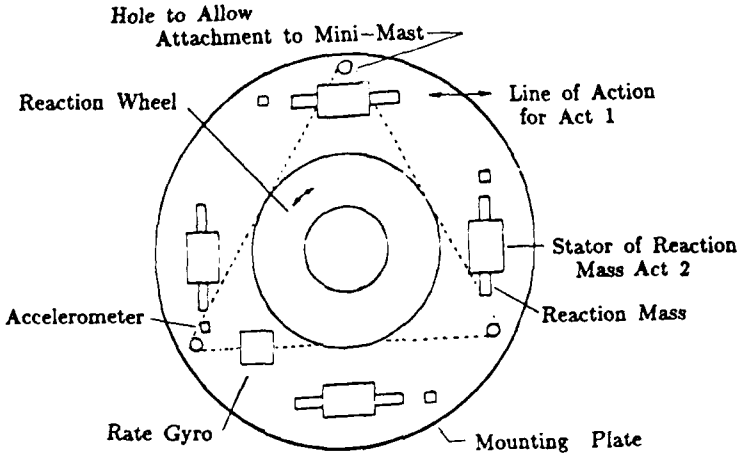

Figure 5. Top View Sketch of the Mini-Mast Control Plate Showing the Locations of the Linear Reaction Mass and Rotary Reaction Wheel Actuators.

Analytic Modeling

Finite element analysis was used for analytic modeling of the test structure. The finite element model (FEM) was developed by the Structural Dynamics Branch of NASA/LaRC. It uses 338 joint locations with 441 beam elements and one circular mounting plate with lumped masses representing the actuator and sensor components at the top. No structural damping was considered. The simulator was developed using modal analysis and extracting only the first ten modes (ref. 1.). The modal equations were expressed in state space and discretized to render them amenable for simulation of the plant and design of the Kalman filter. The equations are shown below in figure 6.

- EQUATIONS OF MOTION :

$$M\ddot{q} + Kq = Du(t)$$

- MODAL SPACE STATE EQUATIONS :

$$\dot{x} = Ax + Bu$$

- DISCRETIZED STATE EQUATIONS :

$$x_{k+1} = \phi x_k + \Gamma u_k$$

- MEASUREMENT MODEL :

$$y_k = Hx_k + v_k$$

Figure 6

Control System Design

Linear Quadratic Regulator theory was used to calculate the controller gains. An estimator was designed using Kalman Filter theory (ref. 2).

- LINEAR QUADRATIC REGULATOR PROBLEM

$$x_{k+1} = \phi x_k + \Gamma u_k$$

$$J_c = \int_0^T (x'Q\,x + u'Ru)\,dt$$

$$J_d = \sum_{k=0}^{n} (x_k \hat{Q} x_k + x_k \hat{w} u_k + u_k \hat{R} u_k)$$

where n is the number of sampled intervals in the interval $0 \le t \le T$

$$u_k = -\,G x_k$$

- OPTIMAL PREDICTOR-ESTIMATOR

$$\hat{x}_{k+1} = \phi \hat{x}_k + \Gamma u_k + F(y_k - H\hat{x}_k)$$

Figure 7.

Problems Associated with Reaction Mass Actuators

Linear reaction mass actuators have a serious problem of stroke limitation that is unique to these control devices. In order to generate a force with an actuator one must accelerate a reaction mass. However, the force must be regulated to keep the reaction mass within its physical confines. A local controller has been designed to deal with stroke limitation. The purpose of this local controller is to force the reaction mass to follow position commands issued by the digital computer. Thus, if the disturbance inputs to the actuator are small enough, the control computer can prevent the reaction mass from striking its stroke limits. The design of the local controller is still in progress and several candidates are being considered. A schematic diagram of the one used herein is shown in figure 10.

- TO GENERATE A FORCE WITH A REACTION MASS ACTUATOR ONE MUST ACCELERATE A REACTION MASS

- THE FORCE MUST BE REGULATED TO KEEP THE REACTION MASS WITHIN ITS PHYSICAL CONFINES

- THE PURPOSE OF THE LOCAL CONTROLLER IS TO FORCE THE REACTION MASS TO FOLLOW POSITION COMMANDS ISSUED BY THE DIGITAL COMPUTER

Figure 8.

Force to Position (FTP) Command Algorithm Using Direct Double Integration

If the control command to an actuator is a sinusoidally decaying type of force command then the displacement of the reaction mass obtained by directly integrating the acceleration twice results in the steady drift of the reaction mass. This shows the need for a local controller.

- CONTROL FORCE COMMAND TO AN ACTUATOR :

$$f(t) = Fe^{-\alpha t}\mathrm{Sin}\omega t$$

- DISPLACEMENT OF REACTION MASS RELATIVE TO ACTUATOR BASE :

$$\delta(t) = \left\{ \frac{F\omega}{(\alpha^2 + \omega^2)m_r} + V_0 \right\} t - \frac{Fe^{-\alpha t}[(\alpha^2 + \omega^2)\mathrm{Sin}\omega t - 2\alpha\omega\mathrm{Cos}\omega t]}{m_r(\alpha^2 + \omega^2)^2} + \frac{2\alpha\omega F}{m_r(\alpha^2 + \omega^2)^2} + \delta_0 - \delta_b(t)$$

- THE LINEAR TERM ON THE RIGHT HAND SIDE OF THE ABOVE EQUATION EXPLAINS THE DRIFT.

Figure 9.

Local Controller

A schematic diagram of the local controller used in this work is shown in figure 10. It consists of a precompensator to shape the input and a relative position feedback loop. The local controller adds damping to the system. This can be observed when the local controller is active and the digital computer issues null displacement commands . Simulation studies showed an added damping of about 4.6 percent in the first mode (ref. 1). When the direct double integration FTP is active the damping is reduced to 0.2 percent. Also the local controller in conjunction with the FTP causes an attenuation of the force command issued by the LQG based controller.

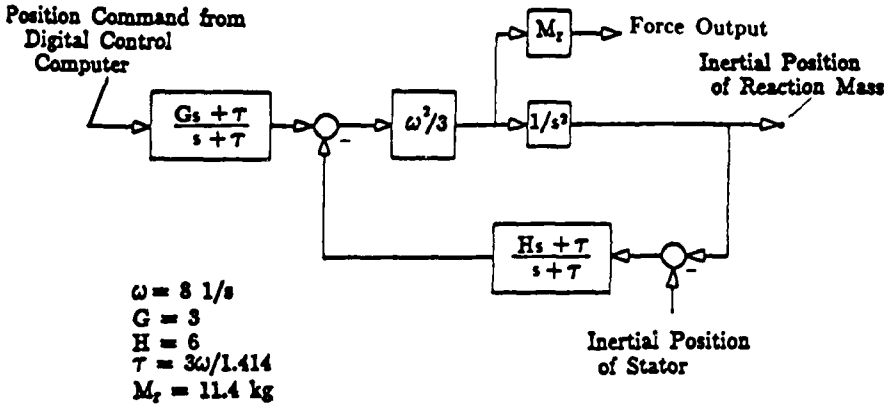

Figure 10. Schematic Diagram of a Local Controller

LQG Test Results

Simulations using idealistic unconstrained pure-force command actuators yielded a logarithmic decrement of 7.2 percent in the first mode (ref. 1). Simulation of the dynamics with the local controller engaged but with the displacement of the reaction mass confined to +/- 15 cm FTP is shown in figure 11. In the control phase the reaction mass drifts to one side, as expected, till saturation is reached. The damping factor in this case is 5 percent before saturation and 4.6 percent afterwards (ref. 1).

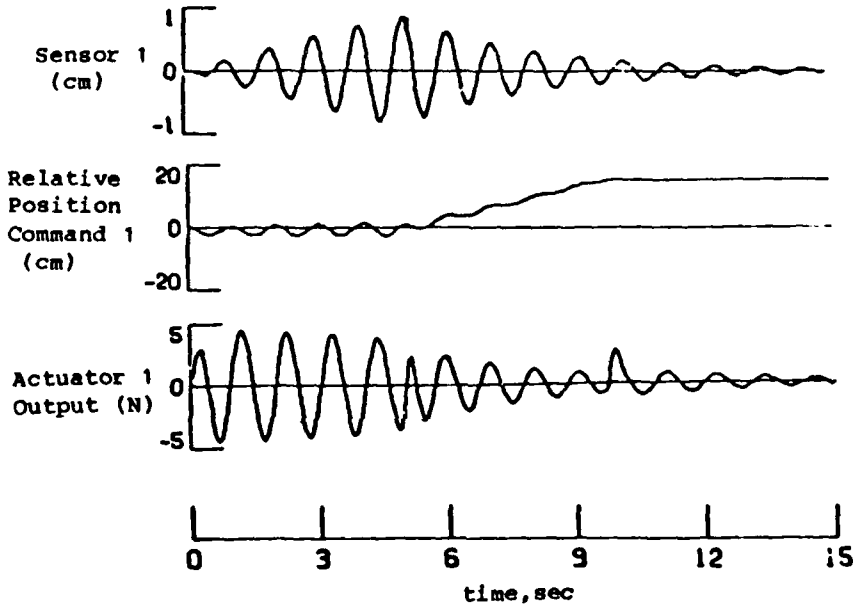

Figure 11. Simulation of Excitation and LQR Control Using the Direct Double Integration FTP Algorithm with Constrained Reaction Mass Actuators.

Modified Force to Position Conversion

To eliminate drift the double integration scheme was replaced by a stabilized scheme shown in figure 12.

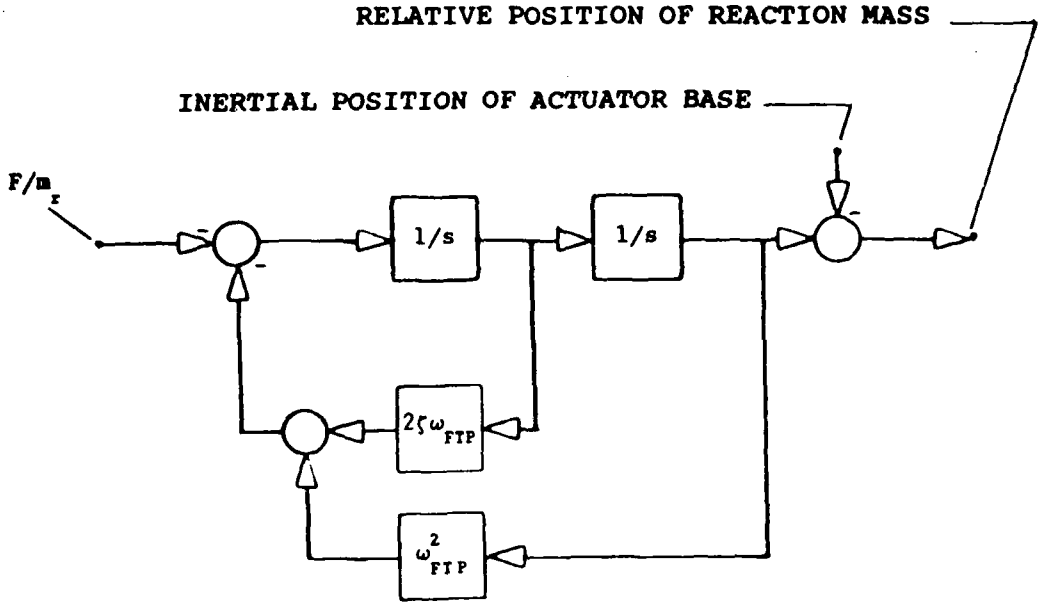

Figure 12. Block Diagram of Modified Force to Position Conversion Loop.

Effects of Modified Force to Position Algorithm

Simulations of the dynamics with the local controller engaged and the modified FTP algorithm active is shown in figure 13. It can be seen that the relative position of the reaction mass does not drift as before and that saturation of the actuator is avoided. The level of damping in the first mode, for the case shown in figure 13, is 7.3 percent.

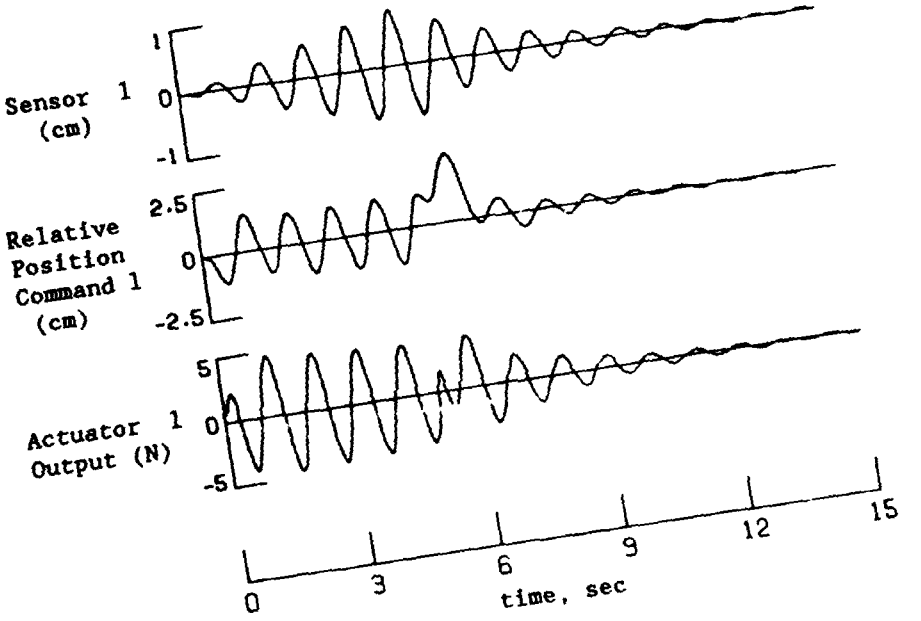

Figure 13 Simulation of Excitation and LQR Control Using the Modified FTP Algorithm with Constrained Reaction Mass Actuators.

Effects of FTP Frequency

When the FTP frequency is increased the logarithmic damping increases as shown in figure 14 below. It can be observed that it is possible to meet or even exceed the design damping. Since the FTP algorithm is in the EDS computer it provides an added advantage of fine-tuning the damping desired.

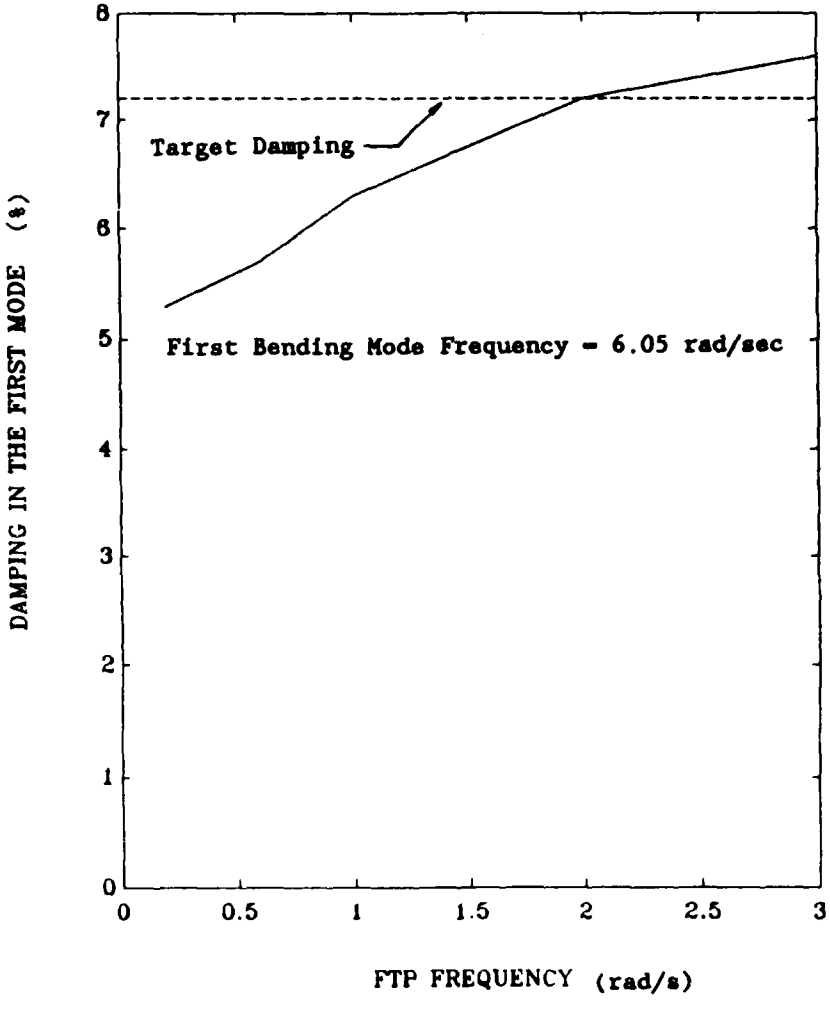

Figure 14. Effect of FTP Frequency on Damping

Concluding Remarks

This paper presented an overview of the work being done at NASA LaRC on developing control laws for the Mini-Mast experimental facility. In particular it was concerned with the problems associated with the stroke limit of the reaction mass actuators. It was shown that the problem could be resolved by converting a force command to a position command of a reaction mass and then use the position command as an input to a local controller so that the relative position of the reaction mass would track the commanded relative position. It was also shown that the position drift arising in the direct double integration method of converting force commands to position commands could be avoided by stabilizing the integration scheme.

- CONTROL LAWS FOR THE MINI-MAST EXPERIMENTAL FACILITY
- PROBLEMS ASSOCIATED WITH REACTION MASS ACTUATORS WHEN USED IN CONJUNCTION WITH LQG CONTROL.
- PROBLEM RESOLVED BY USING FORCE TO RELATIVE POSITION COMMAND CONVERSION IN CONJUNCTION WITH A LOCAL CONTROLLER.

Figure 15.

References

1. Montgomery, R. C. and Ghosh, D.: LQG Control for the Mini-Mast Experiment. Sixth VPI&SU/AIAA Symposium on Control of Large Structures, Blacksburg, Va, 1987

2. Armstrong, E. A.: ORACLS - A Design System for Linear Multivariable Control. Marcel Dekker, Inc., New York, NY, pp. 63-66, 83-91 and 99-104.

U.S. GOVERNMENT PRINTING OFFICE: 1988 548-054/80088

END

DATE

FILMED

DTIC

10-88